

RUSSIAN GEOGRAPHICAL SOCIETY

FACULTY OF GEOGRAPHY,  
LOMONOSOV MOSCOW STATE UNIVERSITY

INSTITUTE OF GEOGRAPHY,  
RUSSIAN ACADEMY OF SCIENCE

Vol. 12

2019

No. 03

# GEOGRAPHY

# ENVIRONMENT

# SUSTAINABILITY

Special Issue «Environmental Change on the Mongolian Plateau: From Challenges to Solution Strategies»

Issue Guest Editors: Daniel Karthe, Sergey Chalov,  
Jerker Jarsjö, Lodoysamba Sereteer, Peter Vossen,  
Alexander Gradel, Antonín Kusbach

# EDITORIAL BOARD

EDITORS-IN-CHIEF:

**Kasimov Nikolay S.**

Lomonosov Moscow State University,  
Faculty of Geography, Russia

**Kotlyakov Vladimir M.**

Russian Academy of Sciences  
Institute of Geography, Russia

DEPUTY EDITORS-IN-CHIEF:

**Solomina Olga N.**

Russian Academy of  
Sciences, Institute of  
Geography, Russia

**Tikonov Vladimir S.**

Lomonosov Moscow  
State University, Faculty of  
Geography, Russia

**Vandermotten Christian**

Université Libre de Bruxelles  
Belgium

**Chalov Sergei R.** (Secretary-General)

Lomonosov Moscow State University,  
Faculty of Geography, Russia

**Alexeeva Nina N.** - Lomonosov Moscow  
State University, Faculty of Geography,  
Russia

**Baklanov Alexander** - World  
Meteorological Organization, Switzerland

**Baklanov Petr Ya.** - Russian Academy of  
Sciences, Pacific Institute of Geography,  
Russia

**Chubarova Natalya E.** - Lomonosov  
Moscow State University, Faculty of  
Geography, Russia

**Daniel Karthe** - German-Mongolian  
Institute for Resources and Technology,  
Germany

**De Maeyer Philippe** - Ghent University,  
Department of Geography, Belgium

**Dobrolubov Sergey A.** - Lomonosov  
Moscow State University, Faculty of  
Geography, Russia

**Ferjan J. Ormeling** - University of  
Amsterdam, Amsterdam, Netherlands

**Sven Fuchs** - University of Natural  
Resources and Life Sciences

**Haigh Martin** - Oxford Brookes University,  
Department of Social Sciences, UK

**Golosov Valentin N.** - Lomonosov Moscow  
State University, Faculty of Geography,  
Russia

**Gulev Sergey K.** - Russian Academy of  
Sciences, Institute of Oceanology, Russia

**Guo Huadong** - Chinese Academy of  
Sciences, Institute of Remote Sensing and  
Digital Earth, China

**Jarsjö Jerker** - Stockholm University,  
Department of Physical Geography and  
Quaternary Geography, Sweden

**Jeffrey A. Nittrouer** - Rice University,  
Houston, USA

**Ivanov Vladimir V.** - Arctic and Antarctic  
Research Institute, Russia

**Kolosov Vladimir A.** - Russian Academy of  
Sciences, Institute of Geography, Russia

**Konečný Milan** - Masaryk University,  
Faculty of Science, Czech Republic

**Kroonenberg Salomon** - Delft University of  
Technology, Department of Applied Earth  
Sciences, The Netherlands

**Kulmala Markku** - University of Helsinki,  
Division of Atmospheric Sciences, Finland

**Olchev Alexander V.** - Lomonosov Moscow  
State University, Faculty of Geography,  
Russia

**Malkhazova Svetlana M.** - Lomonosov  
Moscow State University, Faculty of  
Geography, Russia

**Meadows Michael E.** - University of Cape  
Town, Department of Environmental and  
Geographical Sciences South Africa

**Nefedova Tatyana G.** - Russian Academy of  
Sciences, Institute of Geography, Russia

**O'Loughlin John** - University of Colorado  
at Boulder, Institute of Behavioral Sciences,  
USA

**Paula Santana** - University of Coimbra,  
Portugal

**Pedroli Bas** - Wageningen University, The  
Netherlands

**Radovanovic Milan** - Serbian Academy of  
Sciences and Arts, Geographical Institute  
"Jovan Cvijić", Serbia

**Sokratov Sergei A.**

Lomonosov Moscow State University,  
Faculty of Geography, Russia

**Tishkov Arkady A.** - Russian Academy of  
Sciences, Institute of Geography, Russia

**Wuyi Wang** - Chinese Academy of Sciences,  
Institute of Geographical Sciences and  
Natural Resources Research, China

**Zilitinkevich Sergey S.** - Finnish  
Meteorological Institute, Finland

ASSOCIATE EDITORS:

**Maslakov Alexey A.,**

ASSISTANT EDITORS:

**Litovchenko Daria K.**

**Vlasov Dmitry V.**

# CONTENTS

## GEOGRAPHY

**Alexey S. Victorov, Olga N. Trapeznikova**

STOCHASTIC MODELS OF DYNAMIC BALANCE STATE  
FOR THE MORPHOLOGICAL PATTERNS OF CRYOLITHOZONE  
LANDSCAPES..... 6

**Victor V. Kharitonov**

ICE RIDGES IN LANDFAST ICE OF SHOKAL'SKOGO STRAIT..... 16

## ENVIRONMENT

**Ibrahim M. Ahmed, Eltoum M. Abd Alla**

LANDUSE IMPACT ON ENVIRONMENT OF TUTI ISLAND, SUDAN ..... 27

**Galina Surkova, Aleksey Krylov**

EXTREMELY STRONG WINDS AND WEATHER PATTERNS  
OVER ARCTIC SEAS..... 34

## SUSTAINABILITY

**Zeinab Hazbavi, Seyed Hamidreza Sadeghi  
and Mehdi Gholamalifard**

DYNAMIC ANALYSIS OF SOIL EROSION-BASED WATERSHED HEALTH..... 43

## SPECIAL ISSUE

«ENVIRONMENTAL CHANGE ON THE MONGOLIAN PLATEAU:  
ATMOSPHERE, FORESTS, SOILS AND WATER»

**Daniel Karthe, Sergey Chalov, Alexander Grade,  
Antonín Kusbach**

ENVIRONMENTAL CHANGE ON THE MONGOLIAN PLATEAU:  
ATMOSPHERE, FORESTS, SOILS AND WATER..... 60

## ATMOSPHERIC CHANGE

**Olga Yu. Antokhina, Inna V. Latysheva, Vladimir I. Mordvinov**

A CASES STUDY OF MONGOLIAN CYCLOGENESIS DURING  
THE JULY 2018 BLOCKING EVENTS .....66

# CONTENTS

## FOREST ECOSYSTEMS UNDER CHANGE

**Nikita M. Debkov, Aleksey A. Aleinikov, Alexander Gradel, Anatoly Yu. Bocharov, Nina V. Klimova<sup>1</sup> and Gennady I. Pudzha**

IMPACTS OF THE INVASIVE FOUR-EYED FIR BARK BEETLE  
(*POLYGRAPHUS PROXIMUS* BLANDF.) ON SIBERIAN FIR  
(*ABIES SIBIRICA* LEDEB.) FORESTS IN SOUTHERN SIBERIA.....79

**Antonín Kusbach, Tadeáš Štěřba, Jan Šebesta, Tomáš Mikita,  
Enkhtuya Bazarradnaa<sup>4</sup>, Sarantuya Dambadarjaa, Martin Smola**

ECOLOGICAL ZONATION AS A TOOL FOR RESTORATION  
OF DEGRADED FORESTS IN NORTHERN MONGOLIA..... 98

**Vladimir A. Usoltsev, Igor M. Danilin, Zaandrabalyn Tsogt,  
Anna A. Osmirko, Ivan S. Tsepordey, Viktor P. Chasovskikh**

ABOVEGROUND BIOMASS OF MONGOLIAN LARCH (*LARIX SIBIRICA* LEDEB.)  
FORESTS IN THE EURASIAN REGION..... 117

**Alexander Gradel, Gerelbaatar Sukhbaatar,  
Daniel Karthe, Hoduck Kang**

FOREST MANAGEMENT IN MONGOLIA – A REVIEW OF CHALLENGES  
AND LESSONS LEARNED WITH SPECIAL REFERENCE TO DEGRADATION  
AND DEFORESTATION..... 133

**Dan Altrell**

MULTIPURPOSE NATIONAL FOREST INVENTORY IN MONGOLIA, 2014-2017  
-A TOOL TO SUPPORT SUSTAINABLE FOREST MANAGEMENT.....167

**David Juříčka, Václav Pecina, Martin Brtnický, Jindřich Kynický**

MINING AS A CATALYST OF OVERGRAZING RESULTING IN RISK  
OF FOREST RETREAT, ERDENET MONGOLIA.....184

## SOIL AND WATER RESOURCES UNDER CHANGE

**Elena V. Shabanova, Ts. Byambasuren, G.Ochirbat, Irina E. Vasil'eva,  
B. Khuukhenkhoo and Alexei T. Korolkov**

RELATIONSHIP BETWEEN MAJOR AND TRACE ELEMENTS  
IN ULAANBAATAR SOILS: A STUDY BASED  
ON MULTIVARIATE STATISTICAL ANALYSIS.....199

**Marion Aschmann**

ADDRESSING AIR POLLUTION AND BEYOND IN ULAANBAATAR:  
THE ROLE OF SUSTAINABLE MOBILITY..... 213

**Endon Zh. Garmaev, Anatoly I. Kulikov, Bair Z. Tsydypov,  
Bator V. Sodnomov, Alexander A. Ayurzhanayev**

ENVIRONMENTAL CONDITIONS OF ZAKAMENSK TOWN  
(DZHIDA RIVER BASIN HOTSPOT)..... 224

**Galina L. Shinkareva, Mikhail Yu. Lychagin, Mikhail K. Tarasov,  
Jan Pietroń, Marina A. Chichaeva, Sergey R. Chalov**

BIOGEOCHEMICAL SPECIALIZATION OF MACROPHYTES  
AND THEIR ROLE AS A BIOFILTER IN THE SELENGA DELTA..... 240

**Disclaimer:**

*The information and opinions presented in the Journal reflect the views of the authors and not of the Journal or its Editorial Board or the Publisher. The GES Journal has used its best endeavors to ensure that the information is correct and current at the time of publication but takes no responsibility for any error, omission, or defect therein.*

**Alexey S. Victorov<sup>1</sup>, Olga N. Trapeznikova<sup>1\*</sup>**

<sup>1</sup>Sergeev Institute of Environmental Geoscience of Russian Academy of Science, Moscow, Russia.

\* **Corresponding author:** ontolga@gmail.com

# STOCHASTIC MODELS OF DYNAMIC BALANCE STATE FOR THE MORPHOLOGICAL PATTERNS OF CRYOLITHOZONE LANDSCAPES

**ABSTRACT.** The paper deals with mathematical modeling of a morphological pattern for a broad spectrum of cryolithozone landscapes in a state of a dynamic balance. The state of the dynamic balance means that all the elements of this morphological pattern are in continuous changing while its general parameters as a whole are stable. Two contra-directional processes at the same territory is a precondition for a state of dynamic balance.

We developed a morphological pattern model for lacustrine thermokarst plains with fluvial erosion on the base of the mathematical morphology of landscape using the random process theory. The contra-directional processes here include thermokarst lakes appearing and increasing in size from one side and drainage of the lakes by fluvial erosion, from the other. Thus, the regularities of the structure and dynamics of each landscape morphological pattern are theoretically substantiated. The results of the mathematical modeling were empirically verified at some key sites.

**KEY WORDS:** Morphological pattern; mathematical modeling; dynamic balance; thermokarst lake; khasyrei (alas), landscapes of the cryolithozone

**CITATION:** Alexey S. Victorov, Olga N. Trapeznikova (2019) Stochastic Models Of Dynamic Balance State For The Morphological Patterns Of Cryolithozone Landscapes. *Geography, Environment, Sustainability*, Vol.12, No 3, p. 6-15  
DOI-10.24057/2071-9388-2018-68

## INTRODUCTION

Different researchers studied a dynamic balance state in the cryolithozone, including natural hazard enhancing due to disturbing of the dynamic balance. For instance, these studies include disturbance of tundra landscapes under man-caused impact such as thermal erosion along track lines at bogs, disturbance of vegetation cover, flooding (Novikova et al. 1998; Vinogradov 1999; Mamai 2005); some others dealt with the

thermodynamic balance in the permafrost soil. Some researchers examined changing shares of thermokarst lakes due to climatic change; that can also be regarded as a change of the dynamic balance (Polishuk, Polishuk 2014; Muster et al. 2019; Dneprovskaya et al. 2009; Kipotin et al. 2009; Burn, Smith 1990; Kravtsova, Bystrova 2009). At the same time, we have a lack of works specially devoted to the dynamic balance state of landscape morphological patterns in the cryolithozone.

A broad spectrum of cryolithozone landscapes has the same type of morphological pattern with a possibility of the dynamic balance. Our research shows that this type of landscapes includes lacustrine thermokarst plains with fluvial erosion, alluvial plains, and plains with the extensive development of the landslide process.

The state of the dynamic balance means that all the elements of this morphological pattern, such as thermokarst lakes, khasireis (drained thermokarst lakes), ridges and inter-ridge depressions of alluvial plains, as well as landslide series, are in continuous changing while general parameters of the morphological pattern as a whole are stable.

In the case of these landscapes, the usual methods of analysis and stationary observation do not provide the necessary information about the trends of their evolution. Our research aims to consider the possibility of dynamic balance in the course of development of the morphological pattern of cryolithozone landscapes and assessment techniques for corresponding natural hazards. We analyzed the problem for a case of thermokarst plains with fluvial erosion as an example.

## MATERIALS AND METHODS

The area under consideration is a slight wavy subhorizontal area covered by tundra vegetation, interspersed with lakes and khasyreis and rare fluvial erosion network (Melnikov 2012). Isometric, often roundish shaped lakes are randomly scattered across the plain. Khasyreis are also isometric flat-bottomed and flattened peaty depressions covered with meadow or bog vegetation similar to lakes randomly scattered across the plain. Majority of researchers expect khasyreis to be the result of thermokarst lake drainage, usually due to fluvial erosion (Fig.1).

Thermokarst, thermo-abrasion, and thermo-erosion processes perform in complex interrelations and determine the type of the area (Günther et al. 2013; Liu et al. 2013). Thermokarst depressions separately appear and grow as lakes due to thermos-abrasion after being filled with water. Their growth depends on random factors associated with a meteorological situation of a particular layer and soil condition. At last, at a random point in time, a lake can be lowered by erosion processes and turned into khasyreis, overgrown with meadow and bog vegetation with separate relict lakes; thus the depression stops growing because of lack of water. At the same time, permafrost can reappear within a khasyreis. The whole area appears to be a complex

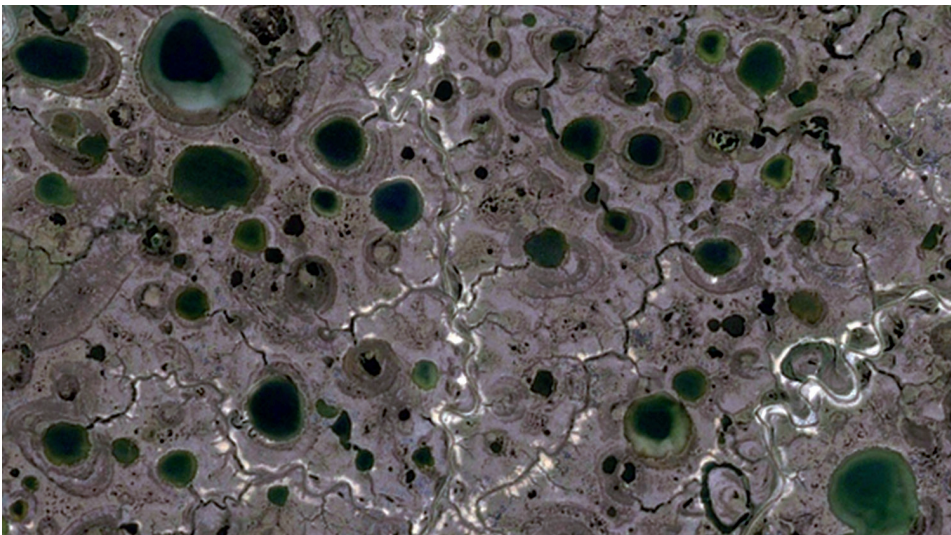


Fig. 1. A typical space image of a thermokarst plain with fluvial erosion

mosaic of sites, which were lakes and khasyreis at a different time. Thus, the morphological pattern of these landscapes changes under two contra-directional processes

- thermokarst lakes appearing and increasing in size,
- drainage of the lakes by fluvial erosion, their turn into khasyreis and stop of their growth.

Two contra-directional processes at the same territory is a precondition for a state of dynamic balance. We made morphological pattern modeling for lacustrine thermokarst plains with fluvial erosion on the base of the mathematical morphology of landscape using the random process theory.

## RESULTS

There are two variants for developing the morphological pattern of the thermokarst plain with fluvial erosion:

- synchronous start of thermokarst lake appearance;
- asynchronous start of thermokarst lake appearance.

In the case of a synchronous start, we suggest that primary thermokarst depressions were appearing within a relatively short period compared with their further development. The model for lacustrine thermokarst plains with fluvial erosion in uniform nature environment in case of the synchronous start is based on the following assumptions:

1. Thermokarst depressions were appearing within a relatively short period (i.e., «synchronous start») independently across the different non-adjacent landscapes; the probability of a new depression appearance within a sample plot was dependent exclusively on the plot area:

$$p_1 = \tau_1^0 \Delta s + o(\Delta s),$$

where  $\tau_1^0$  is an average density lake location (the initial one for the «synchronous start»).

2. The radius of an appeared thermokarst depression is a random variable being a time function; it is undependable of other lakes, and the growth rate is directly proportional to heat losses through the side surface of the lake basin.

3. In the course of its growth, a lake can turn into a khasyreis after draining by the erosion network; the probability of this does not depend on the development of other lakes; if it happens, the depression stops growing.

4. The appearance of new sources of fluvial erosion within a randomly selected area is a random event, and the probability of this depends only on the site area.

The mathematical analysis of the model gives us a set of results (Victorov 1995; Victorov et al. 2017). The simplest of them are the following:

- A quantity of primary thermokarst depressions within a trial plot obeys a Poisson distribution:

$$P(k) = \frac{(\tau_1^0 S)^k}{k!} e^{-\tau_1^0 S},$$

where  $\tau_1^0$  is a parameter,  $S$  is the plot area.

- Change of lake size (area, diameter) in case of unlimited growth without the possibility of lake drainage taken into account should obey the lognormal distribution (probability density):

$$f_0(x, t) = \frac{1}{\sqrt{2\pi\sigma x}\sqrt{t}} e^{-\frac{[\ln x - at]^2}{2\sigma^2 t}},$$

where  $a, \sigma$  are parameters,  $t$  is time.

- The lake drainage due to fluvial erosion and their transformation into khasyreis changes lake size distribution because the lakes have different probabilities of being dried depending on their size.

More sophisticated results deal with the case of the morphological pattern developing for a long time ( $t \rightarrow +\infty$ ).

At any time, the khasyreis radius distribution is determined by the distance to the nearest source of a stream, which stops its growth (the first member under the integral), and the probability that in the

course of its growth the lake reaches the size exceeding this distance. The following formula is used:

$$f_h(x, t) = \frac{2\pi\gamma x e^{-\pi\gamma x^2} [1 - F_0(x, t)]}{\int_0^{+\infty} 2\pi\gamma u e^{-\pi\gamma u^2} [1 - F_0(u, t)] du},$$

where  $F_0(x, t)$  is the radius distribution for a free growing thermokarst lake at the moment  $t$ .

With time increasing ( $t \rightarrow +\infty$ ) the khasyrei radii distribution tends to specific limit distribution. It is easy to see that as far as at any  $x$  the lake radii distribution  $F_0(x, t)$  tends to 0 in case of free growth, the limit distribution density of the khasyrei radii after a long time of development is given by an expression:

$$f_h(x, \infty) = 2\pi\gamma x e^{-\pi\gamma x^2},$$

and the distribution itself is given by a formula:

$$F_h(x, \infty) = 1 - e^{-\pi\gamma x^2},$$

In other words, after a long time of development khasyrei radii distribution should obey the Rayleigh distribution. Hence, the khasyrei areas distribution ( $sh$ ) obeys the exponential distribution:

$$F_{sh}(x, \infty) = 1 - e^{-\frac{x}{\bar{q}}},$$

where  $\bar{q}$  is an average khasyrei area.

Let us examine the radii distribution of thermokarst lakes. At any moment the radii distribution of the thermokarst lakes is determined by the corresponding radii distribution in case of the free growth, but under the condition that the lake has not turned into khasyrei up to this moment, i.e., the distance to the source of a stream is longer than the lake radius. Thus, the distribution density of the thermokarst lake radii is given by the expression:

$$f_l(x, t) = \frac{f_0(x, t) e^{-\pi\gamma x^2}}{\int_0^{+\infty} f_0(x, t) e^{-\pi\gamma x^2} dx}.$$

Using the expression for free growth and simplifying the same terms in the

numerator and denominator depending only on time we get

$$f_l(x, t) = \frac{x^{\frac{a}{\sigma^2}-1} e^{-\pi\gamma x^2} e^{-\frac{\ln^2 x}{2\sigma^2 t}}}{\int_0^{+\infty} x^{\frac{a}{\sigma^2}-1} e^{-\pi\gamma x^2} e^{-\frac{\ln^2 x}{2\sigma^2 t}} dx},$$

where  $a, \sigma$  are the distribution parameters.

After a long time of development ( $t \rightarrow +\infty$ ) this expression tends to a limit distribution:

$$f_l(x, \infty) = \frac{x^{\frac{a}{\sigma^2}-1} e^{-\pi\gamma x^2}}{\int_0^{+\infty} x^{\frac{a}{\sigma^2}-1} e^{-\pi\gamma x^2} dx},$$

in which we can see the known chi-distribution. Taking a roundish shape of the lakes into account, we get that the gamma-distribution is the limit distribution for the lake area ( $sl$ ):

$$f_{sl}(x, \infty) = \frac{\gamma^{\frac{a}{2\sigma^2}} x^{\frac{a}{2\sigma^2}-1} e^{-\gamma x}}{\Gamma\left(\frac{a}{2\sigma^2}\right)},$$

where  $\Gamma(x)$  is the gamma function.

The spatial distribution of lakes is the Poisson one, as well as in the model of the lacustrine thermokarst plains during the whole development period. It results from the first assumption of the model. However, the average density of lake location has been continuously decreasing due to their turn into khasyreis. It depends on the probability that the lake does not reach a size more significant than the distance to the nearest source of a stream and is equal to

$$\tau_l(t) = \tau_l^0 \int_0^{+\infty} \frac{1}{\sqrt{2\pi\sigma}} x^{\frac{a}{\sigma^2}-1} e^{-\pi\gamma x^2} e^{-\frac{\ln^2 x}{2\sigma^2 t}} dx.$$

Thus, the mathematical analysis shows that in this case, we get stable shares between quantities of thermokarst lakes and khasyreis of different size:

- the khasyrei radii distribution after a long enough time of the development should obey the Rayleigh distribution:

$$F_h(x, \infty) = 1 - e^{-\pi\gamma x^2},$$

- the khasyrei area distribution after a long enough time of the development should obey the exponential distribution:

$$F_{sh}(x, \infty) = 1 - e^{-\frac{x}{a}}$$

The spatial distribution of lakes obeys the Poisson law during the whole time of their development; however, the average location density of lake continually decreases due to their turn into khasyreis. Let us consider the second variant, i.e., the variant of the asynchronous start. In this case, we expect the continuous appearance of new initial thermokarst depressions (germs of thermokarst lakes) with the constant density of appearance at that. This approach is based on the fact that we can observe new thermokarst lakes within khasyreis. The roundish shape of these lakes indicates that they are not relict parts of the previously drained thermokarst lake but new thermokarst foci.

In case of the asynchronous start the model for lacustrine thermokarst plains with fluvial erosion in uniform nature environment is based on the following assumptions:

1. The appearance of initial thermokarst depressions during non-overlapping time intervals ( $\Delta t$ ) and at non-overlapping sites ( $\Delta s$ ) are independent random events; the probability for a depression to appear depends only on the duration of the interval and the site area:

$$p_1 = \lambda \Delta s \Delta t + o(\Delta s \Delta t),$$

where  $\lambda$  is a parameter.

2. New lakes do not appear within the already existing thermokarst lakes.
3. The radius of an appeared thermokarst depression is a random variable being a time function; it does not depend on other lakes, and the growth rate is directly proportional to heat losses through the side surface of the lake basin.
4. In the course of its growth, a lake can turn into a khasyrei after draining by the erosion network; the probability of this does not depend on the development of other lakes; if it happens, the depression stops growing.
5. The appearance of new sources of fluvial erosion within a randomly selected area is a random event, and the probability of this depends on the area only.

These assumptions differ from that of the previous model because:

\* the constant average rate of new lake

generation

\* new lakes do not appear within the already existing lakes

It is evident that in the case of an asynchronous start, we also have preconditions for dynamic balance resulting from the development of the landscape morphological pattern under consideration.

The mathematical analysis of this situation is more sophisticated than the previous one, but it gives us a set of conclusions (Victorov 2005):

- after a sufficiently long period ( $t \rightarrow +\infty$ ) since the start of the process a particularly stable state appears under a broad spectrum of conditions;
- a dynamic equilibrium is established between processes of thermokarst lake origination and their turn into khasyreis. Stable quantitative ratios characterize this state of a dynamic balance:
- the limit value for the lake spacing density is

$$\eta(\infty) = -\frac{\lambda}{2a} Ei(-\pi\gamma),$$

where  $a, \lambda$  are parameters,  $\gamma$  is an average spacing density of erosion sources;  $Ei(x)$  is an integral exponential function.

- the limit value of the thermokarst impact is

$$P(\infty) = 1 - \exp\left[-\frac{\lambda}{2a\gamma}\right] e^{-\pi\gamma};$$

- the limit radii distribution for khasyreis is

$$F_h(x) = 1 - e^{-\pi\gamma x^2}.$$

The spatial distribution of lakes obeys the Poisson distribution throughout the whole course of the development. However, the average lakes location density varies because of their constant generation and turning into khasyreis.

## DISCUSSION

### Empirical testing of the models

We empirically tested some of the modeling results at specific key sites located in a different natural environment and permafrost condition (Fig. 2).

The key sites are within different natural and permafrost environments; they are usually characterized by various marine and

alluvial–moraine deposits with different ice content and temperature of permafrost soil.

We have tested the conformity of the khasyreï area empirical distribution to the theoretical exponential distribution (Fig. 3,

Table 1) at all the three key sites with sample volumes from 73 to 122. We verified the results of the comparison using Pearson's fitting criterion. Table 1 demonstrates an accord between empirical data and the exponential distribution at the significance level 0.99.

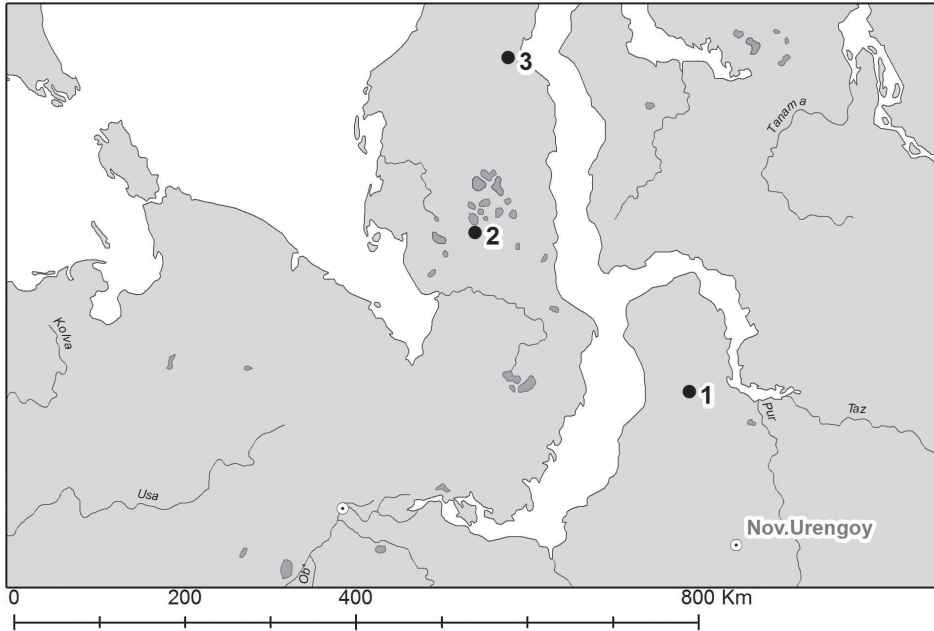


Fig. 2. The overview map of the location of key sites within thermokarst plains with fluvial erosion

Number of observations

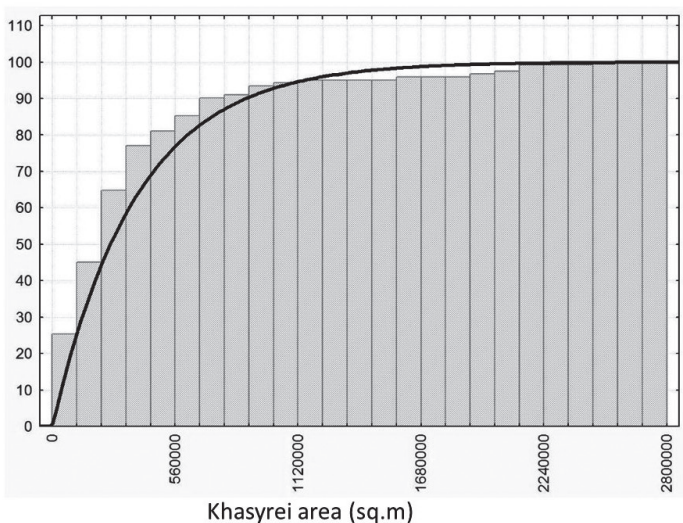


Fig. 3. The correspondence of the distribution of the khasyreï area (sq.m) to the exponential distribution (an example)

**Table 1. The correspondence of the distribution of the khasyrei area to the theoretical distributions (Pearson's criterion) for thermokarst plains with fluvial erosion**

Key sites	The volume of the sample	The theoretical distribution	P value
Site 1	73	The exponential distribution	0.191
		The lognormal distribution	0.044
		The normal distribution	0.000
Site 2	122	The exponential distribution	0.396
		The lognormal distribution	0.353
		The normal distribution	0.000
Site 3	76	The exponential distribution	0.723
		The lognormal distribution	0.012
		The normal distribution	0.000

At these key sites with sample volumes from 53 to 95 we have also investigated the accord between empirical data on the distribution of thermokarst lake areas and gamma distribution, as it is correct for the synchronous start. The obtained data (Fig. 4, Table 2) show that the empirical data do not contradict the suggested model at the significance level 0,99. At the same time, there is a similarity with the lognormal distribution. We regard this situation as pointing on the synchronous start because in this case, an area develops at the first stage as a lacustrine thermokarst plain due to little influence of fluvial erosion until the lakes have not grown in size.

When the lakes become large enough, the situation changes and the lake area distribution tends to the limit gamma distribution, and the appearing khasyreis tends to the exponential distribution, but due to the finite time, the distribution of the lake and khasyrei areas are not exactly equal to them. It should be stressed that according to our research the area distribution of thermokarst lakes within the lacustrine thermokarst plains (without fluvial erosion) usually corresponds to the lognormal distribution while only a few measurements agree with the gamma distribution (Table 3).

**Number of observations**

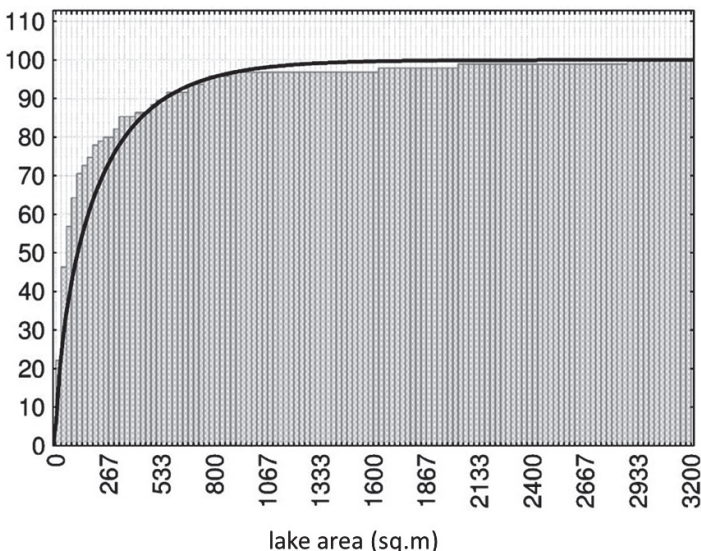


**Fig. 4. The correspondence of the distribution of the thermokarst lake area (sq.m) to the gamma-distribution (an example)**

**Table 2. The correspondence of the distribution of the thermokarst lake area to the gamma-distribution (an example)**

Key sites	The volume of the sample	The theoretical distribution	P value
Site 1	95	The gamma-distribution	0.016
		The lognormal distribution	0.241
		The normal distribution	0.000
Site 2	53	The gamma-distribution	0.051
		The lognormal distribution	0.206
		The normal distribution	0.000
Site 3	93	The gamma-distribution	0.082
		The lognormal distribution	0.012
		The normal distribution	0.001

**Table 3. The correspondence of the thermokarst lake area distribution to the theoretical distributions (Pearson's criterion) for lacustrine thermokarst plains (without fluvial erosion)**

Key site	The volume of the sample	p-value	
		For the lognormal distribution	For the gamma-distribution
Alaska 2	108	0.112	0.000
Taimyr1	345	0.112	0.007
Taimyr2	209	0.631	0.330
Kolyma 1	154	0.216	0.023
Kolyma 2	576	0.000	0.000
Ust'-Lena1-1	145	0.011	0.000
Ust'-Lena1-2	91	0.155	0.006
Ust'-Lena1-3	383	0.00	0.000
Ust'-Lena2	167	0.006	0.000
Yamal1	209	0.00	0.259
Yamal2	176	0.012	0.005
Alaska 1	100	0.023	0.004
West-Siberian2	84	0.088	0.000
Canadian	154	0.127	0.009
West-Siberian1	78	0.587	0.000
Gydansky	74	0.517	0.000

## CONCLUSIONS

Thus, the described research gave us the following results:

- After a long enough time of the development thermokarst plains with fluvial erosion come to the state of dynamic balance. For an asynchronous start, we have confirmed it under a specific broad range of conditions. It reveals in establishing and preserving stable quantitative relationships among elements of the morphological pattern of this landscape.
- This state characterizes with the correspondence of the probabilistic distribution of khasyrei area to the exponential distribution, and their radii to the Rayleigh one despite synchronous or asynchronous start.
- The probabilistic distribution for areas of the thermokarst lakes obeys the gamma-distribution in the case of the synchronous start and a particular distribution in the case of the asynchronous start.

- In case of the asynchronous start the state of dynamic balance results in the stabilization of both the lake location density and the share of lake area within the landscape.

- We are aware that the obtained results need additional empirical testing, but we regard them to be a promising approach.

- The same approach, which we used in the analysis of the lacustrine thermokarst plains, can be involved for assessment of the impact on a linear engineering structure, for instance, at thermokarst plains with fluvial erosion.

## ACKNOWLEDGEMENTS

The research is done with the support of Russian Science Foundation, project # 18-17-00226. ■

## REFERENCES

- Burn C.R., Smith M. W. (1990). Development of Thermokarst Lakes During the Holocene at Sites Near Mayo, Yukon Territory. *Permafrost and Periglacial Processes*, v. 1, pp. 161-176.
- Dneprovskaya V. P., Bryksina N. A., Polishchuk Yu. M. (2009). Study of Thermokarst Changes in Discontinuous Zone of West-Siberian Permafrost Based on Space Images. *Issledovanie Zemli iz Kosmosa*. 4. pp. 88-96 (in Russian).
- Günther F., Overduin P., Baranskaya A., Opel T. and Grigoriev M. N. (2013). Observing Muostakh Island disappear: erosion of a ground-ice-rich coast in response to summer warming and sea ice reduction on the East Siberian shelf // *The Cryosphere Discussions*, 7, pp. 4101-4176.
- Kipotin S.N., Polishchuk Yu. M., Bryksina N. A. (2009). Abrupt changes of thermokarst lakes in Western Siberia: impacts of climatic warming on permafrost melting. *International Journal of Environmental Studies*. v 66, 4, pp. 423-431.
- Kravtsova V.I., Bystrova A.G. (2009). Changes in thermokarst lake size in different regions of Russia for the last 30 years, *Kriosfera Zemli*, v.15, 2, pp. 16-26.
- Liu L., Schaefer K., Gusmeroli A., Grosse G., Jones B. M., Zhang T., Parsekian A. D., and Zebker H. A. (2013). Seasonal thaw settlement at drained thermokarst lake basins, Arctic Alaska// *The Cryosphere Discuss.*, 7, pp. 5793–5822.
- Mamai I.I. (2005). *Landscape dynamics and functioning*. Moscow, MSU publishing house, 138 p. (in Russian).
- Melnikov V.P. ed. (2012). *Kompleksnyy monitoring severotayezhnykh geosistem Zapadnoy Sibiri (Comprehensive monitoring of the northern taiga geosystems of Western Siberia)* Academician publ. house "GEO", 207 p.

Morgenstern A., Grosse, G., Günther F., Fedorova I., and Schirrmeister L. (2011). Spatial analyses of thermokarst lakes and basins in Yedoma landscapes of the Lena Delta, *The Cryosphere*, 5, pp. 849-867.

Morgenstern A., Ulrich M., Günther F., Boike J. and Schirrmeister L. (2012). Evolution of a Thermokarst Basin in Ice-Rich Permafrost, Siberian Lena Delta. // Melnikov, P.I. (ed). Tenth International Conference on Permafrost. Vol. 4: Proceedings of the Tenth International Conference on Permafrost Salekhard, Yamal-Nenets Autonomous District, Russia. Co-edited by D.S. Drozdov and V.E. Romanovsky. The Northern Publisher, Salekhard, Russia, pp. 406-407.

Muster S., Riley W.J., Roth K., Langer M., Cresto Aleina F., Koven C.D., Lange S., Bartsch A., Grosse G., Wilson C.J., Jones B.M. and Boike J. (2019). Size Distributions of Arctic Waterbodies Reveal Consistent Relations in Their Statistical Moments in Space and Time. *Front. Earth Sci.* 7:5. doi: 10.3389/feart.2019.00005.

Novikova N.M., Kust G.S., Kuzmina Zh.V., Trofimova G.U., Dikareva T.V., Avetian S.A., Rozov S.U., Deruzhinskaya V.O., Safonicheva L.F., Lubeznov U.E. (1998). Contemporary Plant and Soil Cover Changes in The Amu-Darya and Syr-Darya River Deltas. Ecological Research and Monitoring of the Aral Sea Deltas: A Basis for Restoration. UNESCO Aral Sea Project 1992-1996 Final Scientific Reports. Paris, 1998. pp. 55-80.

Polishuk Y.M., Polishuk V.Y. (2014). Geo-simulation approach to modelling spatial objects and its application to creating thermokarst lake model using remote sensing data. *BIOCLIMLAND (Biota, Climate, Landscapes)*. 1. pp. 53-69.

Victorov A.S., Kapralova V.N. (2013). Quantitative assessment of natural risks based on satellite observation data (a case study of thermokarst plains). *Izvestiya, Atmospheric and Oceanic Physics*, Vol. 49(9), pp. 1069–1073.

Victorov A.S. (2005). Mathematical Models of Thermokarst Erosion Plains. \ GIS and Spatial Analysis. Proceedings of IAMG2005, Toronto, Canada. v. 1, pp 62-67.

Viktorov A.S. (1995). The Mathematical Model of Thermokarst Lakes Surface as One of the Bases of the Space Survey Interpretation. *Issledovanie Zemli iz Kosmosa*. 5. pp. 42-50 (in Russian).

Viktorov A.S. (1998). The general problems of the mathematical morphology of landscape. Moscow. Tratek. p.191.

Viktorov A.S. (2007). Risk Assessment Based on the Mathematical Model of Diffuse Exogenous Geological Processes. *Mathematical Geology*. V. 39(8). pp. 735-748.

Viktorov A.S., Kapralova V.N., Orlov T.V., Trapeznikova O.N., Arkhipova M.V., Berezin P.V., Zverev A.V., Panchenko E.N., Sadkov S.A. (2017). Consistent patterns of the size distribution of thermokarst lakes. *Doklady Earth Sciences*. v. 474(2). pp. 692-694.

Vinogradov B.V. (1990). The Mapping of Ecosystem Dynamics: A Quantitative Approach. *Mapping Sciences and Remote Sensing*. 27(1), pp. 68-76. DOI: 10.1080/07493878.1990.10641790/.

**Victor V. Kharitonov<sup>1\*</sup>**

<sup>1</sup>Arctic and Antarctic Research Institute, St. Petersburg, Russia

\* **Corresponding author:** [sogra.kharitonov@mail.ru](mailto:sogra.kharitonov@mail.ru)

## ICE RIDGES IN LANDFAST ICE OF SHOKAL'SKOGO STRAIT

**ABSTRACT.** Three first-year ice ridges have been examined with respect to geometry and morphology in landfast ice of Shokal'skogo Strait (Severnaya Zemlya Archipelago) in May 2018. Two of the studied ice ridges were located on the edge of the ridged field and were part of it, because their keels extended for a long distance deep into this field. Ice ridges characteristics are discussed in the paper. These studies were conducted using hot water thermal drilling with computer recording of the penetration rate. Boreholes were drilled along the cross-section of the ridge crest at 0.25 m intervals. Cross-sectional profiles of ice ridges are illustrated. The maximal sail height varied from 2.9 up to 3.2 m, the maximal keel depth varied from 8.5 up to 9.6 m. The average keel depth to sail height ratio varied from 2.8 to 3.3, and the thickness of the consolidated layer was 2.5-3.5 m. The porosity of the non-consolidated part of the keel was about 23-27%. The distributions of porosity versus depth for all ice ridges are presented.

**KEY WORDS:** ice ridge, water thermal drilling, cross-sectional profile, consolidated layer, porosity

**CITATION:** Victor V. Kharitonov (2019) Ice ridges in landfast ice of Shokal'skogo Strait. *Geography, Environment, Sustainability*, Vol.12, No 3, p. 16-26  
DOI-10.24057/2071-9388-2019-43

### INTRODUCTION

Studies of morphometric characteristics of ridged features as the thickest areas of ice cover, unlike similar studies of the morphometry of non-deformed ice, do not have a rich history, and the amount of currently available observational data cannot be considered sufficient (Sudom & Timco 2013). Active studies of ice ridges on the shelf of freezing seas of Russia are conducted, since their morphometric characteristics, primarily the thickness of the ice ridge consolidated layer (CL), should be taken into account at the designing stage in the assessment of possible loads on the structures. And the information about these characteristics is still being supplemented. However, there are very few studies on the morphometry of deformed and ridged ice in the Laptev

and East-Siberian Seas, and for Shokal'skogo Strait, in particular, such information is not available. Under the conditions of changing climate, reduction of ice area in the Arctic Ocean and decreasing ice thickness, any information on the internal structure of modern ice ridges is of undoubted value.

### SITE AND EXPERIMENTAL METHODS

This paper presents the information on morphometric characteristics and the internal structure of three ice ridges in landfast ice of Shokal'skogo Strait in the Severnaya Zemlya Archipelago obtained between April, 13 and May, 31, 2018 (Fig. 1). The working team was accommodated at the "Ice base "Cape Baranov" station belonging to the Arctic and Antarctic Research Institute (AARI).

Investigation of the structure of ice ridges was carried out by means of hot water thermal drilling unit of AARI comprising heater, thermal drill and equipment for penetration rate recording on a logger. The power was supplied by a 4 kW generator. A general view of hot water ice drilling unit is presented in Fig. 2. An example of recording the penetration rate of ice ridge drilling and reconstruction of its structure is presented in Fig. 3. Drilling was carried out along the profile up to reaching level ice. A few boreholes were drilled on the level ice.

The ice ridge geometry and internal structure are retrieved by processing

the thermodrilling records (Morev et al. 2000; Mironov et al. 2003; Kharitonov & Morev 2011). The drilling rate depends on the power supply, ice porosity and ice temperature. The location of voids, hard and porous ice along the drilling hole is identified by the thermodrill penetration rate. The obligatory condition for this identification to be valid is drilling at constant thermal capacity or recording the changes of capacity during drilling. Within the segments of porous ice and, especially, the voids filled by snow, shuga or air, the penetration rate of thermodrill sharply increases. In addition, the distance from snow (ice) surface to the sea level



Fig. 1. Map of the area of work. The 'plus' sign indicates the position of the three ridges



Fig. 2. General view of hot water ice drilling unit UVBL-2. The picture shows the operation of two drilling stations. In 2018, drilling of ice ridges was conducted using one station

is measured. The thermodrilling data processing gives such characteristics as the above-water and under-water parts of the ice cover, the boundaries of the ice ridge CL, the boundaries of the voids and the boundaries of ice layers of various porosities.

## RESULTS AND DISCUSSION

During the period from 13.04.18 to 31.05.18, three ice ridges were examined in detail.

Their main morphometric characteristics are demonstrated in Table 1. The three investigated ridges are labeled in Fig. 4.

On each ice ridge the thermal drilling of boreholes along the profile perpendicularly cutting the ice ridge crest was carried out. To the right of ice ridge 1 there was a first-year ice floe with a thickness of 1.2 m. On the photo, the drilling profile of ice ridge 1 was made along the line connecting the right edge of the snow inflation to the right

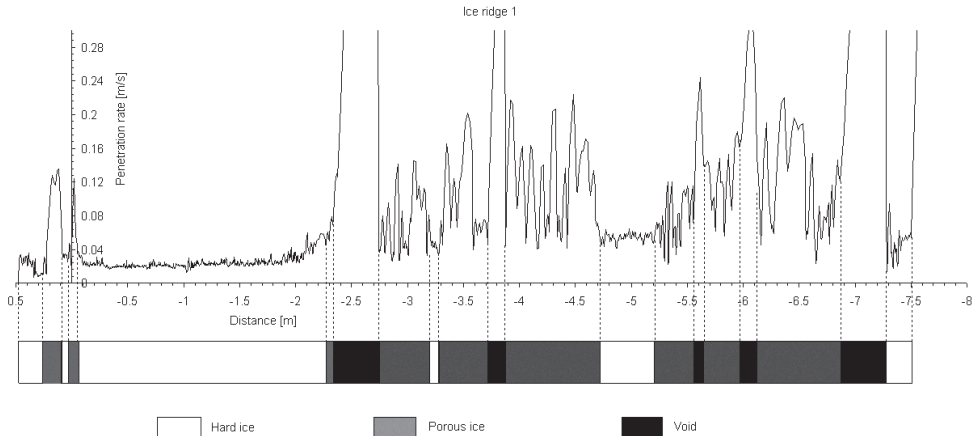


**Fig. 3. Example of thermal drilling record. A strip is drawn under the diagram schematically showing ice ridge structure at the drilling point. White colour shows areas along the borehole corresponding to hard ice; grey colour, areas corresponding to porous ice or drill transition from ice into void; and black colour, voids. Dotted lines show boundaries of these areas**



**Fig. 4. Photo of investigated ice ridges (by Andrey Paramzin). The labels correspond to the ridge' ID. Lines show location of the profiles**

**Table 1. Basic characteristics of investigated ice ridges (by records of hot water thermal drilling)**

	Ice ridge		
	1	2	3
Number of boreholes	267	81	93
Average/maximum ice thickness [m]	7.39/11.22	8.07/10.60	7.64/12.07
Average/maximum sail height [m]	1.82*/3.18	1.61/2.88	1.27/2.87
Average/maximum keel depth [m]	6.62/9.04	7.43/8.49	6.56/9.59
Average position of the upper boundary of CL [m]	-0.11	-0.19	-0.54
Average position of the lower boundary of CL [m]	-2.62	-3.70	-3.48
Minimum/average/maximum CL thickness [m]	1.3/2.5/4.0	2.0/3.5/4.2	1.7/2.9/4.3
Minimum/average/maximum level ice thickness nearby ice ridge [m]	1.20**	1.97***/3.03*** /2.40	1.70***/2.58*** /2.94
Number of measurements of the ice block thickness	54	10	25
Average thickness of ice blocks in the ice ridge sail [m]	0.29* & 0.19****	0.27	0.20* & 0.35****
Sail slope angle [degree]	38.5-52.6*	30.7-84.4	22.7-44.3*
Keel slope angle [degree]	25.0	76.6	38.6-63.6
Average ice ridge porosity	0.17	0.17	0.13
Average porosity of the unconsolidated part of the keel	0.27	0.25	0.23
Ratio of the maximum keel to maximum sail	2.8	3.0	3.3
Average ratio of the CL thickness to total ice thickness	0.34	0.43	0.38
Ratio of the average CL thickness to average level ice thickness	2.09	-	-
Average/maximum snow thickness on the ice ridge [m]	0.41/1.56	0.78/1.60	0.48/1.54

\* Main ice ridge crest.

\*\* Four boreholes were drilled on the level ice 1.20 m thick.

\*\*\* Due to a large size of the rafted ice field, the location of level ice was not reached. The measurements correspond to rafted ice thickness.

\*\*\*\* Second ice ridge crest.

of the ridge and the place where the two ice explorers are. The distance between the leftmost borehole on the profile and the ice ridge crest was 50 m. Drilling profile of ice ridge 2 was approximately parallel to the drilling profile of ice ridge 1. Ridged ice was to the right of the crest of ice ridge 2 and to the left – rafted ice with a thickness of 2-3 m (2.4 m on average). Drilling profile of ice ridge 3 was perpendicular to the drilling profile of ice ridge 2.

Boreholes were spaced at 0.25 m. At the edges of the profiles, where ice ridge consolidation reached 100 %, drilling was performed at a spacing of 0.5-1 m. At each point, snow cover thickness and ice surface elevation above sea level were measured. Besides, 3D-model of upper surface of ice was obtained by processing

of materials of aerial photography survey. Visual examination of the lower surface of ice ridge 1 was also performed using a remotely operated underwater vehicle (ROV) “Gnom” and a sonar (Borodkin et al. 2018). As a result of sonar data processing, it turned out that the crest of the keel of ice ridge 1 is dislocated aside and extends on significant distance perpendicularly to the crest of the sail (Fig. 5). It is a coincidence that the drilling profile runs just along the crest of the keel. Unfortunately, apparently due to an error in the sonar settings the scales are misrepresented to a large degree.

Figs. 6-8 show the profiles of the investigated ice ridges.

Average thickness of ice blocks in the main sail crest of ice ridge 1 was 0.29 m (located

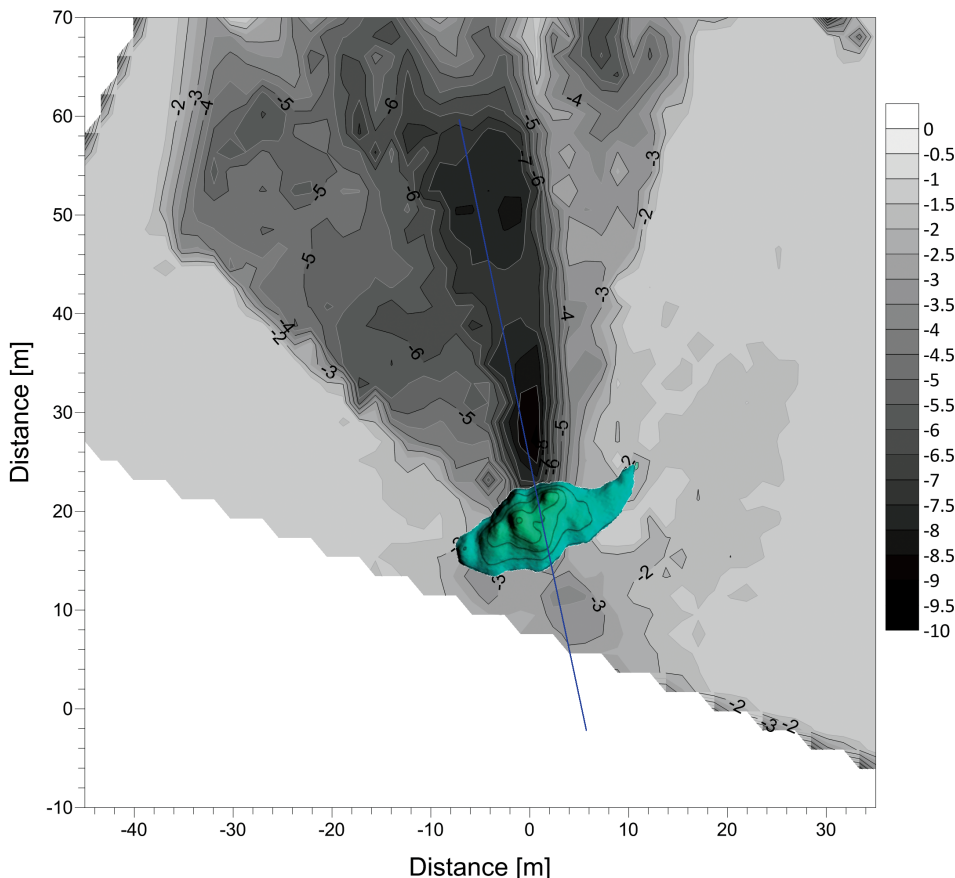


**Fig. 5.**Relief of the lower ice ridge 1 surface. The crest of the ice ridge sail is shown on the diagram in green and cut off along the excess contour of 2 m. The secant line (straight line in the diagram) run perpendicular to the sail crest of ice ridge 1. Keel draft along the drilling profile is shown below

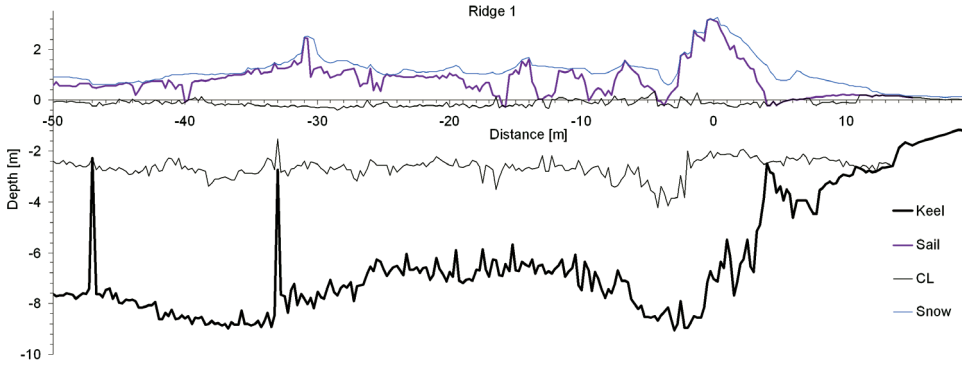


Fig. 6. Resulting cross-sectional profile of thermodrilling of ice ridge 1

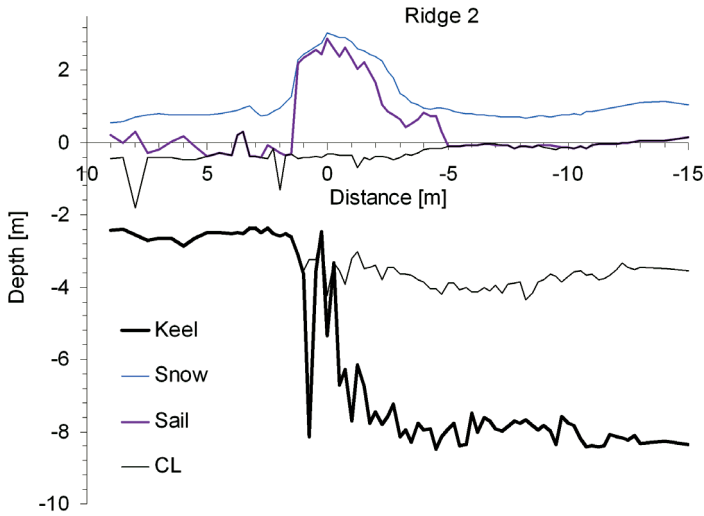


Fig. 7. Resulting cross-sectional profile of thermodrilling of ice ridge 2

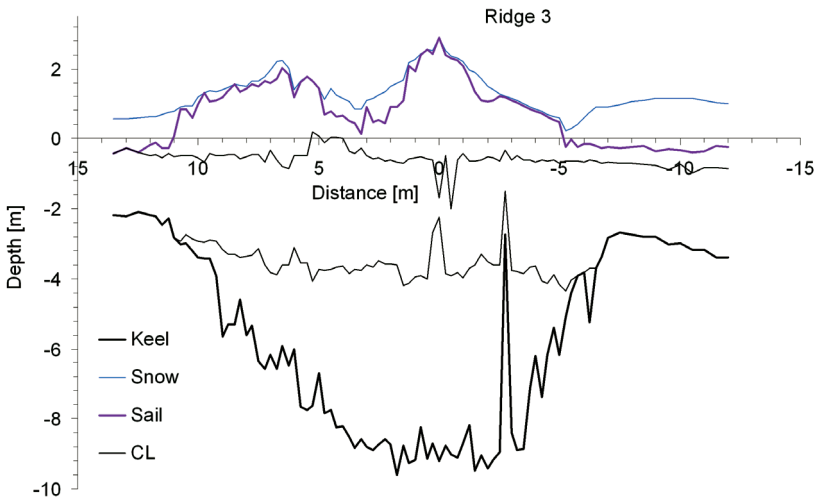


Fig. 8. Resulting cross-sectional profile of thermodrilling of ice ridge 3

at the distance 0 m in Fig. 6), and in the second sail crest (located at the distance of  $-31$  m in Fig. 6)  $-0.19$  m. That means that the main crest of ice ridge 1 is the result of secondary ridging. One of the signs of the secondary ice ridges is a formation of two or several above-water parts of them, located most often at an angle to each other markedly differing in the thickness of the ice fragments (Tyshko and Kharitonov 2011). The crest with a higher sail in the ice ridge 1 was formed later, at the final stage of ridging. Ice ridge 2 has the extremely large angles of sail and keel slope ( $84^\circ$  and  $77^\circ$ ) from the side of rafted ice. Apparently, the keel left slope edge has a fairly loose structure as at a distance of  $-0.25 \dots 0.5$  m. There was almost no ice blocks detected while drilling below the CL. Ice ridge 2 was covered with a thick snow layer. Judging by the block thickness in its sail ( $0.27$  m), the ridge 2 was formed approximately during the same period of time as the main crest of ice ridge 1. Two crests of the sail of ice ridge 3 are also formed from ice of various thickness: the average blocks thickness of the highest pile of ice ridge sail (see Fig. 8) was  $0.20$  m (a mode of distribution was  $0.11$  m), of the more flat pile  $-0.35$  m (a mode of distribution was  $0.32$  m). Hence, the ice ridge 3 was formed in two stages as the two other ridges. There is also a noticeable submerging of the ice ridge 3. In case of ice ridges 1 and 2 it was not succeed to extend the drilling profile in both directions up to reaching level ice. There was an impression that we are on the edge of ridged field of great length. Decisions were made to proceed to the next objects.

Recently, the focus of scientists studying ridged features shifted towards the little-known, but rather interesting problem of CL thickness distribution within a ridged feature. Information for resolving this problem is also provided by our study. Average thickness of the CL of ice ridge 1 is  $2.5$  m; the maximum one is  $4.0$  m; the minimum one is  $1.3$  m. The CL is well developed and non-uniform in its thickness. Unlike the first ice ridge, on ice ridge 2, the thickness of the CL ranges within  $2.0 \dots 4.2$  m; the CL is thick in the right part

of the profile, slightly thinner under the sail, which can be associated with screening by the sail and a barrier for penetration of cold to the ice ridge keel. The CL of ice ridge 3 is slightly thinner ( $1.7 \dots 4.3$  m) than that of ice ridges 1 and 2. However, it is immersed significantly; the average location of the upper CL boundary is at the depth of  $-0.5$  m, at some points up to  $-1$  m. The CL thickness of ice ridges of the Shokal'skogo Strait is noticeably higher than that, for example, near the Spitsbergen archipelago and the Fram Strait. Their CL thickness is  $1.0 \dots 2.8$  m on average (Bonnemaire et al. 2003; Høyland 2002, 2007; Bonath et al. 2018). In the paper (Strub-Klein and Sudom 2012), the average CL thickness of 117 ice ridges equals  $1.6$  m. Mironov and Porubaev (2005, 2012) give the average CL thickness in the range of  $1 \dots 3.6$  m. Undisturbed level ice is located near the ice ridge 1 and the ratio of the average CL thickness to level ice thickness is  $2.1$ . For the ice ridges investigated by Bonath et al. (2018), this ratio is  $1.4 \dots 3$ , predominantly  $2 \dots 3$ . It is suggested in ISO19906 (2010) that the CL thickness can be assumed to be two times the level ice thickness. Nevertheless, from the author's experience of studying 229 ice ridges, this ratio is  $1.6$  on average.

Thickness of the CL does not definitely correlate with the porosity of the unconsolidated portion of the keel and with the snow cover thickness; however, there is a significant reverse correlation with snow/ice elevation above sea level (correlation coefficients  $-0.32$ ,  $-0.72$  and  $-0.31$  for the investigated ice ridges). Therefore, it can be stated that the CL of the studied ice ridges was determined, to a larger extent, by the access of cold to the unconsolidated keel. In most cases, in the portion of the keel covered by the sail or a thick snow cover the CL is slightly thinner. Høyland and Løset observed a similar pattern (1999).

In the central part of the ice ridge 3, the CL has a few voids. Judging by the fact that the CL thickness is rather large in the neighboring boreholes, there should not be sharp differences in the location of CL boundaries between neighboring points. Despite of this, in Fig. 8, the small

CL thickness in this zone is designated approximately. This is, most likely, due to the screening by the sail and preventing cold penetration to the ice ridge keel.

Taking the selected criterion for determination of voids (Mironov et al. 2003) into account, the penetration rate record at every point of drilling can be realised as the staircase curve, where zero corresponds to ice, and one corresponds to voids. All depths are considered in sequence from the maximum ice ridge sail height to the maximum ice ridge keel depth. For all boreholes where the depth under consideration is not beyond the freeboard or the keel lower boundary, values of the staircase curves (0 or 1) are averaged. As a result, the depth-wise distribution of porosity is obtained.

Fig. 9 shows such distribution for the studied ice ridges. In Fig.9c, the porosity below  $-9$  m is cut off at 0.6. The cause of this very high porosity values is the low number of observation for this depth. As may be noticed from Fig. 9 and, especially from Figs. 9b and 9c, the freeboard porosity increases within the layer separating the sail from the CL. It is located at the depth of  $-0.13...0.18$  m (Fig. 9b) and of  $0...0.8$  m

(Fig. 9c). But it is rather a virtual layer in the average ice ridge. As these are averaged curves, it means that there are the voids above the CL in 15-40 % of boreholes. The CL is noted for an abrupt decrease in porosity in the area of water level. The longer the ice ridge was subjected to cold, the greater its CL thickness is and the smaller the variation in the position of its lower boundary is. The porosity curve in the area of the CL lower boundary becomes flatter. The averaged keel porosity below the CL increases with depth. It was noted in (Grishchenko 1988) that in fresh (i. e. at the stage before the CL formation) Arctic ice ridges, the porosity at the sea level was by 0.1-0.2 lower than in the ridge top and keel parts. The author connected this peculiarity of porosity distribution by vertical with the action of the gravity and surfacing forces, contributing to concentration and subsequent compacting of small ice fragments in the sea level area. Surkov (2001(a, b)) showed that the keel porosity in ice ridges of the Sea of Okhotsk and the Baltic Sea below the CL increases with depth from 0.27 to 0.4-0.5 (in the lower keel part) by the linear law. The linear dependence of porosity is also noted in (Pavlov et al. 2016).

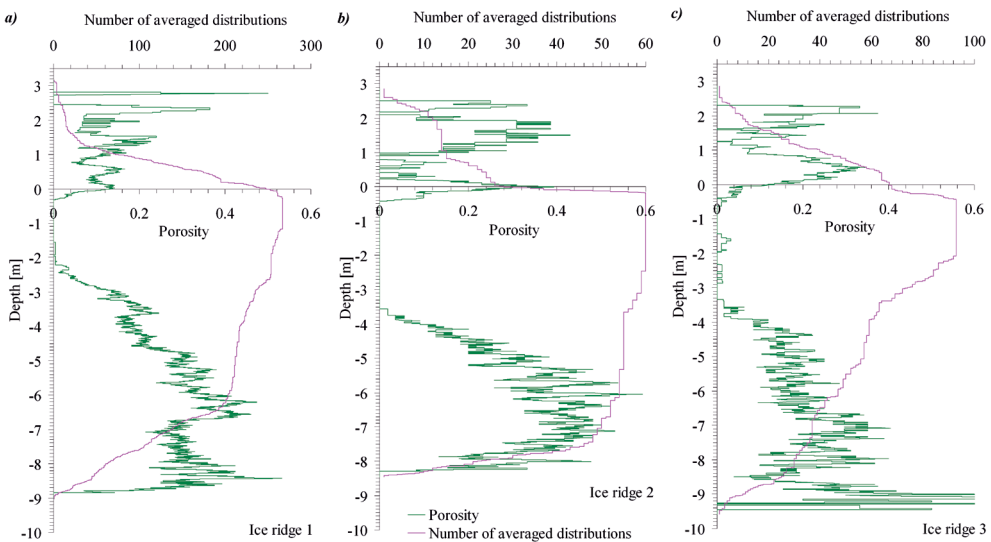


**Fig. 9. Depth-wise distribution of the porosity of ice ridges investigated in the Shokal'skogo Strait (Severnaya Zemlya Archipelago) in 2018 (according to the hot water thermal drilling data)**

The porosity curve increase of ice ridge 1 with depth has discontinuity at the depth of 6.7 m. As core drilling at a distance of 49 m and subsequent study of ice salinity and texture and also the analysis of penetration rate records showed that there was a large block of two-year ice at a distance of –47...–50 m (Fig.6) at a depth below 6.7 m. The number of the distributions used for averaging is not so considerable at a depth below 6.7 m; therefore, the presence of the large ice block leads to a decrease in the average porosity at that depth.

From literary sources it is known that averaged porosity of the unconsolidated portion of the keel can vary from 0.2 (Strub-Klein and Sudom 2012; Ervik et al. 2018) to 0.3 (Beketsky and Truskov 1995; Høyland 2007), reaching in some cases up to 0.5 (Bonath et al. 2018). As can be seen from the graphs in Figs. 9b and 9c, the porosity in the unconsolidated portion of the keel of ice ridge 2 and 3 is depth-wise distributed differently. However, averaged porosities of the unconsolidated portion of the keel of ice ridge 2 and 3 are practically equal (see Table 1). That is, ice in the keels redistributed. Porosity in the ice ridge 2 quickly reaches high values with depth. Porosity below the CL in the ice ridge 3 varies only slightly, but in the lower part of the keel its values increase.

## CONCLUSIONS

The accomplished studies enabled to receive new data on the ice cover of the Shokal'skogo Strait. The following conclusions can be drawn:

- ratios “maximum keel / maximum sail” of the investigated ice ridges were equal to 2.8, 3.0 and 3.3;

- CL thickness of the studied ice ridges varied in the range of 1.3...4.0 m; average values of the CL thickness were 2.5...3.5 m; the formation of CL was owing, to a lesser extent, to the packing density of broken ice in the keel and, to a greater extent, to the access of cold to the unconsolidated keel;

- ratio “average CL thickness / average thickness of level ice”, retrieved for one investigated ice ridge, was equal to 2.1;

- consolidation degree of the investigated ice ridges was about 34-43 %;

- unusual structure of the ice ridge is found, in which the crest of the ice ridge keel is dislocated aside and extends on significant distance perpendicularly to the crest of the sail;

- average porosity of the unconsolidated part of the keel increases with the keel depth.

## ACKNOWLEDGEMENTS

Field research was conducted within the seasonal expedition “Sever-2018” organised by the High-Latitudinal Arctic Expeditions Department, the Arctic and Antarctic Research Institute Roshydromet's. I want to thank my colleagues of AARI Gennady Deshevykh and Andrey Shirshov for the assistance in thermodrilling of ice ridges. I express my gratitude to Andrey Paramzin for kindly providing aerial photographs of ice ridges and special thanks to Stepan Khotchenkov for the sonar data. ■

## REFERENCES

- Beketsky S.P. & Truskov P.A. (1995). Internal Structure of Ice pressure ridges in the sea of Okhotsk. Proc. of the 13th Int. Conference on Port and Ocean Engineering under Arctic Conditions. August 15-18, 1995. Murmansk, Russia, V. 1, pp. 109-111.
- Bonath V., Petrich C., Sand B., Fransson L., Cwirzen A. (2018). Morphology, internal structure and formation of ice ridges in the sea around Svalbard. *Cold Regions Science and Technology* V. 155, pp. 263-279.
- Bonnemaire B., Høyland K.V., Liferov P. & Moslet P.O. (2003). An ice ridge in the Barents Sea, part I: morphology and physical parameters in-situ. Proc. of the 17th Int. Conf. on Port and Ocean Engineering under Arctic Conditions. June 16-19 2003, Trondheim, Norway.
- Borodkin V.A., Paramzin A.S., Khotchenkov S.V. (2018). Joint application of a multirotor unmanned aerial vehicle and a scanning sonar to create a three-dimensional digital model of the ice feature relief. *Rossiiskie poliarnye issledovaniia. Russian polar research*. 2018, 4: 31-35 [In Russian]. [http://www.aari.ru/misc/publicat/sources/34/RPR-34el\\_l\\_30-34.pdf](http://www.aari.ru/misc/publicat/sources/34/RPR-34el_l_30-34.pdf)
- Ervik Å., Høyland K.V., Shestov A., Nord T.S. (2018). On the decay of first-year ice ridges: Measurements and evolution of rubble macroporosity, ridge drilling resistance and consolidated layer strength. *Cold Regions Science and Technology*, V. 151, July 2018, pp. 196-207.
- Grishchenko V.D. (1988). Morphometric characteristics of ice ridges at Arctic basin. Proc. of AARI. V. 401, pp. 46-55 (in Russian with English summary).
- Høyland Knut V. (2007). Consolidation of first-year sea ice ridges. *Journal of Geophysical Research*. 107 (C6, 10.1029/2000JC000526). 15,1-15,15. <https://agupubs.onlinelibrary.wiley.com/doi/10.1029/2000JC000526>
- Høyland K.V. (2007). Morphology and small-scale strength of ridges in the North-western Barents Sea. *Cold Regions Science and Technology*, 48, pp. 169-187.
- Knut V. Høyland & Sveinung Løset. (1999). Experiments and preliminary simulations of the consolidation of a first-year sea ice Ridge. Proc. of the 15th Int. Conf. on Port and Ocean Engineering under Arctic Condition, POAC'99, 1999. Vol. 1, p.49-59.
- ISO19906 (2010). Petroleum and Natural Gas Industries — Arctic Offshore Structures (2010).
- Kharitonov V.V. & Morev V.A. (2011). Method of investigation of internal structure of ice hummocks and stamukhas using the thermal drilling technique. *Russian Meteorology and Hydrology*. V. 36. No. 7: 460-466. <http://mig-journal.ru/archive?id=574>.
- Mironov Y.U., Morev V.A., Porubayev V.S. & Kharitonov V.V. (2003). Study of geometry and internal structure of ice ridges and stamukhas using thermal water drilling. Proc. of the 17th Int. Conf. on Port and Ocean Engineering under Arctic Conditions POAC'03. Trondheim, Norway, June 16-19 2003, V. 2, pp. 623-632.
- Mironov Ye.U. & Porubaev V.S. (2012). Formation of ice ridges in the coastal part of the Kara sea and their morphometric characteristics. *Sovremennye problemy nauki i obrazovaniia. Modern problems of science and education*. No. 4. URL: <http://science-education.ru/ru/article/view?id=6707> (accessed: 05.07.2018).

Mironov Ye.U. & Porubaev V.S. (2005). Structural peculiarities of ice features of the offshore of the Caspian Sea, the Sea of Okhotsk and the Pechora Sea. Proc. of the 18th Int. Conf. on Port and Ocean Eng. under Arctic Conditions (POAC). Potsdam, New York, 26-30 June 2005, Vol. 2, pp. 483-492.

Morev V.A., Morev A.V. & Kharitonov V.V. (2000). Method of determination of ice ridge and stamukha structure, ice features and boundaries of ice and ground. License of Russia № 2153070, Bulletin of inventions № 20 (in Russian).

Pavlov V.A., Kornishin K.A., Efimov Ya.O., Mironov Ye.U. et al. (2016). Peculiarities of consolidated layer growth of the Kara and Laptev Sea ice ridges. Neftyanoe khozyaystvo (Oil industry), No. 11, pp. 49-54 (in Russian with English summary).

Strub-Klein L. & Sodom D. (2012). A comprehensive analysis of the morphology of first-year sea ice ridges. Cold Regions Science and Technology. V. 82, pp. 94–109.

Sodom D. & Timco G. (2013). Knowledge gaps in sea ice ridge properties. Proc. of the 22nd Int. Conf. on Port and Ocean Engineering under Arctic Conditions (POAC). June 9-13, 2013. Espoo, Finland.

Surkov G.A. (2001). Internal structure of first-year hummocks. Proc. of ISOPE, Stavanger, Norway, June 17-22, 2001.

Surkov G.A. (2001). Thickness of the consolidated layer in first-year hummocks. Proc. 16th Int. Conf. on Port and Ocean Engineering under Arctic Conditions. Ottawa, Ontario, Canada. August 12-17, 2001, pp. 245–252.

Tyshko K.P. & Kharitonov V.V. (2011). Some features of one-year ice hummock formation at multiple ice field motions. Russian Meteorology and Hydrology. No. 10, pp. 53-57.

Received on April 3<sup>rd</sup>, 2019

Accepted on August 8<sup>th</sup>, 2019

**Ibrahim M. Ahmed<sup>1</sup>, Eltoum M. Abd Alla<sup>1\*</sup>**

<sup>1</sup> Faculty of Geographical and Environmental Sciences, University of Khartoum, Khartoum, Sudan

\*Corresponding author: mabdallaeltoum@gmail.com

# LANDUSE IMPACT ON ENVIRONMENT OF TUTI ISLAND, SUDAN

**ABSTRACT.** Environmental study was carried out to describe a geographical area and its biodiversity. The example here shows the features of human nutrition habits and quality of life with specific study of negative impact on the environment and Earth resources. Tuti Island in Sudan was prone to this complex problem so it is taken as a case study. The hypothesis is that the use of RS and GIS could help in reconstruction of unused territories so it could help to solve the problem. Changes of land use and land cover were observed using classified Landsat 5 images in 1972, Landsat 7 in 1985 and Landsat 8 in 2018. The results showed that several temporal changes occurred beside turning dense tree cover land into lands with other landuse purposes for 1972, 1985 and 2018. Agricultural zones (crops and trees) were major dominant zones in 1972, 1985 and 2018. In addition, populated residential areas increased through time but not as significantly as trees, sand and cropping landuse areas ( $P=0.89082$ ) as for the classified Landsat 8 image acquired in 2018. Ecosystem planning through GIS and RS could be a good way to solve most of these issues for the future of Tuti Island landuse.

**KEY WORDS:** Ecology, Sudan Islands, Landcover, Agricultural use

**CITATION:** Ibrahim M. Ahmed, Eltoum M. Abd Alla (2019) Landuse Impact On Environment Of Tuti Island, Sudan. *Geography, Environment, Sustainability*, Vol.12, No 3, p. 27-33  
DOI-10.24057/2071-9388-2018-13

## INTRODUCTION

The present and future global environmental challenges bother many world nations, for example the loss of biodiversity, the depletion of the ozone layer, climate change and global warming. In addition, water and soil contamination and food insecurity are the threats for human health in many countries. These problems are multiplied through history and became worse with population increasing. Increased world population affect the Earth resources directly and indirectly. Sudan is one of the most environmentally degraded countries in

the world. Natural resources in Sudan were severely affected by climate change and human interaction. Desertification as an outcome of natural resources degradation and environmental problems was observed through history of the country. Objective of the study is to solve this problem through study of Tuti Island environmental profile. This could give a sustainable solution for its environmental problems and provide food to it is population in a sustainable manner.

## Environmental degradation in Sudan

Eltoum et al. (2015) studied the role of several ecological factors in causing

desertification in Sudan. Eltoum (2017) monitor the state of ecological zones in Sudan since 1958 to 2017 and reported several changes in the country eco zones. Recent researches provide evidence that most of its land was covered by desert and semi-desert zones resulting from severe drought and deforestation (Eltoum et al. 2015; Eltoum 2017). The water resources degraded both qualitatively and quantitatively. The biodiversity decreased due to habitat destruction and weak environmental awareness not only among the public but also among the policy makers (UNEP 2007). Tuti Island is a case of fragile eco system in Sudan where erosion, floods, and landuse conflicts take place. Many researchers take Tuti Island as study area from several perspectives as Lobban (1982) studied the class and kinship of Sudanese urban communities based on Tuti community compared to Burri al Mahas and other Khartoum communities to investigate the effect of urbanization in the Sudan. Although Tuti Island was reported as an isolated area, some changes were observed by researchers latter on. Khidir (1998) reported some social changes between rural and urban communities and divided the life on the island into old village area and new urban one. As researches show, the environment of Tuti Island also changed through history as a response to many factors including human activity and climate changes (Osman 2004; Mohammed 2007; Salah and Idris 2013).

### Geography of Tuti Island

Tuti Island is one of Sudan islands which located in the joint point of the White and blue Nile in Khartoum state at N15.37 E32.29. The three main cities which form Khartoum state are Khartoum, Khartoum North and Omdurman. Tuti Island is located at the central point of these cities. It believed that it was the first populated area in Khartoum region and it may have been established before the 15<sup>th</sup> century during spread of Islam (Osman 2004). Although signs of Arabic language may have presented earlier than 15<sup>th</sup> century in this region (Aldarier 1922). Archaeological studies mentioned that most of Sudan

islands were inhabited by ancient populations which may belong to old Nubian civilization. During Soba kingdom before 15<sup>th</sup> century Tuti island was very famous but there is an information only about one church. Most of the population have appeared after the migration of Arab and Islamic tribe to the Island. Since that time the Island has been isolated from the three cities for many years. In 2009 Tuti bridge was constructed and it linked the island with Khartoum city. Hence, the modern style of life was transferred. Additional two bridges have been suggested by Khartoum Structure Plan to link Tuti Island with Khartoum North and Omdurman cities. The soil of Tuti Island formed from three components which are Nubian sandstones, basement complex, and Rivers deposits which include Sandy soil, Clay soil and Rivers mud, more detailed info could be found in researches of Mohammed (2007).

### Environmental setup

Harison and Jakson (1958) describe Khartoum state as Semi desert area. Later Eltoum (2017) recorded turning Khartoum state into desert. Climate change and desertification were the main reasons of its environmental change. Although Tuti island is isolated by the three rivers (Blue Nile, White Nile and Nile rivers), the climate conditions are described as arid with low rainfall and high evaporation. Accordingly, some changes have occurred in it. Flood disaster was regularly recorded in 1964, 1977 and 1988. Water erosion (Haddam) affects most of its agricultural areas on the rivers sides banks of the Tuti Island. Creeping sand from different parts of the country form seasonal wadies settled in the South part of the island. Population of Tuti Island increased thrice from 5851 in the years 1955/1956 up to 14400 in 1999 with the rate of 10 thousand each 45 years. The continuous increase in the population enhanced amount of waste which directly affected water quality in the river Nile. Animals have been raised for domestic use (meat and milk) while in the past cows had been used for soil cultivation. Group of hunters use many strains of dogs,

specifically the merowe dog and saluki dog strains were found in Tuti Island. Tuti Island is a dense vegetated area in Khartoum state with a high diversity of plants composition. Availability of water from rivers, Nile, Blue Nile and White Nile in addition to clay soil support the vegetation diversity.

### Landuse and Landcover

Bahreldin and Eisa (2014) divided Tuti Island into three zones: old Tuti, central Tuti and farm land. Old Tuti looks like group of small Sudan villages while the central zone has different style. Khartoum Structure Plan in 2014 planned 14 zones for future use of Tuti Island. Since the island is considered as special zone, environmental planning must be taken into account. Historical reports from Islamic civilization have mentioned that Tuti Island and Khartoum city had been forest areas before human beings settled in it. Recently both areas have been used as residential areas beside farms land. While forest areas protection exists in Khartoum city, deforestation on Tuti Island has occurred. Gradual change in land use of both areas has been observed. Many researchers attribute this change to increased population in both areas and settlement activities (Mohammed 2007; Salah and Idris 2013; Bahereidn and Eisa 2014). Agricultural activities on Tuti Island were historically reported since farms have covered most of the area. Several agricultural crops were planted including

vegetables, fruits, citruses and forages (Mohammed 2007).

### MATERIALS AND METHODS

Satellite images were downloaded from USGS web site. These images include recent Aster Dem images for the year 2018: Landsat images for the different periods of time; Landsat 8 which was acquired in 2018; Landsat 7 for 1985 and Landsat 5 for 1972. The images were added to Sudan geo database map which was collected from the Internet. Study area was observed through Google Earth (Fig. 1). To visualize the eco zone component remote sensing and GIS techniques were used, in particular the method of Image supervised classification. The landcover was classified and landuse was identified by using visual interpretation of classified Landsat 5, 7, 8 images and Google earth images. Overlaying techniques were used to identify these classes.

### RESULTS AND DISCUSSION

#### Landcover and landuse map

The landcover and landuse map terms were used generally to describe the geographical patterns of specific area. The new technology which appeared on this century with the use of computers and its software applications provided fast, easy and low cost method to describe these patterns. The geographical information

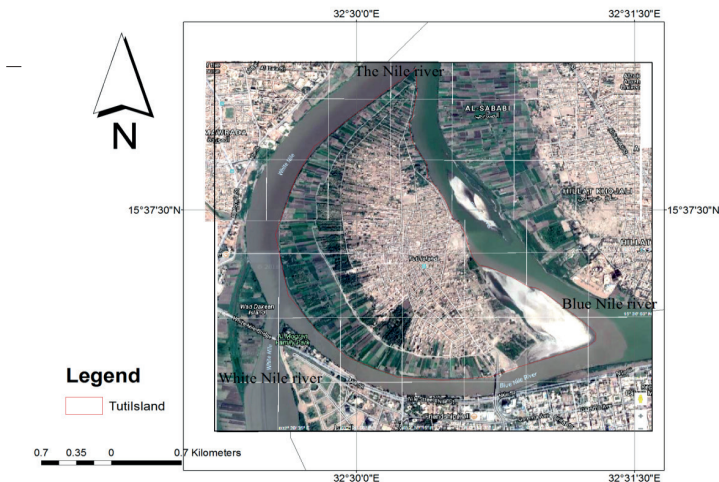


Fig. 1. Tuti Island surrounded by rivers and urban areas of Khartoum state

system and remote sensing stand in front of many branches of science which benefit from them. Supervised classification method in GIS and RS was used to describe the land cover and create landuse map. Fig. 2 shows the land cover classes of Tuti Island in 1972. There were three main classes present in 1972: vegetation, residential area and sand. Most of the Island was covered by vegetation which could be classified as dense and low.

As population increased residential area enlarged and agricultural areas substituted the natural vegetated areas. The sand masses travelled by river water to other location. Fig. 3 represent the change in land use form 1985 to 2018. The residential area has expanded to replace vegetation in some location on the north and west part of the island. The border of the island was reshaped and extended to the south due to sand settlement and water erosion. An increased water area surrounding the island was observed. Increase in some vegetated areas may refer to agricultural activity and shift from trees to low vegetation. A decrease of the Island land in the South part was due to water erosion of the Blue Nile River. The results of classified images in 2018 showed that low vegetated areas were used as agricultural areas for cultivation of crops mainly vegetables and

forages on silt and clay soils. These soils have mainly been formed by the residue of flood which occurred due to the rivers mud moving during floods periods. These fertile soils represent a good base for diverse vegetation through history as it was mentioned (Mohammed 2007).

The high biomass vegetated areas were covered by trees which are fruit and citrus plants with few scattered trees. The soil covered by residential areas was used for settlement of Tuti island population through historical period (Fig. 4). These results are full agreed with spatial classification results (Bahreldin and Eisa 2014) on Tuti Island in addition to the flora of Tuti Island which was classified by Mohammed (2007). The shift and replacement of natural forest trees biomass layer with cultivated citrus and fruit trees may reflect the human activity in this eco system. This may lead to clearance of other forest layers mainly shrubs and grass. This process exposed the soil to water erosion and decreased the land area specifically on the river Nile coast where extensive agricultural practices exist. In general, the land cover present on Tuti Island could be divided into vegetated area including trees area beside cultivated area, water area (Nile, white Nile and blue Nile rivers), residential area and bare area. Landcover

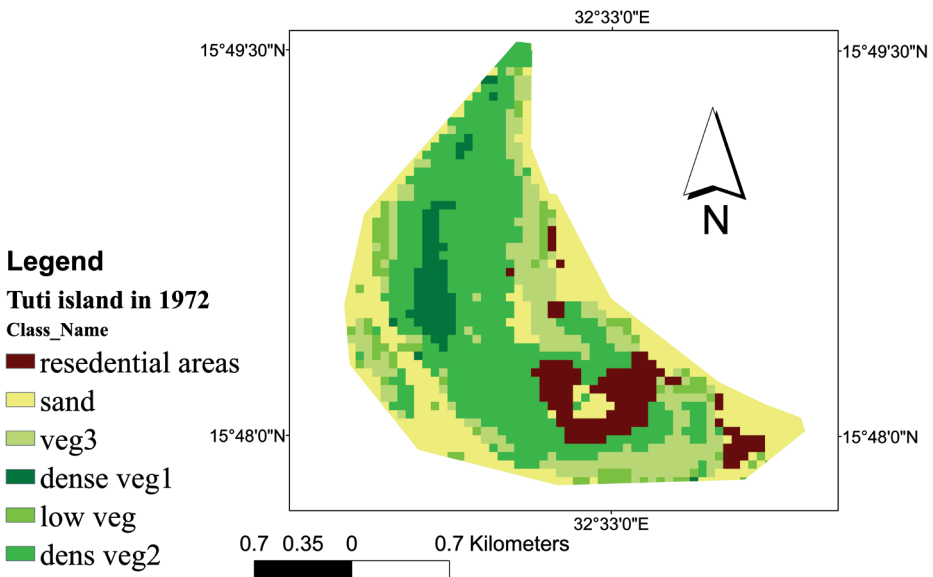
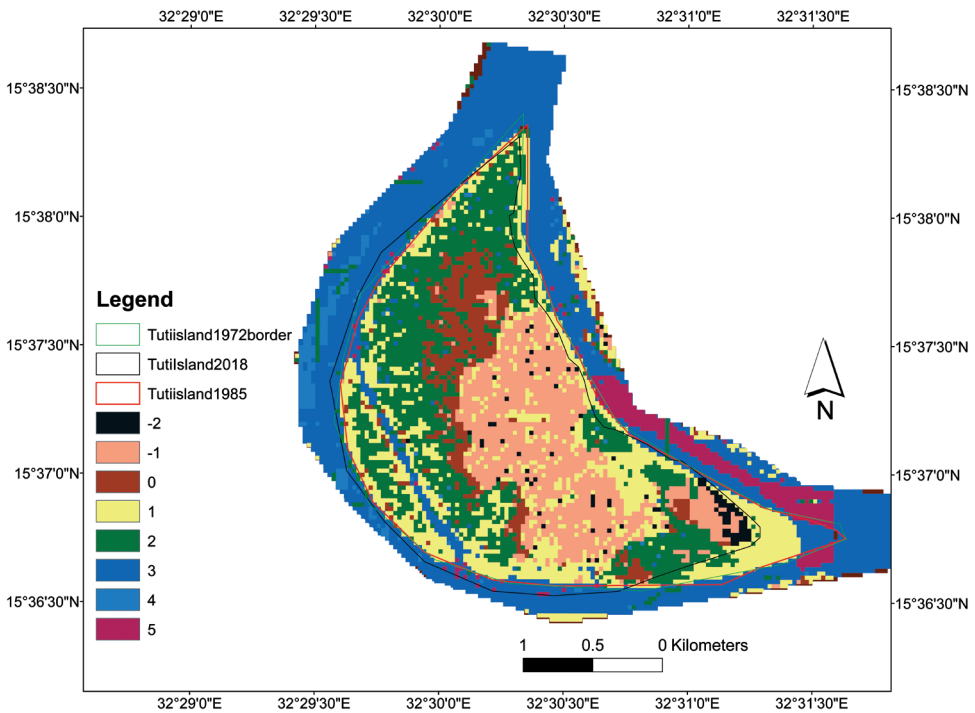


Fig. 2. Land cover classes of Tuti Island in 1972



**Fig. 3. Change of landuse on Tuti Island during 1985-2018**

and landuse of Tuti Island create a critical question about the past formation of this island. Could the island be a part of the Gazera area in the middle of Sudan or stand as an old Delta of the White Nile River which was converted to an island later on due to change in the water course and path way of the Blue Nile river? Further study and investigation may be needed to clarify these assumptions. This may give an opportunity to understand the past environmental system which was present on the island during the past century. Critical investigation of this information will help researchers to plan for sustainable use of this zone.

Landuse classes are occupied with different parts from the total area of Tuti Island (Fig. 5). The high percentage dominant class is crops which represents more than 50% of the total Tuti Island area followed by residential areas which represents 30%. Trees represent only 6% of the total area which is alarming. This means that the area is almost free of trees. Mahmoud et al. (2016) considered Um Dom Island not far from this area in Blue Nile and found that

the forest plant species differ and the tree layer was dominated by acacia and other species. Salah and Idris (2013) reported that environmental state of Alsunut forest in Khartoum city and Tuti Island is controlled by the rivers and human influences. Creeping sands which settled on the river cost on the southern part of the Tuti Island represent an area about 4%. The minimum areas were occupied by wet soil with water from White and Blue Nile rivers - 1% for each area.

### Environmental planning of Tuti Island

In environmental planning for sustainable life on Tuti Island the farms, farmers and farm owners must be involved in any plans for reconstruction of Tuti Island because they represent the major group of the island in 2018. Insignificant difference between the residential areas and other groups (agricultural crops areas, trees and sand) indicate a well-balanced use of land for settlement purpose. Nevertheless, a priority must be given to an incoming generation in the future from the same indigenous population to conserve this

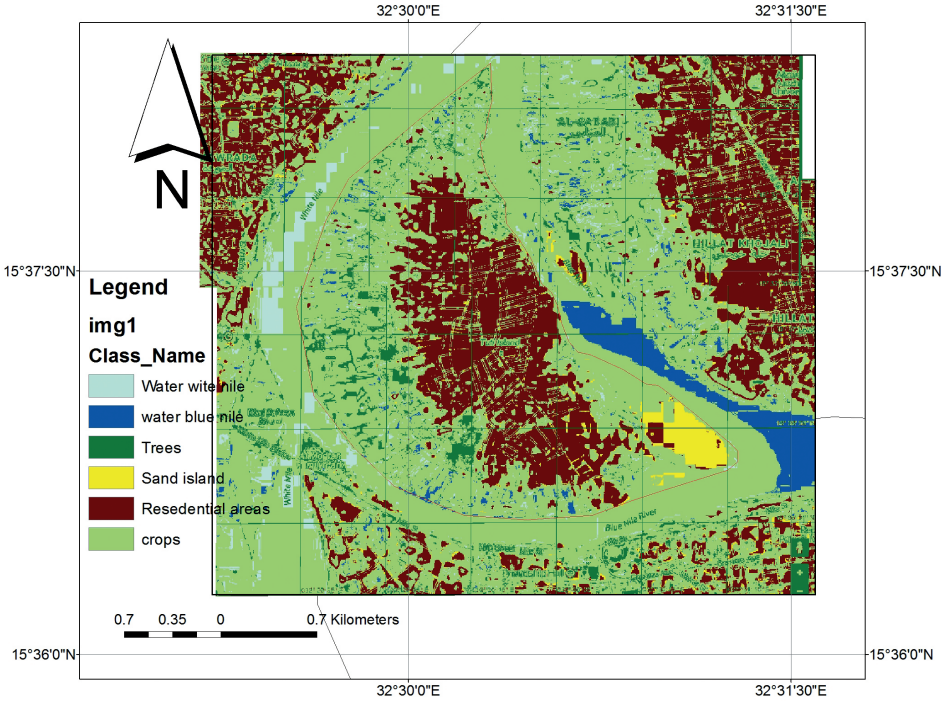


**Fig. 4. Landcover and landuse classes of Tuti Island in 2018**

balance. The prevention of swamp soil area appearing and increasing trees cover will add more environmental values to these areas as in Alsunut forest zone in Khartoum city. These facts agreed with findings of Osman (2004) who reported that there is a high need of principle guide line for sustainable future planning of Tuti Island.

**CONCLUSION AND RECOMMENDATIONS**

In conclusion, Tuti Island was under sever changes due to climate change, desertification, flood disasters and human impact. From 1972 to 2018 the island witnessed several environmental changes and shifts. Temporal increase of human being activity may have adverse impact on

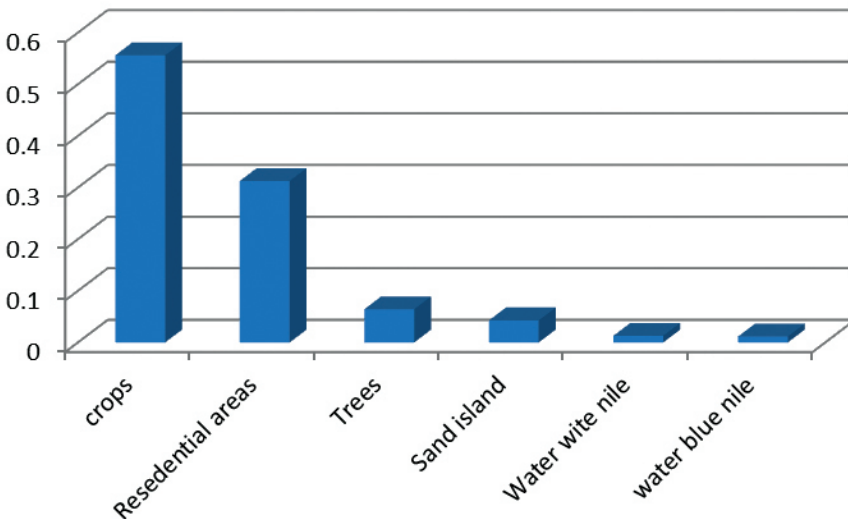


**Fig. 5. Percentage of the landcover classes from the Tuti Island total area**

the environment. Corrective measures must be taken to minimize these changes to serve the need of its residents without damaging the islands environment. Environmental study could help in implementing planning approach to conserve this unique biodiversity area. Environmental degradation are present in several parts of the Earth globe. Increasing population, climate change and urbanization have enlarged the geographical areas where

several environmental systems have crashed. It's clear that corrective measures must take place in these environmental systems for sustainability of live in it. Human beings have played an important role in the environmental systems degradation so changing their behaviour to more positive impact is highly needed. Replanning, organizing and leading of the affected population maybe the first step in achieving sustainability goals. ■

## REFERENCES

- Aldarier A. (1922). Arabic language (AL Arabia) in Sudan. Khartoum. (In Arabic)
- Bahreldin I. and Eisa A. (2014). Spatial changes and urban dynamics in Tuti Island in Tuti Island. International conference on the role of local communities in disaster mitigation Tuti case study. International university of Africa disaster management and refugees studies institute. Khartoum, p. 1-15.
- Eltoum M. (2017). Use of GIS and remote sensing techniques to study the ecological zones of Sudan in 2017. *Sudanese journal on computing & Geoinformatics*, 1(1), pp. 27-48.
- Eltoum M., Dafalla M. and Ibrahim S. (2015). The Role of Ecological factors in causing land surface desertification, the case of Sudan. *Journal of Agriculture and Ecology Research International*, 4(3), pp. 105-116.
- Harrison M. and Jackson J. (1958). Ecological classification of the vegetation of the Sudan. *Forest bulletin*, 2, pp. 1-45.
- Khidir O. (1998). About Tuti the Island and the village. [online]. Available at: <https://vtechworks.lib.vt.edu/bitstream/handle/10919/32246/ch9.pdf?sequence=11&isAllowed=y> [Accessed 04.09.2019]
- Lobban R. (1982). Class and kinship in Sudanese urban communities. *Journal of the International African Institute*, 52(2), pp. 51-76.
- Mahmoud N., Elhakeam M., Abdallah A., Kordofani M. (2016). An inventory of flora in Umdoum Island, Khartoum, Sudan. *Journal of Agriculture and Ecology Research International*, 6(1), pp.1-10.
- Mohammed S. (2007). A study on the flora of Tuti island in Khartoum state. PhD Thesis. Available online: <https://pdfs.semanticscholar.org/cd89/dcc33bef8edf632129dbad33576a75855d52.pdf> [Accessed 04.09.2019].
- Osman M. (2004). Spatial & visual attributes in Tuti Island. MSc Thesis. Available online: <https://core.ac.uk/download/pdf/71676217.pdf> [Accessed 04.09.2019].
- Salah O. and Idris E. (2013). Anote on the bird diversity at two sites in Khartoum, Sudan. *Egyptian Academic Journal of Biological Sciences*. 5(1), pp. 1-10.
- UNEP (2007). Global Environment Outlook. Available online: <https://www.unenvironment.org/global-environment-outlook> [Accessed 04.09.2019].

**Galina Surkova<sup>1\*</sup>, Aleksey Krylov<sup>1</sup>**

<sup>1</sup> Lomonosov Moscow State University, Moscow, Russia

\*Corresponding author: galina\_surkova@mail.ru

# EXTREMELY STRONG WINDS AND WEATHER PATTERNS OVER ARCTIC SEAS

**ABSTRACT.** Strong wind is the main cause of storm sea waves. In order to minimize risks and damages from this phenomenon in the future, precise projections of future climate conditions are necessary. Extremely high wind speed events in the 20<sup>th</sup> - 21<sup>st</sup> centuries over Arctic seas were investigated using ERA-Interim reanalysis data (1981-2010) and CMIP5 models ensemble (RCP8.5 scenario, 2005-2100). Two different approaches were applied to investigate extreme wind events. The first one is traditional and involves direct analysis of wind speed data. It was used for the entire area of the Arctic seas. The second approach is based on an assumption that local and mesoscale extreme weather events are connected with large-scale synoptic processes. As it was shown in previous studies for the Black, Caspian and Baltic seas, it is possible to make climate projection of sea storm waves indirectly, studying the heterogeneity of sea level atmospheric pressure (SLP) fields that are the main factors of strong wind speed and wind waves. In this case, it is not necessary to run long-term simulations with a sea wave model to predict storm activity for the future climate. It is possible to analyze projections of storm SLP fields that are predicted by climate models much better than the wind speed required for a wave model. This method was implemented for the high wind speed events over the Barents Sea. Four major types of SLP fields accompanying high wind speed were revealed for the modern climate. It was shown that the frequency of their occurrence is expected to increase by the end of the 21<sup>st</sup> century.

**KEY WORDS:** wind speed extremes, global warming, Arctic, weather patterns, ocean-atmosphere interaction

**CITATION:** Galina Surkova, Aleksey Krylov (2019) Extremely Strong Winds and Weather Patterns over Arctic seas. *Geography, Environment, Sustainability*, Vol.12, No 3, p. 34-42  
DOI-10.24057/2071-9388-2019-22

## INTRODUCTION

Extreme value analysis is of the great importance in different fundamental and applied scientific areas. High wind speed is one of environmental extremes influencing wide spectrum of human life and activities both from positive and negative points of view. Extreme winds over the seas are very dangerous not only by themselves but they may be considered as a predictor of

storm waves and shore erosion processes. Wind strength and wave energy should be taken into account in shipping and marine engineering (e.g., structural reliability and strength of materials of ships, sea and coastal constructions etc.). On the other hand, wind and wave power can be used for electricity production.

High wind speeds due to cyclonic activity in the Arctic region, are typically observed

there all year around and especially, in cold season (Climate of Russia 2001). Decrease of sea ice coverage during last decades is resulted in lowering of sea surface roughness, and, thus, in higher wind speed and storm waves. The reports of Intergovernmental Panel on Climate Changes (IPCC 2013) showed the prevailed positive tendency of modern wind speed (both mean and extreme) over the Arctic in the areas situated to the north of 70-75 N latitude.

The severe climate of the Arctic region with high cloud cover makes difficult to use remote sensing data for direct atmosphere and ocean observations. In this case the weather and climate models can help to understand the present atmosphere-ocean interaction processes and there physical mechanisms. Earth system modelling is an important tool for future climate projection of extreme weather events that should help managing the risks of extreme events and disasters to advance climate change adaptation (IPCC 2012).

To derive the present and future climate conditions in our study we used the reanalysis and climate model data. Obtained results can be divided into two parts. One is based on direct evaluation of wind speed extremes for the entire Arctic from reanalysis and modeling data. In the second part the main attention is paid to the Barents Sea area. It is well known, that the significant changes of hydrometeorological parameters over the last decades are characterized by increase of strong wind frequency in the Arctic. In our study we analyzed the weather pattern accompanying strong winds, that was described from analysis of the atmospheric sea level pressure (SLP) to derive the frequency of high wind speed events. Such method is appropriate for regional studies, in which the spatial wind pattern is closely associated with regional synoptic processes and the atmospheric pressure field at sea level. Weather conditions accompanying strong winds over the Barents sea are investigated in our study both for the present climate and projected future climate conditions in the 21<sup>st</sup> century.

## MATERIALS AND METHODS

For the first part of our study we used 6-hour wind vector components:  $u$  (zonal) and  $v$  (meridional). The ERA-Interim reanalysis database (Dee et al. 2014) for period of 1981-2010 with grid spacing 0.75x0.75 degree of latitude and longitude was used to derive the present-day weather conditions. As it was shown by Lindsay et al. (2014), this reanalysis provides rather realistic prediction of the wind regime within the Arctic region. It is obvious, that some short-term wind speed extremes cannot be captured with 6-hour time step, but it is completely sufficient to analyze the persistent and constant strong winds causing large-scale sea storms.

For the modern climate the data set of numerical experiments named *Historical* was taken. To derive the future climate conditions we used the results obtained within the Climate Modeling Intercomparison Project CMIP5 (Taylor et al. 2012). The RCP8.5 emission scenario (Moss et al., 2008) supposing the strongest radiation influence of anthropogenic greenhouse gases in comparing to other scenarios for period 2005-2100 was used.

To analyze the spatial wins pattern over whole Arctic we used the results of 14 climate models having data with 6-hours time resolution available in open access (ACCESS1-0, ACCESS1-3, bcc-csm1-1, BNU-ESM, CMCC-CESM, CMCC-CMS, CanESM2, HadGEM2-CC, INM-CM4, IPSL-CM5A-LR, IPSL-CM5A-MR, MIROC-ESM, MPI-ESM-LR, MPI-ESM-MR).

To derive the spatial wind distribution over the Barents Sea, mean daily values of wind speed and atmospheric sea level pressure were used: they were taken from ERA-Interim reanalysis (0.75x0.75 degrees) and modeling results of CMIP5 (*Historical* and RCP8.5 experiments). For daily mean values there are more data in CMIP5 data base. That's why we analyzed the simulation results of 27 climate models (ACCESS1.0, bcc-csm1-1, BNU-ESM, CanESM2, CCSM4, CESM1-

BGC, CESM1-CAM5, CMCC-CESM, CMCC-CMS, CNRM-CM5, CSIRO-Mk3.6.0, GFDL-CM3, GFDL-ESM2G, GISS-E2-H, GISS-E2-R, INMCM4, IPSL-CM5A-LR, IPSL-CM5A-MR, IPSL-CM5B-LR, MIROC-ESM, MIROC-ESM-CHEM, MIROC5, MPI-ESM-LR, MPI-ESM-MR, MRI-CGCM3, MRI-ESM1, NorESM1-M). All model results were interpolated on the grid with the same size of grid cells as reanalysis data had.

Projections of extreme wind speed over the Barents Sea are based on the connection between large-scale circulation and environmental variables and relied upon the “environment to circulation” method (Huth et al. 2008). Unlike the alternative the “circulation to environment” method – which is based on classification of all circulation types with particular attention on calculation of the frequency of extreme events, we focused on investigation and classification of those weather patterns that are associated with extreme events. Nowadays, both approaches are widely used in various fields of the atmospheric sciences. An extensive review of existing classification methods was performed by Huth et al. (2008). For example, there are numerous studies based on the “environment – to circulation” approach (Demuzere et al. 2011; Surkova et al. 2013, Cannon et al. 2002; Yarnal 1993; Brisson et al. 2010; Corte-Real et al. 1998, 1999; Santos et al. 2005; Cassou et al. 2010; Stahl et al. 2006; Philipp et al. 2010; Solman, Menendez 2003). The alternative “circulation – to environment” method is successfully implemented within the framework of the COST733 action (<http://cost733.met.no>) entitled “The harmonization and application of weather types classifications for European regions”.

Atmospheric circulation types for extreme wind episodes over the Barents Sea were obtained by cluster analysis preprocessed by the Empirical Orthogonal Function (EOF) analysis to reveal leading modes that determine their spatial variability. For each case a dataset was prepared which consists of 30 daily SLP grids including the storm day and the 15 days prior and

14 days after. After EOF decomposition of daily SLP grids, the first three eigenvectors explaining more than 70% of the variance were retained, thus filtering any high-frequency perturbations ( $SLP_{EOF}$ ).  $SLP_{EOF}$  fields for storm days were used as input variables to classify circulation patterns.

Weather regimes are traditionally characterized using cluster analysis or classification methods (Wilks 1995). Those organize pressure maps into nested sequences of clusters forming a growing tree association (hierarchical method, (e.g. Cheng, Wallace 1993), or iteratively perform the classification from predefined initial states randomly selected from the total sample, according to a given number of cluster  $k$  (partition method, e.g. the  $k$ -means approach (e.g. Michelangeli et al. 1995)). More complex approaches, e.g. the Self-Organizing Map method arising from the field of artificial neural network (Johnson et al. 2008) have been also recently proposed. From statistical or technical point of view, weather regime types are thus classes of atmospheric circulation patterns gathered together from a similarity criterion. Those classes are defined by their mean conditions, or centroids, by their variance and by their frequency of occurrence.

Definition of circulation types was provided using the  $k$ -mean cluster analysis. When choosing this method, we followed the experience of the previous studies, successfully applied for classification of pressure fields (Cassou 2010). The  $k$ -means algorithm starts with a preset number of clusters  $k$  and then moves objects between clusters with the goal of, first, minimizing the variance within clusters and, second, maximizing the variance between clusters. Cluster centroids (ensemble means of cluster members) were constructed for each circulation type by averaging the SLP grids of all days that belonged to the same circulation type. It was assumed that four clusters will be sufficient for our study.

Projection of the frequency of extreme wind episodes was provided from

correlation analysis of individual “extreme” SLP fields and daily SLP for each climate model. The day is classified as “extreme” wind day if the correlation coefficient was more than threshold value. The threshold value was estimated individually for each model by comparing the frequency of modeled extreme days in *Historical* experiment and reanalysis data for the present climate.

To compare mean SLP-fields simulated by each model during warm and cold seasons (1981-2010) with a reference field derived from ERA-Interim reanalysis data the Taylor diagram was used (Taylor 2001). The diagram showed relatively good correlation between all considered fields.

## RESULTS AND DISCUSSION

An analysis of extreme wind speeds for the RCP8.5 scenario showed that for the large part of Arctic seas there is a positive response to the global warming of the 21st century (Fig.1). Opposite trends were detected in the north Atlantic regions and in some parts of the Barents Sea. Similar trends for the modern climate were discussed in the IPCC report (IPCC 2013) in respect of the mean wind speeds in high latitudes of the Arctic. It can be expected

that these trends can be prolonged and intensified in case of further global warming. As it was shown in our previous study (Surkova, Krylov 2017), based on the results of future climate simulations made in the framework of CMIP5, this region is rather vulnerable to the global warming and their response is differed significantly from other Arctic regions. Due to complex nonlinear connections in the ocean-atmosphere system it is not easy to explain such specific response of different climate characteristics in the Atlantic part of Arctic (Norwegian and Barents seas). One of possible reason can be related to the expected weakening of meridional water transfer from tropical to high latitudes (Volodin et al. 2013). Another reason may be related to the change in cyclonic activity in this region. But at the present time there is no common opinion about the direction and intensity of these changes as well as about their consequences.

Another outcome of the study is that the positive mean and extreme wind speed anomalies provided by most models are confined to the sea boundaries. The exceptions to this are the North Atlantic and adjacent seas where there is an active heat transport from low latitudes.

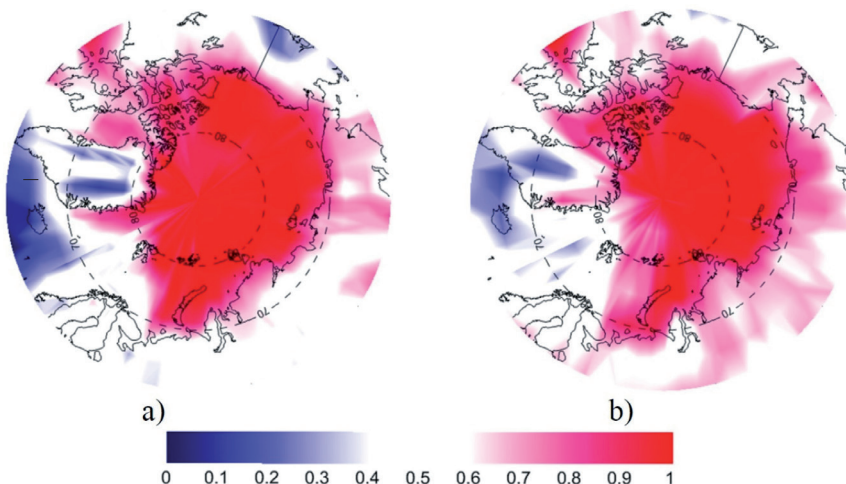


**Fig. 1. The tendency of the anomalies of wind speed quantiles (2081-2100 minus 1981-2010):  $V_{50}$  (left panel),  $V_{99}$  (right panel) according to CMIP5 model ensemble (scenario, RCP8.5). Red-colored values (0.5 – 1) correspond to increased quantiles ( $V_{50}$ ,  $V_{99}$ ), and blue-colored range (0 – 0.5) - to decreased quantiles ( $V_{50}$ ,  $V_{99}$ ) for the majority of the models, respectively**

The same pattern for the Arctic is also observed at the present time – a decrease in the wind speed over the land and a certain increase to the north of 70–75 N. Among the possible reasons for this pattern there is an estimated decrease in the area of sea ice in the Arctic. Following the RCP8.5 scenario, in the warmest months of the year Arctic sea ice can completely disappear for some time (IPCC 2013). Other reasons may be related to the changes of atmospheric baroclinity, restructuring of atmospheric circulation, the displacement of cyclone tracks, etc.

Considering that the values of both the medians and 99th quantiles tend to grow (as well as the 75th and 95th quantiles), we can assume that under RCP8.5 scenario, the entire distribution function of SLP is shifted to eastern Arctic seas. At the same time, the decrease of both currently observed wind speed over land and the wind speed projected by climate models under global warming scenarios have to be pointed out.

Classification of the SLP data for the days with extreme wind speed allows us to create composite maps for each of the four distinguished types (Fig. 2).

Type I is characterized by the most uniform field of the anomalies of atmospheric pressure in comparison with other types (deviation from the mean pressure field does not exceed 12 hPa). The negative anomaly occupies almost the entire territory of the Barents Sea and is most pronounced in the Spitsbergen area, while over the continent the pressure is above the mean values. In this type of synoptic situation, storm wind is usually observed at the southern periphery of cyclones rapidly moving to the east from the North Atlantic (Greenland region) in the direction of the Franz Josef Land. This is one of the most common types of synoptic situations (as well as type 2), causing high values of wind speed in the Barents Sea as it was shown also in the previous studies (Hydrometeorology 1990; Myslenkov et al. 2015).

Type II is distinguished by large anomalies of the pressure field comparing with type I. Two distinct baric formations are clearly visible on the map: the cyclone that emerges into the Barents Sea from the North Atlantic and a powerful anticyclone whose center is located above the Novaya Zemlya archipelago and the eastern part of the Kara Sea. The isolines are oriented almost meridionally. This situation is most consistent with cases when high wind speeds are associated with the southern wind direction, as indicated, for example, by Surkova et al. (2015), where it is noted that the Barents Sea has two priority wind direction sectors, where wind speed reached maximum values – the western and southern ones.

A distinctive feature of type III is a deep cyclone (the pressure gradient from the periphery to the center is about 30 hPa), shifting eastward from Iceland to Scandinavia. Strong east and north-east winds are observed on the eastern periphery of this baric formation. The frequency of this type recurrence is slightly lower than for the first or second types of synoptic situations.

Type IV is characterized by the presence of a particularly deep cyclone (the pressure at the center of the cyclone is 35 hPa below the average). The center of the cyclone is shifted eastward than in type III, and there is no positive anomaly in the pressure field above the north of the European territory of Russia. The frequency of this type is much lower than of the other types. Such circulation can be formed due to the regeneration of the cyclone on the Arctic front.

The right panel of Fig. 2 shows the change in the frequency trend for each type of circulation according to the climate projection based on the RCP8.5 scenario until the end of the 21<sup>st</sup> century. The results show that the frequency of extreme wind speed events will be increased. The main contribution to this growth will be made by the I and III types of SLP distribution (Fig. 3).

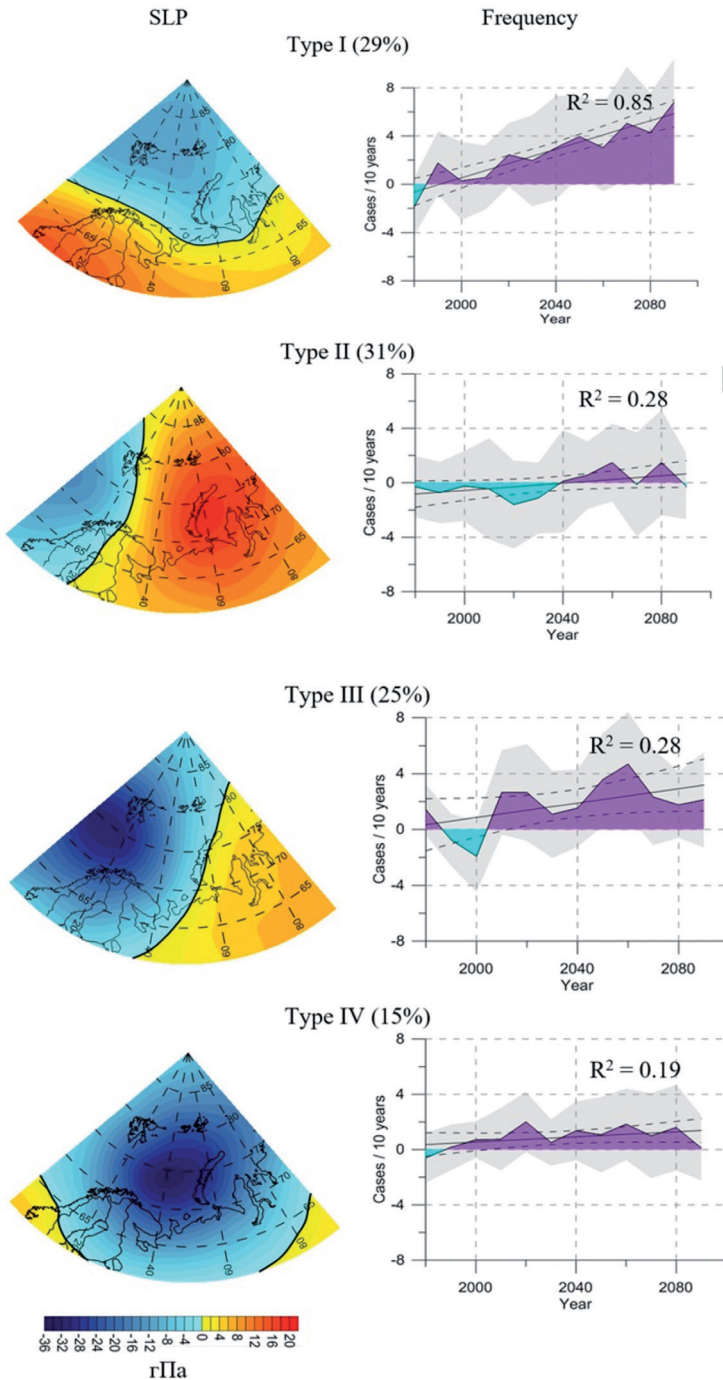
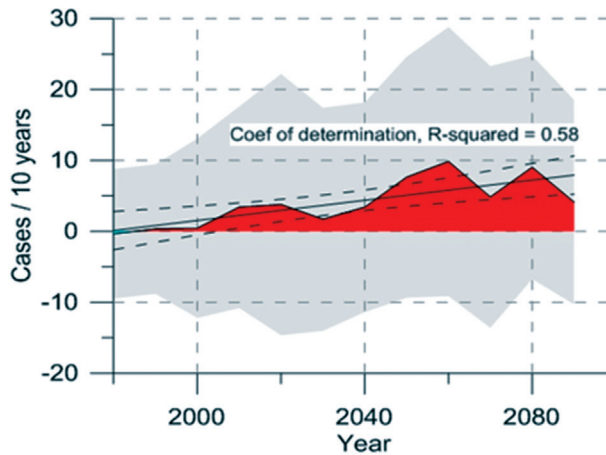


Fig. 2. Weather patterns accompanying strong winds over the Barents Sea (60–90 N, 0–90 E). Left panel – composite maps of SLP pattern types as deviations from climate means, the frequency of different types of weather patterns are given in brackets. Blue-colored areas correspond to negative anomalies (contour lines are drawn for each 2 hPa). Right panel shows temporal variability of decadal frequency of extreme wind speed events as deviation from the long-term mean (1981–2005). Light grey shows the differences between models



**Fig. 3. Interannual variability of synoptic patterns characterized by extremely high wind speed over the Barents seas calculated by model ensemble for all clusters (1-4)**

## CONCLUSIONS

In this study we present the possible trends of extreme wind speed changes during the 21<sup>st</sup> century over Arctic using the results of climate model simulations. Very high temporal resolution (6 hours) allowed us to make consistent comparisons across the Arctic. It was shown that the wind speed extremes can shift towards higher values almost everywhere in the Arctic region. Analysis of daily mean wind speed extremes and the corresponding weather patterns allowed to conclude that the global warming projected by global climate models under scenario RCP8.5 will result in increase of both average and extremely high wind speeds by the end of the 21<sup>st</sup> century over the entire Arctic area. In addition, we show that the frequency of weather patterns over the Barents Sea initiating and accompanying extreme daily mean winds for selected scenario will be higher than under present climate conditions. This study improves our understanding about the spatial patterns of projected warming and its possible influence on changes of extreme winds. Nevertheless,

the problems to explain the mechanisms of the climate system functioning still remain. Because of the complexity and nonlinearity of interaction between the atmosphere and the ocean, as well as teleconnections within the atmosphere itself, it is not easy to explain the reasons of increase of extreme wind speeds and the frequency of such episodes by the end of the 21<sup>st</sup> century in the Arctic.

## ACKNOWLEDGEMENTS

The study was supported by grants of the Russian Foundation for Basic Research: RFBR 18-05-60083 (Modern changes in hydrometeorological conditions in the Barents Sea as an indicator of climatic trends in the Eurasian Arctic in the 21<sup>st</sup> century), RFBR 18-05-60037 (Medical-geographical modeling of spatiotemporal changes in the spatial pattern of naturally-dependent and socially important diseases under the changing climate and economic development of the Russian Arctic) and RFBR 17-05-41153 (Web-atlas of wind and wave available energy in the coastal zones of the Russian seas). ■

## REFERENCES

- Arkhipkin V.S., Gippius F.N., Koltermann K.P., Surkova G.V. (2014). Wind waves in the Black Sea: results of a hindcast study. *Natural Hazards and Earth System Science*, 14 (11), 2883-2897.
- Brisson E., Demuzere M., Kwakernaak B., Van Lipzig N. P. M. (2010). Relations between atmospheric circulation and precipitation in Belgium. *Meteorol Atmos Phys*. DOI 10.1007/s00703-010-0103-y.
- Cannon A.J., Whitfield P.H., Lord E.R. (2002). Synoptic map pattern classification using recursive partitioning and principal component analysis. *Monthly Weather Review*, 130, 1187–1206.
- Cassou C. (2010). Euro-Atlantic regimes and their teleconnections. *Proceedings: ECMWF Seminar on Predictability in the European and Atlantic regions*, 6 – 9 September 2010, 14 pp. <https://www.ecmwf.int/en/learning/workshops-and-seminars/past-workshops/2010-annual-seminar> (July 11, 2019).
- Cheng X.H., Wallace J.M. (1993). Cluster analysis of the northern hemisphere winter 500-hPa height field: spatial patterns. *J. Atmos. Sci.*, 50, 2674–2696.
- Climate of Russia. (2001). Ed.: Kobysheva. 656 pp. (in Russian with English summary).
- Corte-Real J., Qian B., Xu H. (1998). Regional climate change in Portugal: precipitation variability associated with large-scale atmospheric circulation. *International Journal of Climatology*, 18, 619–635.
- Corte-Real J., Qian B. and Xu H. (1999). Circulation patterns, daily precipitation in Portugal and implications for climate change simulated by the second Hadley Centre GCM. *Clim. Dyn.*, 15, 921–935.
- Dee D.P., Uppala S.M., Simmons A.J., et al. (2011). The ERA-Interim reanalysis: configuration and performance of the data assimilation system. *Q. J. R. Meteorol. Soc.*, 137, 553–597.
- Demuzere M., Kassomenos P., Philipp A. (2011). The COST733 circulation type classification software: an example for surface ozone concentrations in Central Europe. *Theor Appl Climatol*, 105, 143–166, DOI 10.1007/s00704-010-0378-4.
- Hydrometeorology and hydrochemistry of the seas of the USSR. Barents Sea. (1990).V.1 (1). Hydrometeorological conditions. Leningrad. Hydrometizdat. 280 p. (in Russian with English summary).
- Huth R., Beck C., Philipp A., et al. (2008). Classifications of Atmospheric Circulation Patterns Recent Advances and Applications. *Trends and Directions in Climate Research*. Ann. N.Y. Acad. Sci. 1146, 105–152.
- IPCC (2013). *Climate Change 2013: The Physical Science Basis*. Contribution of Working Group I to the Fifth Assessment Report of the Intergovernmental Panel on Climate Change. Edited by T. F. Stocker, D. Qin, G.-K. Plattner, M. Tignor, S. K. Allen, J. Boschung, A. Nauels, Y. Xia, V. Bex and P. M. Midgley. Cambridge University Press. Cambridge, United Kingdom and New York, USA, 2013, 1535 pp.
- IPCC 2012 (2012). *Managing the Risks of Extreme Events and Disasters to Advance Climate Change Adaptation*. A Special Report of Working Groups I and II of the Intergovernmental Panel on Climate Change. Eds.: Field C. B., V. Barros, T. F. Stocker, D. Qin, D. J. Dokken, K. L. Ebi, M. D. Mastrandrea, K. J. Mach, G.-K. Plattner, S. K. Allen, M. Tignor, and P. M. Midgley. Cambridge University Press, Cambridge, UK, and New York, NY, USA, 2012, 582 pp.
- Johnson N.L., Kotz S., Balakrishnan N. (1995). *Continuous Univariate Distributions*. Volume 2, 2nd Edition. John Wiley & Sons. 752 pp.
- Johnson N.C., Feldstein S.B., Tremblay B. (2008). The continuum of Northern Hemisphere teleconnection patterns and a description of the NAO shift with the use of self-organized maps. *J. Clim.*, 21, 6354–6371.

Lindsay R., Wensnahan M., Schweiger A., Zhang J. (2014). Evaluation of Seven Different Atmospheric Re-analysis Products in the Arctic, *J. Climate*, 27, 2588–2606.

Michelangeli P., Vautard R., Legras B. (1995). Weather regimes: recurrence and quasi-stationarity. *J. Atmos. Sci.*, 52, 1237–1256.

Moss R. H., Babiker M., Brinkman S., et al. (2008). *Towards New Scenarios for Analysis of Emissions, Climate Change, Impacts, and Response Strategies*. Intergovernmental Panel on Climate Change. Geneva. 132 pp.

Myslenkov S.A., Platonov V.S., Toropov P.A., Shestakova A.A. (2015). Numerical modelling of storm waves in the Barents Sea with the SWAN model on the base of wind data from COSMO-CLM and WRF-ARW. *Vestnik of the Lomonosov Moscow State University, Seria 5, Geography*, No. 6, 65-75.

Philipp A., Bartholy J., Beck C., et al. (2010). Cost733cat - a database of weather and circulation type classifications. *Phys Chem Earth (Special Issue)*, 35, 360–373.

Santos J.A., Corte-Real J., Leite S.M. (2005). Weather regimes and their connection to the winter rainfall in Portugal. *Int. J. Climatol.*, 25, 33–50.

Solman S.A., Menendez C.G. (2003). Weather regimes in the South American sector and neighbouring oceans during winter. *Climate Dynamics*, 21, 91–104.

Stahl K., Moore R.D., McKendry I.G. (2006). The role of synoptic-scale circulation in the linkage between large-scale ocean-atmosphere indices and winter surface climate in British Columbia, Canada. *Int. J. Climatol.*, 26, 541–560.

Surkova G.V. (2015). Climate projection of storm weather patterns. *Proceedings of the Twelfth International Conference on the Mediterranean Coastal Environment MEDCOAST 15*, Özhan, E. (Ed.) 6–10 October, Varna, Bulgaria, 531-540.

Surkova G.V., Arkhipkin V.S., Kislov A.V. (2013). Atmospheric circulation and storm events in the Black Sea and Caspian Sea. *Central European Journal of Geosciences*, 5, № 4, 548-559.

Surkova G.V., Krylov A.A. (2016). Synoptic Patterns Of Extreme Wind Speed Over The Barents Sea. *Vestnik MGU (Moscow University Bulletin). Series 5.Geography*, 6, 18-24 (in Russian).

Surkova G.V., Krylov A.A. (2017). Changes of hydro-thermal climate resources of the Arctic due to global warming of 21 century. *Arctic and Antarctic*, 1, 47-61. DOI: 10.7256/2453-8922.2017.1.22265. [http://e-notabene.ru/arctic/article\\_22265.html](http://e-notabene.ru/arctic/article_22265.html) (in Russian with English summary).

Surkova G.V., Sokolova L.A., Chichev A.R. (2015). Long-term Regime of Daily Wind Speed Maximum over Barents and Cara Seas. *Vestnik MGU (Moscow University Bulletin). Series 5.Geography*, 5, 54-59 (in Russian with English summary).

Taylor K.E. (2001). Summarizing multiple aspects of model performance in a single diagram. *Journal of Geophysical Research (April, 16)* 106, № D7, 7183-7192.

Taylor K.E., Stouffer R.J., Meehl G.A. (2012). The CMIP5 experiment design, *Bull. Amer. Meteor. Soc.* 93, 485–498.

Volodin E.M., Diansky N.A., Gusev A.V. (2013). Simulation and prediction of climate changes in the 19th to 21st centuries with the Institute of Numerical Mathematics. Russian Academy of Sciences, model of the Earth's climate system, *Izv. Atmos. Ocean. Phys.* 49, 347. <https://doi.org/10.1134/S0001433813040105>.

Wilks D.S. (1995). *Statistical methods in the atmospheric sciences*. Academic Press. 476.

Yarnal B. (1993). *Synoptic climatology in environmental analysis*. Belhaven Press, London, 195.

**Zeinab Hazbavi<sup>1</sup>, Seyed Hamidreza Sadeghi<sup>1\*</sup> and Mehdi Gholamalifard<sup>1</sup>**

<sup>1</sup> Tarbiat Modares University, Tehran, Iran

\* **Corresponding author:** sadeghi@modares.ac.ir

## DYNAMIC ANALYSIS OF SOIL EROSION-BASED WATERSHED HEALTH

**ABSTRACT.** Accelerated soil erosion is one of the most important detrimental factors affecting the quality of the watershed health. Due to different environmental pressures and drivers, the effort is needed for ecological health and resilience assessment in regards to erosion changeability. However, this important subject has not been adequately studied yet. Towards this, in the present research, an innovative approach was developed for conceptualizing the watershed health dynamics in viewpoint of soil erosion. A risk-based study was conducted to quantitatively characterize the spatiotemporal variability of erosion-based health in an industrialized watershed i.e., the Shazand Watershed using the conceptual reliability, resilience and vulnerability ( $R_{el}, R_{es}, V_{ul}$ ) framework for four node years of 1986, 1998, 2008 and 2014. To this end, the soil erosion was estimated at monthly scale in 24 sub-watersheds by applying the Revised Universal Soil Loss Equation (RUSLE). The  $R_{el}, R_{es}, V_{ul}$  indicators were then computed according to the threshold defined for the study watershed. A geometric mean was used to combine the three risk indicators and the erosion-based watershed health index was ultimately calculated for each study sub-watershed. Additionally, the change detection analysis was conducted over the years of 1986 to 2014. According to the results of erosion-based the  $R_{el}, R_{es}, V_{ul}$  indices, very healthy, healthy, moderately healthy, un-healthy and very un-healthy conditions in the Shazand Watershed were respectively distributed over some 67, 25, zero, zero and eight percent for 1986; 50, 13, eight, zero and 29 % for 1998; 71, eight, 83, zero, zero and eight percent for 2008 and finally 71, zero, 17, zero and 12 % for 2014. The results of change detection revealed an oscillating trend of erosion-based watershed health index during the whole study period (1986-2014). So that, during periods of 1986-1998, 1986-2008 and 1986-2014, the watershed health decreased at tune of 23, 13 and six percent, respectively. Whilst, the watershed health improved during study periods of 1998-2008 (13 %), 2008-2014 (eight percent) and 1998-2014 (22 %). The results also identified 'hot spots' of the most important index of land degradation and 'bright spots' of land improvement in the Shazand Watershed. The proposed approach would provide a sustainable framework supporting decision makers to comprehend health-related soil erosion targets according to the integrated watershed management plans.

**KEY WORDS:** Dynamic monitoring, Hydrological responses, Land health, Watershed integrity

**CITATION:** Zeinab Hazbavi, Seyed Hamidreza Sadeghi and Mehdi Gholamalifard (2019) Dynamic Analysis Of Soil Erosion-Based Watershed Health. *Geography, Environment, Sustainability*, Vol.12, No 3, p. 43-59  
DOI-10.24057/2071-9388-2018-58

## INTRODUCTION

The extent of land degradation in Iran has been recognized as a pressing challenge for the country economy. It is reported that the soil and water degradation and fertilizers application annually costs the country around than USD12.8 billion about four percent of the total gross domestic product (GDP) (Emadodin et al. 2012). Degradation of land health is distinguished as a foremost global problem, but remains poorly quantified (Shepherd et al. 2015; Hazbavi and Sadeghi 2017; van Noordwijk 2017; Hazbavi et al. 2018a). Soil erosion as the most important indicator of land degradation affect the quality of watershed ecosystems. Numerous approaches have been developed for soil erosion prediction. The Universal Soil Loss Equation (USLE) and the Revised USLE (RUSLE) models (Wischmeier and Smith, 1965; 1978; López-Vicente et al. 2008; Golosov et al. 2014; Pietroń et al. 2017; Van der Knijff et al. 2017; Chatsrimab et al. 2019) have been widely used to efficiently predict the soil erosion under different conditions because of their low data demanding and wide applicability at different scales. RUSLE as an empirical method based on functionalities of the soil erosion processes has been then established. In the last decades, RUSLE has been adopted to watershed scale in integration with Geographic Information Systems (GIS) (Fayas et al. 2019).

A variety of watershed health and protection treatments have been proposed to reduce long-term risks to watershed from accelerated soil erosion (Golrang et al. 2013; Sadeghi et al. 2014; Sadeghi and Hazbavi 2017a; Sadeghi et al. 2018a). However, after more than 40 years, due to increasing degradation, it looks that these activities were not successful (Golrang et al. 2013; Spalevic et al. 2016). Hence, it is essential to advance and improve land health surveillance approaches to target sustainable land management interventions (Hazbavi, 2018). Towards this objective, the dynamic monitoring of the watershed health can help to detect trends over time, identify emerging problems, direct efforts to stressor impacts mitigation for areas where they are most

needed and ultimately track the response of watersheds to different environmental drivers.

Although different approaches were developed to monitor the conditions of the different ecosystems in regards to different environmental stressors (Sadeghi and Hazbavi 2017a and b; Sadeghi et al. 2017; Hazbavi et al. 2019), a risk-focused watershed health monitoring and assessment, which rests on sustainable watershed management approaches has received much less attention. The reliability ( $R_{el}$ ), resilience ( $R_{es}$ ) and vulnerability ( $V_{ul}$ ) framework is one of the most commonly used approach in water resources management perspectives initially introduced by Hashimoto et al. (1982). The  $R_{el}R_{es}V_{ul}$  indicators can be characterized by means of daily, monthly or annual datasets of different determinant factors. This framework simultaneously measures the pressure, state and response of the watershed against to external stressors (Chanda et al. 2014; Hazbavi et al. 2018b and c; Sadeghi et al. 2019). The proficient watershed management would expect improving  $R_{el}$  and  $R_{es}$  of the watershed whereas decreasing  $V_{ul}$  (Alemaw et al. 2016; Hazbavi et al. 2018a and b; Sadeghi et al., 2019). The risk assessment of watershed in the context of health is a topic of great interest to many researches seeking to promote sustainable practices. In this regards, the reliability ( $R_{el}$ ), resilience ( $R_{es}$ ) and vulnerability ( $V_{ul}$ ) framework ( $R_{el}R_{es}V_{ul}$ ) got more attention due to considering the risk-based indicators to mathematically quantify the potential for an entire watershed to fail, the probability of a failed watershed recovering, and the consequences of a watershed lapsing into a failed status (Ahn and Kim 2017; Hazbavi et al. 2018a).

Thereinto, the  $R_{el}R_{es}V_{ul}$  framework in regards to watershed health has been applied for social, environmental and biodiversity criteria (Sood and Ritter 2011), drought management index (Maity et al. 2013; Chanda et al. 2014), water quality data (Hoque et al. 2012; Hoque et al. 2014a; Hoque et al. 2014b, Hoque et al. 2016), hydrological criteria (Hazbavi and Sadeghi 2017; Sadeghi and Hazbavi 2017b) and standardized

precipitation index (Sadeghi and Hazbavi 2017a). Nevertheless, characterization and quantitative risk assessment of watershed health in viewpoint of soil erosion using the  $R_{el} R_{es} V_{ul}$  framework has not been formulated, yet. So, for the present study, a quantitative risk assessment of watershed health with emphasis on soil erosion as an important representative of land degradation was applied to an urbanized and industrialized watershed located in central Iran. Thereinto, the spatiotemporal of watershed health and its change was analyzed during the period of 1986 to 2014.

Recently, the trend of the hydrological health status of the Shazand Watershed has been assessed as un-healthy from 1977 to 2014 (Hazbavi and Sadeghi 2017; Sadeghi et al. 2019; Hazbavi et al. 2019). However, more comprehensive evaluation of determinant index of watershed health is still lacked. The present study has therefore been formulated for better understanding of land degradation situation in the study watershed in time and space hopefully leading to a correct and cost-effective management in the future.

**MATERIALS AND METHODS**

**Study area**

The study area is located in the Markazi Province, in the central plateau of Iran (Fig. 1). The watershed with a total area of almost 1740 km<sup>2</sup> is composed of nearly 44.85 % alluvial sediments and/or sub-mountain gravels and 50.15 % highlands and hard formations. The climate is moderate semi-arid to cold semi-arid (Bsk) and receives about 420 mm rainfall annually (Mokhtari et al. 2011; Darabi et al. 2014; Davudirad et al. 2016). Since 1973, a rapid industrialization has been taken place in the Shazand Watershed. Consequently, the social and economic development in this area was completely changed (Darabi et al. 2014; Davudirad et al. 2016; Sadeghi et al. 2018).

**Soil erosion estimation**

The present study used the predictive empirical model of the Revised Universal Soil Loss Equation (RUSLE) as the simplest model for erosion prediction of an area (Wischmeier and Smith, 1965; 1978; Renard

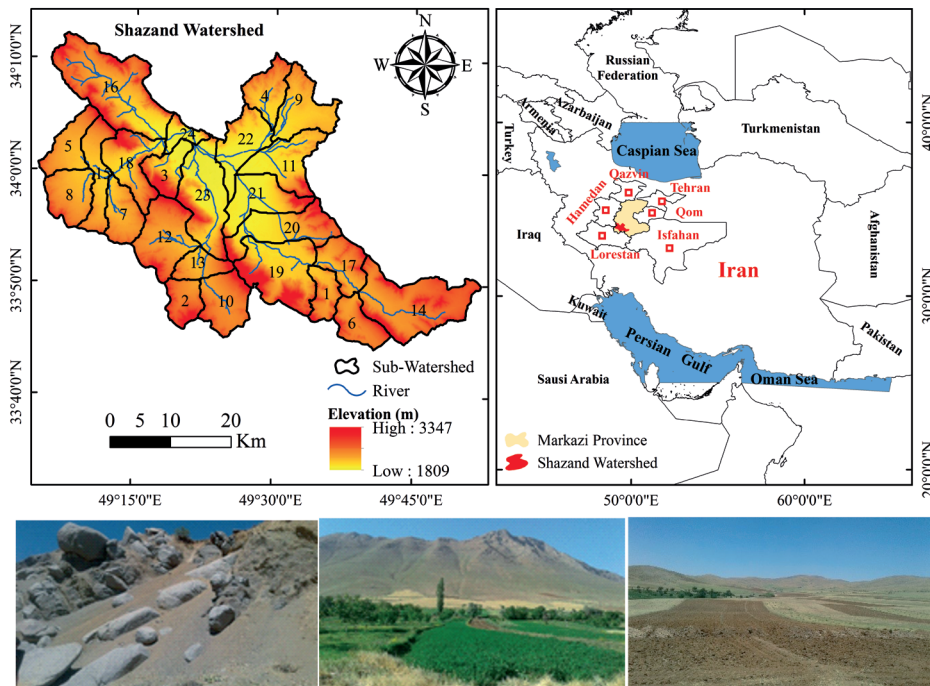


**Fig. 1. Location (Upper) and general governing condition (Bottom) of the Shazand Watershed in Markazi Province, Iran**

et al. 1997). The RUSLE model was applied based on the following equation (Renard et al. 1997).

$$A = R \times K \times L \times S \times C \times P \quad (1)$$

where A is the computed spatial average soil loss over a period selected for R, ( $t \text{ ha}^{-1}$ ); R, K, L, S, C and P are rainfall erosivity [ $(\text{MJ mm}) (\text{ha h})^{-1}$ ], soil erodibility [ $(t \text{ ha h}) (\text{ha MJ mm})^{-1}$ ], slope length, slope steepness, land cover management, and conservation practices factors, respectively. All dimensionless factors were normalized with respect to the unit plot conditions as described in Jain et al. (2001) and Dabral et al. (2008), and has been validated by Ganasri et al. (2016). To determine study factors, the RUSLE was integrated in GIS and Remote Sensing (RS) as successfully reported by many researchers (Millward and Mersey 1999; Prasannakumar et al. 2011; Vijith et al. 2012; Asadi et al. 2017; Mohammadi et al. 2018; Chahrsimab et al. 2019) to improve the accuracy and expedite the estimation. The quantitative output of monthly soil erosion was eventually computed by multiplying the R, K, L, S, C and P factors using the Raster Calculator tool in ArcGIS 10.3.

#### - Rainfall erosivity (r) factor

R factor measures the soil erosion potential caused by rainfall (Wischmeier and Smith 1978; Renard et al. 1997). R factor is often estimated from rainfall intensity if high-resolution of rainfall measurements exist. In the present research, R factor for the Shazand Watershed was estimated on monthly basis according to the calibrated Roose's index developed with reasonable statistical performance (Sadeghi and Tavangar 2015). The primary formula of Roose's model is as follows (Roose 1977).

$$R_{factor} = [0.5 + 0.05P] \quad (2)$$

where R factor and P are rainfall erosivity index [ $(\text{MJ mm}) (\text{ha h})^{-1}$ ] and mean monthly rainfall (mm), respectively.

#### - Soil erodibility (k) factor

The soil susceptibility to erosion could be measured through K factor. The resistance of the soil to particle detachment and soil ability to absorb rainfall affect K factor. For the present study, K factor was computed using data of the

soil types distribution of the study area according to the tables supposed by the USDA (1978).

#### - Topographic (ls) factor

LS factor quantifies the combined impact of slope length (L) and steepness (S) on the soil loss. As the slope length and steepness increase, the progressive runoff accumulation in the downslope direction and runoff velocity and erosivity increase. Thence, the amount of soil loss increases. LS factor was determined using the following approach (Prasannakumar et al. 2011; Vijith et al. 2012) that is verified for Iranian conditions, too (Mohammadi et al. 2018). Flow accumulation denotes the accumulated upslope contributing area for a given cell. The

$$LS = \left( \frac{\text{FlowAccumulation} \times \frac{\text{CellSize}}{22.13}}{\left( \frac{\text{Sin}(\text{Slope}) \times 0.01745}{0.0896} \right)^{1.3}} \right)^{0.4} \quad (3)$$

cell size is the size of the grid cell used for the study and sin (slope) is the sine of the slope angle in degrees. The flow accumulation was obtained with the help of the Digital Elevation Model (DEM) of the study area with a cell size of 30 m. The maps were derived using ArcGIS 10.3 Spatial analyst plus. The following flow-chart (Fig. 2) shows different stages of calculation of LS factor.

#### - Land cover management (c) factor

C factor reflects the protective impact of ground covers against the erosive action of rainfall on reducing soil loss. To estimate C factor, the most widely used index of vegetation of Normalized Difference Vegetation Index (NDVI) was applied according to the following formula (Lin 1997) which is approved for Iranian conditions by Mohammadi et al. (2018).

$$C = \left[ \frac{(-NDVI + 1)}{2} \right] \quad (4)$$

$$NDVI = \frac{(NIR - RED)}{(NIR + RED)} \quad (5)$$

where NDVI is the mean values of Normalized Difference Vegetation Index derived at monthly scale, NIR and RED stand for the spectral reflectance measurements acquired in the near-infrared and visible regions, respectively. All calculation of NDVI were conducted in Terr

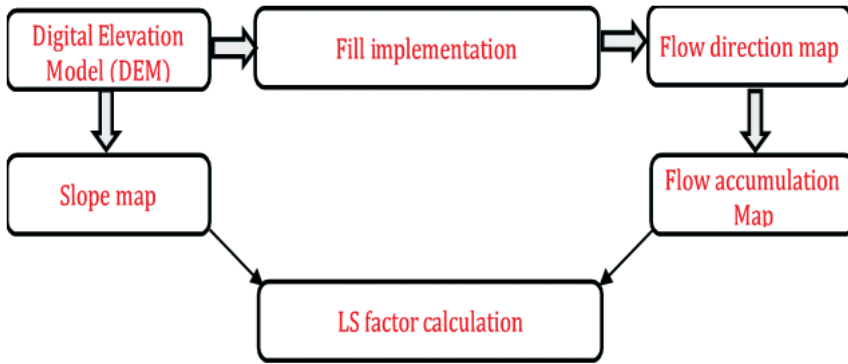


**Fig. 2. Different stages of derivation of topographic (LS) factor (Teh, 2011) for the Shazand Watershed, Iran**

Set 18.21 Software. Forty Landsat TM, ETM+ and OLI images acquired during the years of 1986, 1987, 1998 and 2014 with a spatial resolution of 30 m were used to create NDVI images as detailed in Sadeghi et al. (2019).

**- Conservation practices (p) factor**

P factor is defined as the ratio of soil loss by a conservation practices to that of straight-row farming up and down the slope (Yuan et al. 2016). In the same vein, P factor accounts for the supporting effects of control practices that reduce the erosion potential of runoff. Accordingly, the efficiency of conservation supporting practices depends on slope and land use pattern (Lakkad 2017). Towards this, the P fac-

tor of the Shazand Watershed (Table 1) was determined according to tables proposed by Li et al. (2010), Lu (2011), Yu et al. (2011) and Yuan et al. (2016). Accordingly, the slope map (%) was prepared by DEM and it was merged with land use data using overlay analysis in ArcGIS.

**$R_{el} R_{es} V_{ul}$  framework conceptualization**

A quantitative methodology of reliability, resilience and vulnerability ( $R_{el} R_{es} V_{ul}$ ) initially proposed by Hashimoto et al. (1982) in context of water resources systems was developed for assessing the long term watershed health. The  $R_{el} R_{es} V_{ul}$  framework was conceptualized to an important index of degradation i.e., generated soil erosion in the Shazand Watershed allowing

**Table 1. Used P factor values according to different land use/cover types and slope percentages (Yuan et al. 2016) for the Shazand Watershed, Iran**

Land use/cover	Slope (%)	P factor
Water bodies	0~330	0.00
Irrigated croplands	0~330	0.05
Arable lands	0~5	0.11
	5~10	0.12
	10~20	0.14
	20~30	0.19
	30~50	0.25
	>50	0.33
Forest lands	0~330	0.80
Others	0~330	1.00

conclusions to be drawn for the health analysis of the study watershed.

The  $R_{el}R_{es}V_{ul}$  framework is applicable for different time scales. For the present research, the data were analyzed at monthly scale for soil erosion-based the  $R_{el}R_{es}V_{ul}$  index. The mathematical definitions of reliability, resilience and vulnerability concepts in the  $R_{el}R_{es}V_{ul}$  framework were presented using following formulae. where  $M$  is the number of un-satisfactory

$$Reliability(R_{el}) = 1 - \frac{\sum_{j=1}^M d(j)}{T} \tag{6}$$

$$Resilience(R_{es}) = \left\{ \frac{1}{M} \sum_{j=1}^M d(j) \right\}^{-1} \tag{7}$$

$$Vulnerability(V_{ul}) = \frac{1}{M} \sum_{i=1}^T \left[ \frac{S_{RUSLE}(i) - S_{std}(i)}{S_{std}(i)} \right] H[S_{RUSLE}(i) - S_{std}(i)] \tag{8}$$

events,  $d(j)$  is the duration (the number of months that soil erosion amount exceeds the threshold) of the  $j^{th}$  un-satisfactory event, and  $T$  is the total number of events (here 12). In the context of soil erosion, a satisfactory event was defined beyond a certain threshold of permissible soil erosion for the study watershed as five  $t \text{ ha}^{-1} \text{ y}^{-1}$  (Hosseini and Ghorbani 2005) and the period under consideration.  $S_{RUSLE}(i)$  is the estimated soil erosion at the  $i^{th}$  time step,  $S_{std}(i)$  is the corresponding compliance standard, and  $H[ ]$  is the Heaviside Function, which ensures that only failure events are involved in the vulnerability calculation in Eq. (8). The mathematical and discontinuous Heaviside Function was supposed zero and one for negative and positive arguments, respectively.  $R_{el}$  is controlled by  $d$  and  $T$ . This implies that the duration of failure events was the only factor affecting  $R_{el}$  of watersheds for soil erosion. Whilst,  $R_{es}$  indicator was influenced by  $d$  and  $M$ . Thereafter, interaction of these two factors forms  $R_{es}$  of watersheds against soil erosion process.

The above mentioned concepts were then articulated to describe the performance of the Shazand Watershed against soil erosion long term variations in result of industrial development in the region. The computed  $R_{el}R_{es}V_{ul}$  indicators values were standardized between zero and one (Loucks 1997; Zhao et al. 2006; Wie-

gand et al. 2013; Hazbavi and Sadeghi 2017) using Eqs. (9) and (10) respectively applied for positively and negatively affected indicators of  $R_{el}$  and  $R_{es}$  and  $V_{ul}$ .

$$C_s = \frac{C_i - C_{min}}{C_{max} - C_{min}} \tag{9}$$

$$C_s = \frac{C_{max} - C_i}{C_{max} - C_{min}} \tag{10}$$

where  $C_s$  is the standardized value of each individual indicator;  $C_i$  is the indicators under consideration; and  $C_{min}$  and  $C_{max}$  are the minimum and maximum indicator values respectively.

Then, the soil erosion-based  $R_{el}R_{es}V_{ul}$  index ( $G_A$ ) was then computed using geometric mean by the following formula.

$$G_A = \sqrt[3]{standardizedR_{el} \times standardizedR_{es} \times standardizedV_{ul}} \tag{11}$$

The erosion-based  $R_{el}R_{es}V_{ul}$  index was ranked into five classes of I (0.81-1.00), II (0.61-0.80), III (0.41-0.60), IV (0.21-0.40) and V (0.00-0.20) specified as very healthy, healthy, moderately healthy, un-healthy and very un-healthy watersheds respectively.

**Watershed health change analysis**

Assessments of watershed health change in viewpoint of soil erosion was done through the elementary watershed health index (EWHI) during two time nodes of  $t$  and  $t+1$  of the study period given by Salvati et al. (2014) and Smiraglia et al. (2016) as given below.

$$EWHI_{(t+1)} = \frac{EWHI_{t+1} - EWHI_t}{EWHI_t} \times 100 \tag{12}$$

**RESULTS AND DISCUSSION**

The results of the soil erosion characteristics and  $R_{el}R_{es}V_{ul}$  indicators in the study sub-watersheds and node years have been respectively presented in Tables 2 and 3. The raw data and corresponding calculations of soil erosion for each sub-watershed of the Shazand Watershed have been also presented as supplementary information. The standardized  $R_{el}R_{es}V_{ul}$  indicators for all sub-watersheds and four study years were calculated and the erosion-based  $R_{el}R_{es}V_{ul}$  index was obtained as depicted in Fig. 3. The spatiotemporal maps and the percentage

distribution of different categories of soil erosion-based RelResVul index were also presented in Fig. 4.

The minimum soil erosion-based RelResVul values were 0.50, 0.67 and 12.84 for 1986; 0.58, 0.60 and 11.94 for 1998; 0.58, 0.80 and 0.35 for 2008, and 0.50, 0.67 and 10.71 for 2014. Additionally, the maximum soil erosion-based  $R_{el}R_{es}V_{ul}$  values were obtained 0.67, 1.00 and 1958.47 for 1986; 0.75, 1.00 and 1155.46 for 1998; 0.75, 1.00 and 169.37 for 2008 as well as 0.75, 1.00 and 6985.09 for 2014. The best state of erosion-based  $R_{el}R_{es}V_{ul}$  indicators at all study node years were observed in sub-watershed 9 and the worst situation was obtained for sub-watersheds 7 and 24 (Table 3).

As seen from Table 3, the reliability and resilience indicators are in the good level for most of the study sub-watersheds. It is indicated that the duration of failure of events ( $d$ ) in the Shazand Watershed was short. So that, the maximum duration under failure conditions for the watershed was six months of a year. In addition, these durations were not happening continuously. It was observed that the minimum number of

failure events ( $M$ ) was four. It meant that the six-months failure event was happened in six intervals. This status indicated the high potential of the Shazand Watershed in reliability and resilience. In fact, it can be concluded that the study watershed had a fast reaction to return to a satisfactory state.

The interactions of these indicators resulted in low vulnerability of the Shazand Watershed. According to Fig. 3, the high geometric values of the final index also proved the low vulnerability of the Shazand Watershed to soil erosion process, but the variability of vulnerability was higher than other two study risk indicators, because the vulnerability in addition to “ $M$ ” was influenced by the high variability of soil erosion rates. It is in line with the results obtained for  $SPI-R_{el}R_{es}V_{ul}$  index characterization of the same watershed (Sadeghi and Hazbavi 2017b; Hazbavi et al. 2018a). This finding proved the efficiency of soil erosion from climatic variables. Besides that, the long-term measured sediment concentration of the Shazand Watershed characterized by  $R_{el}R_{es}V_{ul}$  (Hazbavi and Sadeghi 2017) reported the consistent results.

**Table 2. Descriptive statistics of soil erosion for different Shazand Sub-watersheds in the study node years**

Year	Statistical criteria	Soil erosion ( $t\ ha^{-1}\ y^{-1}$ )
1986	Mean	128.25
	Standard deviation	46.17
	Minimum	27.89
	Maximum	219.26
1998	Mean	58.89
	Standard deviation	30.44
	Minimum	17.33
	Maximum	126.04
2008	Mean	28.98
	Standard deviation	12.45
	Minimum	4.98
	Maximum	52.73
2014	Mean	141.65
	Standard deviation	103.94
	Minimum	12.22
	Maximum	360.05

**Table 3. Un-standardized  $R_{el}$ ,  $R_{es}$  and  $V_{ul}$  indicators for the different Shazand Sub-watersheds in the study node years**

Year	1986			1998			2008			2014		
	$R_{el}$	$R_{es}$	$V_{ul}$									
1	0.67	1.00	134.23	0.75	1.00	25.27	0.67	1.00	4.62	0.75	1.00	637.53
2	0.67	1.00	99.92	0.75	1.00	254.85	0.67	1.00	19.65	0.75	1.00	36.12
3	0.67	1.00	68.91	0.75	1.00	57.01	0.75	1.00	3.56	0.75	1.00	188.70
4	0.67	1.00	68.43	0.75	1.00	69.46	0.67	1.00	2.55	0.75	1.00	67.23
5	0.58	1.00	380.73	0.58	0.60	27.93	0.67	1.00	17.45	0.67	1.00	5630.44
6	0.67	1.00	248.62	0.75	1.00	80.67	0.67	1.00	10.36	0.75	1.00	778.74
7	0.50	0.67	1958.47	0.58	0.60	1155.46	0.58	0.80	169.37	0.50	0.67	6985.09
8	0.58	1.00	418.03	0.58	0.60	25.85	0.67	1.00	24.57	0.67	1.00	6036.30
9	0.67	1.00	12.84	0.75	1.00	11.94	0.75	1.00	0.35	0.75	1.00	10.71
10	0.67	1.00	235.61	0.75	1.00	441.41	0.67	1.00	30.08	0.75	1.00	260.81
11	0.67	1.00	30.39	0.75	1.00	82.32	0.67	1.00	0.93	0.75	1.00	24.42
12	0.67	1.00	702.32	0.67	1.00	770.73	0.67	1.00	92.72	0.58	0.80	305.10
13	0.67	1.00	283.40	0.75	1.00	619.02	0.67	1.00	55.62	0.75	1.00	48.75
14	0.67	1.00	73.87	0.75	1.00	28.00	0.67	1.00	2.15	0.75	1.00	128.49
15	0.58	1.00	360.65	0.67	0.75	61.24	0.67	1.00	25.04	0.67	1.00	5407.43
16	0.58	1.00	260.23	0.58	0.60	99.54	0.67	1.00	15.42	0.75	1.00	1923.18
17	0.58	1.00	234.71	0.58	0.60	41.95	0.67	1.00	7.33	0.75	1.00	1077.56
18	0.58	1.00	401.19	0.58	0.60	147.77	0.67	1.00	34.44	0.58	0.60	5980.47
19	0.67	1.00	158.87	0.75	1.00	107.20	0.67	1.00	10.86	0.75	1.00	446.11
20	0.67	1.00	82.43	0.75	1.00	48.26	0.67	1.00	3.15	0.75	1.00	187.50
21	0.67	1.00	19.14	0.75	1.00	71.93	0.67	1.00	0.84	0.75	1.00	16.93
22	0.67	1.00	39.42	0.67	1.00	102.03	0.67	1.00	4.72	0.75	1.00	122.55
23	0.67	1.00	209.66	0.75	1.00	394.42	0.67	1.00	26.87	0.75	1.00	84.76
24	0.50	0.67	988.09	0.58	0.60	931.81	0.58	0.80	79.36	0.50	0.67	2487.68

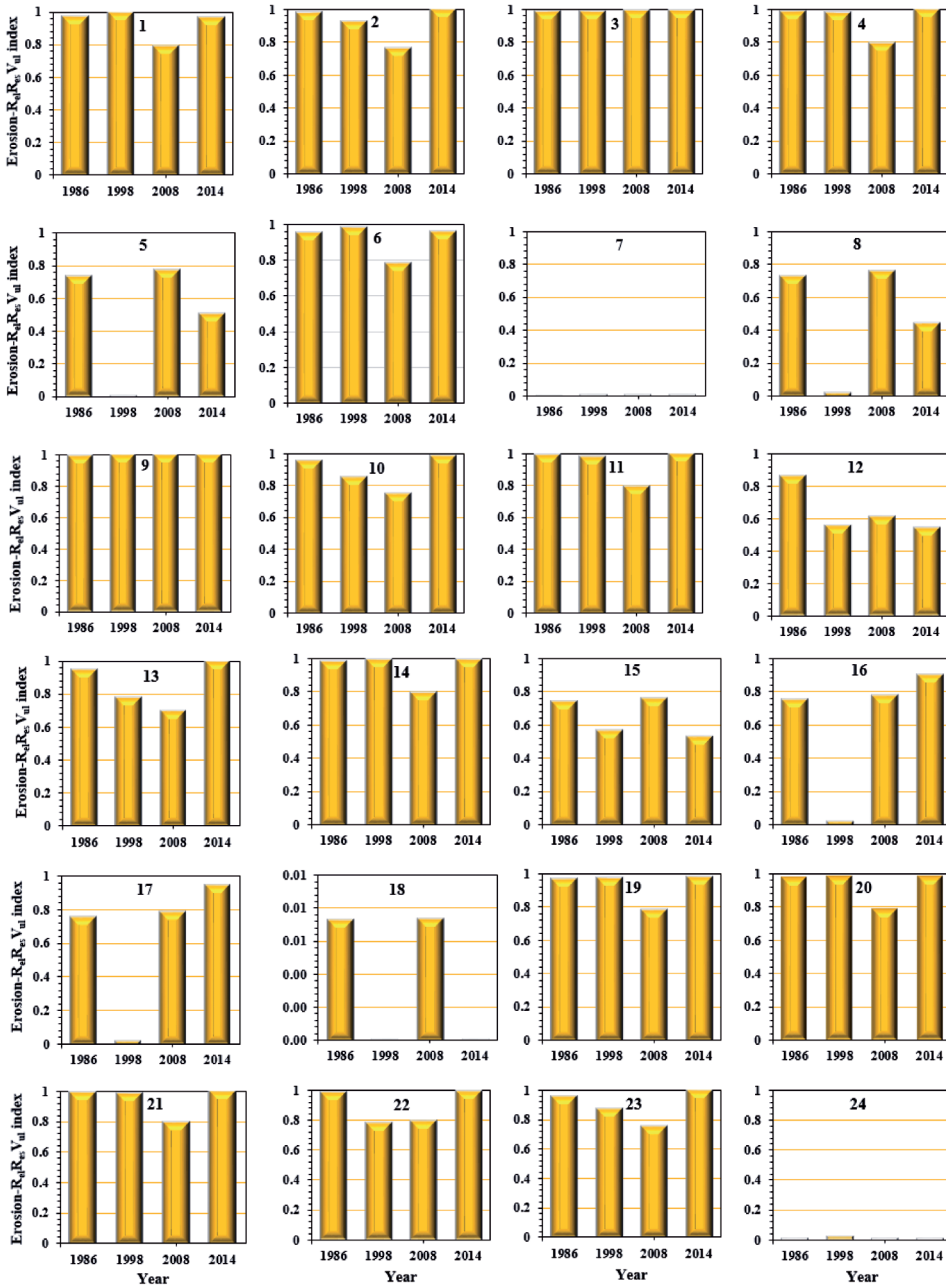


**Fig. 3. Soil erosion-based  $R_{el}R_{es}V_{ul}$  index for the different Shazand sub-watersheds (as numbered) in the study node years**

Analysis of the application of the  $R_{el}R_{es}V_{ul}$  framework also revealed that the distribution of sub-watersheds in viewpoint of soil erosion-based  $R_{el}R_{es}V_{ul}$  index for different status of very healthy (1.00–0.81), healthy (0.80–0.61), moderately healthy (0.60–0.41), and very un-healthy (0.20–0.00) were 67, 25, zero and eight percent for 1986; 50, 13,

eight and 29 % for 1998; eight, 84, zero and eight percent for 2008 and ultimately 71, zero, 17 and 12 % for 2014, respectively, as shown in Fig. 4. No un-healthy (0.40–0.21) condition of soil erosion-based  $RelResVul$  index was found for the Shazand Watershed (Fig. 4). Hereinto, the interchange of  $RelResVul$  have also been summarized in Fig. 5.

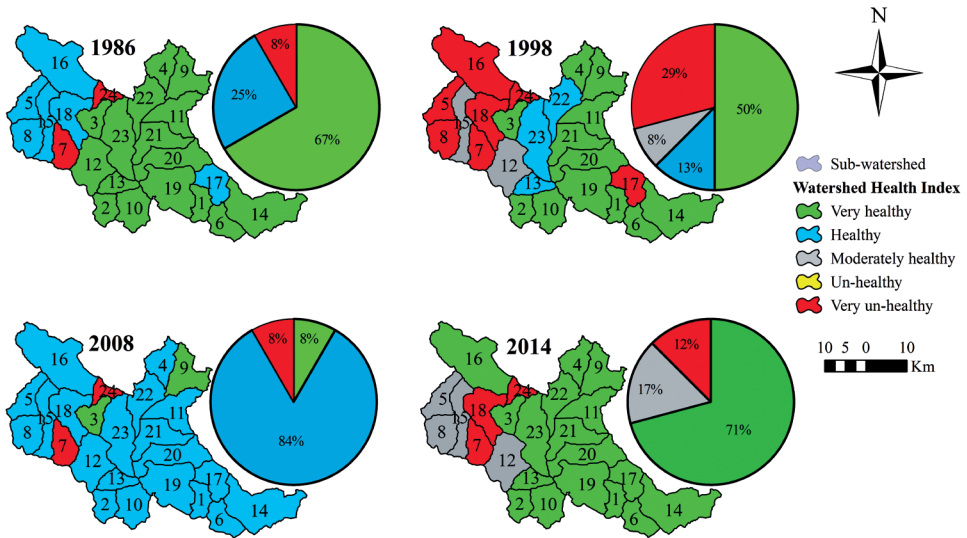


Fig. 4. Spatial distribution of the erosion-based watershed health index for the different Shazand sub-watersheds in the study node years

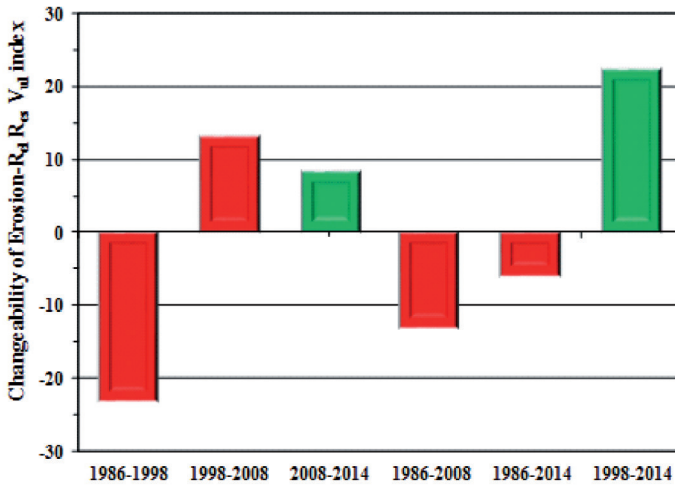


Fig. 5. Change detection of the erosion-based watershed health index in the Shazand Watershed

The sub-watersheds 7 and 24 were found as ‘hot spots’ of land degradation, since they could not recover their ability against soil erosion process in all study node years. This result showed that the soil loss of this sub-watershed was always more than permissible threshold ( $5 \text{ t ha}^{-1} \text{ y}^{-1}$ ). Similar health conditions were verified in the previous researches using other criteria. So that, Hazbavi et al. (2018c) with characterizing the  $R_{el}R_{es}V_{ul}$  framework stated a land cover based watershed health index of 0.36 for sub-watershed 24 indicating an un-healthy state. In addition, the climat-

ic drought state of sub-watershed 24 was quantified less than 0.35 (un-healthy state) according to the  $R_{el}R_{es}V_{ul}$  framework by Sadeghi et al. (2018). Sadeghi et al. (2019) and also reported an un-healthy state during node years of 1986 and 2008 as well as very un-healthy state during 1998 and 2014 for sub-watershed 24 with the help of an integrated watershed health index (IWHI) based on the  $R_{el}R_{es}V_{ul}$  framework. Recently, Hazbavi et al. (2019) also estimated an un-healthy state for this sub-watershed during all study node-years using pressure–state–response (PSR) framework. Ac-

cordingly, they recommended to adapt the immediate managerial measurements to improve and restore the health condition of sub-watersheds located in the north and northeast including the sub-watershed 24. The sub-watershed 18 was also under stress more than other sub-watersheds due to un-stable state during the study period (1986 to 2014). This sub-watershed with land cover based watershed health index of 0.31 for 2014 (Hazbavi et al. 2018c), flow discharge based watershed health index less than 0.40 (Sadeghi and Hazbavi 2017a), climatic drought based watershed health index less than 0.32 (Sadeghi et al. 2018) and IWHI less than 0.40 (Sadeghi et al. 2019) was classified in un-healthy and very un-healthy states. In this context, it is essential to plan the land management strategies and enhance the riparian vegetation.

The sub-watersheds 5, 8, 16 and 17 were in the relatively bad status but they were finally classified in a better status rather than at the end of the study period. These results were in line with Sadeghi et al. (2018) findings who noted that the mentioned sub-watersheds were classified in the fragile and critical classes of Environmental Sensitive Area Index (ESAI) computed for the whole Shazand Watershed. Whilst, Sadeghi et al. (2019) reported a relatively constant state for the mentioned sub-watersheds which could be associated with influence of combination of soil erosion criterion with other criteria of standardized precipitation index, NDVI, and low and high flow discharges in integrated watershed health assessment.

According to the results (Table 3; Fig. 4), sub-watersheds 1, 2, 3, 4, 6, 9, 10, 11, 12, 13, 14, 19, 20, 21, 22 and 23 almost had healthy and very healthy state in terms of the soil erosion-based  $R_{el}R_{es}V_{ul}$  index during study node years. This result reflected a high potential of the stated sub-watersheds in viewpoint of  $R_{el}$  and  $R_{es}$  indicators and their low  $V_{ul}$  to soil erosion. The high soil erosion-based  $R_{el}R_{es}V_{ul}$  index value meant that the sub-watersheds are not prone to soil erosion. However, the state of these sub-watersheds in viewpoint of land cov-

er (Hazbavi et al. 2018c), climatic drought (Sadeghi and Hazbavi 2017b), hydrology (Sadeghi and Hazbavi, 2017a) and integrated watershed health assessment was classified as moderately healthy (0.41-0.60) or un-healthy (0.21-0.40). In overall, Sadeghi et al. (2019) with considering interactive impacts of climatic, hydrologic and anthropogenic activities on watershed health verified a better state of the above mentioned sub-watersheds.

Results of change detection (Fig. 5) revealed that during the study period (1986 -2014), the Shazand Watershed has experienced different condition changes. So that, the rates of changes were not uniform over the study period. The decreasing health trend was found during 1986-1998 (-23 %), 1986-2008 (-13 %) and 1986-2014 (-6%), whilst, the increasing health trend was obtained for periods of 1998-2008 (13 %), 2008-2014 (8%) and 1998-2014 (22 %). As seen in Fig. 5, unpleasant changes in the Shazand Watershed health happened during the periods of 1986-1998, 1986-2008 and 1986-2014. In this regard, Sadeghi et al. (2018) reported an increasing trend in the process of land degradation in the study region. According to their finding, 17, 33, 42, 42 and 50 % of the study area in five year nodes of 1986, 1998, 2008 and 2014, respectively, were in critical condition of land degradation in viewpoint of ESAI. The main factor of land degradation in the Shazand Watershed is vegetation land use change resulted from anthropogenic and managerial factors (Sadeghi et al. 2018). Sadeghi et al. (2019) who assessed the integrated health of the Shazand Watershed noted a deteriorating trend for 1986–1998 and 1986–2008 periods owing to industrialization and urban development.

## CONCLUSION

A novel soil erosion risk assessment-based  $R_{el}R_{es}V_{ul}$  framework was successfully applied in the industrialized and urbanized Shazand Watershed, Central Iran, to map watershed health and to detect changes during node years of 1986, 1998, 2008 and 2014. According to the results, the sub-watersheds 7, 18 and 24 were found

un-healthy in viewpoint of erosion. The emergency managerial strategy is therefore needed to be adopted. However, for major part of other sub-watersheds, the reliability, resilience and vulnerability were in the healthy or moderately healthy status. During the time, the sub-watersheds status was in change. Based on the results, the erosion-based watershed health index in periods of 1986-1998, 1986-2008 and 1986-2014 had decreasing trend of 23, 13 and 6%. The applied technique and conceptualized strategy would provide a sustainable

framework supporting decision making to realize health-related soil and water conservation targets and plans towards the 17 United Nations Sustainable Development Goals (SDGs) from 2015 to 2030. Of course, more research and monitoring programs are required for better understanding of the scale and immediacy of the threatening drivers of soil erosion such as human interventions and climate change to watershed health and to act within a much larger and more comprehensive framework. ■

## REFERENCES

- Ahn S.R., and Kim S.J. (2017). Assessment of watershed health, vulnerability and resilience for determining protection and restoration Priorities. *Environmental Modelling and Software*, 2017, pp. 1-19. <http://doi.org/10.1016/j.envsoft.2017.03.014>.
- Alemaw B.F., Keaitse E.O., and Chaoka T.R. (2016). Management of water supply reservoirs under uncertainties in arid and urbanized environments. *Journal of Water Resource and Protection*, 08(11), pp. 990-1009. <http://doi.org/10.4236/jwarp.2016.811080>.
- Asadi H., Honarmand M., Vazifedoust M., and Mousavi A. (2017). Assessment of changes in soil erosion risk using RUSLE in Navrood Watershed, Iran. *Journal of Agricultural Science and Technology*, 19, pp. 231-244. [http://jast-old.modares.ac.ir/article\\_15958.html](http://jast-old.modares.ac.ir/article_15958.html).
- Chanda K., Maity R., Sharma A., and Mehrotra R. (2014). Spatiotemporal variation of long-term drought propensity through reliability-resilience-vulnerability based Drought Management Index. *Water Resources Research*, 50(10), 7662-7676. <http://doi.org/10.1002/2014WR015703>.
- Chatsimab Z., Ghavimi Panah M.H., Vafaeinejad A.R., Hazbavi Z., and Boloori S. (2019). Prioritizing of the sub-watersheds using the soil loss cost approach (A case study; Selj-Anbar Watershed, Iran). *ECOPERISA*, Accepted for publication.
- Dabral P.P., Baithuri N., and Pandey A. (2008). Soil erosion assessment in a hilly catchment of North Eastern India using USLE, GIS and remote sensing. *Water Resources Management*, 22(12), pp. 1783-1798. <https://doi.org/10.1007/s11269-008-9253-9>.
- Darabi H., Shahedi K., Solaimani K., and Miryaghoubzadeh M. (2014). Prioritization of subwatersheds based on flooding conditions using hydrological model, multivariate analysis and remote sensing technique. *Water Environmental Journal*, 28, pp. 382-392. <https://doi.org/10.1111/wej.12047>.
- Davudirad A.A., Sadeghi S.H.R., and Sadoddin A. (2016). The impact of development plans on hydrological changes in the Shazand Watershed, Iran. *Land Degradation and Development*, 27, pp. 1236-1244. <https://doi.org/10.1002/ldr.2523>.
- Emadodin I., Narita D., and Rudolf Bork H. (2012). Soil degradation and agricultural sustainability: an overview from Iran. *Environment, Development and Sustainability*, 14(5), pp. 611-625. <http://doi.org/10.1007/s10668-012-9351-y>.

Fayas S.M., Abeysingha N.S., Nirmanee G.K.S., Samaratunga D., and Mallawatantri A. (2019). Soil loss estimation using RUSLE model to prioritize erosion control in KELANI river basin in Sri Lanka. *International Soil and Water Conservation Research*, 7(2), pp. 130–137. <http://doi.org/10.1016/j.iswcr.2019.01.003>.

Ganasri B.P., and Ramesh H. (2015). Assessment of soil erosion by RUSLE model using remote sensing and GIS - A case study of Nethravathi Basin. *Geoscience Frontiers*, 7(6), pp. 1-9. <http://doi.org/10.1016/j.gsf.2015.10.007>.

Golosov V.N., Zhang X., Qiang T., Zhou P., and He X. (2014) Quantitative assessment of sediment redistribution in the Sichuan Hilly Basin and the central Russian Upland during the past 60 years. *Geography, Environment, Sustainability*, 2014, 7(3), pp. 39-64. <https://doi.org/10.24057/2071-9388-2014-7-3-35-39>.

Golrang B.M., Lai F.S., Rostami M., Kamurudin M.N., Abd Kudus K., Sadeghi S.H.R., and Mashayekhi M. (2013). The relationship between level of watershed project successful and level of people participation. *World of Sciences Journal*, 3, pp. 1-9.

Hashimoto T., Loucks D. P., and Stedinger J. (1982). Reliability, resilience and vulnerability criteria for water resource system performance evaluation. *Water Resources Research*, 18(1), pp. 14-20. <https://doi.org/10.1029/WR018i001p00014>.

Hazbavi Z. (2018). Importance of geology and geomorphology. *Agriculture & Forestry*, 64(4), pp. 277–287. <http://doi.org/10.17707/AgricultForest.64.4.27>.

Hazbavi Z., Jantiene B., Nunes J.P., Keesstra S.D., and Sadeghi S.H.R. (2018a). Changeability of reliability, resilience and vulnerability indicators with respect to drought patterns. *Ecological Indicators*, 87, pp. 196-208.

Hazbavi Z., Keesstra S.D., Nunes J.P., Jantiene B., Gholamalifard M., and Sadeghi S.H.R. (2018b). Health comparative comprehensive assessment of watersheds with different climates. *Ecological Indicators*, 93, pp. 781–790. <http://doi.org/10.1016/j.ecolind.2018.05.078>.

Hazbavi Z., and Sadeghi S.H.R. (2017). Watershed health characterization using reliability-resilience-vulnerability conceptual framework based on hydrological responses. *Land Degradation and Development*, 28, pp. 1528–1537. <http://doi.org/10.1002/ldr.2680>.

Hazbavi Z., Sadeghi S.H.R., and Gholamalifard M. (2018c). Land cover based watershed health assessment. *AGROFOR International Journal*, 3(3), pp. 47–55. 10.7251/AGRENG1803047H.

Hazbavi Z., Sadeghi S.H.R., Gholamalifard M., Davudirad A.A. (2019). Watershed health assessment using pressure–state–response (PSR) framework. *Land Degradation and Development*, <https://doi.org/10.1002/ldr.3420>.

Hoque Y.M., Hantush M.M., and Govindaraju R.S. (2014a). On the scaling behavior of reliability-resilience-vulnerability indices in agricultural watersheds. *Ecological Indicators*, 40, pp. 136-146. <https://doi.org/10.1016/j.ecolind.2014.01.017>.

Hoque Y.M., Raj C., Hantush M.M., Chaubey I., and Govindaraju R.S. (2014b). How do land-use and climate change affect watershed health? a scenario-based analysis. *Water Quality, Exposure and Health*. 6, pp. 19-33. <http://doi.org/10.1007/s12403-013-0102-6>.

Hoque Y.M., Tripathi S., Hantush M.M., and Govindaraju R. S. (2012). Watershed reliability, resilience and vulnerability analysis under uncertainty using water quality data. *Journal of Environmental Management*, 109, pp. 101–112. <http://doi.org/10.1016/j.jenvman.2012.05.010>.

Hoque Y.M., Tripathi S., Hantush M.M., and Govindaraju R. S. (2016). Aggregate Measures of Watershed Health from Reconstructed Water Quality Data with Uncertainty. *Journal of Environment Quality*, 45(2), 709. <http://doi.org/10.2134/jeq2015.10.0508>.

Hosseini S., and Ghorbani M. (2005). Economics of soil erosion. Ferdowsi University of Mashhad Press. 128 p (in Persian).

Jain S.K., Kumar S., and Varghese J. (2001). Estimation of soil erosion for a Himalayan Watershed using GIS technique. *Water Resources Management*, 15(1), pp. 41-54. <https://doi.org/10.1023/A:1012246029263>.

Lakkad A.P., Nayak, D., Patel, G., and Shrivastava, P.K. (2017). Micro-watersheds prioritization for effective soil conservation planning of sub-watershed. *Research in Environment and Life Sciences*, 10(3), pp. 275-279.

Li H., Chen X., Lim K.J., Cai X., and Sagong M. (2010). Assessment of soil erosion and sediment yield in Liao Watershed, Jiangxi Province, China, using USLE, GIS and RS. *Journal of Earth Science*, 21, 941-953. <https://doi.org/10.1007/s12583-010-0147-4>.

Lin C.Y. (1997). A study on the width and placement of vegetated buffer strips in a mudstone-distributed watershed. *Journal of Chinese Soil and Water Conservation*, 29(3), pp. 250-266 (in Chinese with English abstract).

López-Vicente M., Navas A., and Machín J. (2007). Identifying erosive periods by using RUSLE factors in mountain fields of the Central Spanish Pyrenees. *Hydrology Earth System Sciences Discussion*, 4(4), pp. 2111–2142. <http://dx.doi.org/10.5194/hessd-4-2111-2007>.

Loucks O.L. (1997). Emergence of research on agro-ecosystems. *Annual Review of Ecology and Systematics*, 8, 1730192. <https://doi.org/10.1146/annurev.es.08.110177.001133>.

Lu J. (2011). Soil erosion changes based on GIS/RS and USLE in Poyang Lake Basin. *Transactions of CSAE*, 27, pp. 337-345. <https://doi.org/10.3969/j.issn.1002-6819.2011.02.057>.

Maity R., Sharma A., Kumar D.N., Asce M., and Chanda K. (2013). Characterizing drought using the reliability-resilience-vulnerability concept. *Journal of Hydrologic Engineering*, pp. 859-869. [http://doi.org/10.1061/\(ASCE\)HE.1943-5584.0000639](http://doi.org/10.1061/(ASCE)HE.1943-5584.0000639).

Millward A.A., and Mersey J.E. (1999) Adapting the RUSLE to model soil erosion potential in a mountainous tropical watershed. *Catena*, 38, pp. 109-129. [https://doi.org/10.1016/S0341-8162\(99\)00067-3](https://doi.org/10.1016/S0341-8162(99)00067-3).

Mohammadi S., Karimzadeh H., and Alizadeh M. (2018). Spatial estimation of soil erosion in Iran using RUSLE model. *EcoHydrology*, 5(2), pp. 551-569 (in Persian).

Mokhtari Sh., Babazadeh H., Sedghi H., and Kaveh F. (2011). Long term simulation of Shazand Plain Aquifer under changing resources and applications. *International Journal of Research in Agricultural Sciences and Research*, 2, pp. 1-10. [http://ijasr.srbiau.ac.ir/article\\_5533.html](http://ijasr.srbiau.ac.ir/article_5533.html).

Prasannakumar V., Vijith H., Abinod S., and Geetha N. (2012). Estimation of soil erosion risk within a small mountainous sub-watershed in Kerala, India, using Revised Universal Soil Loss Equation (RUSLE) and geo-information technology. *Geoscience Frontiers*, 3(2), pp. 209-215. <http://doi.org/10.1016/j.gsf.2011.11.003>.

Renard K., Foster G., Weesies G., McCool D., and Yoder D. (1997). Predicting soil erosion by water: a guide to conservation planning with the Revised Universal Soil Loss Equation (RUSLE). US Government Printing Office, Washington, DC. Handbook No. 703, 404 p.

Roose E. (1977) Erosion et ruissellement en Afrique de l'ouest-vingt années de mesures en petites parcelles expérimentales. Pour faire face à ce problème préoccupant, l'ORSTOM et les Instituts Travaux et Documents de l'ORSTOM No. 78, 108 p.

Pietroń J., Chalov S., Chalova A., Alekseenko A., and Jarsjö J. (2017). Extreme spatial variability in riverine sediment load inputs due to soil loss in surface mining areas of the Lake Baikal basin. *Catena*, 152, pp. 82–93. <http://dx.doi.org/10.1016/j.catena.2017.01.008>.

Sadeghi S.H.R., and Hazbavi Z. (2017a). Necessity of watershed health assessment in integrated soil and water resources management. In: Proceedings of 2nd IAHS Panta Rhei International Conference on Water System Knowledge Innovation and Its Practices in Developing Countries, Iran, Gorgan, November 20-22, 2017, pp. 22-23.

Sadeghi S.H.R., and Hazbavi Z. (2017b). Spatiotemporal variation of watershed health propensity through reliability-resilience-vulnerability based drought index (case study: Shazand Watershed in Iran). *Science of The Total Environment*. <http://doi.org/10.1016/j.scitotenv.2017.02.098>.

Sadeghi S.H.R., Davudirad A.A., Sadoddin A., and Paimozd Sh. (2018). Trend of Changes in Land Degradation Index in Shazand Watershed-Markazi Province. *Watershed Engineering and Management*, 9(4), pp. 383-397. <http://doi.org/10.22092/IJWMSE.2017.113459>.

Sadeghi S.H.R., Hazbavi Z., and Cerdà A. (2017). Watershed health assessment to monitor land degradation. *Geophysical Research Abstracts*, EGU General Assembly 2017, Vol. 19, EGU2017-28. <http://adsabs.harvard.edu/abs/2017EGUGA..19...28H>.

Sadeghi S.H.R., Hazbavi Z., and Gholamalifard M. (2019). Interactive impacts of climatic, hydrologic and anthropogenic activities on watershed health. *Science of the Total Environment*, 648, pp. 880-893. <http://doi.org/10.1016/j.scitotenv.2018.08.004>.

Sadeghi S.H.R., Hazbavi Z., and Younesi H. (2014). Sustainable watershed management through applying appropriate level of soil amendments. In *Sustainable Watershed Management - Proceedings of the 2nd International Conference on Sustainable Watershed Management*, SUWAMA 2014.

Sadeghi S.H.R., and Tavangar S. (2015). Development of stational models for estimation of rainfall erosivity factor in different timescales. *Natural Hazards*, 77(1), 429–443. <http://doi.org/10.1007/s11069-015-1608-y>.

Salvati L., Smiraglia D., Bajocco S., Ceccarelli T., Zitti M., and Perini L. (2014). Map of Long-Term Changes in Land Sensitivity to Degradation of Italy. *Journal of Maps*, 10(1), pp. 65-72. <http://doi.org/10.1080/17445647.2013.842506>.

Shepherd K.D., Shepherd G., and Walsh M.G. (2015). Land health surveillance and response: A framework for evidence-informed land management. *Agricultural Systems*, 132, pp. 93-106. <http://doi.org/10.1016/j.agry.2014.09.002>.

Smiraglia D., Ceccarelli T., Bajocco S., Salvati L., and Perini L. (2016). Linking trajectories of land change, land degradation processes and ecosystem services. *Environmental Research*, 147, pp. 590-600. <http://doi.org/10.1016/j.envres.2015.11.030>.

Sood A., and Ritter W.F. (2011). Developing a framework to measure watershed sustainability by using hydrological/water quality model. *Journal of Water Resource and Protection*, 3(11), pp. 788-804. <http://doi.org/10.4236/jwarp.2011.311089>.

Spalevic V., Al-Turki A.M., Barovic G., Silva M.L.N., Djurovic N., Souza W.S., Batista P.V.G., and Curovic M. (2016): Modeling of soil erosion by IntErO model: The case study of the Novsicki Potok Watershed of the Prokletije high mountains of Montenegro. *Geophysical Research Abstracts*. Vol. 18, EGU2016-13864, 2016. EGU General Assembly 2016.

Teh S.H. (2011). Soil erosion modeling using RUSLE and GIS on Cameron Highlands, Malaysia for hydropower development. A 30 ECTS Credit Units MSc Thesis. The School for Renewable Energy Science in affiliation with University of Iceland and University of Akureyri, 71 p.

USDA (1978). Predicting rainfall erosion losses. A Guide to Conservation Planning, Washington DC. *Agricultural Handbook* 537.

Van der Knijff, J.M., Jones, R.J.A., Montanarella, L., 2000. Soil Erosion Risk Assessment in Europe. European Commission Directorate General. Joint Research Centre (JCR), Space Applications Institute, European Soil Bureau.

van Noordwijk M. (2017). Integrated natural resource management as pathway to poverty reduction: Innovating practices, institutions and policies. *Agricultural Systems*, (October), 1-12. <http://doi.org/10.1016/j.agry.2017.10.008>.

Vijith H., Suma M., Rekha V.B., Shiju C., and Rejith P.G. (2012). An assessment of soil erosion probability and erosion rate in a tropical mountainous watershed using remote sensing and GIS. *Arabian Journal of Geosciences*, 5(4), pp. 797-805. <http://doi.org/10.1007/s12517-010-0265-4>.

Wiegand A.N., Walker C., Duncan P.F., Roiko A., and Tindale N. (2013). A systematic approach for modelling quantitative lake ecosystem data to facilitate proactive urban lake management. *Environmental Systems Research*, 2, 12. <https://doi.org/10.1186/2193-2697-2-3>.

Wischmeier W.H., and Smith D.D. (1965). Predicting rainfall-erosion losses from cropland east of the Rocky Mountains: Guide for selection of practices for soil and water conservation. Agricultural Research Service, US Department of Agriculture in cooperation with Purdue Agricultural Experiment Station. 1965.

Wischmeier W.H., and Smith D.D. (1978). Predicting rainfall erosion. Losses: a guide to conservation planning. *Agriculture Handbook*, US Department of Agriculture, Washington, DC. 537, 58 p.

Yu J.X., Zheng B.F., Liu Y.F., and Liu C.L. (2011). Evaluation of soil loss and transportation load of adsorption N and P in Poyang Lake watershed. *Acta Ecologica Sinica*, 14, pp. 3980-3989.

Yuan L.F., Yang G.S., Zhang Q.F., and Li H.P. (2016). Soil erosion assessment of the Poyang Lake Basin, China: using USLE, GIS and remote sensing. *Journal of Remote Sensing and GIS*, 5(3). <http://doi.org/10.4172/2469-4134.1000168>.

Zhao Y.Z., Zou X.Y., Cheng H., Jia H.K., Wu Q., Wang G.Y., Zhang C.L., and Gao S.Y. (2006). Assessing the ecological security of the Tibetan plateau: Methodology and a case study for Lhaze County. *Journal of Environmental Management*, 80, pp. 120-131. <https://doi.org/10.1016/j.jenvman.2005.08.019>.

Received on November 3<sup>rd</sup>, 2018

Accepted on August 8<sup>th</sup>, 2019

**Daniel Karthe<sup>1\*</sup>, Sergey Chalov<sup>2</sup>, Alexander Gradel<sup>3</sup>, Antonín Kusbach<sup>4</sup>**

<sup>1</sup> German-Mongolian Institute for Resources and Technology (GMIT), 2nd Khoroo, Nalaikh District, Ulaanbaatar, Mongolia

<sup>2</sup> Moscow State University, Moscow, Russia

<sup>3</sup> International Forestry Consultancy Gradel, Bad Oeynhausen, Germany

<sup>4</sup> Mendel University in Brno (MENDELU), Faculty of Forestry and Wood Technology, Brno, Czech Republic

\* **Corresponding author:** karthe@gmit.edu.mn

## SPECIAL ISSUE «ENVIRONMENTAL CHANGE ON THE MONGOLIAN PLATEAU: ATMOSPHERE, FORESTS, SOILS AND WATER»

The Mongolian Plateau forms a part of the Central Asian Plateau and covers an area of approximately 3,200,000 square kilometers in Mongolia and adjacent areas in China and Southern Siberia. It contains one of the world's largest grassland areas, with the Gobi desert in the south and a transition via steppe and forest steppe to the taiga and mountain tundra in the North (Dulamsuren et al. 2005; Miao et al. 2015). Due to its location, the Plateau's climate is continental and semi-arid to arid, characterized by low precipitation (about 250 mm on average), high potential evapotranspiration (almost 1000 mm on average), large temperature amplitudes, long and harsh winters and recurrent droughts (Dorjgotov 2009; Liu et al. 2019). The Mongolian Plateau mostly drains into the Arctic Ocean basin, including the system of the Selenga River and Lake Baikal, which is not only the world's largest freshwater lake but also a natural heritage of global importance (Kasimov et al. 2017). Hydrologically, parts of the plateau also belong to the Pacific Ocean and Central Asian internal drainage basins.

Despite being one of the most sparsely populated regions in the world, the Mongolian Plateau has recently started to experience massive socioeconomic and environmental changes (Allington et al. 2017; Fan et al. 2016). Over the past few decades, the region has been warming significantly above the global average rate (Karthe et al. 2017; Törnqvist et al. 2014). Hydrological effects include decreasing runoff trends and desiccation of some streams (Frolova et al. 2017; Moreido and Kalugin 2017) and the shrinkage of lakes across the entire plateau (Tao et al. 2015; Zhou et al. 2019). Land cover changes in the region are related to both climate change (Karthe et al. 2017; Miao et al. 2015) as well as anthropogenic impacts related to urbanization (Allington et al. 2017; Fan et al. 2016), livestock herding (Allington et al. 2017, Sternberg 2012), mining (Batbayar et al. 2019; Jarsjö et al. 2017) and logging (Batkhoo et al. 2011; Tsogtbaatar 2004). In vast parts of the Mongolian Plateau, forest degradation and losses (Gradel et al. 2017; Juříčka et al. 2019a) as well as desertification of grasslands (Khodolmor et al. 2013; Wei et al. 2019) have modified a natural land cover. The key drivers of these processes are mining, agriculture / urbanization and deforestation, which are at the same time major water users and polluters (Batbayar et al. 2019; Jarsjö et al. 2017; Karthe et al. 2017). The above mentioned processes have also had strong effects on the soils, which are affected by anthropogenic impacts

in three major ways: nutrient depletion due to intensive agriculture (Hofmann et al. 2016); soil erosion due to land use change, mining and increasing livestock densities (Sasaki et al. 2018; Sternberg 2012; Wei et al. 2019); and soil pollution (mostly with heavy metals) due to mining, industry and coal combustion in urban areas (Jarsjö et al. 2017; Kosheleva et al. 2019).

The present special issue ENVIRONMENTAL CHANGE ON THE MONGOLIAN PLATEAU: ATMOSPHERE, FORESTS, SOILS AND WATER presents a collection of papers based on two scientific conferences that took place in Ulaanbaatar, Mongolia in August and September 2018. The *International Symposium on Environmental Science and Engineering*, which was held at the German-Mongolian Institute of Resources and Technology, also comprised the *Bringing Together Selenga-Baikal Research Conference*, which continued a tradition of collaborative research and scientific exchange on this unique eco-region. The capacity development workshop *Forestry genetic resources, management and adaption to climate changes*, which took place in Ulaanbaatar and a field station in Domogt Sharyn Gol just a few days later, concluded the most recent Czech-Mongolian forestry project (2015-2018) on introducing advanced forest management and science.

The papers presented in this thematic issue are grouped into three main sections that deal with changes in the atmosphere, forests, soils and water resources respectively.

**Atmospheric change.** Climatic changes and atmospheric pollution are among the main drivers of environmental change on the Mongolian Plateau. In this issue, the paper by *Antokhina et al* analysed the severe droughts observed during the past 20 years. The authors indentified linkages to increased frequency of anticyclogenesis which are related to changing dynamics of long Rossby waves and atmospheric blocking in the middle and upper troposphere. The authors argue that the heavy rain and flooding observed in July 2018 would mark a new period in hydroclimatological development after prolonged drought during the last two decades in Mongolia and Transbaikalia which has a significant impact on the regional environment. The paper by *Aschmann* addresses the relevance of logistics of the transportation sector for air pollution control in Ulaanbaatar. The author proposes a two step approach towards attaining sustainable mobility in Ulaanbaatar, differentiating between short-term and medium- to long-term solutions.

**Forest ecosystems under change.** Forest losses due to fires, timber harvesting, insect outbreaks and conversion of forests into mining or pasture land are the key challenges for forest management in Mongolia. An overview of Mongolia's first national forest inventory by *Altrell* provides baseline information on the current state of forests in Mongolia. A review on forest-related challenges in Mongolia and current perspectives for management is presented by *Gradel et al.* For the Khaan Khentii massif in northern Mongolia, *Kusbach et al.* present a macro-scale ecological zonation of forests. Potentials for larch timber harvesting in Mongolia was assessed by *Usoltsev et al.* who compared single-tree biomass data with other ecoregions in Eurasia. Impacts of the invasive four-eyed fir bark beetle on Siberian fir forests were analyzed by *Debkov et al.* The authors found large and healthy tree individuals to be relatively resistant to this threat, whereas smaller and less healthy individuals were more susceptible to beetle attacks. *Juříčka et al.* (2019b) investigated the suppression of natural forest regeneration due to the livestock grazing and identified nearby mining as one of the explanatory factors.

**Soil and water resources under change.** Pollution of air and soils (Kasimov et al. 2011) are further linked with river systems which is discussed in the following section of the special issue. For the cities of Zakamensk (Russia) and Ulaanbaatar (Mongolia), the papers by *Garmaev et al.* and *Shabanova et al.* assessed soil pollution and erosion problems. *Shinkareva et al.* assessed the effects of water pollution on macrophytes in the Selenga river delta which is the biogeochemical barrier of Lake Baikal. Authors argue that the role of delta as natural filters on the path of flows of substances of natural and anthropogenic origin within the Selenga catchment is driven mostly by biogeochemical or hydrodynamic processes and sufficient to protect Lake Baikal.

## ACKNOWLEDGEMENTS

This special issue contains selected papers from the *Symposium on Environmental Science and Engineering* organized by the German-Mongolian Institute for Resources and Technology (GMIT) and the FAO workshop *Forestry genetic resources, management and adaption to climate changes*. The organizers of this thematic issue would like to thank the sponsors of the conferences for the funding, which was provided by the German Ministry for Economic Cooperation and Development (BMZ) via Gesellschaft für Internationale Zusammenarbeit (GIZ), and the Czech *Development Agency in the framework of the project Development of Forests and the Gene Pool of Local Forest Tree Ecotypes in Mongolia 2015-18* (Grant no. CzDA-RO-MN-2014-6-31210), respectively. The special issue was supported by the Russian Foundation for Basic Research (project 17-29-05027)

DOI-10.24057/2071-9388-2019-1411 ■

## REFERENCES

- Allington G., Li W. and Brown D. (2017). Urbanization and environmental policy effects on the future availability of grazing resources on the Mongolian Plateau: Modeling socio-environmental system dynamics. *Environmental Science & Policy*, Vol. 68, pp. 35-46. doi: 10.1016/j.envsci.2016.11.005
- Altrell D. (2019). Multipurpose national forest inventory in Mongolia, 2014-2017 – A tool to support sustainable forest management. *Geography, Environment, Sustainability*. doi: 10.24057/2071-9388-2019-36
- Antokhina O., Latysheva I. and Mordvinov V. (2019). A cases study of Mongolian cyclogenesis during the July 2018 blocking events. *Geography, Environment, Sustainability*. doi: 10.24057/2071-9388-2019-14
- Aschmann M. (2019). Addressing air pollution and beyond in Ulaanbaatar: the role of sustainable mobility. *Geography, Environment, Sustainability*. doi: 10.24057/2071-9388-2019-30
- Batbayar G., Pfeiffer M., Kappas M. and Karthe D. (2019). Development and application of GIS-based assessment of land-use impacts on water quality: A case study of the Kharaa River Basin. *Ambio*, 48(10), pp. 1154-1168. doi: 10.1007/s13280-018-1123-y
- Batkhuu N., Lee D. and Tsogtbaatar J. (2011). Forest and forestry research and education in Mongolia. *Journal of sustainable forestry*, 30 (6), pp. 600-617. doi: 10.1080/10549811.2011.548761

Debkov N., Aleinikov A., Gradel A., Bocharov A., Klimova N. and Pudzha G. (2019). Impacts of the invasive four-eyed fir bark beetle (*Polygraphus proximus* Blandf.) on Siberian fir (*Abies sibirica* Ledeb.) forests in Southern Siberia. *Geography, Environment, Sustainability*. doi: 10.24057/2071-9388-2019-35

Dorjgotov D. (2009). Vegetation. In: Sh. Tsegmid, V.V. Borobiev, eds., *Mongolian National Atlas*. Ulaanbaatar, Mongolia: Academy of Sciences, Institute of Geography Press, pp. 125-133.

Dulamsuren C., Hauck M. and Mühlenberg M. (2005). Ground vegetation in the Mongolian taiga forest-steppe ecotone does not offer evidence for the human origin of grasslands. *Applied Vegetation Science*, 8, pp. 149-154. doi: 10.1111/j.1654-109X.2005.tb00640.x

Fan P, Chen J. and John R. (2016). Urbanization and environmental change during the economic transition on the Mongolian Plateau: Hohhot and Ulaanbaatar. *Environmental Research*, 144B, pp. 96-112. doi: 10.1016/j.envres.2015.09.020

Frolova N., Belyakova P., Grigor'ev V. et al. (2017). River runoff fluctuations in the Selenga River basin. *Regional Environmental Change*, 17(7), pp. 1965-1976. doi:10.1007/s10113-017-1199-0

Garmaev E., Kulikov A., Tsydypov B., Sodnomov B. and Ayurzhanayev A. (2019). Environmental conditions of Zakamensk town (Dzhida river basin hotspot). *Geography, Environment, Sustainability*. doi: 10.24057/2071-9388-2019-32

Gradel A., Ammer C., Ganbaatar B. et al. (2017). On the effect of thinning on tree growth and stand structure of white birch (*Betula platyphylla* Sukaczew) and siberian larch (*Larix sibirica* Ledeb.) in Mongolia. *Forests*, 8(4), pp. 105. doi: 10.3390/f8040105

Gradel A., Gerelbaatar S., Karthe D. and Kang H. (2019). Forest management in Mongolia – A review of challenges and lessons learned with special reference to degradation and deforestation. *Geography, Environment, Sustainability*. doi: 10.24057/2071-9388-2019-102

Hofmann J., Tuul D. and Enkhtuya B. (2016). Agriculture in Mongolia under pressure of agronomic nutrient imbalances and food security demands: A case study of stakeholder participation for future nutrient and water resource management. In: D. Borchardt, J. Bogardi and R. Ibsch, eds., *Integrated Water Resources Management: Concept, Research and Implementation*. Cham: Springer, pp. 471-514. doi: 10.1007/978-3-319-25071-7\_19

Jarsjö J., Chalov S., Pietroń J. et al. (2017). Patterns of soil contamination, erosion and river loading of metals in a gold mining region of northern Mongolia. *Regional Environmental Change*, 17(7), pp 1991-2005. doi: 10.1007/s10113-017-1169-6

Juříčka D., Kusbach A., Pařílková J. et al. (2019a). Evaluation of natural forest regeneration as a part of land restoration in the Khentii massif, Mongolia. *Journal of Forestry Research*. doi: 10.1007/s11676-019-00962-5

Juříčka D., Pecina V., Brtnický M. and Kynický J. (2019b). Mining as a catalyst of overgrazing resulting in risk of forest retreat, Erdenet, Mongolia. *Geography, Environment, Sustainability*. doi: 10.24057/2071-9388-2019-23

- Karthe D., Abdullaev I., Boldgiv B. et al. (2017). Water in Central Asia: an integrated assessment for science-based management. *Environmental Earth Sciences*, 76(690). doi: 10.1007/s12665-017-6994-x
- Kasimov N., Karthe D. and Chalov S. (2017). Environmental change in the Selenga River – Lake Baikal Basin. *Regional Environmental Change*, 17(7), pp. 1945-1949. doi:10.1007/s10113-017-1201-x
- Kasimov N., Kosheleva N., Sorokina O. et al. (2011). Ecological-geochemical state of soils in Ulaanbaatar (Mongolia). *Eurasian Soil Science*, 44(7), pp. 709-721. doi: 10.1134/S106422931107009X
- Khodolmor S., Tsogtbaatar J., Das D., Batzargal Z. and Mandakh N. (2013). *Desertification Atlas of Mongolia*. Ulaanbaatar, 134 p. (in Mongolian).
- Kosheleva N., Timofeev I., Kasimov N. and Sandag E. (2019). Geochemical transformation of soil cover and woody vegetation in the largest industrial and transport center of Northern Mongolia (Darkhan). *Applied Geochemistry*, 107, pp. 80-90. doi: 10.1016/j.apgeochem.2019.05.017
- Kusbach A., Štěřba T., Šebesta J., Mikita T., Bazarradnaa E., Dambadarjaa S. and Smola M. (2019). Ecological zonation as a tool for restoration of degraded forests in Northern Mongolia. *Geography, Environment, Sustainability*. doi: 10.24057/2071-9388-2019-31
- Liu Z., Yao Z., Huang H. (2019). Evaluation of extreme cold and drought over the Mongolian Plateau. *Water*, 11(1), p. 74. doi: 10.3390/w11010074
- Miao L., Liu Q., Fraser R. et al. (2015). Shifts in vegetation growth in response to multiple factors on the Mongolian Plateau from 1982 to 2011. *Physics and Chemistry of the Earth*, 87-88, pp. 50-59. doi: 10.1016/j.pce.2015.07.010
- Moreido V. and Kalugin A. (2017). Assessing possible changes in Selenga river water regime in the XXI century based on a runoff formation model. *Water Resources*, 44(3), pp. 390-398. doi: 10.1134/S0097807817030149
- Sasaki T., Koyama A., Okuro T. (2018). Coupling structural and functional thresholds for vegetation changes on a Mongolian shrubland. *Ecological Indicators*, 93, pp. 1264-1275. doi: 10.1016/j.ecolind.2018.06.032
- Shabanova E., Byambasuren Ts., Ochirbat G., Vasil'eva I., Khuukhenkhuu B. and Korolkov A. (2019). Relationship between major and trace elements in Ulaanbaatar soils: a study based on multivariate statistical analysis. *Geography, Environment, Sustainability*. doi: 10.24057/2071-9388-2019-18
- Shinkareva G., Lychagin M., Tarasov M., Pietroń J., Chichaeva M. and Chalov S. (2019). Biogeochemical specialization of macrophytes and their role as a biofilter in the Selenga delta. *Geography, Environment, Sustainability*. doi: 10.24057/2071-9388-2019-103
- Sternberg T. (2012). Piospheres and Pastoralists: Vegetation and Degradation in Steppe Grasslands. *Human Ecology*, 40(6), pp. 811-820. doi: 10.1007/s10745-012-9539-7
- Tao S., Fang J., Zhao X. et al. (2015). Rapid loss of lakes on the Mongolian Plateau. *Proceedings of the National Academy of Sciences*, 112(7), pp. 2281-2286. doi: 10.1073/pnas.1411748112

Törnqvist R., Jarsjö J., Pietró J. et al. (2014). Evolution of the hydro-climate system in the Lake Baikal basin. *Journal of Hydrology*, 519, pp. 1953-1962. doi: 10.1016/j.jhydrol.2014.09.074

Tsogtbaatar J. (2004). Deforestation and reforestation needs in Mongolia. *Forest Ecology and Management*, 201, pp. 57-63.

Usoltsev V., Danilin I., Tsogt Z., Osmirko A., Tsepordey I. and Chasovskikh V. (2019). Aboveground biomass of Mongolian larch (*Larix sibirica* Ledeb.) forests in the Eurasian region. *Geography, Environment, Sustainability*. doi: 10.24057/2071-9388-2018-70

Wei H., Wang J., Cheng K. et al. (2019): Desertification information extraction based on feature space combinations on the Mongolian Plateau. *Remote Sensing*, 10(10), pp. 1614. doi: 10.3390/rs10101614

Zhou Y., Dong J., Xiao X. et al. (2019). Continuous monitoring of lake dynamics on the Mongolian Plateau using all available Landsat imagery and Google Earth Engine. *Science of the Total Environment*, 689, pp. 366-380. doi: 10.1016/j.scitotenv.2019.06.341

**Olga Yu. Antokhina<sup>1\*</sup>, Inna V. Latysheva<sup>2</sup>, Vladimir I. Mordvinov<sup>3</sup>**

<sup>1</sup> V.E. Zuev Institute of Atmospheric Optics, SB RAS, Tomsk, Russia

<sup>2</sup> Irkutsk State University, Irkutsk, Russia

<sup>3</sup> Institute of Solar-Terrestrial Physics, SB RAS, Irkutsk, Russia

\* **Corresponding author:** [olgayumarchenko@gmail.com](mailto:olgayumarchenko@gmail.com), [antokhina@iao.ru](mailto:antokhina@iao.ru)

# A CASES STUDY OF MONGOLIAN CYCLOGENESIS DURING THE JULY 2018 BLOCKING EVENTS

**ABSTRACT.** Mongolia and Transbaikalia (M-TB) have experienced severe drought over the past 20 years due to the increased frequency of anticyclogenesis. However, in the summer of 2018, as a result of the formation of a series of cyclones over Mongolia and their move to the Transbaikalia, abnormally high precipitation was observed in the M-TB region. The dynamics of long Rossby waves and atmospheric blocking in the middle and upper troposphere were investigated to identify the causes of cyclogenesis over Mongolia. It was revealed that a sequence of events predefined the extreme precipitation in M-TB in the 2018 summer – the intensification of heat flux over the North Atlantic while maintaining cyclonic vorticity over Central Europe, the development of blocking ridges in the Urals and the Russian Far East, and an upper-level trough oriented to the eastern regions Mongolia. For a long time, the persistent advection of cold air in the rear part of the upper-level trough, as well as increased heat advection during the activation of the East Asian summer monsoon, caused meridional oriented upper-level front strengthening over the eastern regions of Mongolia and extreme precipitation.

**KEY WORDS:** Mongolia, Transbaikalia, rainfall, atmospheric blocking, cyclogenesis

**CITATION:** Olga Yu. Antokhina, Inna V. Latysheva, Vladimir I. Mordvinov (2019) A Cases Study Of Mongolian Cyclogenesis During The July 2018 Blocking Events. *Geography, Environment, Sustainability*, Vol.12, No 3, p. 66-78  
DOI-10.24057/2071-9388-2019-14

## INTRODUCTION

Mongolia and Transbaikalia (M-TB) have experienced severe drought in recent decades due to a decrease in precipitation and an increase in air temperature in summertime (Davi et al. 2006, 2013; Berezhnykh et al. 2012; Erdenebat et al. 2015; Obyazov et al. 2015; Shubert et al. 2014; Hessel et al. 2018). A recent decade-long drought that exceeded the variability in the instrumental record (Hessel et al. 2018) caused economic,

social, and environmental change (Karthé et al. 2014, Kasimov et al. 2017). The changes have affected the discharge of the Selenga River. In the last 20 years (1996-2017) it has decreased significantly (Berezhnykh et al. 2012; Frolova et al. 2017; Moreido and Kalugin 2017). Since the Selenga River is the main tributary of Lake Baikal (Berezhnykh et al. 2012), a decrease in its discharge has caused a reduction of the inflow into the lake, especially in 2014–2015 (Bychkov and Nikitin 2015).

The increase of the anticyclonic circulation over Mongolia is one of the reasons of the growth of aridity in M-TB (Iwasaki and Nii 2006; Zhu et al. 2012; Berezhnyukh et al. 2012; Shubert et al. 2014; Erdenebat and Sato 2015). We suppose that anticyclonic circulation is an attribute of air masses convergence weakening of the midlatitude and East Asia Summer Monsoon (EASM), which is typical for the M-TB region in midsummer (Berezhnykh et al. 2012). Several recent studies (Ding et al. 2008; Li et al. 2009; Chen et al. 2017) showed that EASM had been significantly weakened (decreasing of northward moisture transport). According to Khromov 1956; Yihui and Chan 2005; Chen et al. 2017, there is the evident linkage between cyclonic/anticyclonic activity around the M-TB and North China and intensity of moisture transport by EASM. Chen et al. 2017 have proved the relationship between EASM and East Asian cyclone activity. When the midlatitudes summer cyclone activity over East Asia is strong (weak), EASM tends to be intensified (weakened), and the weak cyclone activity after 1993 generally coincides with the decadal weakening of EASM.

The change in the spatial structure of long quasi-stationary Rossby waves (Iwasaki et al. 2006, Sato et al. 2006, Iwao et al. 2008; Shubert et al. 2014; Li and Ruan 2018) and/or blocking over Eurasia (Antokhina 2019) are reasons for increasing the frequency of anticyclones over Mongolia. Li and Ruan, 2018 discovered the teleconnection, termed the Atlantic–Eurasian (AEA) teleconnection, which is a consequence of a large-scale Rossby wave train that originates in the subtropical North Atlantic Ocean. AEA has five centers of action, in the subtropical North Atlantic Ocean, the northeastern North Atlantic Ocean, Eastern Europe, the Kara Sea, and north China. A positive AEA index (AEAI) is an indicator of anomalously high 500hPa geopotential heights over the subtropical North Atlantic Ocean, Eastern Europe, and Mongolia–north China, and low geopotential heights over

the northeastern North Atlantic Ocean and the Kara Sea–northern Siberia, and vice versa. The AEA shows that the AEA undergoes a high degree of variability from year to year, and the AEA has an increasing trend over the last 30 years. Antokhina, 2019 established that during the high frequency of anticyclogenesis in Mongolia during 1996–2017, the change of Eurasian blocking patterns was observed.

The cause of global changes in circulation may be the weakening of the subtropical jet stream during the summer period (Kwon et al. 2007), due to a decrease in the north-south temperature gradient in the troposphere (Zhang and Zhou 2015). The Arctic amplification may explain the weakening of the north-south temperature gradient in recent decades (Coumou et al., 2018). Wirth et al. 2018 emphasized that ducting property of a jet waveguide (in a climate model) depends on the strength of the jet stream. The weakening of the jet stream can lead to the quasi-stationarity of waves and changing the structure and position of the blocking in midlatitudes. Antokhina, 2019 paid attention to the importance of the jet stream properties because it is waveguide for long Rossby waves. Using (Antokhina 2019) potential temperature on a dynamic tropopause ( $PV-\theta$ ) allowed the author to detect the link between cyclone activity over Mongolia and features of moving along the jet stream the air with high and low potential temperature. The traveling along waveguide of different disturbances can explain teleconnection of far apart regions.

Despite the duration of the drought period and the trend in precipitation change (decrease) and temperature (growth), the situation changed suddenly in July 2018. In July 2018, Mongolia and Transbaikalia were faced with extremal floods (floodlist.com; tass.com 2018). Floods were caused by intense precipitation from July 1 to July 22 (meteo.ru 2018). The greatest amount of precipitation fell in Chita (Transbaikalia),

where the monthly norm was exceeded more than three times (from 1 to 31 July – 330 mm, 320%) (meteo.ru 2018). Extreme rainfall after decades of prolonged drought caused the question – what do these events mean? Is this event evidence of the end of a long drought? Synoptic analysis of the development of cyclogenesis over Mongolia in July 2018 and a comparison with processes causing a large amount of precipitation over M-TB in earlier years may partly shed light on this problem. The study is aimed at finding large-scale features of the atmospheric circulation that could affect the development of the situation in July 2018. Close attention was paid to the development of blocking processes in the middle troposphere since these processes are closely associated with extreme precipitation in Eastern Siberia and Mongolia (Antokhina et al. 2018a,b).

#### **MONGOLIAN CYCLONES CHARACTERISTICS. THE LINKAGE BETWEEN THE MONGOLIAN CYCLOGENESIS AND THE FORMATION OF BLOCKING OVER EURASIA**

According to the report of the weather forecasting center of the Chita (Hydrometcenter of Russia) (meteoinfo.ru 2018), the cause of extreme rain was a series of cyclones originating over Mongolia (also known as Southern cyclones, Mongolian cyclones – MC's). The cyclones originating over Mongolia have a high frequency as compared to all other cyclones in East Asia and have a significant influence on the weather in the Baikal region, Mongolia, and also in the areas located to the northeast (Chen et al. 1990, 1991; Wang et al. 2009). MC's are as a rule deep cyclones with high temperatures and absolute humidity of air masses. These air masses are related to conditions of forced convection, causing cloud cover formation and extreme precipitation. One of the most likely causes of the high frequency of cyclones in Mongolia is the role of a mountain barrier in cyclogenesis. A climatological analysis of cyclogenesis over East Asia revealed that one of the most active

cyclogenesis areas is the lee sides of the Altai-Sayan, Stanovoi, and Great Xinganling mountains. Among these areas, the Altai-Sayan lee side is home to the most active cyclogenesis area in East Asia (Chen et al. 1991).

Weather forecasters extract MC's into a special group of cyclones that develop in the front part of a deep meridional tropospheric trough extending to the south of 50° N (Bukhalova 1959; Loschenko et al. 2010). Researches of synoptic conditions of Mongolian cyclones in Russia formation began in the middle of the 20th century (Arkhangelsky 1956; Bukhalova 1959). Bukhalova, 1959 identified the main trajectories of the Mongolian cyclones and investigated the structure of the upper-level pressure field. According to Bukhalova, 1959, during the formation of Mongolian cyclones in the troposphere, an upper-level trough is observed, oriented from the Ob Bay to the Ulan-Bator areas, characterized by increased advection of cold in the rear and advection of heat in the front. The region of the formation of MC's depends on the localization of the trough line and the associated ridges. If the line of the upper-level trough is oriented in the region of 43-50° N and 90-115° E, over Mongolia the strengthening of the jet stream (upper-level front) is possible. The strengthening of the jet stream causes the development of dynamically unstable baroclinic waves on the tropospheric front and, as a result, the formation of cyclones. Such conditions are more often observed in the summer season. An increase in horizontal geopotential gradients ( $\geq 20$  dkm / 1000 km) on the jet stream axis, convergent advection of cold and heat ( $\geq 4-5$  oC / day), respectively, to the rear and front parts of the cyclone (Loschenko et al. 2010) are considered as predictors of synoptic disturbances development. The structure and dynamics of Mongolian cyclones, as we have already noted, are strongly influenced by orography (large mountain chains) as well as the intensity of energy exchange processes between different layers of the troposphere.

Commonly in the atmospheric circulation researches, wave processes (Rossby long waves) (Wirth et al. 2018) and atmospheric blocking (Mokhov and Semenov 2016) are mentioned as large-scale circulation features responsible for the development of extremal synoptic processes. Rossby waves can be free or forced and maintained either by the energy of the mean flow or by orographic and/or thermal forcing by any region of the globe. In the northern hemisphere, such areas can be the North Atlantic and massive mountains – the Rocky Mountains, Tibet, and the Himalayas. The spatial structure of forced waves differs from the structure of free Rossby waves, which are mostly characterized by waveguide propagation along jet streams. At the nonlinear stage (breaking) Rossby waves can form large-scale quasi-barotropic and stationary pressure anomalies, often called blocking. Long-term intensive advection of heat and/or cold can be responsible for the formation of amplified ridges and troughs, which can block the mean flow in the troposphere. Probably, the wave and advective mechanisms of blocking formation are linked; however, this question, especially for East Asia, requires individual study. With the point of view clarifying the reasons for the activation of cyclonic processes in Mongolia, it is important that, regardless of the formation mechanism, the blocks are closely associated with intensive cold advection in the troughs related to the blocking. Palmen and Newton 1991; Schubert et al. 2014; Antokhina et al. 2018b showed that with the development of ridges and blocking over Europe (Europe-Urals, Europe-Urals-Western Siberia) to the east of the blocking anticyclone (ridge), an advection (intrusion) of polar air occurs, and a deep trough is formed. Under specific development scenarios of blocking over Europe, Urals and Western Siberia, these processes may contribute to the formation of Mongolian cyclones. An example of the development of synoptic and large-scale circulation processes accompanied by intensive precipitation in Mongolia in July 2018 is considered.

## METHOD AND DATA

To identify blocking events, we use GHGS (geopotential height – gradient south) criterion is developed by Lejenäs and Øakland, 1983; Tibaldi and Molteni, 1991; Barriopedro et al., 2006:

$$GHGS = \frac{Z(\varphi_0) - Z(\varphi_s)}{\varphi_0 - \varphi_s},$$

where  $Z$  is the 500 hPa geopotential height,  $\varphi_0 = 60^\circ \text{ N} \pm \Delta$ ,  $\varphi_s = 40^\circ \text{ N} \pm \Delta$ , unlike in (Lejenäs and Øakland 1983; Tibaldi and Molteni 1991), we took the following values for  $\Delta$ :  $\Delta = -5^\circ, -2.5^\circ, 0^\circ, 2.5^\circ$  or  $5^\circ$ , which were first offered for use Barriopedro et al. 2006. The situation when  $GHGS > 0$  is referred to as blocking. A longitude is considered blocked when  $GHGS > 0$  for at least one of the five  $\Delta$  values.

Atmospheric data used in this study are from the European Centre for Medium-Range Weather Forecasts ECMWF Era-Interim (Dee et al. 2011). To identify blocking events, we used 500 hPa geopotential heights. To reveal the origin of the air masses, we analyzed the potential temperature on the dynamic tropopause ( $PV-\theta$ ) (Hoskins 1991) and streamlines at 850 hPa, 500 hPa (The spatial resolution is  $2.5 \times 2.5$  and 4-times-daily for July 2018). According to Hoskins 1991, Masato et al. 2011  $PV-\theta$  is a very good candidate to study the synoptic development of blocking as it is materially conserved in time, providing an excellent tracer for the air masses contributing to blocking formation, and can be inverted to give the balanced component of the flow. In addition, the reversal of the meridional gradient  $PV-\theta$  is associated with Rossby wave-breaking (Masato et al. 2011).

We used daily precipitation data from GPCC (The Global Precipitation Climatology Centre), the spatial resolution is  $1^\circ \times 1^\circ$  for July 2018, version GPCC First Guess Daily Product for July 2018 (Schamm et al. 2013). GPCC Precipitation Climatology Version 2018 (Meyer-Christoffer et al. 2018) was used for estimations of July's mean precipitation (1950–2000).

The Irkutsk Weather Administration provided surface and upper-level weather maps.

RESULTS

Precipitation anomalies and cyclogenesis periods in July 2018

Fig. 1 (a, b) shows maps of precipitation anomalies in July 2018 over Eurasia (Fig. 1a) and the M-TB (Fig. 1b). Two regions with positive precipitation anomalies are visible – Central Europe and most of East Asia (Fig. 1a). It is seen that the greatest amount of precipitation fell in Transbaikalia (Chita station is pointed in Fig. 1b). Over Northern Europe, the Urals and most of Western Siberia, the precipitation anomalies are negative. The

spatial scale of the anomalies in Fig. 1a indicates that they are due to large-scale circulation processes.

Fig. 1 (c) shows the day-to-day histogram of the total daily precipitation in the Selenga basin in July 2018. For comparison, Fig. 1 (d) shows the same histogram for July 1990 – the highest in terms of precipitation in the Selenga River Basin. The calculations showed that July 2018 is in the top five years with the most precipitation in the Selenga basin during the observation period from 1934. At that time, the absolute record for the amount of precipitation in the history of

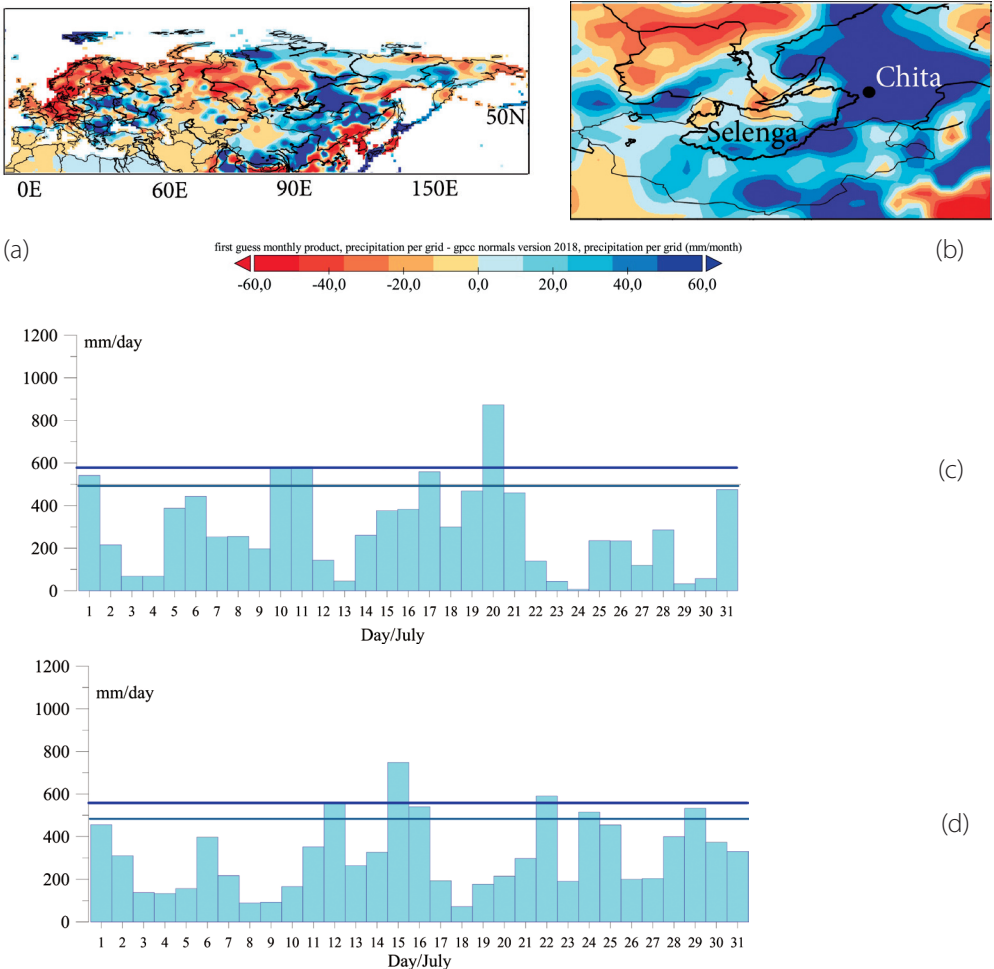


Fig. 1. Precipitation (mm/month) (a,b) deviation from normal 1951-2000, day-to-day total precipitation in Selenga River Basin in 2018 comparison to 1990 (2018 - c, 1990 - d) gray-blue – 90<sup>th</sup> percentile, deep-blue – 95<sup>th</sup> percentile. Event 20 July 2018 – 99<sup>th</sup> percentile. According to GPCC (Schamm et al. 2013)

instrumental observations was recorded at Chita station (Fig. 1b).

Fig. A1 (see Appendix A) on the left shows the maps of precipitation and streamlines at 850 hPa for each day from 1 to 20 July 2018. Fig. A1 on the right shows streamlines at 500 hPa and PV- $\Theta$ . The precipitation and streamlines at 850 hPa maps allow us to compare the dynamics of synoptic disturbances in the lower troposphere and the rainfall associated with them, maps in Fig. A1 on the right – to analyze the large-scale structure of the pressure fields in the period of formation and moving of the MC's. Based on the analysis of Fig. A1, we have identified four intervals, characterized by the formation and moving of the MC's, accompanied by precipitation in the longitude interval of 90-120°E: 4-8, 9-12, 14-17, 18-21 July. All of these cyclones originated in Mongolia and excluding the process of July 14-17, had moved to Transbaikalia.

### Factors contributing to the development of cyclogenesis over Mongolia in July 2018

Fig. 2 shows the time-longitude diagram of the GHGS blocking index. Based on Fig. 2 and Fig. A1, we can more precisely describe the blocking associated with the formation of pressure anomaly. Fig. 3 shows an example of maps which were used to analyze the synoptic processes in July 2018 — AT-700 hPa (3 km) (a) and the surface pressure map (b) for 7<sup>th</sup> July 2018.

As shown by a synoptic analysis of a set of such maps, in July 2018, the Mongolian cyclones more often did not form in the west and north-west of Mongolia, where they most commonly develop in summer, but the east of Mongolia. The conditions of frequent strengthening of the jet stream (upper-level frontal zone) caused precipitation not only in the area of the primary and secondary atmospheric fronts but also in the rear part of the Mongolian cyclones after their moving.

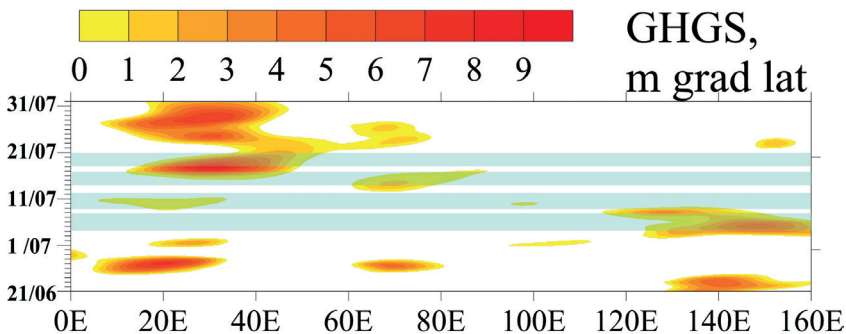


Fig. 2. The time-longitude diagram of the GHGS index (21 June - 31 July 2018), blue belt – periods of precipitation in the M-TB. According to Era-Interim (Dee et al. 2011)

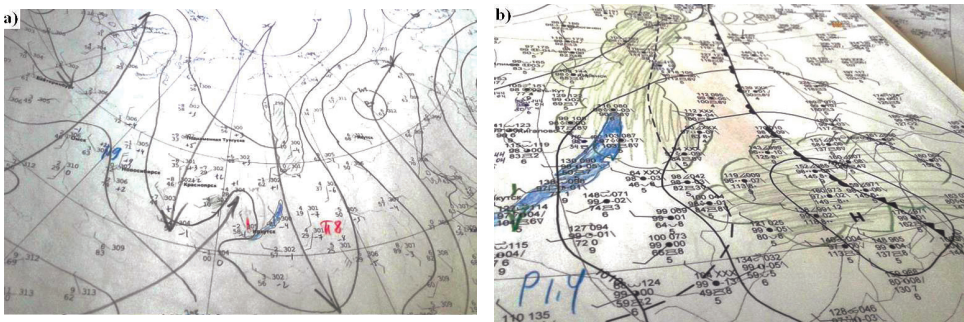


Fig. 3. Maps AT-700 hPa (3 km) (a) and surface pressure (b) for 7 July 2018. According to Irkutsk Weather Administration (<https://www.irmeteo.ru/>)

One of the critical factors that influenced the development of cyclogenesis was the formation of an upper-level trough of large amplitude (Fig 3a, Fig. A1 4-7 July). It can be seen that the orientation of the trough is exceptionally suitable for the formation of MC's (according to Bukhalova 1959 and Loschenko et al. 2010). The combination of intensive advection from the north, the stationary trough for a long time in July played a key role in the formation of the moving cyclogenesis and heavy precipitation in the region M-TB.

The formation of the trough, which was significant for the extreme precipitation over Mongolia in July 2018, was predefined by blocking in Europe (Fig. 2, Fig. A1). It can be seen in the period of displacement of the trough (7-9 July) the blocking over Europe is weakening, and then again is formed over Europe and Western Siberia. The blocking over Europe and Western Siberia persisted for a long time; as a result, the stationary upper-level trough with a line of about 105°E, frontal zone and the development of wave disturbances on it, have been observed almost throughout the July 2018. Intense cold advection in eastern Mongolia and China was observed in the rear part of the trough (Fig. A1 – streamline at 850 hPa and PV- $\theta$ ). The long-lasting heat advection in the front of cyclones contributed to the development and maintenance of a blocking process in the Russian Far East by the synoptic-scale waves. In turn, the blocking over the Far East further contributed to more intense and prolonged precipitation. It should be noted that the development of blocking covered not only the troposphere but also the lower stratosphere and propagated up to 50 hPa.

In general, July's 2018 blocking pattern (Fig. 2) is similar to the type studied earlier in (Antokhina et al. 2018b), which is characterized by the development of blocking over Europe and the Russian Far East (E-RFE). As shown in (Antokhina et al. 2018b), the E-RFE blocking pattern under specific scenarios can contribute to

heavy precipitation in the Selenga River Basin. Several precipitation maxima can accompany the development of E-RFE blocking in July. The first maximum was caused by the strong baroclinicity due to the maximum temperature contrasts in front of the trough (Antokhina et al. 2018b, analysis of 1991 - 6-8 July). The second maximum of precipitation is associated with a northward shift of East Asia monsoon air due to traveling one cyclonic wave after another along the subtropical jet stream (Antokhina et al. 2018b, analysis of 1991 - 19-21 July). In July 2018 advection of moisture from the Pacific Ocean in a layer of 1000–500 hPa contributed to the development of tropospheric frontogenesis in the region of Mongolian cyclones development, especially when Pacific tropical cyclones moved to the coast of Eurasia. The total precipitable water in the eastern areas of the Selenga Basin on July 21 reached 40 kg/m<sup>2</sup>. According to Marchenko et al. 2012, such precipitable water is common for the processes involving monsoon air. The circulation over the North Atlantic, Western Europe, and the Mediterranean has played a significant role in the development of blocking over Europe, the Urals, and Western Siberia, which ultimately determined the anomalous rains over Mongolia. Formed as a result of the intrusion of cold air and deepening of the trough in the last decade of June 2018 (Fig. 4) thermal anomalies and intense cyclonic circulation over Central Europe have persisted until July 20.

The increasing of the North Atlantic heat fluxes could contribute to the amplification of the large-scale waves in the summer of 2018 and their displacement to the east. This is confirmed by the high AO (Arctic oscillation) and NAO (North-Atlantic oscillation) indices (cpc.ncep.noaa.gov 2018) and the positive anomalies of the surface pressure and geopotential at 500 hPa surface in Northern Atlantic, which, according to the Hydrometeorological Center of Russia, reached +7 hPa and +17 dkm (decimeter, 1 dkm=10 m, in synoptic studies is commonly used for geopotential height) over the Atlantic

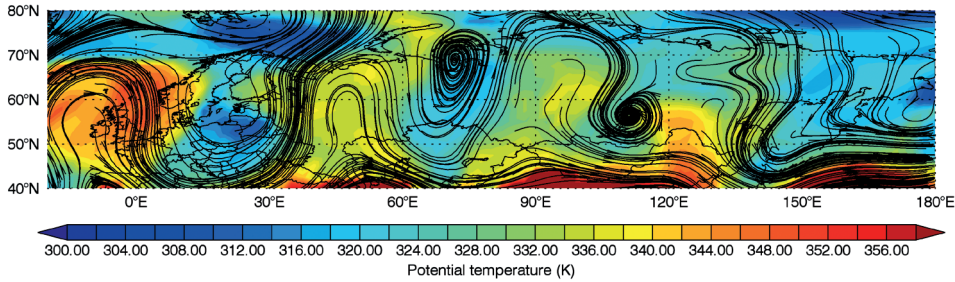


**Fig. 4. Snapshot of the wave-like pattern in Eurasia, 24 June 2018 (PV- $\Theta$  and streamflow at 500 hPa), according to Era-Interim (Dee et al. 2011)**

in July, 2018 (meteoinfo.ru 2018). The development of the thermal and pressure ridge over the North Atlantic has led to a deepening of the adjacent trough and determined the advective-dynamic factors of cyclogenesis over the Mediterranean, where the negative anomalies of the surface pressure in July 2018 reached maximum values in the Northern Hemisphere (-9 hPa). In turn, the heat advection in front of the trough has determined the development of the Urals-Western Siberia blocking ridge while the southern Mediterranean cyclones moved northward. The blocking area in western Eurasia occupied a longitudinal sector equal to 70 degrees (0-70° E Fig. A1, 4 July). The resulting configuration of the baric field in July from 1 to 20 was favorable to ensure that polar air masses were constantly advecting into the Mongolia area.

Fig. 5 shows the altitude-latitude diagrams of the position of the jet streams, dynamical tropopause (2PVU) (Hoskins 1991, Kunz et al. 2011, Masato et al. 2011) and vertical velocity for several days characterizing the different stages of the formation of Mongolian cyclones. On July 6, an extensive area of the upper-tropospheric jet stream formed by a convergence of subtropical and polar jet stream is visible. In the second half of July, mesojets were often observed in the middle and lower troposphere. The positions of the jet streams indicate the convergence of warm and cold air masses and the formation of dynamically significant high-altitude frontal zones over Mongolia and southern Transbaikalia regions with geopotential gradients exceeding 16 dkm / 1000 km.

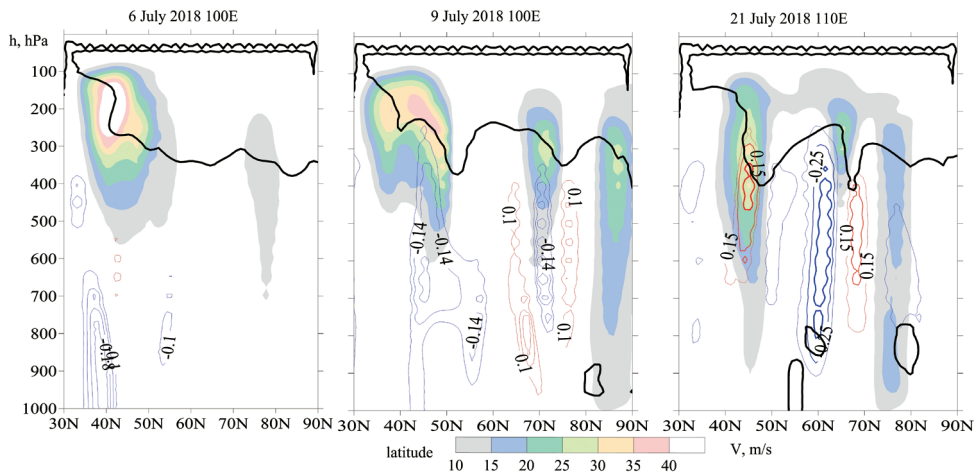


**Fig. 5. Altitude-latitude diagram of the position of jet streams, vertical velocity for 6, 9 and 21 July 2018. The jet stream – rainbow color with color bare, dynamical tropopause position 2 PVU – black line, vertical velocity: blue line – ascending, red – descending (Pa/s). According to Era-Interim (Dee et al. 2011)**

Thermally direct circulation, as evidenced by the ascending motion of the air, which reached the level of the tropopause, also indicates the development of powerful frontogenesis. In the second half of July 2018 (21 July), the strengthening of the ascending motion (up to  $-0.25$  Pa/s) was supported by the descending motion of upper tropospheric air with an intensity of up to  $0.15$  Pa/s. Under such conditions, convection in the area of main and secondary cold atmospheric fronts intensifies, which determined the intense precipitation in the territory of Transbaikalia.

## CONCLUSIONS AND DISCUSSION

After the prolonged drought during the last two decades, in July 2018, Mongolia and Transbaikalia (M-TB) experienced a period of heavy rain and flooding. The paper studied the development of the Mongolian cyclogenesis (MC's) in July 2018. Four intervals were identified associated with the formation of MC's and precipitation: 4-8, 9-12, 14-17, 18-21 July. The paper has shown that intense and prolonged rainfall in the summer of 2018 in M-TB was predefined by the abnormal development of wave processes in the middle troposphere. The abnormal development of wave processes was due to the intensification of heat flux over the North Atlantic, the stationing of a cyclone over central Europe, the development of blocking ridges in the Urals and the Far East, and the adjacent upper-level trough oriented towards the eastern regions of Mongolia. Lasting about twenty days advection of cold air in the rear part of the upper-level trough, and increased heat advection due to the summer East Asian monsoon caused the upper-level front strengthening in the eastern regions of Mongolia, activating cyclonic circulation and extreme precipitation in M-TB in July 2018.

As a discussion of the obtained results, we would like to note the following: we have compared the observed 2018 July blocking pattern to the previously studied

(Antokhina et al. 2018a, 2018b; Antokhina 2019). Previous studies of the link between atmospheric blocking and precipitation in Eastern Siberia and Mongolia have suggested that the 2018 case is rather the exception. We have concluded that it was exceptional even though the development scenario of E-RFE blocking patterns is not exceptional and it was observed by us more than once. Our conclusion is mainly based on an analysis of the details of E-RFE blocking patterns scenario development. We suppose the main feature of circulation in July 2018 is the intensity of cold advection from the Arctic and its trajectory. The permanent cold advection was due to the unusual blocking configuration in western Eurasia. We suppose that further research of changing Rossby wave propagation and atmospheric blocking patterns over Eurasia is the key to figure out rainfall variability which will allow us to find out more about future trends in precipitation in the region M-TB.

## ACKNOWLEDGEMENTS

The study was supported by the Russian Science Foundation Project No. 17-77-10035.

We express our gratitude to Eugene Osipchuk (Ph.D., Melentiev Energy Systems Institute, Siberian Branch, Russian Academy of Sciences) who prepared data on catchment areas of Lake Baikal and Selenga River. We thank The Global Precipitation Climatology Centre (Public Datasets: <https://apps.ecmwf.int/datasets/>), especially Dr. Andreas Becker (Head Precipitation Monitoring Unit (KU42) and Global Precipitation Climatology Centre (GPCC)) and European Centre for Medium-Range Weather Forecasts Public Datasets: <https://apps.ecmwf.int/datasets/>). We are also grateful to Irkutsk Hydrometeorological Administration for the possibility to work with synoptic maps. ■

## REFERENCES

- Antokhina O.Yu., Antokhin P.N., Devyatova E.V., Mordvinov V.I. (2018a). Dynamic Processes In The Atmosphere Determining Summertime Precipitation Anomalies In The Eastern Siberia And Mongolia *Fundamental and Applied Climatology* 5, pp. 10-27 DOI: 10.21513/2410-8758-2018-1-10-27 (in Russian with English summary).
- Antokhina O. Y., Antokhin P. N., Devyatova E. V., Mordvinov V. I., Martynova Yu. V. (2018b). Precipitation in the Selenga River basin during atmospheric blocking over Europe and the Russian Far East in July. *IOP Conf. Series: Earth and Environmental Science* 211, pp. 012054.
- Antokhina O. Yu. (2019). Precipitation in the basin of the Selenga River Basin in July and features of large-scale atmospheric circulation over Eurasia // *Geogr. and Nat. Res.*, 4, in press (in Russian with English summary).
- Arkhangelsky V.L. (1956). Ways and speeds of movement of cyclones and anticyclones in Eastern Siberia and the Far East. *Tr. DVNIGMI* 1, pp. 14 – 23. (in Russian).
- Barriopedro D., García-Herrera R., Lupo A. R., Hernández E. (2006). Climatology of Northern Hemisphere Blocking. *Journal of Climate* 19, pp. 1042–1063.
- Berezhnykh, T.V., Marchenko O.Y., Abasov N.V., Mordvinov V.I. (2012). Changes in the summertime atmospheric circulation over East Asia and the formation of long-lasting low-water periods within the Selenga river basin. *Geogr. Nat. Resour.* 33, pp. 223-229.
- Bychkov I.V., Nikitin V.M. (2015). Water-level regulation of Lake Baikal: Problems and possible solutions. *Geogr. Nat. Resour.* 36, pp. 215- 224.
- Bukhalova L.N. (1959). Southern cyclones in Transbaikalia. *Tr. DVNIGMI* 7, pp. 13 – 25. (in Russian).
- Chen Shou-Jun, Lazić L. (1990). Numerical Case Study of the Altai-Sayan Lee Cyclogenesis over East Asia. *Meteorology and Atmospheric Physics* 42, 3-4 pp. 221–229.
- Chen, Shou-Jun, et al. (1991). Synoptic Climatology of Cyclogenesis over East Asia, 1958-1987. *Monthly Weather Review* 119, 6, pp. 1407–1418.
- Chen H., Teng F., Zhang W., Liao H. (2017). Impacts of Anomalous Midlatitude Cyclone Activity over East Asia during summer on the Decadal Mode of East Asian Summer Monsoon and Its Possible Mechanism. *Journal of Climate.* 30, pp. 739–753.
- Coumou D., Capua G. D., Vavrus S., Wang L., Wang, S. (2018). The influence of Arctic amplification on mid-latitude summer circulation. *Nature Communications* 2018, 9, p. 2959, doi: 10.1038/s41467-018-05256-8.
- cpc.ncep.noaa.gov (2019). North Atlantic oscillation (NAO) [on-line]. Available at: [cpc.ncep.noaa.gov/products/precip/CWlink/pna/norm.nao.monthly.b5001.current.ascii.table](https://cpc.ncep.noaa.gov/products/precip/CWlink/pna/norm.nao.monthly.b5001.current.ascii.table) [Accessed 26.01.2019].
- Davi, N.K., Jacoby G.C., Curtis A.E., Baatarbileg N. (2006). Extension of Drought Records for Central Asia Using Tree Rings: West-Central Mongolia. *J. Climate* 19, pp. 288–299. DOI <https://doi.org/10.1175/JCLI3621.1>.

Davi N. K., Pederson N., Leland C., Nachin B., Suran B., Jacoby G. C. (2013). Is eastern Mongolia drying? A long-term perspective of a multidecadal trend. *Water Resour. Res.* 49, 1, pp. 151–158 doi:10.1029/2012WR011834.

Dee D. P., Uppala S. M., Simmons A. J., Berrisford P., Poli P., Kobayashi S., Andrae U., Balmaseda M. A., Balsamo G., Bauer P., Bechtold P., Beljaars A. C. M., L. van de Berg, Bidlot J., Bormann N., Delsol C., Dragani R., Fuentes M., Geer A. J., Haimberger L., Healy S. B., Hersbach H., Hólm E. V., Isaksen I., Kållberg P., Köhler M., Matricardi M., McNally A. P., Monge-Sanz B. M., Morcrette J.-J., Park B.-K., Peubey C., P. de Rosnay, Tavolato C., Thépaut J.-N., Vitart F. (2011). The ERA-Interim reanalysis: configuration and performance of the data assimilation system. *Q.J.R. Meteorol. Soc.* 137, pp. 553–597, doi:10.1002/qj.828.

Ding Y., Wang Z., Sun Y. (2008). Inter-decadal variation of the summer precipitation in East China and its association with decreasing Asian summer monsoon. Part I: Observed evidences. *Int. J. Climatol.* 28, pp. 1139–1161, doi:10.1002/joc.1615.

Erdenebat E., Sato T. (2015). Recent increase in heat wave frequency around Mongolia: role of atmospheric forcing and possible influence of soil moisture deficit. *Atmospheric Science Letters* 17, pp. 135–140 DOI: 10.1002/asl.616.

floodlist.com (2018). Mongolia – Floods Prompt Rescues and Evacuations [on-line]. Available at: <http://floodlist.com/asia/mongolia-floods-july-2018> [Accessed 26.01.2019].

Frolova N. L., Belyakova P. A., Grigoriev V. Y., Sazonov A. A., Zotov L. V., Jarsjö J. (2017). Runoff fluctuations in the Selenga River Basin. *Regional Environmental Change* 17, pp. 1965–1976.

Hessl A. E., Anchukaitis K. J., Jelsema, C., Cook B., Byambasuren O. (2018). Past and future drought in Mongolia. *Science Advances* 4, 3, pp. e1701832. <http://doi.org/10.1126/sciadv.1701832>.

Hoskins B. J. (1991). Towards a PV- $\theta$  view of the general circulation. *Tellus B: Chemical and Physical Meteorology* 43, 4, pp. 27–35.

Iwao K., Takahashi M. (2008). A Precipitation Seesaw Mode between Northeast Asia and Siberia in Summer Caused by Rossby Waves over the Eurasian Continent *Journal of Climate* 21, pp. 2401–2419.

Iwasaki H., Nii T. (2006). The Break in the Mongolian Rainy Season and Its Relation to the Stationary Rossby Wave along the Asian Jet. *Journal of Climate* 19, pp. 3394–3405.

Karthe, D., Kasimov N. S., Chalov S. R., Shinkareva G. L., Malsy M., Menzel L., Theuring P., Hartwig M., Schweitzer C., Hofmann J., Priess J., Lychagin M. (2014). Integrating Multi-Scale Data For The Assessment Of Water Availability And Quality In The Kharaa - Orkhon - Selenga River System. *Geography, Environment, Sustainability.* 7, 3, pp. 65–86, doi:10.24057/2071-9388-2014-7-3-65-86.

Kasimov N., Karthe D., Chalov S. (2017). Environmental change in the Selenga River—Lake Baikal Basin. *Regional Environmental Change.* 17, 7 pp. 1945–1949.

Khromov S. P. Monsoon in the general circulation of the atmosphere (1956). In book: A.I. Voeikov and modern problems of climatology Hydrometeorological Publishing 283 (in Russian).

Kunz A., Konopka P., Müller R. and Pan L. L. (2011). Dynamical tropopause based on isentropic potential vorticity gradients. *Journal of Geophysical Research* 116, pp. D01110.

Kwon M., Jhun J.-G., Ha K.-J. (2007). Decadal change in East Asian summer monsoon circulation in the mid-1990s. *Geophysical Research Letters* 34, pp. L21706.

Lejenäs H., Øakland H. (1983). Characteristics of Northern Hemisphere blocking as determined from long time series of observational data. *Tellus* 35A, pp. 350–362.

Li J., Cook E. R., Chen F., Davi N., D'arrigo R., Gou X., Wright W. E., Fang K., Jin L., Shi J. Yang T. (2009). Summer monsoon moisture variability over China and Mongolia during the past four centuries. *Geophys. Res. Lett.* 36, pp. L22705, doi:10.1029/2009GL041162.

Li J., Ruan C. (2018). The North Atlantic–Eurasian teleconnection in summer and its effects on Eurasian climates. *Environmental Research Letters* 13, 2, P. 024007.

Loschenko K. A., Latyshev S.V., Potemkin V.L. (2010). Monitoring of dangerous weather phenomena in the territory of the Irkutsk Region. *Bulletin of ISTU* 3, 43, pp. 30–35.

Marchenko O.Yu., Berezhnykh T.V., Mordvinov V.I. (2012). Extremely water content of the Selenga River and features of the summer atmospheric circulation. *Meteorology and hydrology* 10, pp. 81–93 (in Russian with English summary).

Masato G., Hoskins B.J., Woollings T.J. (2011). Wave-breaking characteristics of midlatitude blocking. *Quarterly Journal of the Royal Meteorological Society* 138, 666, pp. 1285–1296.

Meyer-Christoffer A., Becker A., Finger P., Schneider U., Ziese M. (2018). GPCC Climatology Version 2018 at 1.0°: Monthly Land-Surface Precipitation Climatology for Every Month and the Total Year from Rain-Gauges built on GTS-based and Historical Data. DOI: 10.5676/DWD\_GPCC/CLIM\_M\_V2018\_100.

meteo.ru Access to the meteorological database (RIHMI-WDC) (in Russian) Available at <http://aisori.meteo.ru/ClimateR> [Accessed 11.08.2019].

meteoinfo.ru. Main Features Of Atmospheric Circulation (in Russian) Available at: <https://meteoinfo.ru/categ-articles/91-circulation-review/15380-osnovnye-osobennosti-atmosfernoj-tsirkulyatsii-i-pogody-v-severnom-polusharii-v-iyule-2018-goda> [Accessed 26.01.2019].

Mokhov I.I., Semenov V.A. (2016). Weather and Climate Anomalies in Russian Regions Related to Global Climate Change. *Russian Meteorology and Hydrology* 41, 2, pp. 84–92.

Moreido V. M., Kalugin A. S. (2017). Assessing possible changes in Selenga R. water regime in the XXI century based on a runoff formation model. *Water Resources* 44, pp. 390–398.

Obyazov V. A. (2015). Regional response of surface air temperatures to global changes: Evidence from the Transbaikal region. *Doklady Earth Sciences* 461, pp. 375–378 DOI: 10.1134/S1028334X15040054.

Palmén Eric H., Newton C.W. (1969). Atmospheric circulation systems: their structure and physical interpretation. Acad. Press, 606.

Sato N., Takahashi M. (2006). Dynamical Processes Related to the Appearance of Quasi-Stationary Waves on the Subtropical Jet in the Midsummer Northern Hemisphere. *Journal of Climate* 19, pp. 1531–1544.

Schamm K., Ziese M., Becker A., Finger P., Meyer-Christoffer A., Schneider U., Schröder M., Stender P. (2014). Global gridded precipitation over land: a description of the new GPCP First Guess Daily product. *Earth System Science Data* 6, 1, pp. 49–60.

Schubert S.D., Wang H., Koster R. D., Suarez M. J., Groisman P. Y. (2014). Northern Eurasian Heat Waves and Droughts. *Journal of Climate* 27, pp. 3169–207 doi: 10.1175/JCLI-D-13-00360.1.

tass.com. Flood emergency declared in Trans-Baikal Region Available at: <http://tass.com/emergencies/1012380> [Accessed 26.01.2019].

Tibaldi S., Molteni F. (1990). On the operational predictability of blocking. *Tellus V.42A*, pp. 343–365.

Wang X., Zhai P., Wang C. (2009). Variations in extratropical cyclone activity in northern East Asia *Advances in Atmospheric Sciences* 26, pp. 471–479.

Wirth V., Riemer M., Chang E. K. M., Martius O. (2018). Rossby Wave Packets on the Midlatitude Waveguide — A Review. *Monthly Weather Review* 146, pp. 1965–2001.

Yihui D., Chan J. C. L. (2005). The East Asian summer monsoon: an overview. *Meteorology and Atmospheric Physics* 89, pp. 117–42.

Zhang L., Zhou T. (2015). Decadal change of East Asian summer tropospheric temperature meridional gradient around the early 1990s *Science China Earth Sciences* 58, pp. 1609–1622.

Zhu C., Wang B., Qian W., Zhang B. (2012). Recent weakening of northern East Asian summer monsoon: A possible response to global warming. *Geophysical Research Letters* 39, pp. L09701.

Received on February 2<sup>nd</sup>, 2019

Accepted on August 8<sup>th</sup>, 2019

**Nikita M. Debkov<sup>1</sup>, Aleksey A. Aleinikov<sup>2</sup>, Alexander Gradel<sup>3</sup>, Anatoly Yu. Bocharov<sup>1</sup>, Nina V. Klimova<sup>1</sup> and Gennady I. Pudzha<sup>4</sup>**

<sup>1</sup> Institute of Monitoring of Climatic and Ecological Systems, Siberian Branch of the Russian Academy of Sciences, Tomsk, Russia

<sup>2</sup> Center of Forest Ecology and Productivity, Russian Academy of Sciences, Moscow, Russia

<sup>3</sup> Georg-August-Universität Göttingen, Göttingen, Germany

<sup>4</sup> National Research Tomsk State University, Tomsk, Russia

\* **Corresponding author:** nikitadebkov@yandex.ru

# IMPACTS OF THE INVASIVE FOUR-EYED FIR BARK BEETLE (*POLYGRAPHUS PROXIMUS* BLANDF.) ON SIBERIAN FIR (*ABIES SIBIRICA* LEDEB.) FORESTS IN SOUTHERN SIBERIA

**ABSTRACT.** The emergence and spread of non-native invasive forest insects represent a major potential threat to global biodiversity. The present study examines the current invasion of the far eastern four-eyed fir bark beetle *Polygraphus proximus* Blandf. in southern Siberian fir (*Abies sibirica* Ledeb.) forests. We collected data on 38 large sized (2500 m<sup>2</sup>) sample plots, situated in fir forests of the Tomsk region. As a direct result of the four-eyed fir bark beetle infestation, stand density decreased by 34-37%, and stand volume by 30%. The mean height, individual age and diameter at the stand level consequently increased. Our results indicated that stands with complete left-sided or normal ontogenetic structure (composed primarily of late virginal firs or firs in young reproductive stage) are more resistant to invasion by the four-eyed fir bark beetle. By contrast, fir forests characterized by more right-sided ontogenetic structure (composed primarily of mature and old reproductive firs), exhibited the least resistance and, with rare exception, degraded rapidly in response to the invasion. Our results also pointed to a mechanism that initiates invasions of the four-eyed fir bark beetle in fir stands of all types of ontogenetic structure, which is the attack of virginal trees and trees in early reproductive stages. Trees up to average diameter are the most susceptible to invasions of the bark beetle. We identified thicker bark, larger DBH and low occurrence of heart rot as the most important parameters for indicating resistance at the single tree level. DBH and bark thickness ( $p < 0.05$ ) correlated significantly with tree health status in infested stands. Our overall assessment of the potential natural regeneration of damaged stands is that the Siberian fir forests are resilient to invasive species and that the fir ecosystems can potentially recover from this disturbance.

**KEY WORDS:** invasion, stability, resilience, stand structure, taiga ecosystems, natural regeneration

**CITATION:** Nikita M. Debkov, Aleksey A. Aleinikov, Alexander Gradel, Anatoly Yu. Bocharov, Nina V. Klimova and Gennady I. Pudzha (2019) Impacts Of The Invasive Four-Eyed Fir Bark Beetle (*Polygraphus proximus* Blandf.) On Siberian Fir (*Abies sibirica* Ledeb.) Forests In Southern Siberia. *Geography, Environment, Sustainability*, Vol.12, No 3, p. 79-97  
DOI-10.24057/2071-9388-2019-35

## INTRODUCTION

The impact of herbivorous insects on forest ecosystems has interested researchers around the world (Lyamtsev, Isaev 2005; Palnikova et al. 2006; McCullough 2006; Bidart-Bouzat, Imeh-Nathaniel 2008; Rozendaal, Kobe 2016). Particular attention has been given to studying how invasive insects impact different tree species (Binimelis et al. 2007; Hulme et al. 2009; Bacon et al. 2012). The occurrence of invasive insects is particularly pervasive as these organisms are known for their fast growth, rapid reproduction and high dispersal ability (Roques et al. 2010). Ongoing global changes, including warmer temperatures associated with climate change, significantly affect the structural and functional organization of different habitat types that are further intensified when combined with the damaging effects of invasive organisms (Holdenrieder et al. 2004; Brockerhoff et al. 2006; Boyd et al. 2013) and can significantly reduce overall forest biodiversity (Born et al. 2005; Kenis et al. 2009; Straw et al. 2013). Of particular concern is the future of boreal forests, which are characterized by low species biodiversity and susceptibility to external disturbances (Sanderson et al. 2012). It is well known that since the beginning of this millennium, the processes of degradation of coniferous forests in the circumpolar boreal zone has intensified (Aitken et al. 2008; Allen et al. 2009; Worrall et al. 2010; Yousefpour et al. 2010; Martinez-Vilalta et al. 2012; Anderegg 2013). Long-term models of the situation in North America, for example, predict that the frequency of invasions will increase up to the end of the 21<sup>st</sup> century (Aukema et al. 2010; Dukes et al. 2009; Koch et al. 2011). There is strong evidence that globalization has facilitated widespread

outbreaks of invasive alien pests. Given the strong evidence that invasions at the global level are likely to continue, studies focused specifically on the resilience of native habitats against invasive alien pests have become highly important.

Against this backdrop of ongoing global processes, a unique phenomenon in the southern Siberian taiga has been observed, which is large-scale disturbance manifested in dying of large areas of Siberian fir (*Abies sibirica* Ledeb.) forests as a result of the invasion of the four-eyed fir bark beetle (*Polygraphus proximus* Blandf.), a new aggressive far eastern invader (Krivets et al. 2015a). This beetle was first identified in Siberia in 2008, in the vicinity of Tomsk (Baranchikov et al. 2011). The initial emergence of this invasive organism in southern Siberia has largely been attributed with wood importing by way of the Trans-Siberian Railway (Krivets et al. 2015b). In neighboring Mongolia, however, *Abies sibirica* distribution is scattered and limited to few of the northern Mongolian mountain ranges.

The four-eyed fir bark beetle *Polygraphus proximus* Blandford, 1894 is a beetle from the subfamily of bark beetles (Scolytinae) of the weevil family (Curculionidae). *P. proximus* develops under the bark of the tree in four stages: egg, larva, pupa, imago (Krivets et al. 2015b). The primary distribution of this beetle covers the southern part of the Russian Far East (Fig. 1), Northeast China, Korea and Japan. It usually only occurs in forests with trees of the genus *Abies* (Stark 1952). In the primary distribution within the Russian Far East, the local species of harvested fir are susceptible to the four-eyed fir bark beetle – *A. nephrolepis*, *A. sachalinensis*, to a lesser extent *A. holophylla* and *A.*

mayriana (Krivolutskaya 1958). However, especially in its secondary distribution range the impact have only recently become evident and the effects of the invader on the autochthon Siberian fir ecosystems are hardly known.

Our objective therefore was to assess and evaluate (1) the impact of *Polygraphus proximus* on the forest structure in Siberian fir stands in its secondary distribution range, (2) the stability of Siberian fir against the four-eyed fir bark beetle, (3) the renewable potential of fir ecosystems and prediction of their succession dynamics.

## MATERIALS AND METHODS

### Study area

We conducted our research between 2012 and 2018 in the Tomsk region, one of the recipient regions of the four-eyed fir bark beetle invasion. Field studies were conducted in 8 of the 16 administrative districts of the region (Tomsky, Asinovsky, Pervomaysky, Teguldetsky, Shegarsky, Krivosheinsky, Bakcharsky and Chainsky). The course of our field work included

inspecting fir stands located in both harvested forests and in natural forests under different protection categories, including specially protected natural territories (Larinsky, Poskoyevsky, Tomsky and Kaltaysky reserves) (Fig. 1).

The present study builds on previous studies that investigated impacts of the bark beetle on selected sample plots in Siberian fir forests through a more basic analytical approach (Debkov 2018a; 2018b). Our study is aimed at a more comprehensive picture by examining the dynamics of these invasions on Siberian fir using more thorough data and broader analyses. Our database for this study includes 38 sample plots (SP).

### Specific characteristics of the selected stands

In the vast majority of the surveyed stands, Siberian fir is the dominant species. But we also included stands dominated by Siberian spruce (*Picea obovata* Ledeb.; SP 3 and 33), Siberian pine (*Pinus sibirica* Du Tour; SP 2), Aspen (*Populus tremula* L.; SP 31) and Silver birch (*Betula pubescens* Roth;



Fig. 1. Distribution areas map of *Polygraphus proximus* and species of the genus *Abies*

SP 38). The composition of the fir stands in terms of relative distribution varies fairly significantly – from approximately 30 to 100 percent. Most of the stands are even aged (76%). About 24% are uneven aged. Most of the studied stands are of average density (67%), but the proportion of high-density communities is significant (33%). The majority of the studied stands are characterized by high productivity (67%), with the remaining at average productivity (33%). The main forest floor type (hereinafter referred to as forest type) according to the dominating species belong all to so-called “grass-types”: low grass: *Oxalis acetosella* L., *Carex macroura* Meinsh., *Stellaria bungeana* Fenzl., medium grass: *Aegopodium podagraria* L., *Dryopteris Adans.*, *Athyrium filix-femina* (L.) Roth., high grass: *Aconitum septentrionale* Koelle, *Thalictrum minus* L., *Matteuccia struthiopteris* (L.) Tod. All selected stands were observed to be affected by the four-eyed fir bark beetle.

#### Data assessment and classification of stand health via AWTS-index in the sample plots

We established SPs with a size of 0.25 hectares in each of the selected stands. The minimum number of trees of the main canopy in each plot is 100. We assessed the traditional stand parameters (DBH, tree height, and average tree age) and used different methods for measuring additional parameters on the plots. To measure the degree to which individual fir trees were affected by *Polygraphus proximus* outbreaks, we assessed health status of individual trees (TS) using to the scale of categories developed by Krivets et al. (2015b): I – healthy, with no signs of weakening, not attacked by the bark beetle; II – weakened, attacked by the bark beetle, but not settled (unsuccessful attempts at colonization); III – heavily weakened, attacked by the bark beetle, but not colonized; IV – drying (dying), colonized by the bark beetle, while upper crown maintains green needles; V – dead standing tree, from the current year, with discolored needles; and VI – dead standing tree, from past years, with visible signs of

bark beetle infestation on the stems, the entire crown without needles. Based on this evaluation, we derived the *average weight tree health status* (AWTS-index) for all firs in each SP (formula 1).

The surveyed stands belonged to mature age groups and were characterized at the time of the study by varying degrees of health status – from weakened (AWTS is 1.6–2.5 points) to severely weakened (AWTS varies within 2.6–3.5 points) and degraded (AWTS is 3.6 points and above). The calculation of the AWTS-index was performed by the following formula (Krivets et al. 2015b):

$$AWTS = \frac{\Sigma g_1 + 2\Sigma g_2 + 3\Sigma g_3 + 4\Sigma g_4 + 5\Sigma g_5 + 6\Sigma g_6}{\Sigma G} \quad (1)$$

where AWTS is the average weighted category of tree status in the respective stand;  $\Sigma g_1, \Sigma g_2, \Sigma g_3, \Sigma g_4, \Sigma g_5, \Sigma g_6$  is the sum of the basal areas in the SP of the above mentioned respective categories (1-6;  $\Sigma G$  is the sum of basal areas of all fir trees in the SP. See Appendix A.

#### Overview of the current distribution of the invasive bark beetle in Russia

Based on the literature, our data and additional data provided by branches of the Russian Forest Protection Center, we will provide an overview describing recent distribution patterns of the bark beetle and the current extent of outbreaks that, in some cases, have reached widespread epidemic levels.

#### Evaluation of the impact of the invasive bark beetle on the stand structure of fir ecosystems

The experimental material is based on data obtained from 2 permanent SPs (no. 61 and 62), which were established in 2010 on the territory of the Kaltaisky Zoological Reserve and in the harvested forests of the Timiryazevsky forest unit in the Tomsk region. The uniqueness of this material is that the SPs were established before the beginning of the mass invasion of the four-eyed fir bark beetle in this territory, which began in 2011 (Kerchev, Krivets

2012). During the establishment phase of the SPs, we observed abundant resin pitches on the fir trunks, which signals that an invasion has occurred (Krivets et al. 2015b), but there were no signs of excessive dryness.

We made sure that each SP included not less than 200 trees. Tree diameters were measured with an accuracy of 1 mm with a caliper (Haglölf). Model trees outside of the SP perimeter were then selected using the method of proportional representation. The initial number of model trees was 30 pieces within the SP. Felling and bucking trees were carried out using the chainsaw brand STIHL MS 180.

The volume of tree trunks was determined by the complex Huber formula (Anuchin 1982):

$$V = (g_1 + g_2 + \dots + g_n) * L + (g_t + l_t) / 3 \quad (2)$$

where  $g_1, g_2, \dots, g_n$  – basal areas in the middle of the 2-meter sections,  $L$  – section length,  $g_t$  – basal area of the base of the top,  $l_t$  – top length.

### Evaluation of the impact of the invasive bark beetle on the ontogenetic structure of fir ecosystems

Determining the ontogenetic states of Siberian fir trees and regeneration in the foci of the four-eyed fir bark beetle invasion was carried out taking the developed periodization of *Abies sibirica* ontogenesis into account, which represent stages of biological age (Mahatkov 1998; Methodological approach 2010; Evstigneev, Korotkov 2016; Smirnova et al. 2017). In our study, we attributed the ontogenetic features to two levels: regeneration and canopy structure. Early and late immature (im1, im2), early virginal plants (v1) were attributed to regeneration, whereas late virginal (v2) and reproductive trees (young reproductive trees: g1; mature reproductive trees: g2; old reproductive trees: g3) were attributed to the canopy.

The ontogenetic structure was measured on 14 SPs. Overall, 1035 fir trees and 1042

saplings were measured. We hypothesized that attack by the bark beetle can change the proportions of the ontogenetic stages of the stands, and by doing so, can lead to disruption of the regeneration process at tree level.

### Evaluation of the stability of Siberian fir trees to the impact of the invasive bark beetle

In the context of this study the term “stability” is understood on single tree level as the ability of a fir tree to survive a beetle attack, and on the collective level (stand) as the ability of the forest ecosystem to maintain its structure and nature of functioning in space and time under changing environmental conditions, including biotic factors in the form of xylophagous insects. To gauge the stability of fir trees against the bark beetle we collected data pertaining to key variables of fir trees, that we hypothesized to be decisive indicators of the stability against the beetle attacks. These variables are: tree age, DBH, bark thickness, occurrence of heart rot, and radial growth dynamics. We collected the respective data on 22 plots (Appendix A). We used incremental borers (length of 400 mm; diameter of 5.15 mm, Haglölf) to determine the presence of heart rot and determine tree age. DBH and the bark thickness were measured using calipers. All measurements and core sampling were performed at a height of 1.3 m. In that way on each SP, 10 samples were taken from both living trees (AWTS category I-III), and dead trees killed by the bark beetle (AWTS category V-VI). We hypothesized that the selected variables represent key indicators for conducting a rapid assessment of the stability of fir forests against the four-eyed fir bark beetle.

### Evaluation of natural regeneration potential of damaged fir forests

Regeneration was assessed in a modified form according to Pobedinsky (1966) on each of the regeneration plots (RP). Depending on the characteristics of the communities (occupied area and quantitative parameters of regeneration), the assessment was carried out on continuous transects with square-sized RPs of 4 m<sup>2</sup> each, which resulted in 25

RPs or as a discontinuous transects with 30 circular RPs with a size of 10 m<sup>2</sup> each. We assessed species, height, basal diameter, age, density, length and projection of the crown, linear growth of the axial shoot and side shoot of the first order. We additionally selected saplings models composed of 3 individuals per height group to determine the morphological characteristics and age. The distribution pattern of the natural regeneration was estimated by occurrence (the ratio of the number of RPs with at least 1 sapling to the total number of RPs). For studying the spatial distribution of the regeneration, the scattering index, proposed by R.A. Fisher (Svalov 1985) was applied:

$$f = \frac{(\sum x^2 * n_x - N^2 / n) * n}{(n-1) * N} \quad (3)$$

where  $x = 0, 1, 2, \dots$ , regeneration number on RP,  $n_x$  – RP number with  $0, 1, 2, \dots$ , regeneration number;  $n$  – sum RPs on the respective SP;  $N$  – overall regeneration number on SP.

Statistical analysis of our data was carried out using the STATISTICA 10 program (Statsoft 2010). In addition to the standard descriptive statistics (mean±standart error), the non-parametric Mann-Whitney test and Kruskal-Wallis test were used to test the significance of the respective parameter with a level of  $p < 0.05$ . The Kruskal-Wallis one-way analysis of variance by ranks test was used to compare the parameters of stability (occurrence of heart rot, age, DBH, thickness of bark, radial growth) against *P. proximus*. Several independent groups were compared by using the AWTS as dependent variable. The Kruskal-Wallis test is used to detect the differences between several independent groups. In the case of two independent groups the result is equivalent to that of the Mann Whitney U test (Sheskin, 2004).

## RESULTS

### Current distribution of the four-eyed fir bark beetle in Russia

In 2015, the scale of the secondary range of the four-eyed fir bark beetle on the territory of southern Siberia was assessed (Krivets et al. 2015b). At that time, this beetle was observed to be present in 7 regions of

the Siberian Federal District of the Russian Federation: Tomsk, Novosibirsk, Kemerovo, Altai and Krasnoyarsk, the Republics of Altai and Khakassia. The approximate area of the invasive four-eyed fir bark beetle range was 560 thousand km<sup>2</sup>, which is slightly more than the area of a European country such as France. To date, the presence of the four-eyed fir bark beetle has been confirmed on the territory of another constituent entity of the Russian Federation – the Irkutsk Region. On the territory of the Republics of Altai and Khakassia, the invasive beetle is so far absent. The invasion range in Kemerovo (2 administrative districts, 9.1 thousand km<sup>2</sup>), Novosibirsk (1 administrative district, 13.9 thousand km<sup>2</sup>) and Altai (1 administrative district, 2.5 thousand km<sup>2</sup>) increased slightly. The increase in the secondary range on territory of Tomsk (9 administrative districts, 172.7 thousand km<sup>2</sup>) and the Krasnoyarsk (14 administrative districts, 125.5 thousand km<sup>2</sup>) was most pronounced. Thus, for the period from 2015 to 2018 the overall range of invasion appeared to increase by approximately 323.7 thousand km<sup>2</sup> (or 58%).

### General characteristics of damaged forests

The surveyed fir stands are typical for southern Siberia and belong to the common group of the forest floor types – grass. One of the characteristic features of fir forests in the flat plains of the Siberian taiga is that due to their rather narrow ecological amplitude, they are confined to trophic habitats with sufficient moisture regimes. This is confirmed by a slight variation of the yield classes (II–III).

The health status of fir stands varies greatly. AWTS ranged from 1.4 (no degradation, SP 60) to 5.2 (heavy degradation, SP 53). We observed that 29% of the surveyed stands appeared to be weakened, with 25% as severely weakened, and 46% of the stands showed signs of degradation. See appendix A.

### Evaluation of the impact of the invasive beetle on the structure of the fir stands

During the observation period (SP 61 and 62) from 2010 to 2017, stand density increased by 9 and 26%, respectively (Debkov 2018a). This

increase was largely due to ingrowth of young firs into the tree canopy. However, despite the increase of firs in stand composition by 2017, due to damage by the four-eyed fir bark beetle, the number of viable trees decreased by 37 and 34%, respectively. This led to an increase in the share of other species, and the relative share of fir in composition decreased by 11.5% and 14.7%, respectively.

The dynamics of diameter distribution (Fig. 2) showed that throughout the 7 years of the observation period the stands became thicker (increase on the right part of distribution), by about one DBH class. On other hand, it was replenished with new trees (the left part of distribution). The presence of the four-eyed fir bark beetle clearly did not affect the right side of the diameter distribution, but it significantly affected the left side by shifting it from asymmetric and peaked (asymmetry coefficient was  $1.83 \pm 0.15$ , the excess was  $1.73 \pm 0.30$ ) towards a normal distribution (asymmetry coefficient of  $0.08 \pm 0.18$ , the excess –  $0.58 \pm 0.36$ ). The average diameter increased from  $18.6 \pm 0.5$  cm in 2010 to  $21.5 \pm 0.6$  cm in 2017. While the standard deviation remained the same, the variation coefficient decreased from 40 to 35%.

An important indicator of the stand is the standing volume. In 2010, at SP 61, the standing volume of fir trees was  $131 \text{ m}^3/\text{ha}$ . When recalculated in 2017, taking the replenishment with new trees and the increased volume of those existing into account, it should have been  $186 \text{ m}^3/\text{ha}$ . However, as a result of being attacked by

the invasive beetle, the standing volume remained at the same level ( $131 \text{ m}^3/\text{ha}$ ), i.e. the loss of standing volume was  $55 \text{ m}^3/\text{ha}$  or 30%. The ratio of loss of density and productivity also indirectly indicates the nature of the damage itself: fir density decreased by 49%, and standing volume by 30%.

The average age of the studied fir trees in 2010 was  $84.7 \pm 1.6$  years, the average height was  $20.3 \pm 0.4$  m and the average diameter was  $21.2 \pm 0.7$  cm. With normal replenishment of the tree canopy by young fir, by 2017 age should have decreased to  $79.6 \pm 1.5$  years, height to  $19.1 \pm 0.3$  m and diameter to  $18.8 \pm 0.7$  cm. This would be expected since ingrowth of young trees should have taken place. But as a result of the four-eyed fir bark beetle invasion, the average age increased significantly to  $97.5 \pm 2.5$  years, the average height to  $23.3 \pm 0.5$  m and the average diameter to  $27.6 \pm 1.2$  cm. The variation coefficients of the mentioned parameter decreased due to the impact of the bark beetle. The stand structure became more uniform and less diverse.

### Evaluation of the impact of the invasive bark beetle on the ontogenetic structure of fir ecosystems

The percentage of beetle-infested dead trees in the studied stands with a left-sided ontogenetic structure varied significantly (Debkov 2018b), and generally ranged from 23% to 92%. We did, however, observe a connection in terms of the nature of the invasion itself. This is that the initial stage of

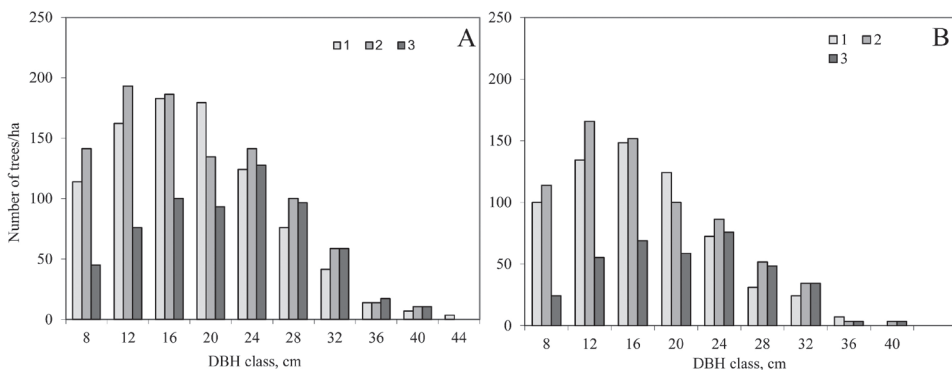


**Fig. 2. Dynamics of the diameter distribution of the whole stand (A) and firs in the stand (B). Numbers refer to assessments in respective years: 1 = 2010; 2 = 2017; 3 = 2017 without dead *A. sibirica***

the bark beetle infestation resulted in damage exclusively limited to late virginal trees (v2) and young reproductive trees (g1). Further, the percentage of dead trees within these ontogenetic stages increased, which then included mature (g2) and old reproductive trees (g3). In our study stands, significant mortality of mature and old reproductive trees exceeding the natural background level was not fixed ( $2.0 \pm 0.7\%$  and  $1.2 \pm 0.7\%$ , respectively). Mortality of younger trees ranged from  $10.0 \pm 2.9\%$  among young reproductive trees to  $38.0 \pm 10.4\%$  in late virginal trees (v2). At the same time, it should be noted that significant decay among mature trees, particularly old reproductive trees (g3), was observed in those fir stands where the percentage of trees within these ontogenetic stages were insignificant (less than 5–10%). See Fig. 3 for an overview of fir forests with different ontogenetic structure of living trees.

The percentage of dead trees in the fir stands characterized by right-sided ontogenetic structure also varied fairly significantly (from 18% to 89%), however this was linked with the percentage of old reproductive trees. While tree mortality was observed among firs across all ontogenetic stages, the breakdown was total loss of late virginal and young reproductive trees,  $6.0 \pm 2.1\%$  of mature reproductive trees, while  $10.7 \pm 1.2\%$  of old reproductive fir trees survived.

A comparative analysis showed that for stands with a left-sided ontogenetic structure the AWTS was  $3.0 \pm 0.6$  (with a range of 1.6 to 4.6), and for ones with a right-sided ontogenetic structure the AWTS value was  $3.6 \pm 0.8$  (with a range of 1.4 to 5.2). However, these differences are not statistically significant.

**Evaluation of the stability of Siberian fir trees to the impact of the invasive bark beetle**

In our analysis on the overall forest stands health during the primary and secondary distribution of the bark beetle invasions in the Tomsk region, no significant differences were found (Mann-Whitney test,  $p = 0.6333$ ). This suggested to us that infestations of the bark beetle affect the entirety of the stand, attacking all available trees at one time, which weakens the forage base for future generations. Overall stand health is largely determined by its growth and vitality. As such, more viable stands merely weakened in response to infestation by the beetle, while less viable stands showed rapid degradation. We found that the residence time of the four-eyed fir bark beetle in specific stands played a secondary role and did not change between the areas of primary and secondary distribution.

The average occurrence of heart rot in living fir trees was  $13.6 \pm 3.6\%$  (Appendix B). The prevalence of rot in dead trees was significantly higher with  $22.6 \pm 4.9\%$ . However, despite these differences, the Mann-Whitney

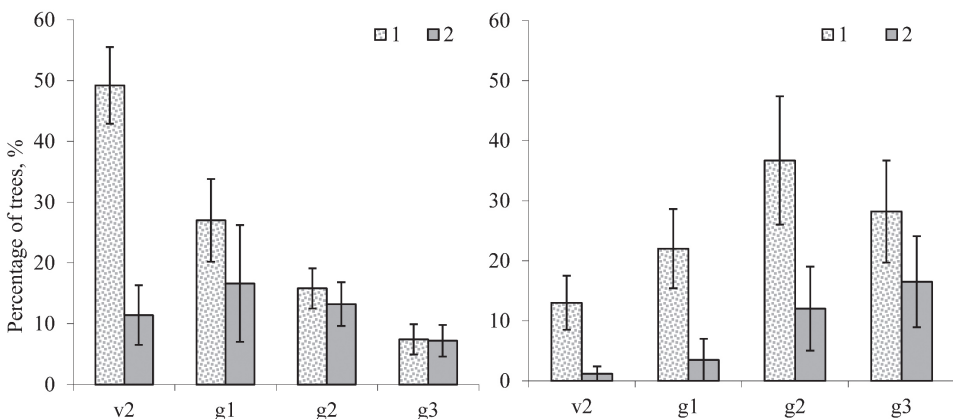


**Fig. 3. Fir forests with left-sided and right-sided ontogenetic structure.**

*v<sub>2</sub>* – late virginal plants; *g<sub>1</sub>*, *g<sub>2</sub>*, *g<sub>3</sub>* – young, mature, and old reproductive plants.  
 1 – before impact, 2 – after impact.

test did not confirm the hypothesis in terms of the effect of rot on tree health ( $p = 0.1995$ ). A significant occurrence of heart rot in living trees in severely damaged stands was not confirmed (Kruskal-Wallis test,  $p = 0.3241$ ). We did, however, note a significant difference in the prevalence of heart rot in dead trees depending on the degree the fir stands had weakened (Kruskal-Wallis test,  $p = 0.0285$ ).

The average age of living trees ( $75 \pm 5$  years) did not differ from that of dead firs ( $73 \pm 3$  years). The range of age variation was greater in living trees (40–132 years) than it was for dead fir trees (42–106 years). The Mann-Whitney test rejected the hypothesis tree age has an influential effect on tree health ( $p = 0.9799$ ). We found no significant relation between age and tree health, in terms of living and dead trees in the series of damaged stands. (Kruskal-Wallis test,  $p = 0.8124$ ,  $p = 0.7728$ , respectively).

We found that the average DBH of living trees was  $28.1 \pm 1.4$  cm. Comparatively, the DBH of dead trees was substantially less, measuring  $23.2 \pm 1.1$  cm. The DBH of living trees varied from between 13.5 and 41.9 cm, whereas DBH for dead firs between ranged from 16.1 to 34.0 cm. The Mann-Whitney test confirmed the significant influence of DBH on the tree health ( $p = 0.0068$ ). The relation between DBH and tree health, in terms of living and dead trees in the series of damaged stands, was not confirmed (Kruskal-Wallis test,  $p = 0.4329$ ,  $p = 0.7112$ , respectively).

The average thickness of bark from living trees was  $8.0 \pm 0.3$  mm, which represented

an absolute range from 5.0 to 11.8 mm. By comparison, the average bark thickness of dead trees was substantially less and measured at  $6.2 \pm 0.2$  mm, within an absolute range of 4.6 to 8.4 mm. The Mann-Whitney test confirmed our hypothesis that bark thickness significantly influences the health status of trees ( $p = 0.0002$ ). The relation between bark thickness and tree health, in terms of living and dead trees in the series of damaged stands, was not confirmed (Kruskal-Wallis test,  $p = 0.1941$ ,  $p = 0.2500$ ). See Appendix B.

The average radial growth in stands in early stages of succession dynamics (SP 32) was  $1.56 \pm 0.06$  mm/year (Fig. 4). The growth gain in dead trees was significantly lower  $1.25 \pm 0.08$  mm/year compared to living firs with  $1.71 \pm 0.07$  mm/year. The Mann-Whitney test confirmed that radial growth is an important indicator of overall tree health ( $p = 0.0001$ ). The average radial growth in late stages of succession (SP 34) was  $2.29 \pm 0.06$  mm/year. The growth gain in dead trees was significantly lower  $1.97 \pm 0.12$  mm/year than in living firs –  $2.38 \pm 0.07$  mm/year. The Mann-Whitney test confirmed the hypothesis that radial growth is an indicator of tree health status ( $p = 0.0025$ ). The value of radial growth on SP 32 was higher than on SP 34, which also affected the degree of damage.

### Evaluation of the natural regeneration potential in damaged fir stands

The species composition of natural regeneration in all studied fir stands is completely dominated (81–100%) by *Abies sibirica*, *Picea obovata* (1–9%),

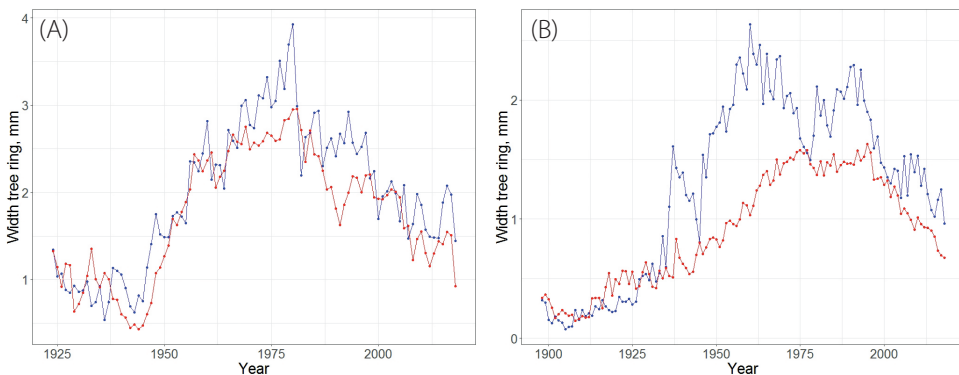


**Fig. 4. Dynamics of radial growth at a later (A) and earlier (B) successional stage of development fir forests. Red line – trees killed by *P. proximus*, blue line – live trees**

*Populus tremula* (1–9%) and *Pinus sibirica* (1–4%) which are most often present as accompanying species. The viability of natural regeneration can be determined by considering morphological indicators given in Appendix C, which characterize the assimilation apparatus (crown) of saplings.

The mean of occurrence rate in the RPs of saplings was  $73 \pm 5\%$  (limits 22–100% on the SPs), and no significant differences were found in the degree of damage of the stand (Fig. 5). The average mean number of saplings was  $5091 \pm 1039$  per ha (range: 260–19200 per ha). We assume a threshold value of 1500 per ha to ensure the natural restoration of fir forests. This value was observed in approximately 76% of the studied stands.

The dynamics of spatial structure of natural regeneration was heterogeneous. The scattering coefficient steadily exceeded 1, while it was higher in mixed stands and dominated by small and medium-sized saplings. This indicates clumped groups of regeneration on one hand (with an occurrence below 65%) and a variable density with regular/uniform occurrence of saplings (above 65%) on the other. For degraded fir forests, the scattering coefficient is  $1.9 \pm 0.3$  (limits 1.1–3.4), for severely weakened with fir trees –  $6.0 \pm 1.8$  (limits 1.4–14.1) and for weakened –  $3.0 \pm 1.0$  (limits 1.0–5.9). We did not find a significant difference in the values of this indicator (Mann-Whitney test,  $p = 0.0530$ ). See appendix C.

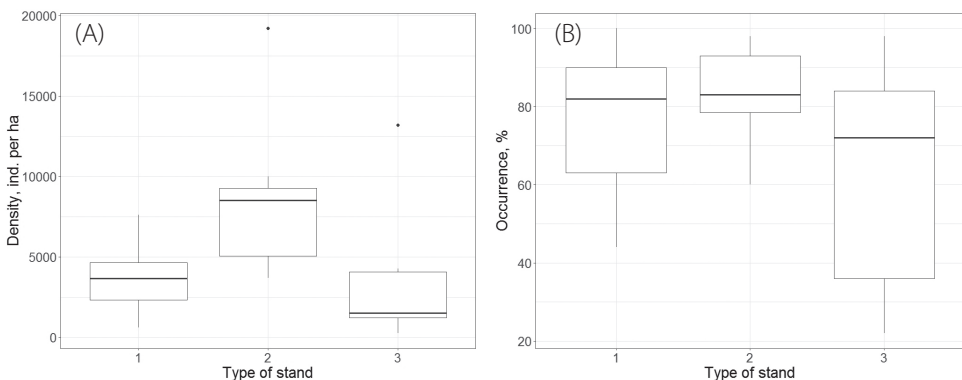


**Fig. 5. The density (A) and occurrence (B) of natural regeneration in fir forests damaged by the four-eyed fir bark beetle. Type of stand: 1 – weakened, 2 – severely weakened, 3 – degraded**

## DISCUSSION

Before discussing our results in the context of single tree - stand- and landscape level, some specific facts on the biology of the beetle should be mentioned. According to Kerchev (2013) the average fertility of the female in the invasive range is  $45,2 \pm 15,3$  eggs, which corresponds to the data in the primary distribution (Yamaguchi 1963). In laboratory, it takes about 50 days under the bark until the first young beetles fly out. Due to sufficient temperatures during the growing season in Western Siberia, as well as in the primary range (Kurentsov 1941; Krivolutskaya 1958), the four-eyed fir bark beetle develops two generations. Most favorable are summer days with sunny calm weather and air temperature above  $15^{\circ}\text{C}$  (Krivets et al. 2015b). Overall 24 species of predatory insects of the four-eyed fir bark beetle have been registered in Western Siberia (Kerchev 2013). Among these, most of the local species are facultative predators of the families *Tenebrionidae*, *Laemophloeidae*, *Colydiidae*, *Histeridae* and *Staphylinidae*. The most popular is the obligate predator of the four-eyed fir bark beetle – the bark beetle *Medetera penicillata* Neg. (Diptera, Dolichopodidae), a species previously unknown to Siberia, described in Japan and Primorsky Krai (Negrobov 1970), and apparently imported together with *P. proximus*. Currently, this species is considered as being the most prominent regulator of the four-eyed fir bark beetle population.

## Tree size matters

The loss of tree species or part of their population changes the local environment, disrupts the main ecosystem processes, including decomposition rates, nutrient movement, carbon uptake and energy flow. In contrast to earlier studies (Baranchikov et al. 2011), we found that the degree of the bark beetle infestation damage in a stand is related to tree diameters. Trees with smaller diameters were clearly more often affected and more seriously damaged than larger trees. Overall, we observed that while invasions by the four-eyed fir bark beetle are systematic and thorough in nature, in that all trees within the stand, including undergrowth, are affected, the most damaging impact is to smaller trees.

Invasions of non-native organisms on native biota often lead to extremely negative consequences that have obvious, direct and measurable economic repercussions. Forest degradation occurs in cases where the impacts of invasions are severe enough to cause a reduction of the host tree species population and relevant, disruptive changes to forest ecological functions and biodiversity. One example of this is the heavy damage to white pine (*Pinus strobus*) forests invaded by white pine blister rust *Cronartium ribicola* (Ostry et al. 2010).

One result we observed in some stands was the increase of several stand parameters (height, age, diameter), while productivity, crown density and stand density decreased. The yield class however was unaffected. Importantly, infestation by the bark beetle appeared to have a homogenizing effect on the stand level in terms of height, age and diameter, which represents one of most consequential, long-term impacts on fir forests. The obtained data characterizing the occurrence of heart rot showed that standing dead fir trees are roughly two times more likely to be infected by heart rot compared to living trees. Some authors (Donyakina et al. 2013) believe that infection by fungal diseases, in particular,

annosus root rot *Fomitopsis annosa*, which leads to the development of rot, is a major factor contributing to the susceptibility of fir trees to infestation by the four-eyed fir bark beetle.

We found no clear connection linking tree age and natural predisposition to attack by the four-eyed fir bark beetle. But one study on the impacts of pine bark beetle *Ips confusus* in forests growing in the southwestern United States dominated by pinyon pine (*Pinus edulis*) showed that it was primarily larger, older trees that suffered the most negative effects (Floyd et al. 2009).

Our study revealed that after infestation the mean DBH compared to dead fir trees is about one DBH class higher (4 cm). The less disturbed stands are characterized by the presence of stronger trees, which, in our case, were firs with a diameter of 30 cm. Based on our results, we can consider trees with diameters of 30 cm as the upper limit for potential attack by the four-eyed fir bark beetle. We should note that one of the first studies on invasions of the four-eyed fir bark beetle (Baranchikov et al. 2011), reported an absence of any association between the reproduction and spread of the beetle with tree diameter sizes. Our own results could not confirm this. This was also the case for other authors (Bleiker et al. 2003), who showed that as a result of impact of western balsam bark beetle *Dryocoetes confusus* on fir state of subalpine fir *Abies lasiocarpa*, trees of medium and above diameter are often damaged, which the authors explained is due to lower resistance levels of old-aged trees. Our data show that tree mortality in fir stands correlated directly to mean diameter.

The assumption that bark thickness plays a crucial role in tree susceptibility to attack by the four-eyed fir bark beetle has been confirmed. We effectively established that strong individuals exhibit higher resistance when bark thickness measures 8–10 mm and higher. Therefore, when the invasive four-eyed bark beetle attacks stands characterized as more stable, it will

necessarily target thin-barked individuals. One aspect of trees growth is the radial growth, which was previously shown to be connected with tree resistance against invasion by the bark beetle (Baranchikov et al. 2014). This was confirmed in our study. We consider radial growth as an indicator of tree health. Healthier trees are more likely to survive an attack.

### **Attacked Siberian fir stands have the potential to regenerate**

The most important element of a forest ecosystem is its capacity for natural regeneration. The impact of invasive organisms can either lead to complete destruction of young generations, or significantly slow down processes of their growth and development to such an extent that there is a change in dominant tree layer (McLaren et al. 2009). Our data indicate that invasion by the four-eyed fir bark beetle represents clear, but not extreme, pressure on regeneration processes. The frequency and quality of fir regeneration in most of stands subjected to invasion of the four-eyed fir bark beetle are generally satisfactory and, in the long-term, will ensure that natural restoration of fir forests continues.

This is particularly important when considering that the effects of an invasive organism can often lead to an increase in regenerative functions of the damaged ecosystems, for example when gaps formed in canopy resulted from the death of eastern hemlock *Tsuga canadensis* trees subjected to invasion of organisms that attacked its undergrowth (Fajvan, Wood 1996; Small, M.J. Small, C.J. Dreyer 2005). At the same time, both in the above-mentioned examples, and according to data (Jenkins 2003) in forests dominated by Fraser fir *Abies frazeri*, a decrease in the frequency of natural regeneration was observed. Accompanying species can strengthen the regeneration process, even if we did not observe this particular dynamic in our own study. However, it was concluded that even these features of regeneration make it possible to continue domination of the main tree

species in long term, eastern hemlock *Tsuga canadensis* (Weckel et al. 2006) and Fraser fir *Abies frazeri* (Stehn et al. 2003), respectively.

Interestingly, one significant impact of the beetle was in the second layer of suppressed trees, of those just beginning to grow into canopy, as well as to some parts of tree canopy itself. The severe damage commonly observed in this category of trees represents a clear disruption of fir forests natural growth dynamics. A critical remaining question pertains to the frequency of such infestations. Indeed, at present, the fir forests in areas where the bark beetle invasions have occurred show strong natural regeneration. This suggests that fir will likely continue as the dominant species in the Tomsk region.

### **The impact of the bark beetle on dark taiga ecosystems in the context of climate change and increased utilization pressure in the region**

Several studies have recently described a general retreat and degradation of dark coniferous forests throughout Northern Asia, parts of Europe and Russia (Zamolodchikov 2012; Kharuk et al. 2013; Kharuk et al. 2016). These authors describe the decline not limited to fir, but include the other two main dark coniferous species (*Pinus sibirica* and *Picea obovata*). Kharuk et al. (2013; 2016) view the bark beetle infestation as secondary disturbance force and one aspect of the large-scale decline of fir and Siberian pine growing in the southern Siberian Mountains. The same authors consider warmer temperatures associated with climate change, and subsequent drought conditions, as the major forces driving forest degradation in the region. In Mongolia, according to Dulamsuren (2004), *Abies sibirica* occurs westwards of Lake Hovsgul and in the Khentey Mountain range and, due to its limited distribution range, it is included in the national Red List of threatened Species. Species like *Abies sibirica* that thrive in humid environments are, in this region, naturally limited to growing at higher elevations with higher precipitation

and on sites with northern or northeastern exposition. Due to their remote distribution, fir stands in Mongolia have relatively high conservation value due to the fact that they have remained largely undisturbed in that they include stands that have never been used for commercial exploitation. There is no evidence to date that invasions of *Polygraphus proximus* have occurred in Mongolia, but this very mobile bark beetle constitutes a potential threat to the valuable Mongolian and Siberian fir stands, especially in the context of current prevailing drivers of forest change in the region, such as forest fires, illegal logging and climate change (Dulamsuren 2011; Kharuk et al. 2013; Gradel 2017; Juříčka et al. 2018). The observed decline of fir in Siberia has primarily occurred in stands subjected to drought stress, which is an underlying factor that weakens the forest stands and make them more susceptible to invasive insects. A relation of increased establishment and spread of bark beetle and climate warming was also found for other regions in the world (Carrol et al. 2003; Dordel 2005; Seidl et al. 2008; Katz 2017). Climate warming is considered to be a main driver for the recent range expansion and accelerated reproduction of the Mountain pine beetle in North America (Carrol et al. 2003; Mitton and Ferrenburg 2012). In Central Europe, artificial spruce plantations have recently facilitated the establishment and spread of *Ips duplicatus*, and more widespread outbreaks are predicted to increase (Petercord and Lemme 2019). Thus, we can also expect further expansion of the four-eyed fir bark beetle to neighboring regions. Due to the specific nature of local climate conditions, such as increasing aridity, Siberian fir forests along the Siberian Mongolian border region are naturally sparse and grow in only few mountain ranges in the region. The occurrence of an invasive bark beetle would add to already existing pressures on these dark coniferous ecosystems. In a study on spruce forests in northern Mongolia, James (2011) found a growth decline of spruce that was significantly connected with higher temperatures. Similarly, Gradel et al. (2018) reported a decline of spruce

during a four-year monitoring interval of a dark coniferous forest outpost situated on a mountain top and surrounded by fire damaged Mountain forest steppe. In this stand, the spruces were gradually replaced by light taiga species, such as birch and larch (Gradel et al. 2018). Possible causes may be changes in water balance, short-term infestations of insects or warmer temperatures associated with global warming (Gradel et al. 2018). Spruce stands are known to be highly sensitive to temperature increase (Zang et al. 2011). Along these same lines, Kharuk et al. (2013) reported in their study of southern Siberia that among several species growing within the same stand, Siberian pines suffered from drought, whereas birch and aspen trees were not affected. The same authors pointed out that stand decline of Siberian pines (> 75 % tree mortality) mainly occurred on southern slopes, where the bark beetle appear to thrive. Exposition is therefore also of importance in terms of stands' susceptibility to disturbance, especially in the context of increasing temperatures. In a study on the relation between wild fires and infestation by the Silk moth (*Dendrolimus sibiricus* Tschetv.) in Siberia, Kharuk and Antamoshkina (2017) found that pest outbreak areas are up to seven times more often affected by fires compared to reference sites. Since fires are also expected to become more frequent throughout the region due to global warming (Tchebakova et al. 2011) we can conclude that the four-eyed fir bark beetle may very well represent an additional, potentially dangerous threat to the disturbance-sensitive dark coniferous ecosystem.

Despite considerable research of the problem of *P. proximus* invasion in Siberian fir forests, there are gaps that require further research. In particular, the mechanism of fir stability to the impacts of the four-eyed fir bark beetle at the physiological and biochemical levels has not been studied sufficiently. Specific features of the feed substrate (for example, its moisture content) on invasive bark beetle population are poorly assessed. In future research, the climatic conditionality

of the mass reproduction of *P. proximus* needs to be understood better.

## CONCLUSIONS

Our results indicate that stands with left-sided ontogenetic structure are less susceptible to invasion by the four-eyed fir bark beetle. Fir forests with right-sided structure are less stable and exhibit rapid degradation as a result of infestation. We established that there is a mechanism that drives invasions by the four-eyed fir bark beetle for stands of all types of ontogenetic structure, which is that these invasive insects primarily attack late virginal and young reproductive trees. Over time, these trees can completely vanish from communities, and mature and old productive trees can suffer extensive damage. During the mass reproduction phase, there is also significant loss of late immature and early virginal fir trees during the invasive insects' expansion phase (up to 50%).

The transformative role of an invasive beetle has its own rules that do not only depend on stand characteristics. Infestation by the four-eyed fir bark beetle largely causes tree death of second layer suppressed trees and thinner trees within the canopy. As a result, the total density of the stand is reduced and exceeds the rate of replenishment with new trees. We also showed that the most significant impact of the invasive bark beetle is on trees with diameters of up to average thickness levels (DBH < 30 cm). Fir trees with heart rot and more radial growth that are relatively

small in diameter and have thinner bark are the first individuals targeted by the invasive four-eyed bark beetle and suffer the greatest damage. These factors that make these trees vulnerable (with the exception of age) should be assigned particular importance when considering the stability of fir forests against the four-eyed fir bark beetle.

Siberian fir forests have a good natural ability to regenerate despite stand weakening or full degradation. This fact leads us to conclude that fir stands in the infestation zone of southern Siberia will likely survive potential expansion of the range of the four-eyed bark beetle.

## ACKNOWLEDGEMENTS

The reported research was funded by the Russian Foundation for Basic Research and the government of Tomsk region, grant № 16-44-700782 and as part of a State Assignment of the Center for Forest Ecology and Productivity, Russian Academy of Sciences (no. AAA-A-A18-118052400130-7).

The authors wish to thank Svetlana A. Krivets, Elvina M. Bisirova, Ivan A. Kerchev and Natalie A. Chernova (Institute of Monitoring of Climatic and Ecological Systems, Tomsk, Russia) for gathering data, branches of the Russian Forest Protection Center (Tomsk, Altai, Novosibirsk, Krasnoyarsk) for providing data on the distribution of the four-eyed fir bark beetle and Aimee Orsini (Berkeley) for language editing. ■

## REFERENCES

- Aitken S. N., Yeaman S., Holliday J. A., Wang T., Curtis-McLane S. (2008). Adaptation, migration or extirpation: climate change outcomes for tree populations. *Evolutionary Applications*, 1(1), pp. 95–111. <https://doi.org/10.1111/j.1752-4571.2007.00013.x>.
- Allen C. D., Macalady A. K., Chenchoun H., Bachelet D., McDowell N., Vennetier M., ... Cobb, N. (2010). A global overview of drought and heat-induced tree mortality reveals emerging climate change risks for forests. *Forest Ecology and Management*, 259(4), pp. 660–684. <https://doi.org/10.1016/j.foreco.2009.09.001>.
- Anderegg L. D. L., Anderegg W. R. L., Berry J. A. (2013). Not all droughts are created equal: translating meteorological drought into woody plant mortality. *Tree Physiology*, 33(7), pp. 672–683. <https://doi.org/10.1093/treephys/tpt044>.
- Anuchin N. P. (1982). *Forest Taxation*. Moscow: Lesnaya promyshlennost'.
- Aukema J. E., McCullough D. G., Von Holle B., Liebhold A. M., Britton K., Frankel S. J. (2010). Historical Accumulation of Nonindigenous Forest Pests in the Continental United States. *BioScience*, 60(11), pp. 886–897. <https://doi.org/10.1525/bio.2010.60.11.5>.
- Baranchikov Yu. N., Demidko D. A., Laptev A. V., Petko V. M. (2014). Dynamics of siberian fir dieback in the outbreak area of the four-eyed fir bark beetle. *Moscow State Forest University Bulletin - Lesnoy Vestnik*, 6, pp. 132–138. (in Russian).
- Baranchikov Yu. N., Petko V. M., Astapenko S. A., Akulov E. N., Krivets S. A. (2011). four-eyed fir bark beetle – a new aggressive pest of fir in Siberia. *Moscow State Forest University Bulletin - Lesnoy Vestnik*, 4, pp. 78–81. (in Russian).
- Bidart-Bouzat M. G., Imeh-Nathaniel A. (2008). Global change effects on plant chemical defenses against insect herbivores. *Journal of Integrative Plant Biology*, 50(11), pp. 1339–1354. <https://doi.org/10.1111/j.1744-7909.2008.00751.x>.
- Bleiker K. P., Lindgren B. S., Maclauchlan L. E. (2003). Characteristics of subalpine fir susceptible to attack by western balsam bark beetle (Coleoptera: Scolytidae). *Canadian Journal of Forest Research*, 33(8), pp. 1538–1543. <https://doi.org/10.1139/x03-071>.
- Born W., Rauschmayer F., Bräuer, I. (2005). Economic evaluation of biological invasions—a survey. *Ecological Economics*, 55(3), pp. 321–336. <https://doi.org/10.1016/j.ecolecon.2005.08.014>.
- Boyd I. L., Freer-Smith P. H., Gilligan C. A., Godfray H. C. J. (2013). The Consequence of Tree Pests and Diseases for Ecosystem Services. *Science*, 342(6160), pp. 1235773–1235773. <https://doi.org/10.1126/science.1235773>.
- Brockerhoff E. G., Liebhold A. M., Jactel H. (2006). The ecology of forest insect invasions and advances in their management. *Canadian Journal of Forest Research*, 36(2), pp. 263–268. <https://doi.org/10.1139/x06-013>.
- Carroll A.L., Taylor S.W., Regniere J., Safranyik L. (2003). Effect of climate change on range expansion by the mountain pine beetle in British Columbia. *The Bark Beetles, Fuels, and Fire Bibliography*. Paper 195. URL: [https://ceaa-acee.gc.ca/050/documents\\_staticpost/cearef\\_21799/2876/schedule\\_e.pdf](https://ceaa-acee.gc.ca/050/documents_staticpost/cearef_21799/2876/schedule_e.pdf).

Donyakina S. S., Kovalev A. V., Tarasova O. V., Palnikova E. N., Astapenko S. A., Sukhovolsky V. G. (2013). The stability of fir trees to xylophages: comparison of visual and instrumental estimations. *Conifers of the boreal area*, XXXI (3-4), pp. 26–30. (in Russian).

Dordel J. (2005) Influences of mountain pine beetle (*Dendroctonus ponderosae*), fire and ungulate browsing on forest stand structure in the southern Canadian Rocky Mountains. Master thesis, University of British Columbia.

Dukes J. S., Pontius J., Orwig D., Garnas J. R., Rodgers V. L., Brazee N., ... Ayres M. (2009). Responses of insect pests, pathogens, and invasive plant species to climate change in the forests of northeastern North America: What can we predict? This article is one of a selection of papers from NE Forests 2100: A Synthesis of Climate Change Impacts o. *Canadian Journal of Forest Research*, 39(2), pp. 231–248. <https://doi.org/10.1139/X08-171>.

Dulamsuren Ch. (2004). Floristische Diversität, Vegetation und Standortbedingungen in der Gebirgstaiga des Westkhentej, Nordmongolei. *Berichte des Forschungszentrum Waldökosysteme, Reihe A, Bd. 191*, Georg-August-Universität Göttingen.

Evstigneev O. I., Korotkov V. N. (2016). Ontogenetic stages of trees: an overview. *Russian Journal of Ecosystem Ecology*, 1 (2). <https://doi.org/10.21685/2500-0578-2016-2-1>.

Fajvan M. A., Wood J. M. (1996). Stand structure and development after gypsy moth defoliation in the Appalachian Plateau. *Forest Ecology and Management*, 89(1–3), pp. 79–88. [https://doi.org/10.1016/S0378-1127\(96\)03865-0](https://doi.org/10.1016/S0378-1127(96)03865-0).

Floyd M. L., Clifford M., Cobb N. S., Hanna D., Delph R., Ford P., Turner D. (2009). Relationship of stand characteristics to drought-induced mortality in three Southwestern piñon–juniper woodlands. *Ecological Applications*, 19(5), pp. 1223–1230. <https://doi.org/10.1890/08-1265.1>.

Gradel A. (2017). Reaktion von Waldbeständen am Rande der südlichen Taiga auf Klimafaktoren, natürliche und waldbauliche Störungen/Response of forest stands at the edge of the southern taiga to climate factors, natural and silvicultural disturbances. Ph.D. Thesis, Georg-August-Universität Göttingen, Göttingen, Germany. Available at: <https://ediss.uni-goettingen.de/handle/11858/00-1735-0000-0023-3F93-C> [Accessed 30 Jan. 2019].

Gradel A., Voinkov A. A., Altaev A. A., Enkhtuya B. (2018). A spatio-structural analysis of intact dark taiga in the southern taiga zone and an interval assessment of a dark conifer mixed forest in the mountain forest steppe zone (Mongolia). *Proceedings of the Kuban State Agrarian University*, 4(73), pp. 36-40. (in Russian).

Holdenrieder O., Pautasso M., Weisberg P. J., Lonsdale D. (2004). Tree diseases and landscape processes: The challenge of landscape pathology. *Trends in Ecology and Evolution*, 19(8), pp. 446–452. <https://doi.org/10.1016/j.tree.2004.06.003>.

Hulme P. E., Pyšek P., Nentwig W., Vilà M. (2009). Will threat of biological invasions unite the european union? *Science*, 324(5923), pp. 40–41. <https://doi.org/10.1126/science.1171111>

James T. M. (2011). Temperature sensitivity and recruitment dynamics of Siberian larch (*Larix sibirica*) and Siberian spruce (*Picea obovata*) in northern Mongolia's boreal forest. *Forest Ecology and Management*, 262(4), pp. 629–636. <https://doi.org/10.1016/j.foreco.2011.04.031>.

Jenkins M. A. (2003). Impact of the balsam woolly adelgid (*Adelges piceae* Ratz.) on an *Abies fraseri* (Pursh) Poir. dominated stand near the summit of Mount LeConte, Tennessee. *Castanea*, 62(2), pp. 109–118.

Juříčka D., Novotná J., Houška J., Pařílková J., Hladký J., Pecina V., Cihlářová H., Burnog M., Elbl J., Rosická Z., Brtnický M., Kynický, J. (2018). Large-scale permafrost degradation as a primary factor in *Larix sibirica* forest dieback in the Khentii massif, northern Mongolia. *Journal of Forestry Research*, 29, pp. 1–12.

Katz C. (2017). Small pests, big problems: the global threat of bark beetles. *Yale environment 360*; Yale School of Forestry and Environment. Available at: <https://e360.yale.edu/features/small-pests-big-problems-the-global-spread-of-bark-beetles> [Accessed 30 Jan. 2019].

Kenis M., Auger-Rozenberg M.-A., Roques A., Timm, L., Péré C., Cock M. J. W., Lopez-Vaamonde C. (2009). Ecological effects of invasive alien insects. In *Ecological Impacts of Non-Native Invertebrates and Fungi on Terrestrial Ecosystems*, Dordrecht: Springer Netherlands, pp. 21–45. [https://doi.org/10.1007/978-1-4020-9680-8\\_3](https://doi.org/10.1007/978-1-4020-9680-8_3).

Kerchev I. A., Krivets S.A. (2012). The outbreak foci of *Polygraphus proximus* Blandf. in fir forests of Tomsk oblast. *Interexpo Geo-Siberia*, 4, pp. 67–72. (in Russian).

Kerchev I. A. (2014). Ecology of four-eyed fir bark beetle *Polygraphus proximus* Blandford (Coleoptera; Curculionidae, Scolytinae) in the West-Siberian region of invasion. *Russ. J. Biol. Invasions*, 5(3), pp. 176–185. <https://doi.org/10.1134/S2075111714030072>.

Kharuk V. I., Antamoshkina O. A. (2017). Impact of silkmouth outbreak on taiga wildfires. *Contemporary Problems of Ecology*, 10(5), pp. 556–562. <https://doi.org/10.1134/S1995425517050055>.

Kharuk V. I., Im S. T., Oskorbin P. A., Petrov I. A., Ranson K. J. (2013). Siberian pine decline and mortality in southern siberian mountains. *Forest Ecology and Management*, 310, pp. 312–320. <https://doi.org/10.1016/j.foreco.2013.08.042>.

Kharuk V. I., Im S. T., Petrov I. A., Dvinskaya M. L., Fedotova E. V., Ranson K. J. (2017). Fir decline and mortality in the southern Siberian Mountains. *Regional Environmental Change*, 17(3), pp. 803–812. <https://doi.org/10.1007/s10113-016-1073-5>.

Krivets S. A., Bisirova E. M., Kerchev I. A., Pats E. N., Chernova N. A. (2015a). Transformation of taiga ecosystems in the Western Siberian invasion focus of four-eyed fir bark beetle *Polygraphus proximus* Blandford (Coleoptera: Curculionidae, Scolytinae). *Russian Journal of Biological Invasions*, 6(2), pp. 94–108. <https://doi.org/10.1134/S2075111715020058>.

Krivets S. A., Kerchev I. A., Bisirova E. M., Pet'ko V. M., Pashenova N. V., Baranchikov YU. N., Demidko D. A. (2015b). Four-eyed fir bark beetle in the forests of Siberia: distribution, biology, ecology, identification and examination of damaged plantings. Tomsk-Krasnoyarsk. (in Russian).

Krivolutskaya G.O. (1958). *Bark beetles of Sakhalin Island*. Moscow –Leningrad: Izd-vo AN SSSR.

Kurentsov A.I. (1950). *Pests of conifers of Primorsky Krai*. Vladivostok: Dal'nevostochnyy filial AN SSSR.

Lyamtsev N.I., Isaev A.S. (2005). Modification of the Gypsy Moth Outbreaks Related to Environmental and Climatic Situation. *Russian Journal of Forest Science*, 5, pp. 3–9.

Makhatkov, I. D. (1991). Polivariantnost' ontogeneza Siberian fir. *Byul. MOIP. Otd. Biol.*, 96(4), pp. 79–88. (in Russian).

Martinez-Vilalta J., Lloret F., Breshears D. D. (2012). Drought-induced forest decline: causes, scope and implications. *Biology Letters*, 8(5), pp. 689–691. <https://doi.org/10.1098/rsbl.2011.1059>.

Methodological approaches to environmental assessment of the forest canopy cover in a small river basin (2010). M: Tovarishchestvo nauchnykh izdaniy KMK. (in Russian).

Mitton J. B., Ferrenberg S. M. (2012). Mountain Pine Beetle Develops an Unprecedented Summer Generation in Response to Climate Warming. *The American Naturalist*, 179(5), E163–E171. <https://doi.org/10.1086/665007>.

Nagel W. (1995). Stoyan D./Stoyan H. *Fractals, Random Shapes and Point Fields. Methods of Geometrical Statistics*. John Wiley & Sons, Chichester 1994, XIV, 389 pp. *Biometrical Journal*, 37(8), pp. 978–978. <https://doi.org/10.1002/bimj.4710370810>.

Negrobov O.P. 1970. A contribution to the knowledge of Medetera of Japan (Dolichopodidae, Diptera) // *Insecta Matsumurana*. Suppl.9. P.1–7.

Ostry M. E., Laflamme G., Katovich S. A. (2010). Silvicultural approaches for management of eastern white pine to minimize impacts of damaging agents. *Forest Pathology*, 40(3–4), pp. 332–346. <https://doi.org/10.1111/j.1439-0329.2010.00661.x>.

Palnikova E.N., Meteleva M.K., Sukhovolsky V.G. (2006). Influence of modifying factors on the forest insect population dynamics and development of their outbreaks. *Russian Journal of Forest Science*, 5, pp. 29–35. (in Russian).

Petercord R., Lemme H. (2019). Der Nordische Fichtenborkenkäfer. LWL aktuell 120. Available at: <http://www.lwf.bayern.de/waldschutz/monitoring/211872/index.php> (in German) [Accessed 28 Feb. 2019].

Pobedinsky A. V. (1966). Study of reforestation processes. M. (in Russian).

Poland T. M., McCullough D. G. (2006). Emerald ash borer: invasion of the urban forest and the threat to North America's ash resource. *Journal of Forestry*, April-May, pp. 118-124.

Rozendaal D. M. A., Kobe R. K. (2016). A Forest Tent Caterpillar Outbreak Increased Resource Levels and Seedling Growth in a Northern Hardwood Forest. *PLOS ONE*, 11(11), e0167139. <https://doi.org/10.1371/journal.pone.0167139>.

Sanderson L. A., Mclaughlin J. A., Antunes P. M. (2012). The last great forest: a review of the status of invasive species in the North American boreal forest. *Forestry*, 85(3), pp. 329–340. <https://doi.org/10.1093/forestry/cps033>.

Seidl R., Rammer W., Jäger D., Lexer M. J. (2008). Impact of bark beetle (*Ips typographus* L.) disturbance on timber production and carbon sequestration in different management strategies under climate change. *Forest Ecology and Management*, 256(3), pp. 209–220. <https://doi.org/10.1016/j.foreco.2008.04.002>.

Silverstein D. (2012). Tornadoes, sepsis, and goal-directed therapy in dogs. *Journal of Veterinary Emergency and Critical Care*, 22(4), pp. 395–397. <https://doi.org/10.1111/j.1476-4431.2012.00784.x>.

Small M. J., Small C. J., Dreyer G. D. (2007). Changes in a hemlock-dominated forest following woolly adelgid infestation in southern New England. *The Journal of the Torrey Botanical Society*, 132(3), pp. 458–470. <https://www.jstor.org/stable/20063785>.

Smirnova O.V., Bobrovsky M.V., Khanina L.G., Zaugolnova L.B., Turubanova S.A., Potapov P.V., Yaroshenko A.Yu., Smirnov V.E. (2017) *Methods of Investigation*. Published in: Smirnova O. V., Bobrovsky M. V., Khanina, L. G. (Eds.). *European Russian Forests* (Vol. 15). Dordrecht: Springer Netherlands. <https://doi.org/10.1007/978-94-024-1172-0>.

Stark V.N. (1952). Bark beetles. In: *USSR fauna. Coleoptera. Vol. XXXI. Moscow – Leningrad: Izd-vo AN SSSR*.

Straw N. A., Williams D. T., Kulinich O., Gninenko Y. I. (2013). Distribution, impact and rate of spread of emerald ash borer *Agrilus planipennis* (Coleoptera: Buprestidae) in the Moscow region of Russia. *Forestry*, 86(5), pp. 515–522. <https://doi.org/10.1093/forestry/cpt031>.

Sheskin JD (2004). *Handbook of parametric and nonparametric statistical procedures*. Third edition. Florida, CRC Press.

Svalov S. N. (1985). Application of statistical methods in forestry. *Forest Science and Forestry*, 4, pp. 1–164. (in Russian).

Tchebakova N. M., Parfenova E. I., Soja A. J. (2011). Climate change and climate-induced hot spots in forest shifts in central Siberia from observed data. *Regional Environmental Change*, 11(4), pp. 817–827. <https://doi.org/10.1007/s10113-011-0210-4>.

Uspensky E. I. (1987). The forest regeneration process under the canopy of small-leaved forests of the middle Volga region. *Forestry Journal*, 3, pp. 116–118. (in Russian).

Weckel M., Tirpak J. M., Nagy C., Christie R. (2006). Structural and compositional change in an old-growth eastern hemlock *Tsuga canadensis* forest, 1965–2004. *Forest Ecology and Management*, 231(1–3), pp. 114–118. <https://doi.org/10.1016/j.foreco.2006.05.022>.

Worrall J. J., Marchetti S. B., Egeland L., Mask R. A., Eage T., Howell B. (2010). Effects and etiology of sudden aspen decline in southwestern Colorado, USA. *Forest Ecology and Management*, 260(5), pp. 638–648. <https://doi.org/10.1016/j.foreco.2010.05.020>.

Yamaguchi H. (1963). Survey and population studies of beetles in wind-swept areas in Hokkaido (II). Beetle infestations on wind-thrown trees in the second year, in 1955 // *Bull. Gov. For. Exp. Sta. Vol. 151. P. 53-73*.

Zamolodchikov D.G. (2012). An estimate of climate related changes in tree species diversity based on the results of forest fund inventory. *Biol Bull Rev*, 2(2), pp. 154–163. <https://doi.org/10.1134/S2079086412020119>.

**Antonín Kusbach<sup>1,2\*</sup>, Tadeáš Štěřba<sup>2</sup>, Jan Šebesta<sup>1</sup>, Tomáš Mikita<sup>3</sup>,  
Enkhtuya Bazarradnaa<sup>4</sup>, Sarantuya Dambadarjaa<sup>4</sup>, Martin Smola<sup>1,5</sup>**

<sup>1</sup>Department of Forest Botany, Dendrology and Geobiocoenology, Faculty of Forestry and Wood Technology, Mendel University, Brno, Czech Republic

<sup>2</sup>Forest Management Institute, Brandýs nad Labem, Czech Republic

<sup>3</sup>Department of Forest Management and Applied Geoinformatics, Faculty of Forestry and Wood Technology, Mendel University in Brno, Brno, Czech Republic

<sup>4</sup>School of Agroecology and Business, Mongolian University of Life Sciences, Darkhan Uul, Mongolia

<sup>5</sup>Lesprojekt Východní Čechy Ltd. Company, Hradec Králové, Czech Republic

\* **Corresponding author:** kusbach@mendelu.cz

## ECOLOGICAL ZONATION AS A TOOL FOR RESTORATION OF DEGRADED FORESTS IN NORTHERN MONGOLIA

**ABSTRACT.** We developed a geo-vegetation zonation in the Khaan Khentii massif, northern Mongolia. Our specific objective was to assess and classify the response of the tree vegetation to environmental factors operating at a coarse climatic level. We sampled forest ecosystem vegetation, climate, physiographic features, and soil properties. Our analysis included clustering, ordination, classification, and ANOVA techniques. Based on the complex data set, we identified three geo-vegetation zones: forest-steppe, montane and dark taiga zone. We characterized them based on the regional environmental factors; (1) climate as indicated by altitude, i.e., precipitation, (2) geomorphology by an index of the vertical distance to channel network and soils by O horizon thickness and soil types. Birch and aspen ecosystems were excluded as discrete zones due to their broad ecological amplitude.

The geo-vegetation zonation outlined in this paper is the first attempt at quantifying vegetation along with the environment at a macroclimatic level in Mongolia. This coarse-scale zonation provides a framework for building a comprehensive ecological classification, a background for sustainable forest management, which is currently unavailable in Mongolia and many central Asian countries. Additionally, it offers a roadmap for a comprehensive ecosystem survey and may act as an information platform and reference for current environmental issues such as forest degradation across Mongolian landscapes.

**KEY WORDS:** Ecological classification; Forest degradation; Sustainable management; Geo-vegetation zone; Zonal concept

**CITATION:** Antonín Kusbach, Tadeáš Štěřba, Jan Šebesta, Tomáš Mikita, Enkhtuya Bazarradnaa, Sarantuya Dambadarjaa, Martin Smola (2019) Ecological Zonation As A Tool For Restoration Of Degraded Forests In Northern Mongolia. *Geography, Environment, Sustainability*, Vol.12, No 3, p. 98-116  
DOI-10.24057/2071-9388-2019-31

## INTRODUCTION

Sustainability is a widely accepted principle in forest ecosystem management (e.g., Barbati et al. 2007). Traditionally, it has been applied through ecological classifications based on knowledge of natural vegetation and environmental conditions (usually defined by important environmental parameters) of a particular area or region (Pfister and Arno 1980; Pojar et al. 1987; Viewegh et al. 2003; Vahálík and Mikita 2011; Kusbach et al. 2017a). This vegetation-environmental relationship can be studied in different spatial-functional settings (Major 1951). It is reflected on a (i) macroscale (macroclimate – regional climate) for example, in biogeoclimatic zonation of British Columbia (Pojar et al. 1987), ecoregions (Bailey 2002), forest types (Caudullo et al. 2016), natural forest areas (Plíva and Žlábek 1986) and forest vegetation zones (Viewegh et al. 2003; Kusbach et al. 2017a), (ii) mesoscale (local climate), e.g., site series (Pojar et al. 1987), climax series (Pfister and Arno 1980), forest site complexes via edaphic series (Viewegh et al. 2003), and (iii) microscale, e.g., site types (Pojar et al. 1987), habitat types (Pfister and Arno 1980), forest site types (Viewegh et al. 2003). Forest ecological classifications exist in territories advanced in forestry such as North America, Europe, and the Asian part of Russia for decades (e.g., Kusbach et al. 2017a). These systems represent an important communication tool for the interested audience and provide an underlying framework for forest policy (decision making) and practice (ecosystem management, restoration and conservation etc.), (e.g., Kotar 1988; Barbati et al. 2007; Sharik et al. 2010; Zenner et al. 2010).

For instance, in the Czech Republic, Regional Plans of Forest Development (RPF) serve as a framework for forestry planning and legislation, practical management, nature protection and conservation, forested land evaluation, tax calculation, subsidies etc. (<http://www.uhul.cz/what-we-do/regional-plans-of-forest-development>). The plans have been developed for natural forest areas, regional

units more or less homogeneous in natural conditions (Plíva and Žlábek 1986). The Czech Forest Ecosystem Classification (CFEC) includes additional structuring of growing conditions typical for forest vegetation zones (Viewegh et al. 2003; Kusbach et al. 2017a).

All worldwide ecological classifications were established based on expert knowledge (Haeussler 2011). While the original idea of zonality (zonality of soils sensu Dokuchaev) has been criticized as old-fashioned and “static” (Johnson et al. 1990), there is still intellectual power and potential in that idea (e.g., the zonal concept), which can serve as a feasible framework for advanced ecological classifications in areas without such systems (Haeussler 2011; Kusbach et al. 2014), especially for use in sustainable close-to-nature forest management.

Based on classic works of e.g., Morozov (1925), Pogrebnjak (1955), Sukachev (1972), Kolesnikov (1974), a tremendous amount of work was done in the field from 1970 during the Joint Russian/Soviet-Mongolian Complex Biological Expeditions and further surveys in terms of forest ecosystem classification and mapping (e.g., Unatov 1950; Lavrenko and Sokolov 1978; Grubov 1982; Karta 1983; Ulziikhutag 1989; Dulamsuren et al. 2005; Vostokova and Gunin 2005; Dorjgotov 2009). However, there is no framework and tools analogical to CFEC and RPF) on the Mongolian territory. Coarse-scale outputs - units of ecosystem surveys and maps (scales 1: 1.5-12 000 000, e.g., Vostokova and Gunin 2005; Dorjgotov 2009) do not provide a sufficient environmental stratification (at least in climate scaling as stated above) for definition of lower forest classification units. Additionally, there is no mapping of particular localities, no site-specific information except a general soil description with the Russian nomenclature (Nogina et al. 1980) used in the phytocoenological typology of Lavrenko and Sokolov (1978) with a brief description of basic forest types. These typological structures used, e.g., in Nyam et al. (2009) are obsolete and broad.

Moreover, no frequent thematic maps such as the map of existing vegetation for the Domogt Shariin Gol Company Ltd. (Kusbach et al. 2017b; Smola et al. 2019) were elaborated within sparse Mongolian descriptive forest management plans. Finally, since there is no legal framework (spatial units similar to the Czech natural forest areas and forest vegetation zones) and tools (a classification system) in Mongolia so far, it is not possible to recommend forest management and implement political decisions systematically (Kusbach et al. 2017b). In Mongolia, the forestry sector, especially forestry legislation, planning, education and extension is under development (Tsedendash 1998; Tsogtbaatar 2007; Batkhuu et al. 2011). Therefore, a formal framework (forest classification with management structures) is necessary to build besides activities such as National Forest Inventory (Altrell and Erdenebat 2016).

Our general objective was to reveal vegetation-environmental interactions in the macroclimate scale in northern Mongolia. We examined the relationships between tree composition and environmental variables (*sensu* Krajina 1965; Bailey 2002). Specific objectives were to (i) assess a response of vegetation to significant environmental factors at a level of regional climate, and (ii) suggest a spatial framework as broad forest/landscape units relatively homogeneous based on that response.

## MATERIALS AND METHODS

### The zonal concept

Late-seral or old-growth, usually minimally disturbed plant communities with intermediate terrain morphology and soil conditions are presumed to best reflect the influence of regional climate (Krajina 1965; Pojar et al. 1987; Bailey 2002). Local climatic, topographical and soil (topoedaphic) extreme sites such as hot steep slopes, cool, shady slopes, cold depressions or skeletal soils are disqualified and only intermediate

environmental conditions are involved in application of the zonal concept and in selection of zonal sites. Together with the local extremes, also disturbed vegetation is disregarded. For details of the concept, see Kusbach et al. (2014).

### STUDY AREA

The study area belongs into the Selenge and Darkhan Uul provinces in northern Mongolia. It is located in the northwest part of the Khaan Khentii massif (Fig 1). The western part of the massif belongs to the vegetation-geomorphologic province of the Daurian-Mongolian forest mountain steppe (Dorjgotov 2009). The lowest parts of the area are as low as 650–700 m a. s. l. and the highest parts reach over 2000 m a. s. l. The majority of the study area is made of uplands (800–1200 m a. s. l.). The Selenge River, the biggest river in Mongolia, with Orkhon, Eröo and Sharyn Gol River tributaries taking water from the study area to the Lake Baikal, Russia.

Mongolia is a landlocked country with climatic extremes, e.g., huge differences between summers and winters in temperatures and rainfall amounts. Winters are long, very cold and relatively dry (little snowy) affecting a relatively short vegetation period (May – September), especially in high elevations. Summers are hot and moister than cold and dry winters (e.g., Tsedendash 1995; Dulamsuren et al. 2005). Springs and falls are short. Mean annual temperature varies between -3 and -1.5°C and mean annual rainfall between 280 and 350 mm within the study area (data obtained from the Mongolia National Agency for Meteorology and Environmental Monitoring). With increasing altitude, the amount of rainfall can reach up to 500 mm per year in the Bugant area, a part of the study area (Oyunsanaa 2011). This general macroclimatic pattern is modified by a local terrain topography causing substantial changes at a mesoclimatic level (Dulamsuren et al. 2005; Hais et al. 2016). This phenomenon of a local climate is distinctive on steep south-facing slopes with enormous temperature differences

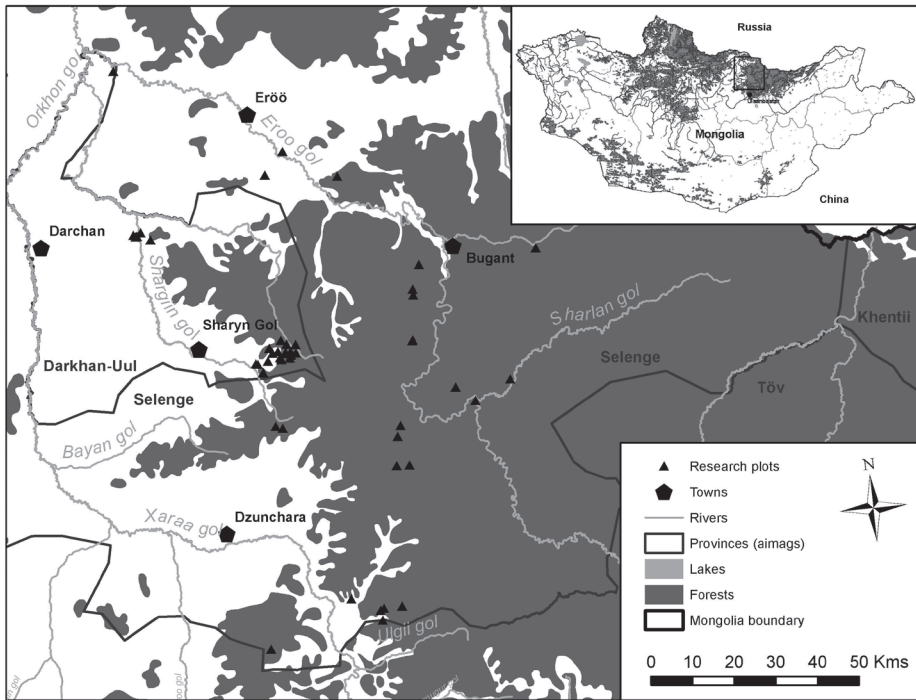


**Fig. 1.** The study area with locations of sample zonal sites

and usually shallow soils contrary to shady north-facing slopes with a low solar radiation. While a forest-steppe or steppe is developed on hot-dry south-facing slopes, a close-canopy forest covers cold-moist north-facing slopes (Dulamsuren et al. 2005, Mühlenberg et al. 2011).

A majority of Khaan Khentii massif consists of plutonic volcanic rocks of the Palaeozoic era, usually metamorphed. These deep and thick bedrocks are combined with Quaternary deposits of loess and eolian sands in lower elevations. In wider valleys of rivers, we can meet young organic soils, alluvial deposits and marches (Geological Map of Mongolia 1998). According to the "World Reference Base for Soil Resources" (WRB 2014) supported by the field pedological experience (Kusbach et al. 2017b), Kastanozems, Chernozems, and Arenosols are the most widespread in the northwest periphery of the study area associated with the steppe zone. On the other hand, Phaeozems, Cambisols, Luvisols, Umbrisol and Fluvisols are the most common soils in the central and eastern part of the study area linked with the forested zone.

The lowest levels of the study area (around 700 – 800 m a.s.l.) are characteristic by steppe and forest-steppe vegetation dominated by *Pinus sylvestris* with locally higher presence of *Ulmus pumila*, and shrubs *Caragana microphylla* and *Spiraea aquilegifolia*. The largest portion of the area is occupied by "light taiga" forest ecosystems dominated by *Larix sibirica*, *Pinus sylvestris*, and *Betula platyphylla* (Ermakov et al. 2002). As subdominants, we can find *Populus tremula* and locally, on the south-facing steep slopes, *Ulmus pumila* with *Spiraea aquilegifolia*. In higher altitudes of the central and eastern part and on north-facing slopes of lower altitudes, stands often belong to "dark taiga" composed of *Abies sibirica*, *Picea obovata* and *Pinus sibirica* (e.g., Knystautas 1987). The presence of *Picea obovata*, *Salix spp.*, *Populus laurifolia*, *Padus asiatica*, *Potentilla fruticosa*, *Betula fruticosa* and *B. fusca* is typical for alluvial vegetation (Dulamsuren et al. 2005; Kusbach et al. 2017b).

Recent dominant landscape disturbances such as timber cutting, livestock overgrazing, wildfires (mostly human-

induced), and mining combined with climate change (causing desertification) result in changes of the structure and age-class distribution of forest stands and depletion and degradation of forests (Khodolmor et al. 2013; Altrell and Erdenebat 2016; Gradel et al. 2017; Kusbach et al. 2017b). In many places, where *Pinus sylvestris* or *Larix sibirica* were cut down, *Betula plathyphylla* and *Populus tremula* stands are now predominant (Dulamsuren et al. 2005; Kusbach et al. 2017b). Forests highly disturbed by overpasturing and logging are thus characterized by low and mid, exceptionally late seral stages where a forest understory including natural regeneration is usually poorly developed (Kusbach et al. 2017b; Juříčka et al. 2019). Species richness along a huge altitudinal gradient is, despite intensive disturbances, very high (Dulamsuren et al. 2005; Chytrý et al. 2012).

### Sampling design and data collection

In summers 2015 to 2018, we established 96 circular sample plots (225 m<sup>2</sup> each) along the altitudinal range in order to get a broad environmental variation of the study area. One soil pit was dug in each plot to the unweathered parent material. A stratified (based on plot vegetation physiognomy, marked as ecosystem) fixed (subjective selection) sampling design was used. (Kusbach et al. 2017b). In this study, applying the zonal concept, we selected 49 zonal sites (Fig. 1), i.e., mature forest stands with intermediate site parameters such as mid-slope position, gentle to moderate slope (< 30 degrees), loamy soils (> 50 cm deep) with coarse rock

fragment content < 50 % by volume and no growing-season ground water table (Damman 1979). We thus avoided those conditions that may substantially modify overall climate, such as frost pockets, cold air drainages and steep slopes. As “mature” we considered vegetation with relatively stable composition of dominant, potential climax tree species, with a clear successional trajectory, e.g., assessed by advance regeneration of climax species (Pfister and Arno 1980; Pojar et al. 1987). True zonal sites with climax (e.g., old growth) vegetation are relatively rare in the Khaan Khentii massif because many forest ecosystems never reach potential climax due to natural disturbances such as fire (e.g., Pojar et al. 1987; Cook 1996) and anthropogenic disturbances such as logging and pasture. Therefore, we compromised this disadvantage by sampling of sites with younger but mature stands (over ca 70 years, Pfister and Arno 1980). Because of not clear status of some mature birch and aspen stands on zonal sites, we accepted them as sites without anthropogenic disturbance.

*Environmental and Soil Data.* We described each sample plot by a forest type (ecosystem) and environmental variables including elevation, slope aspect and slope gradient. Soil properties were assessed based on the Reference Soil Groups (WRB 2014) (Table 1). Parent material or soil substrate observed within the soil pits was verified against a geologic map (Geological Map of Mongolia 1998).

One composite soil sample from 0–30 cm was collected from a pedon in each

**Table 1. Research variables used in the analysis**

Climatic factors	Abbreviation	Units/Values
Total Annual Mean Precipitation	P_year	mm
Annual Mean Temperature	T_year	°C
Physiographic/geomorphometric factors		
Altitude	Alt	meters
Aspect	Aspect	values 0 - 10
Channel Network	Chan_Net	values 0 - 1000

Catchment Area	Catch_A	values 0 - 25 000
Catchment Slope	Catch_Sl	values 0 - 1
Convergence Index	Converg	values - 87 - 89
Diurnal Anisotropic Heating	Diur_Ani	values -0.6 - 0.53
Gradient	Gradient	values 0 - 1
Gradient Difference	Grad_Dif	values -1 - 1
Local Convexity	Convexit	values 0 - 0.8
Mass Balance Index	Mass_Bal	values -1 - 2
Mean Catchment Area	M_Catch	values 0 - 25 000
Midslope Position	M_Slope	values 0 - 1
Normalized Height	Norm_H	values 0 - 1
Protection	Protect	values 0 - 1
Relative Slope Position	R_slope	values 0 - 1
Slope Gradient	Slope	degrees
Slope Aspect Value	av	values 0 - 1 (Roberts and Cooper 1989)
Slope Height	Slope_H	m/0 - 450
Solar Radiation	Solarrad	values 635 000 - 1 400 000
Standardized Height	Stand_H	m/0 - 1500
Topography Wetness Index	TWI	values 0 - 26
Topographic Position Index	TPI	values -11 - 12
Terrain Roughness Index	TRI	values 0 - 60
Valley Depth	Valley_D	m/values 0 - 600
Vertical Distance to Channel Network	Vert_D	values 0 - 762
Wind Exposure	Wind_exp	values 0 - 2
Geologic/Soil Factors		
Available Potassium	aK_A	milligram/100 g of soil
Available Phosphorus	aP_A	milligram/100 g of soil
Carbon Nitrogen Ratio	C/N_A	not applicable
Coarse Rock Fragment Content	skelet	% volumetric
Exchangeable Calcium	eCa_A	milligram/ekv/100 g of soil

Exchangeable Magnesium	eMg_A	milligram/ekv/100 g of soil
Organic Carbon	C_A	%
Soil Substrate	substr	not applicable, categorical
Soil Type	stype	not applicable, categorical
O horizon thickness	Ohor	centimeters
A horizon thickness	Ahor	centimeters
Soil Depth	depth	centimeters
Soil Texture	stext	1-sandy, 2-loamy, 3-clayey
Soil pH	pH_A	1-14 pH scale
Soil Organic Matter	som_A	%
Total Nitrogen	totN_A	%

pit. The fine soil fraction (a particle size < 2 mm) was analyzed for physical and chemical attributes such as soil texture classes (sand, loam, clay) using the feel-method (Thien 1979), pH (1:1 soil in water, Corning pH analyzer), total organic C, total N (LECO CN analyzer, Leco Corp., St. Joseph, MI), exchangeable cations Ca, Mg, K (Holmgren et al. 1977), and available P (Olsen et al. 1954) (Table 1).

In order to detect a site environmental character, we calculated common geomorphometric indices expressing thermic regime of terrain relief, done by its openness and protection of a locality by surrounding relief, and characterizing terrain by hydrological processes. We calculated indices available in the SAGA GIS software for each sample plot (Table 1). We used the Digital Terrain Model (DTM) with a spatial resolution 30×30 m transformed into the coordinate system UTM (the zone north, tier 48). The DTM data derived from the ASTER GDEM (Global Digital Elevation Model) were resampled to achieve: (1) a feasible compromise between a geographical extent of landscape-level units considered and a grain (a pixel size) characterizing an appropriate level of detail of terrain topography, and (2) faster calculation of the indices. Our aim was to filter out microsites (different microclimate or soil moisture conditions).

*Climatic data.* Climatic data in a form of raster data of annual mean air temperature and total annual mean precipitation with resolution of 900×600 m were generated using the free of charge Worldclim database ([www.Worldclim.com](http://www.Worldclim.com)) and interpolated from available climatic stations for the sample sites. Quality climatic data are not available in Mongolia due to a thin network of weather stations and plots (Kusbach et al. 2017b).

### Data analysis

We performed the following analytical steps: (1) ordination of the sample plots/ ecosystems based on environmental data; (2) cluster analysis of ecosystems based on important environmental variables examined in the ordination; (3) discriminant analysis of clusters based on important environmental variables; (4) analysis of variance (ANOVA) of environmental data with clusters. The total dataset was comprised of 49 zonal sites, 26 geomorphic indices, and 21 other environmental variables (including climate and soil).

We used principal components analysis (PCA) ordination to determine the relative importance of the environmental variables and interpret principal components (PC) associated with zonal sites. In the first PCA run, we distinguished among

26 geomorphic indices calculated for each sample plot. Orthogonal rotations and correlation type of a cross-products matrix were used to derive independent, mutually uncorrelated PCs (Lattin et al. 2003). We checked for outliers during the PCA run. Significance of PCs was tested using a Monte Carlo randomization (based on proportion-based p-values for each PC). In order to find the relationship of the variables with the PCs and interpret PCs, we calculated correlation coefficients (loadings) with each ordination axis: the linear (parametric Pearson's *r*) and rank (nonparametric Kendall's *tau*) relationships between the ordination scores and the variables. Our use of *r* and *tau* is suggested to be more conservative than p-values for the null hypothesis of no relationship between ordination scores and variables (McCune et al. 2002). We set the threshold for *r* and *tau* > 0.4 (e.g., Hair et al. 2013). Based on the first PCA run, we selected significant geomorphic indices, which were used together with the environmental variables (climate and soil) in the next PCA run.

To associate the ecosystems with important environmental factors obtained in the PCA, we performed cluster analysis. We used Ward's (1963) linkage method with Sorensen (Bray-Curtis coefficient) distance as suggested by McCune et al. (2002). We transformed the variables with  $|\text{skewness}| > 1$ , standardized the data by adjustment to standard deviate (z-scores) and checked the dataset for outliers. A clustering dendrogram was scaled by a distance objective function (Wishart 1969). Resulting clusters were hereafter considered analytical classes.

Random Forests analysis (Breiman 2001), a machine-learning bootstrapping method, was used to identify the most important environmental variables associated with meaningful clustering to highlight cluster differences. Random Forests is accurate, combines many classification trees, and determines variable importance (e.g., Chen et al. 2004). Results were produced for all classes including among-class partial misclassification errors (taken from the RF

confusion matrix). Important factors (the most influential when assigning classes to observations in the RF algorithm) were ranked in the RF variable importance analysis according to Mean Decrease Accuracy and Mean Decrease Gini. For the machine-learning training (to grow a 'forest'), we used  $n_{\text{tree}} = 1000$  (a number of trees as a function in R) and  $m_{\text{try}} = 1, 2$  and 3 (a number of variables randomly used at each split) (Liaw and Wiener 2002).

Using the most important factors obtained from Random Forests classification and PCA, we confirmed differences between the clusters/classes by the Kruskal-Wallis test (one way non-parametric ANOVA). Finally, using results of the first two PCA runs and meaningful clustering, we displayed broad landscape units as the zones in the third PCA run.

The randomForest and ANOVA analyses were carried out in the program R 3.0.0 (R Core Team, 2014). PC-ORD 6 (McCune and Mefford 2011) was used for PCA ordination and clustering. ArcGIS 10.3 (ESRI, Redlands, LA, USA) software with the Spatial Analyst superstructure and SAGA GIS software (Institute of Geography, University of Hamburg, Hamburg, Germany) were used for the calculation of the geomorphic indices.

Taxonomy and nomenclature of vascular plants followed Grubov (1982).

## RESULTS

We identified the following parent materials and substrates on the zonal sample plots: alcalic granite, para-gneiss, metaquartzite, basic methamorphite, loess, eolian sand, and delluvial deposits.

We identified these soil groups on the zonal sample plots: Arenosols, Cambisols, Chernozems, Kastanozems, Phaeozems, Luvisols, and Umbrisols (WRB 2014).

We calculated correlations (*r*) among 26 geomorphic indices and kept only indices with a strong  $r > 0.8$ . The first PCA ordination (49 plots, geomorphic indices) resulted in three significant PCs ( $p = 0.001$ ),

explaining respectively 31, 21 and 11 % of the total variance within the geomorphic indices (Appendix A). The most important principal component (PC1) was highly associated with macroclimatic indices; Stand\_H ( $r = -0.9$ ,  $\tau = -0.7$ ), R\_Slope ( $r = -0.8$ ,  $\tau = -0.7$ ), Norm\_H ( $r = -0.8$ ,  $\tau = -0.6$ ), Alt ( $r = -0.7$ ,  $\tau = -0.5$ ). PC1 was interpreted as a macroclimate gradient. PC2 was associated with Terrain Roughness (0.9, 0.7), Catchment Slope (0.8, 0.7), Slope (0.6, 0.6), and Protection (0.7, 0.6) (Table 1, Appendix A). We interpreted this as a topographically based soil moisture gradient. (Appendix A).

For the next PCA step, we kept only macroclimatic indices following the zonal concept conditions. We added 21 climatic and soil factors and ran the second PCA. The second PCA (49 plots, 28 environmental factors) resulted in three significant PCs ( $p = 0.001$ ), explaining respectively 31, 13 and 10 % of the total variance within the environmental factors (Appendix B). As in the first PCA run, the most important principal component (PC1) was associated with macroclimatic indices. PC1 was interpreted as a macroclimate gradient. PC2 was highly associated with soil factors, Soil Organic Matter ( $r = 0.6$ ,  $\tau = 0.5$ ), Organic C (0.6, 0.5), and pH (0.5, 0.4). We interpreted this as a soil properties gradient (Appendix B).

In the cluster analysis (47 plots - without two plot outliers, 13 significant environmental factors in the second PCA), there was a stable three-cluster solution based on the distance objective function

and information retained (stability of the three-cluster solution was indicated by the longest horizontal distances of clusters' branches). There was considerable similarity in environmental factors between physiognomically different ecosystems such as *P. sylvestris*, *B. platyphylla* and *P. tremula* (Fig. 2).

The Random Forests classification identified those environmental factors most strongly associated with this three-cluster solution. Four environmental factors were identified as important discriminating the clustering of sites. In order of importance by Mean Decrease Accuracy and Mean Decrease Gini in brackets, we chose two morphometric indices - Vertical Distance to Channel Network (23.1, 5.3), Altitude (21.8, 5.2), one soil factor - O horizon thickness (16.5, 2.8) and one climatic factor - Total Annual Mean Precipitation (10.3, 1.5). The ranking of variable importance was quite stable for solutions with three variables randomly used at each split (mtry function in R), and 1000 trees used to grow a "forest" (ntree function in R, Liaw and Wiener 2002). "Out-of-bag" estimate of error rate as a measure of misclassification was 4 %.

Kruskal-Wallis test confirmed overall significant differences among the zones in: Vertical Distance  $\chi$ -squared value = 34.6, Altitude = 35.7, O horizon thickness = 22.0, Total Annual Mean Precipitation = 20.1 (Fig. 3). We designated low elevation *P. sylvestris* and *U. pumila* forests into the forest-steppe zone, mid elevation *P. sylvestris*, *B.*

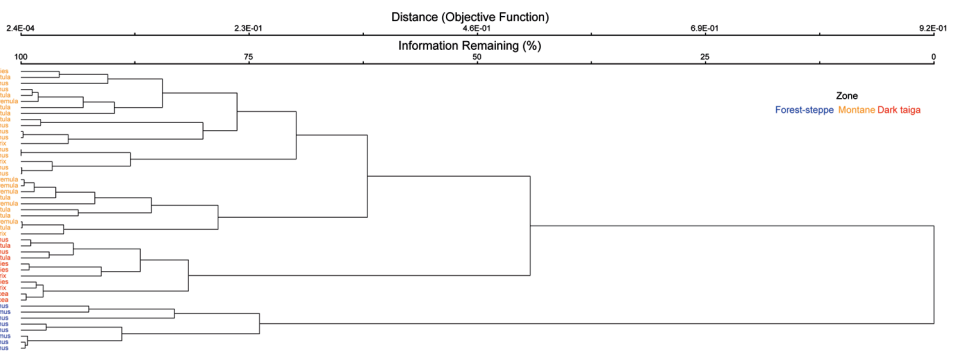


**Fig. 2. The cluster analysis dendrogram with the stable and feasible three-cluster solution. *Abies* = *Abies sibirica*, *Betula* = *Betula platyphylla*, *Larix* = *Larix sibirica*, *Picea* = *Picea obovata*, *Pinus* = *Pinus sylvestris*, *P. tremul* = *Populus tremula*, *Ulmus* – *Ulmus pumila***

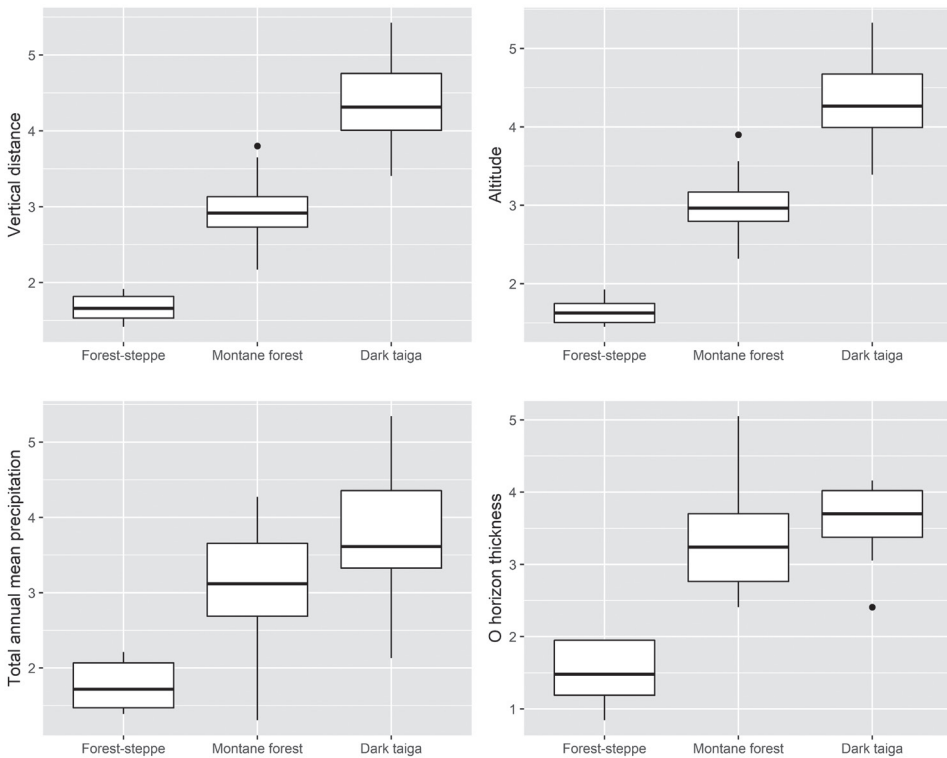


**Fig. 3. Geo-vegetation zones and their significant relationship with the most important environmental factors. For all factors  $p < 0.001$**

*platyphylla*, *P. tremula* and *L. sibirica* forests we referred to as the montane zone, and high elevation *L. sibirica*, *A. sibirica*, *Picea obovata* forests to as the dark taiga zone (Fig. 2). We set up thresholds for the important factors.

Using the most important factors obtained in the Random Forests classification, we constructed a biplot of ecosystems with influential factors in the environmental space in the final PCA run. PC1 was the macroclimatic gradient,  $p = 0.001$ . Envelopes clearly delineated the three distinguish zones (Fig. 4).

## DISCUSSION

### Geo-vegetation zonation

Hilbig and Knapp (1983) presented an altitudinal-based stratification of the lower and upper montane belt in the Khentii Mountains, extended by vegetation classification and floristic description

of Dulamsuren et al. (2005). Similarly, ecosystem mapping for the whole territory of Mongolia (Vostokova and Gunin 2005) offers information on “mesoecosystems” characterized by an ecotope (terrain relief and surface deposits with soil-plant cover in matrix setting) in a basic scale of 1: 8 000 000. Although this mesoscale mapping is supported by “detailed field surveys in stationary field areas” (no scales of those middle-scale maps are provided), this approach differs from ours using the zonal concept. While there is some consistency between the altitudinal structure of forests in Vostokova and Gunin (2005) (scale 1: 8 000 000), and our suggested zonation, Vostokova, Gunin and others (2005) distinguished the forest ecosystems, altitudinal zones and ecosystem types without clear interconnection. They used basic physiognomy for ecosystem and zone naming, e.g., dark taiga, pseudotaiga, subtaiga etc. (similarly to e.g., Korotkov 1976; Tsedendash 1995; Tsogtbaatar 2004; Dulamsuren et al. 2005) and exceptionally

an edicator information, e.g., larch, pine forest for the types. No information on a successional status or disturbances was provided. Other environmental factors except a descriptive relief and soil typing (probably Nogina et al. 1980) stayed unclear.

Our analysis revealed a strong altitudinal pattern based on a broad ecological range of data (climate, geomorphology, soil and vegetation). To our best knowledge, our study is the first attempt to ecologically discriminate vegetation along a relatively comprehensive environmental gradient and quantify significant factors at a macroclimatic level in the Khentii massif. That means the study is data driven, we did not rely on traditional expert knowledge typical for all major worldwide ecological classification systems. We distinguished three **geovegetation zones** characterized by the environmental thresholds: the forest-steppe, montane and dark taiga zone (Fig. 2, 4, Table 2). These zones occur as stacked, vertical belts with distinct climatic, geomorphologic and soil differences. However, when examined in detail, the boundary between these zones is not so abrupt because of local topography, which modifies vegetation at a mesoclimatic level (Dulamsuren et al. 2005; Kusbach et al. 2017b).

In lower elevations, the forest-steppe zone is linked to the true steppe zone without a real tree cover (Karamysheva and Khramtsov 1995). *P. sylvestris* parklands and *U. pumila* woodlands characterize the

zone. Since these ecosystems experience frequent wildfires (Goldammer 2002; Oyunsanaa 2011), *Pinus* can be considered the potential climatic climax species because there is no shade tolerant tree species within the zone (Pojar et al. 1987; Kusbach et al. 2017b). Successional status of *U. pumila* is poorly understood. A heterogeneous substrate and rich steppe (mostly grass) understory vegetation under open canopy forests (Dulamsuren et al. 2005) are reflected by fertile Chernozems, Kastanozems, Phaeozems and Arenosols (almost no O horizon, a thick A horizon rich in soil organic matter and organic carbon). The zone is warmer and drier than the montane zone (Table 2, Fig. 3, 4). Therefore, in general, the forest cover does not exceed 50 % of the total zone area. This cover can be seen almost exclusively on north, northeast-facing slopes within this zone.

*Larix sibirica*, *Pinus sylvestris*, and *Betula platyphylla* are the climatic climax species for the montane zone, which consists of close canopy forests (Fig. 2, 4). Nevertheless, these ecosystems also experience frequent wildfires. Higher potential productivity of prevailing Phaeozems, (less Kastanozems) is indicated not just by higher precipitation, thick O and A horizons with a high amount of soil organic matter (organic carbon), but also by modest pH and presence of important macronutrients Ca, Mg, P and K that were insignificant in the analysis. The zone is cooler and moister than the forest-steppe zone (Table 2, Fig. 3, 4, Appendix B). Therefore, in general, a forest cover is higher than 50% of the total zone

**Table 2. Identification of the geo-vegetation zones. Zones' differences are significant for all factors ( $p = 0.001$ ). For factor abbreviations, see Table 1**

Zone	Altitude (m a.s.l.)	Vertical_D (m)	Precip (mm)	O hor (cm)	Substrate	Soil groups
	Mean (range)					
Forest-steppe	803 (753-875)	61 (6-119)	304 (299-309)	1.3 (0.5-2)	sand, loess	Kastanozems
						Phaeozems
Montane	1130 ( 975-1379)	333 (177-549)	319 (298-331)	6.5 (3-20)	gneiss	Phaeozems
					granite	Kastanozems
Dark taiga	1391 (1090-1744)	590 (322-918)	327 (308- 347)	7.8 (3-11)	gneiss	Cambisols
					granite	Umbrisols

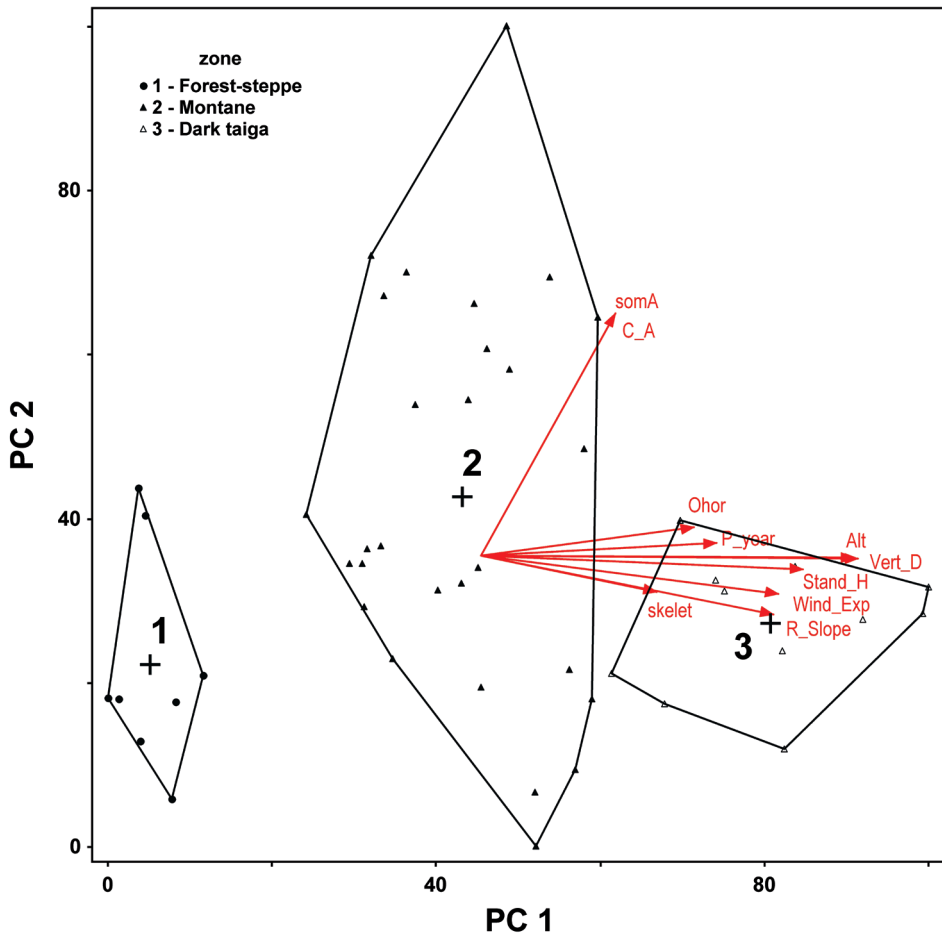


**Fig. 4.** Biplot of the final PCA run with a clear macroclimatic gradient (PC1) and the geo-vegetation zones. For the vector labels, see Table 1 in the text

area. In lower, more accessible parts of the zone, *B. platyphylla* tends to be more abundant than *L. sibirica* or *P. sylvestris* due to logging (since late 1960s up to now), which favored removal of valuable conifers (Dulamsuren et al. 2005; Kusbach et al. 2017b). High intensity logging limits the regeneration of *Pinus* in this area, reduces seedling numbers and creates conditions that are suitable only for the regeneration of deciduous tree species (Gerelbaatar et al. 2019). Thus, the conifers' return into these parts is problematic due to the absence of seed trees, poorly developed or missing natural regeneration and often overgrazing. Artificial planting is usually necessary in those broadleaved ecosystems (Kusbach et al. 2017b; Juříčka et al. 2019).

*Abies sibirica*, *Pinus sibirica* and *Picea obovata* are shade-tolerant and climatic climax tree species of the dark taiga zone, which together with *Betula platyphylla* and *Populus tremula* consist of close canopy forests (Fig. 2, 4). In the highest elevations, we identified Cambisols and Umbrisols (Phaeozems only under broadleaved spp.). The zone is indicated not just by higher precipitation, thick O and thinner A horizons with a high amount of soil organic matter (organic carbon), but also by lower pH and amount of important macronutrients Ca, Mg, P and K. The zone is cool and moist (Table 2, Fig. 3, 4, Appendix B). In general, the forest cover is close to 100 % of the total zone area. Because of lower accessibility of the zone, its vegetation is relatively untouched. Five of our six dark taiga sites were found in an old-growth, never logged forest.

## Birch and aspen communities are off the geo-climatic zonation

The ecological amplitude of *Betulla platyphylla* and *Populus tremula* is extremely broad compared to conifers. In our study area, this amplitude is represented by birch's (1) large altitudinal range, from low azonal sites within the forest-steppe zone (ca 750–800 m a.s.l.) through zonal sites within the montane zone, up to 1473 m a.s.l. within the dark taiga zone, and (2) heterogeneous geomorphology, as indicated by occurrence on diverse substrates and soils (Fig. 2, 3, Table 2). The wide range of climate and geomorphology/soils is associated with large differences in nutrient availability among soils in birch-dominated sites. Birch and aspen occur on rich sites with surpluses of humus and macronutrients such as N, K, Ca, and Mg. It also occurs on relatively poor and more acidic sites in high altitudes, where some macronutrients may be deficient (especially the bases Ca, Mg) (Appendix B). On the other hand, rather than a reflection of the environment, birch-dominated stands in the area are mostly a result of human-induced disturbances such as logging for a valuable conifer timber. Additionally, considerable environmental similarity between physiognomically different ecosystems such as *B. platyphylla*, *L. sibirica*, *P. sylvestris*, and *P. tremula* (Fig. 2) may suggest successional stages of these ecosystems. They, being close in environmental factors, might be distinguished by other than these factors, e.g., disturbance. For example, there was no single environmental factor, important at the level of regional climate that can discriminate birch and aspen ecosystems (secondary small-leaved forests, Vostokova and Gunin 2005) as discrete geo-vegetation zones (Kusbach et al. 2014). Thus, these ecosystems are azonal, driven by disturbance regimes either anthropogenic (logging) or natural (fire).

### Implications for management

In Mongolia, the forestry sector is under development (Tsogtbaatar 2007; Batkhoo

et al. 2011). Except the Resolution by the Parliament of Mongolia No. 49, the State Policy on Forest adopted in May 14, 2015, and the Law on Forest updated in 2012, lower level guidelines (using tools analogical to CFEC and RPF in the Czech Republic) important for starting of sustainable forest management are missing. A state of forests, highly exposed to depletion and degradation especially in a forest-steppe buffer zone is alarming (Vostokova and Gunin 2005; Batkhoo et al. 2011; Kusbach et al. 2017b). Forests generally grow in extreme conditions with low productivity, poor regeneration capacity and over-harvesting (Gerelbaatar et al. 2019). The state forest policy should be changed towards detailed legislation based on ecological and sustainable principles (Altrell and Erdenebat 2016). In regions without earlier ecological classification systems such as Mongolia, our approach has considerable potential for the development of ecologically sound classifications. We suggest that management and ecosystem studies should be viewed in the context of a comprehensive ecological classification (e.g., Haeussler 2011). This framework will facilitate detailed ecosystem structuring at lower ecosystem levels e.g., for a site discrimination.

For example, the geo-vegetation structuring suggested in our analysis was used in development of the first forest management plan in Mongolia based on ecological principles (Smola et al. 2019). Forest management of the forest property of the Domogt Shariin Gol Company Ltd. was recommended for forest development types, the units designed for important landscape environmental gradients. Besides relatively "static" properties (Kusbach et al. 2014), also dynamic indicators (disturbances such as fire) influencing forest ecosystems were considered. Resulting forest development types and subtypes were further structured for age of forest stands (Smola et al. 2019).

At the beginning of regular sustainable management of forests, the systematic classification framework and management

guidelines such as CFEC and RPF, are, within the expert lacking settings of the Mongolian forestry sector, absolutely necessary. The geo-vegetation zonation suggested here, should be expanded and further tested on greater objective data sets, e.g., data coming from the national inventory (Altrell and Erdenebat 2016). Moreover, the forest ecological classification will serve as a reference platform for recent ecological issues such as global climate change resulting in potential changes of ecosystems and important communication tool within and between ecosystem research and management (e.g., Kotar 1988; Kusbach et al. 2014). Besides, it will provide a framework for practical interpretations and decisions such as collecting, organizing and reporting ecological information, e.g., in wildlife, timber, soil and water management, biodiversity, restoration and conservation (e.g., Zenner et al. 2010; Čermák et al. 2019; Smola et al. 2019).

## CONCLUSIONS

Based on complex data and multivariate statistics, we identified three geo-vegetation zones in the study area: (i) forest-steppe, (ii) montane and (iii) dark taiga. The zones were defined as areas with a similar potential overstory composition in climatic climax in order to provide a coarse-scale framework for building comprehensive ecological classification. Our results are in compliance and specify earlier botanical studies of the region. However, we quantified significant factors,

set up macroclimatic environmental limits and characterized these zones by macroclimate, geomorphology, and soils represented by O horizon thickness and soil types. Birch and aspen ecosystems were excluded as the discrete zones from the zonation due to their great ecological amplitude, successional status and predominantly disturbance-based origin.

The geo-vegetation zonation outlined in our study is to our best knowledge, the first attempt at quantifying vegetation along with the environment at a macroclimatic level in Mongolia. A comparable framework is missing in Mongolia, similar approach can be applied elsewhere in central Asia: (i) for development of forest management framework and (ii) as an information platform and reference for current environmental issues in Mongolian landscapes.

## ACKNOWLEDGEMENTS

The paper was supported by the project grants of the Czech Development Agency: (i) Development of Forests and the Gene Pool of Local Forest Tree Ecotypes in Mongolia 2015-18, CzDA-RO-MN-2014-6-31210 realized by the Forest Management Institute, Brandýs nad Labem, Czech Republic, and (ii) Placement of Czech Teachers to Developing Countries, 22-ČRA19-02\_05 realized by the Mendel University in Brno in 2019. We thank all anonymous reviewers for help in improving the paper. ■

## REFERENCES

- Altrell D. and Erdenebat E. (2016). Mongolian Multipurpose National Forest Inventory 2014 – 2016. 1st edition. Ulaanbaatar, Ministry of Environment and Tourism. p. 171.
- Bailey R.G. (2002). Ecoregion-based Design for Sustainability. Springer-Verlag, New York, USA.
- Barbati A., Corona P., and Marchetti M. (2007). A Forest Typology for Monitoring Sustainable Forest Management: The Case of European Forest Types. *Plant Biosystems*, 141, pp. 93–103.
- Batkhuu N-O., Lee D.K., Tsogtbaatar J. (2011). Forest and Forestry Research and Education in Mongolia. *Journal of Sustainable Forestry*, 30, pp. 600–617.

Breiman L. (2001). Random forests. *Machine Learning*, 45, pp. 5-32.

Caudullo G., Pasta S., Giannetti F., Barbati A. and Chirici, G. (2016). European Forest Classifications. In: San-Miguel-Ayaz J., de Rigo D., Caudullo G., Houston Durrant T., and Mauri A. (Eds.), *European Atlas of Forest Tree Species*. Publ. Off. EU, Luxembourg, pp. 32-33.

Chen C., Liaw A., and Breiman L. (2004). Using Random forest to Learn Imbalanced Data. Technical Report 666. Statistics Department of University of California, Berkeley, California, USA.

Chytrý M., et al. (2012). High Species Richness in Hemiboreal Forests of the Northern Russian Altai, Southern Siberia. *Journal of Vegetation Science*, 23, pp. 605-616.

Cook J.E. (1996). Implications of Modern Successional Theory for Habitat Typing: a Review. *Forest Science*, 42, pp. 67-75.

Čermák P., Mikita T., Trnka M., Štěpánek P., Jurečka F., Kusbach A. and Šebesta J. (2018). Changes of Climate Characteristics of Forest Altitudinal Zones within the Czech Republic and their Possible Consequences for Forest Species Composition. *Baltic Forestry* 24(2), pp. 234-248.

Damman A.W.H. (1979). The Role of Vegetation Analysis in Land Classification. *Forestry Chronicle*, 55: pp. 175-182.

Dorjgotov D. (2009). Vegetation. In: Sh. Tsegmid, V.V. Borobiev, eds., *Mongolian National Atlas*. Ulaanbaatar, Mongolia: Academy of Sciences, Institute of Geography Press. pp. 125-133.

Dulamsuren Ch., Hauck M., and Muehlenberg M. (2005). Vegetation at the Taiga Forest-Steppe Borderline in the Western Khentey Mountains, Northern Mongolia. *Ann. Bot. Fennici*, 42, pp. 411-426. Ermakov N., Cherosov M., and Gogoleva P. (2002). Classification of the Ultracontinental Boreal Forests in Central Yakutia. *Folia Geobotanica*, 37 pp. 419-440.

Geological Map of Mongolia. (1998). Mineral Resources Authority of Mongolia, Geological Office, Geological Survey with Mongolian Academy of Science, Institute of Geology and Mineral Resources, Sheet M-48, Scale 1: 1 000 000, Ulaanbaatar, Mongolia.

Gerelbaatar S., Baatarbileg N., Battulga P., Batsaikhan G., Khishigjargal M., Batchuluun T., Gradel A. (2019). Which Selective Logging Intensity is Most Suitable for the Maintenance of Soil Properties and the Promotion of Natural Regeneration in Highly Continental Scots Pine Forests?—Results 19 Years after Harvest Operations in Mongolia. *Forests*, 10(141), doi:10.3390/f10020141.

Goldammer J.G. (2002). Fire Situation in Mongolia. *Int. For. Fire News*, 26, pp. 75–83.

Gradel A., Batsaikhan G., Ochirragchaa N., Batdorj D. and Kusbach A. (2017). Climate-Growth Relationships and Pointer Year Analysis of a Siberian Larch (*Larix sibirica* Ledeb.) Chronology from the Mongolian Mountain Forest-Steppe. *Forest Ecosystems*, 4(22), <https://doi.org/10.1186/s40663-017-0110-2>.

Grubov V.I. (1982). *Opređelitel' Sosudistyh Rastenij Mongolii (s Atlasom)* [Key to the Vascular Plants of Mongolia (with an Atlas)]. – Leningrad, Nauka. p. 442, (in Russian).

Haeussler S. (2011). Rethinking Biogeoclimatic Ecosystem Classification for a Whanging world. *Environmental Reviews*, 19, pp. 254-277, doi: 10.1139/A11-008.

Hair J.F.J., Hult T.G.H., Ringle C. and Sarstedt M. A. (2013). *Primer on Partial Least Squares Structural Equation Modeling (PLS-SEM)*; SAGE Publications, Inc.: Thousand Oaks, CA, USA; p. 307, ISBN 9781452217444.

Hais M., Chytrý M. and Horsák M. (2016). Exposure-Related Rorest-Steppe: A Diverse Landscape Type Determined by Topography and Climate. *Journal of Arid Environments*, 135, pp. 75–84.

Hilbig W. and Knapp H.D. (1983). Vegetationmosaik and Floraelemente an der Wald-Steppen Grenze in Khentey Gebirge 174: (Mongolei). *Flora*, 174, pp. 1-89.

Holmgren G.S., Juve R.L. and Geschwender R.C. (1977). A Mechanically Controlled Variable Rate Leaching Device. *Soil Science Society of America Journal*, 41, pp. 1207-1208.

Johnson D.L., Keller E.A. and Rockwell T.K. (1990). Dynamic Pedogenesis: New Views on Some Key Soil Concepts, and a Model for Interpreting Quaternary Soils. *Quaternary Research*, 33, pp. 306-319.

Juřička D., Kusbach A., Pařilková J., Houška J., Ambrožová P., Pecina V., Rosická Z, Brtnický M. and Kynický J. (2019). Evaluation of Natural Forest Regeneration as a Part of Land Restoration in Khan Khentii Massive, Mongolia. *Journal of Forestry Research*, <https://doi.org/10.1007/s11676-019-00962-5>.

Karamysheva Z.V. and Khramtsov V.N. (1995). The Steppes of Mongolia. *Braun-Blanquetia*, 17, pp. 1-79.

Karta Lesov Mongolskoy Narodnoy Respubliki, M. 1: 1500000 (Map of the Forests of the People's Republic of Mongolia, Scale 1: 1500000). (1983). Updated 2005. Moscow: Glav. Upr. Geodz. Kartogr. Mongol. i Glav. Upr. Geodez. Kartogr. SSSR (Central Directorate for Geodesy and Cartography of Mongolia and Central Directorate for Geodesy and Cartography of the USSR, (in Russian).

Khodolmor S., Tsogtbaatar, J., Das D., Batzargal Z. and Mandakh N. (2013). *Desertification Atlas of Mongolia*. Ulaanbaatar. ISBN: 978-9973-0-065-2, p. 134, (in Mongolian).

Knystautas A. (1987). *The Natural History of the USSR*. McGraw-Hill, New York.

Kolesnikov B.P. (1974). Genetic stage in forest typology and its objectives. *Russian J. For. Sci.* 2: 3–20, (translated from Russian by Lesovedenie, 1974).

Korotkov, I.A. (1976). Geograficheskie zakonomernosti raspredeleniya lesov v Mongol'skoy Narodnoy Respublike (Geographical specifics of forest distribution in the Mongolian People's Republic). *Botanicheskiy Zhurnal (Rus. J. Bot.)*, 61(2), pp. 145-153, (in Russian with English abstract).

Kotar J. (1988). *Ecological Land Classification: the First Step in Forest Resource Management*. In: J.E. Johnson (ed.), *Managing North Central Forests for Non-timber Values*. Proceedings of the Fourth Society of American Foresters Region V Technical Conference, Publication 88-04. Minnesota Extension Service, University of Minnesota, Minnesota, USA, pp. 43-52.

Krajina V.J. (1965). Biogeoclimatic Zones and Classification in British Columbia. *Ecology of Western North America*, 1, pp. 1-17.

Kusbach A., Van Miegroet H., Boettinger J.L., et al. (2014). Vegetation Geo-Climatic Zonation in the Rocky Mountains, northern Utah, USA. *Journal of Mountain Science*, 11(3), pp. 656-673. DOI: 10.1007/s11629-013-2793-3.

Kusbach A., Friedl M., Zouhar V., Mikita T. and Šebesta J. (2017a). Assessing Forest Classification in a Landscape-Level Framework: An Example from Central European Forests, *Forests*, [online], Available at: <http://www.mdpi.com/1999-4907/8/12> [Accessed 9 Jan. 2019].

Kusbach A., Štěřba T., Smola M., Novák J., Lukeš P., Strejček R., Škoda A., Bažant V., and Pondělíčková A. (2017b). Development of Forests and the Gene Pool of Local Forest Tree Ecotypes in Mongolia. *Development of Forests and Landscape in Mongolia, Silviculture, Urban Forestry, Public Relation. Proceedings of the seminar, Sharyn Gol/Darkhan, Mongolia, September 2017. Project CzDA-RO-MN-2014-6-31210. ÚHÚL Brandýs nad Labem, Czech Republic 2017. ISBN 978-80-88184-12-6, (in Czech and Mongolian).*

Lattin J.M., Carrol J.D., et al. (2003). *Analyzing Multivariate Data*. Brooks/Cole, Thompson Learning, Pacific Grove, California, USA.

Lavrenko E.M. and Sokolov V.E. (1978). *Forests of Mongolia- Geography and Typology*. Academy of Science of USSR, Nauka, Moscow, p. 128, (in Russian).

Liaw A., Wiener M. (2002). Classification and Regression by randomForest. *R News*, 2(3), pp. 18–22.

Major J. (1951). A Functional, Factorial Approach to Plant Ecology. *Ecology*, 32(3), pp. 392-412.

McCune B., Grace J.B. and Urban D.L. (2002). *Analysis of Ecological Communities*, 2nd Edition. MjM Software Design, Gleneden Beach, Oregon, USA.

McCune B. and Mefford M.J. (2011). *PC-ORD. Multivariate Analysis of Ecological Data*, Version 6.0 for Windows; MjM Software: Gleneden Beach, OR, USA.

Morozov G.F. (1925). *Theory of forest types*. Leningrad: State Publishing House, p. 367, (translated from Russian from *Ucheniye o tipakh lesa*, 1925).

Mühlenberg M. et al. (2011). *Biodiversity Survey at Khonin Nuga Research Station, West-Khentey, Mongolia*.

Nogina N.A. et al. (1980). *Pocvennaya karta mongolskoy narodnoy respubliky (Soil map of Mongolia) 1: 2 500 000*. Commom Soviet-Mongolian expedition, Pocvennyy institut V. V. Dokuchaeva VASCHNIL (V.V. Dokuchaev Soil Science Institute VASCHNIL), Moscow, Russia, (in Russian).

Nyam L., Otgonsuren B., Ganbaatar Ch., Dashdorj N., Saule A., Tsogbaatar A., and Enkhjargal D. (2009). *Guidelines for forestry workers in Mongolia*. The Forest Agency, Implementing Agency for Government of Mongolia. p. 301.

Olsen S.R., Cole C.V., et al. (1954). Estimation of Available Phosphorus in Soil by Extraction with Sodium Bicarbonate. UDA, Circular 939. U.S. Government Printing Office, Washington, DC, USA. Oyunsanaa, B. (2011). Fire and Stand Dynamics in Different Forest Types of the West Khentey Mountains, Mongolia. PhD Thesis, Georg-August-Universität, Göttingen.

Pfister R.D. and Arno S.F. (1980). Classifying Forest Habitat Types Based on Potential Climax Vegetation. *Forest Science*, 26, pp. 52-70.

Plíva K. and Žlábek I. (1986). Přírodní lesní oblasti ČSR (Natural Forest Areas in the Czech Republic). Státní Zemědělské Nakladatelství Praha: Praha, Czechoslovakia, p. 313, (in Czech).

Pogrebnyak P.S. (1955). Fundamentals of forest typology. Kiev. Publishing house of the Academy of Sciences of the Ukrainian SSR, p. 452, (translated from Russian from *Osnovi lesnoi tipologii*, 1968).

Pojar J., Klinka K. and Meidinger D.V. (1987). Biogeoclimatic Ecosystem Classification in British Columbia. *Forest Ecology and Management*, 22, pp. 119–154.

R Core Team. (2014). R: A Language and Environment for Statistical Computing; R Core Team: Vienna, Austria.

Roberts D.W. and Cooper S.V. (1989). Concepts and Techniques in Vegetation Mapping. In: D.E. Ferguson et al. (eds.), *Proceedings: Land Classifications Based on Vegetation: Applications for Resource Management*. General Technical Report INT-257 USDA, Forest Service, Intermountain Research Station, Ogden, Utah, USA. pp. 90-96.

Smola M., Kusbach A., Štěřba T., Adolt R, Nečas M. (2019). Forest management plan in Domogt Sharii Gol, Mongolia is elaborated on ecological and sustainable principles. *Journal of Landscape Ecology*, 12/2: 92-115. DOI:10.2478/jlecol-2019-0012

Sukachev V.N. (1972). Fundamentals of forest typology and forest biogeocenology. Volume 1. Leningrad. Nauka, p. 408, (translated from Russian from *Osnovi lesnoi tipologii i lesnoi biogeotsenologii*, 1972).

Thien S.J. (1979). A Flow Diagram for Teaching Texture-by-Feel Analysis. *Journal of Agronomic Education*, 8, pp. 54-55.

Tsedendash G. (1995). The Forest Vegetation of the Khentey Mountains. Dissertation, National University of Mongolia, Ulan Bator, (in Mongolian).

Tsedendash G. (1998). Forest Ecological Features of Mongolia. Paper presented at the Open Parliamentary Forum. April 28, 1998, Ulaanbaatar. Mongolia, (in Mongolian).

Tsogtbaatar J. (2004). Deforestation and reforestation needs in Mongolia. *Forest Ecology and Management*, 201, pp. 57–63.

Tsogtbaatar J. (2007). Forest Rehabilitation in Mongolia. In: D.K. Lee, ed., *Keep Asia Green*, Volume II, "Northeast Asia". IUFRO World Series Vol. 20-II. IUFRO, Vienna. ISBN 978-3-901347-76-4. pp. 91-116.

Ulziikhutag N. (1989). Characteristics of flora of Mongolia. In: Ch. Sanchir, ed., *Synopsis of Mongolian flora*. Ulaanbaatar, Mongolia: State Publishing. pp. 107-148, (in Mongolian).

Unatov A.A. (1950). Botanical-geographical district allocation. In: E.M. Lavrenko, ed., The main features of the vegetation cover of Mongolia. Leningrad, Russia: Russian Academy of Sciences Press. pp. 124-189, (in Russian). Vahalík P. and Mikita T. (2011). Possibilities of Forest Altitudinal Vegetation Zones Modelling by Geoinformatic Analysis. *Journal of Landscape Ecology*, 4(2), pp. 49-61.

Viewegh J., Kusbach A. and Mikeska M. (2003). Czech forest ecosystem classification. *Journal of Forestry Science*, 49, pp. 85–93.

Vostokova E.A., Gunin P.D. (2005). Ecosystems of Mongolia. Atlas. Moscow 2005: General Scientific Edition. Institute of Ecology and Evolution, Russian Academy of Science, p. 48.

Ward J.H. (1963). Hierarchical Grouping to Optimize an Objective Function. *Journal of the American Statistical Association*, 58, pp. 236-244.

Wishart D. (1969). An Algorithm for Hierarchical Classifications. *Biometrics*, 25, pp. 165-170.

WRB. (2014). World Reference Base for Soil Resources 2014, update 2015, International Soil Classification System for Naming Soils and Creating Legends for Soil Maps. Report 106. FAO, Rome, [online]. Available at: <http://www.fao.org/3/i3794en/i3794en.pdf> [Accessed 9 Jan. 2019].

Zenner E.K., Peck J.E., et al. (2010). Combining Ecological Classification Systems and Conservation Filters Could Facilitate the Integration of Wildlife and Forest Management. *Journal of Forestry*, 108, pp. 296-300.

Received on February 28<sup>th</sup>, 2019

Accepted on August 8<sup>th</sup>, 2019

**Vladimir A. Usoltsev<sup>1,2</sup>, Igor M. Danilin<sup>3\*</sup>, Zaandrabalyn Tsogt<sup>4</sup>,  
Anna A. Osmirko<sup>1</sup>, Ivan S. Tsepordey<sup>2</sup>, Viktor P. Chasovskikh<sup>1</sup>**

<sup>1</sup> Ural State Forest Engineering University, Yekaterinburg, Russia

<sup>2</sup> Botanical Garden, Russian Academy of Sciences, Ural Branch, Yekaterinburg, Russia

<sup>3</sup> V. N. Sukachev Institute of Forest, Russian Academy of Sciences, Siberian Branch, Krasnoyarsk, Russia

<sup>4</sup> Institute of General and Experimental Biology, Mongolian Academy of Sciences, Ulaanbaatar, Mongolia

\* **Corresponding author:** danilin@ksc.krasn.ru

# ABOVEGROUND BIOMASS OF MONGOLIAN LARCH (*LARIX SIBIRICA* LEDEB.) FORESTS IN THE EURASIAN REGION

**ABSTRACT.** We used our database of tree biomass with a number of 433 sample trees of *Larix* from different ecoregions of Eurasia, involving 61 trees from Mongolia for developing an additive model of biomass tree components. Our approach solved the combined problem of additivity and regionality of the model. Our additive model of tree aboveground biomass was harmonized in two ways: first, it eliminated the internal contradictions of the component and of the total biomass equations, secondly, it took into account regional (and correspondingly species-specific) differences of trees in its component structure. A significant excess of larch biomass in the forest-tundra is found that may be explained by permafrost conditions, by tree growth in low-yielding stands with a high basic density of stem wood and relatively high developed tree crown in open stands. The aboveground biomass of larch trees in Mongolia does not stand out against the background of the most ecoregions of Eurasia. Based on our results, we conclude that the growing conditions of larch in Mongolia are not as tough as it was suggested earlier by other scientists. Biomass relations between regions may be explained by unknown and unaccounted factors and errors of measurements in all their phases (assessment of age, diameter, height of a tree, the selection of supposedly representative samples of component biomass, their drying, weighing, etc.). The question what explains the regional differences in the structure of biomass of trees with the same linear dimensions of their stems, remains open. Undoubtedly, the differences in tree age here play an important role. Also, important factor is the variation in the morphological structure of stands, which, in turn, is determined by both climatic and edaphic factors. The obtained models allow the determination of larch forest biomass in different ecoregions of Eurasia with the help of height and diameter data.

**KEY WORDS:** genus *Larix* spp., aboveground tree biomass, regional differences, equations additivity, allometric models, dummy variables, tables of biomass.

**CITATION:** Vladimir A. Usoltsev, Igor M. Danilin, Zaandrabalyn Tsogt, Anna A. Osmirko, Ivan S. Tsepordey, Viktor P. Chasovskikh (2019) Aboveground Biomass Of Mongolian Larch (*Larix Sibirica* Ledeb.) Forests In The Eurasian Region. Geography, Environment, Sustainability, Vol.12, No 3, p. 117-132  
DOI-10.24057/2071-9388-2018-70

## INTRODUCTION

Forest ecosystems play an important role as sinks of atmospheric carbon. Since a significant part of forest cover has been represented by mixed forests, for the correct estimation of their biological productivity in many cases allometric models of biomass are needed, developed at a tree level. The regression (allometric) method of estimating forest biomass when using the results of sampling of model trees, was represented in the whole range of stem diameters (and sometimes of tree height) is the current standard (Marklund 1983). In conditions of continuously increasing biosphere function of forest cover of the planet, there is a trend related to the harmonization of allometric models of tree biomass, that is fulfilled either by involving dummy variables into a model (Jacobs and Cunia 1980; Fu et al. 2012; Zeng 2015), or by providing additive component composition (Kozak 1970; Parresol 2001; Zheng et al. 2015; Zhang et al. 2016). The additivity of the component composition assumes the consistency of the model by biomass components and means that the total biomass of components (stems, branches, needles) obtained by the component equations is equal to the value of biomass obtained by the equation for total biomass. According to Sanquetta et al. (2015), independent (without additivity) fitting of coefficients for biomass components and total biomass is not satisfactory, but this is not observed in case when the simultaneous fitting is used, accounting the additivity principle and resulting in more effective estimators.

These and other models are usually developed on local (regional) harvest data of tree biomass. As a result, the published models have either regional application

without harmonization with the help of dummy variables and without providing the principle of component additivity composition, or provide additivity of component composition but without any regionalization (Usoltsev 2017). For genus *Larix* spp. a number of models for estimating the aboveground biomass from stem diameter and height data have already been published (Shi et al. 2002; Bjarnadottir et al. 2007; Novák et al. 2011; Zhao et al. 2011; Battulga et al. 2013), but they are of regional nature and do not ensure the additivity of the component composition of the biomass.

The goal of this paper to be combine the mentioned approaches, and to develop a regional additive model (AM) of tree aboveground biomass on the example of the Siberian larch in Mongolia, interfaced with the tree biomass of other regions of Eurasia by involving dummy variables (Draper and Smith 1966) into a model.

## MATERIALS AND METHODS

The database of single-tree biomass created for the forest-forming species of Eurasia provides the data to develop the called modern methodological developments on the trans-continental level (Usoltsev 2016). Harvest data on the biomass of 43 trees were obtained in the forests of the Siberian larch (*Larix sibirica* Ledeb.) of north-eastern Mongolia, the Eastern part of Khentii Mountains, near the village of Mungun-Mort (49°10'N, 110°0'E, 700-1500 m a.s.l.) (Fig. 1).

We established 5 sample plots and measured all trees. Each plot considers an area involving 200-400 trees with the height more 1.5 m and stem diameter at breast height (DBH) more 0.5 cm. Range of diameter classes varies from 0.5 to 32

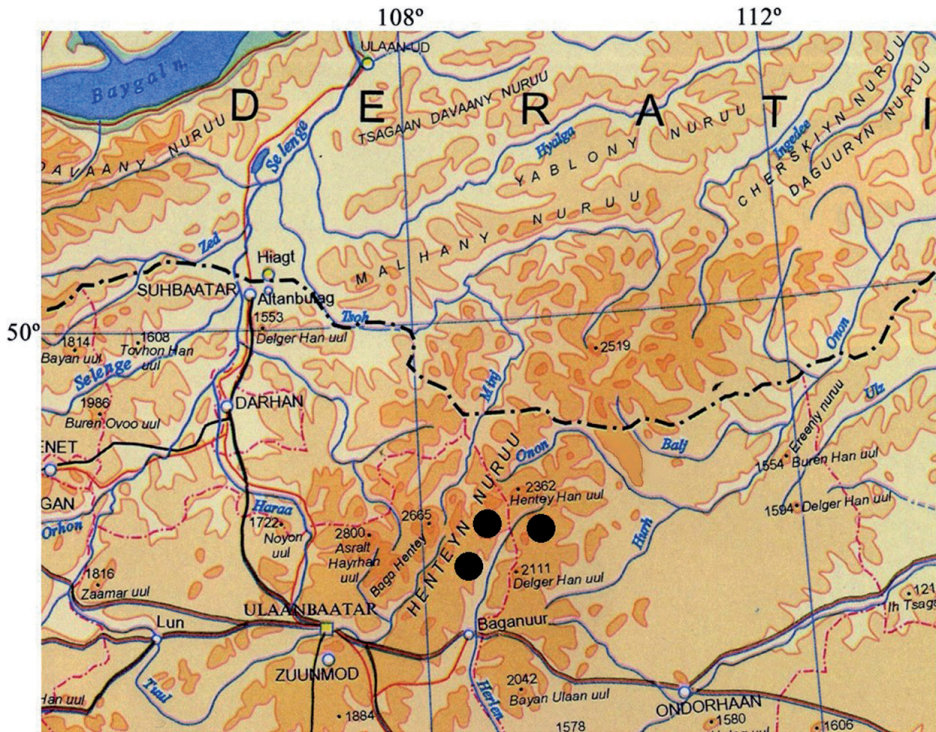


**Fig. 1. The position of the sample area on the map of Khentii Mountains (marked by the black points). Scale 1: 6000000**

cm. On each plot we harvested model trees – one mean value exemplar of each DBH class. Model trees were completely divided into biomass components and weighed in wet state at lever arid balance with an accuracy to  $\pm 1$  g at a weight up to 10 kg and with an accuracy to  $\pm 100$  g at a weight greater than 10 kg. Samples from each component were packed into polyethylene packets, marked, and transported to the laboratory, where to determine moisture content they were dried in a dryer up to an absolutely dry state ( $+105^{\circ}\text{C}$  during three days) and weighed at electronic scale with an accuracy to  $\pm 0.1$  g. The weight of components in an absolutely dry state was equalized analytically, summed according to classes of stem thickness, and reduced to 1 hectare. Bark wood ratio was found from samples cut out of the stem at different heights (according to sections). The length of sections was determined depending on the height of the tree stem. The number of sections for each tree was no less than 10. The calculation of the stem volume

was performed according to the complex Huber's formula (Danilin 2009; Danilin and Tsoigt 2014, 2015). The results of estimating the tree biomass on the sample plots are shown in Table 1. We draw attention to the relatively high density of larch stands, that is typical for larch, growing not only in the harsh mountainous areas of Mongolia, but also in the northern taiga of Russia. In particular, larch has 112 thousand trees per 1 ha at the age of 14 years in Yakutia ( $62^{\circ}\text{N}$ ,  $130^{\circ}\text{E}$ ) (Pozdnyakov 1975), 55 thousand trees per 1 ha at the age of 30 years in the upper Kolyma river ( $62^{\circ}\text{N}$ ,  $147^{\circ}\text{E}$ ) (Pozdnyakov 1975), 4.8 thousand per ha at the age of 40 years near Arkhangelsk ( $64^{\circ}\text{N}$ ,  $40^{\circ}\text{E}$ ) (Molchanov 1971), 2.7-2.9 thousand per ha at the age of 86-87 years in the basin of the Nizhnyaya Tunguska river ( $64^{\circ}\text{N}$ ,  $100^{\circ}\text{E}$ ) (Abaimov et al. 1997).

In another region of Mongolia, on its western border in the mountains of the Mongolian Altai, the biomass structure of Siberian larch trees was studied on 18 sample plots, and allometric models of

**Table 1. Aboveground biomass of larch trees in the eastern part of the Khentii Mountains**

No.	Tree age, years	Stem DBH, cm	Tree height, m	Stem volume, dm <sup>3</sup>		Biomass in absolutely dry condition, kg					Tree numbers per ha	Mean diameter, cm
				Total	Stem bark	Stem		Branches	Foliage	Sum total		
						Total	Bark only					
1	18	8.9	6.5	22.6	7.1	9.6	2.3	6.2	2.6	18.4	56200	1.6
2	18	7.5	5.9	16.9	5.3	7.4	1.8	4.6	1.9	13.9		
3	18	6.3	5.2	11.2	3.5	5.1	1.3	2.7	1.1	8.9		
4	17	4.9	4.9	6.4	2.0	3.1	0.8	1.2	0.7	5.0		
5	18	4.0	4.3	4.3	1.4	2.0	0.6	0.84	0.5	3.34		
6	17	2.9	3.6	2.2	0.9	1.0	0.3	0.42	0.3	1.72		
7	15	1.9	3.3	1.1	0.5	0.4	0.1	0.21	0.1	0.62		
8	14	1.0	2.4	0.2	0.05	0.12	0.05	0.032	0.03	0.182		
9	15	0.5	1.5	0.1	0.05	0.05	0.02	0.021	0.01	0.081		
10	32	17.6	11.3	125.4	37.9	51.4	11.2	19.8	7.5	78.7	5700	5.9
11	35	15.4	11.1	100.6	28.1	40.2	8.8	13.8	5.2	59.2		
12	36	13.2	10.7	75.8	18.4	29.0	6.4	8.0	2.9	39.9		
13	27	9.8	8.3	39.9	9.5	18.4	4.8	8.1	2.7	29.2		
14	27	7.3	7.3	18.3	5.4	8.5	2.3	3.3	1.3	13.1		
15	25	3.9	5.8	4.3	1.2	1.9	0.6	0.5	0.2	2.6		
16	21	1.8	3.0	0.8	0.3	0.4	0.1	0.21	0.04	0.65		
17	15	0.8	2.3	0.2	0.1	0.15	0.05	0.04	0.01	0.20		
18	33	12.5	10.9	73.8	20.8	29.7	6.7	3.7	1.4	34.8		
19	34	11.2	10.4	54.4	16.8	23.5	3.7	3.4	0.9	27.8		
20	32	10.1	10.0	43.9	13.4	19.0	3.6	2.8	0.7	22.5		
21	30	8.8	9.5	33.3	10.0	14.2	3.3	2.1	0.5	16.8		
22	31	8.0	9.2	27.1	8.3	11.5	2.9	1.66	0.44	13.6		
23	35	7.1	8.8	20.8	6.6	8.7	2.4	0.95	0.40	10.05		
24	29	5.6	7.9	10.5	2.2	4.8	1.2	0.23	0.06	5.09		
25	24	4.1	7.1	5.3	0.9	2.7	0.7	0.08	0.03	2.81		
26	27	3.2	6.2	2.9	0.9	1.4	0.4	0.07	0.03	1.5		

27	44	31.0	17.8	618.7	144.0	272.0	38.7	53.2	7.8	333.0	2900	7.5
28	43	27.4	17.6	508.4	114.3	228.9	33.2	36.4	6.2	271.5		
29	39	23.5	17.3	398.0	84.5	185.7	27.7	19.5	4.6	209.8		
30	42	19.8	16.8	288.4	60.5	128.5	20.7	13.8	3.4	145.7		
31	43	15.9	16.2	178.8	36.5	71.2	13.6	7.9	2.2	81.3		
32	41	12.0	12.6	102.4	21.6	40.8	8.1	4.7	1.3	46.8		
33	40	8.1	9.0	25.9	6.7	10.3	2.5	1.4	0.6	12.3		
34	33	4.5	6.6	15.8	4.1	3.1	0.7	1.0	0.5	4.6		
35	75	32.3	20.4	662.4	118.7	273.2	56.2	31.2	7.0	311.4	2100	18.4
36	73	29.7	19.9	587.0	111.6	247.5	49.3	25.8	5.9	279.2		
37	74	27.2	19.3	511.5	104.4	221.6	42.3	20.3	4.8	246.7		
38	73	24.5	18.8	436.0	97.2	195.6	35.2	15.0	3.7	214.3		
39	72	22.0	18.2	360.5	90.0	169.8	28.3	9.6	2.5	181.9		
40	70	18.7	17.5	256.2	66.1	112.6	18.6	5.9	1.7	120.2		
41	70	15.4	16.8	151.9	42.2	55.3	8.9	2.0	0.8	58.1		
42	67	12.2	13.7	92.8	26.2	34.4	5.4	1.6	0.7	36.7		
43	60	8.8	10.5	33.7	10.3	13.5	1.9	1.3	0.6	15.4		

above-ground biomass were calculated according to the diameter and height of the stem (Battulga et al. 2013). We decided to find out whether there are differences in the above-ground tree biomass data of the two mountain regions of Mongolia, and depending on the result obtained we can calculate allometric equations either separately for two regions, or to give one generalized equation.

The harvest tree biomass data of the two regions were obtained in different age ranges: on the Khentii Mountains from 14 to 75 years and on the Mongolian Altai from 55 to 173 years. In order to exclude the influence of age on the comparison result, the tree age was involved into the model as an independent variable, in addition to the stem diameter and height. It is known that allometric equations of different regions have differences not only

in the value of the intercept, but also in the slope of the regression line, i.e. allometric exponent (Battulga et al. 2013). With that said, we coded the harvest data of the two regions by the binary variable and calculated the equation of the following structure:

$$P_a = \exp \left[ a_0 + a_1 \ln A + a_2 \ln D + a_3 \ln H + a_4 (\ln D)(\ln H) + a_5 X + a_6 X(\ln D) + a_7 X(\ln H) \right], \quad (1)$$

where  $P_a$  – aboveground tree biomass in dry condition, kg;  $A$  – tree age, yrs;  $D$  – stem diameter at breast height, cm;  $H$  – tree height, m;  $X$  – the binary variable encoding data belonging to two mountainous regions of Mongolia:  $X=1$  for Khentii and  $X=0$  for Mongolian Altai. According to a geometric interpretation of this result, the constant  $a_5$  characterizes

the difference of the regression intercept values of the two regions on the axis of ordinates,  $a_6$  and  $a_7$ , show the difference in the regression slopes of the two regions via the orthogonal axes of abscissas, respectively along the axes  $D$  and  $H$ . The constant  $a_4$  of the variable  $(\ln D)(\ln H)$  corrects the violation of allometry owing to the shift of  $D$  up the stem for small values of  $H$ , which was shown earlier (Usoltsev et al. 2019).

Calculating regression equations using the standard Statgraphics software showed that only the constants  $a_2$  and  $a_4$  were statistically significant (the value of Student's criterion  $t_{act}$  is 8.2 and 7.8, respectively, that is more than  $t_{05} = 2$ ), and the  $t_{act}$  for the constants  $a_1$ ,  $a_3$ ,  $a_5$ ,  $a_6$  and  $a_7$  are 0.85, 0.54, 0.75, 1.80 and 0.80, respectively, which is less than  $t_{05} = 2$ . This means that there are no statistically significant differences between the regressions of the two regions for the aboveground tree biomass, nor on the values of the intercept or on the slopes for  $D$  and  $H$  regression lines. The resulting equation, common to the mountain environments of Mongolia is obtained:

$$P_a = \exp[-1.4874 + 1.6658 \ln D + 0.1610 (\ln D)(\ln H)], \quad (2)$$

$$R^2 = 0.992, \quad RMSE = 1.18,$$

And in the further comparative transcontinental analysis, *Larix* tree biomass of Mongolia is allocated by one common dummy variable.

For the purpose of comparative analysis of larch biomass of Mongolia in geographical aspect, from the above mentioned database 390 sample trees of six species of the genus *Larix spp.* were additionally taken (respectively *L. decidua* Mill., *L. sukaczewii* N. Dyl., *L. sibirica* L., *L. gmelinii* Rupr., *L. cajanderi* Mayr., and *L. leptolepis* Gord.). The entire quantity of the data for this study is 433 trees, representing eight ecoregions, designated accordingly by eight dummy variables from  $X_0$  to  $X_7$  (Table 2). Sample trees were harvested and processed

in a number from 5 to 10 copies on each sample plot. Then samples were taken from each biomass component to determine the dry matter content (and for wood and bark of stems also to determine the basic density) and after drying the samples at the temperature of 80-100° C, the results were recalculated for the whole tree. The distribution of sample plots in the ecoregions of Eurasia is shown in Fig. 2. In this case we do not consider the biomass of roots, because there is lack of such data, they were determined by researchers not at all sample plots, often without specifying the method of their estimation. The analysis of the world data of underground tree biomass showed that due to the imperfection of methods to estimate fine root biomass, the total underground biomass of trees and stands may be underestimated from two to five times (Usoltsev 2018).

The disaggregation method of two-step proportional weighing based on the principle "from general to particular" is developed as an alternative to the above-mentioned independent (without additivity) fitting approach. It has been implemented in two versions: as a sequential (Zheng et al. 2015) and parallel (Zhang et al. 2016) disaggregating additive systems of equations for aboveground biomass (Fig. 3). According to the structure of the disaggregation model of a two-step additive equation system (Zheng et al. 2015), the aboveground biomass  $P_a$ , estimated by the initial equation, is divided into biomass components estimated by corresponding equations (Table 3).

The coefficients of the regression equations of all two steps are evaluated simultaneously, that ensures the additivity of the biomass of all components (Dong et al. 2015). Since the regression coefficients in the designed model have been calculated on the log-transformed data, a corresponding correction has been introduced in the equations to eliminate the displacements caused by

**Table 2. Aboveground biomass of larch trees in the eastern part of the Khentii Mountains**

Ecoregions	Latitude, North	Longitude, East	Species of the genus <i>Larix</i> spp.	Block of dummy variables							Mean DBH ±SE (cm) and its range (in the brackets)	Mean tree height ±SE (m) and its range (in the brackets)	Number of trees	Sources	
				X <sub>1</sub>	X <sub>2</sub>	X <sub>3</sub>	X <sub>4</sub>	X <sub>5</sub>	X <sub>6</sub>	X <sub>7</sub>					
Western and Central Europe	47°00' - 49°19'	09°00' - 16°40'	<i>L. decidua</i> Mill.	0	0	0	0	0	0	0	0	17.6±11.2 (7.1÷47.8)	17.7±5.5 (9.8÷34.0)	19	Burger, 1945; Vyskot, 1982
European part of Russia	55°20' - 57°50'	37°00' - 48°10'	<i>L. sukaczewii</i> N.Dyl.	1	0	0	0	0	0	0	0	8.2±7.1 (1.0÷35.0)	8.9±5.7 (2.3÷28.0)	25	Dylis, Nosova, 1977; Polikarpov, 1962; Karaseva, 2003
Turgay steppe	53°30'	64°30'	<i>L. sukaczewii</i> N.Dyl.	0	1	0	0	0	0	0	0	16.1±6.2 (6.2÷28.0)	14.6±2.4 (7.9÷17.8)	28	Usoltsev, 2016
Western Siberia, the flood plain of the Pur river	64°03' - 67°00'	78°00' - 101°10'	<i>L. sibirica</i> L.; <i>L. gmelinii</i> (Rupr.) Rupr.	0	0	1	0	0	0	0	0	11.5±7.1 (2.1÷38.0)	11.1±5.0 (2.9÷24.8)	116	Danilin et al., 2015; Usoltsev, 2016
Eastern Siberia, forest-tundra	70°00'	135°49'	<i>L. cajanderi</i> Mayr.	0	0	0	1	0	0	0	0	7.6±4.9 (0.3÷22.7)	6.5±2.8 (1.4÷14.8)	66	Shchepashchenko, 2015
Russian Far East, northern taiga	60°30'	148°00'	<i>L. cajanderi</i> Mayr.	0	0	0	0	1	0	0	0	18.3±11.7 (3.9÷52.8)	13.9±7.0 (2.9÷30.0)	45	Moskalyuk, 2015
Mountains of Mongolia	49°10'	110°00'	<i>L. sibirica</i> L.	0	0	0	0	0	1	0	0	12.7±7.7 (0.5÷32.3)	11.3±5.0 (1.5÷24.3)	61	Battulga et al. 2013; Danilin et al., 2015
Japanese Islands	36°30' - 36°50'	138°10' - 139°40'	<i>L. leptolepis</i> Gord.	0	0	0	0	0	0	0	1	15.2±6.6 (4.0÷35.9)	13.2±5.2 (4.3÷26.7)	73	Research Group..., 1964; Karizumi, 1974



Fig. 2. Distribution of the sample plots on the territory of Eurasia, on which larch trees have been harvested. The sample area in the Khenk Mountains is marked with the black square

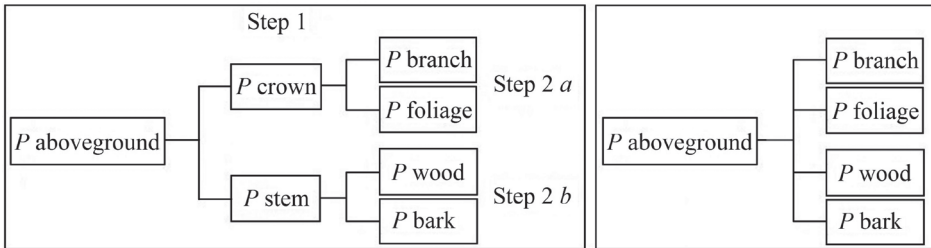


Fig. 3. The pattern of the disaggregating two-step proportional weighting AM of sequential (left) and parallel (right) schemes. The schemes show the relationship between each biomass component, where lines from left to right indicate disaggregation and from right to left indicate summation (Zheng et al. 2015; Zhang et al., 2016)

Table 3. Structure of the two-step additive model (AM), implemented according to the principle of proportional weighting (Zheng et al. 2015; Dong et al., 2015). For symbols here and below see equations (3) and (4)

Step 1	$P_c = \frac{1}{1 + \frac{a_s D^b H^c}{a_c D^b H^c}} \times P_a$	$P_s = \frac{1}{1 + \frac{a_c D^b H^c}{a_s D^b H^c}} \times P_a$
Step 2a	$P_f = \frac{1}{1 + \frac{a_b D^b H^c}{a_f D^b H^c}} \times P_c$	$P_b = \frac{1}{1 + \frac{a_f D^b H^c}{a_b D^b H^c}} \times P_c$
Step 2b	$P_w = \frac{1}{1 + \frac{a_{bk} D^b H^c}{a_w D^b H^c}} \times P_s$	$P_{bk} = \frac{1}{1 + \frac{a_w D^b H^c}{a_{bk} D^b H^c}} \times P_s$

the logarithmic transformation of the variables (Baskerville 1972).

**RESULTS**

Initial regression equations are calculated:

$$\ln P_i = a_i + b_i(\ln D) + c_i(\ln H) + d_i(\ln D)(\ln H) + \sum g_{ij} X_j, \tag{3}$$

where  $P_i$  is biomass of  $i$ -th component, kg;  $i$  is the index of biomass component: aboveground ( $a$ ), crown ( $c$ ), stem over bark ( $s$ ), foliage ( $f$ ), branches ( $b$ ), stem wood ( $w$ ) and stem bark ( $bk$ );  $a_i, \dots, d_i$  are coefficients of numerous independent variables;  $j$  - index (code) of dummy variables, from 0 to 7 (Table 2).  $\sum g_{ij} X_j$  is the block of dummy variables for the  $i$ -th biomass component of the  $j$ -th ecoregion. After anti-log procedure model (1) has the form:

$$P_i = e^{a_i} D^{b_i} H^{c_i} D^{d_i(\ln H)} e^{\sum g_{ij} X_j} \tag{4}$$

According to the standard program of multivariate regression analysis, the coefficients of equations (3) are calculated and their characteristics are obtained, that after their corrections for the logarithmic transformation and its reduction to the form (4) is given in Table A.1 (Appendices). All regression coefficients of equations (4) for numerical variables are significant with a confidence of 0.95. The model is valid in the range of harvest data of tree height and stem diameter of sample trees given

in Table 2. The coefficient of determination for aboveground biomass is 0.991, and for biomass of stem, branches and foliage respectively are 0.992, 0.903 and 0.852 (Table A.1).

By substituting the regression coefficients of the initial equations from the Table A.1 (Appendices) in the structure of the AM presented in Table A.2 (Appendices), according to the two-step scheme of proportional weighing, the transcontinental AM of component composition of larch tree biomass with double harmonization was obtained, the final form of that is given in Table A.3 (Appendices). By tabulation of the resulting model (Table A.3) according to the given values of  $D$  and  $H$  and the value of the dummy variable  $X_6 = 1$ , a regional normative table was obtained, additive in biomass structure and intended for its use in the larch forests of Mongolia (Table 4).

Since the volume of all the tables for eight ecoregions exceeds the format of the journal article, we will limit ourselves to the comparison of some regional features of larch trees biomass structure by the corresponding fragment of the final Fig. 4 for the given diameter and height data.

**Table 4. Elaborated dry biomass table of the Siberian larch in Mongolia by tree height and stem diameter; unit values in kg**

Tree height, m	Biomass components	DBH, cm					
		10	14	18	22	26	30
10	Aboveground	24.14	42.97	66.07	-	-	-
	Tree crown	4.38	10.40	19.55	-	-	-
	Foliage	1.09	2.35	4.12	-	-	-
	Branches	3.29	8.05	15.43	-	-	-
	Stem and bark	19.77	32.57	46.52	-	-	-
	Stem wood	15.64	25.49	36.09	-	-	-
	Stem bark	4.12	7.08	10.43	-	-	-

18	Aboveground	38.99	71.76	113.16	162.80	220.36	-
	Tree crown	2.16	5.67	11.60	20.43	32.59	-
	Foliage	0.55	1.31	2.49	4.12	6.22	-
	Branches	1.60	4.36	9.11	16.32	26.36	-
	Stem and bark	36.83	66.08	101.56	142.37	187.77	-
	Stem wood	30.83	54.72	83.39	116.08	152.18	-
	Stem bark	6.00	11.36	18.17	26.29	35.59	-
26	Aboveground	-	-	156.30	227.40	310.70	405.94
	Tree crown	-	-	7.53	13.66	22.39	34.12
	Foliage	-	-	1.63	2.78	4.30	6.24
	Branches	-	-	5.89	10.89	18.09	27.88
	Stem and bark	-	-	148.77	213.74	288.31	371.81
	Stem wood	-	-	125.80	179.51	240.73	308.86
	Stem bark	-	-	22.97	34.23	47.58	62.95

Evaluation of the model

Since it has been established that the elimination of the internal inconsistency of biomass equations by ensuring their additivity does not necessarily mean the increase in the accuracy of its estimates (Cunia and Briggs 1984; Reed and Green 1985), it is necessary to clarify whether the obtained AM is adequate enough and how its characteristics relate to the indices of the adequacy of initial equations.

The ratio of harvest biomass data and values obtained by the calculation of initial equations and AM of tree biomass, shows the degree of correlation of these values and the absence of visible differences in the structure of residual dispersions obtained from the two models (Fig. 4).

The results of the comparison indicate that there is no absolute superiority in terms of adequacy of either the initial or additive equations (Table 5).

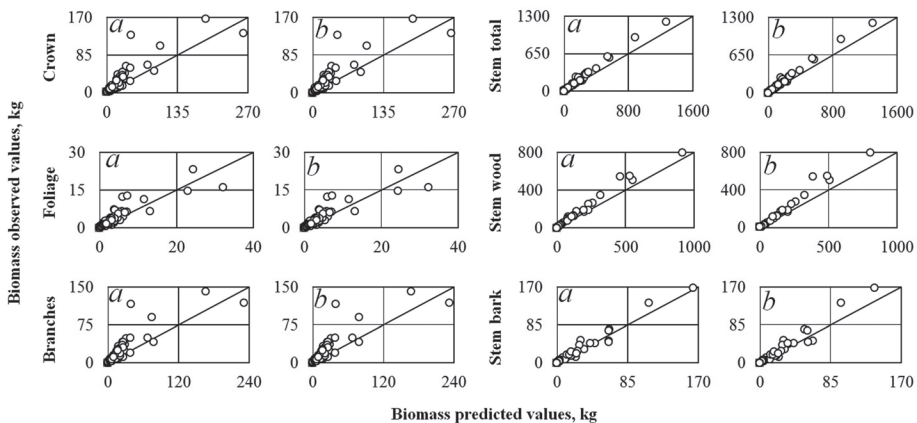


Fig. 4. The ratio of the harvest biomass and its values obtained by calculating the initial (a) and additive (b) models of the larch tree biomass

**Table 5. Comparison of adequacy indices for the initial and additive equations of larch tree biomass**

Adequacy indices	Biomass components*						
	$P_a$	$P_s$	$P_w$	$P_{bk}$	$P_{cr}$	$P_b$	$P_f$
	Initial equations						
R <sup>2</sup>	0,973	0,989	0,974	0,956	0,613	0,585	0,624
RMSE	35,61	19,85	32,42	8,38	18,08	16,35	2,36
Bias	-1,91	-2,20	4,11	-1,79	-19,68	-20,90	-21,89
	AM						
R <sup>2</sup>	0,973	0,988	0,974	0,910	0,594	0,575	0,595
RMSE	35,61	20,63	32,48	11,92	18,53	16,55	2,45
Bias	-1,91	-2,09	-1,90	-8,89	-19,83	-20,91	-21,98

Note. \*Symbols designations see equation (3).

## DISCUSSION

As shown in Table 4, patterns of changes in the structure of tree biomass in dependence of the value of stem diameter and tree height vary significantly. Biomass of all tree components significantly increases as the stem diameter increases, regardless of tree height. The stem biomass of trees having the diameter of 18 cm increases by 3.2 times, with an increase of tree height from 10 to 26 m. But foliage and branches biomass of the same stem diameter decreases with an increase of tree height by 2.5-2.6 times under influence of tree age. A negative relationship between the crown biomass of equal-sized trees and their age in forest stands is well known. For example, the crown mass of the tree with a diameter of 12 cm at the age of 15 years exceeds that at the age of 35 years at the birch by 1.5-2.0 times, and for the aspen – by 2.4-4.4 times (Usoltsev, 1972) due to the age shift of the cenotic position of equal-sized trees: at the age of 15 years such tree is the leader, and at the age of 35 years it is a depressed tree, a candidate for dying. Therefore, the share of participation of one or another biomass component and, accordingly, the cycling rate of larch substances will largely determine its distribution by the diameter

and height of trees.

### Comparison between biomass of larch trees from different Eurasian ecoregions. Ecological considerations

According to Fig. 5 the greatest values of tree aboveground biomass of equal both diameter and height occur in open larch communities growing on permafrost (77 kg), and in the rest of ecoregions the value of biomass is much lower (53-60 kg). Within this range there are trees in the mountains of Mongolia (58 kg). The intermediate position (64 kg) is occupied by the biomass of larch in Central Europe due to the abnormally developed crown of trees in 40-year-old plantations. The significant excess of larch biomass in the forest-tundra may be explained by permafrost conditions, by tree growth in low-yielding stands with a high basic density of stem wood (Hacke and Sperry 2001).

When following our results, the growing conditions of larch in Mongolia are approximately the same as in majority of other regions and not as tough as they are believed by Battulga et al. (2013). Our comparison of aboveground biomass by regions was made for trees with a stem diameter of 14 cm. Battulga et al. conclude

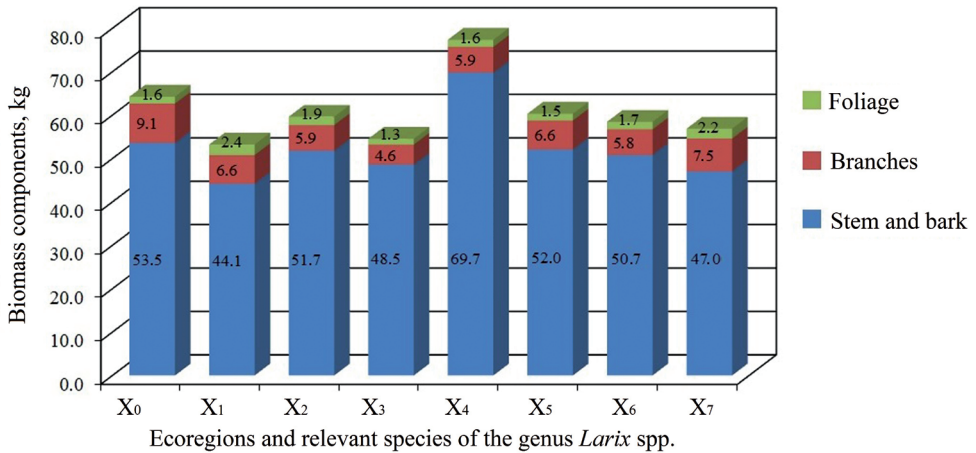


**Fig. 5.** Changes in the structure of the estimated biomass of trees with 14 cm diameter and 13 m height in different ecoregions. Designations: X<sub>0</sub> - Western and Central Europe, X<sub>1</sub> - European part of Russia, X<sub>2</sub> - Turgay steppe, X<sub>3</sub> - Western Siberia, the flood plain of the Pur river, X<sub>4</sub> - Eastern Siberia, forest-tundra, X<sub>5</sub> - Russian Far East, northern taiga, X<sub>6</sub> - mountains of Mongolia, X<sub>7</sub> - Japanese Islands

that there is more aboveground biomass in large trees of Mongolia compared with equal-sized trees of Iceland, and explain this phenomenon by more stringent growth conditions in the steppe compared to the conditions of Iceland. They compare the calculated indices of above-ground biomass. But if we compare the actual values of biomass of the trees having the diameter of 14 cm (see: Battulga et al., Fig. 2), then the differences are virtually absent. It is possible that the underestimation of biomass in Iceland due to the reduced basic density (climatic factor) is compensated by overestimation due to the more developed tree crown in plantations (cenotic factor) compared to the dense natural stands of Mongolia. Thus, some uncertainties in comparison biomass between ecoregions can be result of unaccounted and unknown regional features of age and morphological structures of forest stands.

The main part of the variability in the model (3) is assumed by the stem diameter and height, and the influence of unaccounted factors falls on the residual variance. The dummy variables confined to particular ecoregions extracted some portion of the variability from this residual variance. Belonging of the sample plots to these ecoregions mediates both climatic

and unaccounted ecological traits, and allometric biomass models including air temperature and precipitation, are known as models sensitive to climate variables (Zeng et al. 2017).

Nevertheless, we cannot know what proportion of the variability of the residual variance may be explained by involving climatic (regional) variables in the model, because this residual dispersion accumulates both unknown and unaccounted factors and errors of measurements in all their phases (assessment of age, diameter, height of a tree, the selection of supposedly representative samples of component biomass, their drying, weighing, etc.). The question of what explains the regional differences in the structure of biomass of trees with the same linear dimensions of their stems, remains open. Here, the differences in tree age play an undoubted role, as well as the variation in the morphological structure of stands, which, in turn, is determined by both climatic and edaphic factors. This will be the subject of further research.

The reasons for the relatively large bias values in both types of equations, especially for crown mass, can be seen in Fig. 5, showing the lack of homoscedasticity of

residual variance when the comparison is fulfilled on trivial (not log) coordinates: it extremely increases with increase of the crown biomass value. Accordingly, the biomass variability of the three to four largest trees contributes to the bias greater than the total residual bias of the remaining trees, and this phenomenon determines the large values of the biases. As a result, a slight overestimation or underestimation of the crown biomass of some single largest trees relative to the regression line determines the bias value, not peculiar to the biomass of the community of smallest trees.

The proposed AM, adapted for use in 8 ecoregions of Eurasia, is designed for a more accurate assessment of the carbon stock of larch forests. However, this is a solution to the problem only in the first approximation, because it is based on a limited amount of harvest data. If our database, containing 433 larch sample trees, may be supplemented with harvested (but not yet published) data on 600 larch trees in China (Zeng et al. 2017) and 96 trees in Poland (Jagodzinski et al. 2018), the model will get more consistent.

## CONCLUSIONS

1. On the basis of the obtained harvest biomass data of the Siberian larch trees in Mongolia and in comparison with similar data of other ecoregions of Eurasia,

a Trans-Eurasian AM of the genus *Larix* spp. biomass was developed, and thus the combined problem of additivity and regionality of the model was solved.

2. The AM of tree biomass of *Larix* is harmonized in two ways: it eliminated the internal contradictions of the component and of the aboveground biomass equations, and in addition, it takes into account regional (and correspondingly species) differences of equal-sized trees on its component structure.

3. The aboveground biomass of trees having the same sizes in the mountains of Mongolia is approximately the same as of the majority of the most ecoregions of Eurasia, with except for forest-tundra in the Far North.

4. The results obtained allow to determine larch forest biomass in different ecoregions of Eurasia when using the diameter and height tree measurement.

## ACKNOWLEDGEMENTS

This study was conducted in compliance with the programs of current scientific research of the Ural Forest Engineering University, Botanical Garden of the Ural Branch and V.N. Sukachev Institute of Forestry of Siberian Branch of Russian Academy of Sciences. ■

## REFERENCES

- Abaimov A. P., Prokushkin S. G., Zyryanova O. A., Kaverzina L. N. (1997). Features of formation and functioning of larch forests on permafrost soils. *Lesovedenie*, 5, pp. 13-23. (In Russian).
- Baskerville G.L. (1972). Use of logarithmic regression in the estimation of plant biomass. *Canadian Journal of Forest Research*, 2 (1), pp. 49-53. doi:10.1139/x72-009.
- Battulga P, Tsogtbaatar J, Dulamsuren C., and Hauck M. (2013). Equations for estimating the aboveground biomass of *Larix sibirica* in the forest-steppe of Mongolia. *Journal of Forestry Research*, 24 (3), pp. 431–437. doi:10.1007/s11676-013-0375-4.
- Bjarnadottir B., Inghammar A. C., Brinker M.-M., Sigurdsson B. D. (2007). Single tree biomass and volume functions for young Siberian larch trees (*Larix sibirica*) in eastern Iceland. *Icelandic Agricultural Sciences*, 20, pp. 125-135.

Burger H. (1945). Holz, Blattmenge und Zuwachs. VII. Mitteilung: Die Lärche. Mitteilungen - Schweizerische Anstalt für das Forstliche Versuchswesen, 24 (1), pp. 7-103.

Cunia T., and Briggs R.D. (1984) Forcing additivity of biomass tables: some empirical results. Canadian Journal of Forest Research, 14 (3), pp. 376-384. doi:10.1139/x84-067.

Danilin I.M., and Tsogt Z. (2015). Morphometric parameters and phytomass of the Siberian larch *Larix sibirica* Ledeb. trees in the Eastern Khentii (Northern Mongolia). Siberian Journal of Forest Science, 5, pp. 96-104 (in Russian with English summary). doi: 10.15372/SJFS20150508.

Danilin I.M. (2009). Structural and functional organization of larch phytocenosis in a post-fire progressive succession in the north of Central Siberia. Contemporary Problems of Ecology, 2 (1), pp. 55-65. doi:10.1134/S199542550901010X.

Danilin I.M., and Tsogt Z. (2014). Dynamics of structure and biological productivity of post-fire larch forests in the Northern Mongolia. Contemporary Problems of Ecology, 7 (2), pp. 158-169. doi:10.1134/S1995425514020036.

Danilin I.M., Tsogt Z., and Usoltsev V.A. (2015). Aboveground phytomass of trees of larch and birch in the forests of Central Siberia and the Eastern Khentii Mountains. Eco-Potencial, 1 (9), pp. 33-36. <http://elar.usfeu.ru/bitstream/123456789/4051/1/Danilin.pdf>.

Dong L., Zhang L., Li F. (2015). A three-step proportional weighting system of nonlinear biomass equations. Forest Science, 61 (1), pp. 35-45.

Draper N.R. and Smith H. (1966) Applied Regression analysis. New York, Wiley Publ. Translated under the title "Prikladnoi regressiionnyi analiz". Moscow: "Statistika" Publ., 1973. 392 pp.

Dylis N.V., and Nosova L.M. (1977). Biomass of forest biogeocenoses under Moscow region. Moscow, Nauka Publishing. 143 pp. (In Russian).

Fu L.Y., Zeng W.S., Tang S.Z., Sharma R.P., and Li H.K. (2012). Using linear mixed model and dummy variable model approaches to construct compatible single-tree biomass equations at different scales – A case study for Masson pine in Southern China. Journal of Forest Science, 58 (3), pp. 101-115. doi:10.17221/69/2011-JFS.

Hacke U.G., Sperry J.S. (2001). Functional and ecological xylem anatomy. Perspectives in Plant Ecology, Evolution and Systematics, 4, pp. 97-115.

Jacobs M.W., and Cunia T. (1980). Use of dummy variables to harmonize tree biomass tables. Canadian Journal of Forest Research, 10 (4), pp. 483-490. doi:10.1139/x80-079.

Jagodzinski A.M., Dyderski M.K., Gesikiewicz K., and Horodecki P. (2018). Tree- and stand-level biomass estimation in a *Larix decidua* Mill. Chronosequence. Forests, 9, 587; doi:10.3390/f9100587.

Karaseva M.A. (2003). *Larix sibirica* on the Middle Povolzhye. Ioshkar-Ola, Mari State Technical University. 376 pp. (In Russian).

Karizumi N. (1974). The mechanism and function of tree root in the process of forest production. (I): Methods of investigation and estimation of the root biomass. Bulletin of the Government Forest Experiment Station, 259, pp. 1-99.

Kozak A. (1970). Methods for ensuring additivity of biomass components by regression analysis. *The Forestry Chronicle*, 46(5), pp. 402-405. doi:10.5558/tfc46402-5.

Marklund L.G. (1983). Collecting data for biomass equation development: some methodological aspects (weighing tree components, sampling, statistical, economical and practical aspects) In: *Mesures des biomasses et des accroissements forestiers. Les Colloques de l'INRA (France)*, 19, pp. 37-43.

Molchanov A. A. (1971). Productivity of organic mass in forests of different zones. Moscow, Nauka, 275 pp. (In Russian).

Moskalyuk T.A. (2015). Biomass of sample trees as a basis for studying the forest biological productivity of the Magadan region. *Eco-Potencial*, 2 (10), pp. 17-25 (In Russian). <http://elar.usfeu.ru/bitstream/123456789/4300/1/Moskaliuk.pdf>.

Novák J., Slodičák M., Dušek D. (2011). Aboveground biomass of substitute tree species stand with respect to thinning – European larch (*Larix decidua* Mill.). *Journal of Forest Science*, 57 (1), pp. 8-15.

Parresol B.R. (2001). Additivity of nonlinear biomass equations. *Canadian Journal of Forest Research*, 31(5), pp. 865-878. doi:10.1139/x00-202.

Polikarpov N.P. (1962). Scots pine young forest dynamics on clear cuttings. Moscow, Academy of Sci. USSR, 171 pp. (In Russian).

Pozdnyakov L. K. (1975). Dahurian larch. Moscow, Nauka, 312 pp. (In Russian).

Reed D.D., and Green E.J. (1985). A method of forcing additivity of biomass tables when using nonlinear models. *Canadian Journal of Forest Research*, 15(6), pp. 1184-1187. doi:10.1139/x85-193.

Research Group of Forest Productivity of the Four Universities: Studies on the Productivity of the Forest. Part II. Larch (*Larix leptolepis* Gord.) forests of Shinshu District (1964). Nippon Ringyo Gijyutsu Kyokai, Tokyo. 61 pp.

Sanquetta C.R., Behling A., Corte1 A.P.D., Netto S.P., Schikowski A.B., do Amaral M.K. (2015). Simultaneous estimation as alternative to independent modeling of tree biomass. *Annals of Forest Science*, 72, pp. 1099–1112.

Shchepashchenko D.G. (2015). Aboveground phytomass of *Larix cajanderi* Mayr trees in the North-East of Yakutia. *Eco-Potencial*, 1(9), pp. 37-40 (In Russian). <http://elar.usfeu.ru/bitstream/123456789/4062/1/Schepaschenko.pdf>.

Shi F., Qu L., Wang W., Matsuura Y., Koike T., Sasa K. (2002). Aboveground biomass and productivity of *Larix gmelinii* forests in northeast China. *Eurasian Journal of Forest Research*, 5, pp. 23-32.

Usoltsev V.A. (1972). Birch and aspen crown biomass in forests of Northern Kazakhstan. *Vestnik Selskokhozyaistvennoi Nauki Kazakhstana (Bulletin of Agricultural Science of Kazakhstan)*, 4, pp. 77-80 (In Russian).

Usoltsev V.A. (2016). Single-tree biomass of forest-forming species in Eurasia: database, climate-related geography, weight tables. Yekaterinburg: Ural State Forest Engineering University. 336 pp. (In Russian). (<http://e.lanbook.com/view/journal/91094/>).

Usoltsev V.A. (2017). On additive models of tree biomass: some uncertainties and the attempt of their analytical review. *Eko-Potential*, 2(18), pp. 23-46 (in Russian with English summary). <http://elar.usfeu.ru/handle/123456789/6550>.

Usoltsev V. A. (2018) In basements of the biosphere: What we know about the primary production of tree roots? *Eko-Potencial*, 4 (24), pp. 24-77. (in Russian).

Usoltsev V.A., Zukow W., Osmirko A.A., Tsepordey I.S., Chasovskikh V.P. (2019). Additive biomass models for *Larix* spp. single-trees sensitive to temperature and precipitation in Eurasia. *Ecological Questions*, 30 (2), pp. 57-67. doi: 10.12775/EQ.2019.12.

Vyskot M. (1982). *Larix decidua* Mill. in biomass. *Rozprawy Československé Akademie Véd. Rada Matematických a Přírodních Véd. Praha*, 92 (8), pp. 1-162.

Zeng W.-S. (2015). Using nonlinear mixed model and dummy variable model approaches to construct origin-based single-tree biomass equations. *Trees*, 29(1), pp. 275-283. doi: 10.1007/s00468-014-1112-0.

Zeng W.-S., Duo H.R., Lei X.D., Chen X.Y., Wang X.J., Pu Y. & Zou W.T. (2017). Individual tree biomass equations and growth models sensitive to climate variables for *Larix* spp. in China. *European Journal of Forest Research*, 136 (20), pp. 233–249. doi:10.1007/s10342-017-1024-9.

Zhang C., Peng D.-L., Huang G.-S., Zeng W.-S. (2016). Developing aboveground biomass equations both compatible with tree volume equations and additive systems for single-trees in poplar plantations in Jiangsu Province, China. *Forests*, 7 (2), 32. doi:10.3390/f7020032.

Zhao Q., Liu X. Y., Zeng D. H. (2011). Aboveground biomass and nutrient allocation in an age-sequence of *Larix olgensis* plantations. *Journal Forestry Research*, 22, pp. 71-76.

Zheng C., Mason E.G., Jia L., Wei S., Sun C., Duan J. (2015). A single-tree additive biomass model of *Quercus variabilis* Blume forests in North China. *Trees*, 29(3), pp. 705-716 doi:10.1007/s00468-014-1148-1.

Received on November 29<sup>th</sup>, 2018

Accepted on August 8<sup>th</sup>, 2019

**Alexander Gradel<sup>1,2\*</sup>, Gerelbaatar Sukhbaatar<sup>3,4</sup>, Daniel Karthe<sup>5</sup>, Hoduck Kang<sup>6</sup>**

<sup>1</sup> International Forestry Consultancy Gradel, Bad Oeynhausen, Germany

<sup>2</sup> formerly: Georg-August-Universität Göttingen, Faculty of Forest Sciences and Forest Ecology, Göttingen, Germany

<sup>3</sup> Department of Environment and Forest Engineering, School of Engineering and Applied Sciences, National University of Mongolia, Mongolia

<sup>4</sup> Institute of Forest Science, National University of Mongolia, Mongolia

<sup>5</sup> Engineering Faculty, German-Mongolian Institute for Resources and Technology, Nalaikh, Mongolia

<sup>6</sup> Department of Biological and Environmental Science, Dongguk University, Biomed Campus, Republic of Korea

\* **Corresponding author:** agradel@mail.de

# FOREST MANAGEMENT IN MONGOLIA – A REVIEW OF CHALLENGES AND LESSONS LEARNED WITH SPECIAL REFERENCE TO DEGRADATION AND DEFORESTATION

**ABSTRACT.** The natural conditions, climate change and socio-economic challenges related to the transformation from a socialistic society towards a market-driven system make the implementation of sustainable land management practices in Mongolia especially complicated. Forests play an important role in land management. In addition to providing resources and ecosystem functions, Mongolian forests protect against land degradation.

We conducted a literature review of the status of forest management in Mongolia and lessons learned, with special consideration to halting deforestation and degradation. We grouped our review into seven challenges relevant to developing regionally adapted forest management systems that both safeguard forest health and consider socio-economic needs. In our review, we found that current forest management in Mongolia is not always sustainable, and that some practices lack scientific grounding. An overwhelming number of sources noticed a decrease in forest area and quality during the last decades, although afforestation initiatives are reported to have increased. We found that they have had, with few exceptions, only limited success. During our review, however, we found a number of case studies that presented or proposed promising approaches to (re-)establishing and managing forests. These studies are further supported by a body of literature that examines how forest administration, and local participation can be modified to better support sustainable forestry. Based on our review, we conclude that it is necessary to integrate capacity development and forest research into holistic initiatives. A special focus should be given to the linkages between vegetation cover and the hydrological regime.

**KEY WORDS:** forest management, Mongolia, deforestation, degradation

**CITATION:** Alexander Gradel, Gerelbaatar Sukhbaatar, Daniel Karthe, Hoduck Kang (2019) Forest Management In Mongolia – A Review Of Challenges And Lessons Learned With Special Reference To Degradation And Deforestation. *Geography, Environment, Sustainability*, Vol.12, No 3, p. 133-166  
DOI-10.24057/2071-9388-2019-102

## INTRODUCTION

The development and implementation of sustainable forest management strategies is a key environmental policy issue in Mongolia (Gerelbaatar et al. 2019a). The forests of northern Mongolia not only provide resources such as timber and firewood, but also ecosystem services that are relevant to the well-being of the whole country, such as water purification and retention, erosion control, and biodiversity (Krasnoshhekov 2001; Tsogt et al. 2018; Government of Mongolia 2018). However, nearly 80% of Mongolian territory is exposed to desertification and land degradation (Bulgan et al. 2013). With continuing forest loss and increasing utilization pressure (Tsogtbaatar 2004; Hansen et al. 2013; Government of Mongolia 2018), it is increasingly challenging to establish sustainable forest management practices in Mongolia. It is particularly problematic that forest management in Mongolia often fails to consider science-based standards (Oyunsanaa 2011). This is partly due to a lack of utilizing conclusions from research for regionally adapted management standards and the practical application of suitable management models. Further challenges are related to structural weaknesses in terms of implementation control and administrative oversight (Benneckendorf 2011). Despite nationally and internationally financed initiatives to improve the situation, the overall tendency of forest loss and degradation has been neither stopped nor reversed.

With regard to forest loss and degradation in Mongolia, the phenomena of deforestation and forest degradation need to be distinguished. Deforestation refers to a severe (>90% canopy cover loss) or total loss of

forest cover (Government of Mongolia 2018). In contrast, degradation is characterized by a qualitative loss that affects forest ecosystem functions and is often triggered by specific disturbances. Such disturbances may include a decrease in stocking volume (Government of Mongolia 2018) or a shift toward broad-leaf pioneer tree species after intensive logging (Gerelbaatar et al. 2019a). Continuing degradation can eventually lead to complete deforestation (Government of Mongolia 2018; Gerelbaatar et al. 2019a) and even desertification (Khaulenbek and Kang 2017). Direct drivers of deforestation and forest degradation are disturbances such as fire, pests, unsustainable harvest practices, overexploitation of forest resources, mining activities, and overgrazing (Kondrashov et al., 2008; Ykhanbai 2010; Dulamsuren et al 2011; Khishigjargal et al., 2014; MET 2016; Government of Mongolia 2018; Khongor et al. 2018). Underlying drivers include climate change, which affects the frequency and severity of droughts (Davi et al. 2013) and factors related to socio-economic and political transformation processes in Mongolia (Saladyga et al. 2013), which encompass demographic factors, institutional organization, and the political and legal framework (Government of Mongolia 2018). On local scale permafrost degradation can also trigger forest degradation (Juříčka et al. 2018). All of these aspects need to be understood in order to develop a sustainable forest management framework that can safeguard healthy ecosystem functions and resources, as well as halt or even reverse deforestation and degradation.

We conducted a literature review of the above-mentioned drivers of deforestation and degradation, as well as of the most important ecosystem functions and key

socio-economic demands with the goal of identifying and outlining key challenges and lessons learned for forest management in Mongolia.

## MATERIALS AND METHODS

We reviewed literature from the international scientific community, the Mongolian government, international projects, and other sources relevant to our objective of formulating the following key challenges for forest management in Mongolia: (1) *Adaptation to and mitigation of global warming-induced desertification*; (2) *Resilience against more frequent and severe natural disturbances*; (3) *Linking forest and water resources management*; (4) *Supporting forest regeneration against deforestation and degradation: Afforestation, reforestation, and underplanting*; (5) *Managing the conservation of nature, biodiversity, and wildlife*; (6) *Increased resource utilization and demand in forested areas*; (7) *Consideration of the social and political-cultural background*. In total, 155 publications were reviewed for this study. Of those, 125 sources are directly related to research, development work, or projects in Mongolia or its immediate neighbors, 21 provide a rather general global or theoretical background relevant to the challenges in Mongolia, and 9 provide specific insights from other regions of the world that may be transferable to Mongolia. For each challenge, we provide a short overview of the current situation and of lessons learned from recent studies or projects in the region.

### Challenge 1: Adaptation to and mitigation of global warming-induced desertification

Central Asia is one of the global hotspots of climate change; over the past century, temperatures have risen faster than the world average. This trend is likely to continue in the future (Unger-Sayesteh et al. 2013; Mannig et al. 2013). According to Yu et al. (2003), “the center of the warming zone appears to lie just southeast of Lake Baikal, putting the drylands of northern China and Mongolia near the center of this hot spot”.

In the Mongolian context climate change is usually expected to lead to overall

warmer and drier conditions and more droughts (Batima et al. 2005, Dulamsuren and Hauck 2008, IWRM 2009). In general, the literature sources constitute that mean annual temperature has risen significantly during the last decades. However, because of different data material, time frames and methodologies the information differs, between rather low increase, for example of 0.4 °C between 1951 and 1990 (Yatagai and Yasurani 1995) to moderate, e.g. with a reconstructed increase of about 1.5 °C of growing season temperature compared to previous centuries (Davi et al. 2013), and even strong increase of 2.14 °C during the last 70 years (Oyuntuya et al. 2015). According to Oyuntuya et al. (2015), precipitation has decreased in most regions by at least 0.1 mm/year. Sato et al. (2007) expects a further decrease of precipitation for some parts of northern Mongolia. With regard to future precipitation trends, there is a considerable model uncertainty for this region (Karthé et al. 2014).

A concern raised in many sources is that climate change may exacerbate desertification throughout the country. As northern Mongolia is an extreme and marginal habitat for trees, even minor changes in temperature and water availability may lead to significant changes in forest cover. For the Siberian larch (*Larix sibirica* Ledeb.), which is the dominant tree species throughout most of the Mongolian taiga, Dulamsuren et al. (2011) and Kansaritohreh et al. (2018) observed growth declines since the 1950s and correlated them with increasing drought frequency during the growing period. Climate change impacts are likely to be most drastic in the forest steppe, where conditions may become unsuitable for tree growth (Angerer et al. 2008). Dulamsuren et al. (2010a) even suggested a supra-regional decline of certain tree species, specifically larch. However, not all studies predict such alarming scenarios. In their reconstruction and projection of past and future droughts, Hessler et al. (2018) conclude that the recent extreme drought (in 2000) and pluvial (in 1990) are very rare, but not without precedent in the last 2060 years. Based on comprehensive dendrochronological studies, Slemnev et al. (2012) concluded

that spurts of forest regeneration in Mongolia coincide with especially moist periods that occur approximately every 40-100 years. Thus, climatic conditions and water availability in particular are the main factors shaping the distribution of the main vegetation zones in Mongolia.

From our literature review, we have identified three key areas of action to improve forest management in Mongolia. First, *forest management practices* need to adapt and be adaptable to changing climate conditions, which also includes special consideration of permafrost sites. Second, there needs to be a concerted effort to *combat desertification* along the forest-steppe border zone. Finally, Mongolia needs to assess and improve the *carbon sequestration capacity* of its forests to help offset greenhouse gas emissions.

### Lessons learned

#### *Climate effects on trees and climate-resilient forestry*

A number of recent studies have evaluated the growth performance of tree species and their resilience to droughts and other climatic changes. There is a strong agreement that a minor temperature increase and/or a decrease in precipitation will have mostly negative effects on the growth of larch trees (Dulamsuren et al. 2011; James 2011; Khishigjargal et al. 2014), Scots pines (*Pinus sylvestris* L.; see Demina et al. 2017), Siberian stone pines (*Pinus sibirica* Du Tour; see De Grandpré et al. 2011), and especially spruce (*Picea obovata*, Ledeb.; see James 2011) and birch trees (*Betula platyphylla* Sukaczew.; see Gradel et al. 2017a; Verhoeven et al. 2018). Studies that include dark coniferous trees are, compared to larch, rare for Mongolia. However, some authors have found indication of a potentially climate-induced decline in dark conifers in northern Mongolia (James 2011; Gradel et al. 2018). Overall decline of dark coniferous, for various reasons, is even more evident in neighboring southern Siberia (Kharuk et al. 2013). These conclusions are not yet final and specific long-term research protocols need to be implemented to shed more light. The species-specific demands of spruce and

fir also indicate that stands at the southern distribution border may be more strongly affected by climate change. Dorjsuren (2014) has found that also the quality of larch seeds in Mongolia has decreased since 1980 due to drought. Similarly, Gao et al. (2017) conclude that birch seedlings are more sensitive to water deficit than larch seedlings, and Gradel et al. (2017a) have shown that younger trees are more susceptible to drought than older trees, most likely due to their less-developed root architecture and other factors. These findings indicate which species or development stages of trees may be especially affected if the climate gets drier.

Climate-resilient forestry depends also on the availability of suitable tree species and mechanisms that promote forest regeneration. Due to natural selection, certain provenances of one tree species can be especially valuable for climate-resilient forestry. Extensive research has been conducted on the genetic variation of Siberian tree species such as *Larix sibirica* (Semerikov et al. 2013; Krutovsky et al. 2014) and *Pinus sibirica* (Krutovsky et al. 2014). Research in the framework of the Czech – Mongolian forest cooperation also aims at understanding and improving tolerance to water scarcity (Kusbach et al. 2017). Based on recent research, adapted silvicultural measures for climate-resilient forest management have been proposed. These include analysis and establishment of specific selective harvesting measures and the development of adjusted regeneration and planting concepts (Gradel 2017; Gerelbaatar et al. 2019b). Some European studies, for example, have reported that thinning could be a measure for climate adaptation, since it has a positive impact on the amount of water available to the remaining trees (Gebhardt et al. 2014, Olivar et al. 2014). However, the effects of thinning can vary greatly, particularly when viewed from the level of a single tree to a stand to an entire site (Bolte et al. 2010). Studies that focus solely on the impact of thinning on the water balance in Mongolian forest stands are yet not available.

## Combating desertification

Tree planting is frequently used as a tool for combating desertification at the forest steppe border and often focuses on the establishment or maintenance of scattered woodlands. The Korean-Mongolian *Center for Combating Desertification in Arid and Semi-arid Areas* (CCDASA) is a cooperation platform between key Korean and Mongolian institutions and explores solutions for the recovery of degraded deforested sites. Joint capacity-building measures are combined with field-based research in the southern part of the Bulgan province (see Fig. 1). Research includes the testing and selection of suitable clones (poplar species), agro-forestry experiments, testing of soil improvement and irrigation practices (especially drip irrigation for seedlings and saplings), studies of tree genetics and physiology, GIS analyses, and social-economic analyses (Khaulenbek and Kang 2017).

Planting methods that were adjusted to reduce earthwork costs and enhance tree growth were recently tested, after which the height and crown growth of *Populus sibirica* Tausch seedlings showed significant improvement (Jo and Park 2017a). The authors found that seedling survival rate and height growth improved with shorter irrigation intervals and denser planting (1.5 m spacing compared to 3 m spacing). The results for *Salix rorida* Lacksch., *Populus sibirica*, and *Ulmus pumila* L. were also promising,

with *Salix rorida* showing the fastest growth (Khaulenbek and Kang 2017). Poplar and elm species are particularly suitable because they are relatively fast-growing and well-adapted to difficult environments. They therefore provide important wind-breaking benefits within a fairly short amount of time.

Silviculturists discuss the impact of plantations on groundwater in the desert. According to CCDASA scientists, it is very important to ensure that plantation species are chosen to suit the groundwater conditions at the plantation site. However, some trees, such as *Salix rorida*, can survive as shrubs on sand dunes without any irrigation at all. Planting trees specifically to create windbreaks has also been tested and found significantly increase crop yield (Jo and Park 2017b). On a larger scale, the "green belt" project in the south of the country was established in order to halt degradation and reduce dust and sand storms by establishing a belt of planted trees, such as Saxaul forest plantations in the Gobi Desert (Batkhoo et al. 2017a).

## Carbon sequestration

Undisturbed boreal forests are considered to be carbon sinks. However, major disturbances that result in large-scale degradation can trigger continuous carbon emissions from these forests. Measures that reduce emissions from deforestation and degradation therefore go hand in hand with other objectives for stabilizing

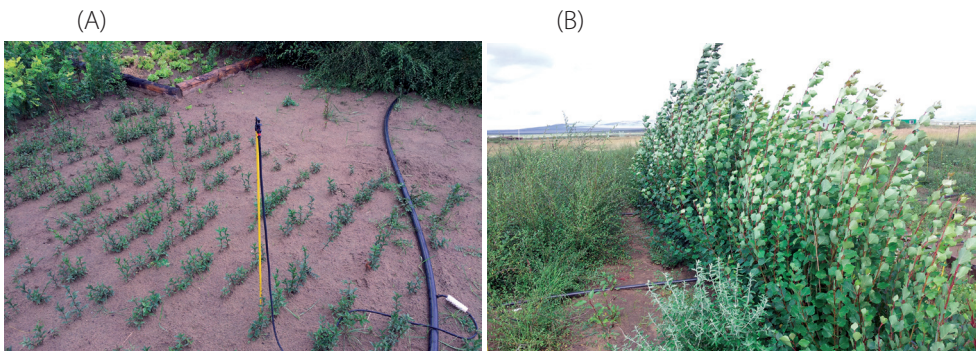


**Fig. 1. Nurseries were established and sites afforested at the Elsentasarkhai Station in Bulgan Province by the ERCCD (Experimental Research Center to Combat Desertification) under the Institute of Geography and Geocology (Mongolian Academy of Sciences). A) Irrigation system in a nursery with seedlings. B) A successful poplar nursery**

forest cover. Sufficient inventory data are important for deriving country-wide information on the extent, density, and quality of forest resources. Dulamsuren et al. (2016) presented one of the earliest comprehensive studies of carbon pool densities in Mongolian forests. Mongolia is the only country with boreal forests under the UN REDD programme (UNFCCC 2019) and has recently submitted a national Forest Reference Level (Government of Mongolia 2018; Khongor et al. 2018). For the 2005-2015 period, carbon removals were much lower than emissions and no clear trend was detected, as emissions and removals varied significantly from year to year (Government of Mongolia 2018). The capacity for carbon sequestration may be improved through certain silvicultural practices (including reforestation). Unsustainable harvest practices and dead wood clearing can trigger negative long-term consequences for the forest carbon pool, for example by reducing the organic matter content of the soil (Gerelbaatar et al. 2019a). By reducing canopy cover, intensive logging and fire can trigger the melting of insular permafrost and the release of soil carbon (Juříčka et al. 2018). Improved control of certain large-scale disturbances (e.g. fire) would also reduce direct carbon emissions. However, climate change is expected to trigger more frequent and severe disturbances, including fires and insect infestations (Ykhanbai 2010; Tchebakova et al. 2011, Dulamsuren et al. 2011). Such disturbances can lead to increased carbon emissions for years after the disturbance (Government of Mongolia 2018). Dulamsuren et al. (2016) predict that the carbon pool of Mongolia's forests will likely decrease further unless strong measures are taken at the national level.

### **Challenge 2: Resilience against more frequent and severe natural disturbances**

In general, disturbances can be characterized by the following criteria (Pickett and White 1985; Puettmann and Ammer 2007): magnitude, intensity/severity, frequency and seasonality. Magnitude refers to the spatial extension

(small scale or large scale). The severity of disturbance can be described by the degree of relative removal of basal area by considering all diameter classes, e.g. in form of an event analysis (see Gadow et al. 2005). Frequency refers to recurrence intervals and seasonality to the likelihood of occurrence of a disturbance during a certain time in the year (Sagwal 1991). Small and large scale disturbances by storms or certain weather events (e.g. snowbreak) are common during late spring and early autumn in Mongolia's mountain forests, but play a less significant role compared to the most eminent natural disturbances, which are fire and insect outbreaks (Tsogtbaatar 2004; Oyunsanaa 2011; Gradel 2017). Therefore, further contemplation in this review is on the latter two disturbances.

### **Lessons learned**

#### *Forest fires*

Fire is the most common disturbance in Mongolia and is often related to dry weather conditions (Goldammer and Furyaev 1996; Kondrashov et al. 2008; Hessel et al. 2016). Approximately 95% of the forest fires in Mongolia are caused by humans; the remainder are largely due to lightning (MET 2017a; 2017b; Government of Mongolia 2018). Fires are most common during spring and to a lesser extent in autumn (Government of Mongolia 2018), when conditions are relatively dry. In Mongolia, heavy rains occur frequently during the summer months, which is the reason why fires do not usually spread at this time of year. Much of the outcome of a fire depends on its intensity. Surface and ground fires are less damaging than crown fires. Short return intervals between more intense fires can lead to the continuing reoccurrence of pioneer stages and prevent forest succession (Makoto et al. 2007; Gradel et al. 2017b). Climate and fuel load are key determinants of the severity of a fire (Tanskanen and Venalainen 2008; Onderka and Melichercik 2010; Government of Mongolia 2018; Keane 2018): higher fuel loads and drier climates facilitate more severe fires.

Oyunsanaa (2011) found that the average frequency of forest fires in the pine forests of the northwestern Khentii Mountains is quite short, with only 11.6 years on average. Hessler et al. (2016) concluded that although overall fire return intervals have not changed considerably since 1900, there has been a trend toward more fires and shorter fire return intervals since the 1500s. The same study concluded that limited fire activity over the last century may be due to the coincidence of drought and intensive grazing, which have reduced fuel continuity and fire spread. However, recent official data (MET 2013; 2017b) suggest that fire has become more frequent in the last two decades in Mongolia (see Fig. 2).

Fire often weakens the resilience of tree stands against secondary disturbances (Government of Mongolia 2018); for this reason, the prevention of forest and steppe fires is mentioned in the very first article in the Forest Law of Mongolia (MOLF 2015). Fire management activities should respect the timely perspective and intensity of the fire disturbance. In this context, some authors refer to three phases of the wildfire cycle: the pre-fire environment, the fire environment, and the post-fire environment. Each phase requires different management actions (Graham et al. 2004; Keane 2018). In Mongolia, the wooden debris is often removed after logging in form of cleanings. If the management goal is to increase stand resilience, silvicultural measures that take into account disturbance history and succession stage (e.g., burned/recently

disturbed, early stage, mid-seral stage, late seral stage, and climax) need to be considered.

At the stand level, different silvicultural measures (thinning, prescribed burning) for increasing fire resilience in Mongolian forests are controversial. A study by Fischborn (2011), for example, did not find a relationship between stand density and fire susceptibility in the upper Eoo basin, and therefore did not support the hypothesis that selective cutting increases fire resistance at the stand level. Prescribed burning has been tested in Mongolia as one means of reducing the fuel load (Kondrashov et al. 2008). In neighboring Buryatia, prescribed burning is at some places practiced in order to reduce grass fuel load (Forestry Agency of Buryatia 2019). The immense input required to implement such a measure (e.g., planning, security, and personnel) also makes the application of, for example, prescribed burning at a broader scale prohibitive. Studies at a larger scale, however, indicate that there is indeed a connection between forest fire intensity and stand density (e.g., Kondrashov et al. 2008; Teusan 2018). The evidence suggests that this is due to higher fuel loads, as Teusan (2018) showed for the northern slopes in Selenge Aimag. For this reason, site-specific selective cutting practices should be evaluated further. As an alternative to prescribed burning, thinning of the larch and birch forests has been shown to have a positive short-term impact on the growth and vigor of the remaining trees, which may increase the resilience of individual trees (Gradel 2017).

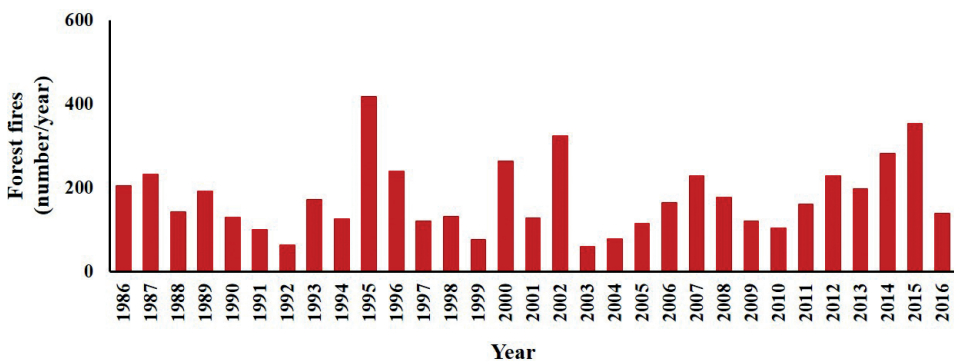


Fig. 2. Mongolian forest fire statistics (1980-2016)

It is important to note, however, that the reduction in canopy cover resulting from tree thinning measures may impact the permafrost; this potential consequence requires further study.

Thinning, however promotes diameter growth and usually bark thickness increases as stem diameter increases (Rosell et al. 2017); thick bark helps to protect the cambium of trees against fire. Recent studies have highlighted the close connection between fire-affected ecosystems and bark thickness, and shown that fire regimes influence whether and to what extent trees invest in bark thickness as a protection against fire (Pausas 2014; Pellegrini et al. 2017). In Mongolia fire frequency and intensity drive processes affecting tree species composition and competition. Recent results from the western Khentii Mountains indicate that fire intensity and frequency may control competition between thick-barked light coniferous trees and thin-barked birch; thus, the fire regime drives interspecific competition to some degree (Gradel et al. 2017b).

Beside intensive logging, fires are considered to be the main cause for the recent compositional shift from one tree species to another. In Mongolia and neighboring regions, this shift is often from coniferous to deciduous forests (Tikhonova et al. 2018; Gerelbaatar et al. 2019a). Birch often dominates after disturbances due to its sprouting ability (Otoda et al. 2013). To prevent the dominance of birch, low-intensity prescribed burning in birch-light coniferous forests may help promote the dominance of light coniferous trees (Gradel et al. 2017b), which may have more silvicultural value. Kondrashov et al. (2008) conclude that susceptibility to forest fires is related to ground vegetation (mainly grass fuel load), as is the resulting intensity of those fires. Thus, measures should focus on suppressing the ignition of fires.

With regard to suppression of an unintended fire outbreak, the intensity and magnitude are main parameter. During the active phase, weather conditions and

fire suppression actions are decisive. Early suppression is reported to be especially successful (Keane 2018). In the Mongolian context, initial attacks on small fires with small groups of locals is one approach. Depending on the regional fire frequency of the respective forest area, the post-fire environment may endure for centuries. In this context, secondary disturbances and forest dynamics (short- and long-term response of the ecosystem) are relevant. The Mongolian government takes a number of forest fire preventing measures during the fire season (spring: late March – mid June, autumn: September – end October) by restricting activities including tourism, timber harvesting, and other silvicultural measures. In the forested regions, local administration pays special attention to firefighting capacities. Finally, restoration of forests after fire and other large scale disturbances is of special importance (Danilin and Tsogt 2012; 2014), which is part of another chapter.

### Insects

Insects are an important part of healthy forest ecosystems. However, insect infestations often exacerbate previous damage (e.g. from fire) and are not uncommon in the boreal forests of northern Asia. Droughts and general forest degradation increase the frequency and severity of insect infestations because they weaken the resilience of the affected forest stands. This does not necessarily need to lead to significant forest dieback, however (Kharuk and Antamoshkina 2017). Important herbivorous insects in the region are currently *Lymantria dispar*, *Erannis jacobsoni*, and *Dendrolimus superans sibiricus* (Dulamsuren et al. 2010b; 2011; Gradel et al. 2017a). The invasive bark beetle (*Polygraphus proximus*) has recently been found in the fir forests of neighboring Siberia, but it has yet to be observed in Mongolia (Kharuk et al. 2017). However, official data show a clear increase in the area affected by insects and diseases in recent years. But the area where control measures are implemented stagnates, as shown by recent statistic data (MET (2017b). See Fig. 3.

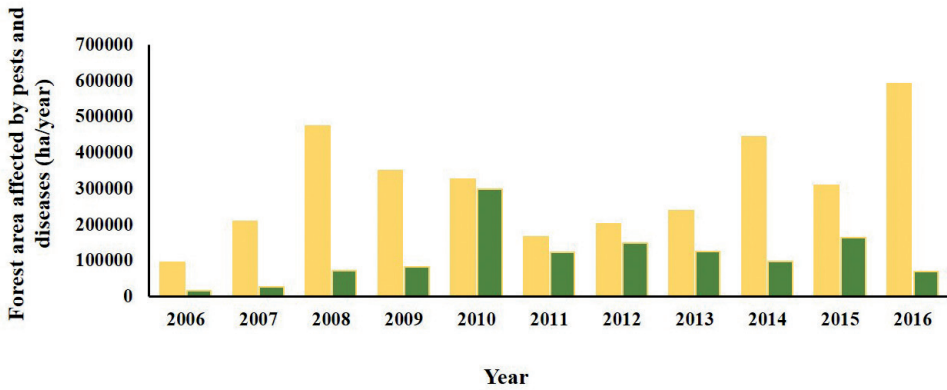


**Fig. 3. Total forest area affected by pests and diseases in Mongolia (2006-2016). Light yellow: overall forest area affected by insects and diseases. Green: area where control measures have been implemented**

Because winter temperatures and snow cover duration influence insect populations, they also (further) influence tree growth. The negative impact of higher mid-winter temperatures or the positive effect of above-average snow cover on insect populations is reflected in the growth rate of larch and birch during the subsequent vegetation period (Dulamsuren et al. 2011; Khishigjargal et al. 2014; Gradel et al. 2017a). Survival rates of eggs of *Lymantria dispar*, for example, can be related to threshold values of the surrounding air temperature (Waggoner 1985). Ongoing and projected climate warming will further exacerbate the current trend of increasing insect infestations. Options for increasing the resilience of forest stands against pests should therefore be considered in the development of Mongolian silviculture. Such options include more effective fire prevention and the regular removal of damaged and diseased trees.

### Challenge 3: Linking forest and water resources management

Mongolia's climate is characterized by its high continentality, which results in limited water availability even in the relatively wettest mountain regions of Northern Mongolia. Consequently, there are strong and bidirectional links between forest cover and hydrology. On the one hand, northern Mongolia is a marginal habitat for trees, and small

regional differences in water availability make the difference between closed taiga forest, open stands of trees or steppe as the dominant land cover (Dulamsuren et al. 2008; 2009). Therefore, any changes not only in precipitation but also in the regional hydrology (e.g. permafrost degradation, changes in the rates of evaporation, surface runoff and water infiltration into soils) are likely to have profound changes on the presence of trees. On the other hand, forest cover itself plays an important role for the regional hydrology – even more so because the headwater zones of all major river systems are located in forested mountain areas. Forest losses in these regions are therefore likely to have profound impacts on ground and surface water availability (Krasnoshhekov 2001; Kopp et al. 2017; Juříčka et al. 2018). These linkages mean that forest and water management should be considered and implemented in an integrated way.

### Lessons learned

*Preservation of the mountain taiga is a prerequisite for ensuring water availability in lowlands*

In a global perspective, Central Asia is one of the regions with the highest proportion of discharge formed in mountain areas (Viviroli and Weingartner 2004) which also contain a significant amount of the region's forest cover (Karthé et al. 2017a).

Mongolia is no exception to this, and the four forested mountain regions of Khentii, Khangai, Khuvsgul and Altai are the sources of the country's most important river and lake systems, comprising amongst others the Selenga and Lake Khuvsgul in Northern Mongolia, the Kherlen and Onon rivers in Eastern Mongolia, and the Khovd river and Valley of Great Lakes in Western Mongolia. For the Selenga, which is in terms of discharge the most important river system in Mongolia, forest cover in different subbasins ranges from a few percent (e.g. 5% in the subbasin of the Tuul river) to about two thirds (e.g. 66% in the subbasin of the Eroo river) and even more along some of its Russian tributaries (Karthé et al. 2017b). At the scale of such subbasins, contrasts become even more evident. For the Kharaa river system, for example, Menzel et al. (2011) showed that the specific runoff generated in forested mountainous headwater regions is about two to four times higher than in steppe-dominated regions. In this specific river basin, about two thirds of the total runoff is generated in those 20% of the catchment that are covered by mountain forests (Menzel et al. 2011).

Whereas the headwater regions are zones of surface runoff and groundwater formation, Mongolia's major water users are the urban and industrial centers of Ulaanbaatar, Erdenet and Darkhan and the agricultural and mining areas, many of which are located along the mid- and downstream sections of major rivers (Karthé et al. 2014; Kasimov et al. 2017). Rapid urbanization, a boom in mining and the intensification of agriculture (and increasing irrigation) have led to an ongoing trend of rising water consumption (Malsy et al. 2016; Park et al. 2017; Priess et al. 2011). In the end, this socio-economic development depends on water resources generated further upstream in the headwater regions of the major river systems which act as 'water towers' (Menzel et al. 2011; Karthé et al. 2015). However, these 'water towers' are under threat due to several pressures, including climate change, frequently recurring forest fires, illegal logging and the conversion of forest into pasture and

agricultural land (Karthé et al. 2015; Priess et al. 2011; Tsogetbaatar 2004).

Even though the relevance of mountain forests for the regional hydrology is not fully understood, a field study in a burnt forest area in the eastern Kharaa river basin (Fig. 4) indicated that forest losses due to forest fires have several hydrologically relevant implications:

- mountain taiga, which typically covers northerly exposed mountain slopes underlain with permafrost soil, plays a key role for regional water availability (Minderlein and Menzel 2015); forest losses are thus likely to reduce freshwater availability in steppe areas further downstream;
- the loss of shading and thick, insulating organic layers contribute to permafrost melt (Lange et al. 2015), which in turn modifies infiltration pattern (for which permafrost acts as a natural barrier);
- losses of forest soils which typically have a high organic matter content and a high water retardation capacity lead to more pronounced hydrological extremes, particularly in case of stormwater flow (Kopp et al. 2017).

#### *Degradation of floodplain forests affects water quality and aquatic ecology*

Besides mountain taiga and forest steppe, over vast parts of Mongolia riparian floodplains constitute the only other areas dominated by woody vegetation. According to Minderlein and Menzel (2015), they contribute to regional freshwater availability at least temporarily during the rainy season, when precipitation exceeds the site-specific evapotranspiration. Even more importantly, woody vegetation in the floodplains plays an important role for erosion prevention and the stabilization of river banks. This is particularly important for the dryland rivers of Northern Mongolia where river bank erosion is the dominant source of fine sediment input into the river system (Theuring et al. 2015).

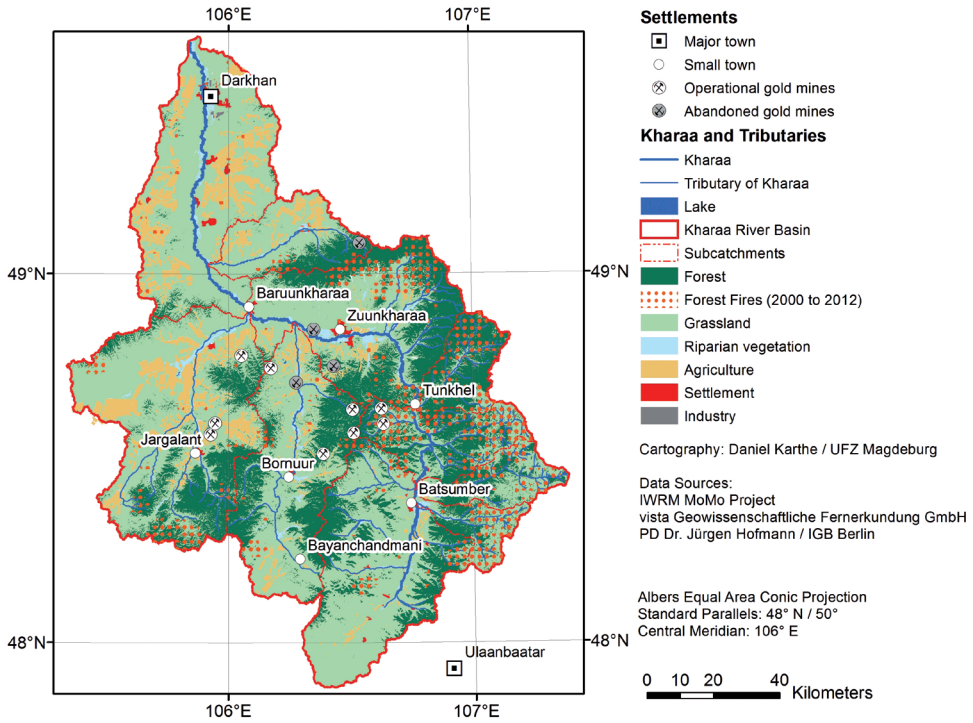


**Fig. 4. Locations of forest fires in the Kharaa River Basin, 2000-2012**

Increasing livestock densities are not only an important cause of grassland degradation (Tuvshintogtokh and Ariungerel 2012), but also puts river banks and their vegetation under growing pressure (Maasri and Gelhaus 2011). Since the 1990s, livestock numbers in Mongolia have increased drastically, reaching 33 million in 1999 (Rao et al. 2015), 44.5 million in 2009 (Maasri and Gelhaus 2011) and is now at the level between 60 and 70 million. Figure 5 illustrates the contrast between vegetated and degraded riverbanks and its relevance for erosion. Whereas dense shrubland (Fig. 5a) helps to

prevent riverbank erosion, high livestock densities and vegetation-free riverbanks lead to significant sediment-input into the river system (Fig. 5b).

The basin of the Kharaa river, just north of Ulaanbaatar, is exemplary for the impacts of high livestock densities on the river system. Based on geochemical and isotope-based fingerprinting techniques, it could be demonstrated that elevated fine sediment loads predominantly originate from riverbank erosion. Moreover, it could be shown that the fine sediments clog the hyporheic interstitial, the ecologically

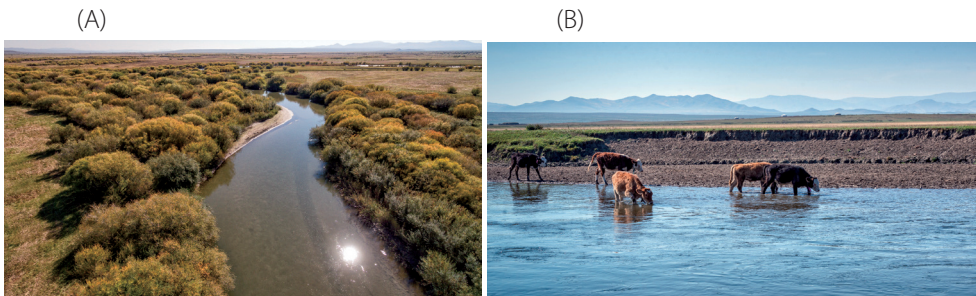


**Fig. 5. A) Natural floodplain vegetation around a tributary to the Kharaa. Photo: André Künzelmann, UFZ. B) Cattle in the Kharaa river**

highly relevant interface zone between surface and groundwater zones. Amongst other problems, this leads to a reduced aquatic macroinvertebrate biodiversity, which coincides with an increased proportion of fine-sediment colonizers (Hartwig and Borchardt 2014). From a management perspective, the stabilization of river banks (which is best achieved by the preservation and restoration of floodplain shrubland) is therefore a high priority (Hartwig et al. 2016).

### *Climate has significant impacts on regional forest cover and hydrology*

For the regional hydrology, climate change has both direct and indirect impacts. In the recent past, several streams in North Mongolia have desiccated and runoff even in major rivers has decreased (Angerer et al. 2008; Batimaa et al. 2008; Karthe et al. 2015). Since the observed and predicted temperature rise is particularly marked for the winter months, sublimation which already equals about 80 % of the total snowfall may increase even further (Wimmer et al. 2009). Even though snowmelt only contributes a small percentage of the annual water supply, reductions in snow water storage affect not only river hydrographs (weaker spring floods) but also plant water availability at the start of the growing season (Hülsmann et al. 2015; Menzel et al. 2011). Similarly, reductions in glaciation of Mongolia's high mountain zones are likely to negatively impact future water availability during the summer months. Even though systematic studies of Mongolia's glaciers are relatively rare, studies from the Altai (Kamp and Pan 2014) and the Tavan Bogd massif (Syromyatina et al. 2015) have shown a considerable shrinkage of glacier areas and volumes. Moreover, it has already been argued that climate change is also likely to have indirect effects on the regional hydrology by leading to changes in forest cover.

Regarding precipitation, global climate models are known to perform

rather poorly in the region, leading to considerable uncertainties about future trends (Malsy et al. 2013; Mannig et al. 2013; Bring et al. 2015). In Mongolia, temperatures have increased by more than 2K since the 1940s, leading to increasing evaporation rates (Karthe et al. 2015) and the thawing of permafrost soils (Sharkhuu et al. 2007; Törnqvist et al. 2014). Even though some models predict a slight increase in future precipitation, it is important to note that changes in rainfall pattern have been observed that are likely to be ecologically relevant. All over Mongolia, a transition from stratiform (moderate but long-lasting) to convective (short but very intensive) rainfall has been observed. Because short and intensive rain showers tend to create more surface runoff, they result in a reduced soil infiltration and therefore plant water availability (Vandandorj et al. 2017).

### **Challenge 4: Supporting forest regeneration against deforestation and degradation: Afforestation, reforestation, and underplanting**

Today, remote sensing and large-scale inventories support the monitoring of deforestation on regional (Teusan 2018), national (MET 2016), or even global levels (Hansen et al. 2013). Depending on the source and methodology, the annual reduction in Mongolian forest area in the first decade of the new millennium was reported to range between 0.21% and 0.7% (FAO 2011; Dorjsuren 2014). The most important and recent baseline data on boreal forest cover southern saxaul forest area are provided by the national forest inventory (MET 2016). A basic question for reforestation initiatives was to what extent the Mountain forest steppe is of natural origin or a product of nomadic pastoralism as touched by Hilbig (2000). Studies showed that the mixture of open grassland and forests, the Mountain forest steppe, with a range of fluctuation over time, is predominantly of natural origin (Zhukov et al. 1978; Dulamsuren et al. 2005).

## Lessons learned

### Afforestation initiatives

Despite increasing reforestation efforts (see Fig. 6), forest quality in terms of species composition, density, and stand health are decreasing, particularly since the 1990s (Tsoigtbaatar 2004; Ykhanbai 2010; Hansen et al. 2013; Khishigjargal 2014). In a study financed by GTZ, the proportion of degraded forest land was estimated to be 25% for the whole country (Kondrashov et al. 2008). This is especially noteworthy since reforestation efforts have increased constantly over the last four decades (see Fig. 6). Although reforestation has been practiced since the 1970s, forest rehabilitation has had relatively limited success around the country (Mühlenberg et al. 2006; MET 2017b). A World Bank study on reforestation in Mongolia found that low survival rates are due to fire, livestock grazing, and water shortages (Mühlenberg et al. 2006).

Species selection depends on a number of factors, such as seed provenance (see also Batkhuu et al. 2010), site conditions, region, and quality of planting materials and their adaptation. Appropriate species selection and soil treatments in reforestation activities facilitate the restoration of land, as shown by Ganchudur (2019) in Bulgan province. Park et al. (2016) found that indigenous Siberian elm trees (*Ulmus pumila*) growing in arid areas are able to substantially alter their morphological and

physiological characteristics to avoid heat stress and increase water conservation. Tree height, leaf size, and stomatal area per unit area decreased with increasing site aridity, while leaf mass per unit leaf area and water-use efficiency increased.

Scots pine (*Pinus sylvestris* L.) and Siberian larch (*Larix sibirica* Ledeb.) are commonly used for boreal conifer forest rehabilitation in Mongolia. This is especially the case in Selenge, Bulgan, and Khentii provinces, where most of the forest timber harvesting and overexploitation has taken place in recent decades. However, these species are also particularly robust, seedlings are readily available, and the mature trees have industrial value. Both species are usually planted as monocultures from two-year old seedlings (Gerelbaatar et al. 2019b). A successful example of reforestation activities are the Scots pine plantations in the Tujyin Nars Special Protected Area (Gerelbaatar et al. 2019b). The forests of Tujyin Nars were depleted sharply during 1960-2000.

On a national level, over 19 thousand hectares of degraded forests have been restored and successfully reforested between 1971 to 2011 (Batkhuu et al. 2017b). In 2005, the Government of Mongolia initiated the National "Green Belt" Programme with the goal of reducing desertification, sand movement, and dust and sand storms caused by climate change and improper land management in the steppe-desert border region.

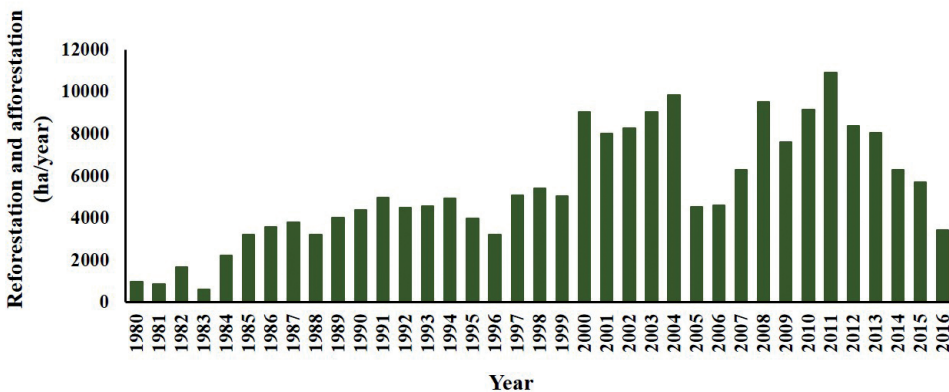


Fig. 6. Reforestation and afforestation in Mongolia between 1980 and 2016 (data source: MET (2017b))

Species were especially selected with respect to tolerance to drought, cold, and salt (Batkhuu et al. 2017b).

### *Timing of reforestation*

The effect of timing of reforestation success has recently been scrutinized by Gerelbaatar et al. (2019b), who found that the survival rate of seedlings in Scots pine plantations is a linear function of the number of dry days (days with air humidity below 30%) during the common planting period in May. The same authors elaborated threshold values of air humidity for the dieback of planted Scots pine seedlings in the Selenge Aimag. Survival rate and relative growth are also the main control parameters regarding reforestation for combating desertification in the frame of the above-mentioned CCDASA initiative (Khaulenbek and Kang 2017). Gerelbaatar et al. (2018a; 2019b) recommended the development of climate-resilient reforestation guidelines, and to test planting during autumn, depending on site conditions possible to consider also other tree species where possible. This includes also underplanting in degraded stands, which so far is not happening. The spectrum of available tree species planting methods and conditions needs to be enlarged (Gerelbaatar et al. 2019b).

### *Examples of natural reforestation after stopping grazing*

Although the overall trend in Mongolia is one of deforestation, there are some local examples of natural reforestation or potentially even forest expansion. There are places, where livestock grazing is the only factor that keeps grasslands open. Small-scale natural forest expansion has been reported following the reduction of livestock pressure in valleys in the eastern Khentii Mountains (Hartwig 2007) and in the Altansumber region, west of Darkhan (Gradel 2017).

### **Challenge 5: Managing the conservation of nature, biodiversity, and wildlife**

The most important criteria for conservation planning are diversity, naturalness, area size and rarity (Spellerberg 1992). Compared to other biomes in the world boreal forests exhibit rather low biodiversity per area unit, but have a relatively high proportion of natural, untouched forest areas (Potapov et al. 2008). In northern Mongolia the boreal forest biome transitions into the open steppe biome (Balandin et al. 2000). This creates a mosaic of different habitats. Therefore, several literature sources value the biodiversity and naturalness of Northern Mongolian forests, especially of the Mountain forest steppe (Dulamsuren et al. 2005; Mühlenberg 2012; Mühlenberg et al. 2012). The studies of Grubov (2001) and Dulamsuren (2004) provide an overview of botany, species and plant communities in the taiga zone and mountain forest steppe. First forest ecological descriptions and botanical studies of the Khangai and Khentii regions were subject of several joint Soviet-Mongolian biological expeditions (e.g. Savin et al. 1983; Savin et al. 1988) and German - Mongolian cooperation (Hilbig and Mirkin 1983).

### **Lesson learned**

#### *High biodiversity in the Mountain forest steppe*

Research at the German-Mongolian research station Khonin Nuga showed that biodiversity is especially high in the Mountain forest steppe. Since the mid 90ies researchers conducted comprehensive interdisciplinary field work in international teams (Mühlenberg 2012), which lead in some cases even to the validation of new species for Mongolia or even new to science (see for example Bayartogtokh (2000). It also provided comprehensive basic descriptions and classification of botanical description and of western Khentii Mountains (Dulamsuren 2004). The naturally fragmented Mountain forest steppe landscape (Dulamsuren et al 2005) is likely to also contain higher biodiversity.

Undisturbed forests contain also higher biodiversity compared to frequently disturbed forests as indicated by studies focusing on forest structure in disturbed light taiga and undisturbed dark taiga forest stands (Gradel and Mühlenberg 2011; Mühlenberg et al. 2012). These forests are also more productive in terms of basal area and volume (Mühlenberg 2012), which is in compliance with recent conclusions about a diversity-productivity relation on global level (Liang et al. 2016). Naturalness and area size are also often connected in Mongolia. Due to its low population density and accessibility ‘untouched, natural’ forests can still be found in Northern Mongolia. Based on criteria related to human alteration, remoteness and the level of fragmentation the remote sensing based worldwide intact forest landscape mapping and monitoring (Potapov et al. 2008; 2017) indicated that in Mongolia especially the Khentii Mountains have still a considerable portion of untouched, so called intact forest landscapes, which is however, constantly decreasing, especially due to fire impact (Potapov et al. 2017). Forest types that are often mentioned as valuable for different conservation reasons are especially types of riparian forests (Bei et al. 2003; Mühlenberg et al. 2004) and types of dark conifer forests (Dulamsuren 2004; Gradel and Mühlenberg 2011; Mühlenberg et al. 2012). *Abies sibirica* is naturally rare and limited to the two main forest regions in Northern Mongolia, namely around Lake Khuvsgul and the Khentii Mountain range (Dulamsuren 2004). *Pinus sibirica* is mentioned as a species with high ecological importance for wildlife (Dulamsuren 2004; Oyunsanaa 2011; Mühlenberg et al. 2012). The nuts of this tree species are an important energy source for wildlife in autumn (Dulamsuren 2004).

### **Approaches of forest conservation**

With regard to realization of forest conservation objectives, two basic approaches exist: segregation and integration. According to the Mongolian law on forests (MOLF 2015), forests are

divided into protection and production forests, which is typical for countries with large forest areas and low population density (e.g. countries of the former Soviet Union, but also North America). Protected forests (such as strictly protected areas, national parks, natural reserves and cultural monuments and local protected areas, where limited use is permitted for the local use of firewood and NTFPs, and other forest areas along rivers, for example) account for approximately 31% of the forest area (MET 2016). The integration of different objectives (e.g. conservation and utilization) in one management unit, often covered under the umbrella term “multifunctional forestry” is another approach developed and applied in Europe and incorporates a wider set of functions (often also recreation) in one forest area. The current approach of segregation (e.g. strictly protected areas for conserving natural landscapes and production forests) allows to protect very large pristine areas. In Mongolia remoteness can be considered as best form of protection of larger natural areas. Clear cuts are forbidden, but some authors suggested considering the integration of ecological values into management practices to some degree (Mühlenberg 2012; Gradel 2017). The review of forest scientific and biological studies indicated that diversity in terms of life forms and forest structure to a considerable extent depend on the amount of overall volume and certain dimensions of dead wood, sufficient number of large sized trees (DBH > 50 cm), certain species (especially Stone Pine), the forest type, amount of dead wood and the succession stage. The disturbance history plays a role in that way, that higher later succession stages with long term undisturbed development consequently lead to higher values of typical old-growth attributes and even diversity levels (Bei et al. 2003; Mühlenberg et al. 2004; Gradel and Mühlenberg 2011; Meyer and Schmidt 2011; Mühlenberg et al. 2012). Certain management practices, such as salvage cutting, which may be useful for other purposes, are considered negative from an ecological viewpoint (Lindenmayer and Noss 2005). Natural

regeneration was found to grow sufficiently in many closed forests (MET 2016) and in some regions, for example around Bugant, even after intensive logging activities and fires (Gradel 2017). However, successful reforestation activities in Mongolia are active measure against degradation and desertification (Ganchudur 2019). In such cases native tree species and if possible local provenances should be given priority. Gerelbaatar et al. (2018b) compared ground vegetation in Scots pine plantations of different age classes with natural stands and found that young plantations were most diverse in terms of species diversity, but lacked certain typical forest species. Recently in a preliminary study Jamyansuren et al. (2018) identified seed regions for the important tree species: 19 regions for Siberian larch, 12 regions for Scots pine, 9 for Siberian pine, 6 for Siberian fir and 9 for Siberian spruce. The same authors recommend that seeds from higher elevated mountainous regions should only be used in a range of about 200-400 m of the original altitude.

#### **Challenge 6: Increased resource utilization and demand in forested areas**

Various sources report a recent increase in forest resource utilization, especially with respect to wood (Tsoigtbaatar 2004; Hartwig 2007; UNREDD 2013), but NTFPs are also shown to be under increased pressure (Sepp and Schüler 2016). The extent, intensity, and frequency of logging-induced degradation is greatest in the most accessible areas, especially in the vicinity of populated and developed regions. These areas are largely dominated by light coniferous trees and now, increasingly, deciduous tree species (Gerelbaatar et al. 2019a). At a regional level, the pressure on forest products is greatest in the more densely populated regions north of Ulaanbaatar, especially in Selenge Aimag (Teusan 2018). Local overuse is one of the reasons why a particularly large number of forest stands grow from birch-rich succession forests in this region. Scots pine and larch (Dugarzhav 1996) are the most preferred

species due to their rapid growth, wood quality, and broad distribution in rather accessible areas.

#### **Lessons Learned**

##### *Management practices, including NTFP collection*

Despite the increasing amount of research concerning forest management in Mongolia, the literature review shows that current practices are largely deemed inadequate. Oyunsanaa (2011), for example, doubts that Mongolian forests have ever been subject to science-based sustainable forest management. Inadequate forest management is frequently mentioned as a driver of forest degradation (UNREDD 2017; Government of Mongolia 2018; Khongor et al. 2018). Although silvicultural guidelines are hardly implemented (Gerelbaatar et al. 2019a), cutting often takes place nowadays as some kind of selective logging. Soum and Aimag authorities typically determine the amount of dead wood to be extracted during a cleaning. The Ministry of Environment and Tourism finally sets an annual quota, which is implemented at the regional level (Sepp and Schüler 2016). In dark taiga forests logging is largely prohibited. Dark coniferous grow also in higher and remote locations, which are more difficult to reach (Gradel et al. 2018).

Commercial forests are managed by private logging companies or with considerable limitations also by forest user groups (FUG), which represent a kind of community forestry. Logging of living trees is carried out only by private companies holding special logging licenses (Gradel and Petrow 2014). FUGs mostly conduct cleanings, collect fuelwood from dead trees and collect NTFPs (MET 2016). These are the most common forest products for local inhabitants of the forested regions; they are also collected by non-FUG members with the respective permissions. NTFP collection is especially practiced at the accessible edge of the forests (e.g. dog-

roses) or for longer trips in the remote dark taiga areas, especially for stone pine nuts, different berries and herbs. Stone pine nuts are considered to be the most important NTFP. According to a study by Sepp and Schöler (2016), the world market price for shelled pine nuts increased by 600% between 2006 and 2014. However, the prevailing method of collection of pine nuts is seriously damaging the stone pine trees. Trees are hit with huge hammers that destroy the bark.

### Logging – scale and practices

Logging data vary widely and are difficult to obtain due to unlicensed (illegal) logging. Since 2000, the FAO has provided estimates of the annual legal production of firewood and industrial round and sawn timber in Mongolia. For 2010, this number was about 974,000 m<sup>3</sup> (FAO 2011). However, especially since the end of the last century, logging has been largely uncontrolled (Tsogtbaatar 2004; UNREDD 2017). Based on the evaluation of additional sources, Gradel and Petrow (2014) estimated an annual fluctuating range of 1 to 4 million m<sup>3</sup>. This number includes an unlicensed logging of between 345,000 and 2 million m<sup>3</sup>. However, the utilization is unregular distributed over the country and a lot of forest stands are actually over-aged (MET 2016). A further increase in the utilization pressure on forests is projected (Ykhanbai 2010).

Most of the harvested timber comes from forest cleanings. According to official sources, about 86.3% of the harvest volume comes from cleaning and sanitation cutting. An additional 4.6% results from thinning, and 9.1% from final harvests (Government of Mongolia 2018). Forest cleaning refers to salvage and sanitation cuttings and consists of the removal of dead trees and fallen limbs (MET 2014). See Fig. 7 for official Mongolian statistics on legally harvested timber through forest cleanings between 2011 and 2014.

According to official sources, only about a fifth of the harvest volume (18.8%) is comprised of commercial timber harvest, whereas about 81.2% is fuelwood. However, fuelwood collection is not usually perceived as a driver of forest degradation. Rather, it is seen as a secondary activity and one that is mostly part of cleanings by forest user groups and locals. For this reason, fuelwood collection is not taxed (Government of Mongolia 2018).

Some sources discuss potential measures to prevent illegal logging. Teusan (2018) reported at least short-term success in working with local people to control illegal logging in the area around Bugant. This is somewhat similar to the basic assumptions of participatory forestry initiatives and forest user groups (e.g. as recommended by FAO, GIZ), which consider participation of local forest users as a prerequisite for protection against illegal logging by

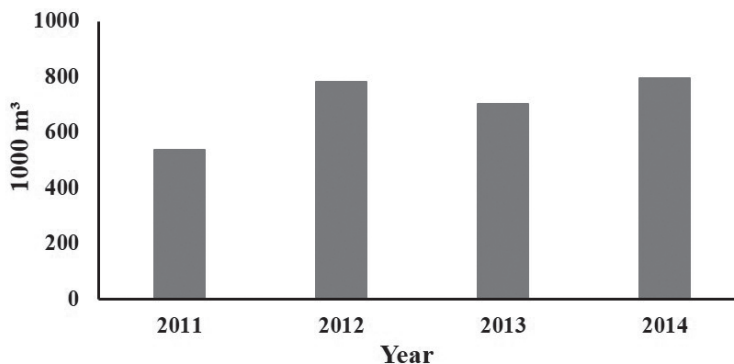


Fig. 7. Official statistic on legally harvested timber through forest cleaning between 2011 and 2014 (MET 2014)

externals (Gradel 2017). In other studies, about Siberian larch, Siberian Pine and Scots Pine it has been shown that genetic timber tracking with molecular markers is possible at regional scale and therefore has been suggested as tool for clarifying illegal logging (Putintseva et al. 2018; Blanc-Jolivet et al. 2018).

Already in the second half of the 20th century, research trials for the evaluation of logging impact concluded that in Mongolia the impact of selective logging is ecologically more positive than clear-cutting (Savin et al. 1988). The short-term effects of thinning from below on individual tree growth was recently studied in larch and birch stands near the steppe border (Gradel et al. 2017c). The authors found that the growth response of the remaining trees was significantly positive and directly related to the reduction of surrounding competitor trees. Interestingly, even medium-aged trees also responded immediately with significant growth increases. These results indicate that in terms of growth reaction and regeneration, low to medium intensity selective logging regimes may be sustainable. The long-term effects of different logging intensities on soil capacity and regeneration in Mongolian Scots pine stands in Selenge province were also recently examined (Gerelbaatar et al. 2019a). The final conclusion was that low intensity (around 25% removal) and, to a lesser extent, even medium intensity (around 50% removal) selective logging triggered regeneration of the main conifer species. The same authors showed that especially high intensity selective logging (around 75% removal) and clear cuts (100% removal) lead to significant decreases in regeneration (especially of the conifer species) and degradation of physical soil properties. However, physical and chemical soil properties indicated that soil capacity was best maintained without any logging at all.

Several authors (Benneckendorf 2011; Schmidt-Corsitto 2014) call for the research and design of improved instruments to promote sustainable forestry, e.g. regionally adapted silvicultural guidelines. Similarly,

measures related to fostering markets for certain products (e.g. charcoal from birch thinning residuals and cleanings) may create incentives for financing silvicultural practices that help promote continuous cover forestry (Gradel 2017). To some degree, this may also shift current utilization away from cutting conifer trees and larger diameters toward harvesting more deciduous trees and trees with smaller diameters. This would help shift utilization to secondary growth succession forests, thereby protecting the remaining old growth forests. The voluntary certification of forest management and NTFPs may also promote a more sustainable utilization. These processes are, however, only in the initial stages in Mongolia; as yet, little regional knowledge is available.

#### *Other relevant forest utilization practices*

On a regional scale, the grazing of cattle can be an important utilization factor (MET 2016). Grazing affects the contact zone between forest and steppe, but mainly plays a role in open forests (UNREDD 2017) with sufficient grass cover. Grazing is reported to play a minor role in more closed forests (MET 2016). In the mountain forest steppe, dense grass layers are common and may hinder forest regeneration (Gradel 2017). Therefore, under certain circumstances grazing could potentially even have a slightly positive impact, if timed properly and managed for the right intensity. On the other hand, grazing in the forest area has most often an adverse effect on the success of forest reproduction and forest establishment when cattle eat or trample seedlings. While the effects of forest fires and logging are relatively clear, the introduction of livestock into forest fringe areas is less well understood in Mongolia. Nevertheless, there are many examples that show, that increasing livestock densities has an adverse effect on the survival of young tree saplings and can totally stop successful forest regeneration (Khishigjargal 2013). There are also examples of natural reforestation after grazing was stopped (see challenge 4 of this review).

Finally, mining also affects forest area. The impact is significant where practiced, but the area in the forested region is in absolute terms relatively little, compared to the area sizes affected by grazing or logging.

### Challenge 7: Consideration of the social and political-cultural background

Mongolia currently faces the simultaneous challenges of transforming from traditional nomadic herding practices to increasingly urban lifestyles, as well as adapting to climate change and increasing utilization pressures. Socio-economic and demographic factors are considered to be indirect drivers of deforestation (Government of Mongolia 2018). We therefore consider the social and political-cultural context as an additional challenge affecting forest management. Factors include population growth, urbanization, and economic growth, all of which lead to more activity in the increasingly accessible forests and a growing demand for wood for construction. At the same time, increasing rural poverty drives unsustainable forest management (Government of Mongolia 2018). These drivers increasingly influence the provision of ecosystem services and management decisions in Mongolia. A schematic presentation of the interdependencies between the forest ecosystem and the social system is presented in Fig. 8.

### Overview of forest historical background in Mongolia

To better understand the relationship between social-political factors and the challenges the forestry sector faces, some historical context is needed. For a long time, the core element of the Mongolian economy was livestock farming in the form of nomadism in the steppe and forest steppe. Both steppe and forest have played a decisive role in the cultural identity of Mongolia and neighboring regions (Filep and Bichsel 2018). For Mongolia, one can argue that steppe-based, subsistence-oriented nomadic pastoralism represents the origin of the Mongolian cultural identity. In this context, forests were perceived as places of shelter, as reported in the national epic from the 13<sup>th</sup> century, the *Secret History*, as well as places for hunting and gathering (Taube 2005; Hartwig 2007).

The background of present-day forest institutions, however, was laid during the socialist period. Although there were early forest use regulations, institutionalization of the forestry sector only took place after the establishment of the Socialist People's Republic of Mongolia in the 1920s. In 1924, the first forestry division was formed in the Ministry of Economic Affairs, and in 1931, the first forest law was passed (Tsogtbaatar 2008). The first national forest inventory took place between 1956 and 1957 (MET 2016). Sovereign rights over forestry and the timber industry

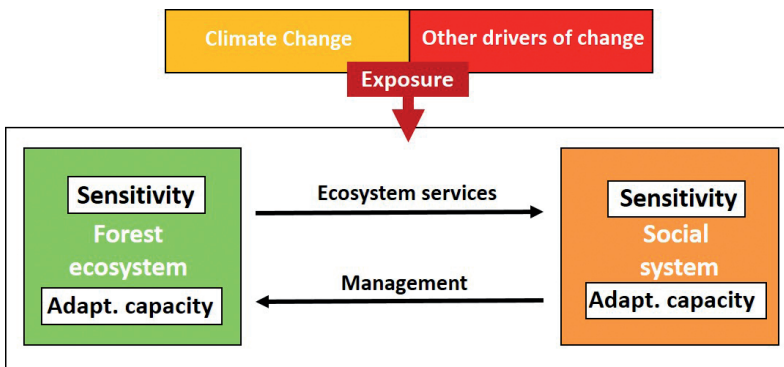


**Fig. 8.** The interdependencies between managed forest ecosystems and the social system. Both systems are exposed to climate change and other drivers of change (based on a general figure from Locatelli et al. 2008)

were consolidated during socialist times in one ministry. Land and forest were state-owned and the Mongolian timber industry was dominated by state-owned enterprises and joint ventures with COMECON members (Council for Mutual Economic Assistance), in particular the USSR, but also Poland and Romania (Gradel and Petrow 2014). The peak of timber use was achieved in the 1980s with a total of sixty sawmills. According to Tsogtbaatar (2008), the total annual volume of timber reached about 2.2 million m<sup>3</sup>. At that time, timber accounted for 4 to 14% of national GDP (Bastian 2000), and several thousand people were employed in the wood combines (Ammann 2002). According to Ykhanbai (2010), the relative share of the forest industry in the GNP was still about 4.1% in 1990, compared with only 0.26% in 2010. With the supply and funding constraints and difficulties faced by COMECON members, the political changes in 1990 brought about drastic changes in the Mongolian forestry sector. Regional forestry units were initially dissolved or integrated into more general environmental authorities (Gradel and Petrow 2014), and a considerable number of sawmill workers lost their jobs. Official annual logging fell significantly (Tsogtbaatar 2008) and unlicensed, illegal logging increased.

## Lessons learned

### *Bridging gaps between different stakeholders, levels and hierarchies*

Today, as in socialist times, woodland remains exclusively in public ownership, while its utilization has been reformed through various models. According to Saladyga et al. (2013), the greatest evidence for an anthropogenic fire regime was found following the transition to a free market economy during the early 1990s, when land-use intensification near the capital city of Ulaanbaatar took place. This indicates the importance of considering increasingly socio-political aspects in the transformation process of land-use management. The Mongolian forest policy sector has been under constant reform.

This ongoing transformation process of the law reflects, to a certain degree, perceived needs, for example putting emphasis on the protection function of forests. Over the last two decades, forest policy has shown the potential for development, such as when a reformed edition of the Forest Act was issued in 2007. Subsequently, a forestry agency was established that was later integrated into the Ministry of Environment as a forestry department. This integration was suggested to give the forestry sector a new framework, to stop the progressive degradation of the forest, and to bring order to the timber business. At regional and local levels, forestry has been re-established to some degree. However, the transfer of policy objectives, formulated for example in the law on forests, into concrete objectives with related implementation guidelines (e.g., guidelines for ecologically adapted silviculture) has not been sufficiently realized yet. There is a gap between policy frameworks, law reformation, and actual implementation and monitoring. Benneckendorf (2011) emphasizes that there is still a need for policy adjustments and capacity buildup within the administrative system. Especially at the local level (soum forest unit), capacities for controlling proper implementation are still lacking.

Some recent initiatives emphasize participatory forestry, especially with regard to the establishment and training of forest user groups (Evans 2008). The introduction of rights and obligations in the context of participatory forest management by forest user groups has been a particular reform approach used in Mongolia. Since the new Forestry Act of 2007, forest user groups (FUG/Nukhurlul), which are mostly associations of local nomads, can acquire usage rights within the scope of approved management plans. Usage is most often related to firewood and NTFPs (Sepp and Schüler 2016). Internationally funded projects have been tailored to facilitate further reforms and capacity development of FUGs. The performance of user groups during a recent FAO project was largely

assessed through methods that involved the participation of all group members (Gradel 2017). This assessment was based on instruments that help to develop group capacities, group identity, and personal ownership (e.g., see Lynam et al. 2007). Local usage rights are combined with duties to protect the forest areas, e.g. from fire and external illegal users. This mechanism should function on the basis of the common interests of the state and the local population. For many forest user groups, staking areas to secure pasture areas plays just as important a role as securing their forest areas. According to recent data presented by UNREDD (2017), a total of 1179 FUGs manage 3,119,635 ha in Mongolia, whereas 83 private forest entities manage about 681,378 ha. In practice, the management impact of these groups varies widely and is not always effective. Community participation and capacity development for agroforestry initiatives for combating desertification are also relevant within the Korean-Mongolian CCDASA initiative (Khaulenbek and Kang 2017). The involvement of locals, e.g. with different user group and community participation approaches, usually has several objectives. These can include balancing the very uneven management impact on a regional scale, protecting and enhancing the protection functions of the ecosystems (e.g., with regard to soil and water), and reducing rural unemployment and poverty by improving or even creating income opportunities. However, the official harvesting of industrial wood continues to be carried out by private companies under concessions acquired by the state (Gradel and Petrow 2014). According to national experts from leading universities in Ulaanbaatar, the establishment of infrastructure for private timber enterprises (e.g., roads and electricity) could also reduce rural unemployment and poverty and balance uneven forest management intensity at the country level.

## CONCLUSIONS

Because forest management in Mongolia faces numerous related and unrelated

challenges, integrated and scientifically-based approaches are urgently needed. These complex problems cannot be solved by focusing on a single topic; rather, synergies need to be identified and utilized to set priorities and guide actions. In Mongolia, the relationship between vegetation cover and the water balance is a particularly urgent issue in the face of advancing climate change and land degradation. The forests and hydrology of a region are connected in manifold ways. The survival or re-establishment of forests requires sufficient water supply, especially in a country like Mongolia where water availability is the most critical factor limiting forest distribution. At the same time, forests play a crucial role in maintaining the hydrological balance and preventing desertification. Forest cover is essential for preventing the loss of permafrost, for example, but this protective function can only be maintained when low-intensity logging practices are used. We therefore recommend that future initiatives emphasize synergetic cross-sectoral approaches that consider the different challenges to forest management, especially with respect to the impact on the hydrological regime. To achieve this, integrated capacity development, forest research, and rehabilitation is needed that works across disciplines and at landscape scales. At the same time, capacity development and legislation need to take into account the specific socio-economic backgrounds of the target regions, and work with local communities, regional and national administrations.

## ACKNOWLEDGEMENTS

We thank Dong Kyun Park (Dongguk University) and Anne Wecking (University of Waikato) for their comments during the initial phase of the manuscript preparation and Ugilkhon Abdullaeva and Aigerim Danilova (Manas University) for their support during the revision. The authors thank two anonymous reviewers for their valuable comments. ■

## REFERENCES

- Ammann H. (2002). Sektorendarstellung Holz. Unveröffentlichter Teilbericht zum GTZ-Projekt: Naturschutz und Randzonenentwicklung, Ulaanbaatar. (in German).
- Angerer J., Han G., Fujisaki I. and Havstad K. (2008). Climate Change and Ecosystems of Asia with Emphasis on Inner Mongolia and Mongolia. *Rangelands*, 30(3), pp. 46-51. DOI:10.2111/1551-501X(2008)30[46:CCAEOA]2.0.CO;2
- Balandin S.A., Basilov V.N., Wilke R.H.B., Camparasa J.M., Coupland R.T., Frade S., Fuller K., Ghilarov A.M., Given D.R., Harcourt C., Hart R.H., Junyent C., Mordkovitch V.G., Pesci R., Petelin D.A., Poch R.M., Porta J., Scott G.A.J., Sheftel B.I., Sokolova Z.P., Tishkov A.A., Beck M., Campillo X. and Vigo M. (2000). *Encyclopedia of the biosphere (Vol. 8), Encyclopedia of the biosphere - Prairies and Taiga*. Gale Group, Detroit (USA), p. 460.
- Bastian O. (2000). Mongolei-Transformation und Umwelt in Zentralasien. *Geographische Rundschau* 52 (3), p. 17-23. (in German).
- Batima P., Natsagdorj L., Gombluudev P. and Erdenetsetseg B. (2005). Observed climate change in Mongolia. AIACC Working Paper, [online] Vol. 13, 26 p. Available at: [http://www.start.org/Projects/AIACC\\_Project/working\\_papers/Working%20Papers/AIACC\\_WP\\_No013.pdf](http://www.start.org/Projects/AIACC_Project/working_papers/Working%20Papers/AIACC_WP_No013.pdf) [Accessed 10 Jun. 2019].
- Batimaa P., Batnasan N. and Bolormaa B. (2008). Climate change and water resources in Mongolia. In: Basandorj, B., Oyunbaatar, D. (Eds). *International conference on uncertainties in water resource management: causes, technologies and consequences*. IHP Technical Documents in Hydrology No. 1, Jakarta, pp. 7–12.
- Batkhuu N.O., Lee D.K., Tsoigtbaatar J. and Park Y.D. (2010). Seed quality of Siberian larch (*Larix sibirica* Ldb.) from geographically diverse seed sources in Mongolia! *Scandinavian Journal of Forest Research*, 2(1), pp. 101-108. DOI:10.1080/02827581.2010.485815
- Batkhuu N.O., Ser-Oddamba B. and Gerelbaatar S. (2017a). Forest and Landscape Restoration in Mongolia. International Conference on Landscape Restoration under Global Change. Poster presentation, San Juan, Puerto Rico, pp. 6-9.
- Batkhuu N.O., Ser-Oddamba B. and Gerelbaatar S. (2017b). Forest and Landscape Restoration in Mongolia. Poster presentation at the International Conference on Forest Landscape Restoration under Global Change. San Juan, Puerto Rico pp.6-7.
- Bayartogtokh B. (2000). New oribatid mites of the genus *Belba* (Acari: Oribatida: Damaeidae) from Mongolia. *International Journal of Acarology* Vol. 26, pp. 297–319.
- Bei M.L., Wichmann F. and Mühlenberg M. (2003). The Abundance of Tree Holes and Their Utilization by Hole-Nesting Birds in a Primeval Boreal Forest of Mongolia. *Acta Ornithologica*, 38(2), pp. 95-102. Available at: <http://www.bioone.org/doi/abs/10.3161/068.038.0205> [Accessed 10 Jun. 2019].
- Benneckendorf W. (2011). Concept for Forestry Sector Development in Mongolia. Interne GIZ-Studie zum GIZ-Projekt: Climate Change and Biodiversity in Mongolia. Zunkharaa, 56 pp.

Blanc-Jolivet C., Yanbaev Y. and Degen B. (2018). Genetic timber tracking of *Larix* ssp. in Eurasia. Published in Degen B, Krutovsky KV, Liesebach M (2018), German-Russian Conference on Forest Genetics - Proceedings – Ahrensburg, 2017 November 21-23. Thünen Report, Vol. 62, pp. 89-93.

Bolte A., Ammer C., Löff M., Nabuurs G.J., Schall P. and Spathelf P. (2010). Adaptive Forest Management: A Prerequisite for Sustainable Forestry in the Face of Climate Change. Published in: Spathelf P (eds.) Sustainable Forest Management in a Changing World: A European Perspective. Springer Netherlands, pp. 115-139. DOI: 10.1007/978-90-481-33017\_8

Bring A., Asokan S.M., Jaramillo F., Jarsjö J., Levi L., Pietroń J., Prieto C., Rogberg P. and Destouni G. (2015). Implications of freshwater flux data from the CMIP5 multimodel output across a set of Northern Hemisphere drainage basins. *Earth's Future*, 3(6), pp. 206–217. DOI:10.1002/2014EF000296

Danilin, I.M. and Tsogt, Z. (2012). Restoration of forests at logging and burned areas in Mongolia. *Problems of Regional Ecology*, N. 1., pp. 7-13 (In Russian with English abstract).

Danilin, I.M. and Tsogt, Z. (2014). Dynamics of structure and biological productivity of post-fire larch forests in the Northern Mongolia. *Contemporary Problems of Ecology*, 7(2), pp. 158-169. DOI: 10.1134/S1995425514020036

Davi N.K., Pederson N., Leland C., Baatarbileg N., Byambagerel S. and Jacoby G.C. (2013). Is eastern Mongolia drying? A long-term perspective of a multidecadal trend. *Water Resources Research*, 49, pp. 151-158. DOI: 10.1029/2012WR011834

De Grandpré L., Tardif J.C., Hessel A., Pederson N., Conciatori F., Green T.R., Oyunsanaa B. and Baatarbileg N. (2011). Seasonal shift in the climate responses of *Pinus sibirica*, *Pinus sylvestris*, and *Larix sibirica* trees from semi-arid, north-central Mongolia. *Canadian Journal of Forest Research*, 41(6), pp. 1242–1255. DOI: 10.1139/x11-051

Dorjsuren Ch (2014). Forest Ecosystems (in Climate change impact and exposure). Published in: Mongolia second assessment report on climate change – MARCC 2014. Ulaanbaatar: pp. 94-100.

Dugarzhav Ch. (1996). Larch Forests of Mongolia (Current Conditions and Reproduction). DSc (Agr.) Thesis (For. Sci. & Silviculture, Ecol.). Krasnoyarsk: V.N. Sukachev Institute of Forest, Rus. Acad. Sci., Siberian Br., 59 pp. (In Russian).

Dulamsuren Ch., Klinge M., Degener J., Khishigjargal M., Chenlemuge T., Bat–Enerel B., Yeruult Y., Saindovdon D., Ganbaatar K., Tsogtbaatar J., Leuschner C. and Hauck M. (2016). Carbon pool densities and a first estimate of the total carbon pool in the Mongolian forest–steppe. *Global Change Biology*, 22, pp. 830-844. DOI:10.1111/gcb.13127

Dulamsuren Ch., Hauck M., Leuschner H.H. and Leuschner C. (2011). Climate response of tree ring width in *Larix sibirica* growing in the drought-stressed forest-steppe ecotone of northern Mongolia. *Annals of Forest Science*, 68(2), pp. 275-282. DOI 10.1007/s13595-011-0043-9.

Dulamsuren Ch., Hauck M. and Leuschner C. (2010a). Recent drought stress leads to growth reductions in *Larix sibirica* in the western Khentey, Mongolia. *Global Change Biology*, 16, pp. 3024-3035. DOI: 10.1111/j.1365-2486.2009.02147.x

Dulamsuren Ch., Hauck M., Leuschner H.H. and Leuschner C. (2010b). Gypsy moth-induced growth decline of *Larix sibirica* in a forest-steppe ecotone. *Dendrochronologia*, 28, pp. 207-213. DOI: 10.1016/j.dendro.2009.05.007

Dulamsuren Ch. and Hauk M. (2008). Spatial and seasonal variation of climate on steppe slopes of the northern Mongolian mountain taiga. *Grassland Science*, 54(4), pp. 217-230. DOI: 10.1111/j.1744-697X.2008.00128.x

Dulamsuren Ch., Hauck M. and Mühlenberg M. (2005). Vegetation at the taiga forest-steppe borderline in the Western Khentey Mountains, northern Mongolia. *Annales Botanici Fennici* Vol. 42, pp. 411-426.

Dulamsuren Ch. (2004). Floristische Diversität, Vegetation und Standortbedingungen in der Gebirgstaiga des Westkhentej, Nordmongolei. *Berichte des Forschungszentrum Waldökosysteme, Reihe A, Bd. 191*, Georg-August-Universität Göttingen, 290 pp. (in German).

Evans P. (2008). Project Status and Recommendations. Report on the project Capacity Building and Institutional Development for Participatory Natural Resources Management and Conservation in Forest Areas of Mongolia (GCP/MON/002/NET), 71 p.

FAO (2011). State of the world's forest 2011. Rome: Food and Agriculture Organization, 164 pp.

Filep E., Bichsel C. (2018). Towards a research agenda on steppe imaginaries in Russia and the Soviet Union. *Geography, Environment, Sustainability*, 11(3), pp. 39-48. DOI:10.24057/2071-9388-2018-11-3-39-48

Forestry Agency of Buryatia (2019). In Buryatia, prescribed burning as prevention against fires begins. [online] Available at: [http://egov-buryatia.ru/ralh/press\\_center/news/detail.php?ID=30110&fbclid=IwAR1r5UTUjMzdn9LICfpS4TT\\_1aXaB2KSDRY66lLeQElzcyoFVUn7OruzM80](http://egov-buryatia.ru/ralh/press_center/news/detail.php?ID=30110&fbclid=IwAR1r5UTUjMzdn9LICfpS4TT_1aXaB2KSDRY66lLeQElzcyoFVUn7OruzM80) [Accessed 10 Jun. 2019].

Gadow K.v. (2005). Forsteinrichtung. Analyse und Entwurf der Waldentwicklung. Universitätsverlag Göttingen, Reihe Universitätsdrucke, Göttingen, 342 S. (in German).

Gao R., Shi X. and Wang R. (2017). Comparative studies of the response of larch and birch seedlings from two origins to water deficit. *New Zealand Journal of Forestry Science*, 47(14). DOI:10.1186/s40490-017-0095-1

Ganchudur T. (2019). Reforestation to Combat Desertification in Degraded Sandy Soil Regions of Central Mongolia. Ph.D. Thesis (Dissertation), Dongguk University, Seoul, Republic of Korea, p. 159 pp.

Gebhardt T., Häberle K.H., Matyssek R., Schulz C. and Ammer C. (2014). The more, the better? Water relations of Norway spruce stands after progressive thinning intensities. *Agricultural and Forest Meteorology*, 197, pp. 235-243. DOI: 10.1016/j.agrformet.2014.05.013

Gerelbaatar S., Batsaikhan G., Tsogtbaatar J., Battulga P., Batarbileg N. and Gradel A. (2018a). Early survival and growth of planted Scots pine (*Pinus sylvestris* L.) seedlings in northern Mongolia. In: *Book of Abstracts*. P. Vossen D., Karthe B., Gunsmaa S., Enkhjargal S., ed., GMIT Symposium on Environmental Science and Engineering, Nalaikh, [online], pp. 8-9. Available at: [http://gmit.edu.mn/site/files/downloads/gmit\\_sese-2018\\_book-of-abstracts.pdf](http://gmit.edu.mn/site/files/downloads/gmit_sese-2018_book-of-abstracts.pdf) [Accessed 18 Feb. 2019].

Gerelbaatar S., Suran, B., Nachin, B. and Chultem D. (2018b). Effects of scots pine (*Pinus sylvestris* L.) plantations on plant diversity in northern Mongolia. *Mongolian Journal of Biological Sciences*, 16(1), pp. 59-70. DOI: 10.22353/mjbs.2018.16.08

Gerelbaatar S., Baatarbileg N., Battulga P., Batsaikhan G., Khishigjargal M., Batchuluun T. and Gradel A. (2019a). Which Selective Logging Intensity is Most Suitable for the Maintenance of Soil Properties and the Promotion of Natural Regeneration in Highly Continental Scots Pine Forests? – Results 19 Years after Harvest Operations in Mongolia. *Forests*, 10 (2): 141. DOI: 10.3390/f10020141

Gerelbaatar S., Batsaikhan G., Tsogtbaatar J., Battulga P., Baatarbileg N. and Gradel A. (2019b). Assessment of early survival and growth of planted Scots pine (*Pinus sylvestris*) seedlings under extreme continental climate conditions of northern Mongolia. *Journal of Forestry Research*. DOI: 10.1007/s11676-019-00935-8

Government of Mongolia (2018). Mongolia's Forest Reference Level submission to the United Nations Framework Convention on Climate Change; UN-REDD Mongolia National Programme; Ministry of Environment and Tourism: Ulaanbaatar, Mongolia.

Gradel A., Voinkov A.A., Altaev A.A. and Enkhtuya B. (2018). A spatio-structural analysis of intact dark taiga in the southern taiga zone and an interval assessment of a dark conifer mixed forest in the mountain forest steppe zone (Mongolia). *Proceedings of the Kuban State Agrarian University*, 4(73), pp. 36-40. (in Russian).

Gradel, A. (2017). Reaktion von Waldbeständen am Rande der südlichen Taiga auf Klimafaktoren, natürliche und waldbauliche Störungen / Response of forest stands at the edge of the southern taiga to climate factors, natural and silvicultural disturbances. Ph.D. Thesis, Georg-August-Universität Göttingen, Germany; 191 pp.

Gradel A., Haensch C., Batsaikhan G., Batdorj D., Ochirragchaa N. and Günther B. (2017a). Response of white birch (*Betula platyphylla* Sukaczew) to temperature and precipitation in the mountain forest steppe and taiga of northern Mongolia. *Asian Dendrochronology Association (ADA) 2015. Dendrochronologia*, 41, pp.24-33. DOI: <http://dx.doi.org/10.1016/j.dendro.2016.03.005>

Gradel A., Batsaikhan G., Ochirragchaa N., Batdorj D. and Kusbach A. (2017b). Climate-growth relationships and pointer year analysis of a Siberian larch (*Larix sibirica* Ledeb.) chronology in the Mongolian mountain forest steppe compared to white birch (*Betula platyphylla* Sukaczew). *Forest Ecosystems*. 4:22. DOI: 10.1186/s40663-017-0110-2

Gradel A., Ammer C., Batsaikhan G., Ochirragchaa N., Batdorj D. and Wagner S. (2017c). On the Effect of Thinning on Tree Growth and Stand Structure of White Birch (*Betula platyphylla* Sukaczew) and Siberian Larch (*Larix sibirica* Ledeb.) in Mongolia. *Forests*, 8 (4), 105.

Gradel A. and Petrow W. (2014). Forstpolitische Entwicklungen im Transformationsland Mongolei. *AFZ-Der Wald*, 17, pp. 36-39. (in German).

Gradel A. and Mühlenberg M. (2011). Spatial characteristics of near-natural Mongolian forests at the southern edge of the taiga. *Allgemeine Forst- und Jagd-Zeitung*, 182(3/4), pp. 40-52. Available at: <http://www.sauerlaenderverlag.com/index.php?id=1234> [Accessed 10 Dec. 2018].

Graham R.T., McCaffrey S. and Jain T.B. (2004). Science Basis for Changing Forest Structure to Modify Wildfire Behavior and Severity; General Technical Report RMRS-GTR-120; USDA Forest Service Rocky Mountain Research Station: Fort Collins, CO, USA, p. 43.

Grubov I.V. (2001). Key to the vascular plants of Mongolia (with an atlas). Volumes I and II. Science Publishers Inc: Enfield, USA. 817 pp.

Hartwig J. (2007). Die Vermarktung der Taiga. Die Politische Ökologie der Nutzung von Nicht-Holz-Waldprodukten und Bodenschätzen in der Mongolei (Erdkundl. Wissen Bnd. 143). (Zugl.: Dissertation, Fakultät für Forst- und Umweltwissenschaften der Albert-Ludwigs-Universität Freiburg i. Br., 2006), [online], p. 445. Available at: <http://www.steiner-verlag.de/titel/56055.html> [Accessed 18 Feb. 2019]. (in German).

Hartwig M., Schäffer M., Theuring P., Avlyush S., Rode M. and Borchardt D. (2016). Cause-effect-response chains linking source identification of eroded sediments, loss of aquatic ecosystem integrity and management options in a steppe river catchment (Kharaa, Mongolia). *Environmental Earth Sciences*, 75: 855. DOI:10.1007/s12665-015-5092-1

Hartwig M. and Borchardt, D. (2014). Alteration of key hyporheic functions through biological and physical clogging along a nutrient and fine-sediment gradient. *Ecohydrology*, 8(5), pp. 961-975. DOI: 10.1002/eco.1571

Hessl A.E., Anchukaitis K.J., Jelsema C., Cook B., Oyunsanna B., Leland C., Baatarbileg N., Pederson N., Tian H. and Hayles L.A. (2018). Past and future droughts in Mongolia. *Science Advances* 4: e1701832. DOI: 10.1126/sciadv.1701832

Hessl A.E., Brown P., Oyunsanna B., Cockrell Sh., Leland C., Cook E., Baatarbileg N., Pederson N., Saladyga T and Byambagarei S. (2016). Fire and Climate in Mongolia (1532-2010 Common Era): Fire and Climate in Mongolia. *Geophysical Research Letters*. *Geophysical Research Letters*. DOI:10.1002/2016GL069059

Hilbig W. (2000). Forest distribution and retreat in the forest steppe ecotone of Mongolia. *Marburger Geographische Schriften* Vol. 135, pp. 171-187.

Hilbig W. and Mirkin B.M. (1983). Entwicklung und Stand der geobotanischen Forschung über die Mongolische Volksrepublik". In: Institut für Biologie der Martin-Luther-Universität Halle-Wittenberg (eds): Erforschung biologischer Ressourcen der Mongolei (3), Halle/Saale: [online], pp. 33-46. Available at: <http://digitalcommons.unl.edu/biolmongol/157> [Accessed 18 Feb. 2019]. (in German).

Hülsmann L., Geyer T., Schweitzer C., Priess J. and Karthe D. (2015). The effect of subarctic conditions on water resources: initial results and limitations of the SWAT Model applied to the Kharaa River Basin in Northern Mongolia. *Environmental Earth Sciences*, 73(2), pp. 581-592. DOI: 10.1007/s12665-014-3173-1

IWRM-MoMo Consortium (2009). Integrated Water Resource Management for Central Asia: Model Region Mongolia. Case Study in the Kharaa River Basin. Final Project Report, 201 pp.

James T. (2011). Temperature sensitivity and recruitment of Siberian larch (*Larix sibirica*) and Siberian spruce (*Picea obovata*) in northern Mongolia's boreal forest. *Forest Ecology and Management*, 262, pp. 629-636. DOI: 10.1016/j.foreco.2011.04.031

Jamyansuren S., Udval B., Batkhuu N., Bat-Erdene J. and Fischer M. (2018). Result of study on developing forest seed region in Mongolia. Proceedings of the Mongolian Academy of Sciences, [online], 58:01(225), pp. 5-14. Available at: <https://www.mongolijol.info/index.php/PMAS/article/view/968> (in Mongolian with abstract in English) [Accessed 18 Feb. 2019].

Jo H. and Park H. (2017a). Effects of pit plantings on tree growth in semi-arid environments. *Forest Science and Technology* 13(2), pp. 66-70. DOI: 10.1080/21580103.2017.1312559

Jo H. and Park H. (2017b). Effects of windbreak planting on crop productivity for agro-forestry practices in a semi-arid region. *Journal of Forest and Environment Science*, 33(4), pp. 348-354. DOI: 10.7747/JFES.2017.33.4.348

Juříčka D., Novotná J., Houška J., Pařílková J., Hladký J., Pecina V., Cihlářová H, Burnog M., Elbl J., Rosická Z., Brtnický M. and Kynický J. (2018). Large-scale permafrost degradation as a primary factor in *Larix sibirica* forest dieback in the Khentii massif, northern Mongolia. *Journal of Forestry Research*, 29, pp. 1–12. DOI: 10.1007/s11676-018-0866-4

Kamp U. and Pan C.G. (2014). Inventory of glaciers in mongolia, derived from landsat imagery from 1989 to 2011. *Geografiska Annaler: Series A, Physical Geography*, 97(4), pp. 653-669. DOI: 10.1111/geoa.12105

Kansaritoreh E., Schuldt B. and Dulamsuren C. (2018). Hydraulic traits and tree-ring width in *Larix sibirica* Ledeb. as affected by summer drought and forest fragmentation in the Mongolian forest steppe. *Annals of Forest Science*, 75:30. DOI: 10.1007/s13595-018-0701-2

Karthe D., Abdullaev I., Boldgiv B., Borchardt D., Chalov S., Jarsjö J., Li L. and Nittrouer J. (2017a). Water in Central Asia: an integrated assessment for science-based management. *Environmental Earth Sciences*, 76, article 690. DOI:10.1007/s12665-017-6994-x

Karthe D., Chalov S., Moreydo V., Pashkina M., Romanchenko A., Batbayar G., Kalugin A., Westphal K., Malsy M. and Flörke M. (2017b). Assessment and Prediction of Runoff, Water and Sediment Quality in the Selenga River Basin aided by a Web-Based Geoservice. *Water Resources*, 44(3), pp.399-416. DOI:10.1134/S0097807817030113

Karthe D., Heldt S., Houdret A. and Borchardt D. (2015). IWRM in a country under rapid transition: lessons learnt from the Kharaa River Basin, Mongolia. *Environmental Earth Sciences*, 73(2), pp. 681-695. DOI:10.1007/s12665-014-3435-y

Karthe D., Kasimov N., Chalov S., Shinkareva G., Malsy M., Menzel L., Theuring P., Hartwig M., Schweitzer C., Hofmann J., Priess J. and Lychagin M. (2014). Integrating Multi-Scale Data for the Assessment of Water Availability and Quality in the Kharaa - Orkhon - Selenga River System. *Geography, Environment, Sustainability*, 3(7), pp. 65-86. DOI: 10.24057/2071-9388-2014-7-3-40-49

Kasimov N., Karthe D. and Chalov S. (2017). Environmental change in the Selenga River – Lake Baikal Basin. *Regional Environmental Change*, 17(7), pp. 1945-1949. DOI:10.1007/s10113-017-1201-x

Keane R.E. (2018). Managing Wildfire for Whitebark Pine Ecosystem Restoration in western North America. *Forests*, 9(10), 648. Available at: <https://www.mdpi.com/1999-4907/9/10/648> [Accessed 18 Feb. 2019]. DOI: 10.3390/f9100648

Kharuk V.I. and Antamoshkina O.A. (2017). Impact of silkmouth outbreak on taiga wildfires. *Contemporary Problems of Ecology*, 10(5), pp. 556–562. DOI: 10.1134/S1995425517050055

Kharuk V.I., Im S.T., Oskorbin P.A., Petrov I.A. and Ranson K.J. (2013). Siberian pine decline and mortality in southern siberian mountains. *Forest Ecology and Management*, 310, pp. 312–320. DOI: 10.1016/j.foreco.2013.08.042

Khaulenbek A. and Kang H. (2017). Collaboration Project to Combat Desertification in Mongolia. PPP on the occasion of the International Conference on Environment and Technology, 27.10.2017, Ulaanbaatar, Mongolia.

Khishigjargal M., Dulamsuren Ch., Leuschner H.H., Leuschner C. and Hauck M. (2014). Climate effects on inter- and intra-annual larch stemwood anomalies in the Mongolian forest-steppe. *Acta Oecologica* Vol. 55, pp. 113-121. DOI: 10.1016/j.actao.2013.12.003

Khishigjargal M. (2013). Response of tree-ring width and regeneration in conifer forests of Mongolia to climate warming and land use. Ph.D. Thesis, Georg-August-Universität Göttingen, Germany; 131 pp.

Khongor T., Bat Ulzii Ch., Yeseul B., Sanaa E., Altangadas J., Khosbayar B., Mahmood A., VanRijn M. and Vickers B. (2018). Carbon emissions and removals from Mongolian boreal forests. In: P. Vossen D., Karthe B., Gunsmaa S., Enkhjargal S., eds, *GMIT Symposium on Environmental Science and Engineering*, Nalaikh, Mongolia, [online] pp. 28-29. Available at: [http://gmit.edu.mn/site/files/downloads/gmit\\_sese-2018\\_book-of-abstracts.pdf](http://gmit.edu.mn/site/files/downloads/gmit_sese-2018_book-of-abstracts.pdf) [Accessed 10 Mar. 2019].

Kondrashov L., Teusan S., Chuluunbaatar T., Nyamjav B., Enkhtur D. and Goldammer J. (2008). Wildland fire disaster risk assessment for Mongolia. Ulaanbaatar: Gesellschaft für technische Zusammenarbeit (GTZ), Global Forest Monitoring Center, Pacific Forest Forum, 80 pp.

Kopp B., Lange J. and Menzel L. (2017). Effects of wildfire on runoff generating processes in northern Mongolia, *Regional Environmental Change*, 17(7), pp. 1951–1963. DOI:10.1007/s10113-016-0962-y

Krasnoshhekov Yu.N. (2001). Special features and protective role of the forests of Mongolia. *Geography of Natural Resources*. N. 1. P. 135-142 (In Russian with English abstract).

Krutovky K.V., Oreshkova N.V., Putintseva Yu.A., Ibe A.A., Deich K. and Shilkina E.A. (2014). Preliminary results of de novo whole genome sequencing of the Siberian Larch (*Larix sibirica* Ledeb.) and the Siberian Stone Pine (*Pinus sibirica* Du Tour). *Siberian Journal of Forest Science*, 1 (4), pp. 79–83. (in Russian with abstract in English).

Kusbach A., Štěřba T., Smola M., Novák J., Lukeš P. and Strejček R. (2017). Rozvoj lesu a krajiny v Mongolsku / Development of forests and landscape in Mongolia. Report for the seminar of the project of the Czech Forest Management Institute Brandýs nad Labem by deputy of the Czech Development Agency in collaboration with Mongolian Authorities, Domogt Sharyn Gol, September 2017, 113 p. (in Czech).

Lange J., Kopp B.J., Bents M. and Menzel L. (2015). Tracing variability of runoff generation in mountainous permafrost of semi-arid northeastern Mongolia. *Hydrological Processes*, 29(6), pp. 1046–1055. DOI:10.1002/hyp.10218

Lindenmayer D.B. and Noss R.F. (2005). Salvage Logging, Ecosystem Processes, and Biodiversity Conservation. *Conservation Biology*, 20(4), pp. 949–958. DOI: 10.1111/j.1523-1739.2006.00497.x

Liang J., Crowther T.W., Picard N., Wiser S., Zhou M., Alberti G., Schulze E.D., McGuire A.D., Bozzato F., Pretzsch H., de-Miguel S. et al. (2016). Positive biodiversity-productivity relationship predominant in global forests. *Science*, 354: 6309, aaf8957. DOI: 10.1126/science.aaf8957

Locatelli B., Herawati H., Brockhaus M., Idinoba M., and Kanninen M. (2008). Methods and Tools for Assessing the Vulnerability of Forests and People to Climate Change – An Introduction. CIFOR Working Paper, [online], No. 43. 28 pp. Available at: [http://www.cifor.org/publications/pdf\\_files/WPapers/WP43Locatelli.pdf](http://www.cifor.org/publications/pdf_files/WPapers/WP43Locatelli.pdf) [Accessed 14 Nov. 2018]

Lynam T., de Jong W., Sheil D., Kusumanto T. and Evans K. (2007). A review of tools for incorporating community knowledge, preferences and values into decision making into natural resources management. *Ecology and Society*, [online], Volume 12(1): 5. Available at: <http://www.ecologyandsociety.org/vol12/iss1/art5/> [Accessed 14 Nov 2018].

Maasri A. and Gelhaus J. (2011). The new era of the livestock production in Mongolia: Consequences on streams of the Great Lakes Depression. *Science of the Total Environment*, 409, pp. 4841–4846. DOI: 10.1016/j.scitotenv.2011.08.005

Malsy M., Flörke M. and Borchardt D. (2016). What drives the water quality changes in the Selenga Basin: climate change or socio-economic development? *Regional Environmental Change*, 17(7), pp. 1977–1989. DOI: 10.1007/s10113-016-1005-4

Malsy M., Heinen M., aus der Beek T. and Flörke M. (2013). Water resources and socio-economic development in a water scarce region on the example of Mongolia. *GeoÖko*, 34(1–2), pp. 27–49.

Mannig B., Müller M., Starke E., Merckenschlager C., Mao W., Zhi X., Podzun R., Jacob D. and Paeth H. (2013). Dynamical downscaling of climate change in Central Asia. *Global Planetary Change*, 110(A), pp. 26–39. DOI:10.1016/j.gloplacha.2013.05.008

MET (2017a). Mongolia's Third National Communication under the United Nations Framework Convention on Climate Change. Ulaanbaatar, Mongolia: Ministry of Environment and Tourism.

MET (2017b). Report on the state of the environment of Mongolia 2015–2016. Ulaanbaatar, Mongolia: Ministry of Environment and Tourism. 264 pp. (in Mongolian).

MET (2016). Multipurpose National Forest Inventory 2014–2016. Mongolian Ministry of Environment and Tourism. 1st ed. Ulaanbaatar: Ministry of Environment and Tourism.

MET (2014). Report on the state of the environment of Mongolia 2013–2014. Ulaanbaatar, Mongolia: Ministry of Environment and Tourism. 75 pp. (In Mongolian).

MET (2013). Report on the state of the environment of Mongolia 2011–2012. Ulaanbaatar, Mongolia: Ministry of Environment and Tourism. 80 pp. (In Mongolian).

Menzel L., Hofmann J. and Ibisch R. (2011). Untersuchung von Wasser- und Stoffflüssen als Grundlage für ein Integriertes Wasserressourcen – Management im Kharaa-Einzugsgebiet (Mongolei). *Hydrologie und Wasserbewirtschaftung*, 55(2), pp. 88–103. (In German).

Meyer P. and Schmidt M. (2011). Accumulation of dead wood in abandoned beech (*Fagus sylvatica* L.) forests in northwestern Germany. *Forest Ecology and Management*, 261(3), pp. 342-352. DOI: 10.1016/j.foreco.2010.08.037

Minderlein S. and Menzel L. (2015). Evapotranspiration and energy balance dynamics of a semi-arid mountainous steppe and shrubland site in Northern Mongolia. *Environmental Earth Sciences*, 73(2), pp. 593–609. DOI:10.1007/s12665-014-3335-1

MOLF (2015). Mongolian Law on Forests (in Mongolian). [online] Available at: <http://www.legalinfo.mn/law/details/12171> [Accessed 14 Nov. 2018]

Mühlenberg M. (2012). Long-Term Research on Biodiversity in West Khentey, Northern Mongolia. *Erforschung biologischer Ressourcen der Mongolei*. Martin-Luther-Universität Halle, Wittenberg, Halle (Saale), [online] pp. 27-32. Available at: <http://digitalcommons.unl.edu/biolmongol/4> [Accessed 15 Jun 2017]. (In German).

Mühlenberg M., Appelfelder J., Hoffmann H., Ayush E. and Wilson K.J. (2012). Structure of the montane taiga forests of West Khentii, Northern Mongolia. *Journal of Forest Science*, 58(2), pp. 45-56.

Mühlenberg M., Batkhashig T., Dashzeveg Ts., Drößler L., Neusel B. and Tsogtbaatar J. (2006). Mongolia - Lessons from tree planting initiatives. *Mongolia Discussion Papers*, East Asia and Pacific Environment and Social Development Department, World Bank, Washington DC, [online], 38 pp., Available at: <http://documents.worldbank.org/curated/en/143891468059947579/Mongolia-lessons-from-tree-planting-initiatives> [Accessed 31 Mar 2019]

Mühlenberg M., Hondong H., Dulamsuren Ch. and Gadow K.v. (2004). Large-scale biodiversity research in the southern Taiga, Northern Mongolia. In: R.C. Szaro, C.E. Peterson, K.v. Gadow, N. Kraeuchi, ed., *Creating a Legacy for Sustainable science-based Forest Management: lessons learned from field experiments*. *Forest Snow and Landscape Research*. Swiss Federal Research Institute WSL, 78 (1–2), pp. 93–118.

Olivar J., Bogino S., Rathgeber C., Bonnesoeur V. and Bravo F. (2014). Thinning has a positive effect on growth dynamics and growth-climate relationships in Aleppo pine (*Pinus halepensis* L.) trees of different crown classes. *Annals of Forest Science*, 71, pp. 395-404. DOI: 10.1007/s13595-013-0348-y

Onderka M. and Melicherck I. (2010). Fire-prone areas delineated from a combination of the Nestorov Fire-Risk Rating Index with multispectral satellite data. *Applied Geomatics*, 2, pp. 1-7. DOI 10.1007/s12518-009-0014-0.

Otoda T., Sakamoto K., Hirobe M., Undarmaa J. and Yoshikawa K. (2013). Influences of anthropogenic disturbances on the dynamics of white birch (*Betula platyphylla*) forests at the southern boundary of the Mongolian forest-steppe. *Journal of Forest Research.*, 18, pp. 82-92. DOI: 10.1007/s10310-011-0324-z

Oyunsanaa B. (2011). Fire and stand dynamics in different types of the West Khentey Mountains, Mongolia. *Dissertation (Ph.D. Thesis)*, Georg-August-Universität Göttingen, Germany; p. 119

Oyuntuya Sh., Dorj B., Shurentsetseg B. and Bayarjargal E. (2015). Agrometeorological information for the adaptation to climate change, in: Badmaev, N.B., Khutakova, C.B. (Eds.): Soils of Steppe and Forest Steppe Ecosystems of Inner Asia and Problems of Their Sustainable Utilization: International Scientific Conference. Buryat State Academy of Agriculture named after V.R. Philipov, Ulan-Ude, pp. 135-140.

Park H., Fan P., John R. and Chen J. (2017). Urbanization on the Mongolian Plateau after economic reform: Changes and causes. *Applied Geography* Vol. 86, pp. 118-127. DOI: 10.1016/j.apgeog.2017.06.026

Park G.E., Lee D.K., Kim, K.W., Batkhuu N.-O., Tsogtbaatar J., Zhu J.-J., Jin, Y., Park P.S., Hyun, J.O. and Kim H.S. (2016). Morphological Characteristics and Water-Use Efficiency of Siberian Elm Trees (*Ulmus pumila* L.) within Arid Regions of Northeast Asia. *Forests*, 7 (11), 280. Available at: <https://www.mdpi.com/1999-4907/7/11/280> [Accessed 10 Jun. 2019] DOI: 10.3390/f7110280

Pausas J.G. (2014). Bark thickness and fire regime. *Functional Ecology*, 29 (3), pp. 315-327. DOI: 10.1111/13652435.12372

Pellegrini A.F., Anderegg W.R.L., Paine C.E.T., Hoffmann W.A., Kartzinel T., Rabin S.S., Sheil D., Franco A.C. and Pacala S.W. (2017). Convergence of bark investment according to fire and climate structures ecosystem vulnerability to future change. *Ecology Letters*, 20 (3), pp. 307-316. DOI: 10.1111/ele.12725

Pickett S.T.A. and White P.S. (1985). The ecology of natural disturbance and patch dynamics. Academic Press, Orlando, FL, USA.: 472 pp.

Potapov P., Yaroshenko A., Turubanova S., Dubinin M., Laestadius L., Thies C., Aksenov D., Egorov A., Yesipova Y., Glushkov I., Karpachevskiy M., Kostikova A., Manisha A., Tsybikova E. and Zhuravleva I. (2008). Mapping the world's intact forest landscapes by remote sensing. *Ecology and Society*, 13(2), p. 51. Available at: <http://www.ecologyandsociety.org/vol13/iss2/art51/> [Accessed 10 Mar. 2019].

Potapov P., Hansen M.C., Laestadius L., Turubanova S., Yaroshenko A., Thies C., Smith W., Zhuravleva I., Komarova A., Minnemeyer S. and Espipova E. (2017). The last frontiers of wilderness: Tracking loss of intact forest landscapes from 2000 to 2013. *Science Advances*, 3(1): e1600821. DOI: 10.1126/sciadv.1600821

Priess J., Schweitzer C., Wimmer F., Batkhisig O. and Mimler M. (2011). The consequences of land-use change and water demands in Central Mongolia. *Land Use Policy*, 28(1), pp. 4-10. DOI:10.1016/j.landusepol.2010.03.002

Puettmann K.J. and Ammer C. (2007). Trends in North American and European regeneration research under the ecosystem management paradigm. *European Journal of Forest Research*, 126, pp. 1-9. DOI: 10.1007/s10342-005-0089-z

Putintseva Yu.A., Oreshkova N.V., Bondar E.I., Sharov V.V., Kuzmin D.A., Makalov S.V. and Krutovky K.V. (2018). Genomics for practical forestry: development of genome-wide markers for timber origin identification and other applications. In: B. Degen, K.V. Krutovsky, M. Liesebach (eds). German-Russian Conference on Forest Genetics - Proceedings – Ahrensburg, 2017 Nov. 21-23. Thünen Report 62: 101-106.

Rao M.P., Davi N.K., D'Arrigo R.D., Skees J., Baatarbileg N., Leland C., Lyon B., Wang S.Y. and Oyunsanaa B. (2015). Dzuds, droughts, and livestock mortality in Mongolia. *Environmental Research Letters*, 10(7), 074012. DOI: 10.1088/1748-9326/10/7/074012

Rosell J.A., Olson M.E., Anfodillo T. and Martinez-Mendez N. (2017). Exploring the bark thickness-stem diameter relationship: clues from lianas, successive cambia, monocots and gymnosperms. *New Phytologist*, 215(2), pp. 569-581. DOI: /10.1111/nph.14628

Sagwal S.S. (1991). *Dictionary of Forest Fires*. Ashish Publishing House, New Delhi, 64 pp.

Saladyga T., Hessel A., Baatarbileg N. and Pederson N. (2013). Privatization, Drought, and Fire Exclusion in the Tuul River Watershed, Mongolia. *Ecosystems*, 16, pp. 1139-1151. DOI: 10.1007/s10021-013-9673-0

Sato T., Kimura F. and Kitoh A. (2007). Projection of global warming onto regional precipitation over Mongolia using a regional climate model. *Journal of Hydrology*, 333, pp.144-154.

Savin E.N., Miljutin L.I., Krasnoshhekov Ju.N., Korotkov I.A., Suncov A.V., Dugarzhav Ch., Cogoo Z., Dorzhsuren Ch., Zhamjansurjen S and Gombosuren N. (1988). *Forests of the Mongolian People's Republic (Larch forests of eastern Khentii)*. Nauka, Moscow, 176 pp. (in Russian).

Savin E.N., Korotkov I.A., Krasnoshhekov Yu.N., Ogorodnikov A.V., Janovskij V.M., Dugarzhav Ch., Dorzhsuren Ch. and Dashzeveg C. (1983). *Forests of the Mongolian People's Republic (Larch forests of Central Khangai)*. Nauka, Siberian branch, Novosibirsk, 150 pp. (in Russian).

Schmidt-Corsitto K. (2014). Case Study on Climate Change Adaptation measures in the North Mongolian forest conducted by the GIZ "Biodiversity and adaptation of key forest ecosystem to climate change" program. In: Natsagdorj L. (2014) *Climate change adaptation strategy and measures*. Published in: Mongolia second assessment report on Climate Change – MARCC 2014. Ulaanbaatar, pp.193-197.

Semerikov V.I., Semerikova S.A., Poleshaeva M.A., Kosintsev P.A. and Lascoux M. (2013). Southern montane populations did not contribute to the recolonization of the West Siberian Plain by Siberian larch (*Larix siberia*): a range-wide analysis of cytoplasmic markers. *Molecular Ecology*, 22, pp. 4958-4971. DOI: 10.1111/mec.12433

Sepp S. and Schüler B. (2016). Value chain analyses for the NTFPs: Pine Nuts, Charcoal, Fuelwood. *ECO Consult Sepp und Busacker*, 42 pp.

Sharkhuu A., Sharkhuu N., Etzelmüller B., Heggem E.S.F., Nelson F.E., Shiklomanov N.I., Goulden C.E. and Brown J. (2007). Permafrost monitoring in the Hovsgol mountain region, Mongolia. *Journal of Geophysical Research*, 102(F12), manuscript F02S06. DOI: 10.1029/2006JF000543

Slemnev, N.N., Sheremetiev, S.N., Gamalei Ju.V., Stepanova, A.V., Chebotareva K.E., Tsogt Z., Tsoozh, Sh. and Yarmishko V.T. (2012). Radial increment variability in Mongolian trees and shrubs under climate dynamics. *Journal of Botany*, 97(7), pp. 852-871. (in Russian).

Spellerberg I.F. (1992). *Evaluation and assessment for conservation: Ecological guidelines for determining priorities for nature conservation*. London / Glasgow / New York / Tokyo / Melbourne / Madras, Chapman and Hall, 260 pp.

Syromyatina M.V., Kurochkin Y.N., Bliakharskii D.P. and Chistyakov K.V. (2015). Current dynamics of glaciers in the Tavan Bogd Mountains (Northwest Mongolia). *Environmental Earth Sciences*, 74(3), pp. 1905-1914. DOI: 10.1007/s12665-015-4606-1

Tanskanen H., Venalainen A., (2008). The relationship between fire activity and fire weather indices at different stages of the growing season in Finland. *Boreal Environment Research*, Vol. 13, pp. 285-302.

Taube M. (2005). *Die Geheime Geschichte der Mongolen. Herkunft, Leben und Aufstieg Dschingis Khans. Aus dem mongolischen übersetzt und kommentiert.* Beck, München, 325 pp. (in German).

Tchebakova N.M., Parfenova E.I. and Soja A.J. (2011). Climate change and climate-induced hot spots in forest shifts in central Siberia from observed data. *Regional Environmental Change*, 11(4), pp. 817-827. DOI: 10.1007/s10113-011-0210-4

Teusan S. (2018). *Analyse der Waldentwicklung in der nördlichen Mongolei seit dem politischen Umbruch im Jahre 1991 unter besonderer Berücksichtigung feuerökologischer Aspekte.* Ph.D. Thesis, FU Berlin, Germany, 171 pp. (in German).

Theuring P., Collins A.L. and Rode M. (2015). Source identification of fine-grained suspended sediment in the Kharaa River basin, northern Mongolia. *Science of the Total Environment*, 526, pp. 77-87. DOI:10.1016/j.scitotenv.2015.03.134

Tikhonova I.V., Korets M.A. and Mukhortova L. (2014). Potential Soil and Climatic Ranges of Pine and Larch in Central Siberia. *Contemporary Problems of Ecology*, 7(7), pp. 752-758. DOI:10.1134/S1995425514070130

Törnqvist R., Jarsjö J., Pietron J., Bring A., Rogberg P., Asokan S.M. and Destouni G. (2014). Evolution of the hydro-climate system in the Lake Baikal basin. *Journal of Hydrology*, 519, pp. 1953–1962. DOI:10.1016/j.jhydrol.2014.09.074

Tsogt Z., Danilin I.M., Tsogtbaatar Zh. and Khongor Ts. (2018). Formation of coniferous forests. Forest inventory structure and productivity. Chapter VI In: *Forests of Mongolia. Vol. 5. Forests of the Eastern Khubsugul, Biological Diversity, Ecosystems, Dynamics, Restoration.* Ulaanbaatar, Mongolia. pp. 158-171. (In Mongolian with Russian summary and contents).

Tsogtbaatar J. (2004). Deforestation and reforestation needs in Mongolia. *Forest Ecology and Management*, 201(1), pp. 57–63. DOI: 10.1016/j.foreco.2004.06.011

Tsogtbaatar J. (2008). *Forest Policy Development in Mongolia.* IUFRO Task Force Science/Policy Interface. [online], Available at: <http://iufro-archive.boku.ac.at/iufro/taskforce/tfscipol/chennai-papers/ftsogtbaatar.pdf> [Accessed 22 Jun. 2019].

Tuvshintogtokh I. and Ariungerel D. (2012). Degradation of Mongolian Grassland Vegetation Under Overgrazing by Livestock and Its Recovery by Protection from Livestock Grazing. In: N. Yamamura, Fujita, N., A. Maekawa, ed., *The Mongolian Ecosystem Network. Environmental Issues Under Climate and Social Changes.* Tokyo: Springer Japan. DOI: 10.1007/978-4-431-54052-6\_10

UNFCCC (2019). REDD + web platform of the UNFCCC for reducing emissions from deforestation and forest degradation in developing countries. [online] Available at: <https://redd.unfccc.int/fact-sheets/forest-reference-emission-levels.html> [Accessed 6 Jun. 2019].

Unger-Sayesteh K., Vorogushyn S., Farinotti D., Gafurov A., Duethmann D., Mandychev A. and Merz B. (2013). What do we know about past changes in the water cycle of Central Asian headwaters? A review. *Global Planetary Change*, 110(A), pp. 4–25. DOI:10.1016/j.gloplacha.2013.02.004

UNREDD (2013) Forest Sector financing flows and economic values in Mongolia. UN REDD Programme, [online], 60 pp. Available at: <http://www.mn.undp.org/content/dam/mongolia/Publications/Environment/UNREDD/Mongolia%20Forest%20Sector%20Valuation%20Report%20Final.pdf> [Accessed 10 Jun. 2019].

UNREDD (2017) Preliminary Assessment of the Drivers of Forest Change in Mongolia: A Discussion Paper for Supporting Development of Mongolia's National REDD+ Strategy. UN-REDD Mongolia National Programme, Ministry of Environment and Tourism, Ulaanbaatar, Mongolia. 127 pp.

Vandandorj S., Munkhjargak E., Boldgiv B. and Gantsetseg B. (2017). Changes in event number and duration of rain types over Mongolia from 1981 to 2014. *Environmental Earth Sciences*, 76(2), manuscript 70. DOI:10.1007/s12665-016-6380-0

Verhoeven D., de Boer W.F., Henkens R.J.H.G. and Sass-Klaassen U.G.W. (2018). Water availability as driver of birch mortality in Hustai National Park, Mongolia. *Dendrochronologia*, 49, pp.127-133. DOI: 10.1016/j.dendro.2018.04.001

Viviroli D. and Weingartner R. (2004). The hydrological significance of mountains: from regional to global scale. *Hydrology and Earth Systems Science*, 8(6), pp. 1016–1029. DOI:10.5194/hess-8-1017-2004

Wimmer F, Schlaffer S, aus der Beek T and Menzel L (2009). Distributed modelling of climate change impacts on snow sublimation in northern Mongolia. *Advances in Geosciences* 21:117-124. DOI:10.5194/adgeo-21-117-2009

Ykhanbai H. (2010). Mongolian forestry outlook study. Asia-Pacific forestry sector outlook study II. Working paper series. No. APFSOS II/ WP/ 2009/ 21 FAO. Bangkok, Kingdom of Thailand, 49 pp.

Zhukov A.B., Savin E.N., Korotkov I.A. and Ogorodnikov A.B. (1978). Forests of the Mongolian People's Republic: Geography and Typology. Biological resources and environmental conditions of the Mongolian People's Republic, Vol. 11, p. 127. (in Russian).

Received on July 7<sup>th</sup>, 2019

Accepted on August 8<sup>th</sup>, 2019

**Dan Altrell\***

<sup>1</sup>Food and Agriculture Organization of the United Nations, Rome, Italy. Formerly Deutsche Gesellschaft für Internationale Zusammenarbeit (GIZ) GmbH, Mongolia\*

**Corresponding author:** Altrell@sajt.se

# MULTIPURPOSE NATIONAL FOREST INVENTORY IN MONGOLIA, 2014-2017 -A TOOL TO SUPPORT SUSTAINABLE FOREST MANAGEMENT

**ABSTRACT.** Mongolia's first Multipurpose National Forest Inventory, 2014-2017, was implemented by the Forest Research and Development Centre, in collaboration with international expertise and the country's main forestry institutions, universities and research organisations.

The long-term objective of the multipurpose NFI is to promote sustainable management of forestry resources in Mongolia, to enhance their social, economic and environmental functions.

The NFI findings show that there are 11.3 million hectares of Boreal Forest in Mongolia. 9.5 million hectares are Stocked Boreal Forest Area, of which 69 percent is located outside of protected areas, 4 percent are designated for green-wood utilisation through forest enterprise concessions, and another 16 percent designated for fallen dead-wood collection through forest user group concessions. The non-protected stocked forests (i.e. production forest) have an average growing stock volume of 115 m<sup>3</sup> per hectare, compared with an optimal growing stock volume of 237 m<sup>3</sup> per hectare, and there is an additional 46.5 m<sup>3</sup> of dead wood per hectare. The growing stock age distribution shows that 24 m<sup>3</sup> per hectare are over 200 years (i.e. economically over-aged). The main tree species in stocked forest are *Larix sibirica* (81%), *Pinus sibirica* (7%), *Betula platyphylla* (6%) and *Pinus sylvestris* (5%), of which all, except for *P. sibirica*, are classified as legally harvestable tree species. Wild fire is the current main environmental factor decreasing the forest tree biomass.

The NFI helped identifying priority areas for the forestry sector, and to guide the implementation of sustainable forest management at the local level. The main forest management challenges of Mongolia's boreal forest will be to address that they are a) under-stocked (less than 50% of production potential), b) over-aged (31% of growing stock volume in stocked production forest is above optimal production age), and c) under-utilised (4% of forest area designated to green-wood utilisation).

**KEY WORDS:** NFI; Forest policy; Forest management

**CITATION:** Dan Altrell (2019) Multipurpose National Forest Inventory in Mongolia, 2014-2017 -A tool to support sustainable forest management. *Geography, Environment, Sustainability*, Vol.12, No 3, p. 167-183

DOI-10.24057/2071-9388-2019-36

## INTRODUCTION

Mongolia's first systematic sample-based national forest inventory (NFI) was conducted in 2014-2017 under the lead of the Ministry of Environment and Tourism (MET). The NFI was implemented by the Forest Research and Development Centre, in collaboration with international expertise and the country's main forestry institutions, universities and research organisations. The inventory covered all of Mongolia's boreal forests and it assessed the forests' multiple functions and also the threats the forest currently is facing. The multipurpose NFI was specifically requested to generate information compatible with the national reporting to UNFCCC and to address the information needs for coherent forest policy development to support sustainable forest management in Mongolia. The background to MET's request was the lack of national-wide holistic forestry information to respond to the many new reporting requirements, and the urgent need to generate necessary baseline information on the status of Mongolia's boreal forest, and to evaluate the challenges ahead in a changing climate (MET 2019).

Existing national-level information on the forestry resources has been derived through compilations of provincial forest assessments, which were based on remote sensing data in combination with ocular inspections (i.e. not objective nor measurement-based) (MET 2019). Other publications on national-level status of ecosystems and their degradation, like the Atlas "Ecosystems of Mongolia" (Vostokova et al. 2005) have not been derived through systematic field data collection, but rather through case study areas, so an objective and systematic national level boreal forest inventory would be the first study presenting country-level representative and accurate information on the status of the boreal forest resources and the actual environmental challenges they are facing.

Mongolia, as many other countries in the region, had previously not implemented

national-level forest inventories based on objective measurements, so new methodologies had to be developed, experts had to be trained, and an inventory organisation had to be mobilised. The German government and the UN-REDD Programme backed MET in mobilising funding and a large pool of both international and national experts, which provided the needed expertise and capacity development to support the design and the implementation of the forest inventory.

Mongolia counts a number of forestry-related universities and research institutes, which together organised to design the NFI, with input from international expertise. The Forest Research and Development Centre (FRDC), under MET, was identified to take the lead and to coordinate the NFI, and in collaboration with international expertise and Mongolia's main forestry institutions, universities, research organisations and private forest inventory companies, the NFI was implemented.

The objective of this article is to present a summary of the forest inventory and derive conclusions from it for the development of sustainable forestry in the country.

## MATERIALS AND METHODS

To address the need to generate information on the multiple functions of forest, also multiple data sources were needed (Fig. 1). A sample-based field inventory and a series of remote sensing surveys form the basis for an accurate and cost-effective multi-purpose forest inventory, and the first cornerstone in Mongolia's forest monitoring system.

### Forest Characteristics Assessment

In order to design the field inventory, a "wall-to-wall" remote sensing survey, based on Landsat 8 ETM data from 2013, generated a "Forest Mask 2013" illustrating the geographic extent of Mongolia's boreal forests (Fig. 2), e.g. "stocked"

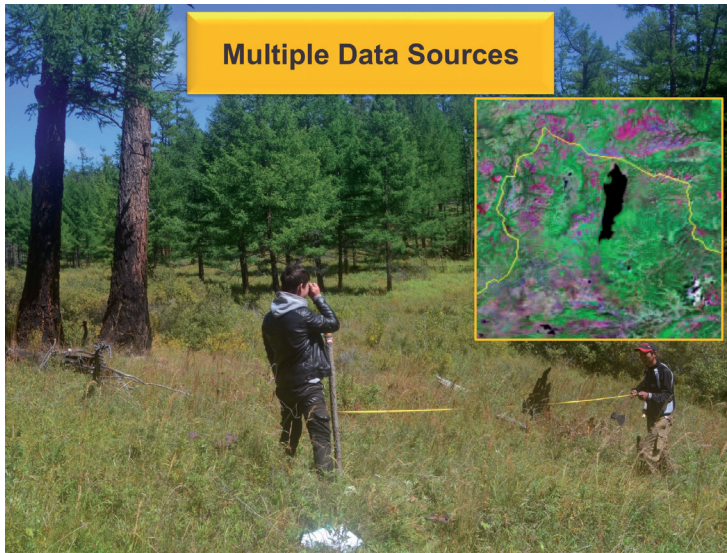


**Fig. 1. Both field inventory and remote sensing surveys were conducted to collect the data for Mongolia’s multi-purpose national forest inventory (Altrel unpublished)**

boreal forest, meaning forest area which currently has a tree canopy cover of at least 10 percent. A team of national and international experts defined the main forest inventory regions (Fig. 3), based on existing national vegetation zones and knowledge on forest typologies.

These forest inventory regions defined the geographic extent for pre-stratification of the field sample, where the Altai region has the densest inventory grid, 1.5 km x 1.5 km, followed by Khuvsgul, Khangai and Khentii regions, 4 km x 4 km, and the remaining boreal forest area 9 km x 9 km.

All of the sample grids are systematic with distribution of sample units (field clusters) North-South and West-East respectively, and totally 4367 field clusters were established throughout Mongolia’s boreal forest, both in stocked forests (Erdenejav 2014) and in temporarily un-stocked forest areas (UN-REDD 2017) (Figure 4).

Each sampling unit for the field data collection represents a cluster of three field plots, where the centre of the first plot is placed on the coordinates of the sampling unit and the centres of the second and third plots are located 100 meters North of the centre of the first

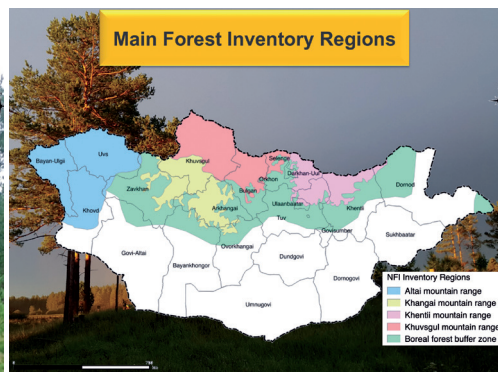


**Fig. 2 (left). Forest Mask 2013, which defined the geographic extent of Mongolia’s stocked boreal forest in 2013 (Altrel unpublished)**

**Fig. 3 (right). Geographic extent of Mongolia’s five boreal forest inventory regions (Altrel unpublished)**

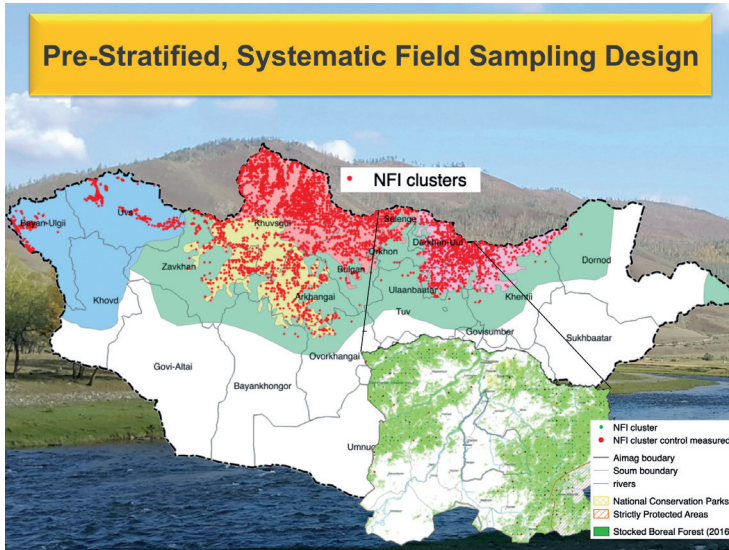


**Fig. 4. Pre-stratified field samples distributed in boreal forests, according to the five forest inventory regions (Altrell unpublished)**

plot, and 50 meters to the West and to the East respectively (Fig. 5). Each of the three field plots is represented by a set of nested circular plots, where the 20-, 12- and 6-meters radius plots have the same centre, and the centres of the two 2-meters radius plots are placed respectively six meters to the West and to the East of the concentric plots' centre (Fig. 6).

The measured and observed plot parameters are described by plot size (plot radius) and Plot Element in Table 1

Internationally standardised methods for data collection (i.e. FAO 2012) were adapted to the Mongolian context and defined in a manual for field data collection, so that the methods were equally applied throughout the country by the inventory teams.

Data from the field inventory were aggregated from tree-level to plot-/cluster-level, and ratio estimation (estimator/area) (McRoberts et al. 2014) was applied to calculate the inventory results at stratum level (Fig. 7), i.e. per-hectare values, and the Variance of the ratio estimates were calculated according Equation 1 (see all related NFI data models in Altrell 2015 and MET 2019).

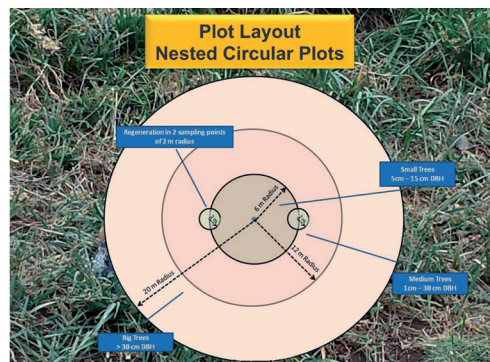
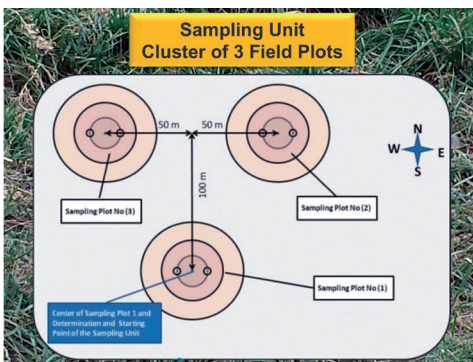


**Fig. 5 (left). Design of field-sampling unit composed by three field plots (MET 2019) Fig. 6 (right). Field plot composed by three concentric circular plots with radius 6 m, 12 m and 20 m respectively, plus two 2-m radius plots located 6 metres to the West and to the East of the centre of the concentric plots (MET 2019)**

**Table 1. Measurement and Observation of Plot Elements by plot size (plot radius) (MET 2019 and Altrell unpublished)**

Plot radius	Plot Elements	Measurements and Observations
20 meter	Trees (standing) with Dbh $\geq$ 30 cm	Dbh, Height, Species, Health, Causative agent, Stem quality, Age class, Position in plot
	Stand Structure	Canopy layers
	Forest Fire	Occurrence
	Grazing	Severity
	Erosion Protection status	Severity
	Slope	Inclination, Aspect
	Landscape	Relief
	Area Protection	Protection status, Protection implementation, Protection recommendations
12 meter	Trees (standing) with Dbh of 15 – 29.9 cm	Dbh, Height, Species, Health, Causative agent, Stem quality, Age class, Position in plot
6 meter	Trees (standing) with Dbh 6 – 14.9 cm	Dbh, Height, Species, Health, Causative agent, Stem quality, Age class, Position in plot
	Red-listed species	Species
	Plant species	Species count
	Ground Vegetation	Coverage by: a) Lichen, b) Mosses, c) Bracken/Fern, d) Herbs, e) Grasses, f) Large lianas, g) Sub-shrubs, h) Shrubs <0.5 m, i) Shrubs 0.5-2 m, j) Shrubs >2 m, k) Trees <0.5 m, l) Trees 0.5-2 m, m) Trees 2-4 m
	Dead Wood (fallen and stumps)	Mid-diameter, Length, Decomposition degree
	Soil	Thickness of Horizon A, B, C, Soil type, Soil texture
	Litter	Layer thickness, Moisture class
2 meter	Tree Regeneration (small) 10 – 50 cm	Stem count by species
	Tree Regeneration (medium) 50 – 150 cm	Stem count by species
	Tree Regeneration (high) >150 cm and Dbh< 6 cm	Stem count by species

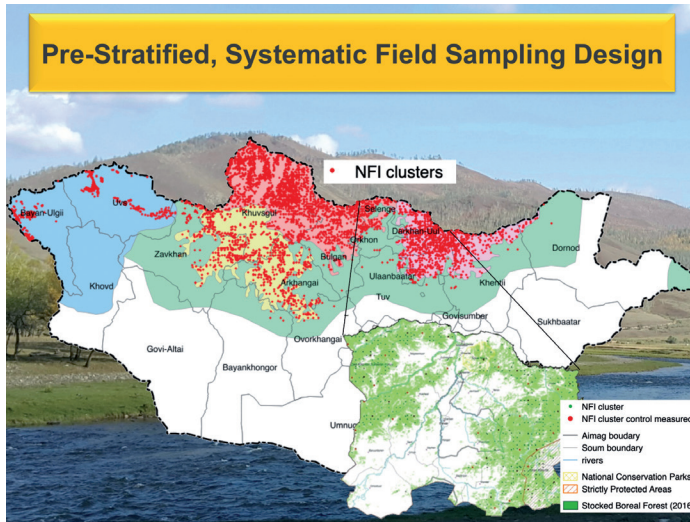


Fig. 7. Illustration of a circular plot with field data, which were aggregated from tree-level to plot-/cluster-level, applying ratio estimation (estimator/area) to calculate the inventory results (Altrell unpublished)

Equation 1: Variance of Ratio estimate (VR).

$$V_R = n * \frac{\sum_1^n (x_i)^2 + \left(\frac{\sum_1^n x_i}{\sum_1^n y_i}\right)^2 * \sum_1^n (y_i)^2 - 2 \frac{\sum_1^n x_i}{\sum_1^n y_i} \sum_1^n x_i y_i}{(\sum_1^n y_i)^2 * (n-1)}$$

Where x is the measured variable (ex. tree volume) in the sample and y is the auxiliary variable (i.e. forest area) in the sample (i.e. plot area with forest). i indicates the individual measurement value of the variable of a total number of n measurements (=sample size). (ex. to estimate tree volume in forest area, n is the number of sample units with forest area).

Totals were extrapolated by multiplying the per-hectare values with the corresponding forest area estimates defined through the remote sensing sampling survey (Figure 8) When available, national data models were applied to calculate the statistical estimates (Equation 2 and 3).

Equation 2 and 3: Examples of national data models for estimation of Growing Stock Volume Density and Biomass Stock Density.

**GS Vol =  $\Sigma(a * D_{bh}^b * H^c) / \Sigma(\text{plot area})$**  - (Equation 2: Growing Stock Volume density [Dorjsuren 2017])

**BS =  $\Sigma(a * D_{bh}^b * H^c) / \Sigma(\text{plot area})$**  - (Equation 3: Biomass Stock density [Dorjsuren 2017])

Where:

- GS<sub>Vol</sub> = Growing Stock Volume density
- D<sub>bh</sub> = Tree Breast-Height Diameter
- H = Tree Total Height
- BS = Biomass Stock density
- A<sub>Plot</sub> =Plot Area
- a = Coefficient of the exponential function D<sub>bh</sub><sup>b</sup> \* H<sup>c</sup>
- b = Exponent of D<sub>bh</sub>
- c = Exponent of H

**Forest Area Assessment**

To estimate the size of the area covered by stocked boreal forests in Mongolia in 2014 a sample-based remote sensing survey was conducted in the northern part of Mongolia, applying the Collect Earth Tool, from the Open Foris Toolbox (FAO 2014), and assessing the remote sensing data available through Google Earth (Erdenejav 2014a). The sampling design was systematic and, applying an equal ground distance between the remote sensing plots within each UTM zone, ranging from 10 km x 10 km to 29 km x 29 km, north-south and west-east respectively, totalling 1,623 sampling plots (Fig. 8). Each sampling plot represented a reference square area of one hectare, in

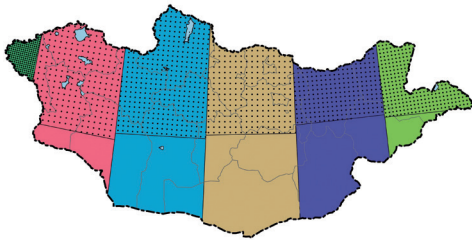


**Fig. 8 (left). Sampling design of remote sensing survey to make a preliminary assessment of the size of the stocked boreal forest area in 2014 (Altrell unpublished)**

**Fig. 9 (right). Remote sensing plot layout with 25 indicative dots, systematically distributed within a reference area of a 1 ha square (Altrell unpublished)**

which 25 equally distributed dots (Fig. 9) indicated where presence of tree canopy cover should be assessed. Applying the threshold of ten percent canopy cover for forest in Mongolia led to defining all plots with at least 3 dots on tree canopy as forest plots.

In order to improve the forest area estimate, and to also include temporarily un- or low-stocked forest area, saxaul forest and other land uses, a nation-wide remote sensing survey was completed in 2017. Also this survey applied the Collect Earth Tool and was sample-based by UTM zone, but applying denser sampling grids (totally 123,577 remote sensing plots) and with the same ground distance 9 km x 9 km between the plots through all UTM zones (Fig. 10). The sampling design was

also pre-stratified with 16 times higher sampling intensity in the boreal forest zone (2,250 m x 2,250 m). Each sampling plot is represented by a reference square area of one hectare, in which there are 49 equally distributed dots (Fig. 11) indicating where the presence of tree canopy cover should be assessed. Applying the threshold of ten percent canopy cover for forest in Mongolia led to defining all plots with at least 5 tree canopy cover dots as forest plots.

### Forest Cover Mapping

A map illustrating the geographic distribution of the boreal forest cover in 2015 was prepared by applying a wall-to-wall remote sensing survey, employing Landsat ETM remote sensing data from

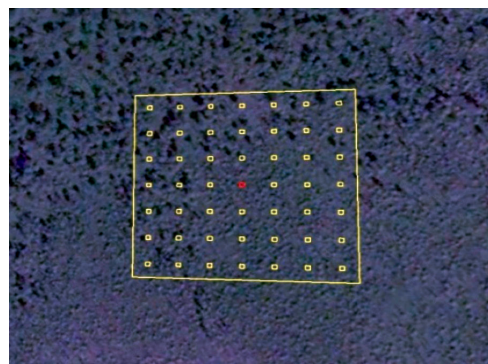
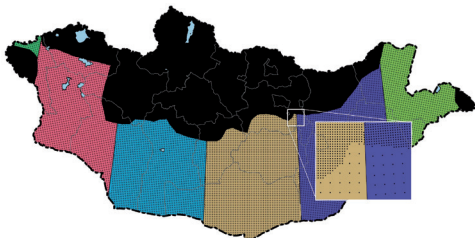


**Fig. 10 (left). Sampling design of nation-wide forest/land use area assessment in 2016 (Altrell unpublished)**

**Fig. 11 (right). Remote sensing plot layout with 49 indicative dots, systematically distributed within a reference area of a 1 ha square (Altrell unpublished)**

2015, and applying machine-learning techniques used by R-studio (RStudio 2015, R 2015) and QGIS (QGIS 2015), where the forest interpreter defined “training areas” of forests that were clearly visible in Google Earth data, to train the R-script “randomForest” (Breiman 2001) in recognising forest areas in the Landsat ETM data. The automatic interpretation was continuously evaluated and the training areas were improved until a satisfactory product was produced, and validated using 1680 reference points chosen in Google Earth data.

### Quality Assurance and Capacity Development

In order to address the quality of the NFI information and to limit the errors of the estimates, the NFI was built on a robust systematic design, national experts were trained to carry out their related NFI duties (field data collection, remote sensing survey, quality assurance, data analysis and reporting) quality controls were carried out for each phase of the NFI, and accurate equipment was used. Experts from private field inventory companies formed field inventory teams and were equipped with high-accuracy measurement equipment and thoroughly trained to conduct the field data collection. Experts at Mongolia’s universities, research institutes and governmental institutions were trained and equipped to conduct the remote sensing surveys and also formed dedicated control teams to carry out re-measurements at five percent of the NFI field clusters. They were also trained to undertake the NFI data analysis, including the scrutinising of collected data to assess the quality of the NFI information. Both national and international experts were taught the capacity developments.

The NFI design errors were limited by applying systematic sampling approaches for both remote sensing surveys and field surveys, and by applying conventional methods that are well tested. The measurement errors (field and remote sensing) were limited by applying a) the high-accuracy measurement equipment

and user-friendly computer applications, b) defining all the measurement and observation procedures in manuals for data collection, and c) thoroughly training all involved experts in conducting the data collection. In addition the field measurement errors were somehow estimated through re-measurements by control teams. Sampling errors were calculated for all per-hectare estimates, even though not all of them have been officially published through the NFI reports.

### Results

The field inventory and the corresponding remote sensing surveys started in 2014, when also the major part of the field data was collected, and concluded in 2017 with the inventory of temporarily un-stocked forest areas. All data, both from field inventory and remote sensing surveys, were compiled in NFI databases and processed to generate the requested information for both national and international reporting.

All reporting from the Multipurpose NFI was done in a transparent manner and the results are published online, at the Forest Research and Development Centre’s web portal <http://www.forest-atlas.mn> (FRDC 2019).

### Forest Area estimates and mapping

Among the main NFI findings are the size of the boreal forest area, which was determined to 11,3 million hectares (UN-REDD 2018), of which 9.5 million hectares correspond to stocked boreal forest (i.e. tree canopy cover  $\geq 40\%$ ) and 1.8 million hectares correspond to un-stocked, or low-stocked, boreal forest (MET 2019) distributed through the northern parts of Mongolia (Fig. 12).

Khuvsgul aimag was the most forested area, with more than 3 million hectares stocked boreal forest, followed by Bulgan and Selenge aimags, with 1.4 million and 1.5 million hectares respectively. Arkhangai, Tuv and Khentii aimags had between 0.7 and 0.8 million hectares of boreal forest, and

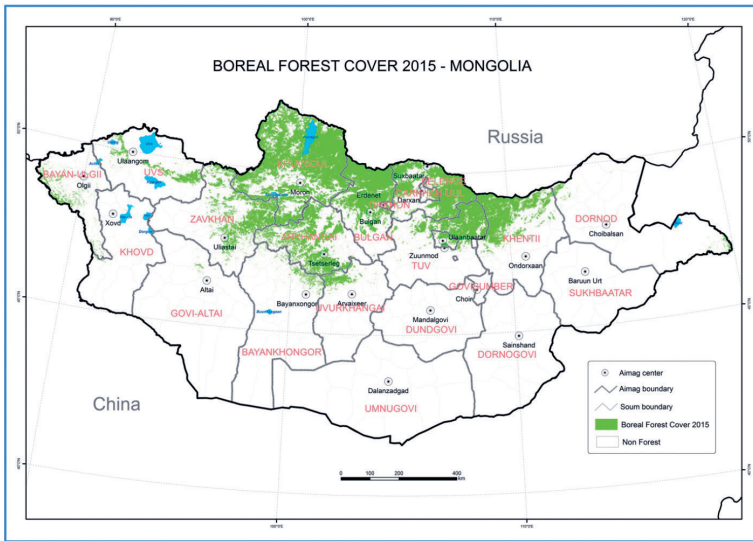


**Fig. 12. Boreal Forest Cover Map 2015 (MET 2019)**

Zavkhan aimag has 0.5 million hectares of stocked boreal forest. In total boreal forest have been registered in 17 country's Aimags. 2.9 million hectares of the boreal forest area were located inside state protected area, which corresponds to 31 percent of the total boreal forest area. 2.0 million hectares (21%) of the forest were designated for production purposes (Fig. 13), of which 1.6 million hectares were managed through agreements with forest user groups (915 officially registered in 2016), and 0.4 million hectares were managed through private enterprise concessions (76 concessions in 2016). The remaining boreal forest area, 4.3 million hectares, was officially not protected and has not yet been designated for any exploitation in 2016.

The area distribution of the different boreal forest (stocked) types is shown in Fig. 14. Siberian Larch (*Larix sibirica*) is the most dominant forest type with 5.7 million hectares, or 62.4 percent of the total stocked boreal forest area, followed by Mixed Coniferous and Mixed Forests with 9.9% and 9.7% respectively.

**Growing Stock Volume**

The Growing Stock Volume per hectare in stocked forest was on average 114 m<sup>3</sup>, or more than totally 1 billion m<sup>3</sup> (MET 2019). The forest regions with the highest average growing stock are Khangai and Khuvsgul with 130 m<sup>3</sup>/ha and 121 m<sup>3</sup>/ha respectively in their stocked forest (Fig. 15). Altai region stands out with the lowest

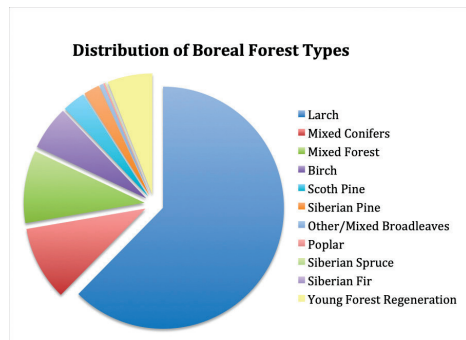
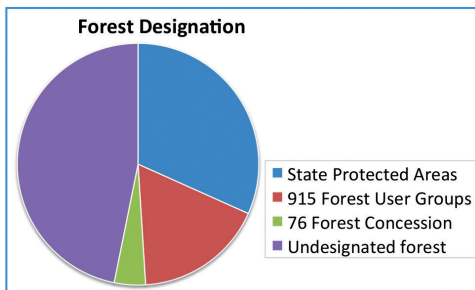


**Fig. 13 (left). Forest Area by Designation (MET 2016)**

**Fig. 14 (right). Boreal Forest Types Distribution, according to Tree Species Composition (MET 2016)**

growing stock, 74 m<sup>3</sup>/ha in stocked forest, mostly due to relatively small volumes in the higher diameter classes.

The national average growing stock volume for the un/low-stocked boreal forest areas is only 31 m<sup>3</sup>/ha, underlining the heterogeneous volume density in Mongolia's boreal forests. The overall national average growing stock volume is 96 m<sup>3</sup>/ha.

Siberian Larch (*Larix sibirica*) is dominant in the boreal forest of Mongolia, and it represents 92 m<sup>3</sup>/ha, or 81 percent of the average growing stock volume (Fig. 16) in stocked boreal forest. Siberian Pine (*Pinus sibirica*) comes on second place with 7.6 m<sup>3</sup>/ha (6.7%), then the White Birch (*Betula*

*platyphylla*) with 7.3 m<sup>3</sup>/ha (6.4%) and Scots Pine (*Pinus sylvestris*) with 5.6 m<sup>3</sup>/ha (4.9%). The other tree species, all together, represent less than 1.5 percent of the growing stock volume in stocked boreal forest (MET 2016).

The volume density of Mongolia's Boreal forest is around 50 percent of the optimal volume density in healthy and well-stocked forest stands, taking into consideration present tree species compositions and stand heights, as defined by the former Botanical Institute in the handbook for forest mensuration (Dorjsuren et. al. 2012). The volume density of forests in the utility zone is similar to the volume density of forests in protected areas, and Fig. 17 illustrates the

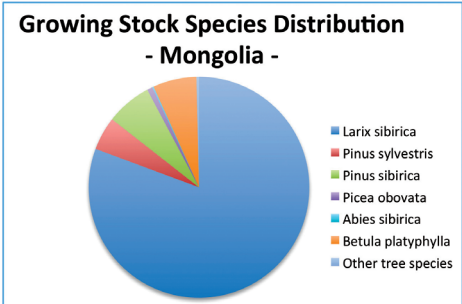
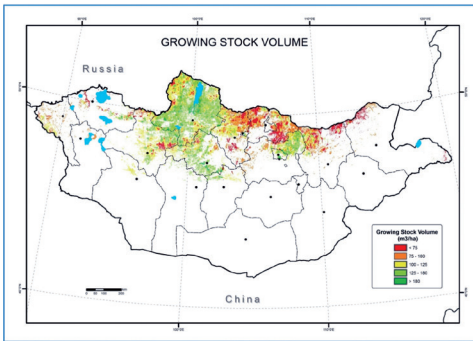


Fig. 15 (left). Distribution of growing stock densities in boreal forest (MET 2019)  
 Fig. 16 (right). Average tree species distribution by stocked GS volume (MET 2016)

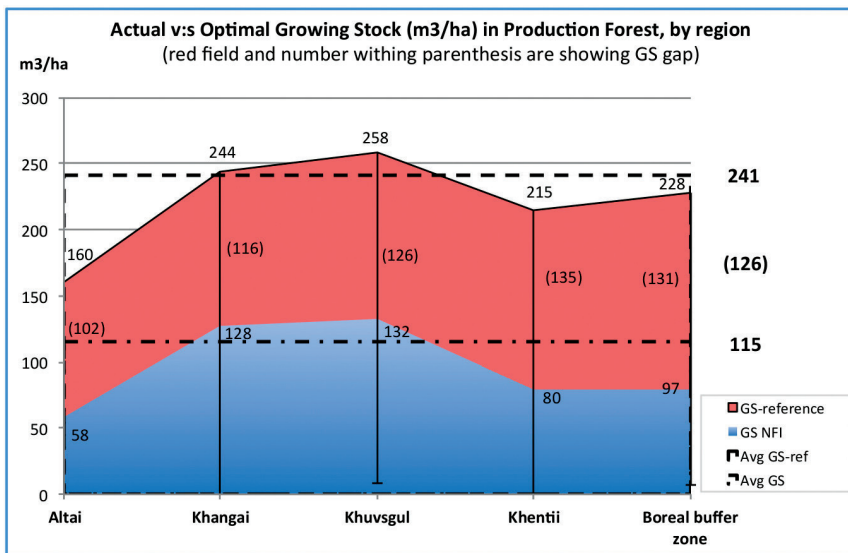


Fig. 17. Actual v:s Optimal Growing Stock Volume in Production Forest, by Forest Inventory Region (MET 2016)

actual and optimal Growing Stock densities by inventory region for forests in the utility zone (production forests).

The optimal national growing stock average in production forest was 237 m<sup>3</sup>/ha, while the actual growing stock density in stocked production forest was 115 m<sup>3</sup>/ha, which leaves a gap of roughly 124 m<sup>3</sup>/ha. The growing stock "gap" was more or less similar in all regions. However, Altai region had the relatively biggest growing stock gap, as its optimal growing stock only was over 190 m<sup>3</sup>/ha (MET 2016).

**Growing Stock Age Distribution**

Most of the growing stock in the stocked boreal forests was found in the age classes between 50 and 200 years, 73.7 m<sup>3</sup>/ha (Fig. 18). 23.8 m<sup>3</sup>/ha is found in the age classes over 200 years, and 15.8 m<sup>3</sup>/ha in the classes less than 50 years (MET 2016).

Harvested wood volume was estimated through the stumps assessed in the field inventory, without considering if the stumps were found in protected forest or in the productive forest area. The degree of decay was assessed for each stump, and this was used as a proxy for the age of the stump, i.e. the time since the tree was harvested.

Assuming that the time for a full decomposition of an average stump in Mongolia's boreal forest is around 50 years

(Shorohova and Kapitsa 2014, 2016), and that the rate of decomposition is constant throughout the stump's lifecycle, then the degree of decay (%) divided by two, is the equivalent to years since the tree was harvested. With this assumption of totally 15 m<sup>3</sup> stem volumes have been logged per hectare in the boreal forest during the last 50 years period (1964-2014), which corresponds to an average annual logging rate of about 0.3 m<sup>3</sup> per hectare per year, or totally 3.4 million m<sup>3</sup>/year. The average wood harvest during the last 10 years (2005-2014) was slightly less, 0.24 m<sup>3</sup> per hectare per year (Fig. 19) (MET 2016). Note that the NFI data cover all stumps independent of their legal or illegal origin, so the results presented do not make any difference between formally (i.e. legally) or informally (i.e. illegally) harvested wood.

**Forest Health**

The health of the stocked boreal forests is similar to other natural boreal forest, and 71 percent of the stocked boreal forest was very healthy, and only 6.8 percent of the forest is damaged (> 90% of the total basal area) (Fig. 20a-b) (MET 2019).

Of the causative agents affecting the health of forest/trees, Wildfire is the environmental hazard most affecting the health of the growing stock, 8.0 m<sup>3</sup>/ha, followed by Snow or Ice 3.7 m<sup>3</sup>/ha (Fig. 21) (MET 2019). Among the assessed causative agents there was also direct human-induced damage (e.g.

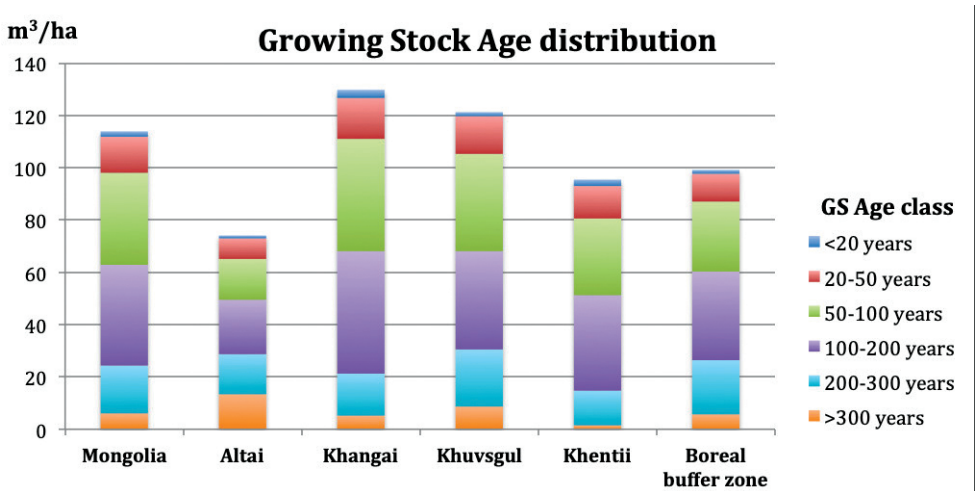


Fig. 18. Growing Stock Volume (m<sup>3</sup>/ha) by Age class (MET 2016)

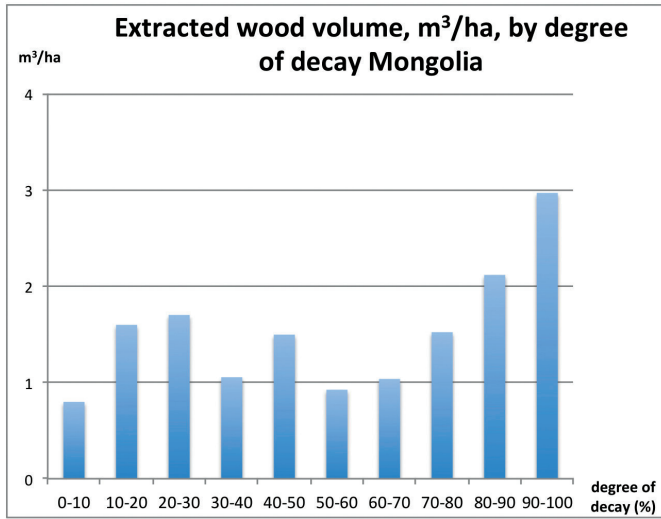


Fig. 19. Average logged wood volume (m³/ha), by degree of decay (MET 2016)

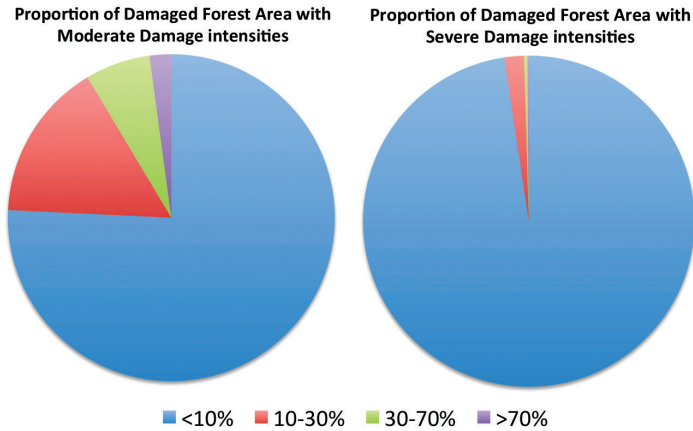


Fig. 20a-b. Damaged Boreal Forest Area Distribution (%), according to Moderate Damage intensities (left) and Severe Damage intensities (right) (MET 2019)

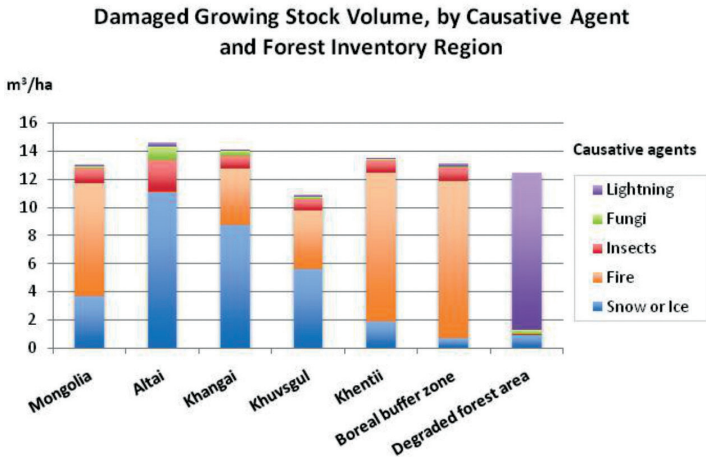


Fig. 21. Damaged Growing Stock Volume (m³/ha), by Causative Agent and Forest Inventory Region (MET 2019)

mechanical damage on tree stems). However, no such damage was recorded during the field survey. Other direct or indirect human-induced damage, like starting wildfires or managing livestock in forest were not assessed.

A summary of the training events related to Mongolia's National Forest Inventory and to Forest Management Planning in Mongolia is presented in Table 2, including the number of training events by topic and the number of trainees by topic.

These findings and many more can be found in the Mongolian Multipurpose National Forest Inventory reports (MET 2016 and MET 2019) and at the Web Portal <http://www.forest-atlas.mn> (FRDC 2019).

## DISCUSSION

### Mongolian forests are overaged and understocked

The new information provided by the Multipurpose NFI reveals that a big proportion of Mongolia's boreal forests biomass is relatively old. The age distribution of the stocked forests indicate that around 30 percent of the commercially viable growing stock volume (Larch, Scots Pine and Birch) in production forest is economically deemed as over-aged (MET 2019), which not

only is economically suboptimal, but also constitutes a potential risk for environmental hazards as pest outbreaks and wildfires, as old-growth trees are weakening and thus producing more dying and dead wood.

The NFI information also shows that Mongolia's boreal forests are significantly under-stocked compared with optimally managed forests, (described in Dorjsuren et. al. 2012), and vast forest areas remain un-stocked for long time, risking being permanently un-stocked (deforestation) or poorly stocked (forest degradation). As indicated in the NFI results, the growing stock densities varies a lot throughout the boreal forest area, which of course partly has to do with the different development stages of the forest, but not only. Some forest areas are very dense. So dense that the natural self-thinning results in a major portion of dead wood in the forest stand. While other forest areas are practically un-stocked, or very poorly stocked in relation to the average tree height (MET 2019). There are no significant differences in the forest characteristics inside or outside of protected areas (MET 2019).

There are many possible reasons for Mongolia's poorly-stocked boreal forest areas; a) unsustainable wood harvesting, where not enough efforts have been made to guarantee a successful regeneration of the forest, b) pest or disease outbreaks

**Table 2. Capacity Development Events for Mongolia's National Forest Inventory and Forest Management Planning**

Training Event	Number of training events	Number of Trainees
National Forest Inventory		
Field Data Collection	3	48
Forest Area Assessment	5	30
Forest Cover Mapping	1	12
Data and Database Management	5	25
Forest Management Planning		
Field Data Collection	2	22
Forest Types Mapping	1	11
Data and Database Management	1	11

decreasing the trees' biomass production, or eventually leading to tree death, c) damage caused by animals (domestic or wildlife) or humans, leading to decreased biomass production or tree death, d) climatic or other natural catastrophes directly damaging the trees, or indirectly by damaging their habitat. However, the causative agent with the overall largest impact on tree biomass degradation is currently the presence of wildfires which is behind most of the damage tree biomass in Mongolia's boreal forests (MET 2019).

### How to tackle environmental problems with silvicultural measures

The estimated mean annual harvesting rate in Mongolia's boreal forest during the last decade corresponds to 0.23 m<sup>3</sup>/ha (MET 2019), which is very much below the mean annual wood increment, estimated at just over 1 m<sup>3</sup>/ha (FRDC 2017). It indicates an underutilisation of the forest production and that the tendency of dead and dying wood will continue increasing, and which creates environmental risks, mainly through the effects of wildfire. There is a very high pressure on the forestry resources close to urban centres and to wood markets (Hijaba 2010), so locally there can be an overexploitation of wood for heating and construction. However, the NFI findings indicate that this overexploitation is geographically very limited, and at a whole a rare event today in Mongolia's boreal forests.

The rational way to solve many present and future environmental problems of Mongolia's boreal forests, and at the same time increase their productivity in terms of living tree biomass, would be to actively manage the forests towards a more species-diverse, vital and resilient tree composition (Schmidt-Corsitto et al 2019). Much of the forest should undergo some kind of logging activity: a) to curb self-thinning in over-dense forest stands with high inter-tree competition (crown thinning), b) to remove "old wolfs" (e.g. big old-growth trees) and over-aged trees, which inhibit a homogeneous development of the forest stand, c) to remove dying trees (sanitary cutting) to curb potential pest outbreaks, d) to guide a more diverse tree species composition (selective cutting), e) to rehabilitate poorly stocked forest areas

(clearcutting) f) to harvest wood from mature forest stands (selective-, shelterwood-, or clearcutting) to stimulate forest regeneration. However, current legislation and government directive needs to be amended to allow a wise and adequate management of the boreal forests. Like many other boreal forests, Mongolia's Larch- and Pine- dominated forests are well adapted to fire dynamics, and thus naturally often regenerate after huge wildfires. Clearcutting mimics severe wildfires, in the sense that it decreases, if not all, large parts of the living biomass in an area. Contrary to wildfires, which can affect up to several thousands of hectares, clearcutting restricts its impact to a limited area, and the wood is used as valuable greenwood for timber instead of literally going up in smoke. Light-loving pioneer species are favoured by clearcutting, which initially clears the area from competitive vegetation and opens up for full sun exposure, which benefit these species, which quickly get re-established. However, not all boreal forest areas are apt for final harvesting through clearcutting due to the topography, soil characteristics, microclimate, and not least the species composition. Shade tolerant species often benefit from a protecting canopy layer to regenerate. Selective cutting maintains continuous, and possibly, multiple canopy layer, to protect the new regenerations from direct sun exposure. For forests in-between the extremes of sun loving species and shade tolerant species shelterwood systems can then be the best option, where the dominating canopy layer(s) are being phased out little by little in order not to lose too much of the protective impact of the tree canopies before a successful regeneration has been well established. Worth noticing is that clearcutting is currently not allowed in Mongolia, so a revision in related legislation would be necessary to allow large parts of the boreal forest to be managed in a close-to-nature manner.

The removal of weak and dying trees will decrease the risk of pest outbreaks, and will not add more deadwood to Mongolia's boreal forests, which is already well-represented there. By thinning the over-dense forest stands and by removing over-ages trees, the growth of the remaining trees will be stimulated, and their vitality will be strengthened.

It might sound strange, but totally removing remaining tree biomass on very degraded forest areas and assisting the regeneration to create homogeneous well-stocked forest stands is a long-term approach to increase the forest biomass production, and thereby also the carbon sequestration which was described in the Forest Act of Sweden in 1948 (SKS 2019) as a tool to successfully rehabilitate degraded forest areas in Sweden.

## OUTLOOK

In a future, when climatic changes are foreseen, and the market for forestry products and services are yet to be confirmed, it is wise to diversify, to be prepared for whatever outcome. So, by guiding a diversified tree species composition, not only in the regeneration phase of the forest, but also in its young and premature phases, by selective cutting the forest would become more resilient to future climatic changes and to changes in the market of forestry products and services.

To better satisfy future information needs on the status and trends of Mongolia's forestry resources, the national forest inventory should consider all of the countries forests, i.e. also include the southern semidry "saxaul forests". The sampling design should also be stricter and should not allow shifting of cluster or plot locations, in order to avoid bias. To permit full flexibility for post-stratification, the sampling design, preferably based on the uniform 9 km x 9 km grid, should also cover the whole territory, where the non-forestry clusters can be excluded from field inventory after a pre-assessment using very high resolution remote sensing data (e.g. Collect Earth application). This would also make the field inventory data representative for direct area, i.e. the totals could be estimated without further auxiliary information.

## CONCLUSIONS

Mongolia's Multipurpose National Forest Inventory aimed at stimulating Sustainable Forest Management in Mongolia, not only by feeding policy formulation processes with accurate information, but also by supporting the development of assessment methods for

forest management planning. Drawing from the experiences and the information from the NFI, recommendations and guidelines on measurement-based forest management planning were made to prepare more reliable forest management plans, and silviculture guidelines for Mongolian forestry were developed to direct forest management measures towards a more effective and adequate treatments.

Mongolia's boreal forests produce less than half the biomass of well-managed boreal forests. Less than one fourth of the yearly biomass production is being cut, resulting in a lot of selfthinned- (dead trees) and over-aged trees, posing a potential risk for pest outbreaks and severe wildfires. There is a need to revise Mongolia's forest policies to address the overall suboptimal state of the boreal forest, and at the same time the under-utilisation of their boreal forests, by actively manage the forests for healthy green-wood production.

Current multipurpose national forest inventory is part of a continual process and is the first one of a series of consecutive assessments to monitor Mongolia's boreal forest resources. The value of the NFI data will increase with every cycle, as information on trends and changes (increment and losses) will be generated.

## ACKNOWLEDGEMENTS

Funding from the Mongolian government, the German government and from the Food and Agriculture Organization of the United Nations, and a massive commitment from all related stakeholders in- and outside Mongolia made it possible to reach the enormous achievement of planning and implementing Mongolia's Multipurpose National Forest Inventory. None mentioned and none forgotten, but I extend my special recognition to the Forest Department at MET, to the Climate Change Project Implementation Unit at MET, to the UN-REDD National team in Mongolia and also to their international support, to the dedicated researchers at Mongolia's Forestry Universities and Forest Research Institutes, and of course to my close colleagues at GIZ in Mongolia. ■

## REFERENCES

- Altrell D. (2015). NFI Estimation Methods and Data Models. Ulaanbaatar. GIZ.
- Breiman, L. (2001). Random Forests. Machine Learning: 5–32.
- Dorjsuren Ch. (2017). Estimation of Aboveground Biomass and Carbon stock in Mongolian Boreal Forest. Ulaanbaatar. GIZ.
- Dorjsuren Ch., Dugarjav C., Tsogt Z., Tsedendash G., and Chuluunbaatar T. (2012). Forest Mensuration Handbook of Mongolia. Ulaanbaatar. Institute of Botany at the Mongolian Academy of Science. Mongolian Forest Agency.
- Erdenejav, E. (2014a). Assessment of Boreal Forest Area in Mongolia Using Dot-Grid Sampling. Ulaanbaatar. GIZ
- Erdenejav E. (2014b). Multipurpose National Forest Resources Inventory of Mongolia: Allocation sampling clusters NFI Mongolia. Ulaanbaatar. GIZ.
- Food and Agriculture Organization of the United Nations (FAO) (2012). Field Manual for Integrated Field Data Collection. National Forest monitoring and Assessment. Forestry Department NFMA Working Paper No.37. Available at: <http://www.fao.org/3/ap152e/ap152e.pdf>. Rome. FAO.
- FAO (2014). Food and Agriculture Organization of the United Nations Open Foris Initiative. Available at: <http://www.openforis.org>.
- FRDC (2017). Mongolia's Forest Fund Report. Ulaanbaatar. Ministry of Environment and Tourism.
- FRDC (2019). Mongolia's Multipurpose National Forest Inventory on-line Forest Atlas. Available at: [www.forest-atlas.mn](http://www.forest-atlas.mn). Ulaanbaatar. Ministry of Environment and Tourism.
- Hijaba Y. (2010). Mongolia Forestry Outlook Study. Asia-pacific Forestry Sector Outlook study II - Working Paper No. APFSOS II/WP/ 2009/ 21. Bangkok. FAO
- IB (2012). Forest mensuration handbook of Mongolia. Institute of Botany at the Mongolian Academy of Science. Ulaanbaatar. Mongolian Forest Agency. (Mongolian)
- McRoberts R.E., Tomppo E.O., Czaplewski R.L. (2014). Sampling designs for national forest assessments. Knowledge Reference for National Forest Assessments. <http://www.fao.org/forestry/44859-02cf95ef26dfdc86c6be2720f8b938a8.pdf>. Rome. FAO.
- Mongolian Ministry of Environment and Tourism (MET) (2019). Mongolian Multipurpose National Forest Inventory 2014-2017. 2nd ed. Ulaanbaatar. Ministry of Environment and Tourism.
- Mongolian Ministry of Environment and Tourism (MET) (2016). Mongolian Multipurpose National Forest Inventory 2014-2016. 1st ed. Ulaanbaatar. Ministry of Environment and Tourism.
- QGIS Development Team (2015). QGIS Geographic Information System. Open Source Geospatial Foundation Project. Available at: <http://qgis.osgeo.org>

R Development Core Team (2015). R: A language and environment for statistical computing. R Foundation for Statistical Computing, Vienna, Austria. ISBN 3-900051-07-0, Available at: <http://www.R-project.org>.

RStudio Team (2015). RStudio: Integrated Development for R. RStudio, Inc., Boston, MA. Available at: <http://www.rstudio.com/>.

Schmidt-Corsitto K., Altrell D., Kenjibai S. (2019). *Silviculture Guidelines for Mongolian Forestry*. Ulaanbaatar. GIZ.

Schultz M. (2016). *Mapping Mongolia's Boreal Forest Cover 2015*. Ulaanbaatar. GIZ

Shorohova E. and Kapitsa E. (2016). The decomposition rate of non-stem components of coarse woody debris (CWD) in European boreal forests mainly depends on site moisture and tree species. *European Journal of Forest Research*. 2016, 135(3), pp 593–606.

Shorohova E. and Kapitsa E. (2014). Mineralization and fragmentation rates of bark attached to logs in a northern boreal forest. *Forest Ecology and Management* 315, pp. 185–190.

Swedish Forest Agency (SKS) (2019). The Forest Act. Para. 5:3. (SWE). Available at: <https://www.skogsstyrelsen.se/globalassets/lag-och-tillsyn/skogsvardslagen/skogsvardslagstiftning-2019-.pdf>. ISBN 978-91-87535-14-7. Skogsstyrelsen. Jönköping. (Swedish)

United Nations programme to Reduce emissions from Deforestation and forest Degradation (UN-REDD) (2018). *Annual Forest Change Matrix, incl. CE Forest Area statistics*. Ulaanbaatar. UN-REDD.

United Nations programme to Reduce emissions from Deforestation and forest Degradation (UN-REDD) (2017). *Methodology for Selection of Additional NFI Plots in Degraded Forest*. Ulaanbaatar. UN-REDD.

Vostokova E.A., Gunin P.D., Andreev A.V., Bazha S.N., Vorobyov C.A., Drobyshev Yu.I., Prischepa A.V. (2005). *Ecosystems of Mongolia - Atlas*. Moscow. Russian Academy of Sciences and Mongolian Academy of Sciences.

Received on March 5<sup>th</sup>, 2019

Accepted on August 8<sup>th</sup>, 2019

David Juříčka<sup>1\*</sup>, Václav Pecina<sup>1</sup>, Martin Brtnický<sup>1,2</sup>, Jindřich Kynický<sup>2</sup>

<sup>1</sup> Mendel University in Brno, Faculty of Forestry and Wood Technology, Department of Geology and Pedology, Brno, Czech Republic

<sup>2</sup> Central European Institute of Technology, Brno University of Technology, Brno, Czech Republic

\* Corresponding author: david.juricka@mendelu.cz

## MINING AS A CATALYST OF OVERGRAZING RESULTING IN RISK OF FOREST RETREAT, ERDENET MONGOLIA

**ABSTRACT.** This paper provides information on long-term suppression of natural forest regeneration due to the livestock grazing in the vicinity of one of the world largest open-pit ore mine close the city of Erdenet in Mongolia. The area is characterized by high concentration of herder's households where the 52% were found only up to 1 km distance from the forest edge. Forest grazing causes extensive damage to seedlings and significant reduction of their growth. Within the 30–99 cm height category, up to 61% *Larix sibirica*, 90% *Betula platyphylla* and 68% *Populus tremula* individuals are grazing-damaged. *L. sibirica* and *P. tremula* seedlings with heights over 99 cm were absent, and no individuals of any species were found within 136–200 cm height category. In addition to the seedlings, only 7 or more meters high *L. sibirica* individuals are found in the forest structure, which means the absence of successfully growing forest regeneration for at least 40 years. In 2017, the defoliation of *L. sibirica*, reaching locally up to 100%, occurred in the stands east of the mine. Total defoliation represents a high risk of mortality of affected individuals. The stands cannot be successfully regenerated under the conditions of current intensive grazing. Mine metal stocks are calculated to provide for at least another 25 years of mining. Over that time, neither significant population decline nor decreasing grazing pressure on forests can be expected. If effective protection measures are not implemented, there is a risk of transforming threatened forest into steppe.

**KEY WORDS:** overgrazing, forest regeneration, *Larix sibirica*, herders, defoliation, mining

**CITATION:** David Juříčka, Václav Pecina, Martin Brtnický, Jindřich Kynický (2019) Mining As A Catalyst Of Overgrazing Resulting In Risk Of Forest Retreat, Erdenet Mongolia. *Geography, Environment, Sustainability*, Vol.12, No 3, p. 184-198  
DOI-10.24057/2071-9388-2019-23

### INTRODUCTION

Mongolian forests are located predominantly in the northern part of the country (between 47–52°N and 89–116°E.), on the southern border of the vast Siberian taiga and the Mongolian

steppes with the total area over 19 million ha. (Ykhanbai et al. 2010; Batkhuu et al. 2011). The forests are mostly composed of *Larix sibirica* covering 60% of the forest territory. Another significant species are pines (*Pinus sylvestris* and *Pinus sibirica*) and *Picea sibirica* covering about 5 up to 8% of

the forest area. Furthermore, a significant species proportion is represented by the *Betula* genus, occupying approximately 9% of the Mongolian forest territory (Batkhoo et al. 2011; MET 2019).

A very important part of Mongolian forest ecosystems are the extremely sensitive mountain forest-steppe ecosystems. They play an irreplaceable role for preventing soil erosion and desertification (James 2011; Priess 2015), they have a positive effect on the soil water regime, play an invaluable role for the regional hydrology (Menzel et al. 2011; Karthe et al. 2015; Batbayar et al. 2018), and serve as important biodiversity centres (Sankey et al. 2006).

Unfortunately, Mongolian forests have been subjected to strong negative impact of illegal timber logging, forest fires and overgrazing for a long time (Tsogtbaatar et al. 2004). The combination of anthropogenic disturbance and climate change (Sato et al. 2007; Marin 2010; Oyuntuya et al. 2015) causes serious change in moisture conditions of the ecosystems leading to deterioration of the forests health (Juříčka et al. 2018). Weakened Mongolian forests are then exposed extensively to pests (Hauck et al. 2008; Dulamsuren et al. 2010a). A consequence of these factors can result in large-scale mortality of *L. sibirica* at affected sites (Juříčka et al. 2018).

Above all, heavy grazing pressure poses a serious threat to tree regeneration and thereby to the long-term existence of Mongolian forests. The beginning of the primary anthropogenic degradation on the territory of Mongolia is connected especially with the onset of intensive grazing at the early of the second millennium (Saizen et al. 2010). Grazing livestock significantly disturbs forest ecosystems (Lkhagvadorj et al. 2013), causes reducing of litter, compacting and disturbing of soils, reducing water infiltration rates, soil erosion, and it also can be significant factor of species changes in forest vegetation (Belsky and Blumenthal 1997). The long-term intensive forest grazing changes quantity

and height structure of seedlings and saplings. Thereby, it prevents successful forest regeneration for decades (Sankey et al. 2006; Khishigjargal et al. 2013). On the contrary, decrease in the number of grazing cattle in the forest leads to significant increase of number of seedlings and saplings (Buffum et al. 2009).

Mongolia is one of the most overgrazed countries in the world (Asner et al. 2005). Nevertheless, grazing livestock does not long provide just food self-sufficiency for migrating nomads. Currently, it is an important factor of the Mongolian economy (Janzen 2005). Agriculture sector in Mongolia (livestock forms nearly 90%; FAO 2015) created 10.4% of GDP in 2017 (The World Bank 2019) although it was up to 41% in 1996 (The Global Economy 2019). Pastoralism presents not only production of meat and dairy products. There is a growing proportion and number of goats, which form the backbone of a dynamically growing and highly profitable cashmere industry (Berger et al. 2013). However, at the same time, they cause the most critical damage to seedlings (Fernández-Giménez et al. 2012; Lkhagvadorj et al. 2013). Goats make 41.2% in the total number of livestock (National Statistics Office of Mongolia 2019).

The situation got fundamentally worse after 1990's with political and economic changes in Mongolia. The planned economy turned into market economy and, therefore, the number of livestock increased (Yoshihara et al. 2008; Saizen et al. 2010). In 1992, the number of livestock was 25.6 million in Mongolia. However, the number increased to 44.5 million in 2009 (Sankey et al. 2006; Maasri et al. 2011) and the number reached up to 66.2 million in 2019 (Mongolian Statistics Information Service 2019). Political changes and in some regions environmental deterioration have led to decline in nomad's migration. The herders concentrate around water resources, forests and large settlements. Therefore, the grazing pressure occurs for a longer time on a relatively smaller area (Sternberg 2008).

Our objectives were: (i) to provide information on long-term disturbance of forest regeneration in the vicinity of Erdenet city and to assess the role of mining in this unfavourable situation, (ii) to assess survival perspective of forest in the surrounding of Erdenet in the context of serious defoliation detected in 2017, (iii) to propose effective measures to ensure long-term survival of the forest.

## MATERIALS AND METHODS

### The study area

The research was conducted in forests in the vicinity of Erdenet city. The city is currently the second largest and populated in the Mongolia. The city began to grow in 1975 following the start of ore mining. Erdenet's population has increased from 29,100 inhabitants in 1979 (Quandal 2017) to current approximately 100,000 inhabitants (Enkhbayar 2019). It is a model example of population extension in Mongolia's mining areas.

In the centre of the area of interest there is a significant landscape element - a large Cu-Mo open-pit mine. The mine

is surrounded by older urbanized area with block buildings in the north and younger yurt household area in the west. The central part of the locality around the mine consists of steppe (1,300 m a.s.l.), which turns into mountain with mountain forest-steppe ecosystem (max. 1,700 m a.s.l.) (Fig. 1). The warmest month is July with average temperature of 17 °C; the coldest month is January with -21 °C. The average annual precipitation is about 350 mm (TimeAndDate 2019).

To determine the amount of yurt households in the study area, actual satellite image (26 May 2016) was used from GoogleEarth. Positions of herder households was exported to ArcGIS 10.4.1. Distance of herder's households from forest edge was found using buffer-zones, which were established around the edge of forest stands by utilization multiple ring buffer analyses in ArcGIS 10.4.1.

### Design of measurements

A total of 20 plots (1,376–1,653 m a.s.l.) of a size 10 x 10 m each were evaluated (Mühlenberg et al. 2012; Bellingham

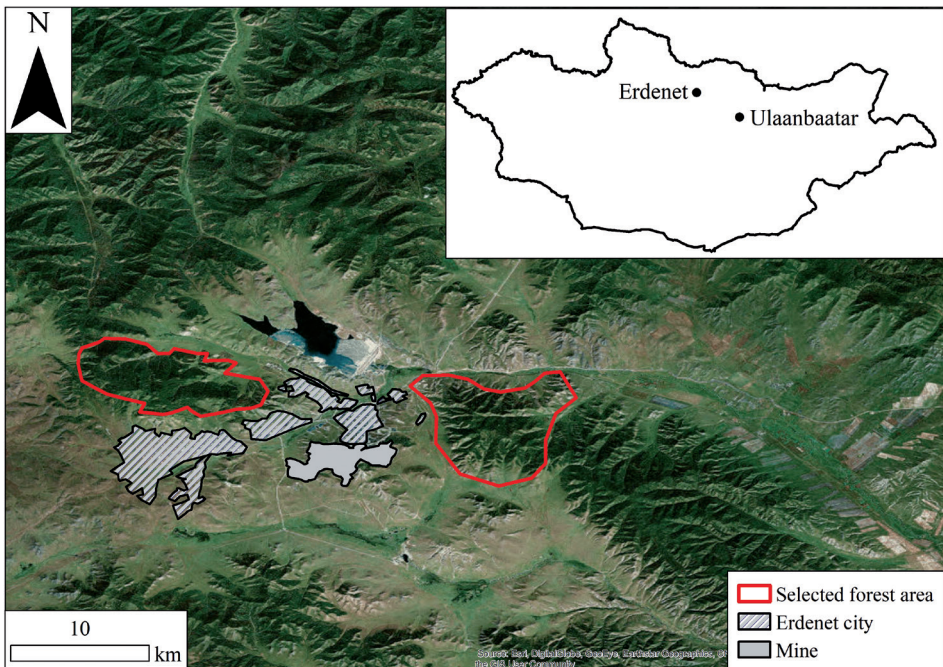


Fig. 1. Map of the area of interest

et al. 2016) in July 2016. The distance between individual sites is 0.7–2.2 km. Individual research plots were situated 0.1–2.5 km from forest edge. Each plot had been selected as a representative sample of local mature stands. We conducted grazing pressure evaluation, qualitative and quantitative evaluation of forest regeneration, dendrometric measurements and deadwood mapping. There were noted: position on the slope, altitude and slope aspect of each plot, as a background for evaluation of the influence of environmental factors.

### Forest mapping

In the locality, there are goats, sheep, cattle, yaks and horses grazing. The overall grazing pressure on the site was evaluated through the Reimoser et al. (1999) (none to very heavy) and Ludwig et al. (2014) (degree 1–4) methodologies.

Forest regeneration evaluation included the measurement of the heights of the seedlings and saplings present and character of their damage (non-injured, lateral, terminal, lateral + terminal). Heights of forest regeneration of the individual species are classified into the categories <10, 10–29, 30–99, 100–136 cm and 136–200 cm (Acker et al. 2017). Summary of all plots was counted per 1 ha (individuals, ha<sup>-1</sup>).

Species composition and number of individuals were determined within dendrometrics measurement. For each individual the height, girth, physiological vitality and biomechanical vitality were measured. Height of trees was measured using an altimeter Sylva CM-1015-2025 and a Nikon Laser Forestry rangefinder. Physiological vitality gauges tree health and cause of damage ranging from 1 to 5. Biomechanical vitality expresses the potential degree of reduced or threatened viability caused by mechanical failure of an individual, ranging from 1 to 5 (Pejchal and Šimek 2012, 2015). Stand basal area (SBA) was calculated by summing basal area (0.00007854 x diameter<sup>2</sup> at breast height) from all site locations and then

converted to a one-hectare area (Hédli et al. 2009). The position of a tree, its altitude and slope exposure were recorded using the GPS (Garmin GPSMAP 62 st). Position on the slope was later determined in program ArcGIS 10.4.1. according to Ludwig et al. (2014).

In order to confirm the defoliation of the stands, recorded in the field in August 2017, and to determine its extent, satellite images by GoogleEarth from May 16, 2017 and September 7, 2018 were used. Images were exported to ArcGIS 10.4.1 where defoliation was marked by visual detection. The limited image size in 2018 allowed only a minority of Erdenet forest stands to be explored.

### Data analyses

Relation of forest regeneration to environmental factors (position on the slope, altitude and slope aspect) has been tested using Monte Carlo test in the Canoco programme. The evaluation of the significance of single research plots distance from the edge of the forest was not made due to the high risk of results distortion due to the factor of "privileged cattle routes", which cannot be accurately evaluated from the satellite images. The horizontal distance between the plots and the forest edge is not a suitable variable.

## RESULTS

In the area around the mine, 126 herder households were counted and mapped in 2016. 52% of them have been found to be located in distance from forest edge less than 1 km (Fig. 2).

The assessment of the grazing intensity has confirmed that forests around Erdenet city are under heavy grazing pressure (Fig 3). The level of grazing pressure at research plots have been indicated as "very heavy" according Reimoser et al. (1999) and "degree 4" as reported by Ludwig et al. (2014). Both authors report it as a maximum level of grazing pressure on a locality.

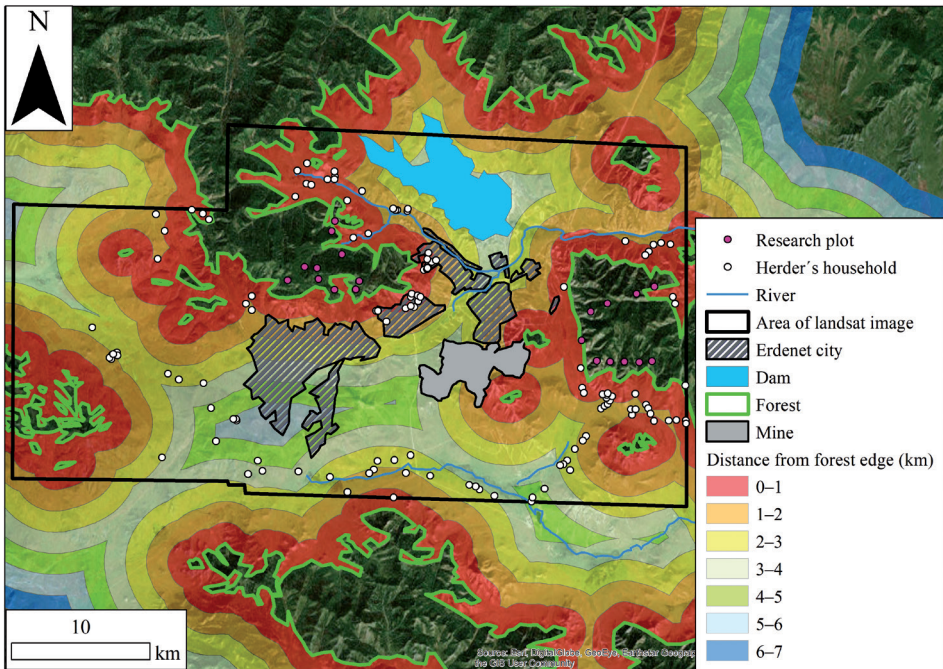


Fig. 2. Distribution of herder households depending on the forest stands distance

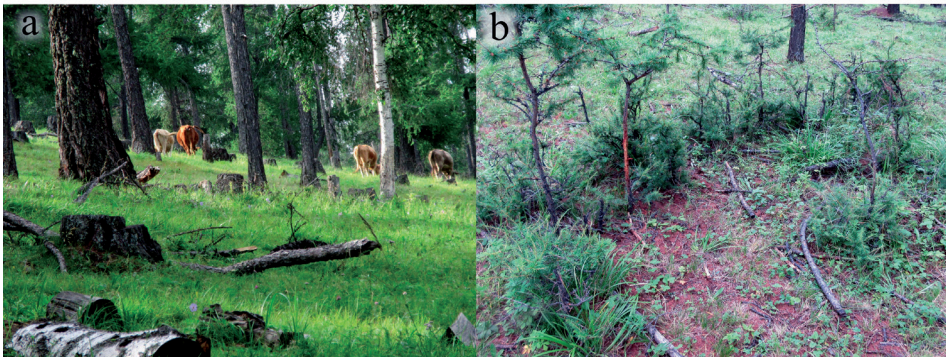


Fig. 3. Forest grazing (a) and damage of natural forest regeneration (b)

The occurrence of seedlings was sporadic in the stands. Tree seedlings were found in 8 of the 20 sites. *L. sibirica* was regenerated only in 4 sites, *B. platyphylla* in 3 sites and *P. tremula* in 4 sites out of 20. The most regenerated tree species is the main late successional species of the local forest, *L. sibirica*, forming 69% of the total counts of 2,190 individuals, ha<sup>-1</sup> higher than 10 cm.

Height category of 10–29 cm prevails in terms of *L. sibirica* and *P. tremula* height structure. Only 13% of the individuals of *L. sibirica* and 16% of *P. tremula* were

found within 30–99 cm height category. No individuals of these two species were found in higher height categories. *B. platyphylla* was found mostly in the 30–99 cm height category in a number of 165 individuals, ha<sup>-1</sup>. In the 100–136 cm height category, there were only 10 individuals, ha<sup>-1</sup> of *B. platyphylla* and no individuals in 136–200 cm height category.

The structure of damage to individuals is shown in Fig. 4. Individuals in 30–99 cm height category are damaged significantly more than those in category of 10–29 cm. Within 10–29 cm height

category, only 8% of *L. sibirica* individuals are damaged; within 30–99 cm height category, 61% of *L. sibirica* individuals are already damaged. In total, 14% of *L. sibirica* individuals are damaged. Deciduous trees show distinctly higher damage in all height categories than *L. sibirica*. 90% of *B. platyphylla* individuals in 30–99 cm height category are damaged. In total, 88% of the individuals are damaged. *P. tremula* showed a total damage in 66% of individuals: 65% within 10–29 cm height category and 68% within 30–99 cm height category. The characteristics is similar in all species; terminal damage was the most frequent.

The influence of environmental factors on data variability was excluded. Monte Carlo test did not confirm any correlation between the environmental factors with number, tree species and type of regeneration seedlings damage in the locality.

The observed stands were mainly composed of larch with sporadic occurrence of birch. Their predominant status was assessed as satisfactory on the basis of parameters evaluated in 2016 (Table 1). Physiological vitality at level 2 of *L. sibirica* showed slight deviations from the optimum and the assumption of possible long-term existence. The biomechanical vitality of *L. sibirica* at level 2 was only slightly reduced, with the assumption of a long-term existence. The dead individuals of *L. sibirica* occupied only 15% of the total number of living and dead trees. There was recorded occurrence of gypsy moth (*Lymantria dispar*) as a potential risk factor, which sporadically caused different degrees of crown defoliation. There was also visible evidence of timber logging throughout the area with a character of either selection harvesting in the stand (Fig. 3a) or clearcutting (Fig. 5). Efforts of targeted forest management with its sustainability

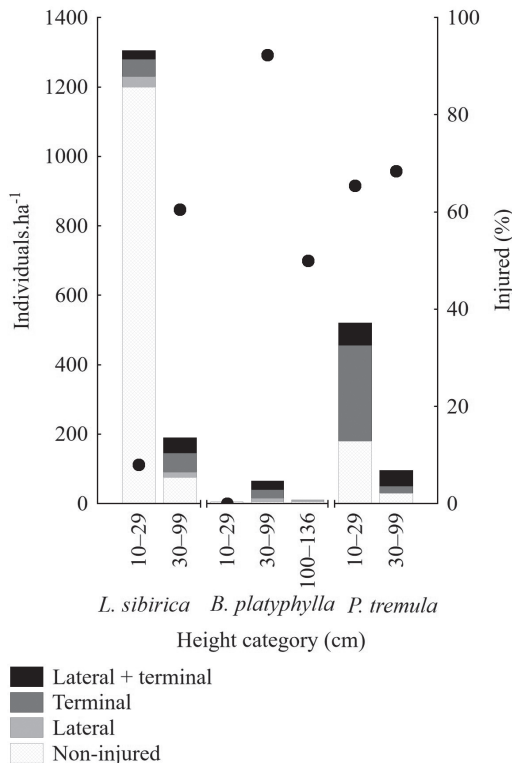


Fig. 4. Numbers (individuals, ha<sup>-1</sup>) and structure of damage (%) of the seedlings



**Fig. 5. Patch cutting without natural or artificial regeneration**

**Table 1. Forest characteristics. Growing stock SBA ( $\text{m}^3, \text{ha}^{-1}$ ), number of trees (individuals,  $\text{ha}^{-1}$ ), height (m): median (min–max), physiological and biomechanical vitality (degree), deadwood (individuals,  $\text{ha}^{-1}$ ) in 2016**

	<i>L. sibirica</i>	<i>B. platyphylla</i>
Growing stock SBA	33.25	0.33
Number of trees	405	10
Height	21 (7–35)	16 (9–23)
Physiological vitality (1–5)	2	1
Biomechanical vitality (1–5)	2	1
Standing deadwood $\varnothing$ 10–50 cm	15	0
Standing deadwood $\varnothing$ > 50 cm	5	0
Fallen deadwood $\varnothing$ 10–50 cm	20	0
Fallen deadwood $\varnothing$ > 50 cm	30	0

principles in the study area can be ruled out, because no artificial regeneration of forests was found and the protection of forests practically does not exist there.

In August 2017, 100% defoliation of *L. sibirica* was detected with focal area character east from the mine (Fig. 6a). Large-scale extend was confirmed by the analysis of satellite images (Fig. 6b).

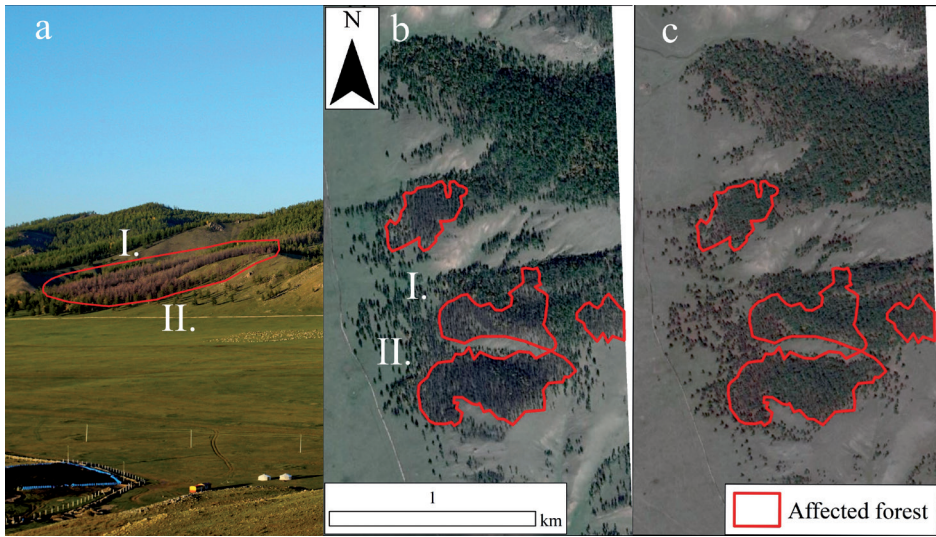


**Fig. 6. Defoliation of forest near the mine. (a) situation from terrain 08.2017, (b) situation 09.2018, (c) situation 05.2017**

The defoliation occurred between May (Fig. 6c) to August 2017. There were only standing individuals; no fallen timber was found. These stands did not show any damage caused by fire. Individual focal areas were of size 6–18 ha.

## DISCUSSION

The city of Erdenet is the second most populated city in Mongolia (Enkhbayar 2019). As such, it represents an important market of livestock products and resources for herders, which is used by herders as they concentrate (Fig. 2) in large quantities around the city. However, this is a serious problem for local forest ecosystems as they are subjected to heavy grazing pressure.

The yurt household factor is also presented as significant by Sankey et al. (2006), as they found a lower grazing intensity in sites with lower number of yurt households. Very heavy grazing pressure, as it is described by Reimoser et al. (1999), was found in the whole study area. Local opening of stands by selection harvesting and clearcutting (Fig 3a, 5) simulates natural disturbances and processes typical for boreal forest, as Bondarev (1997) describes them. This creates ideal conditions for forest regeneration, but long-term intensive

grazing around Erdenet has not allowed the successful growth of seedlings and thereby prevented the natural forest regeneration in the area. Poor condition of the seedlings is reflected in particular by low count of *L. sibirica*, *B. platyphylla* and *P. tremula* seedlings in height category of 30–99 cm and by the absence of these species in height categories over 99 cm. Similar situation is also described by Sankey et al. (2006), who indicate the absence of forest regeneration within the intensively grazed forest-steppe ecotones in Darhad Valley for the period of up to 30 years. Khishigjargal et al. (2013) also states the absence of *L. sibirica* saplings in excessively grazed forest of Altai Tavan Bogd National Park since the late 1970's. This observation is further confirmed by Hauck and Lkhagvadorj (2013) who report that long-term grazing pressure can totally stop successful forest regeneration for decades.

In contrast to the low number of seedlings in height category above 99 cm, there is a high number of *L. sibirica* seedlings within 10–29 cm height category (Fig. 4). This can point to suitable conditions for regeneration through opening of crown canopy, but it is also a direct consequence of overgrazing. In the affected forest, there is very low internal species competition (Khishigjargal et al. 2013), where 100–

200 cm height category individuals are missing and only mature trees are present. Therefore, seedlings have enough light: *L. sibirica* seedlings have extremely high light demand (Abaimov 2010). Only 8% of damage of 10–29 cm height *L. sibirica* seedlings is due to the fact that livestock do not prefer small seedlings, as it focuses on taller individuals (Khishigjargal et al. 2013). However, 61% was damaged within 30–99 cm height category.

The beginning of intensive grazing in the locality of Erdenet can be approximately deduced from height structure of the stand (Khishigjargal et al. 2013), because typically there is very common multi-aged tree age pattern for Siberian larch forests (Bondarev 1997), and in the studied stands next to Erdenet trees 1–7 m high are missing (Fig. 4, 7; Tab 1). From initial mapping of *L. sibirica* held in similar natural conditions of southern Khentii (unpublished data), cambial age of trees 8–13 m high was determined to be 36–52 years (true age plus 10–20 years, Dulamsuren et al. 2010). Even Koizumi et al. (2003) state age of *L. sibirica* individuals

high 12.3–20.4 m in south Siberia to be in range of 40–80 years. Kharuk et al. (2018) report age of *L. sibirica* high  $9.8 \pm 0.6$  m  $46 \pm 3$  years in the same area. From already mentioned, it can be assumed that the last generation of *L. sibirica* in the Erdenet locality has exceeded height 1 m approximately in 1980s, i.e. at the beginning of ore mining in Erdenet mine. In this southern part of boreal forests, age distribution can be a result of periodic catastrophic fires (Bondarev 1997). This fact can be avoided due to distribution of the plots and absence of fire damage of the remaining trees.

During 2017–2018, east from the mine, there has been noticed *L. sibirica* defoliation of focal area character confirmed by landsat image. Defoliation of larch can cause significant tree mortality in the dry sites (Jardon et al. 1994), thus, we assume there will be massive mortality of the stands in future years. Meanwhile, the confirmed scale of such damaged stands is more than 49 ha. Based on occurrence of gypsy moth, detected in 2016, we suggest that defoliation of *L.*

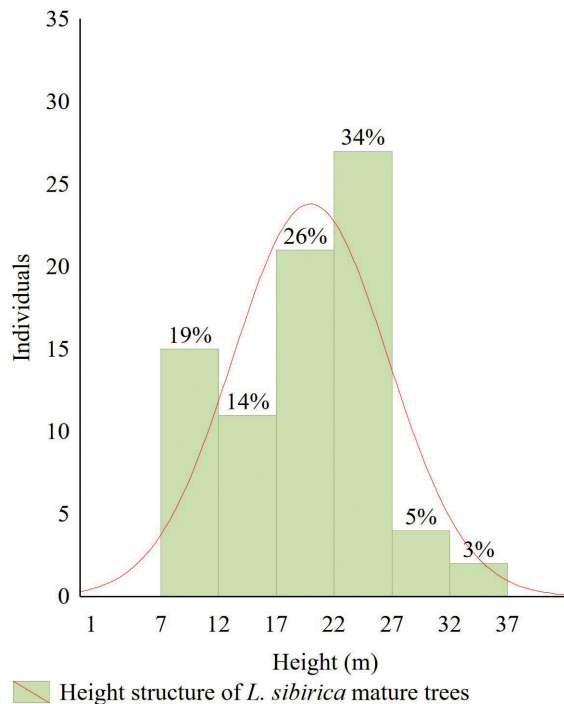


**Fig. 7.** Height structure of *L. sibirica* individuals

*sibirica* individuals is caused by increasing numbers of the pest. It can indicate influence of another stress factor, which has caused primary weakening of the stands, e.g. drought stress (Dulamsuren et al. 2010). Outbreak of gypsy moth causing extensive mortality of *L. sibirica* is described by Hauck et al. (2008) and Dulamsuren et al. (2010a) in the Khentii Mountains in the north of the Mongolia. Due to intensive grazing, there are not young individuals in the locality which would fill an ecological niche. Systematic artificial restoration of the stands cannot be expected as it is only very limited in Mongolia (FAO 2015) and it is very inefficient (Ykhanbai et al. 2010).

We assume that the current negative trend of forest regeneration inhibition due to overgrazing will further continue depending on the Cu-Mo mining in the Erdenet Ovoo mine. Mine metal stocks are calculated to provide for another 25 years of mining, at minimum until 2040 (Seltmann et al. 2004). Over that period, there is no assumption of significant population decline, and therefore no foreseen reduction in grazing livestock, which is needed to reduce the pressure on the overgrazed forests.

Herders do not respect forest grazing prohibition, neither in strictly protected area (our experience). Therefore, it is imperative to ensure the protection of the affected forest stands from further grazing, e.g. by fencing. It is currently the only truly effective measure, which is verified in the Mongolian environment at the stands of Domog Sharin Goll in the Khentii Mountains (Kusbach et al. 2017). Fencing physically prevents access of livestock to selected forest stands and thus protects them from further damage. Assuming that protective measures are implemented, the natural restoration of the heavily affected areas can also be realized by pioneer species of *B. platyphylla* and *P. tremula*. Pioneer species will prepare the habitat for the growth of the late successional species of *L. sibirica*, as it happens in conditions of natural succession, such as in the case of habitats

affected by the fire (Abaimov 2010). If no action is taken, there will be a risk of cutting dead trees after forest dieback in the short term, and since the defoliation of *L. sibirica* affects mainly forest edge, an immediate shift of the tree line will occur there. In the degraded stands, there will be a gradual change of environmental conditions (James 2011), which in the background of the Mongolian climate changes (Sato et al. 2007; Marin 2010; Oyuntuya et al. 2015) in synergy of intensive grazing, can represent a real threat of transformation of the affected forest ecosystems into steppe.

## CONCLUSIONS

Erdenet city has become aim of the urbanization process due to ore mining. We assume that the high number of yurt households in Erdenet surroundings results from socioeconomic reasons, because the city presents a constant market for herder's products. Herders in the city surroundings prefer sites located close the forest: 52% yurt households were found within 1 km distance from the forest edge. As a result of their accumulation, an intensive overgrazing of larch forest occurs in the vicinity of the city.

Very heavy grazing pressure prevents successful growing of *L. sibirica* seedlings as the late succession tree species. *L. sibirica* individuals within 99–200 cm height category are completely missing in the stands. Further, seedling of pioneer tree species *B. platyphylla* and *P. tremula* do not grow well as no individuals were found in 137–200 cm height category. Individuals within 10–29 cm height category were found in large quantities and are generally less damaged, as livestock doesn't prefer to feed on very small seedlings. High amount of lower seedlings was also allowed by increasing resource availability resulting from absence of intraspecific competition for light through the timber logging and by the absence of a higher height category seedlings. Disturbed height structure of mature trees indicates the beginning of

the intensive grazing from 1980s. In the forests located east of the mine, extensive defoliation of *L. sibirica* was found on more than 49 ha. Under current grazing pressure there will not be any natural regeneration to maintain actual tree line of threatened forest. The grazing pressure will not drop for at least 25 years, which is the remaining time of mining operation according to current plans. If the measures for the physical protection of natural forest regeneration against

livestock grazing, such as forest fence, are not implemented, there is a real threat of forest transforming into steppe. Such a change would be difficult to reverse due to the resulting alterations of microclimate and soil hydrology.

#### ACKNOWLEDGEMENTS

E!7614 international project of applied research solved within EUREKA program.

#### REFERENCES

- Abaimov A.P. (2010). Geographical Distribution and Genetics of Siberian Larch Species. In: Osawa A., Zyryanova O.A., Matsuura Y., Kajimoto T. and Wein R.W. ed., Permafrost ecosystems: Siberian larch forests. New York: Springer, pp. 41-58. doi: 10.1007/978-1-4020-9693-8\_3.
- Acker S.A., Kertis J.A. and Pabst R.J. (2017). Tree regeneration, understory development, and biomass dynamics following wildfire in a mountain hemlock (*Tsuga mertensiana*) forest. *Forest Ecology and Management*, 384, 72-82. doi: 10.1016/j.foreco.2016.09.047.
- Asner G.P., Elmore A.J., Olander L.P., Martin R.E. and Harris T. (2005). Grazing systems, ecosystem responses, and global change. *Annu. Rev. Environ. Resour.*, 29, pp. 261-99. doi: 10.1146/annurev.energy.29.062403.102142.
- Batbayar G., Pfeiffer M., Kappas, M. and Karthe D. (2018). Development and application of GIS-based assessment of land-use impacts on water quality: A case study of the Kharaa River Basin. *Ambio*. doi:10.1007/s13280-018-1123-y.
- Batkhuu N., Lee D.K. and Tsogtbaatar J. (2011). Forest and Forestry Research and Education in Mongolia. *Journal of Sustainable Forestry*, 30(6), 600-617. doi: 10.1080/10549811.2011.548761.
- Bellingham P.J., Richardson S.J., Mason N.W., Veltman C.J., Allen R.B., Allen W.J., Baker. R.J. and Ramsey D.S. (2016). Introduced deer at low densities do not inhibit the regeneration of a dominant tree. *Forest Ecology and Management*, 364, 70-76. doi: 10.1016/j.foreco.2015.12.013.
- Belsky A.J. and Blumenthal D.M. (1997). Effects of Livestock Grazing on Stand Dynamics and Soils in Upland Forests of the Interior West. *Conservation Biology*, 11, pp. 315-327. doi: 10.1046/j.1523-1739.1997.95405.x.
- Berger J., Buuveibaatar B. and Mishra C. (2013). Globalization of the Cashmere Market and the Decline of Large Mammals in Central Asia. *Conservation Biology*, 27(4), 679-689. doi:10.1111/cobi.12100.
- Bondarev A. (1997). Age distribution patterns in open boreal Dahurican larch forests of Central Siberia. *Forest Ecology and Management*, 93(3), pp. 205-214. doi: 10.1016/S0378-1127(96)03952-7.

Buffum B., Gratzter G. and Tenzin Y. (2009). Forest grazing and natural regeneration in a late successional broadleaved community forest in Bhutan. *Mountain Research and development*, 29(1), pp. 30-35. doi: 10.1659/mrd.991.

Dulamsuren C., Hauck M. and Leuschner C. (2010). Recent drought stress leads to growth reductions in *Larix sibirica* in the western Khentey, Mongolia. *Global Change Biology*, 16(11), pp. 3024-3035. doi: 10.1111/j.1365-2486.2009.02147.x.

Dulamsuren C., Hauck M., Leuschner H.H. and Leuschner C. (2010a). Gypsy moth-induced growth decline of *Larix sibirica* in a forest-steppe ecotone. *Dendrochronologia*, 28(4), pp. 207-213. doi: 10.1016/j.dendro.2009.05.007.

Enkhbayar T. (2019). Urban Housing Policy and Country Profile of MONGOLIA. [online] Available at: <https://www.unescap.org/sites/default/files/Session%202B%20-%20Tsolmon%20Enkhbayaar.pdf> [Accessed 30 Jan. 2019].

FAO (2015) Mongolia - Global Forest Resources Assessment 2015 – Country Report. [online] Available at: <http://www.fao.org/3/a-az278e.pdf> [Accessed 4 Jan. 2019].

Fernández-Giménez M., Batjav B. and Baival B. (2012). Lessons from the dzud: adaptation and resilience in Mongolian pastoral socio-ecological systems. Washington, World Bank.

Hauck M., Dulamsuren C. and Heimes C. (2008). Effects of insect herbivory on the performance of *Larix sibirica* in a foreststeppe ecotone. *Environmental and Experimental Botany*, 62(3), pp. 351-356. doi: 10.1016/j.envexpbot.2007.10.025.

Hauck M. and Lkhagvadorj D. (2013). Epiphytic lichens as indicators of grazing pressure in the Mongolian forest-steppe. *Ecological Indicators*, 32, pp. 82-88. doi: 10.1016/j.ecolind.2013.03.002.

Hédl R., Svátek M., Dančák M., Rodzay A.W., Salleh A.B. and Kamariah A.S. (2009). A new technique for inventory of permanent plots in tropical forests: a case study from lowland dipterocarp forest in Kuala Belalong, Brunei Darussalam. *Blumea-Biodiversity, Evolution and Biogeography of Plants*, 54(1-3), pp. 124-130. doi: 10.3767/000651909X475482.

James T.M. (2011). Temperature sensitivity and recruitment dynamics of Siberian larch (*Larix sibirica*) and Siberian spruce (*Picea obovata*) in northern Mongolia's boreal forest. *Forest Ecology and Management*, 262(4), pp. 629-636. doi: 10.1016/j.foreco.2011.04.031.

Janzen J. (2005). Mobile livestock-keeping in Mongolia: present problems, spatial organization, interactions between mobile and sedentary population groups and perspectives for pastoral development. *Senri. Ethnol. Stud.*, 69, pp. 69-97. doi: 10.15021/00002641.

Jardon Y., Filion L. and Cloutier C. (1994). Long-term impact of insect defoliation on growth and mortality of eastern larch in boreal Québec. *Ecoscience*, 1(3), pp. 231-238. doi: 10.1080/11956860.1994.11682247.

Juříčka D., Novotná J., Houška J., Pařílková J., Hladký J., Pecina V., Cihlářová H., Burnog M., Elbl J., Rosická Z., Kynický J. and Brtnický M. (2018). Large-scale permafrost degradation as a primary factor in *Larix sibirica* forest dieback in the Khentii massif, northern Mongolia. *Journal of Forestry Research*, 88, pp. 1-12. doi: 10.1007/s11676-018-0866-4.

Karthe D., Heldt S., Houdret A. and Borchardt D. (2015). IWRM in a country under rapid transition: lessons learnt from the Kharaa River Basin, Mongolia. *Environmental Earth Sciences*, 73(2), 681-695. doi:10.1007/s12665-014-3435-y.

Kharuk V.I., Petrov I.A., Dvinskaya M.L., Im, S.T. and Shushpanov A.S. (2018). Comparative Reaction of Larch (*Larix sibirica* Ledeb.) Radial Increment on Climate Change in the Forest Steppe and Highlands of Southern Siberia. *Contemporary Problems of Ecology*, 11(4), pp. 388-395. doi: 10.1134/S1995425518040042.

Khishigjargal M., Dulamsuren Ch., Lkhagvadorj D., Leuschner Ch. and Hauck M. (2013). Contrasting responses of seedling and sapling densities to livestock density in the Mongolian forest-steppe. *Plant Ecology*, 214(11), pp. 1391-1403. doi: 10.1007/s11258-013-0259-x.

Koizumi A., Takata K., Yamashita K. and Nakada R. (2003). Anatomical characteristics and mechanical properties of *Larix sibirica* grown in south-central Siberia. *IAWA journal*, 24(4), pp. 355-370. doi: 10.1163/22941932-90000341.

Kusbach A., Štěrba T., Smola M., Novák J., Lukeš P., Strejček R., Škoda A., Bažant V. and Pondělíčková A. (2017). Development of forests and the gene pool of local forest tree ecotypes in Mongolia. part: Development of forests and landscape in Mongolia, silviculture, urban forestry, public relation. Proceedings of the seminar, Sharyn Gol/Darkhan, Mongolia, September 2017. Project CzDA-RO-MN-2014-6-31210. ÚHÚL Brandýs nad Labem, Czech Republic 2017. ISBN 978-80-88184-12-6.

Lkhagvadorj D., Hauck M., Dulamsuren C. and Tsogtbaatar J. (2013). Pastoral nomadism in the forest-steppe of the Mongolian Altai under a changing economy and a warming climate. *Journal of Arid Environments*, 88, pp. 83-89. doi: 10.1016/j.jaridenv.2012.07.019.

Ludwig R., Dorjsuren Ch. and Baatarbileg N. (2014). Manual for multipurpose national forest inventory field assessment. Ulaanbaatar: Internationale Zusammenarbeit (GIZ) GmbH.

Maasri A. and Gelhaus J. (2011). The new era of the livestock production in Mongolia: Consequences on streams of the Great Lakes Depression. *Science of The Total Environment*, 409(22), pp. 4841-4846. doi: 10.1016/j.scitotenv.2011.08.005.

Marin A. (2010). Riders under storms: Contributions of nomadic herders' observations to analysing climate change in Mongolia. *Global Environmental Change*, 20(1), pp. 162-176. doi: 10.1016/j.gloenvcha.2009.10.004.

Menzel L., Hofmann J. and Ibsch R. (2011). Untersuchung von Wasserund Stoffflüssen als Grundlage für ein Integriertes Wasserressourcen – Management im Kharaa-Einzugsgebiet (Mongolei). *Hydrologie und Wasserbewirtschaftung*, 55(2), 88-103.

MET (2019) Multipurpose National Forest Inventory 2nd edition. [online] Available at: <http://www.forest-atlas.mn/Documentation.aspx> [Accessed 7 Jan. 2019].

Mongolian statistics information service (2019). Number of livestock. [online] Available at: [http://www.1212.mn/statHtml/statHtml.do?orgId=976&tblId=DT\\_NSQ\\_1001\\_021V1&conn\\_path=i2&language=en](http://www.1212.mn/statHtml/statHtml.do?orgId=976&tblId=DT_NSQ_1001_021V1&conn_path=i2&language=en) [Accessed 9 Jan. 2019].

Mühlenberg M., Appelfelder J., Hoffmann H., Ayush E. and Wilson K. (2012). Structure of the montane taiga forests of West Khentii, Northern Mongolia. *Journal of forest science*, 58(2), pp. 45-56. doi: 10.17221/97/2010-JFS.

National Statistics Office of Mongolia (2019). Number of livestock, by type, by region, bag, soum, aimag and the Capital. [online] Available at: [http://1212.mn/tables.aspx?TBL\\_ID=DT\\_NSQ\\_1001\\_021V1](http://1212.mn/tables.aspx?TBL_ID=DT_NSQ_1001_021V1) [Accessed 7 Jan. 2019].

Oyuntuya S., Dorj B., Shurentsetseg B. and Bayarjargal E. (2015). Agrometeorological information for the adaptation to climate change. In: Badmaev N.B. and Khutakova C.B., eds., *Soils of Steppe and Forest Steppe Ecosystems of Inner Asia and Problems of Their Sustainable Utilization*, 1st ed. Ulan-Ude: Buryat State Academy of Agriculture, pp. 135-140. doi: 10.1016/S0168-1923(00)00110-6.

Pejchal M. and Šimek P. (2012). Evaluation of potential of woody species vegetation components in objects of landscape architecture. *Acta Universitatis Agriculturae et Silviculturae Mendelianae. Brunensis*, 60(24), pp. 199-204. doi: 10.11118/actaun201260080199.

Pejchal M. and Šimek P. (2015). Methodology of wood evaluation for monument care supplies (certified methodology). Mendel University in Brno, Lednice, pp. 29-53 (in Czech).

Priess J., Schweitzer C., Batkhisig O., Koschitzki T. and Wurbs D. (2015): Impacts of land-use dynamics on erosion risks and water management in Northern Mongolia. *Environmental Earth Sciences*, 73(2), pp. 697-708 doi: 10.1007/s12665-014-3380-9.

Quandal (2017). Population of Erdenet. [online] Available at: [https://www.quandl.com/data/CITYPOP/CITY\\_ERDENETORMONGOLIA-Population-of-Erdenet-OR-Mongolia](https://www.quandl.com/data/CITYPOP/CITY_ERDENETORMONGOLIA-Population-of-Erdenet-OR-Mongolia) [Accessed 9 Jan. 2019].

Reimoser F., Armstrong H. and Suchant R. (1999). Measuring forest damage of ungulates: what should be considered. *Forest Ecology and Management*, 120(1), pp. 47-58. doi: org/10.1016/S0378-1127(98)00542-8.

Saizen I., Maekawa A. and Yamamura N. (2010). Spatial analysis of time-series changes in livestock distribution by detection of local spatial associations in Mongolia. *Applied Geography*, 30(4), pp. 639-1304. doi: 10.1016/j.apgeog.2010.01.002.

Sankey T.T., Montagne C., Graumlich L., Lawrence R. and Nielsen J. (2006). Lower forest-grassland ecotones and 20th Century livestock herbivory effects in northern Mongolia. *Forest Ecology and Management*, 233(1), pp. 36-44. doi: 10.1016/j.foreco.2006.05.070.

Sato T., Kimura F. and Kitoh A. (2007). Projection of global warming onto regional precipitation over Mongolia using a regional climate model. *Journal of Hydrology*, 333(1), pp. 144-154. doi: 10.1016/j.jhydrol.2006.07.023.

Seltmann R., Gerel O. and Kirwin D. (2004). *Geodynamics and Metallogeny of Mongolia with a special emphasis on copper and gold deposits*. London: IAGOD.

Sternberg T. (2008). Environmental challenges in Mongolia's dryland pastoral landscape. *Journal of Arid Environments*, 72(7), pp.1294-1304. doi:10.1016/j.jaridenv.2007.12.016.

The Global Economy (2019). Mongolia: GDP share of agriculture. [online] Available at: [http://www.theglobaleconomy.com/Mongolia/Share\\_of\\_agriculture/](http://www.theglobaleconomy.com/Mongolia/Share_of_agriculture/) [Accessed 7 Jan. 2019].

The World Bank (2019). World Development Indicators. [online] Available at: <https://databank.worldbank.org/data/source/world-development-indicators> [Accessed 7 Jan. 2019].

Time and Date (2019). Climate & Weather Averages in Erdenet, Mongolia. [online] Available at: <https://www.timeanddate.com/weather/mongolia/erdenet/climate> [Accessed 4 Jan. 2019].

Tsogtbaatar J. (2004). Deforestation and reforestation needs in Mongolia. *Forest Ecology and Management*, 201(1), pp. 57-63. doi: 10.1016/j.foreco.2004.06.011.

Ykhanbai H. (2010). Mongolia forestry outlook study. Asia-pacific forestry sector outlook study II: working paper no. APFSOS II/WP/2009/21, Retrieved 2010. [online] Available at: <http://www.fao.org/docrep/014/am616e/am616e00.pdf> [Accessed 3 Jan. 2019].

Yoshihara Y., Chimeddorj B., Buuveibaatar B., Lhagvasuren B. and Takatsuki S. (2008). Effects of livestock grazing on pollination on a steppe in eastern Mongolia. *Biological Conservation*, 141(9), pp. 2376-2386. doi: 10.1016/j.biocon.2008.07.004.

Received on February 20<sup>th</sup>, 2019

Accepted on August 8<sup>th</sup>, 2019

**Elena V. Shabanova<sup>1</sup>, Ts. Byambasuren<sup>2,3</sup>, G.Ochirbat<sup>3</sup>, Irina E. Vasil'eva<sup>1</sup>, B. Khuukhenkhoo<sup>3</sup> and Alexei T. Korolkov<sup>2</sup>**

<sup>1</sup> A.P. Vinogradov Institute of Geochemistry SB RAS, Irkutsk, Russia

<sup>2</sup> Irkutsk State University, Irkutsk, Russia

<sup>3</sup> Institute of Physics and Technology of MAS, Ulaanbaatar, Mongolia

\* **Corresponding author:** tsagaanbyambasuren@gmail.com

# RELATIONSHIP BETWEEN MAJOR AND TRACE ELEMENTS IN ULAANBAATAR SOILS: A STUDY BASED ON MULTIVARIATE STATISTICAL ANALYSIS

**ABSTRACT.** This article focuses on the relationships between major (Si, Al, Mg, Fe, Ca, Na, K, S, P and Ti) and potentially toxic trace (Ag, As, B, Ba, Bi, Co, Cd, Cr, Cu, F, Ge, Mo, Mn, Li, Ni, Pb, Sb, Sn, Sr, Tl, V and Zn) elements in Ulaanbaatar surface soils and also sources of the trace elements in the soils distinguished by the methods of multivariate statistical analysis. Results of exploratory data analysis of 325 Ulaanbaatar soil samples show the accumulation of Ca, S, B, Bi, Cu, Mo, Pb, Sb, Sn, Sr and Zn in urban soils. The major elements were grouped by cluster analysis in tree associations characterizing main soil fractions: sandy P-(K-Na-Si), clayey (Mg-Ti-Fe-Al) and silty (S-Ca). The factor analysis shows that silty fraction is enriched in major elements of both natural and anthropogenic origin. The principal component analysis from 32 variables extracted nine principal components with 82.49% of the cumulative explained variance. The results of cluster and factor analyses well agree and reaffirm the enrichment causes of potentially toxic elements are a coal combustion at thermal power stations (B, Bi, Ca, Mo, S and Sr) and traffic emissions (Cu, Pb, Sn and Zn). Spatial distributions of trace elements in the districts of Ulaanbaatar city were obtained by ordinary kriging. It is illustrated that the different principal components define the various origins and patterns of accumulation of trace elements in soils. The supplementation of data set by the concentration of organic carbon and the species of elements could help to identify the sources of such elements as P, Ni, Al, Fe, Ca, Ba, Bi, Cr, Zn, Sr and Sb in urban soils more completely.

**KEY WORDS:** urban surface soils; major and trace element; clayey, silty and sandy fractions; multivariate statistical analysis; ordinary kriging

**CITATION:** Elena V. Shabanova, Ts. Byambasuren, G.Ochirbat, Irina E. Vasil'eva, B. Khuukhenkhoo and Alexei T. Korolkov (2019) Relationship between major and trace elements in ulaanbaatar soils: a study based on multivariate statistical analysis. *Geography, Environment, Sustainability*, Vol.12, No 3, p. 199-212  
DOI-10.24057/2071-9388-2019-18

## INTRODUCTION

Environmental pollution is a worldwide problem that humanity is facing today. It is well known that the soil pollution can affect human health. Soil is considered as a dynamic ecosystem, able to accumulate and transport many components (including trace elements). Some of those trace elements are natural components of the environment and are healthy for humans, animals and plants. However, if the concentrations of these elements are significantly elevated in ecosystems, they are recognized as harmful. Different anthropogenic (wastes from different industries and transportation) and natural (soil-forming processes) sources influence the soil composition and the ability of soil for self-restoration (Kabata-Pendias 2011). The urban soils are much more vulnerable to pollution due to a low capacity of natural self-purification processes.

When studying the urban soils with wide spatial variations of features, lower buffer capacity and fertility loss, it is important to know both the concentrations of chemical elements and the geochemical structure in order to understand the relationships between soil and underlying rocks, and also to reveal the potential pollutants (Norra et al. 2006; Maurice 2009; Zinkutė et al. 2011; Chai et al. 2015; Byambasuren et al. 2018). In addition, the major element composition of soils is useful for studying the geochemical barriers, where mechanisms of trace element fixing by minerals are conditioned by sorption and oxidation-reduction processes, and by formation of new minerals-carriers (Vodyanitskii 2008; Kosheleva et al. 2015). However, many studies are limited by a narrow set of trace elements despite the clayey, silty or sandy fractions affect the soil elemental composition and the trend of biogeochemical processes (Norra et al. 2006; Maurice 2009; Zinkutė et al. 2011). Nowadays, the methods of multivariate statistical analysis are widely used to identify the sources of environmental pollution and to reveal the relationships between elements in the soil cover (Norra et al. 2006; Wong et al. 2006; Chen et al. 2008; Chai et al., 2015; Luo et al. 2015; Steinnes and Lierhagen

2018; etc.). Besides multivariate statistical analysis is often employed to develop measures for soil fertility improvement by the geostatistical modeling of under study areas mapping (Armstrong 1998; Facchinelli et al. 2001; Lee et al. 2006; Christensen et al. 2018; etc.).

Like in other big industrial cities, the surface soils of Ulaanbaatar city (Mongolia) are exposed to a strong anthropogenic impact due to the growth of the urban population and number of industries, industrial and domestic wastes, and thus have to be subject of continuous environmental monitoring. Therefore, the aim of the present study was to investigate and interpret the relationships between major (Si, Al, Mg, Fe, Ca, Na, K, S, P and Ti) and potentially toxic trace (Ag, As, B, Ba, Bi, Co, Cd, Cr, Cu, F, Ge, Mo, Mn, Li, Ni, Pb, Sb, Sn, Sr, Tl, V and Zn) elements of Ulaanbaatar surface soils to identify the sources of element supply into urban soils. The study included:

statistical description of sets containing 32 elements representing the urban surface soils;

revealing the relationships between major elements via the cluster analysis;

interpretation of relationships between major and trace elements with the Pearson's correlation coefficient;

use of factor analysis to identify the groups of elements demonstrating similar behavior;

revealing possible sources of element supply into the soil using the spatial methods of geostatistical modeling.

## OBJECTS AND METHODS

The present study investigated soils from Ulaanbaatar city in Mongolia. The city lies at an elevation of about 1300-1500 m above the sea level in north central Mongolia, in an intermountain basin, drained by the Tuul River (106°55 E and 47°55 N). The climate is sharply continental with large amplitude fluctuations in annual and daily

temperatures. Nowadays, the area of the city is 4704.4 sq. km; it refers to the Khangai soil-bioclimate province, the Prekhentei (Cis-Khentei) district with chestnut and dark-chestnut soils under eluvial and trans-eluvial positions and alluvial stony-pebble soils in accumulative landscapes of river valleys. Carbonate dark-chestnut soils are neutral in reaction and poor in humus (2-3%) with carbonate-free upper horizons in the soil profile and occurs in the valley of the Tuul River and on the south slopes of Chingeltei Uul with wormwood-herb-grass communities (Gerasimov et al. 1984; Kasimov et al. 2011).

The parent rocks here include the Archean granites, Carboniferous metamorphic shales and Neogene mottled clays often containing readily soluble salts and gypsum, sand and conglomerates. The Quaternary pebbly sand-loamy alluvial deposits predominate in the river valleys. The shales and clays are enriched in Fe, Mn, Cr, Co, Pb, Ni and Ti; while granites, sandy sediments and river alluvium are poor in these elements; Mn, Mo, V, Co and Pb contents are at the Clarke level (Batkishig 1999; Vasilyeva et al. 2013).

Ulaanbaatar city currently is an integrated industrial-transport-residential area with the population of 1 417 396 people (Capital statistics 2018). The central area of the city is occupied by multi-storied buildings (residential houses, buildings for different industrial enterprises and institutions), while most of the city's outskirts are occupied by unplanned ger (yurt) districts. Such ger residences lack sanitary conditions and accessible transportation; gers are heated with firewood or coal, being an important source of air pollution.

In total 325 soil samples subjected to different anthropogenic impact were collected in Ulaanbaatar using a non-regular sampling network in 2010-2011 (Vasilyeva et al. 2013; Byambasuren et al. 2018): close to thermal power plants, highways, residential areas and parks (Fig.1). The samples were collected and prepared using the normative documents (ISO 2008). The atomic-emission spectrometry with a.c. arc discharge (Vasil'eva and Shabanova 2012) was used to determine concentrations of 30 elements (Si, Al, Mg, Fe, Ca, Na, P, Ti, Ag, As, B, Ba, Bi, Co, Cd, Cr, Cu, F, Ge, Mo, Mn, Li, Ni, Pb, Rb, Sb, Sn, Sr, Ti, V и Zn), while the concentrations of K

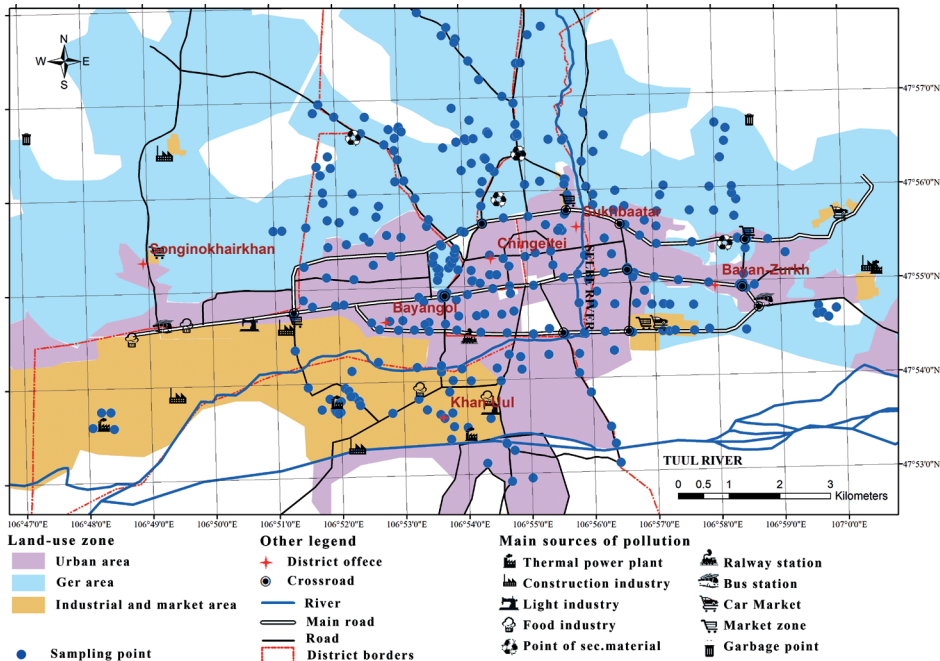


Fig. 1. Scheme of soil sampling with the characterization of different Ulaanbaatar districts

and S were defined by X-Ray fluorescence analysis (Gunicheva 2012).

This analytical information was sequentially treated by exploratory data analysis (calculation of minimum, maximum, median, average, geometric mean, coefficients of variation, skewness and kurtosis under 95 % confidence intervals); Shapiro-Wilk test (checking normality of each element concentration distribution in a set); cluster and factor analysis (classification of soil fractions in terms of major element composition and identification of soil pollution source). As the distribution of each element analyzed in the topsoil can be different from normal distribution, the analytical data were additionally transformed by Box-Cox method. The hierarchical relationships between major elements were described via the cluster analysis, where the Euclidian distance between primary transformed analytical data was used as a similarity measure and the distance between two clusters was calculated with Ward's method. Matrix of Pearson's correlation coefficients was calculated in order to describe the coupling strength between major and trace elements without identifying the causes and consequences of gotten geochemical associations. Factors describing the similarities and differences in the behavior of elements were distinguished by the principal component analysis. Amount of principal components (PC) was selected via Kaiser's criterion, i.e. the factors having eigen-values over 1 were taken into account. The normalized factor loadings (the varimax rotation strategy) increased the data interpretability. The spatial distributions of element groups (factors) were established by the ordinary kriging, where an index expressing the similarity degree of a PC to the association of elements in the sample was used. Some features of the land use and the geological structure of the territory of Ulaanbaatar city as well as the element distributions in the surface soil were taken into account when interpreting the geostatistics results and identifying sources of elements. The statistical procedures were calculated

and generalized via Microsoft Office Excel 2013 and STATISTICA 13; the geostatistical modeling was done with ArgGIS 13.

## RESULTS AND DISCUSSION

Table 1 shows statistical features in trace element distribution in surface soils of Ulaanbaatar city. The concentrations of major (Si, Al, Fe, Mg, Ca, Na, K, P, S, Ti) and trace (F, Ba, Sr, Li, P, B, Mn, Ni, Co, V, Cr, Mo, Cu, Pb, Zn, Ge, As, Sn, Sb, Ag, Tl, Bi, Cd) elements vastly varied. Concentrations of major elements (Si, Al, K and Ti) appear to be similar to the geochemical background in Mongolia (Vasilyeva et al. 2013) while the concentrations of other elements exceed their regional background values. The regional background values of the majority of the above elements are significantly different from their abundances in the lithosphere due to specific features in geology and landscape (Soil cover... 1984). The ratio of an average concentration of element in urban soil to regional background value of the same element more than 1 suggests the existence of some local anomalies on geochemical barriers which could, in certain conditions, lead to the enrichment by this element, i.e. a combination of higher concentrations and wide element variations suggests an anthropogenic or pedogenic origin of the element (Wei et al. 2010). Therefore, the available data for the urban soils indicate the accumulation of Ca, Na, S, B, Bi, Cu, Mo, Pb, Sb, Sn, Sr и Zn and removal of Mg, V, Co and Cd.

Sets of initial data for all elements (Table 1) demonstrate the consistency of median, average and geometric mean of total concentrations; a wide spread of data; asymmetric and sloping-like distributions. The Shapiro-Wilk test revealed the lack of normal distribution for elements throughout the city area. Such behavior is typical of urban topsoil with a layer thickness of about 50 cm, produced by mixing, filling or by burial of land surfaces in urban and suburban areas. The skewness significantly reduced for transformed data elements; though most elements (Si, Fe, S, As, B, Ba, Bi, Cr,

Cu, Sb, Mo, Mn, Ge, Co, Li, V, Ba and Sr) still preserved the sloping-like shape of their distribution. The transformed data only for Al, Ca, Na, P, Ag, Cd, Ni, Pb, Sn, F and Sr can be regarded as normally distributed in terms of three criteria (skewness and kurtosis, calculated indicator of Shapiro-Wilk test at  $p > 0.05$ ).

The relationships of major elements in Ulaanbaatar soils were characterized by means of cluster and factor analyses. Both analyses revealed the same groups of elements [P-(K-Na-Si)]-[(S-Ca)-(Mg-Ti-Fe-Al)], which are related to certain soil fractions (Fig. 2). A group of elements P-(K-Na-Si) represents a sandy fraction. Sands formed as a result of mechanical weathering under dry climatic conditions of Mongolia often contain quartz, feldspar, clay and gypsum fragments (Gerasimov et al. 1984; Norra et al. 2006). Terrigenous clastic rocks with high content of sodium and potassium are mainly distributed in this area. Silicon in this association occurs as quartz and characterizes sandy soil. The presence of phosphorus in this group can be best explained by increasing

phosphate adsorption of soils enriched in sodium at pH over 6.5 (Maurice 2009). The similarity in chemical composition of clayey and silty soil fractions complicates distinguishing the remaining major elements between fractions. It has been suggested that clayey fraction including the following group of elements (Mg-Ti-Fe-Al) predominates in the Ulaanbaatar topsoil. This fraction is hard to separate from the silty fraction that contains Ca and S. However, elements of (S-Ca) group could be of anthropogenic origin as well, as sulfur is regarded as an air pollutant in areas, which widely use combustion of brown coal (Amgalan et al. 2016). Nowadays, 90 % of electricity in Mongolia is produced by thermal power stations which burn brown coal with sulfur content varying from 0.2 to 3.2 wt. % (Erdenetsogt et al. 2009).

Table 2 shows correlation coefficients between major and trace elements. Positive correlation between Mn, Ba, Li, B, Ge and major elements of sandy and clayey fractions indirectly suggests a natural origin of these trace elements.

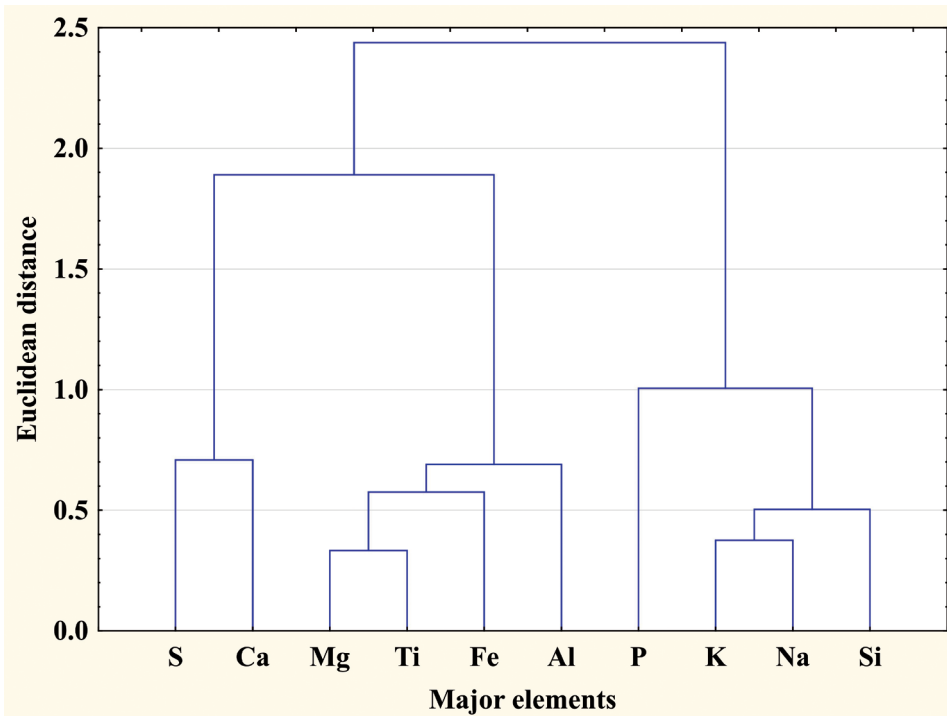


Fig. 2. Dendrogram of relationships between major elements in urban soils

Table 1. Results of exploratory data analysis for each chemical element in the data set

Element	Measure unit	$C_{BG}$	Statistics of set of obtained concentrations					Statistics of data spread		Coefficients, describing data					
			$\mu$	M	$C_{GM}$	$C_{min}$	$C_{max}$	$\sigma$	V	Initial			transformed		
										S	K	W	S	K	W
Si	% wt.	30	28.76	28.83	28.64	19.51	34.79	2.58	9	-1.19	3.65	0.00	0.18	2.42	0.00
Al		6.7	6.99	7.02	6.92	4.1	9	0.94	13	-0.47	0.6	0.15	0.00	0.19	0.77
Mg		0.9	0.68	0.66	0.65	0.21	1.12	0.21	31	-0.66	0.31	0.00	-0.02	-0.44	0.15
Ca		1.6	2.26	2.00	2.08	1.00	6.7	1.08	48	2.25	5.59	0.00	0.01	0.19	0.54
Fe		2.9	2.89	2.8	2.75	1.05	7.5	0.98	34	1.67	5.2	0.00	-0.01	1.23	0.33
Ti		0.38	0.37	0.37	0.35	0.11	1.00	0.13	35	2.55	11.68	0.00	0.02	3.68	0.00
Na		1.5	2.1	2.2	2.03	0.63	3	0.48	23	-0.96	1.11	0.00	-0.11	-0.09	0.31
K		2.2	1.99	2.08	1.95	0.64	2.69	0.38	19	-1.37	1.97	0.00	-0.12	0.45	0.01
P		0.105	0.12	0.098	0.1	0.038	0.32	0.058	51	1.4	1.85	0.00	0.01	-0.24	0.68
S		0.092	0.19	0.11	0.12	0.023	2.52	0.34	182	6.08	40.62	0.00	-0.11	1.76	0.30
Ag	ppm	-	0.29	0.18	0.2	0.05	10	0.61	208	13	202	0.00	0.00	0.04	0.35
As		12	11	9.7	10	2.6	64	6	55	5	35	0.00	-0.21	4.46	0.00
B		35	56	51	53	28	230	20	37	4	23	0.00	-0.1	1.36	0.00
Ba		700	671	705	656	364	1055	140	21	-0.1	0.9	0.00	0.05	1.15	0.00
Bi		0.50	0.72	0.68	0.7	0.4	3.6	0.25	35	6	57	0.00	-0.09	1.17	0.00
Cd		1	0.82	0.72	0.75	0.36	3.1	0.42	50	3	9	0.00	0.02	-0.14	0.25
Co		18	12	12	11	3.9	34	3.8	32	1	5	0.00	0.01	0.75	0.01
Cr		45	59	51	53	24	960	60	101	12	64	0.00	-0.18	2.08	0.00
Cu		25	48	39	41	17	1400	82	171	14	230	0.00	-0.11	1.12	0.00
F		450	479	450	459	240	2100	166	35	4	32	0.00	-0.05	0.58	0.06
Ge		-	1.9	1.7	1.8	0.85	6.8	0.69	37	3	15	0.00	-0.11	1.66	0.00
Li		32	23	22	23	10	49	5.1	22	0.9	2.4	0.00	0.01	0.92	0.01
Mn		710	629	580	594	360	5500	406	65	11	128	0.00	-0.16	1.26	0.00
Mo		1.9	2.8	2.3	2.5	0.6	17	2.2	76	4	19	0.00	-0.18	3.06	0.00
Ni		33	35	34	34	15	73	8.5	24	1.00	1.00	0.00	0.00	0.26	0.12
Pb		20	67	50	51	19	1370	110	164	10	110	0.00	-0.03	0.22	0.05
Sb		1.2	4.3	3	3.1	0.62	200	11	264	16	278	0.00	-0.16	2.55	0.00
Sn		2.8	5.7	4.7	5	2.7	96	6.1	106	11	156	0.00	-0.01	0.34	0.06
Sr		290	428	421	424	296	671	59	14	0.6	2.5	0.01	0.00	0.99	0.12
Tl		-	0.79	0.7	0.73	0.3	2.2	0.33	41	2.00	3.00	0.00	0.00	0.07	0.00
V	83	66	66	65	31	180	14	22	1.6	11.8	0.00	0.01	1.83	0.00	
Zn	60	149	130	135	61	1600	115	77	10	110	0.00	-0.07	0.68	0.01	

Note.  $C_{BG}$  – regional background value;  $\mu$  – average; M – median of data distribution;  $C_{GM}$  – geometric mean;  $\sigma$  – scattering; V – coefficient of variation; S – skewness; K – kurtosis; W – calculated indicator of Shapiro-Wilk at  $p > 0.05$ .

A more significant correlation between elements of the clayey fraction and Mn and Li is found. The sources of these elements are carbonaceous metamorphic shales and Neogene mottled clays. The negative correlations between major elements ((Mg-Ti-Fe-Al) and (K-Na-Si)) and typical pollutants ((Pb-Sb-Ag-Cu-Zn-Sn) and (Ni-Co-V-As-F)-(Mo-Bi-Cd-Cr-Tl)) are mainly observed. Elements (Cu-Sb)-

(Mo-Bi-Cd-Cr-Tl) show significant positive correlations with sulfur. Concentrations of the above trace element for 50-90% of samples are higher than the regional geochemical background and connected with sulfur. Thus, it can be suggested that the contamination by these elements are due to combustion of brown coal and automobile petroleum (Chou 2012; Chai et al. 2015). A positive correlation of P

**Table 2. Correlations between major and trace elements (The significant correlations at the 0.05 level are marked in bold)**

Major element Trace element	Si	Na	K	P	Al	Fe	Mg	Ti	Ca	S
Ag	-0.09	-0.22	-0.05	<b>0.61</b>	0.08	0.08	0.09	0.05	0.07	0.19
As	<b>-0.63</b>	<b>-0.44</b>	<b>-0.41</b>	-0.06	-0.20	0.30	-0.14	-0.23	0.09	0.24
B	0.07	0.16	<b>0.25</b>	0.04	<b>0.33</b>	<b>0.36</b>	0.22	0.11	-0.05	<b>-0.38</b>
Ba	-0.12	0.06	0.09	<b>0.31</b>	0.03	0.03	0.05	0.00	-0.08	0.12
Bi	<b>-0.32</b>	<b>-0.38</b>	<b>-0.32</b>	-0.11	<b>-0.29</b>	0.21	<b>-0.26</b>	-0.24	0.09	<b>0.46</b>
Cd	<b>-0.65</b>	<b>-0.39</b>	<b>-0.51</b>	0.12	<b>-0.36</b>	0.17	-0.19	<b>-0.41</b>	<b>0.35</b>	<b>0.58</b>
Co	<b>-0.67</b>	<b>-0.29</b>	<b>-0.29</b>	<b>0.41</b>	-0.07	<b>0.25</b>	0.12	-0.05	0.14	0.07
Cr	-0.02	<b>-0.41</b>	<b>-0.39</b>	-0.19	<b>-0.44</b>	0.02	<b>-0.39</b>	<b>-0.30</b>	-0.06	<b>0.50</b>
Cu	<b>-0.42</b>	<b>-0.41</b>	<b>-0.47</b>	-0.11	<b>-0.29</b>	0.06	<b>-0.26</b>	<b>-0.29</b>	<b>0.34</b>	<b>0.49</b>
F	<b>-0.76</b>	<b>-0.33</b>	<b>-0.36</b>	0.14	-0.20	<b>0.30</b>	-0.18	<b>-0.31</b>	0.10	0.24
Ge	0.03	-0.05	0.00	0.19	<b>0.30</b>	<b>0.33</b>	0.24	-0.06	0.14	-0.15
Li	<b>0.28</b>	0.09	<b>0.35</b>	<b>0.33</b>	<b>0.62</b>	<b>0.51</b>	<b>0.73</b>	<b>0.43</b>	<b>-0.33</b>	<b>-0.37</b>
Mn	-0.08	<b>-0.26</b>	-0.02	<b>0.31</b>	<b>0.40</b>	<b>0.72</b>	<b>0.75</b>	<b>0.48</b>	0.03	-0.19
Mo	<b>-0.34</b>	<b>-0.46</b>	<b>-0.60</b>	<b>-0.34</b>	<b>-0.48</b>	0.12	<b>-0.32</b>	<b>-0.57</b>	<b>0.34</b>	<b>0.73</b>
Ni	<b>-0.39</b>	-0.05	-0.17	<b>0.26</b>	0.03	0.08	0.01	0.06	0.22	0.16
Pb	<b>0.25</b>	-0.17	-0.09	0.15	0.06	-0.08	0.06	0.12	0.05	0.23
Sb	0.00	-0.23	<b>-0.25</b>	-0.22	-0.18	0.05	-0.11	0.00	-0.01	<b>0.28</b>
Sn	-0.08	<b>-0.27</b>	-0.24	0.02	-0.12	0.04	-0.15	<b>-0.25</b>	0.20	0.18
Sr	-0.11	0.10	-0.17	0.17	0.10	-0.14	-0.15	0.05	<b>0.37</b>	0.11
Tl	<b>-0.37</b>	<b>-0.31</b>	<b>-0.40</b>	0.01	<b>-0.37</b>	0.01	-0.22	<b>-0.45</b>	<b>0.32</b>	<b>0.45</b>
V	<b>-0.40</b>	-0.12	-0.12	<b>0.44</b>	<b>0.25</b>	<b>0.45</b>	<b>0.42</b>	<b>0.27</b>	-0.10	<b>-0.38</b>
Zn	-0.20	<b>-0.29</b>	<b>-0.34</b>	0.01	-0.09	0.18	0.02	-0.13	<b>0.25</b>	0.20

and Ca with trace elements Ni, Co, V, As, F and Ag characterizes them as pedogenic elements, which were involved into natural formation of surface soils during the sedimentation of organic substances.

The study of correlations between major and potentially toxic trace elements in surface soils via the factor analysis revealed nine principal components (PC) out of 32 variables (Table 3). Each PC considers not more than 24.5% of cumulative explained variance, which

in total can account for 82.49% of the cumulative explained variance. Variance and cumulative explained variance for each factor varies from 7.79 to 1.01 and from 24.3 to 3.16, correspondingly. The coefficients of communality show the completeness of the description of each element (variable) via the distinguished principal components. For the majority of elements, except of Al, Ba, Bi, Ca, Cr, Fe, Ni, P, Sb, Sr and Zn, these coefficients are rather high; therefore the variables are well represented by the PCs. However,

**Table 3. Results of factor analysis showing relative loading of total concentrations of major and trace elements of surface soils (The loadings over 0.45 are marked in bold)**

Statistics	PC-1	PC-2	PC-3	PC-4	PC-5	PC-6	PC-7	PC-8	PC-9	Communality
Eigenvalue	7.79	5.08	3.25	2.37	2.13	1.90	1.57	1.30	1.01	
Cumulative explained variance (%)	24.33	40.22	50.38	57.78	64.43	70.37	75.28	79.33	82.49	
Element	Loading									
Si	<b>-0.829</b>	0.021	-0.033	0.035	0.123	-0.328	-0.201	-0.074	-0.013	0.94
Na	-0.349	-0.275	-0.258	0.194	0.295	<b>-0.428</b>	0.202	-0.331	-0.168	0.93
K	<b>-0.408</b>	-0.082	-0.232	0.304	0.340	<b>-0.462</b>	-0.316	-0.167	-0.190	0.89
P	0.185	0.227	-0.023	<b>0.822</b>	0.031	-0.137	0.076	-0.133	-0.035	0.84
Al	-0.180	<b>0.487</b>	-0.039	0.197	0.309	-0.403	0.093	-0.184	-0.099	0.77
Fe	0.307	<b>0.784</b>	0.048	-0.167	0.199	0.112	-0.160	0.209	0.017	0.86
Ti	-0.143	<b>0.547</b>	-0.105	0.143	-0.182	<b>-0.527</b>	0.118	-0.092	0.114	0.88
Mg	-0.009	<b>0.869</b>	-0.013	0.046	-0.013	-0.187	0.103	-0.282	0.028	0.95
Ca	0.142	0.020	0.279	-0.179	-0.116	0.183	<b>0.805</b>	-0.148	-0.038	0.86
S	0.110	-0.200	0.046	0.027	-0.247	<b>0.655</b>	0.193	0.373	0.290	0.96
Ag	0.022	0.184	<b>0.469</b>	<b>0.715</b>	-0.152	0.105	-0.001	0.205	-0.055	0.89
As	<b>0.778</b>	-0.054	0.110	-0.186	0.190	0.137	-0.056	0.164	0.263	0.94
B	0.169	0.229	-0.033	-0.201	<b>0.820</b>	-0.259	0.025	0.011	-0.057	0.90
Ba	0.230	-0.058	0.031	<b>0.443</b>	0.406	0.033	-0.059	-0.119	<b>0.605</b>	0.81
Bi	0.158	-0.042	0.266	-0.057	0.155	0.204	0.056	<b>0.786</b>	0.101	0.78
Cd	<b>0.487</b>	-0.056	0.178	0.192	-0.081	<b>0.680</b>	0.211	0.147	-0.089	0.96
Co	<b>0.819</b>	0.138	0.021	0.348	-0.061	0.095	0.079	-0.091	-0.143	0.92

Cr	-0.109	-0.148	0.014	-0.014	-0.215	0.307	-0.086	<b>0.761</b>	0.119	0.87
Cu	0.281	-0.167	<b>0.751</b>	0.023	-0.120	0.232	0.170	0.268	0.085	0.92
F	<b>0.846</b>	-0.087	0.146	0.070	0.254	0.216	-0.029	0.130	-0.060	0.95
Ge	-0.004	0.302	<i>0.445</i>	0.141	<b>0.709</b>	0.135	0.089	-0.104	0.068	0.91
Li	-0.226	<b>0.782</b>	-0.150	0.257	0.128	-0.104	-0.244	-0.082	-0.125	0.92
Mn	0.175	<b>0.873</b>	0.048	0.149	0.136	-0.019	0.032	0.038	-0.028	0.95
Mo	0.078	-0.148	0.290	-0.259	0.095	<b>0.773</b>	0.133	0.264	0.197	0.97
Ni	<b>0.465</b>	-0.015	0.118	0.323	-0.130	-0.302	0.349	<b>0.490</b>	-0.131	0.80
Pb	-0.384	0.100	<b>0.576</b>	0.370	-0.123	0.124	0.056	0.095	<b>0.460</b>	0.94
Sb	-0.074	-0.052	0.187	-0.179	-0.151	-0.023	0.008	0.199	0.800	0.87
Sn	-0.027	-0.074	<b>0.847</b>	0.102	0.197	0.317	-0.012	0.029	-0.063	0.93
Sr	-0.053	-0.076	-0.101	0.225	0.192	0.101	<b>0.772</b>	0.124	0.024	0.77
Tl	0.122	-0.094	0.272	0.140	-0.090	<b>0.783</b>	0.128	0.006	<i>-0.411</i>	0.97
V	<b>0.712</b>	0.384	-0.117	0.140	0.012	-0.275	-0.161	-0.260	0.011	0.95
Zn	0.209	0.023	<b>0.699</b>	-0.049	0.145	-0.008	0.037	0.108	<b>0.466</b>	0.81

the lower coefficients of communality indicate an incomplete statistical model and necessity to consider more variables (chemical elements and compounds; e.g. organic matter concentrations and/or speciation of elements).

Significant positive loadings are observed in each factor for the following elements: F>Co>As>V>>Cd>Ni – PC-1; Mn>Mg>Fe>Li>Ti>>Al – PC-2; Sn>Cu>Zn>Pb>>Ag>Ge – PC-3; P>Ag>>Ba – PC-4; B>Ge>>Ba – PC-5; Tl>Mo>Cd>S – PC-6; Ca>Sr – PC-7; Bi>Cr>Ni – PC-8; Sb>Ba>>Zn>Pb – PC-9. Negative loadings are typical of only three factors: Si>K in PC-1; Ti>>K>Na>Al – PC-6; Sb>Ba>Zn≈Pb – PC-9. Some elements are simultaneously dominated in several factors accordingly to their loadings: K (negative loadings in PC-1 and PC-6); Cd (positive loadings in PC-1 and PC-6); Ni (positive loadings for PC-1 and PC-8); Al and Ti (positive loading in PC-2 and negative loading for PC-6); Ag (positive loadings for PC-3 and PC-4); Ge (positive loadings for PC-3 and PC-5); Pb and Zn

(positive loadings for PC-3 and PC-9); Ba (positive loadings for PC-4, PC-5 and PC-9); Tl (positive loading for PC-6 and negative loading for PC-9). Thus, it implies that the above elements occur in several mineral phases of Ulaanbaatar soil samples. Fig. 3 demonstrates the spatial distributions of those factors.

As regard to geochemical classification, out of 32 elements analyzed in the urban soil cover, the most widespread elements in the Earth's crust are present in five factors: PC-1 (Si, K), PC-2 (Al, Mg, Fe, Mn, Ti); PC-4 (P), PC-6 (Na, K, Ti, S) and PC-7 (Ca), while the lithogenic elements, which characterize the composition and structure of sedimentary rocks and soils, are included in factors of PC-1 and PC-2. These factors include both major and trace elements (Si, K, F, Co, As, V, Cd, Ni and Mn, Mg, Fe, Li, Ti, Al, correspondingly) thus providing the greatest contribution to the cumulative explained variance. The first factor reveals the siderophile elements, while the second one identifies major elements of soil clayey fraction.

Trace elements from PC-1 tend to be associated with manganese phases from PC-2 (Vodyanitskii 2008). Therefore, X-ray diffractometry, NIR-spectrometry or extraction methods are required for studying such relationships and mineral phases in soil samples. Additionally, the coefficients of communality for Al, Fe and Ni suggest some organic-biological processes, which were not taken into consideration in the present study, but influence the chemical composition of the clayey fraction. Geographical distribution of elements of PC-1 and PC-2 can be closely related to the landscape of the city area (Christensen et al. 2018; Steinnes and Lierhagen 2018). Positive loadings for F, As, V, Co, Ni; Mn and Li of PC-1 and PC-2 reflect their geochemical affinities and indicate their pedogenic and lithogenic origin in soils.

PC-3 (Sn-Cu-Zn-Pb-Ag-Ge) reflects the accumulation of heavy metals Cu, Pb, Sn and Zn in soils (Table 2) and indicates their spatial distribution along central transport highways and in the vicinity of bus terminal (Fig. 3). However, the soil pollution of these elements cannot be explained by motor transport emissions only, as lead and zinc were presented in PC-9, and silver and germanium – PC-4 and PC-5, correspondingly.

Elements (P-Ag-Ba) of PC-4 highlighted three zones of the city: along the Selbe River and in ger districts (Khailaast and Chingerltei) (Fig. 3). It should be noted that the maximum contributions of PC-4 are located in places of illegal dumping. The coefficients of communalities for phosphorus and barium are low and suggest the associations of these elements with the soil organic matter (Maurice 2009), which is beyond the scope of the present study.

Other two factors (PC-5 and PC-6, and correspondingly groups of (B-Ge-Ba) and (Ti-Mo-Cd-S-Na-K-Ti) elements) have similar spatial distributions in ger districts. It indicates that the soils contain minerals formed by coal combustion. During rains, garbage and ash migrate from ger districts

located on elevated sites to low-lying areas where the element-contaminants are accumulated. Note, that sulfur from PC-6 can create complexes with toxic elements, that have high coefficient of biological absorption (over 70%) and any their speciation are highly toxic for organisms occurring in soils with poor organic matter abundance (Chou 2012). These features could be weaker if the concentrations of potassium, sodium, aluminum and titanium increase.

PC-7 and PC-8 characterize the relationships between (Ca-Sr) and (Bi-Cr-Ni) elements with lower communality coefficients, which can be possibly related to the formation of compounds with the soil organic matter. Amongst 5 key elements of PC-7 and PC-8 only nickel occurs in another factor (PC-1). Calcium, strontium and bismuth tend to accumulate in the soil cover (Table 2). PC-7 is distributed in two big areas occupied by unplanned ger districts: Bayankhushuu (north-west district) and Shark-Khad (north-east district). An increase level of soil contamination is only observed at the sale sites of firewood and coal from various deposits (Baga-nuur, Nalaikh, Shivee-Ovoo, etc.). Elements of PC-8 are distributed in the industrial area with thermal power stations # 2, 3, 4 as well as close to old inoperative station. Small plants of wool and leather processing which use reagents with bismuth, chromium and nickel, are located close the thermal power stations under operation.

The PC-9, correspondingly Sb-Ba-Zn-Pb-Tl elements, is difficult to relate to any natural or technogenic phenomena. However, based on its spatial distribution (closeness to wholesale markets), accumulation of specific wastes containing these elements could be suggested.

## CONCLUSIONS

Therefore, the relationships between major (Si, Al, Mg, Fe, Ca, Na, K, S, P and Ti) and potentially toxic trace elements (Ag, As, B, Ba, Bi, Co, Cd, Cr, Cu, F, Ge, Mo,

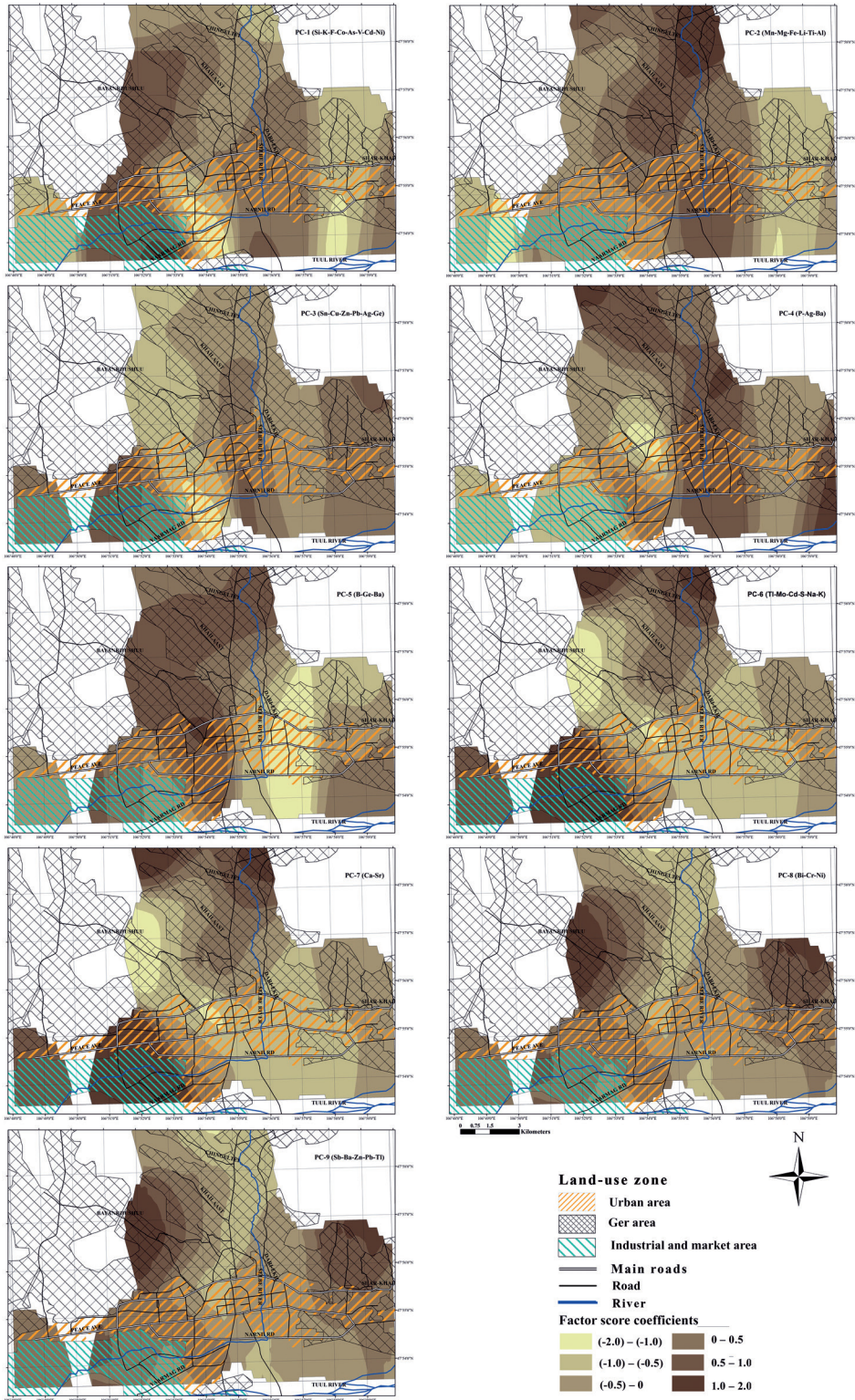


Fig. 3. Geographical distributions of the distinguished principal components

Mn, Li, Ni, Pb, Sb, Sn, Sr, Ti, V and Zn) were studied in 325 Ulaanbaatar soil samples. Results of exploratory data analysis show accumulation of Ca, S, B, Bi, Cu, Mo, Pb, Sb, Sn, Sr and Zn in urban soils (Kasimov et al. 2011; Vasilyeva et al. 2013; Amgalan 2016; Byambasuren et al. 2018). The cluster analysis distinguished associations of major elements which characterize main soil fractions: sandy P-(K-Na-Si), clayey (Mg-Ti-Fe-Al) and silty (S-Ca). The factor analysis shows that silty fraction is enriched in major elements of both natural and anthropogenic origin. From 32 variables the principal component analysis extracted nine PCs with 82.49% of the cumulative explained variance. The obtained principal components describe the most elements well, except of Al, Ba, Bi, Ca, Cr, Fe, Ni, P, Sb, Sr and Zn. The results of cluster and principal component analyses well agree with data (Kasimov et al. 2011; Vasilyeva et al. 2013; Amgalan 2016; Byambasuren et al. 2018) and reaffirm that the enrichment causes of potentially toxic elements are coal combustion at thermal power stations (B, Bi, Ca, Mo, S and Sr) and traffic emissions (Cu, Pb, Sn and Zn). Spatial distributions of trace elements were obtained by ordinary kriging. This

method also helped to identify the districts of Ulaanbaatar city being the most vulnerable to antropogenic impact (ger districts, central transport highways, areas close to bus terminal and factories of wool and leather processing). Some elements occur in the different factors thus implying various origin and pattern of accumulation of these elements in soils. The supplementation of data set by the concentration of organic carbon and the speciation could help to identify the sources of elements such as P, Ni, Al, Fe, Ca, Ba, Bi, Cr, Zn, Sr and Sb in urban soils more completely. Besides, toxic elements contamination of Ulaanbaatar soils requires a continuous monitoring, planning and conducting practical measures to improve soil fertility.

#### ACKNOWLEDGMENTS

The study was fulfilled within the framework of the Agreement on scientific cooperation between the A.P. Vinogradov Institute of Geochemistry of Siberian branch of the Russian Academy of Sciences and Institute of Physics and Technology of the Mongolia Academy of Sciences. ■

#### REFERENCES

- Amgalan N., Narantsetseg T. and Shagjamva D. (2016). Valuations of elemental concentrations of particle matter in Ulaanbaatar, Mongolia. *Open Journal of Air Pollution*, 5(4), pp. 160-169. doi: 10.4236/ojap.2016.54012
- Armstrong M. (1998). *Basic Linear Geostatistics*. Springer-Verlag Berlin Heidelberg GmbH.
- Batkhisig O. (1999). *Extended Abstract of Candidate's Dissertation in Geography*. Ulaanbaatar (in Russian).
- Byambasuren Ts., Shabanova E.V., Korolkov A.T., Vasilyeva I.E., Ochirbat G. and Khuukhenkhuu B. (2018). Distribution of Trace Elements in Soils of Ulaanbaatar. *The Bulletin of Irkutsk State University. Series Earth Sciences*, 26, pp. 31-45. (in Russian with English summary)
- Capital statistics. (2018). Official Website. [online] Available at: <http://www.ubstat.mn/> [Accessed 01 Oct. 2018] (in Mongolian).
- Chai Y., Guo J., Chai Sh., Cai J., Xue L. and Zhang Q. (2015). Source identification of eight heavy metals in grassland soils by multivariate analysis from the Baicheng-Songyuan area, Jilin Province, Northeast China. *Chemosphere*, 134, pp. 67-75. doi: 10.1016/j.chemosphere.2015.04.008

Chen T., Liu X.M., Zhu M.Z., Zhao K.L., Wu J.J., Xu J.M. and Huang P. (2008). Identification of trace element sources and associated risk assessment in vegetable soils of the urban-rural transitional area of Hangzhou, China. *Environmental Pollution*, 151(1), pp. 67-78. doi: 10.1016/j.envpol.2007.03.004

Chou C.-L. (2012). Sulfur in coals: A review of geochemistry and origins. *International Journal of Coal Geology*, 100, pp. 1-13. doi: 10.1016/j.coal.2012.05.009

Christensen E.R., Steinnes E. and Eggen O.A. (2018). Anthropogenic and geogenic mass input of trace elements to moss and natural surface soil in Norway. *Science of the Total Environment*, 613-614, pp. 371-378. doi: 10.1016/j.scitotenv.2017.09.094

Erdenetsogt B.-O., Lee I., Bat-Erdene D. and Jargal L. (2009). Mongolian coal-bearing basins: Geological settings, coal characteristics, distribution, and resources. *International Journal of Coal Geology*, 80, pp. 87-104. doi: 10.1016/j.coal.2009.08.002

Facchinelli A., Sacchi E. and Mallen L. (2001). Multivariate statistical and GIS-based approach to identify heavy metal sources in soils. *Environmental Pollution*, 114, pp. 313-324. doi: 10.1016/S0269-7491(00)00243-8

Gunicheva T. (2012). Application of nondestructive X-Ray fluorescence method (XRF) in soils, friable and marine sediments and ecological materials. In: Panagiotaras D., ed., *Geochemistry – Earth's System Processes*. InTech, pp. 371-388. Available from: <http://www.intechopen.com/books/geochemistry-earth-s-system-processes/application-of-nondestructive-wavelength-dispersive-x-ray-fluorescence-wd-xrf-method-in-soils-friabl> [Accessed 09 Feb. 2019].

ISO 10381-2008: Soil quality, Sampling, Part 1-5: Guidance on the procedure for the investigation of urban and industrial sites with regard to soil contamination.

Kabata-Pendias A. (2011). *Trace elements in soils and plants*. 4th ed. CRC Press, Boca Raton, FL, 2011.

Kasimov N.S., Kosheleva N.E., Sorokina O.I., Bazha S.N., Gunin P.D. and Enkh-Amgalan S. (2011). Ecological-geochemical state of soils in Ulaanbaatar (Mongolia). *Eurasian Soil Science*, 44(7), pp. 709-721. doi: 10.1134/S106422931107009X

Kosheleva N.E., Kasimov N.S. and Vlasov D.V. (2015). Factors of the Accumulation of Heavy Metals and Metalloids at Geochemical Barriers in Urban Soils. *Eurasian Soil Science*, 48(5), pp. 476-492. doi: 10.1134/S1064229315050038

Lee C.S., Li X., Shi W., Cheung S.C. and Thornton I. (2006). Metal contamination in urban, suburban and country park soils of Hong Kong: a study based on GIS and multivariate statistics. *Science of The Total Environment*, 356(1-3), pp. 45-61. doi: 10.1016/j.scitotenv.2005.03.024

Luo X.-S., Xue Y., Wang Y.-L., Cang L., Xu B. and Ding J. (2015). Source identification and apportionment of heavy metals in urban soil profiles. *Chemosphere*. 127, pp. 152-157. doi: 10.1016/j.chemosphere.2015.01.048

Maurice P.A. (2009). *Environmental surfaces and interfaces from the nanoscale to the global scale*. John Wiley & Sons, Inc.

Norra S., Lanka-Panditha M., Kramar U. and Stüben D. (2006). Mineralogical and geochemical patterns of urban surface soils, the example of Pforzheim, Germany. *Applied Geochemistry*, 21, pp. 2064-2081. doi: 10.1016/j.apgeochem.2006.06.014

Soil cover and soils of Mongolia. (1984). In: I.P. Gerasimov, N.A. Nogina, Dorjgotov D., ed. Moscow: Science. (in Russian).

Steinnes E. and Lierhagen S. (2018). Geographical distribution of trace elements in natural surface soils: Atmospheric influence from natural and anthropogenic sources. *Applied Geochemistry*, 88, pp. 2-9. doi: 10.1016/j.apgeochem.2017.03.013

Vasil'eva I.E. and Shabanova E.V. (2012). Arc atomic-emission analysis in geochemical research. *Industrial laboratory. Diagnostics of materials*, 78(1-II), pp. 14-24. (in Russian with English summary).

Vasilyeva I.E., Shabanova E.V., Doroshkov A.A., Proydakova O.A., Otgontuul Ts., Khuukhtnkhuu B., Byambasuren Ts. (2013) Distribution of toxic and essential elements in soils of Ulaanbaatar city. *Environment and sustainable development in Mongolian plateau and surrounding regions*, vol. 1, pp. 67-71. Available at: <https://docs.google.com/viewer?a=v&pid=sites&srcid=ZGVmYXVsdGRvbWFpbntb25wbGF0ZWZlMjMjAxM3xneDoyMzJmWJlNjRmNTU3NmM> [Accessed 09 Feb. 2019].

Vodyanitskii Yu.N. (2008). Heavy metals and metalloids in soils. Moscow: V.V. Dokuchaev Soil science Institute. (in Russian).

Wei B.G. and Yang L.S. (2010). A review of heavy metal contaminations in urban soils, urban road dusts and agricultural soils from China. *Microchemical Journal*, 94(2), pp. 99-107. doi: 10.1016/j.microc.2009.09.014

Wong C.S.C., Li X. and Thornton I. (2006). Urban environmental geochemistry of trace metals. *Environmental Pollution*, 142(1), pp. 1-16. doi: 10.1016/j.envpol.2005.09.004

Zinkutė R., Taraškevičius R. and Želvys T. (2011). Major elements as possible factors of trace element urban pedochemical anomalies. *Central European Journal of Chemistry*, 94(2), pp. 337-347. doi: 10.2478/s11532-011-0012-z

Received on February 13<sup>th</sup>, 2019

Accepted on August 8<sup>th</sup>, 2019

**Marion Aschmann<sup>1\*</sup>**

<sup>1</sup> University of Stuttgart, Institute for Economics and Law, Stuttgart, Germany

\* **Corresponding author:** aschmann@ivr.uni-stuttgart.de

# ADDRESSING AIR POLLUTION AND BEYOND IN ULAANBAATAR: THE ROLE OF SUSTAINABLE MOBILITY

**ABSTRACT.** All over the world the transport sector contributes to local air pollution as well as CO<sub>2</sub>-emissions and transportation related problems such as congestion especially in urban agglomerations. In Ulaanbaatar traffic is currently not the most important source of air pollution but it will gain importance due to a growing demand for transport and related effects. A transformation towards sustainable mobility is therefore needed which is pursued by reduction of the number of trips, influencing the modal split towards more sustainable modes and more efficient handling of mobility.

This paper discusses different characteristics of air pollution, traffic congestion and CO<sub>2</sub>-emissions and respective suitability of policy instruments. It is argued that conducting mobility more efficient will be not enough to address all relevant effects of growing demand. In doing so special attention is given to the interaction of built environment, land use and transport as well as related planning approaches which is particularly important in a situation when urban growth has to be managed.

A transfer towards sustainable mobility needs a two-step approach: a more short-term improvement related to a more environmentally friendly transport system and a long-term approach to organise urban mobility in a sustainable way by adopting an integrated urban and transport planning and influencing transport behaviour.

**KEY WORDS:** External costs of transport, sustainable mobility, integrated urban and transport planning, transit oriented development, policy mixes for sustainable mobility

**CITATION:** Marion Aschmann (2019) Addressing Air Pollution And Beyond In Ulaanbaatar: The Role Of Sustainable Mobility. Geography, Environment, Sustainability, Vol.12, No 3, p. 213-223  
DOI-10.24057/2071-9388-2019-30

## INTRODUCTION

The air pollution problem on the Mongolian plateau is long known and experienced every year especially during the heating period. Main sources of pollution in the capital city of Ulaanbaatar are identified as coal burning in gers (the traditional local tents), industrial emissions, household heating as well as emissions from public and private transport among other sources (Amarsaikhan et al. 2014, p. 124). The contribution of motor vehicles is estimated at around 10 % (WHO 2018, p.2). A specifically high contribution of the transport sector can be stated regarding NO<sub>x</sub>, the share of transport amounts to 33 % in 2010 (see Guttikunda et al. 2013, p. 594), with a strongly growing number of vehicles (see also under 2.). A recent study conducted to prepare an air quality improvement program states the causes for the low level of air quality on a general level: the study identifies the increasing number of private vehicles and polluting public buses as a part of a highly polluting urban system among inconsistent energy and environmental policy as well as uncoordinated urban development (ADB 2017, p.9).

Additional to the man-made sources there also is a specific sensitivity of the area, in Ulaanbaatar the local air pollution is enhanced by location and topography. The weather phenomenon known as thermal inversion occurs frequently (Amarsaikhan et al. 2014, p. 125). It is characterised by a layer of cooler air near ground level which is covered by a layer of warmer air. This leads to a low degree of mixing of the layers and pollutants remain in the lower layer.

But addressing the transport system is not only important because it contributes to local air pollution and causes accompanying CO<sub>2</sub>-emissions. The rapid growth of the Ulaanbaatar urban area together with a growing number of private vehicles and the existing overloaded public transportation system cause undesirable effects other than emissions. It is also the root of congestion and traffic safety problems.

The next section discusses the existing situation regarding urban mobility and its related problems and derives the goal of sustainable urban mobility as a long term development opportunity.

## GOAL OF SUSTAINABLE MOBILITY

Mobility of persons and goods is generally associated with positive effects: mobility of persons is crucial for social co-existence whereas mobility of goods is a precondition for a functioning economy based on division of labour. These effects of mobility regarding persons or goods are strongly related to the concept of accessibility: activities (e.g. home, work, leisure activities) take place in different locations whereas goods need to be transported between production facilities or to the consumers. Mobility then represents those movements conducted as trips between origins and destinations.

Negative effects of mobility relate to road traffic with private and heavy-goods vehicles. This also puts a strain on the environment and health of people especially in metropolitan areas and restricts the quality of life of urban residents. Quite often especially lower income neighbourhoods are affected, whose residents show a high degree of vulnerability which means that they are less able to cope with the situation. This is also the case for Ulaanbaatar and lower income ger districts (see ADB 2017, p. 9).

Though the situation in metropolitan areas differs according to the local conditions, local air pollution along with heavy congestion is seen as major challenges in many Southeast Asian cities by the International Transport Forum (ITF 2017a, p. 158). There is additionally an increasing transport demand with no signs of slowing down plus high vehicle growth rates for cars. Projections say that the share of private cars continues to increase strongly in developing regions and falls only slightly in developed countries (ibid, p. 13). Though increases in motorisation will bring positive benefits and contribute to economic growth, high levels of

congestion, energy consumption, local air pollution, and CO<sub>2</sub>-emissions will often follow (ibid, p. 157). Although this analysis is related to Southeast Asian countries, the results most likely also hold for Mongolia and especially Ulaanbaatar. Empirical research shows increasing car ownership rates with increasing income as a global trend.

This trend can be confirmed on the basis of information on registered vehicles in Ulaanbaatar though the data source is limited. Zhamsueva et al. state an increase in vehicles from 2005 to 2013 from 75 000 to 300 100 (see Zhamsueva et al. 2018, p. 270), which corresponds to a compound annual growth rate of 18.93 %. More recent information from the Ulaanbaatar Traffic Control Centre states more than 480 000 registered vehicles in Ulaanbaatar in 2017 (see Seaniger 2017). Correspondingly the compound annual growth rate equals 12.46 % for the time period 2013-2017, still representing a high growth rate fuelled by population growth on the one hand and growing income on the other. A huge increase in car ownership especially for middle-income Mongolians is also attributed to the low price of imported right-hand drive vehicles (see ibid).

Regarding the importance of mobility as well as the continuing growth of the transport sector a transformation towards sustainable mobility is needed to overcome the negative side effects. The transport related targets can be linked to the UN Sustainable Development Goals. Since transport and mobility are cross-cutting issues there is no single mobility target but a number of goals which are affected by transport. Transport and mobility in general should be organised in a way that the sustainability goals are supported without restricting the possibility for economic development.

The higher-order sustainability goals need to be translated into operational targets. The most relevant goal related to urban mobility is "Good Health and Well-being". It is pursued with the targets to reduce accidents and their consequences as well

as to reduce deaths and illnesses from pollution. Another very important goal is "Sustainable Cities and Communities" with the targets to provide access to safe, affordable, accessible and sustainable transport systems for all and to reduce the adverse environmental impact of cities. Beyond that transport related targets focus on climate change and energy efficiency (High-level Advisory Group on Sustainable Transport 2016, p. 11). As argued, sustainable mobility is an important field of action in a long term strategy to achieve a more sustainable city. Though sustainable transport also encompasses social and economic aspects such as affordability or operational efficiency the main focus of this paper lies on the ecological dimension.

## EXTERNAL COSTS AND POLICY INSTRUMENTS

### Characteristics of external costs

In the first place an efficient strategy should combine various instruments to reduce the negative impacts of mobility and transportation. These negative impacts are often so called external costs: in economic terms negative externalities are costs that affect a third party who did not choose to take it and which are not reflected in the prices. Related activities impose costs on society which are not or only partly taken into account when making the decision. For the transport sector the focus usually lies on negative externalities such as accidents, local and global emissions as well as noise and congestion costs. Some externalities occur within the transportation sector (such as congestion) whereas others arise locally and harm the respective residents within the area of influence (such as pollution by particulate matter) or even have a global impact (such as CO<sub>2</sub>-emissions).

The priority of reduction should be targeted to those external costs which are seen as most pressing for rapidly growing cities in Asia as aforementioned. The following tables base on this selection and show the different types of external costs.

Shown are the related cost aspects and valuation issues as well as their functional relationship with the transportation system and by which factors they are mainly influenced or determined. The variation in the characteristics, especially regarding the linkage to the transport system and main drivers, lead to the fact that policy instruments vary in their suitability to address the different external effects. The differentiation is therefore needed to determine policy or policy mixes. The characteristics listed below base on a detailed study on external costs of transport for the European commission (edited based on Ricardo-AEA 2014, p. 8f.).

Currently these effects are the main concern in Ulaanbaatar and cause an urgent demand for action, all main cost drivers are a critical issue. Congestion costs as well as CO<sub>2</sub>-emissions will become more pressing as transportation demand will increase over the next years.

To fully understand the problem with congestion costs it is necessary to distinguish among social costs and private

costs in more detail. Private costs incur at the transport user and are considered during the decision process, such as fuel cost or transport fare, but also own time costs (Ricardo-AEA 2014, p. 8f.). The impact on other transport users is not included in these private costs. The time costs by an additional vehicle (so called marginal costs) imposed on the other road users (and additional operating costs due to congestion) are therefore external costs. These costs of time losses affect private as well as commercial users can amount to a significant total welfare loss of a society. Both types of additional costs so far discussed are born by users within the transport sector. Outside the transport sector e.g. environmental costs occur in a congested situation: increased air pollution due to higher fuel consumption and noise harm the nearby residents. These cost types have strong distributional effects.

For CO<sub>2</sub>-emissions efforts and related costs to reduce them occur on a local level whereas the benefits of reduction ensue on a global scale which limits the readiness

**Table 1. Local air pollution**

Cost elements	Functional relationship	Main cost drivers
<ul style="list-style-type: none"> <li>• Health costs, years of life lost, crop losses, biosphere costs ...</li> <li>• Critical valuation issues, especially regarding long-term risks</li> </ul>	<ul style="list-style-type: none"> <li>• Correlation with traffic volume, level of emission and location</li> <li>• Strong spatial and temporal effects (hotspots)</li> </ul>	<ul style="list-style-type: none"> <li>• Population and settlement density</li> <li>• Geographical situation / sensitivity of an area</li> <li>• Level of emissions depend on</li> <li>• Type and condition of vehicles</li> <li>• ...</li> </ul>

**Table 2. Traffic Congestion**

Cost elements	Functional relationship	Main cost drivers
<ul style="list-style-type: none"> <li>• Time and operating costs (within transport sector)</li> <li>• Safety and environmental costs</li> <li>• Critical valuation issues, especially regarding value of time</li> </ul>	<ul style="list-style-type: none"> <li>• Increasing marginal cost in relation to traffic amount</li> <li>• Depending on time / location</li> </ul>	<ul style="list-style-type: none"> <li>• Type of infrastructure</li> <li>• Relation of traffic volume and capacity, mainly depending on</li> <li>• Time of the day, location, accidents ...</li> </ul>

**Table 3. CO<sub>2</sub>-Emissions**

Cost elements	Functional relationship	Main cost drivers
<ul style="list-style-type: none"> <li>• Prevention costs and damage costs</li> <li>• Critical valuation issues, esp. long-term risks</li> </ul>	<ul style="list-style-type: none"> <li>• Costs are proportional to traffic amount and fuel used</li> <li>• Effects are independent from location or time of emission</li> </ul>	<ul style="list-style-type: none"> <li>• Level of emissions depending on</li> <li>• Type of vehicles and additional equipment (e.g. air conditioning)</li> <li>• Speed characteristics</li> <li>• Fuel use and type ...</li> </ul>

to cut back these emissions. Reduction might not be a major concern in Mongolia right now but gain importance in the long term and should therefore be considered.

Detailed knowledge about these effects is required to judge the suitability of policy approaches which deal with the main cost drivers but also the functional relationship and a necessary precondition for the design of strategies need to be considered.

Measurement of these external costs is driven by the need for action or monitoring requirements regarding the evaluation of policy instruments at a later stage. Additional monetary assessment of physical indicators is no precondition though it shows the relative importance of the related issues and helps to evaluate instruments regarding their cost efficiency. The total welfare loss of a society is not only determined by the total impact but also by the valuation decisions. For congestion cost the value of time for private as well as commercial users in the transport system has to be estimated, the latter e.g. on the basis of respective average labour cost. Due to this aspect all cost rates have to be determined or adapted for a specific region or country.

**External costs and policy instruments**

Goals of sustainable mobility are pursued by three general approaches: reducing the number of trips, influencing the modal split towards more sustainable modes and conducting trips more environmentally friendly, usually by increased efficiency of vehicles.

The most important direct approach to address negative external effects of transportation is the introduction of legally binding regulations. Regulations such as EU emission standards for new vehicles limit polluting emissions and aim at enhancing specific technological progress, other regulations such as the EU directive standardising the quality of petrol and diesel fuels define standards and focus on quality control. The other prevalent approach is public spending with the objective of increasing the share of public transportation, e.g. provision or extension of infrastructure capacity or subsidies for public transport operation. To be distinguished from these are market-based instruments which influence relative prices such as taxation of energy sources or motor vehicle taxes (Brenck et al. p.418). Additional instruments can be adopted on the local level, e.g. driving restrictions or parking regulations.

The advantage of regulatory instruments is that the reduction in terms of ecological effects is more reliable and the occurrence of hot spots can be prevented; both aspects make them suitable for local air pollution. Another positive aspect is the implementation which is comparatively easy and cheap if institutional capacity is available (ibid, p.418). Notwithstanding regulatory instruments also have a main disadvantage, there is no or only a weak link to abatement costs. This can lead to a low cost efficiency, especially for CO<sub>2</sub>-emissions where reduction in the transport sector is comparatively expensive (and correspondingly reductions in other sectors cheaper). For other pollutants there are well established solutions with a high penetration of the respective vehicle markets.

Main concern of public spending in terms of public transport provision and related subsidies is to provide accessibility for urban residents, investment in public transport support indirectly affects external effects by influencing the modal share. Though this is always a costly option, increased capacity and utilisation of rail-bound systems e.g. in Europe, as well as introduction of new mass transportation systems in other parts of the world is a necessary precondition to enable the choice of a more sustainable mode.

Economic instruments aim at the price of using environmental resources, related instruments are input or pollution taxes, e.g. differentiation of petroleum tax or motor vehicle tax varying according to emission levels. An advantage of these policy instruments is that they influence demand not only related to the buying decision but also the general demand in terms of kilometres travelled. This advantage is only lost if the respective markets barely respond to pricing or high transaction costs (e.g. for implementation or enforcement of this policy) occur (ibid, p.418). But depending on the price elasticity of demand also leads to the fact that demand reaction can only be anticipated and the ecological effect cannot be controlled. Pricing instruments therefore should only be part of a strategy to reduce local air pollution.

A benefit of pricing strategies is that they are able to generate public revenues which can be used to for improving the public transport situation; on a local level this is one of the main arguments in favour of road pricing schemes.

As already mentioned regulative instruments can reliably reduce local air pollution: in Europe emission regulations regarding emission levels of new vehicles and regulation of the quality of petrol and diesel fuels effectively reduced air pollution. The legislative authority required stepwise lower emission levels for new vehicles and thereby caused the manufacturers to develop a more efficient technology for motors and emission control. Secondly, the quality of fuel was improved by an EU directive. This led to a significant decrease of specific emissions by pollutants and CO<sub>2</sub>-emissions relative to the person kilometres travelled during the last twenty years as shown for Germany in Fig. 1 (German Environmental Agency eds. 2018). A similar relationship could be illustrated by showing the increasing efficiency of freight traffic with an even more distinct decrease. In both cases the increase in trips consumes the efficiency gains and correspondingly the total emission reduction is always lower than reduction in specific emissions.

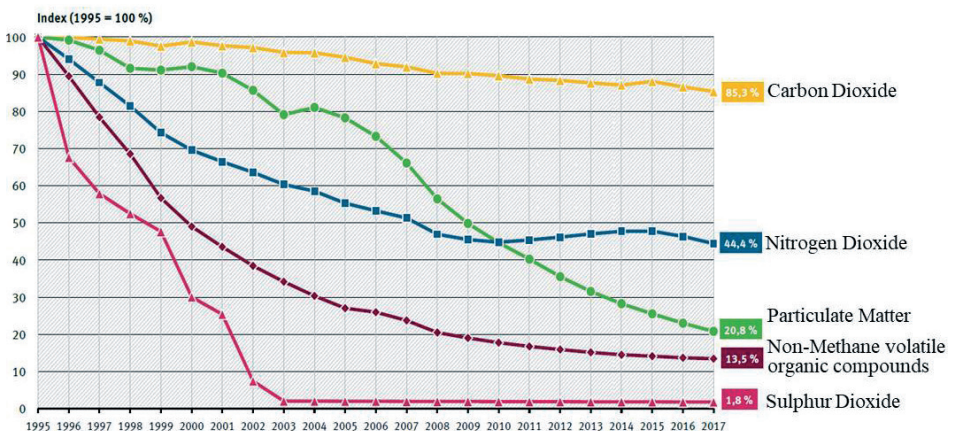


**Fig. 1. Specific emissions by private vehicles (direct emissions/person kilometres travelled). Source: German Environmental Agency (eds. 2018), URL see references Data and calculation model TREMOD Transport Emission Model, Version 5.81 (01/2018) based on standardized emission factors for road transport**

As can be seen in figure 1 the transport sector remains to be an important source of NO<sub>x</sub> and particulate matter as well as CO<sub>2</sub>. The effort to influence the modal split by public investment in sustainable modes is increasingly successful in an urban context, but emission reduction within the transport sector remains a crucial issue.

Transformation towards sustainable mobility especially in the context of urban mobility therefore requires more than better vehicle and fuel technology, relying on efficiency only will not be sufficient. Efficiency gains reduce the vehicle operating costs, which encourages an increase of total annual kilometres travelled, the actual fuel saving lies below the theoretically possible. This so called "rebound effect" has been identified and estimated by a number of empirical studies. The size of the effect reflects the elasticity of vehicle travel with respect to fuel price. Although there remains a net reduction in fuel consumption, the increased demand tightens other transport related problems such as pollution, congestion, road and parking facility costs and urban sprawl (VTPI 2017). The rebound effect thereby intensifies the problems of a continuously growing motorisation rate. The saturation level regarding the vehicle kilometres travelled can only be estimated for Mongolia but is most likely far from being reached yet, the same holds for the car ownership (motorisation) rate.

Ignoring the above characterised rebound effect leads to overestimate the impact of instruments which influence the efficiency of new vehicles, such as fuel efficiency standards, and to undervalue the effect of instruments which address vehicle use, such as transport management and pricing strategies, as part of an emission reduction policy mix.

### Transport and built environment

The policy instruments discussed so far aim at two of the three mobility goals: efficient handling and thereby reducing

external costs directly as well as a shift towards more sustainable modes. These instruments should be backed up by a mid to long-term strategy which aims at an integrated land-use and transport planning since built environment is a major determinant of travel demand and mode choice. „If travel distances, traffic congestion and traffic pollution are to be reduced there must be coordination between transportation, housing and land use programmes. Urban development should be managed so as to reduce future traffic loads and promote growth travel efficiencies“ (Cervero 2003, p. 66).

As stated above there is a strong relationship between land use and transport demand in terms of trips and kilometres travelled: Distribution of land uses in a city determines the distribution of activities and this creates demand for transport. Transportation infrastructure enables transport and provides accessibility of the different activities. Accessibility on the other hand also determines location decisions and influences changes regarding the land use.

If growth is not managed by integrated planning a trend to higher car dependency arises over time: the settlement structure becomes more scattered and users as well as planners become less sensitive to distance (and time). Growing car dependency results in a growing motorisation rate followed by investment in infrastructure for private transport which leads to increasing distance travelled.

A higher car dependency of the settlement structure is reflected in a lack or uncomfortable access to public transport, an unfavourable travel time ratio (public versus private transportation) and inconvenient accessibility of opportunities for activities by public transportation. This again fuels car dependency but also leads to low accessibility of satellite towns or scattered settlements.

Shaping settlement growth therefore is a crucial issue especially in areas with a high rate of urbanisation. The way how and where growth is accommodated determines to a large extent if a region is transit-supportive. An integrated strategy to manage settlement growth bases on "transit oriented development". With the backbone of a functioning mass transit system this planning approach focuses on built environment factors which positively influence the reduction of private trips and vehicle kilometres per capita as well as enhance public transit ridership. The most important factors are "five D's": Settlement Density, Diversity of land-uses, Design of urban environment (walkability), Destination Accessibility and Distance to transit (Ewing and Cervero 2010). Transport oriented development is often based on rail-bound systems, but other mass transit systems such as grade separated bus rapid transit systems provide a cost-efficient urban mobility solution and require a lower optimal residential density (Falcocchio and Levinson 2015, p. 367).

Pursuing the integration of land use planning as well as development on the one hand and transport planning on the other for a "Transit Oriented Development" is the aim of many planning authorities: concentrating urban development next to mass transit stations to support public transit ridership and developing transport systems to connect existing and planned development hubs. By increasing PuT accessibility alternatives to land uses based on private motorised transport accessibility are created and current urban mobility becomes more sustainable, which has the positive side effect of improving urban quality of life (Bertolini et al. 2016, p. 3).

There is extensive literature discussing the background reasoning of integrated planning as well as pursuing "smart growth" or "transit oriented development". Increasingly there are also best practice examples related to coordinated approaches of land development and transportation (Curtis et al 2016, Falcocchio and Levinson 2015). Recommendations

refer to measures such as zoning (concentrated retail activities instead of strip development along major transport arteria) or how activity centres can be designed to provide of multi-modal access (Falcocchio and Levinson 2015, p. 378ff.).

## RESULTS AND DISCUSSION: POLICY MIXES FOR SUSTAINABLE MOBILITY

To move towards an environmentally friendly transport system and in the long run to achieve sustainable mobility two goals can be identified: enhancing the efficiency in handling transport activities and influencing the demand for transport in terms of number of trips and modes used. Regulatory instruments such as efficiency standards influence external costs directly: they reduce air pollution, avoid the emergence of hotspots and can lead to a significant decrease of specific emissions for both private and commercial vehicles (see the positive effects of EU emission levels for new vehicles and regulation of the quality of petrol). The disadvantage refers to the fact that these measure only relate to the buying decision, there is no influence on the use.

In the long run for Ulaanbaatar regulatory measures will not be sufficient regarding growing population as well as a growing motorisation rate and rebound effects: Greenhouse gases will not be reduced substantially and the problem of congestion and parking remains unsolved. There is additionally a partly low accessibility of housing areas, which calls for improvement of public transportation as a backbone. Additional to regulation direct impact on behaviour and transport demand is necessary to reduce the number of trips or conduct them with a sustainable mode: suitable is a policy mix of improvement of land-use planning together with investment in public transport and economic instruments. Mixes are necessary to take spatial and temporal effects of emissions into account (see different characteristics of the external costs of transport).

A policy mix with ambitious public transport improvement and regulation of car use is able to reduce car dependency and increase accessibility within a city and at the same time cuts back emissions and congestion (ITF 2017a, p.54). On the contrary sprawling cities enhance car dependency and require investment in transport infrastructure; the International Transport Forum judges this investment as not environmentally and financially sustainable especially in Asia and Latin America (ibid, p.54).

If the modal split is to be influenced towards a higher share of public transport the capacity of the currently existing system in Ulaanbaatar needs to be enlarged. As discussed provision and access to an affordable and sustainable transport system is a precondition for sustainable mode choice. For Ulaanbaatar there is a long history of planning activities to improve the public transport system which is currently based on a bus network. A city-wide Bus Rapid Transit Scheme (BRT) is planned as a backbone of Ulaanbaatar's public transportation system, which should provide an efficient, environmentally friendly as well as accessible and affordable mass transit system. This should especially connect satellite towns and traditional ger areas with predominantly lower income residents.

At present the BRT concept together with a traffic management system is part of an urban transport investment program (ADB 2018, p.3).

The general recommendations regarding the policy mix have to be adapted to the local conditions and in doing so knowledge can be gained from international best practice examples e.g. Mexico City, which has a similar geographic situation in which air pollutants are trapped over the city. From the mid-1980s onwards the city succeeded in cutting back pollution by comprehensive air quality management addressing private households and industry (Molina et al. 2009). Although air quality has substantially improved throughout the last thirty years the city

still experiences regular problems. The air pollution mitigation strategies currently discussed as suitable policy mix ranges from state-of-the-art emission standards and mandatory vehicle inspection, differentiated economic instruments (taxes and incentives) to investment in sustainable modes and integrated land-use planning which involves tools such as a Mobility Master Plan (ITF 2017b).

## CONCLUSION

In European and American agglomerations transport is a major source of pollution whereas high emission levels in Asian and African metropolitan areas are rather caused by the use of materials and fuels for heating and cooking. Nevertheless, with increasing economic wealth the motorisation rate grows continuously and leads to congestion and pollution (Baklanov et al., p. 245).

This analysis also holds for Ulaanbaatar, currently the focus is on air quality improvement by making domestic cooking and heating more efficient. There also is awareness regarding the necessity of directly influencing the external cost with improving the quality of fuel as well as the provision of an improved system of public transportation (see below), though there are also ideas which go beyond this improvement strategy. Approaches discussed also encompass improvement and enforcement of existing regulations (traffic laws, number plate restrictions) as well as pricing strategies (introduction of a congestion charge) a.o. (see Seaniger 2017). Regarding the growing demand of private motorised transport and related consequences in the long run strong focus is required on behaviour related instruments and a change in land-use planning backed up by infrastructure investments.

Planning the new BRT system and related improvement of the management capacity of the transport agencies is an important step towards more sustainable mobility. Up to now assistance for capacity development to improve the

ability of the urban transport agencies to plan and manage urban mobility in an integrated and sustainable way has been completed in 2018 (ADB 2018, p. 3). This approach was complemented with the recommendation to centralise transport planning and policy in one agency (ibid, p.4).

This potential reorganisation would also offer the opportunity to move towards an integrated planning approach to implement the above discussed long-term strategy. Currently there is only limited attention on the need for action to take care of a growing demand of private motorised transport and related consequences in the long run which would require behaviour related instruments together with a change in land-use planning.

An implementation requires a strategic planning framework for interlinking urban and transportation planning, preferably

implemented by a specialised institution (Newman 2016). Whether a process towards sustainable urban mobility is started and how it is shaped is determined by the local agencies and needs to be based on the local frame conditions: a short term policy mix related to transport efficiency gains should be backed up by measures to influence modal split and transport demand.

Knowledge regarding barriers and challenges on the one hand and best practices or promising approaches on the other can be transferred. Especially regarding the suggested integrated planning approach barriers like overlapping responsibilities between different agencies or limited planning competences will have to be overcome. All authors nevertheless state that moving towards sustainability in transportation needs integration of various subjects as well as awareness and cooperation of all stakeholder groups. ■

## REFERENCES

- Amarsaikhan D., Battsengel V., Nergui B., Ganzorig M. and Bolor, G. (2014). A Study on Air Pollution in Ulaanbaatar City, Mongolia. *Journal of Geoscience and Environment Protection*, 2, pp. 123-128. doi: 10.4236/gep.2014.22017
- Asian Development Bank ADB (2017). Proposed Policy-Based Loan Mongolia: Ulaanbaatar Air Quality Improvement Program. Concept Paper. [online] Available at: <https://www.adb.org/sites/default/files/project-documents/51199/51199-001-cp-en.pdf> [Accessed 26 Feb. 2019].
- Asian Development Bank ADB (2018). Mongolia: Ulaanbaatar Urban Transport Capacity Development. Completion Report. [online] Available at: <https://www.adb.org/projects/documents/mon-45140-001-tcr> [Accessed 26 Feb. 2019].
- Baklanov A., Molina L.T. and Gauss M. (2016). Megacities, air quality and climate. *Atmospheric Environment*, 126, pp. 235-249. doi: 10.1016/j.atmosenv.2015.11.059
- Bertolini L., Curtis C. and Renne J.L. (2016). Introduction, In: Curtis C., Renne J.L. and Bertolini L. (eds.). pp. 3-12.
- Brenck A., Mitusch K. and Winter M. (2016). External Costs of Transport. In: Schwedes et al. (eds.). *Handbook Transport Policy*. 2nd ed. Wiesbaden, Springer, pp. 401-429 (in German).
- Cervero R. (2003). Growing smart by linking transportation and land use: Perspectives from California. *Built environment*, 29(1), pp. 66-78.
- Curtis C., Renne J.L. and Bertolini L. (2016). *Transit oriented development: making it happen*. New York, Routledge.

Ewing R. and Cervero R. (2010). Travel and the Built Environment. A Meta-Analysis. *Journal of the American Planning Association*, 76(3), pp. 265-294. doi: 10.1080/01944361003766766

Falcochio J.C. and Levinson H.S. (2015). *Road Traffic Congestion: A Concise Guide*, Springer Tracts on Transportation and Traffic 7. Cham, Springer Nature Switzerland.

German Environmental Agency (eds. 2018). Emissions of the Transport Sector (in German), [online] Available at: <https://www.umweltbundesamt.de/daten/verkehr/emissionen-des-verkehrs#textpart-1> [Accessed 26 Feb. 2019].

Guttikunda S.K., Lodoysamba S., Bulgansaikhan B. and Dashdondog B. (2013). Particulate pollution in Ulaanbaatar, Mongolia. *Air Quality, Atmosphere and Health*, 6(3), pp. 589-601. doi: 10.1007/s11869-013-0198-7

High-level Advisory Group on Sustainable Transport (2016). *Mobilizing Sustainable Transport for Development. Analysis and Policy Recommendations from the United Nations Secretary-General's High-Level Advisory Group on Sustainable Transport*, [online] Available at: <https://sustainabledevelopment.un.org/topics/sustainabletransport/highleveladvisorygroup> [Accessed 26 Feb. 2019].

ITF (2017a). *ITF Transport Outlook 2017*. Paris, OECD Publishing.

ITF (2017b). *Strategies for Mitigating Air Pollution in Mexico City*, [online] Available at: <https://www.itf-oecd.org/strategies-mitigating-air-pollution-mexico-city> [Accessed 26 Feb. 2019].

Molina L.T., de Foy B., Vázquez Martínez O. and Páramo Figueroa V.H. (2009). Air Quality, Weather and Climate in Mexico City. *World Meteorological Organisation Bulletin*, 58 (1), [online] Available at: <https://public.wmo.int/en/bulletin/air-quality-weather-and-climate-mexico-city> [Accessed 26 Feb. 2019].

Newman P. (2016). Planning for Transit Oriented Development: Strategic Principles. In: Curtis C., Renne J.L. and Bertolini L. (eds.), pp.12-22.

Ricardo-AEA (2014). *Update of the Handbook on External Costs of Transport. Final Report. Report for the European Commission DG Move*, [online] Available at: [https://ec.europa.eu/transport/sites/transport/files/handbook\\_on\\_external\\_costs\\_of\\_transport\\_2014\\_0.pdf](https://ec.europa.eu/transport/sites/transport/files/handbook_on_external_costs_of_transport_2014_0.pdf) [Accessed 26 Feb. 2019].

Seaniger C.-A. (2017). 8-Step Solution to Solving Ulaanbaatar's Traffic Nightmare. *The UB Post* 25. Jan. 2017, [online] Available at: <https://www.pressreader.com/mongolia/the-ub-post/20170125/281509340899617> [Accessed 14 June 2019].

Victoria Transport Policy Institute VTPI (2017). *Rebound Effects. Implications for Transport Planning*. TDM Encyclopedia, [online] Available at: <http://www.vtpi.org/tdm/tdm64.htm> [Accessed 26 Feb. 2019].

World Health Organisation WHO (2018). *Air Pollution in Mongolia: Policy Brief*, [online] Available at: [http://www.wpro.who.int/mongolia/publications/20180228\\_policy\\_brief\\_on\\_air\\_pollution.pdf](http://www.wpro.who.int/mongolia/publications/20180228_policy_brief_on_air_pollution.pdf) [Accessed 26 Feb. 2019].

Zhamsueva G.S., Zayakhanov A.S., Starikov A.V., Balzhanov T.S., Tsydyпов V.V., Dementyeva A.L., Khodzher T.V., Golobokova L.P., Khuriganova O.I., Azzaya D. and Oyunchimeg D. (2018). Investigation of chemical Composition of Atmospheric Aerosol in Ulaanbaatar During 2005-2014. *Geography and Natural Resources*, 39(3), pp. 270-276. doi: 10.1134/S1875372818030113

**Endon Zh. Garmaev<sup>1</sup>, Anatoly I. Kulikov<sup>2</sup>, Bair Z. Tsydypov<sup>1\*</sup>,  
Bator V. Sodnomov<sup>1</sup>, Alexander A. Ayurzhanaev<sup>1</sup>**

<sup>1</sup> Baikal Institute of Nature Management SB RAS, Ulan-Ude, Russia

<sup>2</sup> Institute of General and Experimental Biology SB RAS, Ulan-Ude, Russia

\* **Corresponding author:** bz61@binm.ru

## ENVIRONMENTAL CONDITIONS OF ZAKAMENSK TOWN (DZHIDA RIVER BASIN HOTSPOT)

**ABSTRACT.** Ecological problems of Zakamensk town are associated with sand deposits that were formed as a result of mining activities of former Dzhidinsky tungsten-molybdenum plant. Sands are accumulated in large quantities and they contain dangerous concentrations of heavy metals. Desertification in an urbanized area is manifested locally, but it differs from agricultural desertification by a profound and comprehensive destructive change in the components of the environment. Maps of soils, vegetation, types of lands, as well as ecological zoning maps of Zakamensk were created. The basis for the creation of electronic maps using GIS were stock, archive and own materials, topographic maps and remote sensing data. Urbanized desertification in Zakamensk is caused by chemical contamination of sandy eluvium, the spreading of pollutants by water flows and wind currents. Erosion occurs both in the form of flat flushing and linear erosion. The most intensive is gully erosion. Quantitative parameters of temporal variability of the erosive rainfall potential for the Zakamensk town are received. The quantitative characteristics of loads of pollutants on the territory of the town are determined on the basis of the erosion-deflation models. The calculations showed that 204 tons/ha of contaminated sand annually falls into the settlement area with water-erosion flows (Pb – 3.7 tons, W – 4.3 tons). Moreover, active wind activity led to the deposition of more metals (Pb – 5.6 tons, W – 6.5 tons) in the town.

**KEY WORDS:** erosion, deflation, residual soils, water streams, erosion rainfall potential, relief erosion index

**CITATION:** Endon Zh. Garmaev, Anatoly I. Kulikov, Bair Z. Tsydypov, Bator V. Sodnomov, Alexander A. Ayurzhanaev (2019) Environmental Conditions Of Zakamensk Town (Dzhida River Basin Hotspot). Geography, Environment, Sustainability,

Vol.12, No 3, p. 224-239

DOI-10.24057/2071-9388-2019-32

## INTRODUCTION

The use of mineral deposits lies at the heart of our civilization. Mineral extraction is one of the most powerful types of technogenesis. Its impact on the natural environment is increasing and spreading over large areas. In mining regions, huge amounts of waste are generated during the extraction of minerals (Karthe et al., 2014). These are the large areas of almost complete destruction of natural landscapes, occupied by mines, wells, quarries, rock dumps, wastes of primary ore beneficiation (tailings), heaps, transport trunk lines, etc. In recent decades, one of the main problems of environmental safety is the elimination of the consequences of past economic activity.

This paper considers urban ecosystem of Zakamensk, and within its boundaries, the area of activity of the former Dzhidinskyy tungsten-molybdenum plant (DTMP). The town is located on the south-west of the Republic of Buryatia near state border with Mongolia in 404 km from Ulan-Ude in the central part of the Dzhida ridge (Fig. 1). The research subject is located in the mountain-taiga area of the valley of the river Modonkul, the right tributary of the Dzhida river which belongs to the largest Baikal Lake drainage system – the Selenga River (Chalov et al., 2013; Chalov et al., 2015; Karthe et al., 2017; Environmental Atlas-monograph ..., 2019). The height of the mountain valley bottom is about 1100 meters above sea level; the mid-altitude

mountains with absolute height of 1300-1400 meters are adjacent to the town.

The emergence of Zakamensk is inextricably connected with the activity of DTMP, which was established in 1934 by order of the USSR People's Commissariat of Heavy Industry on the basis of the Dzhidinsky ore cluster, which unites Pervomaiskoye molybdenum deposit and Holtoson and Inkur tungsten deposits. In the pre-war and war years, the plant was a leader in tungsten concentrate production. Thus, its production in 1934 was 73.5 %, in 1935 65.7 %, in 1937 50 %, in 1944 40 % of the total volume of tungsten concentrate produced in the USSR (Implementation ..., 2007). In the postwar years, the plant increased its production capacity of tungsten and molybdenum concentrates. In 1992, in connection with the conversion of the military industry, the production decreased by 70 %. February 26, 1998 Dzhidinsky tungsten-molybdenum plant ceased to exist (Implementation ..., 2007).

During the shutdown of the plant, the sanitary and environmental requirements for the closing enterprises were not met. Mining operations were stopped, but the mine workings were not eliminated (after the plant was shut down, toxic tailings known as "Gidrootval" (Hydro Dump) and "Lezhaliye peski" (Deserted Sands) remained); reclamation of disturbed lands was not carried out; issues of stopping the discharge of polluted mine water into surface water bodies were not resolved;

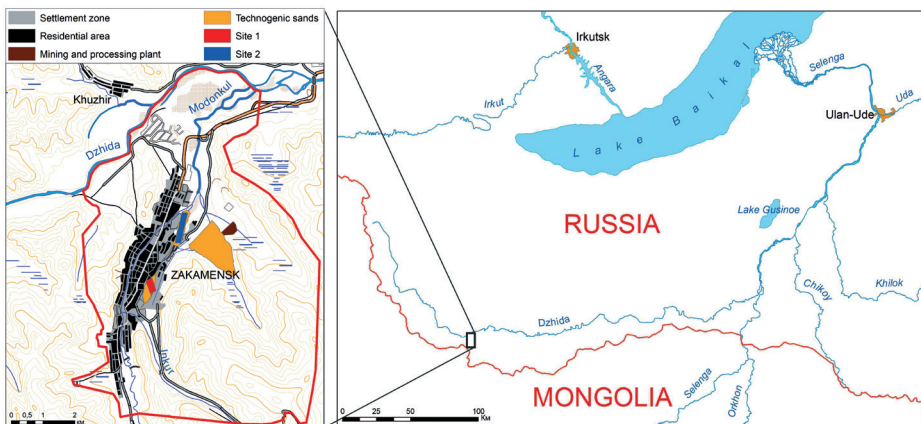


Fig. 1. Geographical location of Zakamensk town

design environment protection solutions in the area of Zakamensk and adjacent territories were not implemented, etc. All this led to the fact that with the suspension of the plant's activities, the negative impact of its waste on the environment and the population not only did not decrease, but also significantly increased (Timofeev et al., 2018).

During the period of the plant's operation, 44.5 million tons of enrichment waste were stored in tailing dumps.

The goal of the study is a quantitative assessment of the transfer of pollutants (heavy metals) to the territory of Zakamensk from technogenic sands by water and wind flows.

The following tasks were set:

- 1) to determine the boundaries and geographical location of the polluted territory of Zakamensk;
- 2) to develop large-scale cartographic models of soils, vegetation, land types and ecological zoning of the town;
- 3) to identify the quantitative parameters of heavy metal pollution due to water-erosion processes, as well as deflation.

## MATERIALS AND METHODS

Ecological problems of Zakamensk are associated with sand deposits (technoeluvium) – the consequences of mining activities. Concentrating plants are located here, and the tailing dump of the former Dzhidinsky tungsten-molybdenum combine adjoins the residential area. Sands are accumulated in large quantities and contain dangerous concentrations of heavy metals. Desertification in an urbanized area (urban desertification) appears locally, and differs from agricultural one by a profound and comprehensive destructive change in the environment components.

In this paper maps of soils, vegetation, types of lands, as well as ecological zoning maps of Zakamensk were created with the help of geoinformation system ArcGIS 10.2. The basis for the creation of electronic maps using GIS were stock, archive and own materials, topographic maps and remote sensing data (Khamnaeva et al., 2013).

In Zakamensk urban desertification is associated with chemical pollution of sandy techno-eluvium and the spreading of pollutants by water and



**Fig. 2. Sheet erosion of the techno-eluvium surface**



**Fig. 3. Gully erosion of the techno-eluvium surface**

wind currents (Kulikov et al., 2012; Khamnaeva et al., 2013; Kasimov et al., 2016). Erosion occurs both in the form of sheet (Fig. 2) and linear erosion (Fig. 3). The most impressive is gully erosion (Tulokhonov et al., 2018).

In Russia, up to 7 million hectares of land are affected by gully erosion, the number of gullies is approaching 15 million, the annual increase in the length of the gully network is more than 20,000 km. Over 700 cities in Russia are exposed to gully erosion (Osintseva, 2001; Kovalev, 2009). Moreover, gully formation in urban area cannot be considered obviously dangerous. There is an interdependent system: city – gully-draw network.

Technoeluvium of Zakamensk refers to loose or loosely connected sands (Table 1). The density of sands is considerable, so the total porosity is low, as is the

porosity factor. For erosion it is important that the sands are characterized by a large filtration of moisture.

Among the particle-size fractions, particles larger than 0.2 mm predominate (Table 2). Thin fractions are contained in an amount of about 12 %. By origin and soil texture (GOST (State standard) 25100-95), the deposits of technoeluvium belong to the class of technogenic dispersed soils, to the group of disconnected ones, to a subgroup of natural bulk dislocated formations, to the type of production and economic waste, to the type of sand (GOST, 2001). Since the content of fractions is larger than 0.25 mm and exceeds 50 %, then the sands of technoeluvium have an average size. According to this parameter, sands of techno-eluvium are similar to natural aeolian sands (Ivanov, 1971).

**Table 1. Some physical properties of the techno-eluvium sands of Zakamensk**

Type	$\rho_s, \text{g/cm}^3$	$\rho_d, \text{g/cm}^3$	Void content, vol. %	$K_{\phi}, \text{cm/day}$	$e$
Loose sand	2.5	1.67	33	140	0.50
Sand connected	2.5	1.60	36	120	0.56

Note:  $\rho_s$  – density of the solid phase,  $\rho_d$  – density of the soil,  $K_{\phi}$  – filtration coefficient,  $e$  – porosity coefficient, i.e. the ratio of the pore volume to the volume of the solid phase,  $e = (\rho_s - \rho_d) / \rho_d$

**Table 2. The granulometric composition of the techno-eluvium**

Size of fractions, mm	Content, %
1-0.5	36.98
0.5-0.2	39.28
0.2-0.074	12.06
0.074-0.044	5.30
< 0.044	6.38
Total:	100

In general, erosion begins if the condition is met:

$$r_{\bar{a}} > q \quad (1)$$

where  $r_{\bar{a}}$  is the precipitation rate;  $q$  is the water absorption rate by the surface of the techno-eluvium.

The rate of water flow ( $Q$ ) at different slope sections ( $x$ ) is determined by the law:

$$dQ/dx = r_{\bar{a}} - q \quad (2)$$

so, it depends on the flow loss as it moves down the slope to absorb, and the erosion loss of the soil ( $V$ ) will depend on  $w$  – the cross-sectional area of the drain and  $l$  – the runoff length:

$$V = \int_0^l w dl \quad (3)$$

The shear force of the water flow ( $F_{cd}$ ) depends on the flow rate ( $v$ ), the water layer ( $h$ ), and the ratio of the mass of the particle ( $m$ ) to its cross-sectional area ( $S$ ):

$$F_{cd} = f(F_{cu}, v, h, m/S) \quad (4)$$

The value of  $F_{cd}$  increases with increasing  $v$  and  $h$  and decreasing  $m/S$ .  $F_{cu}$  (the adhesion of soil particles) is a function of the particle density ( $\rho$ ) and the strength of its bond with other particles  $F_{cb}$ .  $F_{cb}$  depends on the content of colloids in the soil and many other factors:

$$F_{cu} = f(\rho, F_{cb}) \quad (5)$$

Erosion occurs under the condition  $F_{cd} > F_{cu}$ . The rate of the water flow at which the separation of solid particles from the soil surface begins is called the critical

velocity of the flow ( $V_{kp}$ ). At the same density, the total cross-section of the particles per volume unit increases with decreasing of size. Therefore, the critical flow velocity is lower for soils with smaller microaggregates and particles than on soils with large particles.

For predictive calculation of erosion of Zakamensk technogenic sands we use the Universal Soil Loss Equation (USLE), developed in the USA (Wischmeier and Smith, 1978). The USLE model has been adapted for the territory of north part of Eurasia in a number of works (Larionov, 1993; Kuznetsov and Glazunov, 2004).

The equation has the form

$$Q = 0.224 \cdot R_{30} \cdot K \cdot LS \cdot C \cdot P \quad (6)$$

where  $Q$  – soil loss during erosion, kg/m<sup>2</sup>/year;  $R_{30}$  – rainfall erosion index;  $K$  – a complex characteristic of soil properties (erodibility or soil washability);  $LS$  – relief erosion potential;  $C$  – complex characteristics of the soil use;  $P$  – complex characteristics of anti-erosion measures. For our case, the last two terms are equated to unity, because technoeluvium is not used in agriculture.

The Universal Soil Loss Equation makes it possible to determine the soil loss from slopes in a wide range of time scales from one erosive event to the entire period of development. Disadvantage: the inability to calculate the amount of accumulation and redeposition of sediments within the slopes.

Rainfall erosion index is calculated (Wischmeier, 1959):

$$R_{30} = E \cdot I_{30} / 100 \tag{7}$$

where  $I_{30}$  – 30-minute rainfall intensity, mm/hour;  $E$  is the kinetic energy of the drops for 1 mm of rainfall falling out on 1 m<sup>2</sup>, kg<sub>f</sub>·m.

Energy of rainfall is determined by the formula (Wischmeier and Smith, 1958):

$$E = 1.213 + 0.8901 \cdot 1gr_r \tag{8}$$

where  $r_r$  – rainfall intensity, mm/hour.

To determine the layerwise kinetic energy of rain and, in general, the rainfall erosion index is rather difficult. Moreover, approaches and design schemes should be unified for conducting a comparative analysis. The rainfall erosion index ( $R_{30}$ ) is based on the multiply of the precipitation layer on a maximum 30-minute intensity:

$$R_{30} = 0.258 \cdot H \cdot I_{30} - 0.149 \tag{9}$$

where  $H$  – precipitation depth, mm.

Index  $I_{30}$  is determined by the following equation :

$$I_{30} = 0.121 \cdot \exp(0.0529 \cdot H) \tag{10}$$

Calculations are made separately for each rainfall with 10 mm layer or more. Rainfalls

in a smaller amount do not cause a noticeable washout (Tolchel'nikov, 1990). Next is the summation of  $R_{30}$  individual rainfalls during the season with liquid precipitation.

RESULTS AND DISCUSSION

Thematic mapping

Soil is one of the main depositing elements of the ecosystem. According to the soil zoning, the territory of Zakamensk belongs to the Malo-Khamar-Daban mountain district, the East Sayan mountain province of the deciduous forest zone of slightly frozen soils. Sod-forest and floodplain meadow soils dominate. Fig. 4 is a map of the soil cover of the territory of Zakamensk. The following types of soil are identified: 1) sod-calcareous; 2) forest sod; 3) alluvial meadow; 4) anthropogenically transformed; 5) non-soil formations (technogenic sands).

Fig. 5 is a map of the main types of vegetation in Zakamensk, it highlights: 1) valley and floodplain meadows with a combination of shrubs; 2) larch forests with an admixture of birch and aspen; cowberry-forb, forb-gramineous, steppe restoration series in place of light coniferous forests; 3) larch on the

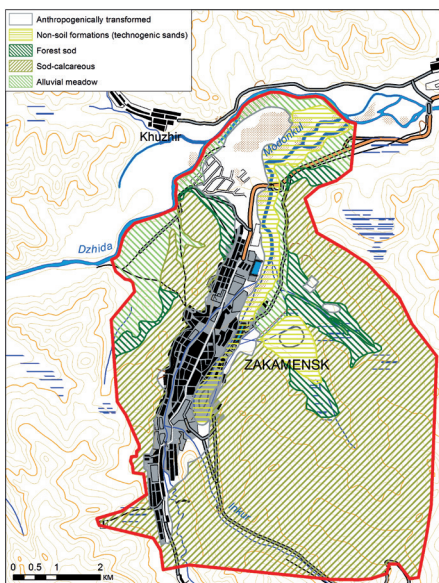


Fig. 4. Soil cover

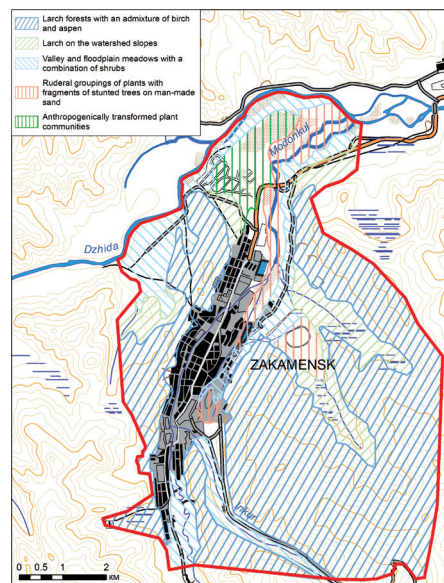


Fig. 5. Vegetation cover

watershed slopes: grass-lingonberry, grass-moss, shrub; 4) ruderal groupings of plants with fragments of stunted trees on man-made sand; 5) anthropogenically transformed plant communities.

The typology of lands on the town territory is based on their functional purpose. There are 3 groups of land: 1) nature conservation; 2) active economic use; 3) extensive economic use. Among them there are types and subtypes. Types of lands with the intensive use are used to carry out economic activities: processing of natural resources, creating housing, life support systems, transport, communications, etc. There are residential, residential on sands, agricultural, agricultural on overgrown sands, badlands, overgrown badlands and industrial types (Fig. 6). The lands of inconveniences and wastelands (badlands) take a special place, they constitute a reservoir for engaging in economic activity. For Zakamensk these are the areas with technogenic sand. As it can be seen in Fig. 6, the main structural center of the complex, formed in the lower reaches of the river Modonkul, consists of two spatial formations: residential lands and sandy badlands of tailing dumps, which have the properties of spatial neighborhood and adjunction. The adjunction is caused by the system-forming stream of the channel waters of the river Modonkul. This is especially true of the fluvial flow bed re-deposition of the material of the Kholtoson

deposit and Inkur mining and processing plants. As a result, a plume of sands containing heavy metals in high quantities formed a sub-parallel residential area.

In addition to creating maps of vegetation, soil cover, and types of urban areas, an ecological zoning map has been created for Zakamensk town (Fig. 7). The boundaries of the zones of ecological status are determined on the basis of a total indicator of soil pollution (Kulikov et al., 2012). The maps of Zakamensk (scales 1:3500 and 1:10000) served as a basis of ecological mapping. The ecological zoning map shows that the territory of Zakamensk is differentiated into areas of ecological disaster and an environmental emergency. The rest of the town belongs to the zone of relatively satisfactory situation. One particular transit area was identified, associated with pollution of bottom silts of the river Modonkul. It is determined by the bottom accumulation coefficient of heavy metals and belongs to the zone of ecological disaster.

**EROSION**

In Zakamensk for one rainfall ( $i$ ) with the layer  $H_i = 14.1$  mm following numbers were obtained:  
 $I_{130} = 0.121 \cdot \exp(0.0529 \cdot 14.1) = 0.121 \cdot \exp(0.718) = 0.121 \cdot 2.142 = 0.259$ .  
 Single rainfall erosion index:  $R_{130} = 0.258 \cdot 14.1 \cdot 0.259 - 0.149 = 0.793$ .

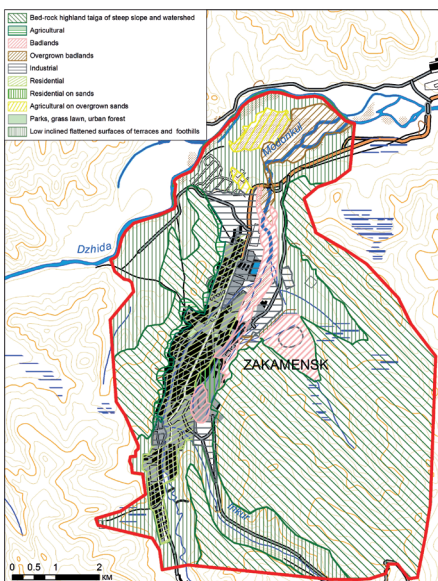


Fig. 6. Types of urban areas

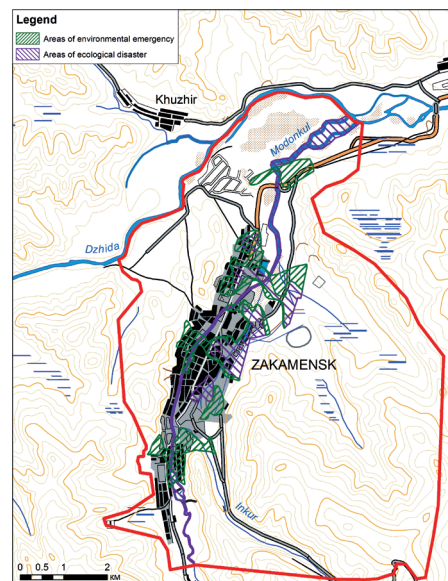


Fig. 7. Zones of ecological disadvantage

For all rainfalls of one year  $SR_{130} = 8$ . To obtain the climatic norm, averaging is usually used for 30 years (in the USA, 22 years). For Zakamensk the average value of  $R_{30}$  for 1966-2013 is 21.4 units. According to the sketch map of the rainfall erosion index, Zakamensk area is located between the values of 6 and 10 units (Larionov, 1993).

The distribution of precipitation in the multi-year cycle is affected by global climate change. In Zakamensk changes in erosion rainfall potential (ERP) in 1966-1975 are in the range of 9-37 with an average value of 18.0 units. In the next decade (1976-1985) the fluctuations range expanded to 10-42 with an average value of 16.7 units. In 1986-1995 there was a further extension of the extremum to 6-111 with an average ERP of 23.6 units. ERP maximum is 111 units was observed in 1992. If we exclude the abnormal year, then we obtain fluctuations in the range 6-28 and an average of 13.9 units. In the next decade (1996-2005) there is a further increase in the average value of ERP to 26 units at extreme values of 3.5-42. In the years 2006-2013 the amplitude of the fluctuations of the ERP continued to increase from 3 to 61, and the average value reached 25.5 units.

Particularly unstable is the beginning of the 21st century. It follows from the regression equation that the growth of ERP is 2.5 units/10 years (Fig. 8). The general growth of ERP, and especially its instability over the years, indicates that erosion-hazardous rain showers are becoming more likely.

The *LS*-factor shows how many times the intensity of loss on a given slope with its morphometric characteristics exceeds the loss intensity per unit of precipitation index from the runoff site with the reference length and slope parameters. To calculate the *LS* relief erosion index, you must have actual values for the steepness and length of the slope. The length of the drainage line of any one type of land is usually taken for the length of the slope from its upper boundary, watershed or artificial drainage boundary (profiled road, ditch, forest belt, etc.) to the lower boundary or thalweg of the ravine (girder), or an artificial drainage boundary. The slope is measured along the steepest part of the slope between two adjacent or several contiguous horizontals.

Erosion contamination sites (Table 3) are located in the eastern part of the city.

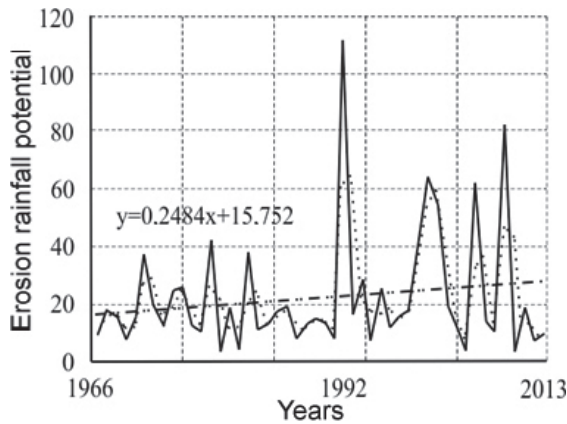


Fig. 8. Long-term dynamics of erosion rainfall potential (R30) from 1966 to 2013 in Zakamensk with a trend, a trend formula and a smoothing curve

Table 3. Morphometric characteristics of the key sites

Sites	Square, ha	Relative height, m	Drainage line length, m	Average slope steepness, °
Site 1	30.43	37	480	9.5 (tg 9.5° = 0.167)
Site 2	170.4	86	920	21 (tg 21° = 0.384)

The first key site of technoeluvium is an area of 30.43 hectares with the relative height of 37 m, the length of flow line of 480 m, an average steepness of the slope towards the watercourse and an urban area of 9.5° (tg 9.5° = 0.167).

The second site has an area of 170.4 hectares, the height of 86 m, the length of 920 m, an average steepness of the slope towards the drainage stream 21° (tg 21° = 0.384).

In view of artificial origin and relatively short (on a geological scale) time after dumping, the slopes of sites are even in the longitudinal profile and rugged by erosion ruts, furrows and gullies in the cross direction profile.

$$LS = L^{0.4} \cdot S^{1.45} \tag{11}$$

To determine the relief erosion index, we use expression:

For Site 1  
 $LS_1 = 480^{0.4} \cdot 0.167^{1.45} = 11.817 \cdot 0.075 = 0.89$   
 For Site 2  
 $LS_2 = 920^{0.4} \cdot 0.384^{1.45} = 15.329 \cdot 0.250 = 3.83$

For an approximate rapid determination of LS, a nomogram deserves attention (Fig. 9).

From the table values (Kuznetsov and Glazunov, 2004) it follows that the anti-erosion resistance of bare sand technoeluvium can be taken as equal to  $K = 0.42$ .

Taking the received parameters into account, erosion losses of technogenic sands will be on the first site:

$$Q_1 = 0.224 \cdot R \cdot K \cdot LS_1 = 0.224 \cdot 8 \cdot 0.42 \cdot 0.89 = 0.670 \text{ kg/}$$

$$\text{m}^2/\text{year} = 6.7 \text{ t/ha/year.}$$

Then, from the entire area of the first site up to 204 tons of contaminated sands fall annually in the city limits.

On the second site:

$$Q_2 = 0.224 \cdot R \cdot K \cdot LS_2 = 0.224 \cdot 8 \cdot 0.42 \cdot 3.83 = 2.883 \text{ kg/}$$

$$\text{m}^2/\text{year} = 28.8 \text{ t/ha/year,}$$

so, pressing of pollution on the hydroecosystem of the local water flow is 4907 tons per year.

Soil-erosion pollution of the environment is an independent phenomenon. It is characterized by special soil-erosion migration routes of pollutants in the catchment area. Transport of the substance occurs with slope deposits. Slope deposits undergo hydromechanical selection by fractions and a specific chemical transformation along the slope.

In the area of Lake Baikal the conditional concentration of total phosphorus was 6.0 mg/l at a soil washout rate of 15.8 tons/ha/year, a loss module of 3.2 t/ha/year and an annual water flow layer of 43 mm (Litvin and Kiryukhina, 2004). The information given by Belotserkovsky M.Yu. and Topunov M.V. (1996) is of a great interest. So, as the latter authors say, in the 90s of the XX century, in Buryatia, with an average plowland area of 1019.2 thousand hectares the average loss was 10.5 t/ha/year, and the allowable loss was 4.5 t/ha/year. In general, in the East Siberian region, the intensity of soil erosion from arable land is one of the highest among the economic regions of Russia – 8.1 t/ha/year. In general, in Russia, the washout intensity is 4.3 t/ha/year. The annual gross erosion from the territory of Eastern

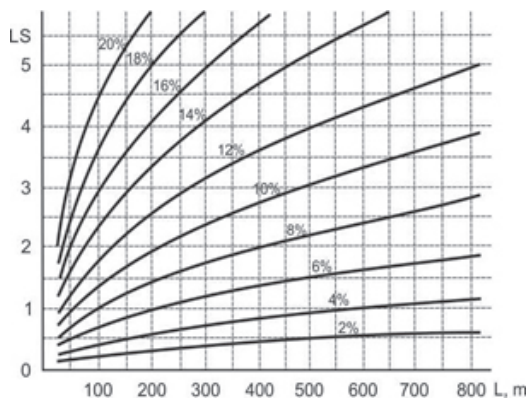


Fig. 9. Nomogram for approximate rapid determination of erosion potential of the relief

Siberia is 77926.1 thousand tons, and from the territory of Russia – 566240.2 thousand tons.

Khirsanov N.I. and Osipov G.K. (Litvin and Kiryukhina, 2002) developed an empirical formula for the input of phosphorus into the natural environment with products of erosion

$$W_p = 0.02 \cdot G^{0.58} \quad (12)$$

where  $G$  – soil erosion module (t/ha),  $W_p$  – phosphorus output (kg). The exponent in this dependence reflects the relative decrease in the intensity of phosphorus output with increasing soil erosion intensity. Phosphorus is taken as an indicator element.

For technogenic sands of Zakamensk, priority pollutants are Cd, Pb, Zn, Cu, and also Mo and W

**Table 4. Erosion contamination of the territory of Zakamensk by heavy metals**

Element – Pollutant	Concentration	Site 1	Site 2
Cd	a) sands of technogenic eluvium in situ, %	0.001	0.001
	b) eroded sands, t/t	$1 \cdot 10^{-5}$	$1 \cdot 10^{-5}$
	c) gross pressing on the urban ecosystem, t/year	$2.04 \cdot 10^{-3}$	0.049
	d) pressing for 1996-2011 period, t	0.030	0.700
Pb	a) sands of technogenic eluvium in situ, %	0.120	0.210
	b) eroded sands, t/t	$1.2 \cdot 10^{-3}$	$2.1 \cdot 10^{-3}$
	c) gross pressing on the urban ecosystem, t/year	0.245	10.305
	d) pressing for 1996-2011 period, t	3.700	154.600
Zn	a) sands of technogenic eluvium in situ, %	0.080	0.100
	b) eroded sands, t/t	$8 \cdot 10^{-4}$	$1 \cdot 10^{-3}$
	c) gross pressing on the urban ecosystem, t/year	0.163	4.907
	d) pressing for 1996-2011 period, t	2.400	73.600
Cu	a) sands of technogenic eluvium in situ, %	0.040	0.020
	b) eroded sands, t/t	$4 \cdot 10^{-4}$	$2 \cdot 10^{-4}$
	c) gross pressing on the urban ecosystem, t/year	0.082	0.981
	d) pressing for 1996-2011 period, t	12.300	14.700
W	a) sands of technogenic eluvium in situ, %	0.140	0.080
	b) eroded sands, t/t	$1.4 \cdot 10^{-3}$	$8 \cdot 10^{-4}$
	c) gross pressing on the urban ecosystem, t/year	0.286	3.926
	d) pressing for 1996-2011 period, t	4.300	58.900
Mo	a) sands of technogenic eluvium in situ, %	0.015	0.020
	b) eroded sands, t/t	$1.5 \cdot 10^{-4}$	$2 \cdot 10^{-4}$
	c) gross pressing on the urban ecosystem, t/year	0.031	0.981
	d) pressing for 1996-2011 period, t	0.500	14.700

(Kasimov, 2013; Chalov et al., 2015). For these elements, the erosion contamination of the urban area and water bodies is calculated (Table 4).

As established by soil-geochemical studies (Kulikov et al., 2012), the cadmium content in the techno-eluvium of both sites was 0.001 %, or 10 g/t. The small content of cadmium is explained by its relative scarcity and diffusion. Clark cadmium in the earth's crust is 0.13 mg/kg (Vinogradov, 1962).

It is conventionally accepted that in the sediment yield the cadmium content remains the same as in the sands of technoeuvium. Under these assumptions the amount of cadmium in the urban district of Zakamensk from the area of the first site is 0.002 tons per year. From the time of the closure of the mining industry (1998) to the city it decreased to 0.03 tons with erosive runoff. Liquid and solid flows from the second site fall into the watercourse. Therefore, the cadmium contamination of the hydroecosystem from the side of the second site is an order of magnitude higher. Other metals in the sands of techno-eluvium are contained in much larger quantities. So, mercury after the termination of industrial work in the hydroecosystem was in the amount of 3.7 and 155 tons from the first and second sites respectively. Other metals in the pollution of the water system in absolute terms participate to a lesser extent.

### Soil drifting

Another type of desertification in an urbanized area is soil drifting. The critical wind speed is different for particles of different diameters. This explains the sorting of mineral particles along the diameter. Sorting of particles leads to the formation of sand deserts in one case, and clay soils, as well as loess deposits in the surrounding desert territories, in the other. Usually, particles of less than 0.01 and more than 1 mm remain in place, and coarse particles weighing 0.01-0.05 mm are carried out over long distances and settle in the form of loess. According to Dolgilevich M.I. (1978), the range of transport of finely dispersed material in dust storms reaches 4000 km. It is as a result of this sorting that loess formed on the periphery of the deserts. It can be rightly

argued that the loess plateau and the fertile heylutu soils formed over more than 4000 years of cultivation are due to aeolian material from the Central Asian steppes. The similarity of the material of dust storms of Central Asia, China and Primorye by chemical composition is established (Tolchelnikov, 1990). It is important in the future to show the commonality of the sands of Central Asia and the floodland loess of the Yellow River on microelement composition and the presence of rare elements. According to NASA materials it is established that every year 56 million tons of dust reaches North America from the Central Asian region. Particularly active dust flies in spring in connection with the activation of cyclones and strong western winds, prevailing in the middle latitudes.

From the central and western parts of the Sahara, dust storms penetrate the airspace over the Atlantic Ocean. Taken samples show that dust can spread to South and Central America. For many Asian countries, including Korea, the forecast for the maintenance of Yellow Dust (Yellow Sand, Asian Dust) in the spring with the development of the so-called yellow dust storms becomes actual. To prevent dust storms that disrupt the work of many electronic tools in Mongolia, in the Gobi Desert, the Green Belts program is organized with the help of the international community and research on phytomeliorative sand fixation is beginning.

In the modern era, the problem of forecasting dust storms becomes more urgent. The development of recognition techniques and the conduct of their space monitoring have been carried out since the late 90s. The deciphering of dust storms and evaluation of their main characteristics are carried out with the help of a special Normalized Differential Dust Index (NDDI), which was implemented by Chinese scientists in the study of dust storms in Northern China and Mongolia according to MODIS data (Qu et al., 2006).

Deflationary potential of a wind (DPW) is calculated by the following formula (Pushkarev, 1984):

$$r_i = 0.001 \cdot V_i^3 \cdot f_i \quad (13)$$

where  $V_i^3$  is the wind speed in the speed group  $i$ ,  $f_i$  – duration of the wind in percent of the total period in the direction of  $j$  and with the group of

velocities  $i$ . The calculation of DPW is carried out for each month as a sum for each direction from eight rhumbs.

When predicting the deflation of soils, it is assumed that the kinetic energy of the wind is directly proportional to the cube of its velocity and inversely proportional to the moisture content of the soils. The deflationary work of the wind, having, for example, a speed of 4 m/s, will exceed the work of a wind having a speed of 2 m/s, not two but eight times.

Climate index of soil drifting (Chepil et al., 1963):

$$C = 10^2 \cdot V^3 / (H / T + 10)^2 \quad (14)$$

where  $V, H, T$  – the average annual values of wind speed, precipitation, air temperature, respectively. The cube of wind speed is in the

numerator, the square of humidity is in the denominator.

The climatic factor of soil drifting can also be determined by expression:

$$C = 34.486 \cdot 10^2 \cdot V^3 (P - E)^2 \quad (15)$$

where  $P$  – precipitation and  $E$  – evaporation.

With an annual erosive wind potential of 50-100, an average of 2-5 dust storms occur annually in the region (Bazhenova et al., 1997; Tyumentseva, 2013). For sands of technoeuvium, anti-deflation resistance is minimal and equal to 15. The probability of soil deflation is estimated by score 4 or high. Aeolian accumulation reaches 10 t/ha/year.

During the soil drifting with contaminated sand, the same elements are found in the city and in

**Table 5. Deflation pollution of the territory of Zakamensk by heavy metals**

Element – Pollutant	Concentration	Site 1	Site 2
Cd	a) eroded sands, t/t	$1 \cdot 10^{-5}$	$1 \cdot 10^{-5}$
	b) gross pressing on the urban ecosystem, t/year	$3.04 \cdot 10^{-3}$	$17.04 \cdot 10^{-3}$
	c) pressing for 1996-2011 period, t	0.05	0,24
Pb	a) eroded sands, t/t	$1.2 \cdot 10^{-3}$	$2.1 \cdot 10^{-3}$
	b) gross pressing on the urban ecosystem, t/year	0.37	3.58
	c) pressing for 1996-2011 period, t	5.60	53.70
Zn	a) eroded sands, t/t	$8 \cdot 10^{-4}$	$1 \cdot 10^{-3}$
	b) gross pressing on the urban ecosystem, t/year	0.24	1.70
	c) pressing for 1996-2011 period, t	3.60	25.50
Cu	a) eroded sands, t/t	$4 \cdot 10^{-4}$	$2 \cdot 10^{-4}$
	b) gross pressing on the urban ecosystem, t/year	0.12	0.34
	c) pressing for 1996-2011 period, t	1.80	5.10
W	a) eroded sands, t/t	$1.4 \cdot 10^{-3}$	$8 \cdot 10^{-4}$
	b) gross pressing on the urban ecosystem, t/year	0.43	1.36
	c) pressing for 1996-2011 period, t	6.50	20.40
Mo	a) eroded sands, t/t	$1.5 \cdot 10^{-4}$	$2 \cdot 10^{-4}$
	b) gross pressing on the urban ecosystem, t/year	0.05	0.34
	c) pressing for 1996-2011 period, t	0.80	5.10

the hydroecosystem, which are contained in the techno-eluvium (Table 5). Since the closure of the mining enterprise (1998), deflation tungsten contamination has reached 6.5 tons in the first site. The hydroecosystem received 20 tons of tungsten from this site. Also great are the aerial incomes of lead, copper, etc.

## CONCLUSIONS

The retrospective analysis of the available materials on the assessment of the environmental condition in Zakamensk, personal observations and especially the analysis of the latest research result on remote and ground-based sensing of the state of the day surface revealed the following:

1. The main source of the environment pollution are tailings and mine water.
2. The main factor of pollution is toxic substances, primarily, heavy metals, inheriting high concentrations from ore rock, and currently deposited in the tailings material, as well as pollutants contained in mine waters.
3. The main processes contributing to the expansion of the pollution area are: a) wind separation covering a vast territory; b) plane washout and linear erosion, especially intense during spring and summer floods; c) lateral underground filtration and outlets of the mine water; d) alluvial demolition of the river Modonkul redeposited material; e) anthropogenic dispersion, consisting in the occasional use of sand for dumping roads, playgrounds, in construction, etc.

The scheme for grouping the adverse effects of the DTMP waste by source, factor and process has been developed. The territory of Zakamensk is differentiated into areas of ecological disaster and an extreme ecological situation. The whole other territory of the town refers to the zone of satisfactory situation. One special transit area associated with the pollution of the bottom sediments of the river Modonkul was identified. It is determined by the coefficient of the bottom accumulation

of heavy metals and refers to the zone of ecological disaster.

Desertification processes in the territory of Zakamensk (urban desertification ) manifest themselves in the form of sheet and linear erosion and redeposition (erosion), soil drifting and redeposition (contamination) of sands contaminated with heavy metals, the legacy of the mining activity of the now closed Dzhidinsky tungsten-molybdenum plant.

The long-term dynamics of such an important indicator as the rainfall erosion index occurs with a positive trend – 2.5 units/10 years, i.e. the probability of erosion-hazardous rains in the region is increasing.

With the use of modern calculation methods, it has been established that the city limits with water-erosion flows to 204 t / ha of contaminated sands each year, and only after the closure of the plant in 1996, priority pollutants such as lead 3.7 t, tungsten – 4.3 t.

Active wind activity led to the deposition of even more metals in the city. Urban ecosystems of Zakamensk are under deflation metal pressing (for lead is equal 5.6 t, and tungsten - 6.5 t).

Qualitative characteristics of the surface waters of the river Modonkul belong to the very dirty class (VI), while the river remains the most polluted water object in the republic as a result of the discharge of mine waters of the frozen DTMP.

Wastewater from tunnels is characterized by an increased content of chromium, zinc, cadmium, iron and other metals.

Pollution by heavy metals has a negative impact on the health of the residents of Zakamensk. Air pollution caused the risk of increasing such diseases as cardiovascular, lung cancer, chronic and acute respiratory, including asthma among the citizens (Kulikov et al., 2012). Therefore, urgent reclamation and remediation of contaminated sands of technoeluvium,

rehabilitation of the territory of Zakamensk of the Republic of Buryatia is necessary.

The ecological situation in Zakamensk and in its adjacent territory is qualified as an ecological disaster, and for the general morbidity (according to the population's consultation in medical institutions) – as a crisis.

## ACKNOWLEDGEMENTS

This work was carried out within the framework of a state assignment of the Baikal Institute of Nature Management of Siberian Branch of Russian Academy of Sciences (project No. AAAA-A17-117021310251-4) and partially supported by the Russian Foundation for Basic Research under research project No. 19-55-53026. ■

## REFERENCES

- Bazhenova O.I., Lyubtsova E.M., Ryzhov Yu.V., Makarov S.A. (1997). Spatio-temporal analysis of the dynamics of erosion processes in the south of Eastern Siberia. Novosibirsk: Nauka. 203 p. (in Russian with English summary)
- Belotserkovskiy M.Yu. and Topunov M.V. (1996). The cost of anti-erosion measures to preserve soil fertility with the existing agricultural use of arable land. In: R.S. Chalov, ed., Erosion and channel processes. Issue 2. Materials of coordination meetings of universities in 1991-1995, Moscow: MSU, pp. 48-54. (in Russian with English summary)
- Chalov S., Jarsjö J., Kasimov N., Romanchenko A., Pietróń J., Thorslund J., Promakhova E. (2015). Spatio-temporal variation of sediment transport in the Selenga River Basin, Mongolia and Russia. *Environmental Earth Sciences*, 73, pp. 663-680. doi: 10.1007/s12665-014-3106-z
- Chalov S., Kasimov N., Lychagin M., Alexeevsky N., Belozerova E., Theuring P., Shinkareva G., Romanchenko A., Garmayev E. (2013). Water resources assessment of the Selenga–Baikal river system. *Geoöko*, 34, pp. 77-102.
- Chepil W.S., Siddoway F.N., Armbrust D.V. (1963). Climatic index of wind erosion conditions in the Great Plains. *Soil Science Society of America Journal*, 27, pp. 449-452.
- Dolgilevich M.I. (1978). Dust storms and agroforestry meliorative events. Moscow: Kolos. 159 p. (in Russian with English summary)
- Environmental Atlas-monograph "Selenga-Baikal" (2019). Edited by N. Kasimov. M.: Faculty of Geography, MSU. 208 p. Available at: [https://www.researchgate.net/publication/335567904\\_Environmental\\_Atlas-monograph\\_Selenga-Baikal](https://www.researchgate.net/publication/335567904_Environmental_Atlas-monograph_Selenga-Baikal)
- GOST 25100-95. Soils. Classification (2001). Moscow. 23 p. (in Russian)
- Implementation of environmental measures related to the shutdown of the Dzhidinsky tungsten-molybdenum plant in Zakamensk: assessment of the environmental situation in the adjacent area of the former DTMP: economic agreement report (interim) (2007). In: A.I. Kulikov, ed., Ulan-Ude: Buryat State Academy of Agriculture. (in Russian)
- Ivanov A.D. (1971). Some results of studying of aeolian sands and soil deflation in Transbaikalia. Wind erosion and control measures. *Bulletin of Institute of natural sciences of Buryat subbranch of Siberian branch of USSR Academy of sciences*, 9, pp. 131-137. (in Russian with English summary)

Karthe, D., Kasimov, N., Chalov, S., Shinkareva, G., Malsy, M., Menzel, L., Theuring, P., Hartwig, M., Schweitzer, C., Hofmann, J., Priess, J., Lychagin, M. (2014) Integrating Multi-Scale Data for the Assessment of Water Availability and Quality in the Kharaa - Orkhon - Selenga River System. *Geography, Environment, Sustainability*, 3(7) pp. 65-86. doi: 10.24057/2071-9388-2014-7-3-40-49

Karthe D., Chalov S., Moreido V., Pashkina M., Romanchenko A., Batbayar G., Kalugin A., Westphal K., Malsy M., Flörke M. (2017). Assessment of runoff, water and sediment quality in the Selenga River basin aided by a web-based geoservice. *Water Resources*, 44 (3), pp. 399-416. doi: 10.1134/S0097807817030113

Kasimov N., Kosheleva N., Gunin P., Korlyakov I., Sorokina O., Timofeev I. (2016). State of the environment of urban and mining areas in the Selenga Transboundary River Basin (Mongolia Russia). *Environmental Earth Sciences*, 75 (1283), pp. 1-20. doi: 10.1007/s12665-016-6088-1

Kasimov N.S. (2013). *Landscape Ecogeochemistry*. Moscow: publisher Filimonov M.V. 208 p. (in Russian with English summary)

Khamnaeva G.G., Kulikov A.I., Tsydypov, B.Z. (2013). Current ecological state of the Zakamensk city environment and its adjacent territory. *Bulletin of Buryat State Academy of Agriculture*, 3(32), pp. 79-85. (in Russian with English summary)

Kovalev S.N. (2009). *Development of gully in urban areas*. Ph.D. author's abstract. Moscow. 25 p. (in Russian)

Kulikov A.I., Mangataev A.Ts., Kulikov M.A., Hamnaeva G.G., Plyusnin A.M. (2012). Ecological zoning and statistical parameters of ecologically dangerous zones of Zakamensk (the Republic of Buryatia). *ESSUTM bulletin*, 3 (38). pp. 221-227. (in Russian with English summary)

Kuznetsov M.S. and Glazunov G.P. (2004). *Soil erosion and protection*. Moscow: MSU. 352 p. (in Russian with English summary)

Larionov G.A. (1993). *Soil erosion and deflation: basic patterns and quantitative assessments*. Moscow: MSU. 198 p. (in Russian with English summary)

Litvin L.F. and Kiryukhina Z.P. (2002). *Erosion dangerous lands and spatio-temporal patterns of soil erosion. Natural-anthropogenic processes and environmental risk*, Moscow: Gorodets. pp. 196-202. (in Russian with English summary)

Litvin L.F. and Kiryukhina Z.P. (2004). *Soil-erosion migration of nutrients and pollution of surface waters. Soil erosion and channel processes*, 14, pp. 45-64. (in Russian with English summary)

Osintseva N.V. (2001). *Physico-geographical factors of development of gully erosion of urban lands*. Ph.D. author's abstract. Tomsk. (in Russian)

Pushkarev M.F. (1984) *Soil Erosion (Translation from English)*; Kolos: Moscow, Russia. 415 p. (in Russian)

Qu John, Hao Xianjun, Kafatos Menas, Wang Lingli (2006). Asian Dust Storm Monitoring Combining Terra and Aqua MODIS SRB Measurement. *IEEE Geoscience and Remote Sensing Letters*, 3(4), pp. 284-486.

Timofeev I., Kosheleva N., Kasimov N. (2018). Contamination of soils by potentially toxic elements in the impact zone of tungsten-molybdenum ore mine in the Baikal region: A survey and risk assessment. *Science of the Total Environment*, 642, pp. 63-76. doi: 10.1016/j.scitotenv.2018.06.042

Tolchelnikov Yu.S. (1990). Soil erosion and deflation. Ways to control. Moscow: Agropromizdat. 158 p. (in Russian with English summary)

Tulokhonov A.K., Tsydygov B.Z., Sodnomov B.V., Gurzhapov B.O., Ayurzhanayev A.A., Batotsyrenov E.A., Togmidon V.V., Ayusheev Ch.Yu., Zharnikova M.A., Alymbaeva Zh.B., Garmaev E.Zh. (2018). Assessment of the linear erosion development through the example of a gully in the Selenga Middle Mountains. *Izvestiya vuzov «Geodeziya i aerofotosyemka»*. *Izvestia vuzov «Geodesy and Aerophotosurveying»*, 62 (3): 327-336. (in Russian with English summary)

Tyumentseva E.M. (2013). The use of statistical methods in the study of aeolian processes. *Bulletin of the Department of Geography of ESSAE*, 1-2 (7), pp. 38-46. (in Russian with English summary)

Vinogradov A.P. (1962). The average content of chemical elements in the main types of igneous rocks of the earth's crust. *Geochemistry*, 7, pp. 555-571. (in Russian with English summary)

Wischmeier W.H. (1959). A rainfall erosion index for universal soil-loss equation. *Soil Science Society of America Journal*, 23, pp. 246-249. doi: 10.2136/sssaj1959.03615995002300030027x

Wischmeier W.H. and Smith D.D. (1958). Rainfall energy and its relationship to soil loss. *Eos, Transactions American Geophysical Union*, 39, pp. 285-291. doi: 10.1029/TR039i002p00285

Wischmeier W.H. and Smith D.D. (1978). Predicting rainfall erosion losses. *USDA Agr. Handbook 537*, Washington. 65 p.

Received on March 1<sup>st</sup>, 2019

Accepted on August 8<sup>th</sup>, 2019

**Galina L. Shinkareva<sup>1\*</sup>, Mikhail Yu. Lychagin<sup>1</sup>, Mikhail K. Tarasov<sup>1</sup>, Jan Pietroń<sup>2</sup>, Marina A. Chichaeva<sup>3</sup>, Sergey R.Chalov<sup>1</sup>**

<sup>1</sup> Lomonosov Moscow State University, Leninskie Gory, Moscow, Russia

<sup>2</sup> WSP Sverige AB, Ullevigatan 19, Gothenburg, 411 40, Sweden

<sup>3</sup> Peoples Friendship University of Russia (RUDN University), 6 Miklukho-Maklaya St., Moscow, Russia

\* **Corresponding author:** galina.shinkareva@gmail.com

## BIOGEOCHEMICAL SPECIALIZATION OF MACROPHYTES AND THEIR ROLE AS A BIOFILTER IN THE SELENGA DELTA

**ABSTRACT.** This study aims to evaluate the biofiltration ability of higher aquatic vegetation of the Selenga delta as a barrier for heavy metals and metalloids (HMM) flows into the Lake Baikal. Main aquatic vegetation species have been collected from deltaic channels and inner lakes: *Nuphar pumila*, *Potamogeton perfoliatus*, *P. pectinatus*, *P. natans*, *P. friesii*, *Butomus umbellatus*, *Myriophyllum spicatum*, *Ceratophyllum demersum*, *Phragmites australis*. Analysis of the obtained data showed that regardless of the place of growth hydrotrophs spiked water-milfoil (*M. spicatum*) and the fennel-leaved pondweed (*P. pectinatus*) most actively accumulate metals. Opposite tendencies were found for helophytes reed (*Ph. australis*) and flowering rush (*B. umbellatus*), which concentrate the least amount of elements. This supports previous findings that the ability to concentrate HMM increases in the series of surface – floating – submerged plants. Regarding river water, the studied macrophyte species are enriched with Mn and Co, regarding suspended matter – Mo, Mn and B, regarding bottom sediments – Mn, Mo and As. We identified two associations of chemical elements: S-association with the predominant suspended form of migration (Be, V, Co, Ni, W, Pb, Bi, Mn, Fe and Al) and D-association with the predominant dissolved form of migration (B, U, Mo, Cr, Cu, Zn, As, Cd, Sn and Sb). Due to these associations three groups of macrophytes were distinguished – flowering rush and reed with a low HMM content; small yellow pond-lily and common floating pondweed with a moderate accumulation of S-association and weak accumulation of D-association elements; and clasping-leaved pondweed, fennel-leaved pondweed, and pondweed Friesii accumulating elements of both S and D groups. The results suggest that macrophytes retain more than 60% of the total Mn flux that came into the delta, more than 10% – W, As, and from 3 to 10% B, Fe, Co, Mo, Cd, V, Ni, Bi, Be, Cu, Zn, Cr, U, Al. The largest contribution is made by the group of hydrotrophs (spiked water-milfoil and pondweed), which account for 74 to 96% of the total mass of substances accumulated by aquatic plants.

**KEY WORDS:** biogeochemistry, deltaic environment, heavy metals and metalloids in aquatic systems, macrophytes, hyperspectral images.

**CITATION:** Galina L. Shinkareva, Mikhail Yu. Lychagin, Mikhail K. Tarasov, Jan Pietroń, Marina A. Chichaeva, Sergey R.Chalov (2019) Biogeochemical Specialization Of Macrophytes And Their Role As A Biofilter In The Selenga Delta. Geography, Environment, Sustainability, Vol.12, No 3, p. 240-263  
DOI-10.24057/2071-9388-2019-103

## INTRODUCTION

In recent years, the growing attention has been paid to ecology and geochemistry of river deltas and their wetland systems (Cui et al. 2009; Iqbal 2010; Thorslund et al. 2017; Wang et al. 2014). Due to increasing anthropogenic pressure on the catchments, the role of deltas as natural filters on the path of substance flows of natural and anthropogenic origin is becoming increasingly important (Thorslund et al. 2017). Aquatic vegetation significantly influences turbulent flow field (Nepf 2012) and thus became an important driver of wetlands hydrological impacts. Through various processes, the aquatic plants provide important environmental services, such as storage of pollutants. Hence, they are often utilized in constructed wetlands to reduce contaminant loads in rivers (Rai 2009; Patel and Kanungo 2010; Leto et al. 2013; Sun et al. 2013; Guittonny-Philippe et al. 2014). Higher aquatic plants, or macrophytes, play an important role in the processes of deposition of substances in river deltas (The Selenga River Delta... 2008; Carbiener et al. 1990; Underwood et al. 2006; Coops et al. 1999; Khedr and El-Demerdash 1997; Kröger et al. 2009; Chaplin and Valentine 2009). For instance, studies in the Volga River delta showed that the accumulation of chemical elements by aquatic plants depends on their ecological and morphological characteristics, biogeochemical specialization, the content of chemical elements in the components of aquatic systems, and migration conditions, determined primarily by the flow characteristics of water streams and bodies (Lychagina et al. 1998; Lychagin et al. 2015).

This study considers Selenga River delta which is the largest freshwater delta in the World and which plays protective role for the Lake Baikal which is the oldest and deepest lake of the planet and a UNESCO World Heritage Site (2019). Selenga accounts for 60% of the total river water flow and 82% of sediment load to Lake Baikal (Pietroń 2017). The

anthropogenic impact on ecosystems in the Selenga River basin has increased in the recent decades, e.g., by the extraction of minerals, primarily gold, urbanization, and agricultural development, especially in the upper, Mongolian, part of the basin (Pietroń et al. 2017; Jarsjö et al. 2017; Malsy et al. 2013). In addition, changing climatic conditions in the basin, such as increasing air temperatures (0.022°C/year, nearly two times faster than the global average; Törnqvist et al. 2014) can also significantly affect the regional ecosystems.

The Selenga River delta acts as a “geochemical filter” by dispersion and storage of metal. According to the previous studies suspended sediment particles are important in heavy metals and metalloids in the Selenga River basin transport (Thorslund et al. 2012; Chalov et al. 2015; Chalov et al. 2017). These particulate matter fluxes can be significantly altered by macrophytes in the Selenga River delta. It was observed that the most effective removal of contaminants occurs along relatively narrow distributary channels adjacent to vast wetland areas (Chalov et al. 2017). In the submerged parts of the delta, affected by the backwater from the Lake Baikal, the sediment can be transported outside the deltaic channels to the nearest water bodies in conditions with water discharge from moderate to high (Pietroń et al. 2018). However, the detailed quantitative characteristics of flows of potentially toxic elements and their amounts deposited in the Selenga River delta are still poorly understood. Moreover, despite the observed hydrological and geochemical patterns little is known about the role of aquatic vegetation in the metal storage function of the Selenga River delta. Hydrofauna and hydroflora of Selenga basin related to algae, fish, plankton, benthos, amphibian fauna species, microbial communities along rivers have been investigated since the end of 19th century within its Mongolian part (Dgebuadze et al. 2010). In the Russian part of Selenga basin a lot of work in aquatic vegetation studies was done by V.V. Chepinoga and co-authors (Chepinoga 2012; Chepinoga

and Rosbach 2012; Lane et al. 2015). However, there is a lack of knowledge regarding the accumulation of chemical elements by different species of aquatic plants due to environmental conditions. This paper considered aquatic vegetation of Selenga River delta to study its ability and effectiveness in filtering of riverborn metals and metalloids. Hence, the working hypothesis is that the storage processes of macrophytes play an important role in the accumulation of the contaminant loads along the deltaic channels.

**STUDY AREA**

The Selenga river carries out 2.5 million tons per year of suspended matter to the Lake Baikal, forming a delta with an area of about 540 km<sup>2</sup>. Thickness of sediment layer in the Selenga delta is up to 5000–5500 meters. It was formed by the river sediment flow towards the steep slope of the Baikal rift over 500 thousand years. Such a large amount of sediment inflow of the Selenga allows the delta to protrude into the Lake Baikal (Rogozin 1981): the delta and its underwater continuation divide the Lake into the Southern and

Central basins with average depths about 1100-1500 m (Tulokhonov 2001). Selenga delta is undergoing an active phase of regression (Dong et al. 2013), the closest coastal distance of the Lake (26 km) is still registered across from the Selenga estuary.

Three sectors are commonly distinguished in the delta (Korytny et al. 2012; Il'icheva 2015; Chalov et al. 2017): the Western – Selenginsky, the Central – Sredneustevsky, and the Eastern – Lobanovsky (Fig. 1). The distribution of runoff across the sectors is uneven: an average of 45% passes through the Lobanovsky sector, 20% along the Sredneustevsky and 35% along the Selenginsky (Korytny et al. 2012).

The Selenginsky sector includes the main channel of the Selenga River, the Levoberezhnaya, Glubokaya, Shumikhka, Shamanka, and Galutai channels. These channels (Fig. 2a) are characterized by a large water discharges (32–157 m<sup>3</sup>/s). The growth of the delta in this sector reaches 2 km per 100 years (Korytny et al. 2012). Bottom sediments in large channels are often sandy or sandy-pebble, whereas

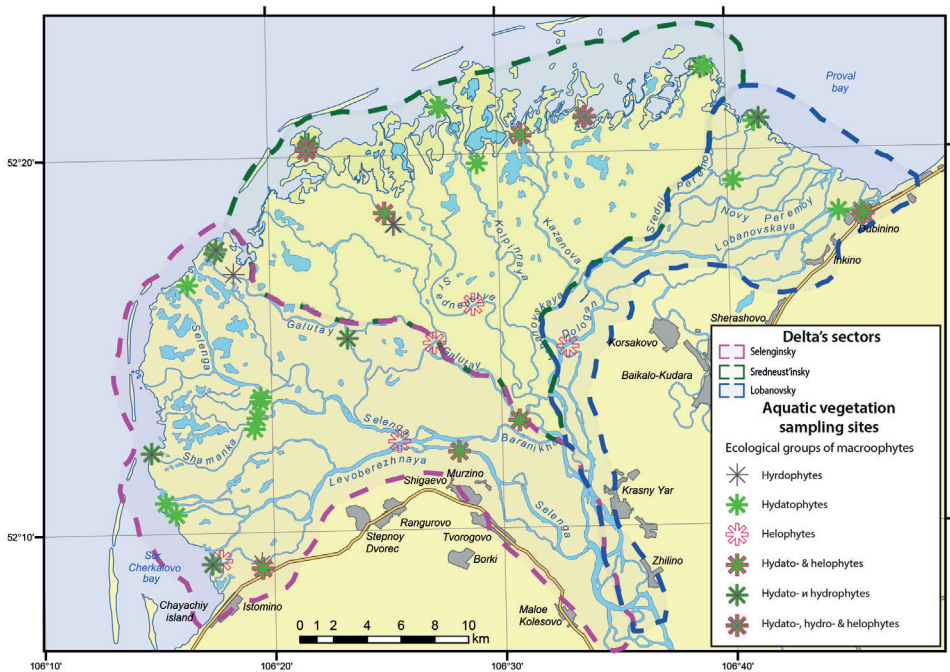


**Fig. 1. Sampling sites of macrophytes in the Selenga delta**

silt dominates (~52%) in floodplain lakes and permanently submerged marshlands (~64%). The submerged channel bank areas of the channels in this part of the delta are characterized by similar content of silt (~57%; Pietron et al. 2018).

The Sredneustievsky sector includes the small channels Krivaya, Kolpinnaya, Sredneustye, Casanova, Severnaya (Fig. 1) with low water discharge (up to 35 m<sup>3</sup>/s). In this parts, content of silt in sediment deposited on banks increases up to 26% (Pietron et al. 2018) and it has been observed that some of the channels dry out in rainless periods. In most recent years, this sector is experiencing flooding along the outer edge, which causes an increase in the area of intra-delta lakes with abundant aquatic vegetation (Chalov et al. 2017).

The Lobanovsky sector consists of the Lobanovskaya channel and its branches Novy Peremoy and Sredniy Peremoy. This part of the delta experiences progradation towards Lake Baikal at a speed of 30–40 m per year (Korytny et al. 2012). The channels are characterized by the moderate water discharge (30–50 m<sup>3</sup>/year) and a small amount of aquatic plants. Sand fractions prevail in bottom sediments (about 47%). At the mouth area of the Lobanovskaya channel bottom sediments are finer, with the silt content exceeding 50% (Kasimov et al. 2019).

## MATERIALS AND METHODS

This work is based on the data collected on field during summer growing period of: (1) 8<sup>th</sup>–14<sup>th</sup> of August 2011, (2) 30<sup>th</sup> of June to 2<sup>nd</sup> of July 2012 and (3) 13<sup>th</sup>–26<sup>th</sup> of July 2013. Areas with the most typical geochemical conditions within the Selenga delta channels were chosen as the sampling locations. At every sampling station field measurements of the physicochemical parameters of river waters and bottom sediments were measured on site by Hanna field instruments (e.g. pH, mineralization, redox potential). In addition, dissolved oxygen content using the Winkler method was

determined. At some locations Van Veen grab was used to take samples of bottom sediments.

Water samples were taken in 2 and 5 liter bottles, after which they were filtered on a Millipore vacuum station with a Millivac Mini Vacuum Pump (230v 50Hz) through pre-weighed membrane filters with a diameter of 47 mm and a pore size of 0.45 µm. To preserve river water samples for further HMM determination 0.1 ml of HNO<sub>3</sub> (concentrated) was added to new 15 ml Saerstedt tubes and filled up to the mark with filtered water. All tubes were carefully closed. The filters and bottom sediments were dried at room temperature (~21°C). Filters were afterwards weighed again to determine the mass of the suspended sediments.

In the coastal part of inner lakes and water channels the sampling of prevailing macrophyte species was carried out: small yellow pond-lily (*Nuphar pumila*), pondweeds (*Potamogeton perfoliatus*, *P. pectinatus*, *P. natans*, *P. friesii*), flowering rush (*Butomus umbellatus*), spiked water-milfoil (*Myriophyllum spicatum*), hornwort (*Ceratophyllum demersum*), reed (*Phragmites australis*). Those samples have been dried in the oven at a temperature of 60°C. Collection of aquatic vegetation samples from premeasured sites (usually 0.25 x 0.25 m) within typical areas where one dominant plant species grow was done separately. Macrophytes collected from those sampling locations were weighed in the laboratory, after which a smaller amount have been taken for further HMM concentrations determination. Each of these smaller samples have been weighed, dried in an oven, and weighed again after drying.

In estuarine vegetation and other components of aquatic systems the content of 21 chemical elements (Table 1) was analyzed using the ICP-MS (ICP-AES) methods. Those elements are Be, B, V, Cr, Co, Ni, Cu, Zn, As, Mo, Cd, W, Pb, Bi, U, Sn, Sb, Mn, Fe and Al.

A total amount of 144 river water, 146 suspended sediments, 118 bottom sediments and 143 macrophytes samples have been analyzed.

To characterize the relationship of the content of elements in aquatic plants and other components of aquatic systems coefficients  $K_w$ ,  $K_s$  and  $K_b$  were used:  $K_w = C_n / (1000 \times C_w / a)$ ,  $K_s = C_n / C_s$ ,  $K_b = C_n / C_b$ , where,  $C_n$  – metal concentration in the aquatic plant (mg/kg of dry matter),  $C_w$  – metal concentration in the river water ( $\mu\text{g/L}$ ),  $a$  – mineralization of water (mg/kg),  $C_s$  – metal content in suspended matter (mg/kg),  $C_b$  – metal concentration in bottom sediments (mg/kg).

Due to a possible high variability of the HMM content in components of aquatic systems, to fully reflect the relationship of the contents of elements in the plant-habitat system we propose to use a multiplicative accumulation coefficient

$$K_{wsb} = \sqrt[3]{K_w \times K_s \times K_b}$$

Furthermore, to assess the evaluation of the total accumulation of chemical elements by macrophytes we also suggest the coefficient

$$Z_{veg} = \sum K_{wsb} \text{ at } K_w > 1.5; K_s > 1.5; K_b > 1.5$$

In addition, remote sensing data obtained during 28/07/2014 – 16/08/2014 when shooting the delta from ultralight aviation (ULM) with sensing platform ULM/Headwall mounted on it was used to compile distribution maps of the main groups of macrophytes. Two main groups of aquatic plants were distinguished: 1) plants with floating leaves with predominance of small yellow pond lily (*N. pumila*) and 2) submerged plants with predominance of pondweeds (*Potamogeton perfoliatus*, *P. pectinatus*, *P. natans*, *P. friesii*) and spiked water-milfoil (*Myriophyllum spicatum*).

Sensing platform ULM/Headwall is a hyperspectral pushbroom sensor. Its original data contains 250 spectral channels with 0.7 m spatial resolution. In our case total amount of bands was reduced to 151 (509.74 nm to 778.74 nm)

and spatial resolution to 5 m to increase processing speed. After geometric, radiometric and atmospheric correction (Cubero-Castan et al. 2015) remote sensed images were processed with Spectral Angle Mapper (SAM) algorithm in ENVI GIS. From total amount of 143 field vegetation sites 90 was used for supervised classification and 53 for its verification. Total accuracy of classification was 79% for classified sites and 64% for verification sites. Based on image classification area of aquatic vegetation distribution was estimated. Water plants with a predominance of small yellow pond-lily (group 1) occupy about 41 sq km of delta, and pondweeds and spiked water-milfoil (group 2) occupy about 11 sq km. The elements accumulation in the  $N$  group (group 1 or group 2) of aquatic vegetation ( $HM_N$ , kg) from the beginning of growing season till the sampling date was determined as follows:

$$HM_N = C_N^{HM} \times B_N \times P_N \times 10^{-6}$$

where  $C_N^{HM}$  is the average concentration of an element in the  $N$  group of aquatic vegetation at the sampling date (mg/kg, wet weight),  $B_N$  is the average phytomass of plants of the  $N$  group at the sampling date,  $\text{kg/m}^2$ ;  $P_N$  is the distribution area of group  $N$  in the delta,  $\text{m}^2$ ,  $10^{-6}$  is the conversion factor from mg to kg.

The HMM fluxes in dissolved ( $W_c$ ) and suspended ( $W$ ) forms per day have been calculated using the following equations:

$$W_{ci} = Q \times C_{ci} \times 86400 \times 10^{-9},$$

$$W_i = R \times C_i \times 86400 \times 10^{-6}$$

where  $W_{ci}$  is the flux of the  $i$ -element in dissolved form, kg/day;  $W_i$  – flux of the  $i$ -element in suspended form, kg/day;  $Q$  – water discharge,  $\text{m}^3/\text{s}$ ;  $R$  – suspended matter discharge,  $\text{kg}/\text{s}$ ;  $C_{ci}$  – concentration of the  $i$ -element in river water,  $\mu\text{g}/\text{m}^3$ ;  $C_i$  – concentration of the same  $i$ -element in suspended matter,  $\text{mg}/\text{kg}$ ; 86400 – conversion factor seconds to days;  $10^{-9}$  – conversion factor  $\mu\text{g}$  to  $\text{kg}$ .

Taking into account the length of the growing season at the time of sampling, the total flux of elements brought into

the delta in dissolved and suspended forms for this hydrological period the proportion of HMM precipitated in the delta due to the activity of each group of aquatic plants ( $HM_{N\%}$ ) was estimated as follows:

$$HM_{N\%} = \frac{NM_N \times 100}{(W_{Ci} + W_i) \times T},$$

where  $HM_N$  is elements accumulation in the  $N$  group of aquatic vegetation (kg);  $W_{Ci}$  and  $W_i$  are the fluxes of the  $i$ -element in dissolved and suspended form respectively (kg/day);  $T$  – time period from the beginning of the growing season to the time of sampling (days).

## RESULTS AND DISCUSSION

### Spatial distribution of aquatic vegetation

Variation of hydrological conditions of three sectors of the Selenga delta (Fig. 1) has a great influence on the development of aquatic vegetation species. Large water discharges of the Selenginsky sector cause a rare presence of aquatic plants in the channels (mostly reed and small yellow pond-lily) and a large number of macrophytes in the intra-delta lakes Zavernyaekha and Tolstonozhikha (different pondweeds, small yellow pond-lily, spiked water-milfoil, Fig. 2b), and also at the water-stream mouths in the Sor Cherkalov bay (pondweeds, small yellow pond-lily, Fig. 2c). The Sredneustievsky sector with small

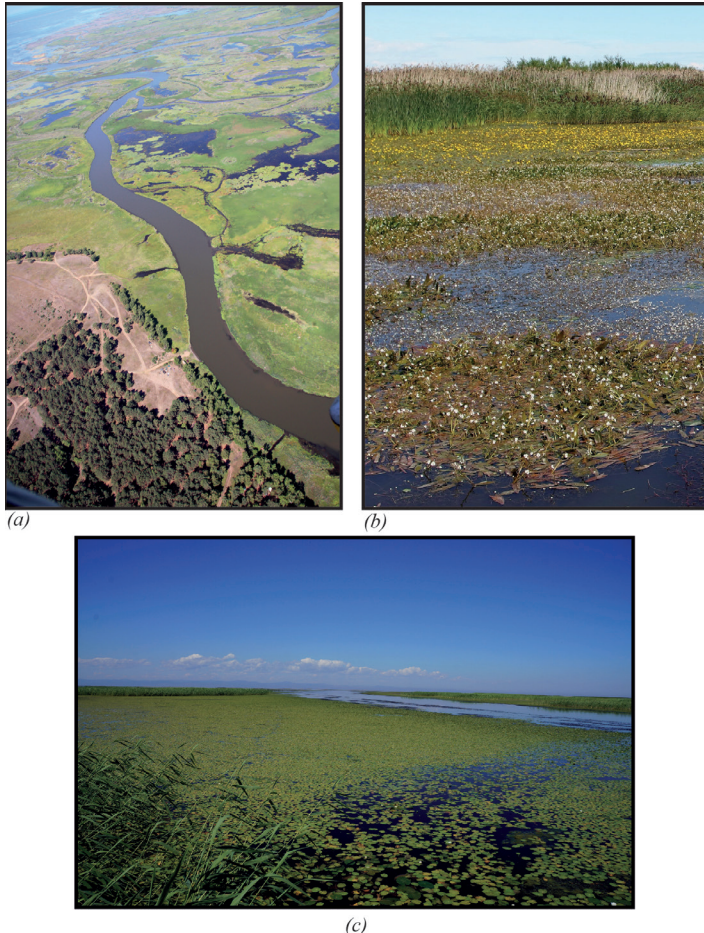


**Fig. 2. Aquatic vegetation of the Selenga delta:**  
 (a) – macrophyte-free large channel; (b) – macrophyte communities in delta lakes;  
 (c) – dense fields of macrophytes in the mouth area of the small channel

channels and low water discharges stands out with the greatest distribution of aquatic vegetation. Main species of this sector are small yellow pond-lily, pondweeds and spiked water-milfoil. The Lobanovsky sector with moderate water discharges is characterized with small amount of aquatic plants. The curtains of small yellow pond-lily, clasping-leaved pondweed, spiked water-milfoil were found there.

### Water chemistry of the Selenga delta

Elements migration factors within Selenga delta are weakly variable. Thus, mineralization values ( $M$ ) in the channels is quite stable (110–144 mg/L) and not dependent on the hydrological season. Spatial variability in the delta sectors is also small: about 110–130 mg/L. Differences in mineralization of the waters of the Proval Bay and the Sor Cherkalov Bay are insignificant: 80–104 mg/L. The highest  $M$  values were found at the mouth of the Casanova channel (130 mg/L), which apparently is associated with the supply of mineralized groundwater (Khazheeva and Pronin 2007). Beyond the island bar where river water is diluted by lake waters there is a decrease in mineralization to 77–84 mg/L. Mineralization in Lake Baikal is quite constant and amounts to about 100 mg/L (State Report... 2014). Alkaline conditions are stable too. The average pH value for deltaic river waters is 8.15 with extreme values from 7.0 to 9.91. The lowest pH was noted in the inner delta lakes of the Selenginsky sector and highest in the small channels of the Selenginsky and Sredneustievsky sectors with a lot of aquatic vegetation. Dissolved oxygen is quite evenly distributed over the delta area and varies from 7.7 to 16.2 mg/L. Minimum values were found in the Selenginsky sector of the delta in the Shamanka and Levoberezhnaya channels (7.7–9.8 mg/L), maximal values were found in the Lobanovskaya channel and the Sor Cherkalov Bay (13.2–15.6 mg/L).

### Heavy metals and metalloids in aquatic plants

The data demonstrated high variability of the chemical elements content in plants: the ratio of maximum and minimum contents in various species is up to 70 times for Cu, Zn, Mo, Cd and up to 1000 times or even higher for Co, V, Al, Be, W, Sn, U. Such differences are due to the ecological and morphological features of the species.

According to ecological and biological characteristics developed in the process of adaptation, all macrophytes are divided into three groups (Katanskaya 1981). The first group, hygrophytes (helophytes), is related to coastal-aquatic rooting plants with stems and leaves rising above the surface of the water that can exist and develop both in water and on the wet shores of water bodies. In the Selenga delta this group includes reed (*Phragmites australis*), flowering rush (*Butomus umbellatus*), and bur reed (*Sparganium*). Due to the simultaneously existence of these macrophytes in aqueous and air environments, they do not lack in light nutrition. Hydrophytes are aquatic plants, subdivided into freely floating non-rooting and rooting with freely floating leaves. In the delta, this is a small yellow pond-lily (*Nuphar pumila*), water lily (*Nymphaea tetragona*), limnanth (*Nymphoides peltata*) and Canadian pondweed (*Elodea canadensis*). Hydatophytes are submerged plants; hence, their entire development cycle takes place in water. They are pondweeds (*Potamogeton*), hornwort (*Ceratophyllum demersum*) and spiked water-milfoil (*Myriophyllum spicatum*).

Reed (*Phragmites australis*) is a typical helophyte and characterized by a wide range of habitat conditions (Ye et al. 1997; Baldantoni et al. 2004; Quan et al. 2007). It forms dense thickets both along the banks of delta channels and intra-delta lakes with water depth of up to 2 m. Contents of the most heavy metals and metalloids (except Mo) in reed are the lowest among macrophytes of the Selenga delta (Table 1).

**Table 1. The average content of chemical elements in macrophytes of the Selenga delta (mg/kg of dry matter)**

Elements	<i>Ph. australis</i> (n=8)	<i>B. umbellatus</i> (n=7)	<i>N. pumila</i> (n=27)	<i>P. natans</i> (n=8)	<i>P. perforliatus</i> (n=21)	<i>P. friesii</i> (n=6)	<i>P. pectinatus</i> (n=5)	<i>M. spicatum</i> (n=14)	<i>C. demersum</i> (n=8)
Fe	409	379	929	1011	2306	10863	8014	9079	2246
Al	312	304	808	703	2312	5225	5297	5196	1872
Mn	393	760	330	1064	1328	1873	1486	3700	2697
Zn	30	25	17	16	22	33	31	25	17
Cu	4.1	6.1	3.8	4.71	6.7	8.9	11	10	5.6
Pb	0.23	0.29	0.6	0.59	1.2	2.3	2.9	3.0	0.98
Bi	0.001	0.01	0.0	0.02	0.03	0.06	0.07	0.08	0.03
Ni	0.72	1.3	1.7	1.78	5.1	6.5	9.4	8.8	6.3
Co	0.17	0.28	0.9	1.25	2.9	2.8	3.7	5.0	4.7
Sn	0.04	0.06	0.0	0.02	0.07	0.1	0.28	0.1	0.08
Cd	0.01	0.04	0.0	0.05	0.16	0.06	0.13	0.15	0.12
Cr	0.62	0.82	1.7	1.38	3.5	8.4	9.9	8.6	3.0
V	0.99	0.9	2.7	2.7	6.2	16	19	17	5.7
Be	0.01	0.01	0.03	0.03	0.08	0.14	0.19	0.19	0.07
W	0.05	0.08	0.1	0.001	0.06	0.25	0.1	0.12	0.16
B	5	11	16	10	12	9	56	26	25
As	0.17	0.23	0.5	1.11	1.6	8.9	4.3	7.3	4.3
Mo	2.5	1.01	0.9	0.58	1.3	2.0	1.6	1.8	0.87
U	0.04	0.08	0.3	0.35	1.27	1.3	1.5	1.7	0.65
Sb	0.001	0.01	0.001	0.001	0.02	0.03	0.05	0.02	0.02

In the Volga delta, reed was also characterized by the lowest HMM contents (Lychagina et al. 1998; Kazmiruk 2008; Brekhovskikh et al. 2009; Tkachenko 2011). However, the average contents of Mn, Fe, Cu, Zn in reed of the Selenga delta are 7–15 times higher than ones in the Volga delta. These metals are closely related to organic matter, amount of which in water of the Selenga delta is significantly higher. At the same time

in the Selenga delta the contents of Ni, Co, Pb, Cd are 2–59 times lower due to lower content in components of aquatic systems.

*Flowering rush (Butomus umbellatus)* in the Selenga delta was found in the Glubokaya, Severnaya channels and the main Selenga channel. This is a rather large plant with a thick, fleshy rhizome, basal upright leaves, and umbellate inflorescences at the top

of the stem, usually growing in water bodies 0.5–0.7 m deep. A flowering rush is a helophyte, as well as a reed, with a similar low content of HMM (table 1).

*Small yellow pond-lily (Nuphar pumila)* is most often found in the mouth areas of water streams, low-flow sections of the channels, and also along the shores of the intra-delta lakes. Water-lily family consists of perennial aquatic plants with a long rhizome, rounded floating leaves and yellow flowers. The species belongs to large-leaved hydrophytes and is characterized by a higher accumulation of HMM than the helophytes (Table 1).

*Pondweeds (Potamogetons)* are widespread within the Selenga delta. These are floating plants with leaves of various shapes and sizes, inflorescence-spike of grayish-green or brownish-green colour. They belong to the group of hydatophytes and generally accumulate HMM more actively than helophytes and hydrophytes (Table 1). Pondweeds form the following range according to increase of HMM content: common floating pondweed (*P. natans*) – clasping-leaved pondweed (*P. perfoliatus*) – pondweed Friesii (*P. friesii*) – fennel-leaved pondweed (*P. pectinatus*). The difference is significant: average content of Mn, Cu, Pb, Ni, Co in *P. pectinatus* is 2-5 times higher than in *P. natans*, Fe, Al, As, U, Be – 5–7 times. *P. friesii* stands the greatest accumulation W, As, Mo, and Zn.

Common floating pondweed was found mainly in the Selenginsky sector of the delta. Fennel-leaved pondweed is widespread in the Lobanovsky sector. Pondweed Friesii is common for small shallow channels of the Sredneustevsky sector. Clasping-leaved pondweed is the most widespread in the whole delta, grows fairly evenly and is characterized by moderate accumulation of HMM.

*Hornwort (Ceratophyllum demersum)* is a perennial herbaceous aquatic plant with thin branches, a rigid stem with sessile leaves. The plant does not form a

root system and, provided the bottom is close to retain in the bottom sediments, specific rhizoid branches can develop. This is a shade-loving plant, sensitive to light, which, nevertheless, grows to a depth of 9 m. Often, the hornwort forms quite dense clusters, freely drifting in the water column. Since photosynthesis at a depth is difficult, the hornwort is more in need of chemical elements necessary for photosynthesis and respiration (Fe, Mn, Zn, etc.) than other types of macrophytes (Lychagina et al. 1998). It has air cavities (70% of the volume), which creates favorable conditions for the concentration of the elements. In the Selenga delta, the hornwort is often found in the mouths of the channels of the Sredneustevsky sector with low flow rates and hindered water exchange. It is characterized by a high content of B, to a lesser extent Ni and Co (Table 1). Due to the fact that the hornwort does not form the root system, it receives the necessary substances and elements from the surrounding water, actively accumulating Zn, Pb, and Cu (Keskinkan et al. 2004). It should be noted that the hornwort plays an important role as a biofilter precipitating suspended particles. This was previously noted in the Volga delta (Lychagina et al. 1998), where the hornwort is characterized by a high content of Mn, Ni, Co, and Cd.

*Spiked water-milfoil (Myriophyllum spicatum)* is a genus of perennial aquatic plants with ascending shoots rising above the surface, creeping rhizomes. Water-milfoil has long and flexible stems up to 2 m length, pinnate leaves, dissected into very narrow, threadlike lobes, green or brown color. The flowers are small, collected in spike-shaped inflorescences towering above the water. Spiked water-milfoil is widespread throughout the delta. Due to the strongly dissected cirrus leaves, water-milfoil is the best trap of the suspended substances among all considered species. Compared to the other plant species, water-milfoil mostly concentrates B, Cr, Co, Ni, Pb, and U (Table 1). It was reported for

Muraviovka Park located in the southern part of Zeya-Bureya Depression (Amur Region, Russia) that spiked water-milfoil accumulates Cu, Zn and Pb in larger quantities than other submerged and rooted hydrophytes with floating leaves (Pakusina et al. 2018).

These results indicate that regardless of the hydroclimatic conditions and the place of growth, hydrophytes spiked water-milfoil and the fennel-leaved pondweed (*P. pectinatus*) most actively accumulate metals, and opposite tendencies were found for helophytes reed and flowering rush which concentrate the least amount. A similar trend of increasing contents of HMM in the following series: helophytes – hydrophytes – hydrophytes was observed for aquatic plants of the Volga delta, as well as an increase in the contents of HMM from large-leaved species to diverse-leaved (Tkachenko et al. 2016). The average HMM concentrations in macrophytes of the Selenga and Volga deltas are generally close, only the content of Mn, Cu, Ni, and Pb are 1.5–3 times higher in the Volga delta, and Fe and Zn are 1.2 times higher in the Selenga delta.

Content of heavy metals and metalloids in aquatic plants is, in general, different from terrestrial plants (Table 2). The latter ones show wider range of Cu, Zn, Pb, Ni, Co values due to the stronger variability of environmental geochemical conditions in terrestrial ecosystems. However, content of Fe and Mn in aquatic plants in many cases exceeds content in terrestrial species. It is less pronounced for marine and more for freshwater plants. This is clearly seen in the Volga and Selenga deltas. The reason is the widespread development of reducing conditions in bottom sediments and wetlands of river deltas, which are very favorable for the migration of Fe<sup>2+</sup> and Mn<sup>2+</sup> compounds.

Generally, HMM levels in macrophytes of the Selenga delta are similar to macrophytes of the Volga delta and aquatic plants of unpolluted estuaries (Table 2).

#### Biogeochemical specialization of macrophytes

The content of HMM in aquatic plants is largely determined by their physiological characteristics and ecological group to which this plant belongs. Due to the

**Table 2. Heavy metals content in plants, mg/kg of dry weight**

Elements	Terrestrial plants <sup>1</sup>	Marine plants <sup>2</sup>	Aquatic plants of unpolluted estuaries <sup>3</sup>	Macrophytes of the Selenga Delta <sup>4</sup>	Macrophytes of the Volga Delta <sup>5</sup>
Fe	18–100	20–5000	50–40000	67–43000	64–36000
Mn	16–1840	7–1740	70–15000	72–47000	54–13000
Cu	1–150	1.2–86	4.5–8.9	1–20	2–32
Zn	12–300	1.4–165	10–100	4–85	2–72
Ni	0.07–48	1–154	3–40	0.1–20.0	0.8–60
Co	0.01–200	0.1–1090	–	0.01–15.0	0.7–15
Pb	0.1–300	2.6–19	2–49	0.05–7.4	0.5–12
Cr	–	–	0.2–50	0.2–30.0	0.02–318

<sup>1</sup> according to Kabata-Pendias and Pendias (1984); <sup>2</sup>Saenko (1992); <sup>3</sup>Moore and Ramamurthy (1987); <sup>4</sup>authors data; <sup>5</sup>Lychagina et al. (1998)

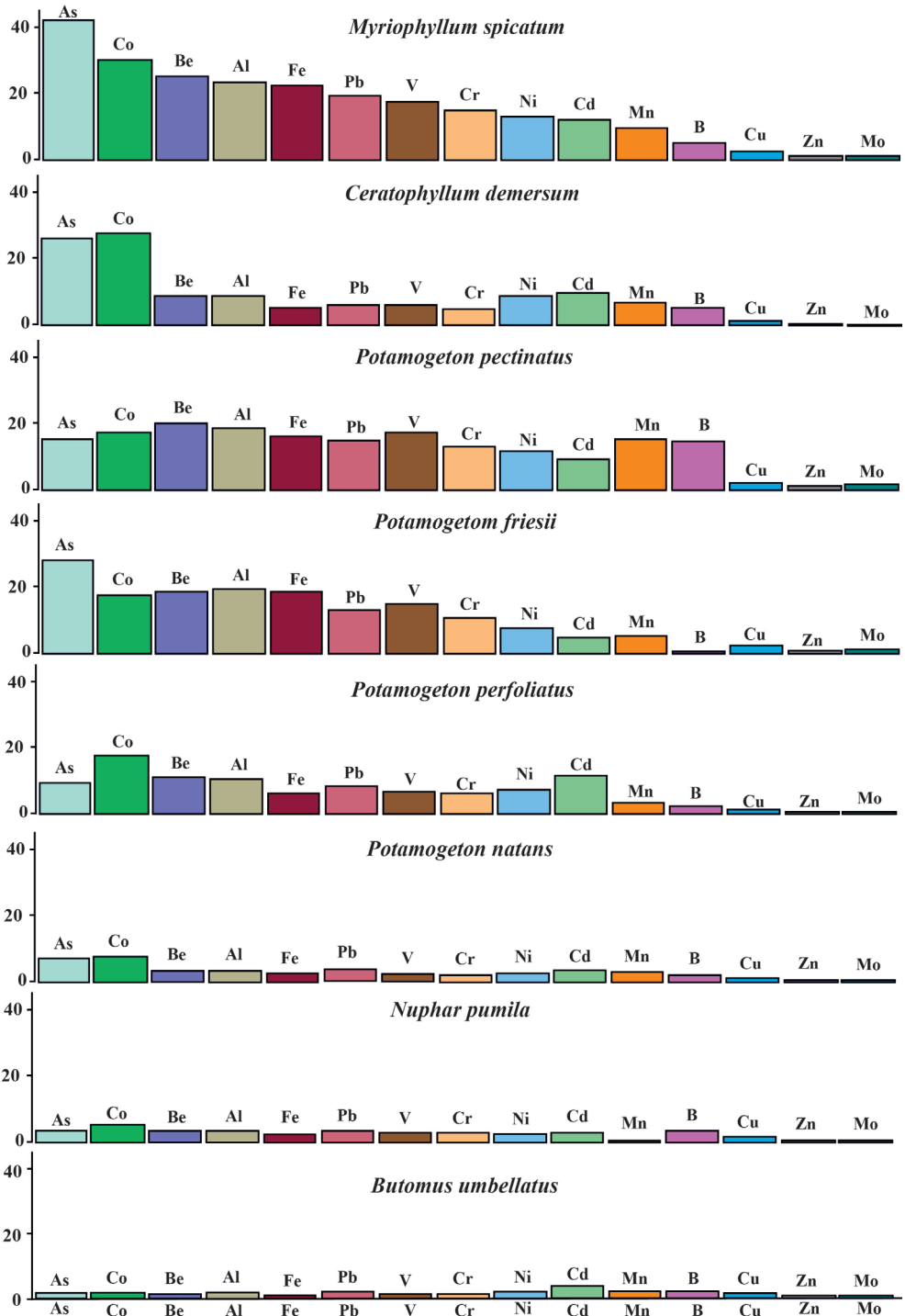


Fig. 3. Enrichment factor  $EF_r$  of chemical elements in various macrophyte species regarding content in reed

high variability of the contents exceeding for the most chemical elements 100%, it is difficult to compare species among themselves. For this, the Enrichment Factor  $EF_r = C_n/C_r$  was calculated (Fig. 3), where  $C_n$  is the content of a chemical element in a particular plant species, and  $C_r$  is the content of this element in a reference species.

Reed has been selected as the latter for several reasons. It has the widest ecological amplitude of growth and participates in a wide variety of plant associations. Reed receives nutrients mainly from bottom sediments through the root system. Content of HMM in reed leaves weakly related to the content in river water. It determines the lowest HMM content in reed among macrophyte species in the Selenga delta. Previously reed was used as a reference species in biogeochemical studies in the Volga delta (Lychagina et al. 1998).

Sviridenko with co-authors (2017) studied ecotopes of aquatic macrophytes of the West Siberian Plain. They reported that some species could be found within areas with high concentrations of dissolved metals. This fact could stand for this species high tolerance to certain element. Thus small yellow pond-lily could withstand rather high concentrations of dissolved Pb, Ni; hornwort – Pb, Ni, Zn, Cu, Mn; pondweeds – Pb, Ni, Mn and to a lesser extent Zn, Cr, Cu; reed – Pb, Ni, Zn, Cd, Cr, Cu, Mn; spiked water-milfoil – Zn; flowering rush – Zn and to a lesser extent Mn. This data confirms previous conclusions about the possibility of using reed as a reference species.

The maximum  $EF_r$  values are common for U. This is due to its very low content in a reference species, as well as high migratory ability in alkaline water and easy accessibility to aquatic plants. Submerged macrophytes fennel-leaved pondweed, clasping-leaved pondweed, pondweed Friesii, spiked water-milfoil, hornwort are characterized with the highest content of U and As, which generally corresponds to the published data (Reay 1972; Outridge and Noller 1991; Favas et al. 2012; Favas et al. 2014).

Analysis of  $EF_r$  values makes it possible to identify the features of biogeochemical specialization of various aquatic plant species (Fig. 3). As clearly seen in Fig. 3, *Myriophyllum spicatum* is characterized by the greatest accumulation ( $EF_r > 10$ ) of a wide group of chemical elements, including both elements that are highly soluble (U, As, B, Cd) and slightly soluble (Fe, Al, Pb, Ni, Co, Be, Cr, V) in the waters of the Selenga delta. Obviously, this plant species has a high ability to accumulate both dissolved and suspended forms of chemical elements. The ability to group concentration of chemical elements is slightly less pronounced for *Ceratophyllum demersum*.  $EF_r$  values for this plant are lower, for most elements are in the range of 5 to 10. As already noted, the high ability to accumulate elements in the Selenga delta is distinguished by pondweeds, among which *Potamogeton pectinatus* and *P. friesii* stand out. For the both species  $EF_r$  values mainly exceed 10.

Weak accumulation of chemical elements is characterized by *Nuphar pumila* and *Butomus umbellatus* species. The average content of Fe, Mn, Pb, Ni, Cr, V, U, As in *Nuphar pumila* is 2–3 times higher than in *Phragmites australis*. For *Butomus umbellatus*, this is noted only for U, Cd and Pb.

### Environmental impacts on metal accumulation in macrophytes

Aquatic plants can receive nutrients mainly in two ways: via the root system from bottom sediments and through the stem and leaf surface from the river water (Sawidis et al. 2001). The wider root system development contributes to the absorption of chemical elements from a larger area, enhancing their accumulation by macrophytes (Wang et al. 1997). The presence of underwater and floating leaves provides a large area for capturing solid suspended particles from the water flow, as well as sorption of the dissolved HMM (Bonnano and Giudice 2010). Macrophytes of wetlands are known to have a greater or comparable ability to accumulate metals compared to other

plant species and biota (Jana 1988). Moreover, the ability to concentrate HMM increases in the series of surface – floating – submerged plants.

The relationship of the contents of elements in aquatic plants and other components of aquatic systems can be characterized using the coefficients  $K_w$ ,  $K_s$  and  $K_b$ . Mean values of HMM are given in the Table 3.

Regarding river water, the studied macrophyte species are enriched with Mn ( $K_w$  up to 26.3) and Co (2.7), regarding suspended matter – Mo ( $K_s$  up to 2.9), Mn (2.8) and B (1.4), regarding bottom sediments – Mn ( $K_b$  up to 9.9), Mo (4.2) and As (1.5).

According to  $K_{wsb}$  values (Table 4) all plant species accumulate mainly Mn and Mo. The widest range of accumulating elements is characteristic for spiked water-

**Table 3. Average content of HMM in components of aquatic systems of the Selenga Delta**

Elements	Suspended sediment, mg/kg (n=83)	Bottom sediment, mg/kg (n=70)	River water, µg/L (n=83)
Be	1.6	2.1	0.03
B	51	–	7.28
V	109	95	1.58
Cr	54	39	3.37
Co	20	11	0.23
Ni	38	23	1.11
Cu	43	18	1.69
Zn	116	63	8.33
As	20	4.8	0.96
Mo	1.67	1.2	1.17
Cd	0.50	0.28	0.02
W	0.90	2.3	0.03
Pb	33	19	1.15
Bi	0.66	0.26	0.00
U	2.8	2.9	0.97
Sn	2.4	2.8	0.06
Sb	0.30	0.85	0.07
Mn	2077	585	25.9
Fe	41125	26365	408
Al	38207	74571	275

**Table 4. Series of HMM accumulation factor by macrophytes according to the values of the coefficient  $K_{wsb}$** 

Species	$K_{wsb}$ value				
	> 10	10–1.0	1.0–0.5	0.5–0.1	< 0.1
<i>M. spicatum</i>	Mn	As, Co, Mo, Fe, Cd	Bi, Cu, Ni, U, V, Zn, Al	Cr, Be, Pb, W, Sn	Sb
<i>C. demersum</i>	–	Mn, Co	As, Cd, Mo, Ni, Cu	Zn, W, U, Fe, Bi, V, Al, Cr, Be, Sn, Pb	Sb
<i>P. friesii</i>	–	Mn, Mo, As	Zn, Cu, Fe, Co, U, Bi, V, Ni	Al, Cd, W, Cr, Be, Pb, Sn	Sb
<i>P. perfoliatus</i>	–	Mn, Cd	Mo, Co, U, Cu, Zn, Ni	Bi, As, Fe, Al, V, Be, Cr, Pb, W	Sn, Sb
<i>P. pectinatus</i>	Mn	Mo	Cu, Zn, Fe, Co, Cd, Ni, U, V, As, Bi	Al, Cr, Be, Sn, Pb, W, Sb	–
<i>P. natans</i>	–	Mn	–	Mo, Cu, Zn, Co, Cd, As, Ni, U, Bi, Fe, V	Al, Cr, Pb, Be, Sn, Sb, W
<i>N. pumila</i>	–	Mn	Mo	Zn, Cu, Cd, Co, Ni, U, Bi, Fe, As, W, V	Al, Cr, Be, Pb, Sn, Sb
<i>B. umbellatus</i>	–	Mn, Mo	Zn, Cu	Cd, W, Ni	Co, Sn, Bi, Fe, U, V, As, Al, Cr, Pb, Sb, Be
<i>Ph. australis</i>	–	Mo, Mn	Zn	Cu, W	Cd, Ni, Sn, Fe, Co, Bi, V, As, Al, Cr, Pb, U, Be, Sb

milfoil:  $Mn_{11.5}, As_{1.6}, Co_{1.4}, Mo_{1.3}, Fe_{1.2}, Cd_{1.1}$ . The shorter series found for the pondweed Friesii  $Mn_{6.4}, Mo_{3.3}, As_{1.1}$ , clasping-leaved pondweed ( $Mn_{4.2}, Cd_{1.1}$ ), fennel-leaved pondweed ( $Mn_{18.4}, Mo_{3.7}$ ) and hornwort ( $Mn_{8.5}, Co_{1.3}$ ). Reed and flowering rush are characterized by the lowest  $K_{wsb}$  values (1.2–2.3), which confirms the relatively weak relationship of these plant species with the habitat.

The highest  $Z_{veg}$  values are common for the fennel-leaved pondweed (22.1) and spiked water-milfoil (13.1), followed by the pondweed Friesii (9.7), hornwort (8.5), clasping-leaved pondweed (4.2), and flowering rush (4.1), common floating pondweed (3.4) and reed (1.9).

To identify the peculiarities of accumulation of suspended and dissolved forms of HMMs

by aquatic plants, we examined the ratio of decimal logarithms of the products of the concentrations of chemical elements migrating in aquatic systems of the Selenga delta mainly in suspended or dissolved forms. Two associations of chemical elements were identified:

1) S-association with the predominant suspended form of migration – Be, V, Co, Ni, W, Pb, Bi, Mn, Fe and Al;

2) D-association with the predominant dissolved form of migration – B, U, Mo, Cr, Cu, Zn, As, Cd, Sn and Sb.

Due to these associations three groups of macrophytes were distinguished (Fig. 4):

1) helophytes flowering rush and reed with a low HMM content (green zone in the figure);

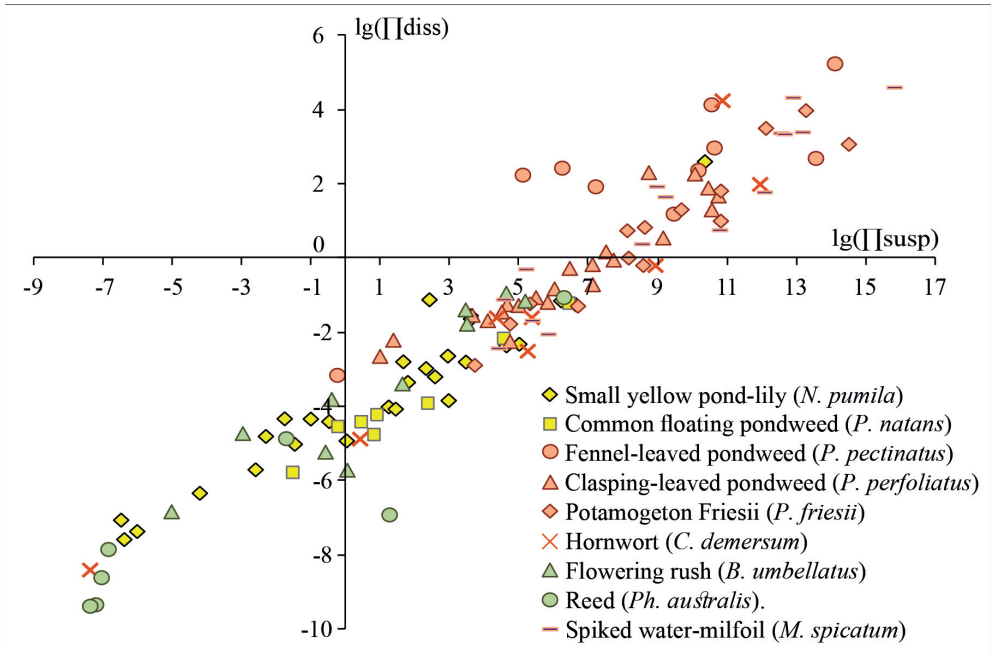


**Fig. 4. Accumulation of suspended and dissolved forms of HMM by macrophyte species**

2) hydrophyte small yellow pond-lily and hydathophyte common floating pondweed with a moderate accumulation of S-association elements and weak accumulation of D-association elements (yellow zone);

3) hydathophytes submerged with a large leaf area, accumulating both elements of group S and D – claspingleaved pondweed, fennel-leaved pondweed, and pondweed Friesii (orange zone).

In the I quarter of the field in Figure 4 (orange zone) with active accumulation of both dissolved and suspended forms of elements, with the predominance of the latter, there are spiked water-milfoil, hornwort and pondweeds. Flowering rush and reed are located in IV и III quarters. They are characterized by weak accumulation of both dissolved and suspended forms of elements, which is caused by the prevailing root nutrition from the bottom sediments. Common floating pondweed and small yellow pond-lily (yellow zone) are mainly located in the IV quarter. They show relatively weak accumulation of suspended forms of elements because they do not have

such dissected leaves as spiked water-milfoil and hornwort, and cannot precipitate the suspended matter with the same intensity.

Mn, which actively accumulates in macrophytes of the Selenga delta, migrates mainly in suspended form. This element is necessary for plants to build large molecules (proteins), and is also involved in the photosynthesis of oxygen in chloroplasts (Kabata-Pendias and Pendias 1984). The highest concentrations of Mn were found in spiked water-milfoil (3700  $\mu\text{g/g}$ ) and hornwort (2697), and the smallest – in the small yellow pond-lily (330) and reed (393).

#### Spatial features of HMM distribution

The main spatial features of the spatial distribution of HMM can be shown by example of Mo. This is one of the main elements concentrating in aquatic plants to a greater extent than in other components of aquatic landscapes, presented in the Selenga water mainly in dissolved form. It is accumulated by macrophytes 70 times more intensively than Co and As. The great demand of macrophytes in Mo is associated with its functions in their body: it is a part

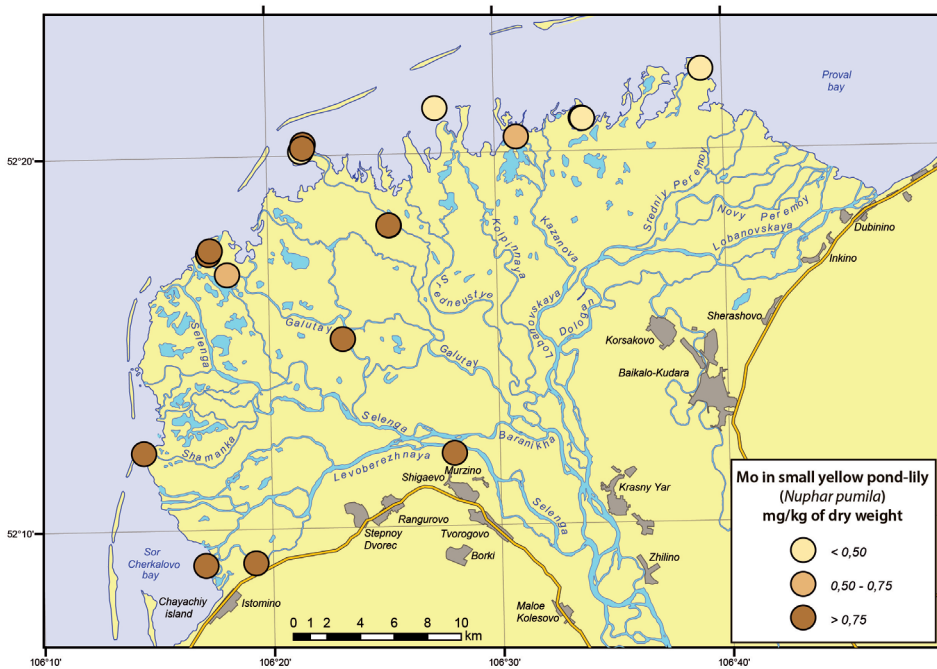


**Fig. 5. Mo content in the small yellow pond-lily (*Nuphar pumila*)**

of proteins and enzymes, participates in nitrogen fixation and redox reactions (Kabata-Pendias and Pendias 1984). Most of all Mo was found in reed (2.5  $\mu\text{g/g}$ ) and spiked water-milfoil (1.8), and least of all in common floating pondweed (0.6) and small yellow pond-lily (0.9).

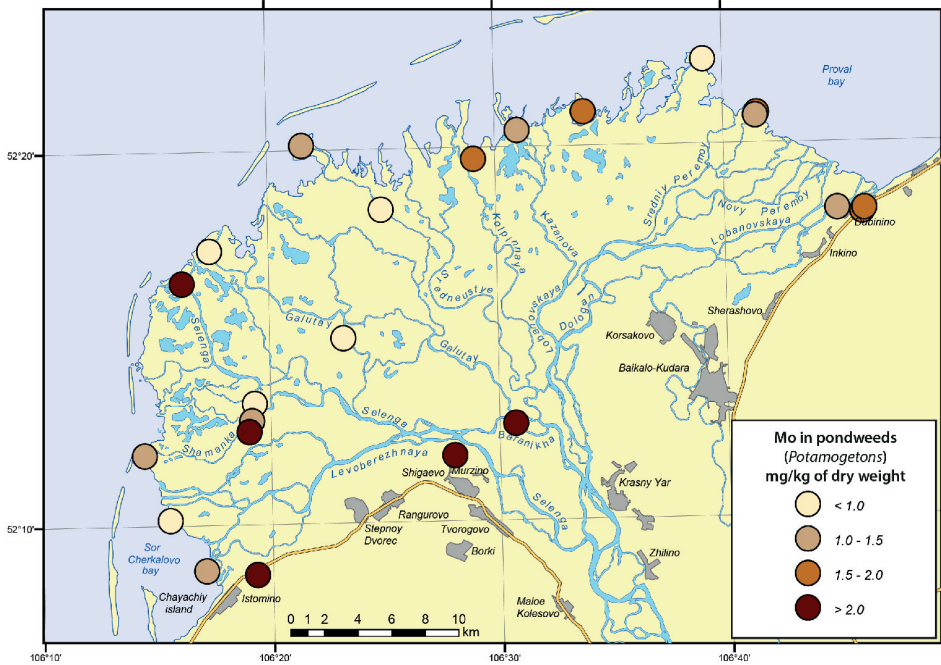
*Nuphar pumila*. Relatively high concentrations of HMM in *Nuphar pumila* were observed in the Selenginskiy sector of the delta (Fig. 5) during the summer low water season, when fine particles sedimentation processes occur in the mouths of large channels. Reduced contents were noted in the Lobanovskaya channel during the flood period.

*Potamogetons*. On the whole, they more actively accumulate HMM than water lilies, reeds, and flowering rush (Table 1), but each species has its own peculiarities. Common floating pondweed was found mainly in the Selenginskiy sector of the delta and in small quantities in the Sredneustevsky sector (Fig. 6a). It accumulates only small amounts of suspended matter. Fennel-leaved pondweed, widespread in the Lobanovsky sector, is characterized by the highest content of a number of metals. Pondweed

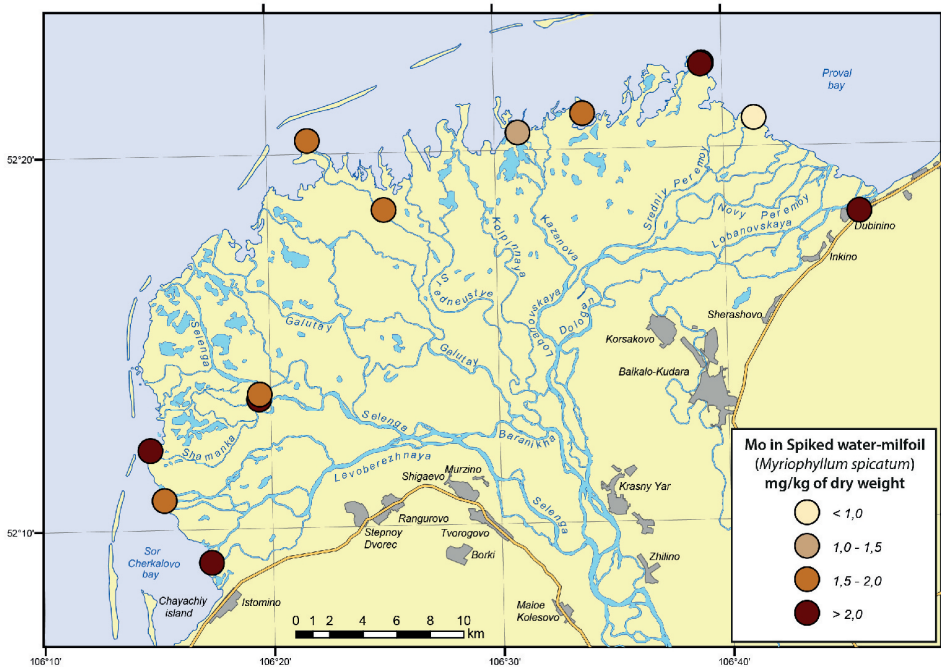
*Friesii*, common in small shallow channels of the Sredneustevsky sector, accumulates mainly Cu and Zn, which are necessary for the synthesis of chlorophyll.

Clasping-leaved pondweed is most widespread in the whole delta, grows fairly evenly and is characterized by moderate accumulation of HMM. Local maximum of the elemental abundances in pondweeds (Fig. 6a) were noted in the Severnaya (common floating pondweed), Srednyy Peremoy (fennel-leaved pondweed), Lobanovskaya (clasping-leaved pondweed) and Galutay (pondweed *Friesii*) channels.

*Myriophyllum spicatum*. Spiked water-milfoil (with a stem up to 2 m long) was found throughout the Selenga delta; its largest accumulations are characteristic for the western end of the delta (Fig. 6b). The highest metal content in spiked water-milfoil was found at the mouths of the Severnaya and Srednyaya channels of the Sredneustevsky sector. Due to the strongly dissected cirrus leaves, water-milfoil is the best trap of river suspended sediments among all considered species.



(a)



(b)

Fig. 6. Mo content in (a) pondweeds (*Potamogetons*) and (b) spiked water-milfoil (*Myriophyllum spicatum*)

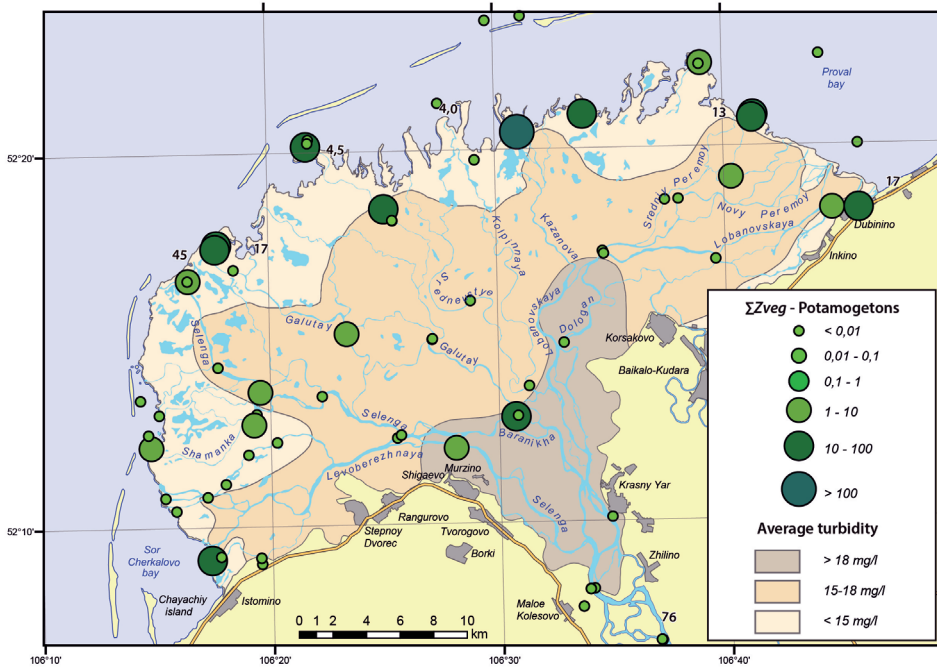


Fig. 7. Spatial distribution of the additive coefficient  $\Sigma Z_{veg}$  in hydatophytes by the example of pondweeds

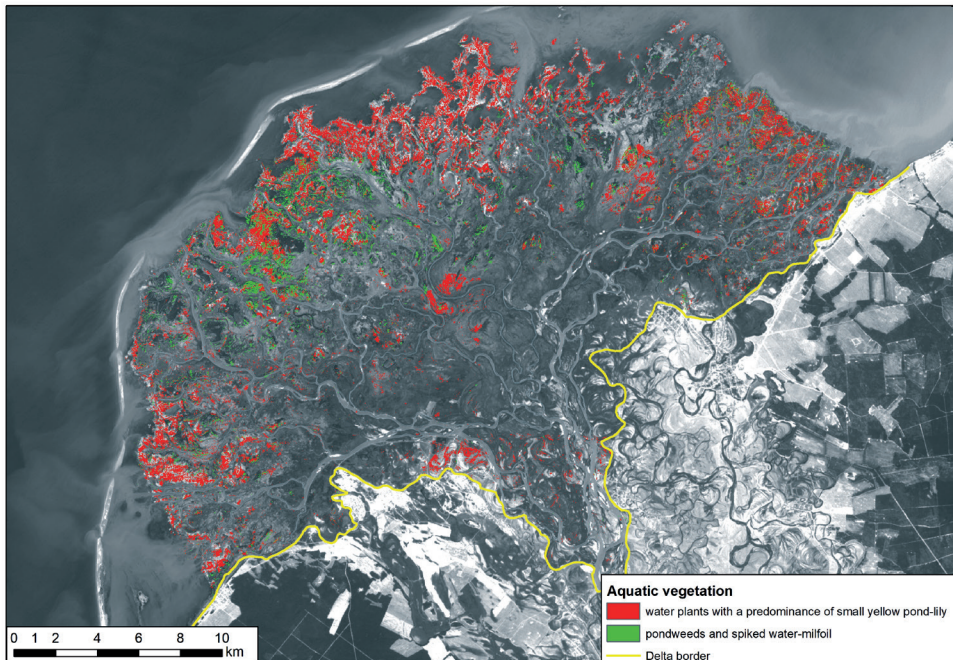


Fig. 8. Distribution scheme of the main groups of macrophytes: red shows the distribution of associations of water plants with a predominance of small yellow pond-lily, green shows the distribution of pondweeds and spiked water-milfoil

Total accumulation coefficient  $Z_{veg}$  (Fig. 7) increases at the delta-lake edge where the accumulation of HMM by macrophytes is significant. Small backwaters of large channels and intra-delta lakes where under low flow conditions both with shallow depths and highwater temperature rapid development of aquatic plants occurs, especially of hydato- and hydrophytes. These plants as a biofilter in a large extent participate in the deposition of suspended matter. Hydatophytes are characterized by higher  $Z_{veg}$  values than hydrophytes. This is caused by the active accumulation of suspended particles on the leaf surface. The result of the remote sensing data can be seen in Fig. 8. The analysis made it possible to compile a series of HMMs on the intensity of biofiltration by macrophytes: they retain more than 60% of the total Mn flux that came into the delta, more than 10% – W, As, and from 3 to 10% B, Fe, Co, Mo, Cd, V, Ni, Bi, Be, Cu, Zn, Cr, U, Al. The largest contribution is made by the group of hydatophytes (spiked water-milfoil and pondweed), which account for 74 to 96% of the total mass of substances accumulated by aquatic plants.

## CONCLUSIONS

The study reveals the biogeochemical specialization of higher aquatic vegetation which is dominated by accumulation of Mn and Mo. These elements are part of proteins and are necessary for the reaction of photosynthesis and redox reactions.

Macrophyte accumulation levels of HMM are determined by plant species. The reed with low  $Z_{veg}$  coefficients (1.2–2.3) was used as a reference plant. HMM accumulation in macrophytes in relation to reed was revealed for U, As, Cd and B. These elements dominated in dissolved form in the Selenga delta regardless of hydroclimatic conditions.

Species with a very weak accumulation of elements were distinguished (reed and flowering rush) from well-accumulating species (a group of pondweeds, small yellow pond lily, hornwort and spiked water-milfoil). Spiked water-milfoil accumulates the maximum number of elements in relation to

other components of aquatic systems. The accumulation series according to  $Z_{veg}$  for it are as follows:  $Mn_{11.5}, As_{1.6}, Co_{1.4}, Mo_{1.3}, Fe_{1.2}, Cd_{1.1}$ . Among pondweeds the group concentration of HMMs is common for the pondweed Friesii ( $Mn_{6.4}, Mo_{3.3}, As_{1.1}$ ). Claspingleaved pondweed ( $Mn_{4.2}, Cd_{1.1}$ ), fennel-leaved pondweed ( $Mn_{18.4}, Mo_{3.7}$ ) and hornwort ( $Mn_{8.5}, Co_{1.3}$ ) accumulate only 2 elements each. The active concentration of elements by well-accumulating species is explained by the physiological characteristics of these plants: they have very dissected leaves, a large area of which allows them to retain a significant amount of suspended matter. Moreover, immersed species are more in need of trace elements due to lack of light.

Delta macrophytes precipitate more than 60% of Mn, more than 10% of W, As, and from 3 to 10% of B, Fe, Co, Mo, Cd, V, Ni, Bi, Be, Cu, Zn, Cr, U, Al from the total flux of the element that came into the epic part of the delta. The largest role in the accumulation of suspended matter enriched with HMMs is played by hydatophytes, which capture a large amount of suspended matter and act as biological "traps".

## ACKNOWLEDGEMENTS

Work was done with financial support of following grants: "Comprehensive assessment of the impact of the Selenga basin on Lake Baikal" (RGS, No. 06/2015-И), "Development of the atlas-monograph "The Selenga Basin: hydrological and landscape-geochemical analysis" (RGS, 13/2016-P), Spatio-temporal analysis of the migration of chemical elements and compounds in natural and anthropogenic landscapes" (No. 14-27-00083), RGS-RFBR "Geochemical barrier zones in freshwater river deltas of Russia" (No. 23/2017 / RGS-RFBR), RFBR "Long-term river variability the influx of water, sediment and chemicals into Lake Baikal" (No. 17-29-05027). In addition, the work was supported by WSP Sverige AB (project K3502010). The field visits were also done as a part of expedition Selenga-Baikal and the Baikal expedition of the Russian Geographical Society in 2011-2018. ■

## REFERENCES

- Baldantoni D., Alfani A., Di Tommasi P., Bartoli G. and Virzo De Santo A. (2004). Assessment of macro and microelement accumulation capability of two aquatic plants. *Environmental Pollution*, 130, pp. 149-156. doi: 10.1016/j.envpol.2003.12.015
- Brekhovskikh V.F., Volkova Z.V. and Savenko A.V. (2009). Higher aquatic vegetation and accumulation processes in the delta of the river Volga. *Arid ecosystems*, 15(3(39)), pp. 34-45. (In Russian)
- Carbiener R., Trémolières M., Mercier J. L. and Ortscheit A. (1990). Aquatic macrophyte communities as bioindicators of eutrophication in calcareous oligosaprobe stream waters (Upper Rhine plain, Alsace). *Vegetatio*, 86(1), pp. 71-88. doi: 10.1007/BF00045135
- Chalov S., Bazilova V. and Tarasov M. (2017). The balance of suspended sediment in the Selenga delta at the end of the 20th - beginning of the 21st centuries: modeling according to LANDSAT images. *Water resources*, 44(3), pp. 332-339. (In Russian). doi: 10.7868/S0321059617030075
- Chalov S., Jarsjö J., Kasimov N., Romanchenko A., Pietron J., Thorslund J. and Promakhova E. (2015). Spatio-temporal variation of sediment transport in the Selenga River Basin, Mongolia and Russia. *Environmental Earth Sciences*, 72(2), pp. 663-680. doi: 10.1007/s12665-014-3106-z
- Chalov S., Thorslund J., Kasimov N., Aybullatov D., Ilyicheva E., Karthe D., Kositsky A., Lychagin M., Nittrouer J., Pavlov M., Pietron J., Shinkareva G., Tarasov M., Garmaev E., Akhtman Y. and Jarsjö J. (2017). The Selenga River delta: a geochemical barrier protecting Lake Baikal waters. *Regional environmental change*, 17(7), pp. 2039-2053. doi: 10.1007/s10113-016-0996-1
- Chaplin G. and Valentine J. (2009). Macroinvertebrate production in the submerged aquatic vegetation of the Mobile–Tensaw Delta: effects of an exotic species at the base of an estuarine food web. *Estuaries and Coasts*, 32(2), pp. 319-332. doi: 10.1007/s12237-008-9117-9
- Chepinoga V. (2012). Wetland vegetation database of Baikal Siberia (WETBS). *Biodiversity & Ecology*, 4, p. 311. doi: 10.7809/b-e.00107
- Chepinoga V. and Rosbach S. (2012). Aquatic vegetation of Lemnetaea class on the territory of Baikal Siberia. *Russian vegetation*, 21, pp. 106-123. (In Russian)
- Coops H., Hanganu J., Tudor M. and Oosterberg W. (1999). Classification of Danube Delta lakes based on aquatic vegetation and turbidity. *Hydrobiologia*, 415, pp. 187-191. doi: 10.1023/A:1003856927865
- Cubero-Castan M., Constantin D., Barbieux K., Nouchi V., Akhtman Y. and Merminod B. (2015). A new smoothness based strategy for semi-supervised atmospheric correction: application to the Léman-Baikal campaign. 7th Workshop on Hyperspectral Image and Signal Processing: Evolution in Remote Sensing, EPFL-CONF, pp. 1-4. doi: 10.1109/WHISPERS.2015.8075379
- Cui B., Tang N., Zhao X. and Bai J. (2009). A management-oriented valuation method to determine ecological water requirement for wetlands in the Yellow River Delta of China. *Journal for Nature Conservation*, 17(3), pp. 129-141. doi: 10.1016/j.jnc.2009.01.003

Dgebuadze Y., Dorofeyuk N. and Krylov A. (2010). Contributions of Russian Scientists to the Research of Aquatic Ecosystems in Mongolia. *Mongolian Journal of Biological Sciences*, 8(1), pp. 59-69. doi: 10.22353/mjbs.2010.08.07

Dong T., Il'icheva E., Nittrouer J. and Pavolv M. (2013). Morphology and sediment transport dynamics of the Selenga River delta, Lake Baikal, Russia. In AGU Fall Meeting Abstracts.

Favas P., Pratas J. and Prasad M. (2012). Accumulation of arsenic by aquatic plants in large-scale field conditions: opportunities for phytoremediation and bioindication. *Science of the Total Environment*, 433, pp. 390-397. doi: 10.1016/j.scitotenv.2012.06.091

Favas P., Pratas J., Varun M., D'Souza R. and Paul M. (2014). Accumulation of uranium by aquatic plants in field conditions: prospects for phytoremediation. *Science of the Total Environment*, 470, pp. 993-1002. doi: 10.1016/j.scitotenv.2013.10.067

Guittonny-Philippe A., Masotti V., Höhener P., Boudenne J., Viglione J. and Laffont-Schwob I. (2014). Constructed wetlands to reduce metal pollution from industrial catchments in aquatic Mediterranean ecosystems: A review to overcome obstacles and suggest potential solutions. *Environment International*, 64, pp. 1-16. doi: 10.1016/j.envint.2013.11.016

Il'icheva E. (2015). Runoff in the river delta Selenga. Materials of the XV meeting of geographers of Siberia and the Far East. Ulan-Ude. Irkutsk: Institute of Geography named after V.B. Sochava SB RAS. pp. 91-93. (In Russian)

Iqbal I. (2010). *The Bengal Delta: Ecology, state and social change, 1840–1943*. Springer.

Jarsjö J., Chalov S., Pietroń J., Alekseenko, A. and Thorslund, J. (2017). Patterns of soil contamination, erosion and river loading of metals in a gold mining region of northern Mongolia. *Regional environmental change*, 17(7), pp. 1991-2005. doi: 10.1007/s10113-017-1169-6

Kabata-Pendias A. and Pendias H. (1984). *Trace elements in soils and plants*. Boca Raton: CRC Press.

Kasimov N., Kosheleva N., Lychagin M. et al. (2019). *Environmental Atlas-monograph "Selenga-Baikal"*. Moscow: Faculty of Geography, MSU. Available at: [https://www.researchgate.net/publication/335567904\\_Environmental\\_Atlas-monograph\\_Selenga-Baikal](https://www.researchgate.net/publication/335567904_Environmental_Atlas-monograph_Selenga-Baikal). (In Russian)

Katanskaya V. (1981). *Higher aquatic vegetation of the continental reservoirs of the USSR. Study methods*. Leningrad: Nauka. (In Russian)

Keskinkan O., Goksu M., Basibuyuk M. and Forster C. (2004). Heavy metal adsorption properties of a submerged aquatic plant (*Ceratophyllum demersum*). *Bioresource Technology*, 92 (2), pp. 197-200. doi: 10.1016/j.biortech.2003.07.011

Khazheeva Z. and Pronin N. (2007). The influence of Canadian Elodea on the chemical composition of water and bottom sediments in the Selenga river delta. *Bulletin of BSU*, 3, pp. 177-179. (In Russian)

Khedr A. and El-Demerdash M. (1997). Distribution of aquatic plants in relation to environmental factors in the Nile Delta. *Aquatic Botany*, 56(1), pp. 75-86. doi: 10.1016/S0304-3770(96)01090-X

- Korytny L., Il'icheva E., Pavlov M. and Amosova I. (2012). Hydrologo-morphological approach to regionalization of the Selenga river basin. *Geography and Natural Resources*, 33(3), pp. 212-217. doi: 10.1134/S1875372812030055
- Kröger R., Moore M., Locke M., Cullum R., Steinriede Jr., R., Testa III S., Bryant C. and Cooper C. (2009). Evaluating the influence of wetland vegetation on chemical residence time in Mississippi Delta drainage ditches. *Agricultural Water Management*, 96(7), pp. 1175-1179. doi: 10.1016/j.agwat.2009.03.002
- Lane C.R., Anenkhonov O., Liu H., Autrey B.C. and Chepinoga V. (2015). Classification and inventory of freshwater wetlands and aquatic habitats in the Selenga River Delta of Lake Baikal, Russia, using high-resolution satellite imagery. *Wetlands Ecology and Management*, 23(2), pp. 195-214. doi: 10.1007/s11273-014-9369-z
- Leto C., Tuttolomondo T., La Bella S., Leone R. and Licata M. (2013). Effects of plant species in a horizontal subsurface flow constructed wetland–phytoremediation of treated urban wastewater with *Cyperus alternifolius* L. and *Typha latifolia* L. in the West of Sicily (Italy). *Ecological Engineering*, 61, pp. 282-291. doi: 10.1016/j.ecoleng.2013.09.014
- Lychagina N., Kasimov N. and Lychagin M. (1998). Biogeochemistry of macrophytes of the Volga delta. Moscow: Geography Department of Moscow State University. (In Russian)
- Malsy M., Heinen M., aus der Beek T. and Flörke M. (2013). Water resources and socio-economic development in a water scarce region on the example of Mongolia. *Geo-Öko*, 34 (1-2), pp. 27-49
- Nepf H. (2012). Flow and transport in regions with aquatic vegetation. *Annual review of fluid mechanics*, 44, pp. 123-142. doi: 10.1146/annurev-fluid-120710-101048
- Outridge P. and Noller B. (1991). Accumulation of toxic trace elements by freshwater vascular plants. *Reviews of Environmental Contamination and Toxicology*. New York: Springer. doi: 10.1007/978-1-4612-3196-7\_1
- Pakusina A., Platonova T., Lobarev S. and Smirenski S. (2018). Chemical and Ecological Characteristics of Lakes Located in the Muraviovka Park. *Asian Journal of Water, Environment and Pollution*, 15(4), pp. 27-34. doi: 10.3233/AJW-180054
- Patel D. and Kanungo V. (2010). Phytoremediation potential of duckweed (*Lemna minor* L. a tiny aquatic plant) in the removal of pollutants from domestic wastewater with special reference to nutrients. *Bioscan*, 5(3), pp. 355-358.
- Pietroń J. (2017). Sediment transport from source to sink in the Lake Baikal basin: Impacts of hydroclimatic change and mining (Doctoral dissertation, Department of Physical Geography, Stockholm University).
- Pietroń J., Chalov S., Chalova A., Alekseenko A. and Jarsjö J. (2017). Extreme spatial variability in riverine sediment load inputs due to soil loss in surface mining areas of the Lake Baikal basin. *Catena*, 152, pp. 82-93. doi: 10.1016/j.catena.2017.01.008
- Pietroń J., Nittrouer J., Chalov S., Dong T., Kasimov N., Shinkareva G. and Jarsjö J. (2018). Sedimentation patterns in the Selenga River delta under changing hydroclimatic conditions. *Hydrological processes*, 32(2), pp. 278-292. doi: 10.1002/hyp.11414

Quan W., Han J., Shen A., Ping X., Qian P., Li C., Shi L. and Chen Y. (2007). Uptake and distribution of N, P and heavy metals in three dominant salt marsh macrophytes from Yangtze River estuary, China. *Marine Environmental Research*, 64, pp. 21-37. doi: 10.1016/j.marenvres.2006.12.005

Rai P. (2009). Heavy metal phytoremediation from aquatic ecosystems with special reference to macrophytes. *Critical Reviews in Environmental Science and Technology*, 39(9), pp. 697-753. doi: 10.1080/10643380801910058

Reay P. (1972). The accumulation of arsenic from arsenic-rich natural waters by aquatic plants. *Journal of applied ecology*, 9(2), pp. 557-565. doi: 10.2307/2402453

Rogozin A. (1981). The history of the relief development of the Selenginsky coast zone of the Lake Baikal. Fishery value of the coastal zone of the Lake Baikal. Irkutsk. pp. 3-18. (In Russian)

Sawidis T., Chettri M., Papaionnou A., Zachariadis G. and Stratis J. (2001). A study of metal distribution from lignite fuels using trees as biological monitors. *Ecotoxicology and Environmental Safety*, 48, pp. 27-35. doi: 10.1006/eesa.2000.2001

State report "The state of the Lake Baikal and measures for its protection in 2013". (2014). Irkutsk: Siberian branch of the Federal State-Funded Scientific-Practical Enterprise "Rosgeolfond". (In Russian)

Sviridenko B., Murashko Yu., Sviridenko T., Efremov A. and Tokar O. (2017). Content of heavy metals in ecotopes of hydromacrophytes of the West Siberian plain. *Bulletin of Surgut State University*, (4), pp. 81-96. (In Russian)

Sun H., Wang Z., Gao P. and Liu P. (2013). Selection of aquatic plants for phytoremediation of heavy metal in electroplate wastewater. *Acta physiologiae plantarum*, 35(2), pp. 355-364. doi: 10.1007/s11738-012-1078-8

Thorslund J., Jarsjö J., Belozerova E. and Chalov S. (2012). Assessment of the gold mining impact on riverine heavy metal transport in a sparsely monitored region: the upper Lake Baikal Basin case. *Journal of Environmental Monitoring*, 14, pp. 2780-2792. doi: 10.1039/C2EM30643C

Thorslund J., Jarsjö J., Jaramillo F., Jawitz J., Manzoni S., Basu N., Chalov S., Cohen M., Creed I., Goldenberg R. and Hysin A. (2017). Wetlands as large-scale nature-based solutions: Status and challenges for research, engineering and management. *Ecological Engineering*, 108, pp. 489-497. doi: 10.1016/j.ecoleng.2017.07.012

Tkachenko A. (2011). Geochemistry of aquatic landscapes of the Volga estuary region. PhD thesis synopsis. Moscow: Lomonosov Moscow State University (In Russian)

Tkachenko A., Gerasimova M., Lychagin M., Kasimov N. and Kroonenberg S. (2016) Bottom sediments in deltaic shallow-water areas – are they soils? *Geography, Environment, Sustainability*, 9(3), pp. 39-52. doi: 10.15356/2071-9388\_03v09\_2016\_03

Tulokhonov A. (2001). Field environmental workshop for students of natural sciences. Ulan-Ude: Publishing House of the BSC SB RAS. (In Russian)

Törnqvist R., Jarsjö J., Pietron J., Bring A., Rogberg P., Asokan S. and Destouni G. (2014). Evolution of the hydro-climate system in the Lake Baikal basin. *Journal of Hydrology*, 519, pp. 1953-1962. doi: 10.1016/j.jhydrol.2014.09.074

Underwood E., Mulitsch M., Greenberg J., Whiting M., Ustin S. and Kefauver S. (2006). Mapping invasive aquatic vegetation in the Sacramento-San Joaquin Delta using hyperspectral imagery. *Environmental Monitoring and Assessment*, 121(1-3), pp. 47-64. doi: 10.1007/s10661-005-9106-4

Unesco.org, (2019). UNESCO's Official Website. [online] Available at: <https://whc.unesco.org/en/list/754>

Wang W., Gorsuch J. and Hughes J. (1997). *Plants for Environmental Studies*. New York: CRC Press.

Wang B., Wang Y. and Wang W. (2014). Retention and mitigation of metals in sediment, soil, water, and plant of a newly constructed root-channel wetland (China) from slightly polluted source water. *SpringerPlus*, 3(1), p. 326. doi: 10.1186/2193-1801-3-326

Ye Z., Baker A., Wong M. and Willis A. (1997). Zinc, lead and cadmium tolerance, uptake and accumulation by the common reed, *Phragmites australis* (Cav.) Trin. ex Steudel. *Annals of Botany*, 80(3), pp. 363-370. doi: 10.1006/anbo.1997.0456

Received on July 7<sup>th</sup>, 2019

Accepted on August 8<sup>th</sup>, 2019

# AUTHOR GUIDELINES

1. Authors are encouraged to submit high-quality, original work: scientific papers according to the scope of the Journal, reviews (only solicited) and brief articles.
2. Papers are accepted in English. Either British or American English spelling and punctuation may be used.
3. All authors of an article are asked to indicate their names (with one forename in full for each author, other forenames being given as initials followed by the surname) and the name and full postal address (including postal code) of the affiliation where the work was done. If there is more than one institution involved in the work, authors' names should be linked to the appropriate institutions by the use of 1, 2, 3 etc superscript. Telephone and fax numbers and e-mail addresses of the authors could be published as well. One author should be identified as a Corresponding Author. The e-mail address of the corresponding author will be published, unless requested otherwise.

## EXAMPLE:

**Ivan I. Ivanov<sup>1</sup>, Anton A. Petrov<sup>1\*</sup>, David H. Smith<sup>2</sup>**

<sup>1</sup>University/Organization name, Street, City, ZIP-code, Country

<sup>2</sup>University/Organization name, Street, City, ZIP-code, Country

\* **Corresponding author:** example@example.com

4. The GES Journal style is to include information about the author(s) of an article. Therefore we encourage the authors to submit their portrait photos and short CVs (up to 100 words).
5. Article structure should contain further sections:
  - Abstract.
  - Keywords (Immediately after the abstract, provide a maximum of 6 keywords, avoiding general and plural terms and multiple concepts (avoid, for example, 'and', 'of'). Be sparing with abbreviations: only abbreviations firmly established in the field may be eligible. These keywords will be used for indexing purposes.)
    - Introduction (State the objectives of the work and provide an adequate background, avoiding a detailed literature survey or a summary of the results.)
    - Material and methods (Provide sufficient details to allow the work to be reproduced by an independent researcher. Methods that are already published should be summarized, and indicated by a reference. If quoting directly from a previously published method, use quotation marks and also cite the source. Any modifications to existing methods should also be described.)
      - Results (Results should be clear and concise.)
      - Discussion (This should explore the significance of the results of the work, not repeat them. A combined Results and Discussion section is often appropriate. Avoid extensive citations and discussion of published literature.)
      - Conclusions (The main conclusions of the study may be presented in a short Conclusions section, which may stand alone or form a subsection of a Discussion or Results and Discussion section.)
      - Acknowledgements (List here those individuals who provided help during the research and funds which provided financial support of your research.)
      - References (Make a list of references according to guidance provided below).
      - Appendices (If there is more than one appendix, they should be identified as A, B, etc.

Formulae and equations in appendices should be given separate numbering: Eq. (A.1), Eq. (A.2), etc.; in a subsequent appendix, Eq. (B.1) and so on. Similarly for tables and figures: Table A.1; Fig. A.1, etc.).

6. Sections and sub-sections shouldn't be numbered, but divided into sub-levels. If you would like to refer to a particular section, name it without any numbers (for example: see "Materials and methods")

7. Math equations should be submitted as editable text and not as images (use appropriate tool in text editor). Present simple formulae in line with normal text where possible and use the solidus (/) instead of a horizontal line for small fractional terms, e.g., X/Y. In principle, variables are to be presented in italics. Number consecutively any equations that have to be displayed separately from the text (if referred to explicitly in the text).

8. Figures and figure captions. Number the illustrations according to their sequence in the text. Regardless of the application used, when your figure is finalized, please 'save as' or convert the images to one of the following formats: TIFF, JPG. Supply files that are optimized for screen use. **The resolution should be at least 300 dpi.** Besides inserting figures into your manuscript, you must also upload appropriate files during paper submission. Ensure that each illustration has a caption. A caption should comprise a brief title (not on the figure itself) and a description of the illustration beginning from "Fig. 1..." (note: no any dots in the end of the capture!). Keep text in the illustrations themselves to a minimum but explain all symbols and abbreviations used.

Example of referring to the figure in text: (Fig. 1)

Example of figure caption: Fig. 1. The distribution of the family Monimiaceae

9. Tables. Please submit tables as editable text and not as images. Tables can be placed either next to the relevant text in the article, or on separate page(s) at the end. Number tables consecutively in accordance with their appearance in the text, place table caption above the table body and place any table notes below the body. Be sparing in the use of tables and ensure that the data presented in them do not duplicate results described elsewhere in the article. Please avoid using vertical rules and shading in table cells.

Example of table caption: Table 1. Case studies and used methods

10. The optimum size of a manuscript is about 3,000–5,000 words. Under the decision (or request) of the Editorial Board methodological and problem articles or reviews up to 8,000–10,000 words long can be accepted.

11. To facilitate the editorial assessment and reviewing process authors should submit "full" electronic version of their manuscript with embedded figures of "screen" quality as a **PDF or DOC file.**

12. We encourage authors to list three potential expert reviewers in their field. The Editorial Board will view these names as suggestions only.

13. Original reviews of submitted manuscripts remain deposited for 3 years.

# SCIENTIFIC AND PRACTICAL PEER-REVIEWED JOURNAL “GEOGRAPHY, ENVIRONMENT, SUSTAINABILITY”

No. 03 (v. 12) 2019

**FOUNDERS OF THE MAGAZINE:** Russian Geographical Society, Faculty of Geography, Lomonosov Moscow State University and Institute of Geography of the Russian Academy of Sciences

The magazine is published with financial support of the Russian Geographical Society.

The magazine is registered in Federal service on supervision of observance of the legislation in sphere of mass communications and protection of a cultural heritage. The certificate of registration: ПИ № ФС77-67752, 2016, December 21.

## **PUBLISHER**

Russian Geographical Society  
Moscow, 109012 Russia  
Novaya ploshchad, 10, korp. 2  
Phone 8-800-700-18-45  
E-mail: [press@rgo.ru](mailto:press@rgo.ru)  
[www.rgo.ru/en](http://www.rgo.ru/en)

## **EDITORIAL OFFICE**

Lomonosov Moscow State University  
Moscow 119991 Russia  
Leninskie Gory,  
Faculty of Geography, 1806a  
Phone 7-495-9391552  
Fax 7-495-9391552  
E-mail: [ges-journal@geogr.msu.ru](mailto:ges-journal@geogr.msu.ru)  
[www.ges.rgo.ru](http://www.ges.rgo.ru)

## **DESIGN & PRINTING**

Agency «CONNECT»  
Moscow, 117452,  
Artekovskaya str., 9, korp. 1  
Phone: +7 (495) 955-91-53  
E-mail: [info@connect-adv.ru](mailto:info@connect-adv.ru)

Sent into print 04.06.2019  
Order N gi319

Format 70 ½ 100 cm/16  
11,4 p. sh.  
Digital print  
Circulation 20 ex.